Topics in Organometallic Chemistry 63

Pierre H. Dixneuf
Jean-François Soulé *Editors*

Organometallics for Green Catalysis

Springer

63
Topics in Organometallic Chemistry

Aims and Scope

The series *Topics in Organometallic Chemistry* presents critical overviews of research results in organometallic chemistry. As our understanding of organometallic structure, properties and mechanisms increases, new ways are opened for the design of organometallic compounds and reactions tailored to the needs of such diverse areas as organic synthesis, medical research, biology and materials science. Thus the scope of coverage includes a broad range of topics of pure and applied organometallic chemistry, where new breakthroughs are being achieved that are of significance to a larger scientific audience.

The individual volumes of *Topics in Organometallic Chemistry* are thematic. Review articles are generally invited by the volume editors. All chapters from Topics in Organometallic Chemistry are published Online First with an individual DOI. In references, Topics in Organometallic Chemistry is abbreviated as Top Organomet Chem and cited as a journal.

More information about this series at http://www.springer.com/series/3418

Pierre H. Dixneuf • Jean-François Soulé
Editors

Organometallics for Green Catalysis

With contributions by

M. Beller · K. Beydoun · C. Bruneau · N. Chatani · J. G. de Vries · P. H. Dixneuf · R. A. Farrar-Tobar · C. Fischmeister · M. F. Hertrich · P. Hu · W. D. Jones · J. Klankermayer · A. Lei · W. Leitner · Y. Liu · D. Milstein · M. Schmitz · M. V. Solmi · J.-F. Soulé · S. Tin · M. Tobisu · H. Yi

Springer

Editors
Pierre H. Dixneuf
Organométalliques, matériaux et Catalyse
Univ Rennes, CNRS, (UMR 6226)
Institut Sciences Chimiques
Rennes, France

Jean-François Soulé
Organométalliques, matériaux et Catalyse
Univ Rennes, CNRS, (UMR 6226)
Institut Sciences Chimiques
Rennes, France

ISSN 1436-6002 ISSN 1616-8534 (electronic)
Topics in Organometallic Chemistry
ISBN 978-3-030-10954-7 ISBN 978-3-030-10955-4 (eBook)
https://doi.org/10.1007/978-3-030-10955-4

Library of Congress Control Number: 2019931921

This Springer imprint is published by the registered company Springer Nature Switzerland AG
The registered company address is: Gewerbestrasse 11, 6330 Cham, Switzerland

Preface

Climate change, resource depletion, and environmental protection create new challenges for the scientific community. In order to maintain quality of life by developing novel technologies and sciences, chemists have to find new catalytic processes toward green and sustainable chemistry and to offer useful industrial applications. One consensus already reached is that organometallic chemistry and related catalysts constitute a strength in the development of green chemistry. Indeed, organometallic catalysis plays a crucial role in straightforward access to complex molecules and novel molecular materials with the discovery of unprecedented reactivities and has been a pillar of industrial chemistry. While both energy and green chemistry fields are still under development, the emergence of concepts and strategies based on organometallics that contribute lasting value is beginning to be observed.

This volume of *Topics in Organometallic Chemistry* is dedicated to giving an overview of the most important aspects of the applications of transition metal complexes in green chemistry, including the transformation of renewables and the formation of bulk chemicals as well as some examples of the storage or production of energy.

Developing new strategies to recycle carbon dioxide into useful resources is becoming increasingly crucial. The valorization of carbon dioxide into useful products or its use as an energy carrier can now be achieved owing to the development of novel transition metal complexes. The first chapter of this volume, written by Beller and Hertrich, focused on hydrogenation of carbon dioxide into methanol, which is one of the most important reactions related to the "methanol economy" concept. The prospect of utilizing carbon dioxide as a C1 feedstock for synthetic applications is also discussed in two chapters. Leitner et al. give an outline of catalytic pathways to synthesize a variety of useful compounds on reactions of carbon dioxide as C1 building block with simple alkenes, while Klankermayer and Beydoun summarize the recent applications of carbon dioxide for the formation of

C–N and C–O bonds within the syntheses of formamides, methyl amines, and dialkoxymethanes.

Sustainable production of bulk chemicals from renewables is not limited to the use of carbon dioxide as the valorization of bio-based raw materials is also an important green catalysis research topic. Recent progress was made using organometallic catalysts. The chapter by Bruneau and Fischmeister reveals the state of the art for the valorization of oils by olefin metathesis, where specific organometallic catalysts are now performant to be used for low purity renewable materials transformations. Among renewables or bio-based raw materials, phenol derivatives have attracted significant attention as a renewable aromatic feedstock for the production of organic compounds that are useful for our society. Chatani and Tobisu give a comprehensive overview of recent advances in the area of catalytic transformations of phenol derivatives via the activation of C(aryl)–O bonds of aryl esters, carbamates, ethers, as well as phenols.

Pincer complexes have recently brought revolutions in catalysis and especially in the way to generate and activate hydrogen, leading to new catalytic processes with high TON never reached before. The contribution of Jones points out the predominant role of low-cost iron pincer complexes as sustainable catalysts for the hydrogenation and dehydrogenation reactions of common organic compounds. By contrast, Milstein and Hu, employing water instead of hazardous oxidants, reveal the eco-friendly oxidation of alcohols into carboxylic acids with the use of catalytic amount of pincer complexes. De Vries et al. point out the advantages of hydrogen transfer reactions as green and selective processes for the preparation of allylic alcohols, which are versatile compounds useful in a large variety of industrial processes.

C–H bond activation and functionalization, which is one of most useful eco-friendly processes in organic synthesis, and recently presented in two volumes of *Topics in Organometallic Chemistry* by Dixneuf and Doucet, can now be achieved with the help of photoredox systems enabling valorization of sunlight as a clean energy source. Dixneuf and Soulé give an overview of the advantages of the use of photoredox systems for the formation of C–C bonds from C(sp^2)–H bonds under green conditions, whereas Lei et al. present the contribution of C–H bond oxidation using visible light for the formation of C–O and C–N bonds.

This volume of *Topics in Organometallic Chemistry* offers a versatile point of view on the recent progress of organometallic catalysis for valorization of bulk chemicals into the high-value daily-life products and/or energy vector using green catalytic processes, which is of growing importance for academic and industrial scientists. The green catalytic processes presented in this volume are likely to highlight the profit brought by catalysis for a better environment but also to the improved knowledge of teachers and students in this developing field. Many catalytic processes presented in this volume will initiate the design of new organometallics as more efficient catalysts and find further applications attractive for industry and economy.

We are grateful to all the contributors, experts in various complementary fields, who have contributed with us to create this multiple-facet volume.

We dedicate this volume to all chemists and students who are contributing to discover new organometallic catalysts and new green and sustainable catalytic processes increasing scientific knowledge for our societal profit.

Rennes, France — Pierre H. Dixneuf
Rennes, France — Jean-François Soulé
24 September 2018

Contents

Top Organomet Chem (2019) 63: 1–16
DOI: 10.1007/3418_2018_13

Published online: 12 October 2018

Metal-Catalysed Hydrogenation of CO_2 into Methanol

Maximilian Franz Hertrich and Matthias Beller

Contents

Abstract The conversion of carbon dioxide into value-added chemicals is of growing importance for academic and industrial scientists. Regarding scale, the reduction of carbon dioxide to methanol is the most important reaction, not only for chemical products but also as a potential energy vector. Herein, we describe recent developments in carbon dioxide reduction to methanol focusing on the use of organometallic catalysts.

Keywords Carbon dioxide · Homogenous catalysis · Methanol

1 Methanol: From Platform Chemical to "Methanol Economy"

One of the main problems we have to face in the next decades is the climate change caused by the increase of carbon dioxide and other greenhouse gases in the atmosphere, which will even more accelerate in the future due to the growing world economy and population. In order to reduce emissions and to overcome intensive

M. F. Hertrich and M. Beller (✉)
LIKAT, Rostock, Germany
e-mail: Matthias.beller@catalysis.de

consumption of fossil energy carriers, society, politics and economy all over the world focus on "energy turnaround" and "traffic turnaround". For example, in Europe, Belgium, Germany, Italy, Denmark, Norway, Switzerland and other countries not only ban coal, oil and natural gas as energy sources but also ban nuclear power. Therefore new value chains and technologies for a renewable energy supply are highly desired [1].

A key issue for the transformation of the current global energy system is the storage of flexible and dynamic renewable energy in form of more stable chemical energy carriers. In this context the concept of a so-called methanol economy was established by Olah [2]. In this concept, methanol is proposed as a universal energy storage medium, either to use it (directly) or its derivative dimethylether (DME) as fuel for engines and fuel cells, respectively. In general, methanol is biologically easily degradable and has advantageous properties with respect to handling and storage infrastructure [3]. In this concept methanol should be produced through hydrogenation of carbon dioxide, which can be obtained via separation from air directly [4], from flue gas or other sources [5]. The required hydrogen for the reduction of the carbon dioxide should be produced by electrolysis with renewable electricity. This also opens the possibilities for economic development of countries with large deserts in the global south [6]. In that way a closed cycle for the production of energy carriers and fuels based on renewable resources could be achieved. However, currently the synthesis of methanol with hydrogen produced by electrolysis is not competitive under the economic conditions of 2018 [7]. Therefore, most of the methanol is still fabricated from fossil resources based on synthesis gas [8].

Beside its use as fuel, methanol is widely applied as platform chemical in today's chemical industry. More specifically, methanol is used for the production of formaldehyde, acetic acid (*Monsanto* process), methyl *tert*-butyl ether, olefins and specialities [9]. Hence, in principle starting from methanol, a variety of industrially relevant products could be obtained from this C_1 building block [3, 8]. For this reason, methanol from carbon dioxide can be a significant substitute for oil in the chemical industry [10].

2 Physicochemical Approach: Nature of CO_2 Hydrogenation to Methanol

Hydrogenation of carbon dioxide to methanol in the gas phase is closely related to the (reverse) water-gas shift reaction and the hydrogenation of carbon monoxide to methanol (Eqs. I–III, Scheme 1). These reactions are typically catalysed by heterogeneous materials composed of different metal oxides [11]. All three reactions will occur simultaneously and are in chemical equilibria. Since the reaction steps and the formation of possible intermediates on the surface of a heterogeneous catalyst are still not fully understood, the research in that field concentrates on fundamental

Scheme 1 Hydrogenation of carbon dioxide to methanol and related reactions

$$CO_2 + 3\,H_2 \rightleftharpoons CH_3OH + H_2O \quad (I)$$

$$CO_2 + H_2 \rightleftharpoons CO + H_2O \quad (II)$$

$$CO + 2\,H_2 \rightleftharpoons CH_3OH \quad (III)$$

thermodynamic and kinetics of the corresponding reactions. In this context, Graaf et al. have made great efforts to describe the thermodynamic equilibria properly and find the equilibria constants [12, 13]. Moreover, they investigated the kinetics of carbon dioxide reduction catalysed by a commercial Cu-Zn-Al mixed oxide [14].

The reductions of carbon oxides to methanol are both exothermic, whereas the water-gas shift reaction is endothermic. Obviously, the gas phase reactions to methanol can be positively influenced by applied pressure and decreased temperature following the principle of Le Chatelier [15]. However, with regard to practicability, carbon dioxide reduction is normally carried out at 50 bar and 220–270°C, which limits the yield for thermodynamically reasons to under 35% [16]. Besides increasing pressure, some groups pointed out that the separation of either water or methanol via condensation or sorption can improve the methanol yield up to about 70% [16, 17].

In contrast to heterogeneously catalysed gas phase reactions, the formation of methanol from carbon dioxide in liquid phase is better understood [18]. In general, there are three steps with three different intermediates for the hydrogenation of carbon dioxide assumed: initial reduction to formic acid or formates, respectively, followed by the reductive formation of formaldehyde or related formyl species coupled with dissociation of water and, finally, further hydrogenation and release of methanol. The first two steps have a higher activation barrier, whereas the reduction of formaldehyde to methanol is kinetically easier. Typically, the hydrogenation of formic acid or the formate species is supposed to be the rate determining step [19].

3 Industrial Relevant Catalysts and Established Processes

Notably until the 1920s, methanol was synthesised mainly out of wood as a by-product of the coking process [3]. In contrast, all currently applied industrial methanol processes are based on synthesis gas using heterogeneous catalysts. In general, synthesis gas for methanol is mostly produced via steam reforming, partial oxidation of natural gas or coal gasification. As early as 1924, BASF took out the first patent in this field [20]. In this first industrial process, a mixture of carbon monoxide and dioxide was reduced with hydrogen at 200 bars and 400°C in the presence of zinc-chromium-oxides doped with other metals. Nowadays, Cu/ZnO/Al_2O_3 systems constitute state-of-the-art catalysts with or without different additives. Almost 80% of the presently used catalysts belong to this type of materials. In

addition, palladium and bimetallic catalysts have been studied to a lesser extent [21]. For this reason, the copper-based systems are relatively well understood. As an example, Schlögl, Behrens and co-workers investigated in detail the active sides of this latter heterogeneous catalysts [22], whereas the group of Słoczyński pointed out the influence of different transition metal additives to the established system [23, 24]. Besides different palladium-based materials [25–28], also platinum [29–31] and nickel [32, 33] were shown to be active for carbon monoxide/carbon dioxide hydrogenation. Interestingly, not only oxidic species but also carbides were shown to catalyse this reaction [34]. Nonetheless, most of the currently used catalysts belong to the $Cu/ZnO/Al_2O_3$ type [21]. Typical reaction conditions vary from 190°C to 270°C and 15 bar to 90 bar pressure [35]. It should be clearly pointed out that the present processes use synthesis gas as feedstock vide supra, which is transformed with water to carbon dioxide in situ. Nevertheless, different life cycle assessment studies for carbon dioxide hydrogenations [11] and concept studies [36] suggest methanol production directly from carbon dioxide. Indeed, besides some pilot plants [10], the "George Olah CO_2 to Renewable Methanol Plant" in Iceland with a capacity of about 4,000 tons per year [37] demonstrates the feasibility of this approach. It produces methyl alcohol electrochemically from flue gas of a geothermic power plant. The special conditions for low-cost geothermal energy in Iceland are essential for the competitiveness of this demonstration unit. Due to the low oil and natural gas prices in recent years, methanol production from syngas out of fossil resources will still dominate in industry in the coming decade [38].

Nonetheless, direct carbon dioxide hydrogenation is a research field of high interest and is not confined to heterogeneous catalysis. Organometallic well-defined complexes catalyse the reduction of carbon dioxide at lower temperatures [39] and in some cases even at ambient pressures [40] which is positive with respect to the thermodynamics or costs of the reaction. Additionally, such processes might be beneficial for decentralised small-scale production units for methanol, which may play a role as part of a storage technology for an energy supply system in the future. Although homogenous catalysts are prone to a more rational design, currently their performance is far away from being practically relevant. Also other approaches for the formation of methanol from carbon dioxide based on photo- [41] or plasma-catalysts are interesting but yet not applicable [42].

4 Organometallic Catalysed Hydrogenation of CO_2

4.1 First Active System

In 1993, the group of Tominaga reported that carbon dioxide can be reduced with hydrogen in the presence of ruthenium dodecacarbonyl and alkalimetal iodides to form methanol, methane and carbon monoxide, respectively [43]. The reaction was performed in *N*-methylpyrrolidone at 240°C under 20 bar of carbon dioxide and 60 bar of hydrogen. The presence of dissolved iodide ions was essential for the

stabilisation of the active species: Without addition of iodide, the ruthenium complex decomposed to ruthenium metal particles, which gave methane as main product. In a follow-up publication, Tominaga et al. described the proposed mechanism for the hydrogenation of carbon dioxide with that system based on results from IR experiments [44]. First, the tetranuclear complex $[H_2Ru_4(CO)_{12}]^{2-}$ is formed under reaction conditions. This complex releases carbon monoxide in the presence of iodide in a reverse water gas shift reaction. Next, carbon monoxide reacts with $[H_2Ru_4(CO)_{12}]^{2-}$ and iodide to form the trinuclear $[HRu_3(CO)_{11}]^{-}$ and mononuclear $[Ru(CO)_3I_3]^{-}$ complex, which undergo in a following catalytic cycle the hydrogenation of carbon monoxide to methanol (Scheme 2).

At the optimal reaction temperature (240°C), a TON of 32 (based on ruthenium) was obtained with that system. At lower temperatures only formation of carbon monoxide or no reaction and at higher temperatures formation of methane took place. Other precursors as $Fe_2(CO)_8$, $Co_2(CO)_8$, $Mo(CO)_6$, $Rh_3(CO)_{12}$, $W(CO)_6$ or $Ir_4(CO)_{12}$ were not active in the reaction, whereas different iodide sources can be applied. Although the ruthenium carbonyl-based system has significant disadvantages such as high reaction temperature, low selectivity and low stability, it was state-of-the-art in this homogeneous transformation for over 15 years.

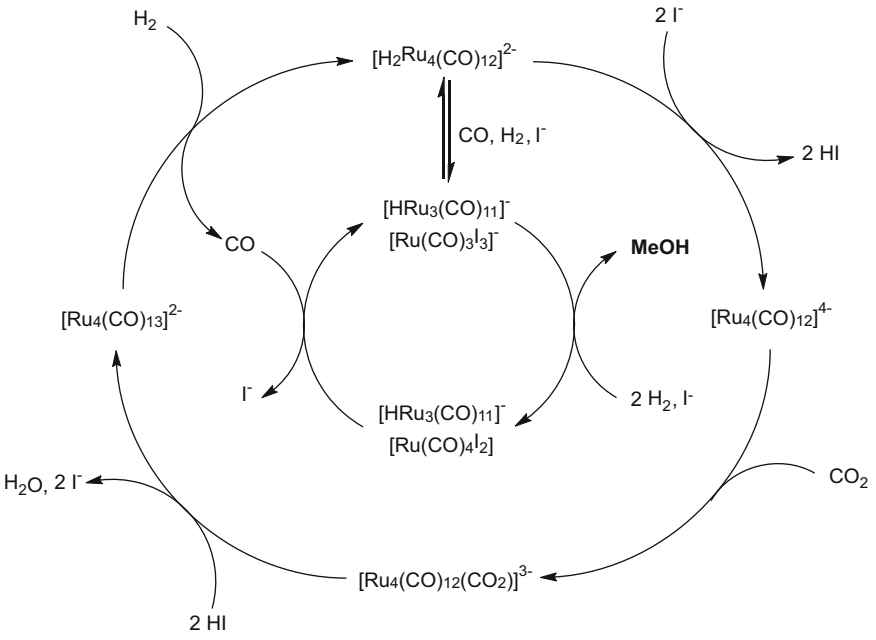

Scheme 2 Proposed mechanism for the first homogeneous carbon dioxide hydrogenation (adapted from Tominaga et al. [44])

4.2 *Indirect or Stepwise CO_2 Hydrogenation*

More recently, different groups suggested an indirect pathway for the methanol synthesis out of carbon dioxide via reduction of carbonates, carbamates or other more activated carbon dioxide derivatives, which can be easily prepared from carbon dioxide with amines or alcohols [45]. In 2011, based on previous efforts in the hydrogenation of amides [46] and urea derivatives [47], Milstein and co-workers described ruthenium PNN pincer-type catalysts (Scheme 3) for hydrogenation of carbonates, carbamates and formates to methanol as indirect method for carbon dioxide reduction [48]. The ability of the so-called non-innocent ligand metal complex to split hydrogen to form an active dihydride species is essential for that reaction. The thermodynamically favoured aromatisation of the pyridine moiety in the ligand backbone is considered to be responsible for that reactivity (Scheme 3). For the hydrogenation of urea derivatives, carbonates, carbamates and formates, Milstein et al. achieved with catalyst **1** TONs of methanol production up to 57 [47] and 4400, 98, 4700 [48], respectively. Despite these interesting results, it should be mentioned that this system is not able to hydrogenate carbon dioxide directly.

In the same year, Huff and Sanford described a so-called cascade catalysis process, which overcomes this problem [49]. The individual three steps are (1) reduction of carbon dioxide to formic acid with $[Ru(PMe_3)_4(OAc)Cl]$, (2) formation of methyl formate catalysed by $Sc(OTf)_3$ and (3) hydrogenation of methyl formate to methanol by Milstein's catalyst (**1**, see Scheme 3). The reaction was performed under 30 bar of hydrogen and 10 bar of carbon dioxide at 135°C in methanol for 16 h. However, the TON for methanol is with 2.5 significantly too low for any application. The authors pointed out that the deactivation of Milstein's catalyst by $Sc(OTf)_3$ is the main reason for that. In a control experiment where they separated

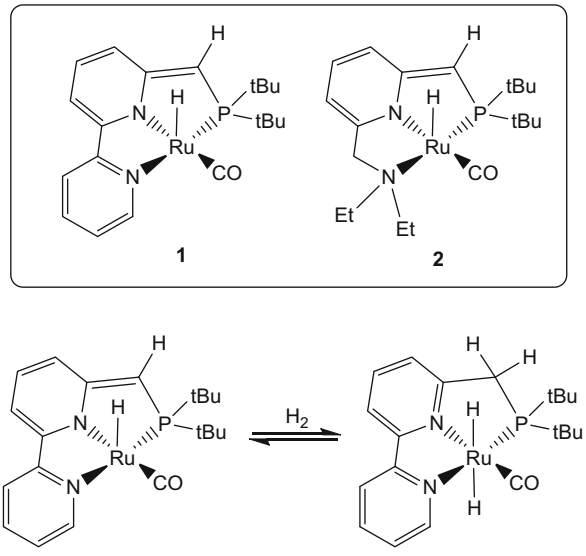

Scheme 3 Different hydrogenation catalysts prepared by Milstein's group and proposed formation of the catalytic active species for the hydrogenation of carbon dioxide derivatives [48]

the third from the two former reaction steps via transferring the volatile, generated methyl formate from a first to a second reaction vessel, they improved the TON to 21.

An interesting approach for indirect carbon dioxide hydrogenation was developed by Ding and co-workers, who reduced cyclic carbonates at 140°C with different ruthenium PNP pincer catalysts and KOtBu (1 eq. regarding the catalyst) as co-catalyst under 50 bar of hydrogen [50]. As shown in Scheme 4, the stable pre-catalyst **3** forms the active ruthenium complex **3′**. This species activates hydrogen under generation of dihydride complex **3″** which transfers in a consecutive reaction step the activated hydrogen to the cyclic carbonate. After rearrangement it is reduced again by **3″** to give ethylene glycol and formaldehyde. Finally, the generated formaldehyde is reduced in a third hydrogenation step to methanol. It should be mentioned that Gordon recently assumed a more elaborated mechanism for this type of reactions [51].

Catalyst **3** was identified to be the most active one for this reaction with a maximum TON of 84000 and has not only the ability to hydrogenate cyclic carbonates but also polycarbonates. The authors suggest for an industrial application to link their reaction with the well-established *Shell Omega* process which is carried out to produce ethylene carbonate out of ethylene oxide and carbon dioxide.

In 2015, Milstein's group reported a further development of the system described above [52]. In a two-step process, carbon dioxide was captured with different amino alcohols forming oxazolidinones in the presence of caesium carbonate. Consecutive hydrogenation proceeded with ruthenium pincer complexes (e.g. **1**, **2**) and KOtBu as

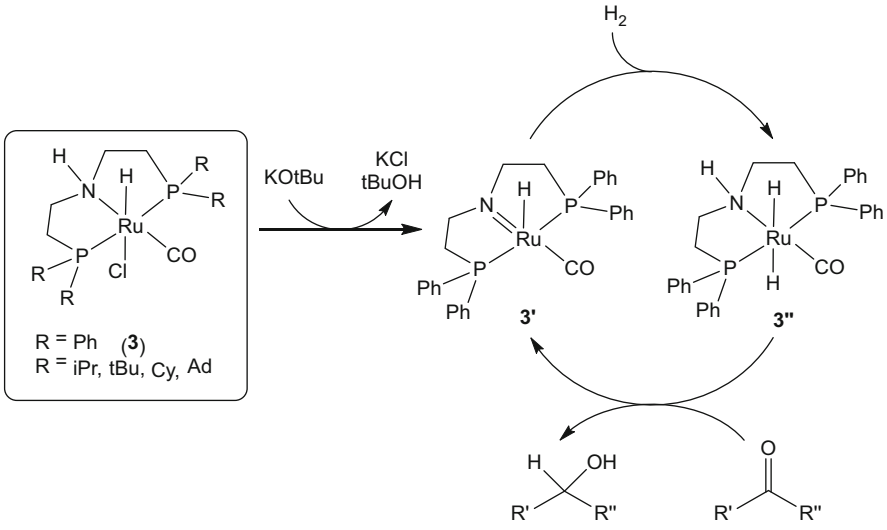

Scheme 4 Different hydrogenation catalysts prepared by Ding's group, proposed formation of the catalytic active species and simplified depiction of the catalytic cycle for the hydrogenation of cyclic carbonates [50]

(co-)catalyst. For the optimal capturing of carbon dioxide, valinol (1-isopropyl-2-hydroxylamine) was reacted in DMSO for 24 h under 1 bar of carbon dioxide in the presence of caesium carbonate as catalyst. After cooling to room temperature, degassing and filtering the reaction mixture, the ruthenium catalyst **1** and KOtBu were added and the hydrogenation was carried out (60 bar hydrogen, 135°C, 72 h). Under these optimal conditions, 53% overall yield for methanol was achieved. Based on the success of these indirect carbon dioxide hydrogenations, recently more efforts focused also on the direct carbon dioxide hydrogenation.

4.3 Direct CO_2 Hydrogenation

In 2012, the group of Klankermayer and Leitner published an interesting study for direct carbon dioxide hydrogenation [53]. In their work, ruthenium complexes of the special tridentate ligand triphos were applied as catalyst. In addition, strong acids (methane sulfonic acid, *p*-toluene sulfonic acid, bis(trifluoromethane) sulfimide) were required as co-catalyst. More specifically, the reaction was carried out at 140°C, 80 bar pressure (H_2:CO_2 = 3:1) with ethanol as additive and THF as solvent. As active species the ruthenium complex **4′** was postulated, which can be formed in situ from $Ru(acac)_3$ and triphos (Scheme 5). Notably, applying **4** as isolated direct precursor improved results for hydrogenation of carbon dioxide can be obtained. The authors assumed ethanol as a stabiliser by in situ formation of ethyl formate. Best yields for methanol were achieved when bis(trifluoromethane) sulfimide ($HNTf_2$) was used as co-catalyst. A reason for that might be the weakly coordinating character of the anion compared to methane sulfonate and *p*-tosylate anions. A ratio of 1:1 of catalyst and co-catalyst was pointed out to be optimal for the reaction. With optimal parameters a maximum TON of 221 was achieved.

Later, the same group investigated the reaction mechanism of this transformation using NMR, MS and computational studies [54]. In addition to their former findings regarding the role of ethanol, the authors describe another mechanism without formation of a formate ester as intermediate. As a starting point, they obtained some methanol in an NMR experiment without addition of any alcohol in the presence of catalyst **4**. Further in situ measurements of the solution pointed out

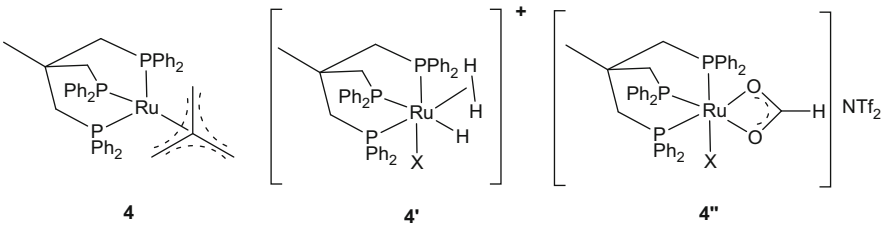

Scheme 5 Catalyst precursor, catalytic active species and intermediate/resting state of the carbon dioxide hydrogenation catalyst from Klankermayer and Leitner [53, 54]

complex **4**″ as active intermediate or resting state of the catalyst. In the same study, the TON of the catalyst could be improved by increasing the pressure or lowering the catalyst concentration up to 442. Additionally, recycling of the catalyst was provided applying the aqueous biphasic system 2-methyl tetrahydrofuran/water. The catalyst retained at least four times with 50% loss in activity.

In 2015, the group of Sanford described a homogeneous catalyst system for carbon dioxide hydrogenation under basic conditions [55]. This is of interest as the capturing of carbon dioxide and formation of more activated intermediates are usually carried out under basic and not acidic conditions. Hence, a catalytic process for carbon dioxide fixation in basic media can be advantageous [56]. Sanford and co-workers disclosed known ruthenium catalysts (**1**, **2**, **5**, see Schemes 3 and 7) and potassium phosphate as co-catalyst for their carbon dioxide reduction. First, they studied the ability of different ruthenium catalysts to reduce dimethylammonium dimethylcarbamate (DAMC) to methanol. Here, the commercial available complex **5** was successful to give methanol in addition to dimethylformamide (DMF) and dimethylammonium formate (DAF) as by-products. The addition of potassium phosphate as co-catalyst was essential for obtaining activity. The authors suggested two different mechanistic pathways for overall reaction, which are shown in Scheme 6: (a) direct reduction of DAMC via DMF to methanol and dimethyl amine (pathway I) or (b) decomposition of DAMC to carbon dioxide and dimethyl amine, consecutive reduction to formic acid, followed by substitution reaction to generate DMF and, finally, hydrogenation to methanol (pathway II). According to the second pathway, the addition of dimethyl amine should accelerate the formation of DMF from formic acid. Indeed, under optimal conditions 96% conversion of carbon dioxide and TONs of 220 for methanol and 740 for DAF/DMF were reached,

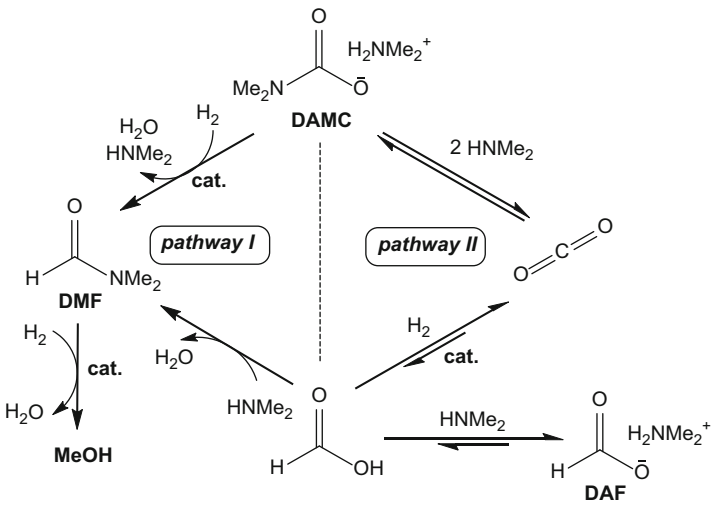

Scheme 6 Two possible reaction pathways for DAMC hydrogenation to methanol described by Sanford's group [55]

respectively. As major drawback of that system, the authors pointed out that the catalyst starts to decompose at 155°C.

Ding et al. discussed a related approach for carbon dioxide reduction under basic conditions with morpholine as capturing agent [57]. In this work, different ruthenium pincer complexes were tested for the *N*-formylation reaction of different amines using carbon dioxide and hydrogen (120°C, 40 h, 35 bar hydrogen, 35 bar carbon dioxide). Then, hydrogenation of methanol continued in the same pot at 160°C and 50 bar hydrogen pressure for 1 h. Ru-MACHO (**3**) as catalyst and THF as solvent were used for both steps.

Another interesting example for amine-assisted carbon dioxide fixation was published by Prakash's group in 2016 [40]. Herein, they reported different ruthenium PNP pincer complexes (Scheme 7), which were active for carbon dioxide hydrogenation with amine intermediates. The polyamine pentaethylenehexamine (PEHA) was used as capturing agent and triglyme as solvent. The process proceeded best at 75 bar (CO_2:H_2 = 1:3) and 155°C with **5** as catalyst. Again, relatively long reaction times were needed (40 h). When potassium phosphate was used as additive, TONs up to 690 could be reached – without an additive the TON decreased to 520. The bifunctional catalyst is essential for the reaction, and the corresponding

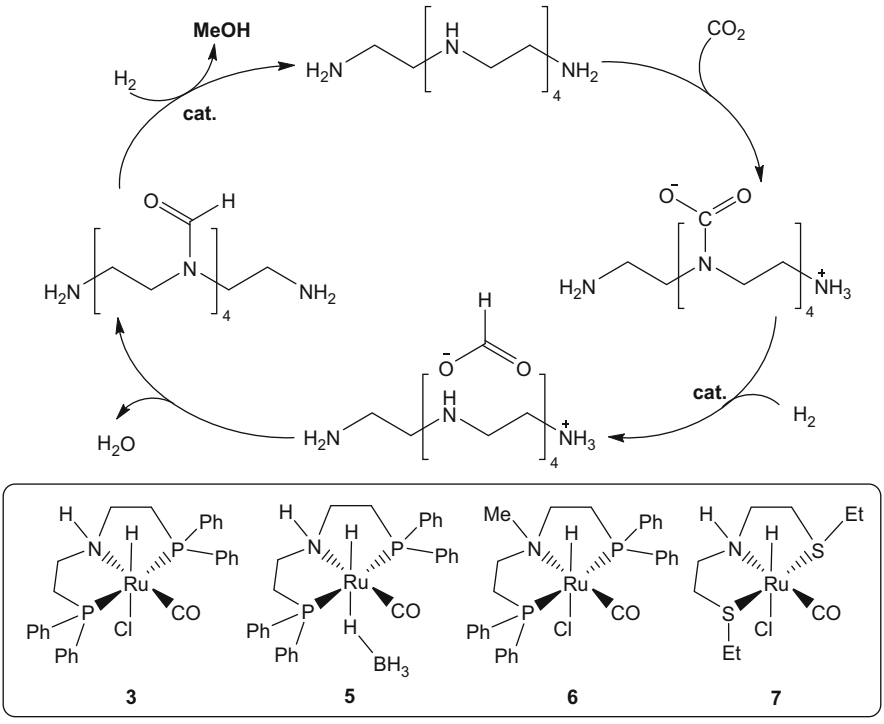

Scheme 7 Different ruthenium pincer catalysts and proposed reaction cycle for carbon dioxide hydrogenation with PEHA as capturing agent (adapted from Prakash et al. [40])

N-methylated derivative of **5** is not active in this reduction at all. Since PEHA and triglyme both have a high bowling point, water and methanol as main products can be easily separated by distillation from the reaction mixture. Using this strategy, the catalyst was recycled several times and was still active after the fifth cycle.

Notably, Prakash et al. captured carbon dioxide directly from synthetic air by passing it through an aqueous solution of PEHA at ambient pressure and room temperature. Afterwards a triglyme solution of **5** was added, and the captured carbon dioxide derivatives were reduced for 55 h at 155°C and 50 bar of hydrogen to give a yield of 79% methanol (with reference to captured carbon dioxide).

It is worth mentioning that the same group reported recently a system for sequential hydrogenation of carbon dioxide in aqueous media using pincer complexes as catalyst and PEHA as capturing agent [58]. The hydrogenation was carried out in a two-step process: First, carbon dioxide (partial pressure of about 0.07 bar) was captured in a mixture of catalyst, PEHA and water at 70°C for 4 h. Second, 2-methyl tetrahydrofuran was added, and the carbon dioxide derivatives were hydrogenated at 145°C and 70 bar of hydrogen for 72 h. Using **5** as catalyst, a maximum TON of 520 was achieved, and the catalyst and the auxiliary amine were recycled successfully multiple times.

In 2016, the groups of Himeda and Laurenczy disclosed a new concept for carbon dioxide reduction to methanol based on the disproportionation of formic acid [59]. The authors suggested as strategy the reduction of carbon dioxide to formic acid followed by the disproportionation of the formed formic acid to methanol and back to carbon dioxide. It was demonstrated that the iridium catalyst **8** (see Scheme 8) catalysed both reactions in water with sulfuric acid as co-catalyst. Under optimal conditions (20 bar CO_2, 60 bar H_2, 70°C, 2.5 mol/kg molality of sulfuric acid), the system was still active after 45 h, and the selectivities for the disproportionation products were >95% for methanol. Based on NMR and GC/MS experiments, the authors assumed an inner sphere mechanism for the reaction and direct hydrogenation of carbon dioxide to formic acid and consecutive disproportionation. Notably, this is the only methodology described in literature for carbon dioxide fixation to methanol in water, until now. Moreover, in a follow-up study, the authors

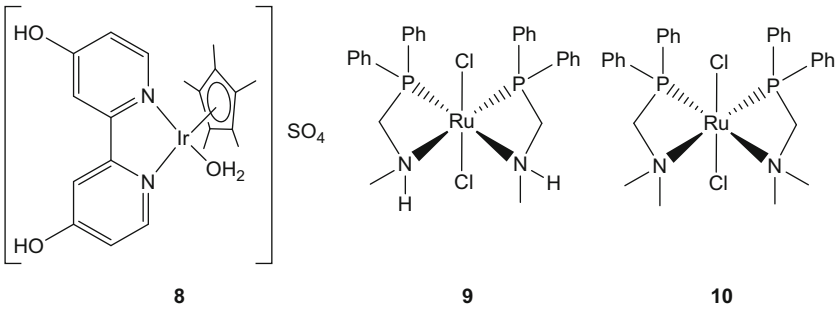

8 **9** **10**

Scheme 8 Different iridium and ruthenium complexes used as catalyst for carbon dioxide fixation by Sordakis et al. [59] and Everett and Wass [60]

demonstrated the recycling of their catalyst multiple times under aerobic conditions without a loss in activity [61].

In the same year, Everett and Wass identified ruthenium complexes based on bidentate phosphinoamine ligands to be active in carbon dioxide hydrogenation (Scheme 8) [60]. Once again, different amines were used as capturing agent for carbon dioxide and the reaction proceeded stepwise via formamides as intermediates. The hydrogenation was carried out at 180°C at a pressure of 10 bar carbon dioxide and 30 bar hydrogen in a mixture of toluene and amine as solvents with sodium ethanolate as additive. Most efficiently, complex **9** catalysed the reaction (TON of 8900) at very low catalyst loading of 50 nmol with di-isopropyl amine as auxiliary reagent. Based on their results the authors assumed an outer sphere mechanism according to Gordon's studies [51]. Furthermore, they hypothesised that a more steric demanding amine as capturing agent decelerates the generation of the formamide, whereas it increases the reaction rate of the hydrogenation of the formamide to methanol.

Up to this point, all discussed catalyst systems for homogeneous hydrogenation of carbon dioxide to methanol are based on different noble metal complexes. Recently, some groups made some efforts to overcome this problem. In 2017, Beller and co-workers described the first non-noble metal-based homogeneous catalyst for carbon dioxide hydrogenation [62]. Inspired by Leitner's and Klankermayer's ruthenium-based system [53], the catalytic active species is formed in situ from a mixture of cobalt(III) acetylacetonate, triphos and $HNTf_2$. The optimised reaction was performed at 100°C for 24 h and at a pressure of 20 bar carbon dioxide and 70 bar hydrogen. Under these conditions a maximum TON of 50 for methanol was achieved. Different cobalt precursors and additives were tested, and NMR and MS studies were carried out to investigate the mechanism of the reaction. As a result of that, a cationic cobalt triphos complex with the weakly coordinating NTf_2^- as anion was suggested as active species which is formed after an induction period from the cobalt precursor. Shortly after that, Klankermayer's group showed for a slightly different cobalt triphos system that substation of THF by a fluorinated isopropanol can improve the catalyst productivity. Both systems are working under non-basic conditions [63].

As another class of non-noble metal catalysts, Prakash and co-workers described manganese PNP pincer complexes for the title reaction (Scheme 9) [64]. The methodology followed a two-step process: (1) *N*-formylation of the amine (110°C, 30 bar CO_2, 30 bar H_2) and (2) hydrogenation of the in situ generated formamide

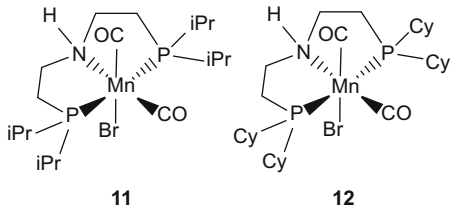

Scheme 9 Different manganese complexes used as catalyst for carbon dioxide hydrogenation by the group of Kar et al. [64]

(150°C, 70–80 bar hydrogen). Complex **11** was found to be most active under the optimised conditions with morpholine as capturing agent, KOtBu as activating base and THF as solvent. With **11** a TON for methanol up to 36 was reached.

5 Outlook

The catalytic hydrogenation of synthesis gas to methanol constitutes a major industrial process with fundamental importance for today's chemical industry. Currently, in this process also small amounts of carbon dioxide, which constitutes the active substrate, are present. In the future, larger amounts of carbon dioxide might be added to this process, which makes it also interesting for hydrogen storage technologies. However, the vision of a "methanol economy" is still far away from realisation since until now there are no economical competitive processes to produce methanol from carbon dioxide. The development of catalysts enabling much higher TONs and TOFs is crucial to overcome this problem. Besides that objective, costs of the catalysts have to be low, and the materials should be abundant. Moreover, other hurdles like carbon dioxide supply and water tolerance have to be addressed in the future. Although none of these problems has been solved in satisfying manner, interesting concepts and catalysts have been developed which are working under relatively mild conditions. In the future, work for homogeneous carbon dioxide valorisation should include more easily available feedstocks such as CO_2 streams directly from power plants.

References

1. Schlögl R (2011) Chemistry's role in regenerative energy. Angew Chem Int Ed 50:6424–6426. https://doi.org/10.1002/anie.201103415
2. Olah GA (2005) Beyond oil and gas: the methanol economy. Angew Chem Int Ed 44:2636–2639. https://doi.org/10.1002/anie.200462121
3. Olah GA, Goeppert A, Prakash GKS (2009) Chemical recycling of carbon dioxide to methanol and dimethyl ether: from greenhouse gas to renewable, environmentally carbon neutral fuels and synthetic hydrocarbons. J Org Chem 74:487–498. https://doi.org/10.1021/jo801260f
4. Sanz-Pérez ES, Murdock CR, Didas SA, Jones CW (2016) Direct capture of CO2 from ambient air. Chem Rev 116:11840–11876. https://doi.org/10.1021/acs.chemrev.6b00173
5. Boot-Handford ME et al (2014) Carbon capture and storage update. Energy Environ Sci 7:130–189. https://doi.org/10.1039/C3EE42350F
6. Offermanns H, Effenberger FX, Keim W, Plass L (2018) Solarthermie und CO2: methanol aus der Wüste. Chem Ing Tech 89:270–273. https://doi.org/10.1002/cite.201600169
7. Asif M, Gao X, Lv H, Xi X, Dong P (2018) Catalytic hydrogenation of CO2 from 600 MW supercritical coal power plant to produce methanol: a techno-economic analysis. Int J Hydrog Energy 43:2726–2741. https://doi.org/10.1016/j.ijhydene.2017.12.086
8. Goeppert A, Czaun M, Jones J-P, Surya Prakash GK, Olah GA (2014) Recycling of carbon dioxide to methanol and derived products – closing the loop. Chem Soc Rev 43:7995–8048. https://doi.org/10.1039/C4CS00122B

9. Ali KA, Abdullah AZ, Mohamed AR (2015) Recent development in catalytic technologies for methanol synthesis from renewable sources: a critical review. Renew Sust Energ Rev 44:508–518. https://doi.org/10.1016/j.rser.2015.01.010
10. Olah GA (2013) Towards oil independence through renewable methanol chemistry. Angew Chem Int Ed 52:104–107. https://doi.org/10.1002/anie.201204995
11. Artz J et al (2018) Sustainable conversion of carbon dioxide: an integrated review of catalysis and life cycle assessment. Chem Rev 118:434–504. https://doi.org/10.1021/acs.chemrev.7b00435
12. Graaf GH, Sijtsema PJJM, Stamhuis EJ, Joosten GEH (1986) Chemical equilibria in methanol synthesis. Chem Eng Sci 41:2883–2890. https://doi.org/10.1016/0009-2509(86)80019-7
13. Graaf GH, Winkelman JGM (2016) Chemical equilibria in methanol synthesis including the water–gas shift reaction: a critical reassessment. Ind Eng Chem Res 55:5854–5864. https://doi.org/10.1021/acs.iecr.6b00815
14. Graaf GH, Stamhuis EJ, Beenackers AACM (1988) Kinetics of low-pressure methanol synthesis. Chem Eng Sci 43:3185–3195. https://doi.org/10.1016/0009-2509(88)85127-3
15. Gaikwad R, Bansode A, Urakawa A (2016) High-pressure advantages in stoichiometric hydrogenation of carbon dioxide to methanol. J Catal 343:127–132. https://doi.org/10.1016/j.jcat.2016.02.005
16. Zachopoulos A, Heracleous E (2017) Overcoming the equilibrium barriers of CO2 hydrogenation to methanol via water sorption: a thermodynamic analysis. J CO2 Util 21:360–367. https://doi.org/10.1016/j.jcou.2017.06.007
17. Stangeland K, Li H, Yu Z (2018) Thermodynamic analysis of chemical and phase equilibria in CO2 hydrogenation to methanol, dimethyl ether, and higher alcohols. Ind Eng Chem Res 57:4081–4094. https://doi.org/10.1021/acs.iecr.7b04866
18. Li Y-N, Ma R, He L-N, Diao Z-F (2014) Homogeneous hydrogenation of carbon dioxide to methanol. Cat Sci Technol 4:1498–1512. https://doi.org/10.1039/C3CY00564J
19. Ge H, Chen X, Yang X (2017) Hydrogenation of carbon dioxide to methanol catalyzed by iron, cobalt, and manganese cyclopentadienone complexes: mechanistic insights and computational design. Chem Eur J 23:8850–8856. https://doi.org/10.1002/chem.201701200
20. Mittasch A, Pier M, Winkler K (1923) Ausführung organischer Katalysen. Germany Patent DE415686, 24.07.1923
21. Alvarez A et al (2017) Challenges in the greener production of Formates/formic acid, methanol, and DME by heterogeneously catalyzed CO2 hydrogenation processes. Chem Rev 117:9804–9838. https://doi.org/10.1021/acs.chemrev.6b00816
22. Behrens M et al (2012) The active site of methanol synthesis over Cu/ZnO/Al2O3 industrial catalysts. Science 336:893–897. https://doi.org/10.1126/science.1219831
23. Słoczyński J, Grabowski R, Kozłowska A, Olszewski P, Lachowska M, Skrzypek J, Stoch J (2003) Effect of Mg and Mn oxide additions on structural and adsorptive properties of Cu/ZnO/ZrO2 catalysts for the methanol synthesis from CO2. Appl Catal A 249:129–138. https://doi.org/10.1016/S0926-860X(03)00191-1
24. Słoczyński J, Grabowski R, Olszewski P, Kozłowska A, Stoch J, Lachowska M, Skrzypek J (2006) Effect of metal oxide additives on the activity and stability of Cu/ZnO/ZrO2 catalysts in the synthesis of methanol from CO2 and H2. Appl Catal A 310:127–137. https://doi.org/10.1016/j.apcata.2006.05.035
25. Fujitani T, Saito M, Kanai Y, Watanabe T, Nakamura J, Uchijima T (1995) Development of an active Ga2O3 supported palladium catalyst for the synthesis of methanol from carbon dioxide and hydrogen. Appl Catal A 125:L199–L202. https://doi.org/10.1016/0926-860X(95)00049-6
26. Liang X-L, Dong X, Lin G-D, Zhang H-B (2009) Carbon nanotube-supported Pd–ZnO catalyst for hydrogenation of CO2 to methanol. Appl Catal B 88:315–322. https://doi.org/10.1016/j.apcatb.2008.11.018
27. Bahruji H et al (2016) Pd/ZnO catalysts for direct CO2 hydrogenation to methanol. J Catal 343:133–146. https://doi.org/10.1016/j.jcat.2016.03.017

28. Malik AS, Zaman SF, Al-Zahrani AA, Daous MA, Driss H, Petrov LA (2018) Development of highly selective PdZn/CeO2 and Ca-doped PdZn/CeO2 catalysts for methanol synthesis from CO2 hydrogenation. Appl Catal A 560:42–53. https://doi.org/10.1016/j.apcata.2018.04.036
29. Shao C, Fan L, Fujimoto K, Iwasawa Y (1995) Selective methanol synthesis from CO2/H2 on new SiO2-supported PtW and PtCr bimetallic catalysts. Appl Catal A 128:L1–L6. https://doi.org/10.1016/0926-860X(95)00109-3
30. Khan MU et al (2016) Pt3Co octapods as superior catalysts of CO2 hydrogenation. Angew Chem Int Ed 55:9548–9552. https://doi.org/10.1002/anie.201602512
31. Bai S, Shao Q, Feng Y, Bu L, Huang X (2017) Highly efficient carbon dioxide hydrogenation to methanol catalyzed by zigzag platinum-cobalt nanowires. Small 13. https://doi.org/10.1002/smll.201604311
32. Studt F et al (2014) Discovery of a Ni-Ga catalyst for carbon dioxide reduction to methanol. Nat Chem 6:320–324. https://doi.org/10.1038/nchem.1873
33. Hengne AM et al (2018) Ni–Sn-supported ZrO2 catalysts modified by indium for selective CO2 hydrogenation to methanol. ACS Omega 3:3688–3701. https://doi.org/10.1021/acsomega.8b00211
34. Rodriguez JA, Liu P, Stacchiola DJ, Senanayake SD, White MG, Chen JG (2015) Hydrogenation of CO2 to methanol: importance of metal–oxide and metal–carbide interfaces in the activation of CO2. ACS Catal 5:6696–6706. https://doi.org/10.1021/acscatal.5b01755
35. Dang S, Yang H, Gao P, Wang H, Li X, Wei W, Sun Y (2018) A review of research progress on heterogeneous catalysts for methanol synthesis from carbon dioxide hydrogenation. Catal Today. https://doi.org/10.1016/j.cattod.2018.04.021
36. Van-Dal ÉS, Bouallou C (2013) Design and simulation of a methanol production plant from CO2 hydrogenation. J Clean Prod 57:38–45. https://doi.org/10.1016/j.jclepro.2013.06.008
37. www.carbonrecycling.is/george-olah/. Accessed 23 May 2018
38. www.methanol.org/the-methanol-industry/. Accessed 23 May 2018
39. Alberico E, Nielsen M (2015) Towards a methanol economy based on homogeneous catalysis: methanol to H2 and CO2 to methanol. Chem Commun 51:6714–6725. https://doi.org/10.1039/C4CC09471A
40. Kothandaraman J, Goeppert A, Czaun M, Olah GA, Prakash GKS (2016) Conversion of CO2 from air into methanol using a polyamine and a homogeneous ruthenium catalyst. J Am Chem Soc 138:778–781. https://doi.org/10.1021/jacs.5b12354
41. Sun Z, Talreja N, Tao H, Texter J, Muhler M, Strunk J, Chen J (2018) Catalysis of carbon dioxide photoreduction on nanosheets: fundamentals and challenges. Angew Chem Int Ed Engl 57:2–20. https://doi.org/10.1002/anie.201710509
42. Wang L, Yi Y, Guo H, Tu X (2018) Atmospheric pressure and room temperature synthesis of methanol through plasma-catalytic hydrogenation of CO2. ACS Catal 8:90–100. https://doi.org/10.1021/acscatal.7b02733
43. Tominaga K-i, Sasaki Y, Kawai M, Watanabe T, Saito M (1993) Ruthenium complex catalysed hydrogenation of carbon dioxide to carbon monoxide, methanol and methane. J Chem Soc Chem Commun:629–631. https://doi.org/10.1039/C39930000629
44. Tominaga K-i, Sasaki Y, Watanabe T, Saito M (1995) Homogeneous hydrogenation of carbon dioxide to methanol catalyzed by ruthenium cluster anions in the presence of halide anions. Bull Chem Soc Jpn 68:2837–2842. https://doi.org/10.1246/bcsj.68.2837
45. Du XL, Jiang Z, Su DS, Wang JQ (2016) Research progress on the indirect hydrogenation of carbon dioxide to methanol. ChemSusChem 9:322–332. https://doi.org/10.1002/cssc.201501013
46. Balaraman E, Gnanaprakasam B, Shimon LJW, Milstein D (2010) Direct hydrogenation of amides to alcohols and amines under mild conditions. J Am Chem Soc 132:16756–16758. https://doi.org/10.1021/ja1080019
47. Balaraman E, Ben-David Y, Milstein D (2011) Unprecedented catalytic hydrogenation of urea derivatives to amines and methanol. Angew Chem 123:11906–11909. https://doi.org/10.1002/ange.201106612

48. Balaraman E, Gunanathan C, Zhang J, Shimon LJW, Milstein D (2011) Efficient hydrogenation of organic carbonates, carbamates and formates indicates alternative routes to methanol based on CO2 and CO. Nat Chem 3:609. https://doi.org/10.1038/nchem.1089
49. Huff CA, Sanford MS (2011) Cascade catalysis for the homogeneous hydrogenation of CO2 to methanol. J Am Chem Soc 133:18122–18125. https://doi.org/10.1021/ja208760j
50. Han Z, Rong L, Wu J, Zhang L, Wang Z, Ding K (2012) Catalytic hydrogenation of cyclic carbonates: a practical approach from CO2 and epoxides to methanol and diols. Angew Chem Int Ed 51:13041–13045. https://doi.org/10.1002/anie.201207781
51. Dub PA, Gordon JC (2017) Metal–ligand bifunctional catalysis: the "accepted" mechanism, the issue of concertedness, and the function of the ligand in catalytic cycles involving hydrogen atoms. ACS Catal 7:6635–6655. https://doi.org/10.1021/acscatal.7b01791
52. Khusnutdinova JR, Garg JA, Milstein D (2015) Combining low-pressure CO2 capture and hydrogenation to form methanol. ACS Catal 5:2416–2422. https://doi.org/10.1021/acscatal.5b00194
53. Wesselbaum S, vom Stein T, Klankermayer J, Leitner W (2012) Hydrogenation of carbon dioxide to methanol by using a homogeneous ruthenium–phosphine catalyst. Angew Chem 124:7617–7620. https://doi.org/10.1002/ange.201202320
54. Wesselbaum S et al (2015) Hydrogenation of carbon dioxide to methanol using a homogeneous ruthenium-Triphos catalyst: from mechanistic investigations to multiphase catalysis. Chem Sci 6:693–704. https://doi.org/10.1039/C4SC02087A
55. Rezayee NM, Huff CA, Sanford MS (2015) Tandem amine and ruthenium-catalyzed hydrogenation of CO2 to methanol. J Am Chem Soc 137:1028–1031. https://doi.org/10.1021/ja511329m
56. Kar S, Kothandaraman J, Goeppert A, Prakash GKS (2018) Advances in catalytic homogeneous hydrogenation of carbon dioxide to methanol. J CO2 Util 23:212–218. https://doi.org/10.1016/j.jcou.2017.10.023
57. Zhang L, Han Z, Zhao X, Wang Z, Ding K (2015) Highly efficient ruthenium-catalyzed N-formylation of amines with H2 and CO2. Angew Chem 127:6284–6287. https://doi.org/10.1002/ange.201500939
58. Kar S, Sen R, Goeppert A, Prakash GKS (2018) Integrative CO2 capture and hydrogenation to methanol with reusable catalyst and amine: toward a carbon neutral methanol economy. J Am Chem Soc 140:1580–1583. https://doi.org/10.1021/jacs.7b12183
59. Sordakis K, Tsurusaki A, Iguchi M, Kawanami H, Himeda Y, Laurenczy G (2016) Carbon dioxide to methanol: the aqueous catalytic way at room temperature. Chem Eur J 22:15605–15608. https://doi.org/10.1002/chem.201603407
60. Everett M, Wass DF (2017) Highly productive CO2 hydrogenation to methanol - a tandem catalytic approach via amide intermediates. Chem Commun 53:9502–9504. https://doi.org/10.1039/C7CC04613H
61. Sordakis K, Tsurusaki A, Iguchi M, Kawanami H, Himeda Y, Laurenczy G (2017) Aqueous phase homogeneous formic acid disproportionation into methanol. Green Chem 19:2371–2378. https://doi.org/10.1039/C6GC03359H
62. Schneidewind J, Adam R, Baumann W, Jackstell R, Beller M (2017) Low-temperature hydrogenation of carbon dioxide to methanol with a homogeneous cobalt catalyst. Angew Chem Int Ed Engl 56:1890–1893. https://doi.org/10.1002/anie.201609077
63. Schieweck BG, Klankermayer J (2017) Tailor-made molecular cobalt catalyst system for the selective transformation of carbon dioxide to dialkoxymethane ethers. Angew Chem Int Ed 56:10854–10857. https://doi.org/10.1002/anie.201702905
64. Kar S, Goeppert A, Kothandaraman J, Prakash GKS (2017) Manganese-catalyzed sequential hydrogenation of CO2 to methanol via formamide. ACS Catal 7:6347–6351. https://doi.org/10.1021/acscatal.7b02066

Top Organomet Chem (2019) 63: 17–38
DOI: 10.1007/3418_2018_24

Published online: 28 November 2018

Catalytic Processes Combining CO_2 and Alkenes into Value-Added Chemicals

Synthesis of Cyclic Carbonates, Lactones, Carboxylic Acids, Esters, Aldehydes, Alcohols, and Amines

Marc Schmitz, Matilde V. Solmi, and Walter Leitner

Contents

Abstract The present chapter comprises an overview on catalytic pathways to synthesize a highly desired variety of common compounds/chemicals starting from carbon dioxide as C1 building block and simple alkenes. After a summary of the corresponding pioneering work of the past, the authors focus on state-of-the-art

M. Schmitz
Institut für Technische und Makromolekulare Chemie, RWTH Aachen University, Aachen, NRW, Germany

M. V. Solmi
Institut für Technische und Makromolekulare Chemie, RWTH Aachen University, Aachen, NRW, Germany

CPE Lyon and CNRS, Université de Lyon, ICL, C2P2 UMR 5265 LCOMS (CNRS – CPE Lyon – Univ. Lyon 1), ESCPE Lyon, Villeurbanne, France

W. Leitner (✉)
Institut für Technische und Makromolekulare Chemie, RWTH Aachen University, Aachen, NRW, Germany

Max Planck Institute for Chemical Energy Conversion, Mülheim an der Ruhr, Germany
e-mail: walter.leitner@cec.mpg.de

protocols. New transformations based on simple and non-activated starting materials containing a C–C double bond functionality leading to a broad product portfolio are covered. Overall, this chapter embraces sustainable routes, reagents, and apparatus to produce value-added products starting from CO_2 and alkenes as cheap and readily available building blocks.

Keywords Alcohols · Aldehydes · Alkenes · Amines · Carbon dioxide · Carbonates · Carbon–carbon bond formation · Carboxylic acids · Esters · Homogeneous catalysis · Lactones · Reverse water-gas shift reaction

1 General Introduction

Fossil fuels are currently the world's main source of carbon, with 93% used for energy and transportation purposes and the remaining 7% being used for chemical production [1]. Challenges associate with the use of fossil fuels are their finite nature and their release of greenhouse gases into the atmosphere by combustion. To address these problems, researchers have turned to CO_2 as an alternative, abundant, and green carbon source. While enormous amounts of CO_2 are released annually from anthropogenic sources, only about 0.3% is being utilized today [2]. Pursuing new routes to utilize CO_2 would allow further exploitation of the vast and ubiquitous carbon source.

Researchers have successfully incorporated CO_2 into simple compounds like urea and formic acid and into complex compounds like polyurethanes [3, 4]. In addition, CO_2 has reacted effectively with numerous substrates, including alcohols, epoxides, aromatics, and alkynes, to produce molecules of industrial importance. In detail, this embeds the synthesis of fuels, bulk chemicals, commodities, and even fine chemicals and pharmaceuticals [5, 6]. The use of CO_2 in their synthesis can significantly reduce the carbon footprint of chemical production, when coupled with renewable energy input [3, 7–10].

Among many conceivable target products, carbonates, lactones, carboxylic acids, esters, aldehydes, alcohols, and amines appear highly attractive. Their general structure implies a close relationship to the CO_2 molecule. At the same time, their synthesis is particularly challenging as they mostly require formation of new carbon–carbon bonds. While CO_2 reacts readily with *O*- and *N*-nucleophiles to give carbonic and carbamic acids, reactions to form C–C bonds require typically stoichiometric use of carbanions such as Grignard reagents or other metal alkyl and aryl species. Alternative pathways involving catalytic combinations of alkenes with CO_2 are of great interest to synthesize the mentioned target molecules (Scheme 1), especially when the transformed alkene can be provided from biomass, e.g., by selective dehydration of the corresponding alcohol [11, 12]. According to the principles of Green Chemistry and Engineering, the synthesis of the target molecules will involve essentially a (molecular metal) catalyst and a highly intensified process scheme. Different classes of highly important chemical products are outlined in the next sections.

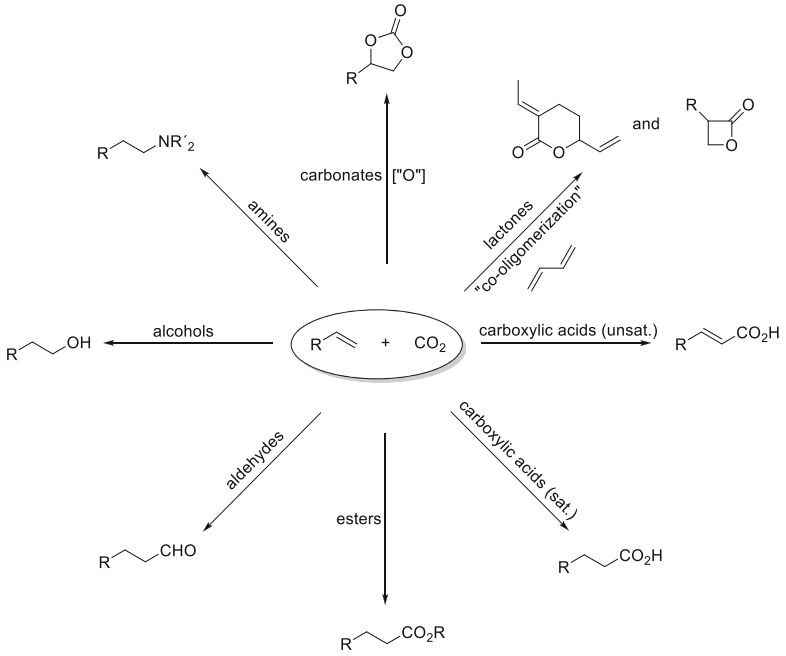

Scheme 1 Schematic overview of the target molecules and the systems illustrated in this book chapter

2 Reaction Products from CO_2 and Alkenes

2.1 Cyclic Carbonates

Cyclic carbonates are generally stable compounds which can guarantee a long-term fixation of CO_2 [13]. Carbonates are employed in a wide variety of industrial applications. Fluorinated carbonates are used in batteries production (as electrolytes additives) [14, 15]. Other carbonates, i.e., dimethyl carbonate, are used as solvents, considered greener compared to traditional VOCs [13, 16]. They are employed for the synthesis of compounds such as diols (i.e., ethylene glycol), carbamates, methanol, heterocyclic compounds, and ionic liquids [13]. In addition, carbonates are useful precursors for the synthesis of different polymers for various applications [17, 18]. Polycarbonates are thermoplastic polymers of high importance, finding application in the electrical sector, building, and automotive fields as well as data storing (i.e., CDs) and optical equipment (i.e., laboratory goggles) [19].

Traditionally, the production of carbonates requires the use of the highly toxic phosgene [16]. Recently, many protocols coupling epoxides and CO_2 have been reported leading to a greener synthesis of carbonates [16, 18, 20, 21]. Nevertheless, some of the used epoxides (i.e., propylene oxide) are considered toxic, and they usually require to be synthesized from alkenes [16, 22]. Starting directly from alkenes,

a safe oxidant, and CO_2 can lead to a greener synthesis of these useful compounds, eliminating the need of toxic reagents such as phosgene and corresponding epoxides.

The synthesis of carbonates from alkenes is considered as oxidative carboxylation since it involves an oxidation step (to epoxides) followed by the carboxylation of the intermediate (Fig. 1). Different oxidants and different catalysts (homogeneous, heterogeneous, and nonmetallic) have been reported in the literature. The present literature deals mainly with the production of cyclic carbonates starting from alkenes, while other types of carbonates synthesis are not well represented by the current research. Linear carbonates can also be obtained by coupling CO_2 with alcohols; however, this approach is reviewed elsewhere [23, 24]. Herein, the authors report a list of significant examples dealing with the production of cyclic carbonates starting from alkenes, CO_2, and different types of oxidants.

The group of Aresta reported about a rhodium complex able to perform the transformation of olefins to carbonates in the presence of O_2 and CO_2 [25]. The homogenous system suffered from very low activity (TON = 3); therefore they decided to implement the system using a heterogeneous catalyst. Different heterogeneous catalysts known to perform a first epoxidation step and a following carboxylation were tested. Nb_2O_5 showed good catalytic activity but resulted in only low yields of the desired product (4.5%) [26]. Titanosilicate molecular sieves coupled with H_2O_2 or *tert*-butyl hydroperoxide (TBHB) oxidants were able to catalyze the oxidative carboxylation of alkenes in organic solvents with yields up to 52% [27]. The system was further implemented using ionic liquids as solvents, abolishing the need of organic volatile solvents [28]. More elaborated heterogeneous catalytic systems were developed more recently based on the gained mechanistic knowledge. In 2015, Jain et al. reported the immobilization of a cobalt complex and triphenylphosphonium bromide on chitosan [22]. The catalyst was able to convert alkenes, CO_2, and O_2 into carbonates, providing yields up to 85%. In addition, the catalyst was recyclable up to four times by simple magnetic separation. The same year the group of Han developed a polyoxometalate-based homochiral metal-organic framework (MOF) able to produce even enantiomerically pure carbonates [29]. The catalyst consists of a pyrrolidine moiety as chiral organocatalyst and Keggin-type anions (Zn(II)-based polyoxometalate) as oxidation catalyst. This moiety can convert the alkene into a chiral epoxide, using TBHB as oxidant. The MOF contains an amine-bridged ligand to adsorb and activate CO_2 and therefore be able to perform the following transformation of the epoxide into the carbonate. Yields up to 92% for

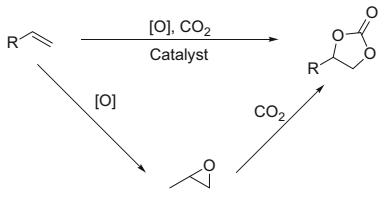

Fig. 1 General oxidative carboxylation of alkenes to carbonates. [O] = general oxidant (i.e., H_2O_2, O_2, etc.)

enantiomerically pure carbonates were achieved using this multifunctional catalytic system [29].

In addition to metal-based catalyst, other systems were reported. In 2007, Li et al. reported the transformation of alkenes to carbonates using CO_2, H_2O_2 as oxidizing agent and bromides in catalytic amounts to activate the transformation [30]. The system is highly active and can lead to yields of carbonates of 89%. Recently, other examples of nonmetallic catalysts performing similar transformations were reported. For example, homoallylic alcohols and CO_2 can lead to the enantioselective synthesis of cyclic carbonates with the aid of a dual Brønsted acid/base organocatalyst [31].

The reported examples represent an interesting step forward toward the development of technologies able to fix CO_2 in valuable chemicals such as cyclic carbonates. In addition, the use of alkenes and CO_2 for these processes would lead to substitute processes using highly toxic reagents (phosgene) and allow to elude the additional transformation step of alkenes via epoxides.

2.2 *Lactones*

Due to the formal relation in their synthetic pathway from CO_2 and an alkene functionality or diene moiety, respectively, lactones and co-oligomerization products like 3-ethylidene-6-vinyltetrahydro-2*H*-pyran-2-one are discussed together within this section. Both products embody a 1-oxacycloalkan-2-one unit which is known to be abundant within comonomers for plastics, in flavors and fragrances, or for sesquiterpenoids in plants and in drugs. Apart from α- and β-lactones, these compounds are mostly made by an internal esterification of an alcohol and a carboxylic acid functionality under the release of one equivalent of water. Another typical method of producing lactones is the Baeyer-Villiger oxidation. Cyclic ketones are oxidized with peroxycarboxylic acids under ring expansion. The Baeyer-Villiger oxidation of cyclohexanone provides ε-caprolactone, which is industrially produced in considerable quantities as starting material for the preparation of polyesters and polyethers. However, the formation of lactones starting from simple alkenes in combination with renewable CO_2 is so far rare in literature. Yet, the formation of β-lactones has never been observed experimentally.

Early catalytic reactions with CO_2 in the formation of γ-lactones were carried out by Inoue et al. in 1979 [32]. For methylenecyclopropanes, 2.4 mol% of, e.g., [Pd(dpa)$_2$] (dba = dibenzylideneacetone), in the presence of a phosphine ligand (2.0–4.0 eq.) catalyzed the reaction with CO_2 (40 atm) and provided successfully a mixture of five-membered lactones in good yields (Fig. 2, up to 77%, **2** and **3**). They were able to influence the selectivity between **2** and **3** by changing from PPh_3 to a chelating dppe ligand. They suggest that the transformation with CO_2 proceeds via a trimethylenemethane species **4** (Fig. 2) which has been suggested for the Pd-catalyzed cycloadditions of methylenecyclopropanes to alkenes before [33]. However, a methyl-substitution in positions 3 and 3′ instead of position 1 was not tolerated

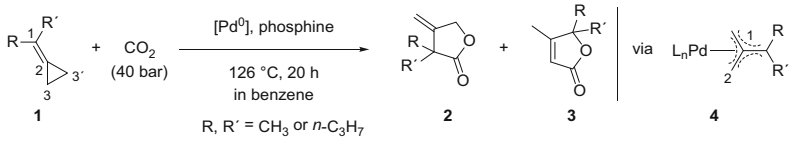

Fig. 2 Reaction of methylenecyclopropanes with CO_2 catalyzed by palladium(0) complexes [32]

since no conversion was observed. Further details on the mechanism and on catalyst reusability remain unknown.

Subsequently, Binger and Weintz described the dependence on the reaction conditions like temperature, pressure, ligand concentration, and substrate amount on the desired formation of products **2** and **3**. During their investigations, even co-oligomerization products from **3** and **1** were observed which were already known for Pd^0-catalyzed alkylations of CH-acidic compounds [34, 35]. Based on their experiments and optimizations (precursor, cyclopentadienyl allyl palladium, DMF, 165°C, PPh_3), they were even able to yield compound **3** (R, R = H) with 80% yield from methylenecyclopropane and proposed a plausible reaction pathway involving the insertion of CO_2 into a Pd–C bond forming a palladalactone with the mentioned consecutive reactions. The few protocols herein reported are still unique examples to produce simple five-membered γ-lactones **2** and **3** from monoenes and CO_2 under catalytic conditions.

Compared to monoenes, reactions of dienes with CO_2 have been studied more deeply. Regarding the coupling of dienes with CO_2, lactones can be synthesized in the so-called co-oligomerization or telomerization ("linear dimerization") reactions. In particular with conjugated dienes, transition metal compounds can readily form complexes via coupling reactions with CO_2. Early publications from the 1970s reported about the first telomerization of dienes with CO_2. In general, telomerizations can be considered as dimerization of two dienes in the presence of a suitable nucleophile, for example, alcohols, resulting in the case of 1,3-butadiene in substituted octadienes (1-substituted-2,7-octadienes, 3-substituted 1,7-octadiene). These products are useful intermediates, for example, in the total synthesis of natural products, precursors for plasticizer alcohols, solvents, corrosion inhibitors, and herbicides. From an industrial point of view, 1,3-butadiene and methanol are the most attractive starting materials due to their availability and low price. However, carbon dioxide can be used as suitable coupling partner as well for this reaction. Thus, Inoue et al. and Musco et al. found in the 1970s that highly functionalized organic compounds, γ- and δ-lactones, can be prepared by homogeneously Pd-catalyzed telomerization of 1,3-butadiene with CO_2 [36–38]. In 1980, Döhring and Jolly introduced 1,2-butadienes (methylallene) as substrates [39]. However, theses transformations suffered from low selectivity for the lactone products, since open esters, carboxylic acids, and higher alkenes can be formed, too [40]. With immobilized palladium catalysts, prepared from [Pd(η^5-Cp)(η^3-C_3H_5)] and polymer-bound phosphines, the group around Dinjus was able to produce up to 72% selectivity of δ-lactone 2-ethylidene-6-heptene-5-olid, albeit at low conversion

(7%) [41]. The resulting δ-lactone is a highly functionalized compound and may be used for producing various products and as intermediate for consecutive reactions, e.g., like hydrogenations, hydroformylations, hydroaminations, or polymerizations [42, 43].

Recently, Behr et al. discussed in detail the mechanistic pathways for the synthesis of γ- and δ-lactones with palladium-phosphine catalysts [42, 44] (Fig. 3). After coupling of two butadiene molecules, the equilibrium between bis-η^3allyl- and mono-allyl-species complex allows insertion of carbon dioxide to the allylic carbonate species. Reductive elimination leads to the lactone isomers depending on the C–O formation. During an intensive investigation of this reaction [41], the same group published about their improvements toward a mini-plant with up to 95% selectivity of the δ-lactone at a conversion rate of 45% butadiene (Fig. 4) [42].

The group developed a stable and robust process enabling recycling of the by-products and closing all solvent and catalyst loops. In a continuously stirred tank reactor, butadiene and carbon dioxide are mixed together with acetonitrile and the catalyst system $Pd(acac)_2/PPh_3$. The product mixture is continuously fed into a thermal separation and a connected distillation unit to remove the gaseous phase and recycle the feeds. Thus, in their mini-plant, δ-lactone was obtained maintaining the catalyst activity over 70 h of continuous operation and with a constant product stream of 8 g h^{-1} with an overall yield of 30% and a selectivity of 85% [45].

In the rhodium-catalyzed reaction of butadiene and carbon dioxide, a C13 γ-lactone-2-ethyl-2,4,9-undecatrien-4-olide is formed by a combination of three molecules of butadiene with one CO_2, besides the C9-lactones generated as in the case of palladium catalyst system [46]. Inspired by the given literature basis and results of the group of Nozaki in 2014 (Pd-catalyzed one-pot/two-step co-/terpolymerization

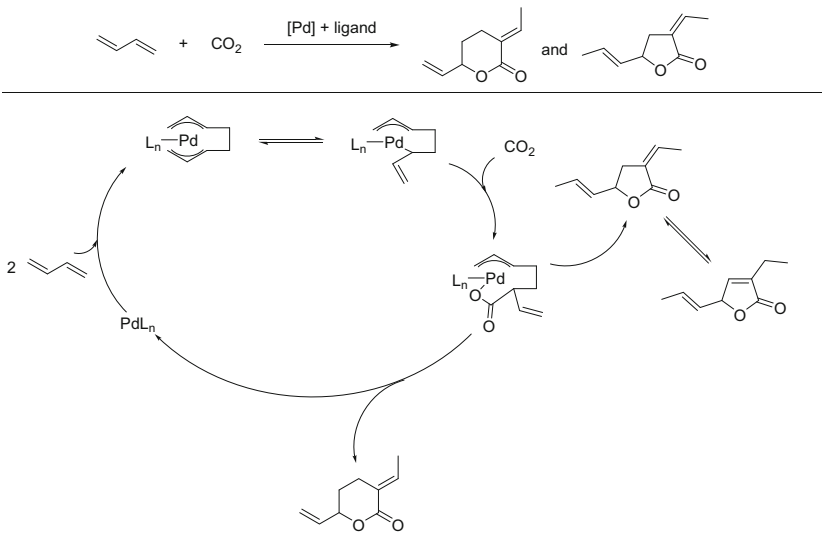

Fig. 3 Pd-catalyzed transformation of 1,3-butadienes into lactones [42]

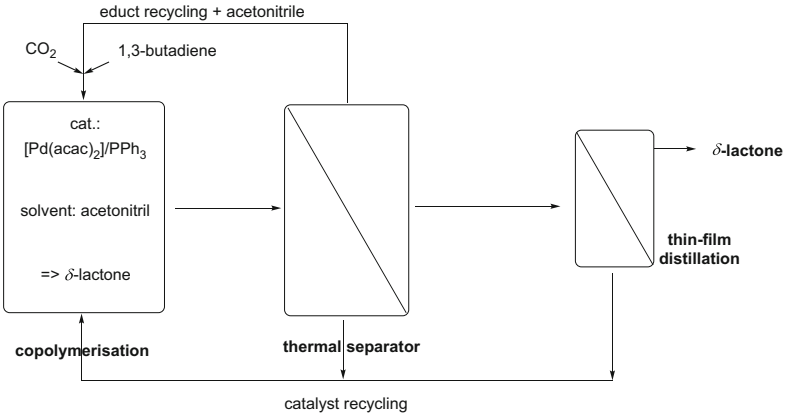

Fig. 4 Flow scheme of the production process for the δ-lactone (6 h, 80°C) [42, 44, 45]

of carbon dioxide and 1,3-dienes) [47], the group of Beller improved the yield of the δ-lactone up to 67% [48]. They reported a system comprised of Pd_2dba_3/TOMPP (tris-(o-methoxyphenyl)-phosphine) as catalyst showing high productivity at low loadings and under mild conditions (0.06 mol% [Pd], 0.18 mol% ligand, 80°C, TONs up to 1,500). Most recently, Bayón and Dupont developed a similar catalyst system, in the presence of an ionic liquid additive giving an increased TON of 4,540 of lactone with 96% selectivity after 5 h at 70°C [49].

2.3 Carboxylic Acids and Derivatives

Carboxylic acids and their derivatives are highly important for the synthetic utilization in the production of, e.g., polymers, pharmaceuticals, solvents, and food additives (commodities) [50]. Presently, the global market for carboxylic acids is predicted to grow each year ca. 5% [51]. Carboxylic acids are especially produced for applications in polymer industry as both monomers and additives, e.g., as polyvinyl acetate (glue) from acetic acid [52, 53], PET (polyethylene terephthalate) [54], nylon fibers (polyamides) [55] based on adipic acid, and amines or acrylic/methacrylic polymers [56]. For modifying the properties of synthetic polymers, long-chain carboxylic acids ($>C_9$) are used as additives for alkyd resin films [57]. Apart from the polymer sector, carboxylic acids are widely used as solvents [58], for the textile and leather industry [59, 60]; in agrochemical industry to provide herbicides, fungicides, and rodenticides [58]; in pharmaceutical industry [51, 61, 62]; and for the food and feed industry [58, 63]. Moreover, Shell reported the use of valeric acid derivatives as biofuels [64], while formic acid is discussed as hydrogen carrier/storage [7, 65, 66]. Today, the majority of aliphatic (C_4–C_{13}), aromatic carboxylic, and dicarboxylic acids are produced via oxidation of the corresponding aldehydes usually obtained by the oxo synthesis (alkene hydroformylation).

Oxidation catalysts are usually Co or Mn salts, and O_2 (or HNO_3, $KMnO_4$) is used as oxidant [58, 67]. Small-chain acids like formic acid or acetic acid [53, 68, 69] are mainly produced by carbonylation, using, e.g., alcohols [70] or alkenes [71, 72], as substrates. Pivalic acid and other tertiary carboxylic acids can be obtained from alkenes by the Koch synthesis [58, 73]. Industrially, carboxylic acid esters can be synthesized by alkoxycarbonylations of alkenes, since it produces esters in a single step without coupling agents [74], or more generally via esterification reactions [75]. Stereoselective hydroesterification processes, mostly palladium- or rhodium-catalyzed, also enable the access to a variety of compounds which are widely used not only in the pharmaceutical field [76, 77]. For production of biodiesel, large quantities of fatty acid methyl esters are produced by transesterification of vegetable oils (mostly soybean, rapeseed or palm oil) with methanol [78].

The use of CO_2 as C1 building block for industrial production of carboxylic acids is implemented for decades in the synthesis of salicylic acid according to Kolbe [79] and Schmitt [80], converting phenol with CO_2 in the presence of a base (NaOH). However, this reaction has limited synthetic scope being applicable to phenolic type substrates and is based on a stoichiometric approach.

The examples discussed in this section focus on catalytic reactions where free acids are isolated as the products (if appropriate, after acidic hydrolysis) using mainly simple and non-activated alkenes as substrates.

According to Fig. 5, two basic routes **(1)** and **(2)** toward carboxylic acids based on an alkene moiety in combination with CO_2 can be envisaged.

Following pathway **(1)**, acrylic acid as important platform chemical is one of the major target molecules provided by this transformation [81]. Preliminary work in this field was carried out in particular by the group of Hoberg. They studied the oxidative coupling of different alkenes like ethene [82], 1,3-butadiene [83], or styrene [84] with CO_2-forming metalla-latone intermediates in the presence of [Ni(cod)$_2$] and a stabilizing base additive (DBU, 1,8-diazabicyclo[5.4.0]undec-7-ene). Starting from the isolated and stabile Ni-lactone, further saturated (e.g., propionic acid) and unsaturated carboxylic acids were accessible after hydrolysis. However, β-H elimination toward acrylic acid was not feasible at that time. These kinetic and thermodynamic constraints were computationally investigated by DFT calculations in 2007 [85]. A breakthrough for the catalytically Ni-promoted synthesis of acrylates was shown by Lejkowski et al. in 2012 [86, 87]. They developed a robust nickel catalyst for the direct carboxylation of simple alkenes, like ethene, styrene, and

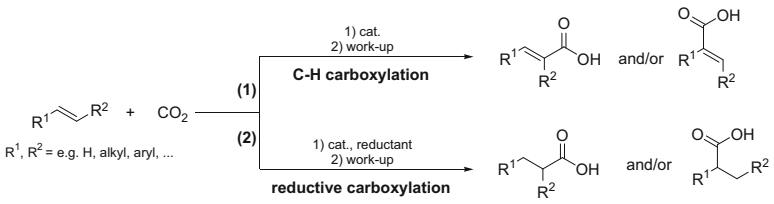

Fig. 5 Possible routes to carboxylic acids from alkenes and CO_2

1,3-dienes with CO_2 to their corresponding linear α,β-unsaturated carboxylic acid salts (TONs up to 116 for butadiene carboxylation) by the usage of an electron-rich bisphosphine ligand (BenzP*) and a suitable base (sodium 2-fluorophenoxide).

Vogt and coworkers were also able to develop a catalytic procedure for the synthesis of acrylate with diphosphine nickelalactones in the presence of Et_3N as base (with TONs up to 21) [88].

In addition to transition metal catalysts, such as Ni, Mo, and W, especially Pd offers new promising strategies to generate acrylic acid [88–90]. Most recently, the group of Schaub enhanced the TON to sodium acrylate to 514 using a Palladium system in an amide solvent (CHP: *N*-cyclohexylpyrrolidone) with a basic additive (alcoholates) [91, 92]. Additionally, the system was found suitable for other alkenes like propene and cyclopentene (TONs up to 92). In a semicontinuous reaction setup, they could show good results for the ethene conversion to acrylate with a total TON from 2 cycles of 235 in combination with an integrated catalyst recycling stream (Fig. 6).

The second pathway **(2)** to combine alkenes with CO_2 to yield carboxylic acids involves an overall reductive process, whereby saturated aliphatic acids are obtained as the final products (Fig. 5). One of the first examples in literature for the homogeneous catalytic conversion of ethene with CO_2 to the free propionic acid dates back to 1978. Lapidus et al. carried out the transformation in 38% yield in the presence of Wilkinson's catalyst under harsh reaction conditions (180°C, 700 bar) [93]. An exact mechanism of this transformation has so far remained unclear as no reduction equivalents required for product formation are specified in the described protocol.

Based on the approach from pioneering work by Hoberg [82–84] as well as Walther and Dinjus [94] to regenerate reactive metal species for alkene/CO_2 coupling, Rovis and coworkers reported about the first nickel-catalyzed reductive

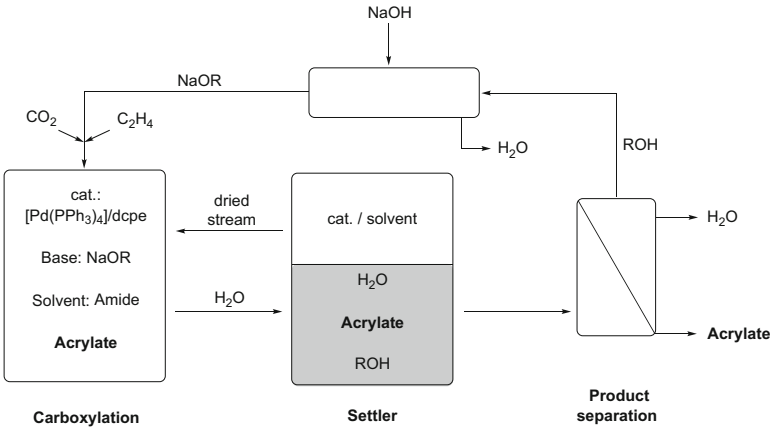

Fig. 6 Semicontinuous process scheme for Pd-catalyzed synthesis of sodium acrylate from ethene and CO_2 [91]

carboxylation of styrenes using CO_2 under ambient conditions (23°C, 1 bar CO_2) [95]. The transformation led regioselectively to saturated α-substituted carboxylic acids (phenylacetic acid derivatives). However, transmetallation of nickel by Et_2Zn was required to regenerate the active species in this hydrocarboxylation. Under comparable reaction conditions (r.t., 1 bar CO_2, THF), an iron-catalyzed system with similar regioselectivities of the formed α-aryl carboxylic acids has been reported in 2012 using an excess of a Grignard reagent (EtMgBr) as reductant [96, 97]. For aryl carboxylation reactions, light-driven transformations [98] or generally photo-redox catalytic systems [99, 100] have also attracted interest recently.

In 2013 the group of Leitner reported the rhodium-catalyzed formal hydrocarboxylation of alkenes. The reaction of olefins with CO_2 and H_2 leads to the corresponding one-carbon-atom elongated carboxylic acids (Fig. 7) [101]. Saturation of the C–C double bond provides an important energetic driving force, but competing hydrogenation poses also mechanistic challenges on the transformation [102].

With a $[RhCl(CO)_2]_2/PPh_3$ system and a promoting iodide reagent, very high to excellent yields (up to 92%) for the free acids were obtained for a range of cyclic and linear alkenes. For internal olefins, the ratio of regioisomeric acids is largely independent of the original position of the double bond. Mechanistic studies including isotopic labeling studies with $^{13}CO_2$, D_2, and $H_2{}^{18}O$ demonstrated that the formal hydrocarboxylation results from the effective interconnection of two catalytic cycles. In the first step, catalytic reverse water-gas shift reaction (*r*WGSR) generates carbon monoxide and water, which consecutively get converted in a subsequent Reppe-type hydroxycarbonylation cycle to yield the free carboxylic acid (Fig. 7).

In 2016 the group of Mikami published ambient synthesis of α-aryl carboxylic acids from CO_2 and styrene derivatives via rhodium-catalyzed hydrocarboxylation (precursor, $[RhCl(cod)_2]$) [103]. Depending on the substrate, yields up to 95% were obtained. As reduction equivalents, 1.2 eq. of $ZnEt_2$ per mol substrate was most suitable. Remarkably, they were able to perform the catalytic asymmetric hydrocarboxylation of α,β-unsaturated esters synthesize with ee values up to 66% employing a

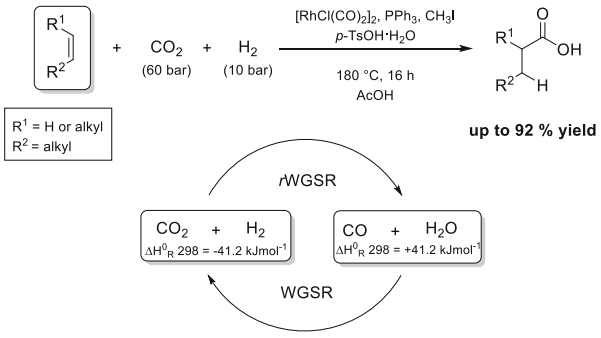

Fig. 7 Overall hydrocarboxylation of alkenes involving the *r*WGSR followed by the consecutive hydroxycarbonylation [101]

cationic rhodium complex with (*S*)-(−)-4,4′-bi-1,3-benzodioxole-5,5′-diylbis (diphenylphosphine) [(*S*)-SEGPHOS] as a chiral diphosphine ligand (Fig. 8).

The group of R. Martin has reported a variety of carboxylation reactions of divers starting materials like allylic alcohols [104], styrenes [105], 1,3-dienes [106], halogenated aliphatic hydrocarbons [107, 108], unsaturated hydrocarbons [109–111], and others [112, 113]. They were able to control regioselective hydrocarboxylation of aryl- and alkyl-substituted C–C bonds with a catalytic system based on a nickel precursor, a bipyridine-based ligand, and a reducing reagent (metallic manganese) (Fig. 9) [109]. Even more recently, the same group published about the 1,4-dicarboxylation of 1,3-dienes (e.g., butadiene) using the Ni-based reaction system in Fig. 9 [106]. This multiple CO_2 incorporation into abundant 1,3-dienes gives access to adipic acids from simple and available precursors. The salient features of this method are its excellent regio- and chemo-selectivity, mild conditions, and ease of execution. The (over-)stoichiometric use of a metal-based reducing agent is, however, a major limitation for large-scale application.

Clearly, the principle outlined in Fig. 7 utilizing a combination of CO_2 and H_2 as source for in situ formed CO (and H_2O, respectively) offers the most attractive strategy for alkene transformations. Meanwhile, protocols were published about carboxylation-, alkoxycarbonylation- or hydroformylation-related reactions and may open new strategies in CO_2 utilization [89, 114, 115]. Notably, the required hydrogen may also come from organic substrates, in particular alcohols, as most catalysts active in these reactions are generally active for dehydrogenation or reforming processes.

In 2012 the group of García reported the first example of catalytic reductive hydroesterification reaction of styrenes using CO_2 as a C1 source and methanol as a reductant catalyzed by nickel complexes [116]. Yields up to 71% for the linear isomer were obtained using complex [(dippe)Ni(μ-H)]$_2$ for styrenes bearing σ-electron-withdrawing groups. The corresponding TON was limited, however, as high catalyst loadings (20 mol%) were required.

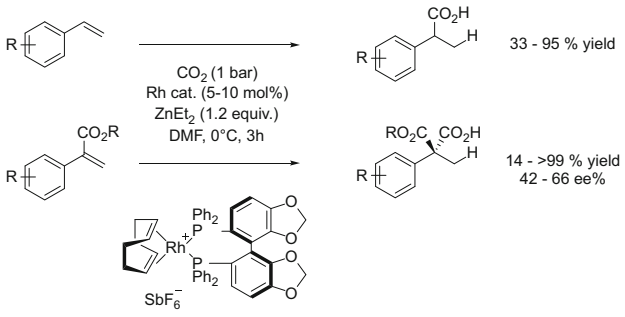

Fig. 8 Rh-catalyzed hydrocarboxylation of alkenes with CO_2 and $ZnEt_2$ [103]

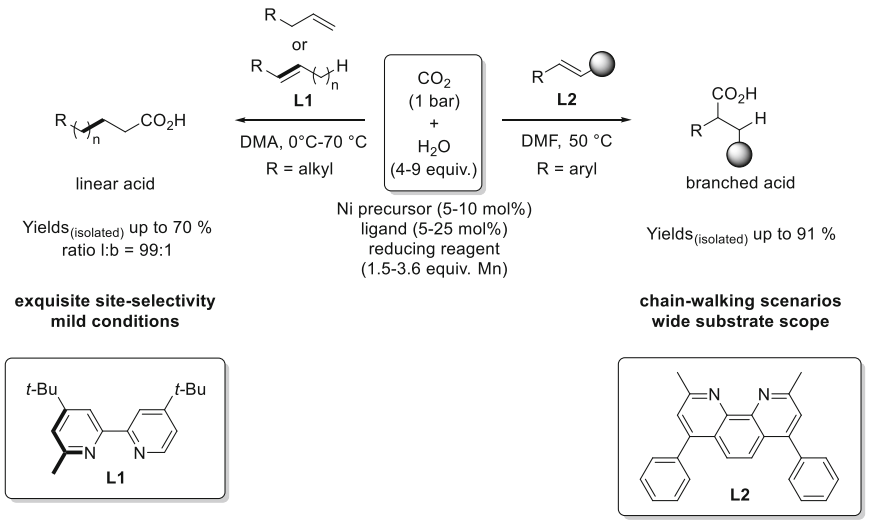

Fig. 9 Site-selective incorporation of CO_2 to a wide range of unsaturated hydrocarbons utilizing water as formal hydride source [109]

In 2014, the group of Beller published a Ru-based conversion of alkenes, CO_2, and alcohols into carboxylic acid esters (Fig. 10) [117]. Essential for their transformation is the activity of the catalytic system $[Ru_3(CO)_{12}]$/[BMIM]Cl in the rWGSR (reverse water-gas shift reaction), coupled with alkoxycarbonylation. A variety of linear and cyclic alkenes afforded the corresponding carboxylic acid esters with a yield range of 41–95% in the presence of different alcohols. No external hydrogen is required since the reduction of CO_2 is proceeded by hydrogen transfer from the alcohol used in excess as solvent [118]. Investigations including isotopic labeling experiments provided experimental evidence for this catalytic pathway, similar to the previous reports on Rh-catalyzed hydrocarboxylation [101]. In case of the use of an internal alkene, isomeric mixtures of the ester products were obtained, whereby the distribution of product isomers seemed independent of the original substitution pattern, albeit with a slight preference toward the linear product.

In 2015, Fleischer et al. described the indirect utilization of CO_2 as a C1 source under ambient reaction conditions by using *N*-formylsaccharin as a CO transfer reagent with an integrated recycling approach of the CO-surrogate (Fig. 11) [119]. The carbonylation proceeds in a highly region-selective manner yielding the desired branched ester from styrene derivatives in yields up to 97%. In contrast, linear esters were obtained in yields up to 91% with exclusive formation of the *n*-product from alkyl-substituted alkenes. The catalyst system is based on a Pd^0 precursor, a bidentate phosphine ligand, and a Brønsted acid.

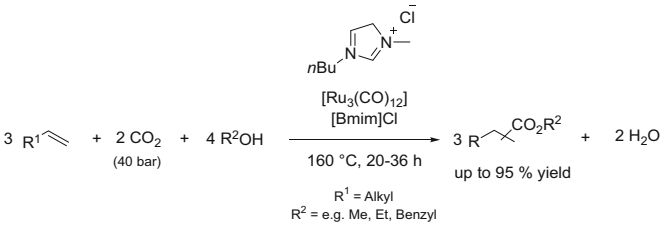

Fig. 10 Ru-catalyzed alkoxycarbonylation of alkenes with carbon dioxide and methanol [117]

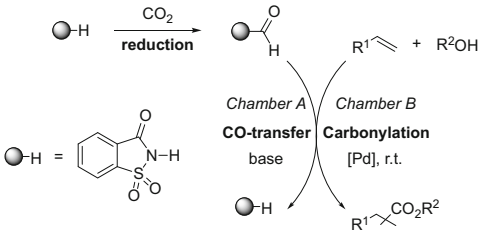

Fig. 11 Indirect utilization of CO_2 as a C1 source under ambient reaction conditions using *N*-formylsaccharin as a CO transfer reagent [119]

2.4 Further Reduced Target Molecules

The following section summarizes the state of the art for the use of CO_2 as a C1 building block in combination with alkenes for the generation of more strongly reduced functional groups such as aldehydes, alcohols, and amines. It covers synthetic protocols comprising, e.g., hydroformylation, hydrohydroxymethylation, and hydroaminomethylation, using CO_2/H_2 as synthon to generate useful compounds. The target molecules are highly important for a lot of different applications like pharma, agriculture, or health care as well as for further chemical transformations by addressing compounds like APIs, solvents, lubricants, dyeing reagents, or plastics. Considering their usual synthetic routes, a change from common C1 building blocks to CO_2 opens new fields and opportunities for upcoming synthetic pathways and transformations.

2.4.1 Aldehydes

While CO_2 is long known as a possible C1 source in technical hydroformylation, its application has found more widespread attention in organic synthesis only most recently. In 2017, the research groups of Xia and Ding used the readily available and inexpensive poly(methylhydrosiloxane) (PMHS, $M_W = 1900$) as alternative

reductant to high pressure H_2 for hydroformylation of alkenes and CO_2 [120]. The desired aldehydes from alkyl- and aryl-based substrates were isolated in moderate to good yields (up to 70%) and with good selectivity to the linear product (l:b = up to 89:11). From their mechanistic studies, they found that CO_2 was inserted preferentially into the Si–H bond to form the corresponding silyl formate [Si]OC(O)H which either decomposes into CO and silanols [Si]OH or is hydrolyzed to formic acid subsequently releasing CO and H_2O. With the production of CO, aldehydes could then be formed by established Rh-catalyzed hydroformylation chemistry [121]. Interestingly, an excess of CO_2 hindered the further reduction of the formed aldehyde toward the alcohol moiety (Fig. 12) [120].

2.4.2 Alcohols

Pioneering work in this area has been reported in 2000 by Tominaga and Sasaki, who used CO_2 as building block with various ruthenium cluster complexes to obtain C_1-elongated alcohols from different alkenes (Fig. 13) [122]. The highest yield of 88% alcohol was achieved using $[H_4Ru_4(CO)_{12}]$, a well-known rWGSR catalyst. The nature and performance of the required alkali salt additive were intensively studied together with investigations about the active species [123–126]. An immobilized system was also reported [127]. Although the inferred primary product of this reaction is the aldehyde obtained by hydroformylation of the alkene, these intermediates were not observed in high yield due to rapid further reduction. This system proved effective for several substrates. When CO was used instead of CO_2, the yield of the alcohol was either significantly decreased or comparable to the

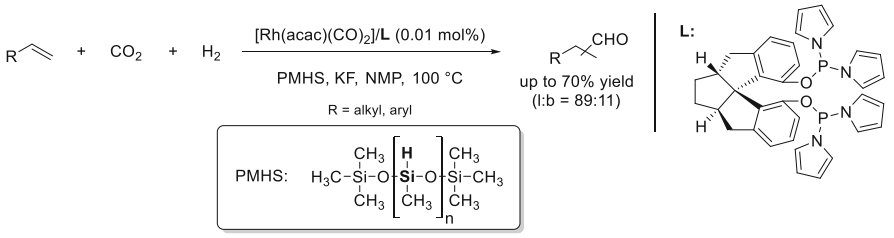

Fig. 12 Hydroformylation of alkenes with CO_2, silane, and H_2 [120]

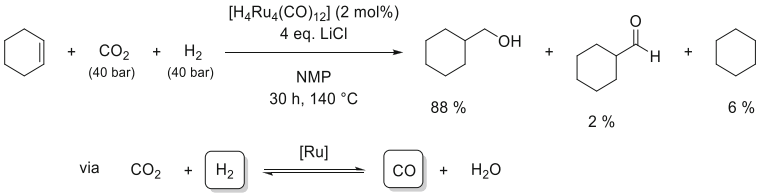

Fig. 13 Ru-catalyzed hydroformylation/reduction of cyclohexene using CO_2 [122]

system with CO_2, showing that this catalyst was rather negatively affected by a large presence of CO in the system.

More recently, the Beller group used a ruthenium catalyst comprising a (bulky) phosphite for this reaction, allowing the use of CO_2 to afford alcohols from terminal and internal alkenes (Fig. 14) [128, 129]. The optimization of the catalyst and ligand allowed slightly lower temperatures to be used while suppressing the undesired hydrogenated product formed from the alkene. In the same year, the group of Dupont developed a catalytic system in which the ionic liquids [BMI·Cl] or [BMMI·Cl] reacted in the presence of H_3PO_4 with $[Ru_3(CO)_{12}]$ to generate Ru-hydride-carbonyl-carbene species as further efficient catalysts for this transformation [130]. Thus, even lower temperatures (120°C) and shorter reaction times (12 h) were feasible.

In 2017, Yu and coworkers realized a highly regio- and enantioselective copper-catalyzed hydrohydroxymethylation of alkenes with CO_2 as the C1 source and $(EtO)_3Si$-H as reductant (Fig. 15) [131]. A series of chiral homobenzylic/allylic alcohols from styrenes and 1,3-dienes were obtained under mild conditions. In this transformation, many functional groups, including halides, amine, ether, and ester, were tolerated. The isolated products were directly applied for the further synthesis of bioactive compounds like (*R*)-(−)-curcumene and (*S*)-(+)-ibuprofen. Mechanistic studies suggested that the key step was the formation of the active L*CuH catalyst which gave an alkyl copper species after subsequent insertion of the alkene into the Cu–H bond. Carboxylation of this complex with CO_2 formed the copper carboxylate. Further reduction of the carboxylate by two equivalents of hydrosilane produced first

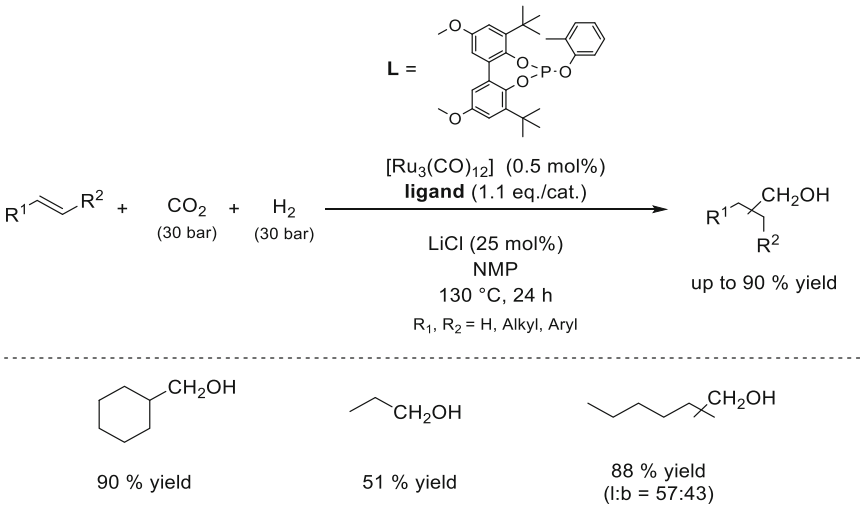

Fig. 14 Ru-catalyzed hydroformylation/reduction of alkenes with carbon dioxide (hydrohydroxymethylation) [128]

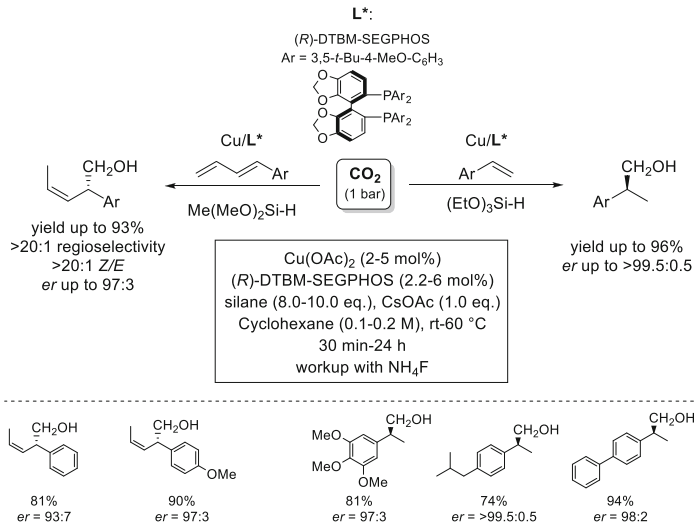

Fig. 15 Enantioselective hydrohydroxymethylation with CO_2 to give chiral alcohols [131]

the silyl ether which released the alcohol product after treating with NH_4F. Thus, these studies suggest that pathways without involving the *r*WGS equilibrium may also be possible to exploit the CO_2/H_2 synthon.

2.4.3 Amines

Amines are large-scale industrial products or intermediates that are often produced by multistep processes [70]. To provide amines in a single-unit operation, the hydroaminomethylation reaction approach can lead to the formation of C1-elongated amines from alkenes [132]. An initial hydroformylation of the alkene forms the aldehyde that gets further converted in a second step with an amine toward an enamine/imine from which the final amine is formed through subsequent reduction. The group of Eilbracht demonstrated already in 2009 the possibility to use CO_2 as a CO surrogate for the conversion of alkenes with secondary amines and aniline [133]. The use of the rWGSR catalyst system $[Ru_3(CO)_{12}]$/LiCl/BTAC (BTAC = benzyltrimethylammonium chloride) proved to be an efficient system for the in situ formation of CO from CO_2 and H_2. Optimization of the four-step tandem reaction was successfully demonstrated using cyclopentene and morpholine as substrates (Fig. 16). The combination of promoting salts revealed a synergetic effect on the yield and selectivity, with the phase-transfer catalyst enhancing the solubility of LiCl in toluene. Isomeric mixtures (l:b up to 64:36) of secondary and tertiary amines were formed effectively from a variety of alkenes with yields in the range of 35–98%.

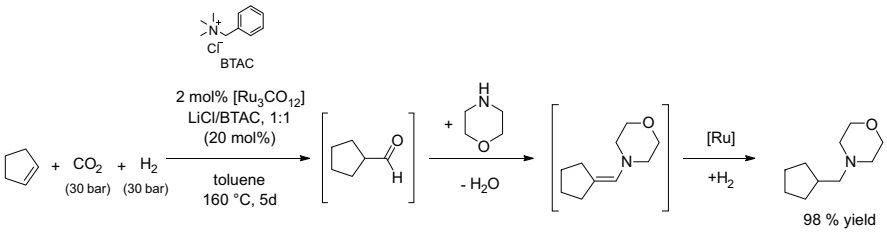

Fig. 16 Hydroaminomethylation of cyclopentene with morpholine applying carbon dioxide as C1 building block [133]

In 2016, Dupont and coworkers reported about further development of this system that was able to perform more efficient under milder reaction conditions (120°C, 24–36 h). Similar to the alcohol synthesis mentioned above, the imidazolium salt-based ionic liquid [BMMI]Cl in the presence of H_3PO_4 was used to generate the active Ru catalyst for the CO_2-based hydroaminomethylation [134].

3 Conclusion

The development of new processes to address a broad spectrum of chemicals starting from simple non-activated alkenes and CO_2 has been an active field of research that has seen a high dynamic progress in the past decades. Many new synthetic pathways have been reported by groups all around the world. The reported protocols show a basis for processes reducing the dependence on fossil by incorporating CO_2 into useful chemicals. Although many systems are still in an early stage of development, they set the stage for opening new perspectives in the development of processes that follow the "Green Chemistry" principles. At present, however, the need of organometallic (reducing) reagents in stoichiometric quantities is still a limiting factor. In this context, protocols relying on the use of CO_2 and H_2 as CO surrogate via the rWGSR appear very attractive, as they can capitalize on the established knowledge in organometallic carbonylation catalysis. These strategies offer alternatives to replace fossil-based CO by CO_2, without changing drastically the chemistry of the following transformation. With the rapidly growing implementation of renewable electricity, the required H_2 may be generated by electrolysis exploiting and buffering fluctuating energy sources. To develop these protocols toward practical procedures, deeper knowledge about the molecular transformations has to go hand in hand with the development of advanced reaction engineering solutions right from the beginning. Assessment tools beyond established life cycle assessment (LCA) methods are necessary to critically analyze the potential of using CO_2 in combination with catalysis to lower the carbon footprint for industrial synthesis and, by that, provide more sustainable alternatives to conventional petrochemical productions.

References

1. Centi G, Quadrelli EA, Perathoner S (2013) Energy Environ Sci 6:1711
2. News (2014). Carbon Manage 5:13
3. Peters M, Kohler B, Kuckshinrichs W, Leitner W, Markewitz P, Muller TE (2011) ChemSusChem 4:1216
4. Langanke J, Wolf A, Hofmann J, Böhm K, Subhani M, Müller T, Leitner W, Gürtler C (2014) Green Chem 16:1865
5. Aresta M, Dibenedetto A, Angelini A (2014) Chem Rev 114:1709
6. Leitner W, Klankermayer J (2015) Science 350:629
7. Klankermayer J, Wesselbaum S, Beydoun K, Leitner W (2016) Angew Chem Int Ed 55:7296
8. Alper E, Yuksel Orhan O (2017) Petroleum 3:109
9. Artz J, Muller TE, Thenert K, Kleinekorte J, Meys R, Sternberg A, Bardow A, Leitner W (2018) Chem Rev 118:434
10. Cokoja M, Bruckmeier C, Rieger B, Herrmann WA, Kühn FE (2011) Angew Chem Int Ed 50:8510
11. Byun J, Han J (2017) Green Chem 19:5214
12. Bond JQ, Alonso DM, Wang D, West RM, Dumesic JA (2010) Science 327:1110
13. Shaikh RR, Pornpraprom S, D'Elia V (2017) ACS Catal 8:419
14. McMillan R, Slegr H, Shu Z, Wang W (1999) J Power Sources 81:20
15. Komaba S, Ishikawa T, Yabuuchi N, Murata W, Ito A, Ohsawa Y (2011) ACS Appl Mater Interfaces 3:4165
16. Schaffner B, Schaffner F, Verevkin SP, Borner A (2010) Chem Rev 110:4554
17. Gregory GL, Lopez-Vidal EM, Buchard A (2017) Chem Commun (Camb) 53:2198
18. Besse V, Camara F, Voirin C, Auvergne R, Caillol S, Boutevin B (2013) Polym Chem 4:4545
19. Abts G, Eckel T, Wehrmann R (2014) Polycarbonates. Ullmann's encyclopedia of industrial chemistry. Wiley-VCH, Weinheim, p 1
20. Vaitla J, Guttormsen Y, Mannisto JK, Nova A, Repo T, Bayer A, Hopmann KH (2017) ACS Catal 7:7231
21. Scharfenberg M, Hilf J, Frey H (2018) Adv Funct Mater 28:1704302
22. Kumar S, Singhal N, Singh RK, Gupta P, Singh R, Jain SL (2015) Dalton Trans 44:11860
23. Shukla K, Srivastava VC (2016) RSC Adv 6:32624
24. Kindermann N, Jose T, Kleij AW (2017) Top Curr Chem 375:15
25. Aresta M, Dibenedetto A (2002) J Mol Catal A Chem 182:399
26. Aresta M, Dibenedetto A, Tommasi I (2000) Appl Organomet Chem 14:799
27. Srivastava R, Srinivas D, Ratnasamy P (2003) Catal Lett 91:133
28. Sun JM, Fujita S, Arai M (2005) J Organomet Chem 690:3490
29. Han Q, Qi B, Ren W, He C, Niu J, Duan C (2015) Nat Commun 6:10007
30. Eghbali N, Li C-J (2007) Green Chem 9:213
31. Vara BA, Struble TJ, Wang W, Dobish MC, Johnston JN (2015) J Am Chem Soc 137:7302
32. Inoue Y, Hibi T, Satake M, Hashimoto H (1979) J Chem Soc Chem Commun 982
33. Binger P, Schuchardt U (1977) Angew Chem Int Ed 16:249
34. Binger P, Weintz HJ (1984) Chem Ber 117:654
35. Trost BM (1980) Acc Chem Res 13:385
36. Inoue Y, Sasaki Y, Hashimoto H (1978) Bull Chem Soc Jpn 51:2375
37. Musco A, Perego C, Tartiari V (1978) Inorg Chim Acta 28:L147
38. Sasaki Y, Inoue Y, Hashimoto H (1976) J Chem Soc Chem Commun 605
39. Döhring A, Jolly P (1980) Tetrahedron Lett 21:3021
40. Musco A (1980) J Chem Soc Perkin Trans 1:693
41. Holzhey N, Pitter S, Dinjus E (1997) J Organomet Chem 541:243
42. Behr A, Henze G (2011) Green Chem 13:25
43. Omae I (2012) Coord Chem Rev 256:1384
44. Behr A, Bahke P, Becker M (2004) Chem Ing Tech 76:1828

45. Behr A, Becker M (2006) Dalton Trans 2006:4607
46. Behr A, He R (1984) J Organomet Chem 276:c69
47. Nakano R, Ito S, Nozaki K (2014) Nat Chem 6:325
48. Sharif M, Jackstell R, Dastgir S, Al-Shihi B, Beller M (2017) ChemCatChem 9:542
49. Balbino JM, Dupont J, Bayón JC (2018) ChemCatChem 10:206
50. Wu X-F, Zheng F (2017) Top Curr Chem 375:4
51. Juliá-Hernández F, Moragas T, Cornella J, Martin R (2017) Nature 545:84
52. Cordeiro CF, Petrocelli FP (2002) Vinyl acetate polymers. Encyclopedia of polymer science and technology, vol 12. Wiley, Hoboken, p 416
53. Budiman AW, Nam JS, Park JH, Mukti RI, Chang TS, Bae JW, Choi MJ (2016) Catal Surv Jpn 20:173
54. Reese G (2001) Polyesters, fibers. Encyclopedia of polymer science and technology, vol 3. Wiley, Hoboken, p 652
55. Anton A, Baird BR (2002) Polyamides, fibers. Encyclopedia of polymer science and technology, vol 3. Wiley, Hoboken, p 584
56. Swift G (2002) Acrylic (and Methacrylic) acid polymers. Encyclopedia of polymer science and technology, vol 1. Wiley, Hoboken, p 79
57. Wicks ZW (2007) Alkyd resins. Encyclopedia of polymer science and technology, vol 1. Wiley, Hoboken, p 1
58. Kubitschke J, Lange H, Strutz H (2014) Carboxylic acids, aliphatic. Ullmann's encyclopedia of industrial chemistry. Wiley, Hoboken, p 1
59. Moret S, Dyson PJ, Laurenczy G (2014) Nat Commun 5:4017
60. Riemenschneider W, Tanifuji M (2011) Oxalic acid. In: Chemistry UsEoI (ed) Ullmann's encyclopedia of industrial chemistry, vol 25. Wiley, Hoboken, p 529
61. Boullard O, Leblanc H, Besson B (2000) Salicylic acid. Ullmann's encyclopedia of industrial chemistry, vol 32. Wiley, Hoboken, p 127
62. Kantor TG (1986) Pharmacotherapy 6:93
63. Szilagyi M (2012) Aliphatic carboxylic acids: saturated. Patty's toxicology. Wiley, Hoboken, p 471
64. Lange JP, Price R, Ayoub PM, Louis J, Petrus L, Clarke L, Gosselink H (2010) Angew Chem Int Ed Engl 49:4479
65. Álvarez A, Bansode A, Urakawa A, Bavykina AV, Wezendonk TA, Makkee M, Gascon J, Kapteijn F (2017) Chem Rev 117:9804
66. Supronowicz W, Ignatyev IA, Lolli G, Wolf A, Zhao L, Mleczko L (2015) Green Chem 17:2904
67. Röhrscheid F (2000) Carboxylic acids, aromatic. Ullmann's encyclopedia of industrial chemistry, vol 7. Wiley, Hoboken, p 113
68. Haynes A (2010) Adv Catal 53:1
69. Noriyuki Y, Takeshi M, Joe W, Ben S (1999) The chiyoda/uop acetica™ process: a novel acetic acid technology. In: Hideshi H, Kiyoshi O (eds) Studies in surface science and catalysis, vol 121. Elsevier, Amsterdam, p 93
70. Weissermel K, Arpe HJ (2008) Industrial organic chemistry, vol 3. Wiley, Weinheim
71. Reppe W, Kröper H (1953) Justus Liebigs Ann Chem 582:38
72. Samel U-R, Kohler W, Gamer AO, Keuser U, Yang S-T, Jin Y, Lin M, Wang Z (2014) Propionic acid and derivatives. Ullmann's encyclopedia of industrial chemistry. Wiley, Weinheim, p 1
73. Koch H, Haaf W (1958) Justus Liebigs Ann Chem 618:251
74. Kiss G (2001) Chem Rev 101:3435
75. Batoux N (2004) Synthesis 2004:2766
76. Konrad TM, Durrani JT, Cobley CJ, Clarke ML (2013) Chem Commun (Camb) 49:3306
77. Kollár L (2008) Modern carbonylation methods. Wiley-VCH, Weinheim
78. Meher L, Sagar DV, Naik S (2006) Renew Sust Energ Rev 10:248
79. Kolbe H (1874) Adv Synth Catal 10:89

80. Schmitt R (1885) J Prakt Chem 31:397
81. Limbach M (2015) Acrylates from alkenes and CO2, the stuff that dreams are made of. In: Pérez PJ (ed) Advances in organometallic chemistry, vol 63. Elsevier, Amsterdam, p 175
82. Hoberg H, Peres Y, Krüger C, Tsay YH (1987) Angew Chem Int Ed 26:771
83. Hoberg H, Gross S, Milchereit A (1987) Angew Chem Int Ed 26:571
84. Hoberg H, Peres Y, Milchereit A (1986) J Organomet Chem 307:C38
85. Graham DC, Mitchell C, Bruce MI, Metha GF, Bowie JH, Buntine MA (2007) Organometallics 26:6784
86. Lejkowski ML, Lindner R, Kageyama T, Bódizs GÉ, Plessow PN, Müller IB, Schäfer A, Rominger F, Hofmann P, Futter C, Schunk SA, Limbach M (2012) Chem Eur J 18:14017
87. Huguet N, Jevtovikj I, Gordillo A, Lejkowski ML, Lindner R, Bru M, Khalimon AY, Rominger F, Schunk SA, Hofmann P, Limbach M (2014) Chemistry 20:16858
88. Hendriksen C, Pidko EA, Yang G, Schaffner B, Vogt D (2014) Chemistry 20:12037
89. Kirillov E, Carpentier JF, Bunel E (2015) Dalton Trans 44:16212
90. Aresta M, Pastore C, Giannoccaro P, Kovács G, Dibenedetto A, Pápai I (2007) Chem Eur J 13:9028
91. Manzini S, Cadu A, Schmidt AC, Huguet N, Trapp O, Paciello R, Schaub T (2017) ChemCatChem 9:2269
92. Manzini S, Huguet N, Trapp O, Paciello RA, Schaub T (2017) Catal Today 281:379
93. Lapidus A, Pirozhkov S, Koryakin A (1978) Bull Acad Sci USSR 27:2513
94. Dinjus E, Walther D, Schuetz H, Schade W (1983) Z Chem 23:303
95. Williams CM, Johnson JB, Rovis T (2008) J Am Chem Soc 130:14936
96. Greenhalgh MD, Thomas SP (2012) J Am Chem Soc 134:11900
97. Greenhalgh MD, Kolodziej A, Sinclair F, Thomas SP (2014) Organometallics 33:5811
98. Murata K, Numasawa N, Shimomaki K, Takaya J, Iwasawa N (2017) Chem Commun 53:3098
99. Seo H, Liu A, Jamison TF (2017) J Am Chem Soc 139:13969
100. Seo H, Katcher MH, Jamison TF (2017) Nat Chem 9:453
101. Ostapowicz TG, Schmitz M, Krystof M, Klankermayer J, Leitner W (2013) Angew Chem Int Ed 52:12119
102. Ostapowicz TG, Hölscher M, Leitner W (2012) Eur J Inorg Chem 2012:5632
103. Kawashima S, Aikawa K, Mikami K (2016) Eur J Org Chem 2016:3166
104. van Gemmeren M, Borjesson M, Tortajada A, Sun SZ, Okura K, Martin R (2017) Angew Chem Int Ed 56:6558
105. Yatham VR, Shen Y, Martin R (2017) Angew Chem Int Ed Engl 56:10915
106. Tortajada A, Ninokata R, Martin R (2018) J Am Chem Soc 140:2050
107. Julia-Hernandez F, Moragas T, Cornella J, Martin R (2017) Nature 545:84
108. Liu Y, Cornella J, Martin R (2014) J Am Chem Soc 136:11212
109. Gaydou M, Moragas T, Julia-Hernandez F, Martin R (2017) J Am Chem Soc 139:12161
110. Wang X, Nakajima M, Martin R (2015) J Am Chem Soc 137:8924
111. Correa A, León T, Martin R (2014) J Am Chem Soc 136:1062
112. Martin R, Tortajada A, Julia-Hernandez F, Borjesson M, Moragas T (2018) Angew Chem Int Ed. https://doi.org/10.1002/anie.201803186
113. Juliá-Hernández F, Gaydou M, Serrano E, van Gemmeren M, Martin R (2016) Top Curr Chem 374:1
114. Wu L, Liu Q, Jackstell R, Beller M (2014) Angew Chem Int Ed 53:6310
115. Porosoff MD, Yan B, Chen JG (2016) Energy Environ Sci 9:62
116. González-Sebastián L, Flores-Alamo M, García JJ (2012) Organometallics 31:8200
117. Wu L, Liu Q, Fleischer I, Jackstell R, Beller M (2014) Nat Commun 5:3091
118. Dibenedetto A, Stufano P, Nocito F, Aresta M (2011) ChemSusChem 4:1311
119. Gehrtz PH, Hirschbeck V, Fleischer I (2015) Chem Commun 51:12574
120. Ren X, Zheng Z, Zhang L, Wang Z, Xia C, Ding K (2017) Angew Chem Int Ed 56:310
121. Dong K, Wu XF (2017) Angew Chem Int Ed 56:5399
122. Tominaga K-I, Sasaki Y (2000) Catal Commun 1:1

123. Kontkanen M-L, Oresmaa L, Moreno MA, Jänis J, Laurila E, Haukka M (2009) Appl Catal A Gen 365:130
124. Jaaskelainen S, Haukka M (2003) Appl Catal A 247:95
125. Tominaga K-I, Sasaki Y (2004) J Mol Catal A Chem 220:159
126. Tsuchiya K, Huang J-D, Tominaga K-I (2013) ACS Catal 3:2865
127. Tominaga K-I (2006) Catal Today 115:70
128. Liu Q, Wu L, Fleischer I, Selent D, Franke R, Jackstell R, Beller M (2014) Chem Eur J 20:6888
129. Fritschi S, Korth W, Julis J, Kruse D, Hahn H, Franke R, Fleischer I, Chowdhury AD, Weding N, Jackstell R, Beller M, Jess A (2015) Chem Ing Tech 87:1313
130. Ali M, Gual A, Ebeling G, Dupont J (2014) ChemCatChem 6:2224
131. Gui Y-Y, Hu N, Chen X-W, Liao LL, Ju T, Ye J-H, Zhang Z, Li J, Yu D-G (2017) J Am Chem Soc 139:17011
132. Boerner A, Beller M, Wünsch B (2009) Sci Synth 40:111
133. Srivastava VK, Eilbracht P (2009) Catal Commun 10:1791
134. Ali M, Gual A, Ebeling G, Dupont J (2016) ChemSusChem 9:2129

Top Organomet Chem (2019) 63: 39–76
DOI: 10.1007/3418_2018_16

Published online: 1 September 2018

Recent Advances on CO_2 Utilization as C1 Building Block in C-N and C-O Bond Formation

Synthesis of *N*-Formyl Amines, *N*-Methylamines, and Dialkoxymethanes

Kassem Beydoun and Jürgen Klankermayer

Contents

Abstract In the last decade, enormous efforts have been initiated to establish catalytic transformations with carbon dioxide (CO_2) as a C_1 building block toward the synthesis of value-added products. The scientific development was largely based

K. Beydoun and J. Klankermayer (✉)
Institut für Technische und Makromolekulare Chemie, RWTH Aachen University, Aachen, Germany
e-mail: jklankermayer@itmc.rwth-aachen.de

on the design of tailored molecular catalysts and ligands, making novel synthetic pathways with CO_2 as substrate achievable. Herein, recent applications using CO_2 for the homogeneous catalyzed formation of C-N and C-O bonds within the synthesis of formamides, methylamines, and dialkoxymethanes are summarized, focusing on the construction of value-added intermediates and products.

Keywords CO_2 utilization · Ligand development · Molecular catalysis · Sustainable chemistry

1 General Introduction

In addition to the established efforts dedicated to the direct reduction of carbon dioxide (CO_2) to methanol, novel approaches with molecular catalysts for the sustainable utilization of CO_2 were initiated in the last years. These synthetic efforts are summarized and visualized in pathway diagrams, showing the possibility to utilize CO_2 via reduction, functionalization, or combinations thereof [1]. This structural synthetic approach is assisted by the concept of synthesizing complex molecular products from CO_2 via multiple bond cleavage and bond-forming events. The coupling partner is a hydrogenated CO_2 building block with varying reduction levels, enabling innovative reaction with amines, alcohols, and olefin substrates (see also "Catalytic Chess at the Interface of Chemistry and Energy" [2]) [3–12]. Three scenarios emerge from this concept where CO_2 is either incorporated into products (1) without formal reduction of the oxidation state at carbon, (2) with partially reduced carbon by the removal of one oxygen atom, or (3) by reduced carbon to saturated hydrocarbons under removal of both oxygen atoms (Fig. 1).

The development of molecular transition metal-based catalysts has made enormous progress in the last decade, enabling to activate challenging functionalities or molecules and to tailor the organometallic species with the ligand environment for unprecedented reactions and transformations. Alongside, great efforts have been dedicated to explore versatile synthetic pathways for the formation of CO_2-based value-added products for pharmaceutical, industrial, and fuel applications. Within this approach, the exploration of sustainable reducing agents for CO_2 activation and the combination with bio-based feedstock have been in the research focus. This methodology would minimize the overall carbon footprint of the envisaged transformations via the integration of renewable energy and could foster the reduction of fossil-based substrates. In this manner, the utilization of bio-based feedstock in combination with CO_2 together with "green hydrogen" (from water photo- or electrolysis) [13–19] as the reducing partner would represent a sustainable approach toward the recently introduced "biohybrid" fuels or materials [20–22].

In this chapter, we will discuss three application fields of CO_2 as a building block for the synthesis of formamides, methylamines, and dialkoxymethanes, as these compounds represent value-added products for diverse interesting applications [2].

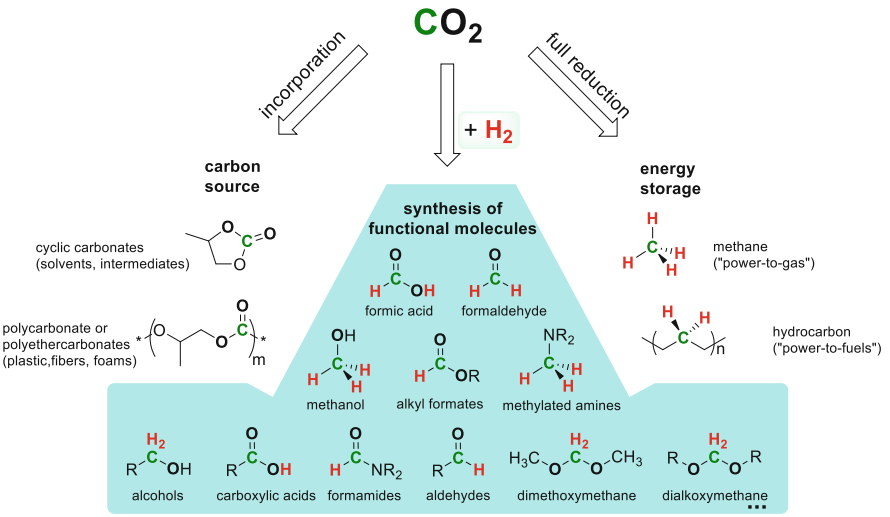

Fig. 1 Classification of utilization of carbon dioxide as a carbon source at the interface of the chemical and energetic value chains: incorporation of the CO_2 molecule without formal reduction (left), complete reduction of CO_2 to methane and saturated hydrocarbons (right), or combined reduction and bond formation to result in a large synthetic diversity (middle)

2 *N*-Formylation of Amines

2.1 Formamides

Formamides are considered as valuable platform chemicals for the synthesis of many important chemical products such as fragrances, pharmaceuticals, agrochemicals, industrial solvents, and dyes [23–27]. Moreover, formyl moieties are found in many natural product analogues as important amine protecting groups [28]. Among several methods developed for the synthesis of formamides, the general method involves the use of excess amount of a formylating reagent (e.g., alkyl formate, formic acids, or formamide) in the presence of the corresponding amine [29, 30]. However, most traditional methods are showing drawbacks such as high costs, toxicity, poorly accessible starting materials, sensitivity, high waste streams, and long reaction times [30]. One other pathway to formamide synthesis comprises the use of carbon monoxide CO as the C1 building block. This is the case for the two formamide derivatives with the highest industrial relevance [27], formamide ($HCONH_2$) and *N*,*N*-dimethylformamide ($HCON(CH_3)_2$, DMF), that can be synthesized starting from CO in a two-step process or in a direct synthesis (Scheme 1a, $b_{1,2}$) [27, 31, 32]. Other *N*-substituted formamides have also been documented with commercial significance [27, 31] such as *N*-methylformamide (used as solvent or intermediate of insecticide formation), *N*-formylmorpholine (as solvent or anticorrosive agent), and formanilide (used as an antioxidant in the rubber industry and as intermediate in the pharmaceutical industry).

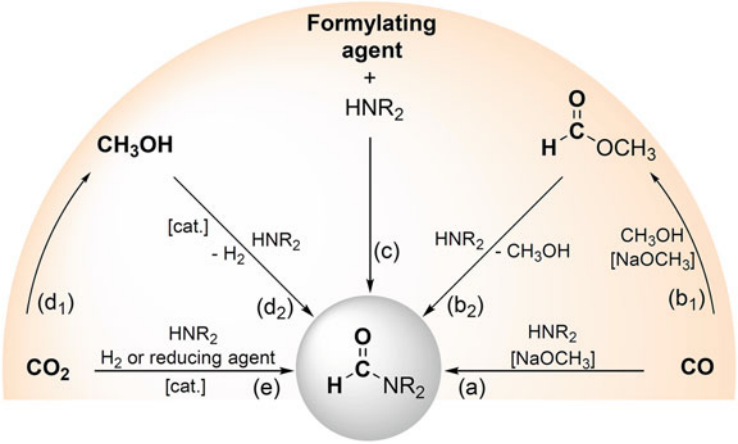

Scheme 1 Diverse approaches for the production of formamides

In the last few years, many researchers reported the use of more sustainable routes for the synthesis of formamides starting from the abundant feedstock methanol as the C1 source of the formyl group (Scheme 1d_2) [33–37]. These routes can also use methanol from renewable resources (biomass) or CO_2, thus further reducing the environmental impact [38]. However, the direct use of CO_2 as a C1 building block for the formyl group in amides is gaining more attention in terms of reducing the overall energy demand and the number of process units compared to the use of biomass- or CO_2-based methanol as the C1 building block. The formation of formamides from CO_2 and amines comprises a one-equivalent reduction step of CO_2 (using H_2 or reducing agent) and the subsequent condensation with the amine substrate via a new C-N bond formation resulting in a formamide product in a one-pot procedure (Scheme 1e). All this triggered researchers from different groups to deeply focus on the development of different catalytic systems to perform this CO_2-based reaction under more sustainable conditions. Many methods have been reported, employing the use of solid catalysts for *N*-formylation [39–46]; however, only recent homogeneous approaches will be discussed in this chapter.

2.2 *Production of Formamides Using CO_2 and Reducing Agents (Excluding Molecular H_2)*

2.2.1 Metal-Free Systems

Formamides can be synthesized from CO_2 and amines in the presence of a variety of reducing agents. This might not be the most atom-economic procedure compared to the use of hydrogen gas; however, milder reaction conditions with low reaction pressures and temperatures and extended substrates scope are broadly applied. The

most used reducing agents for the reductive formylation of amines with CO_2 are hydrosilanes, which are mild and easily handled reagents, possessing in many cases high reactivity due to lower bond dissociation energy. Moreover, they are inexpensive, nontoxic, and more resistant to air and moisture compared to other reducing agents (e.g., aluminum and boron hydrides). The first examples of formamide synthesis using amines, CO_2, and hydrosilanes were reported by the group of Cantat in 2012 [1]. The organocatalyst 1,5,7-triazabicyclo[4.4.0]dec-5-ene (TBD) was chosen as a base to promote the insertion of CO_2 to N-H bonds [47] under low CO_2 pressure (<3 bar), forming the [TBDH][O_2CNR_2] intermediate (Scheme 2). Subsequently, the presence of phenylhydrosilane reduces the carbamate moiety to afford the formamide products in yields up to 99% and the corresponding siloxane as by-product (Scheme 2) with the favor of amine substrates having higher basicity.

Outstanding developments were then achieved by the use of readily available 1-alkyl-3-methylimidazolium ionic liquids (ILs) (specifically 1-butyl-3-methylimidazolium chloride ([BMIm]Cl)), as highly efficient nonmetal catalyst for the formylation of amines using CO_2 and phenylsilane $PhSiH_3$ at room temperature (Scheme 3a) [48]. In this approach, the ILs acted as bifunctional catalysts, which can in a first step catalyze the activation of the Si-H bond of $PhSiH_3$ to react with CO_2, forming the silyl formate intermediate. In a second step, an IL-activated amine (R_2N-H:IL) reacts with the silyl formate intermediate to form the formamide product [48]. This metal-free approach to formamides from CO_2 is promoted by the ILs with a synergetic effect of both, the corresponding anions and cations, to afford the resultant formamide products in moderate to excellent yields. On the other hand, as it is well-known for phosphorus ylide (P-ylides) to be powerful and versatile nucleophilic reagents in organic synthesis [49–51], the use of P-ylide-CO_2 adducts as an efficient metal-free catalyst for CO_2 utilization reactions was also investigated. The P-ylide-CO_2 adduct catalysts, which can be obtained by the nucleophilic addition of P-ylides to CO_2 [52], proved to be very efficient for CO_2 utilization as C1 building

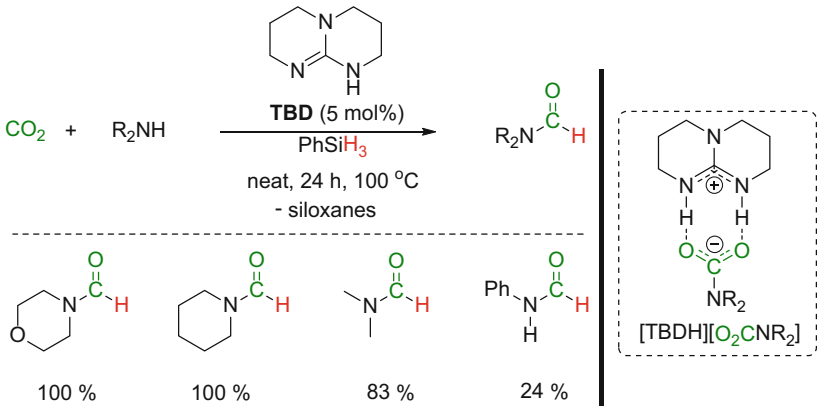

Scheme 2 Metal-free approach for the formylation of amines using CO_2 as C1 building block and TBD as catalyst

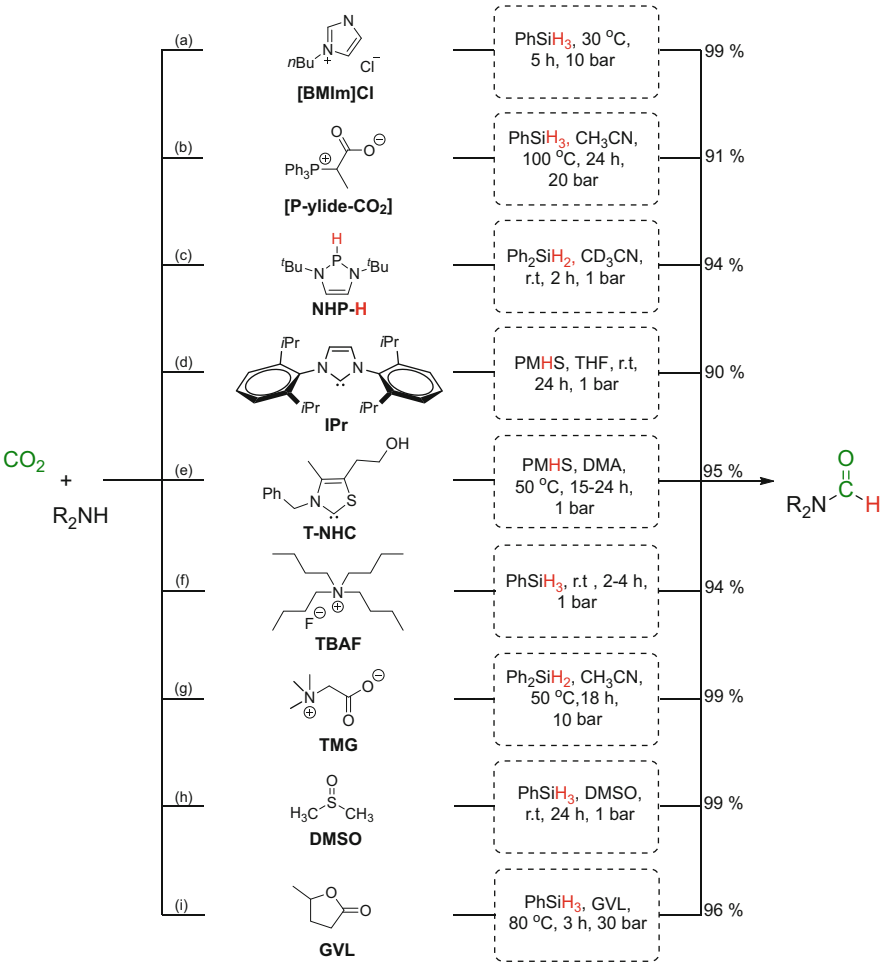

Scheme 3 Recent applications of metal-free catalytic systems for the *N*-formylation of amines using CO_2 with the corresponding maximum yields obtained

block for the synthesis of functionalized cyclic α-alkylidene carbonate and oxazolidinone derivatives [53]. Moreover, the P-ylide-CO_2 adducts were also applied to CO_2 reduction to form *N*-formylated (or *N*-methylated) compounds with moderate activity, using $PhSiH_3$ (or 9-BBN) as reductant [53]. The silyl formate intermediate is catalytically formed and converted in the presence of amines to the corresponding formamide product in up to 91% yield (Scheme 3b). Another metal-free approach to formamides synthesis from CO_2 was described in 2016 [54, 55]. In this work, the use of 1,3,2-diazaphospholene (NHP-H) as a catalyst in the presence of diphenylhydrosilane as reducing agent showed to be highly reactive for the stepwise reduction of CO_2, following the sequence hydrophosphination/P-to-Si formate transfer/*N*-formylation. More precisely, hydrophosphination of CO_2 with

NHP-H afforded phosphorus formate (NHP-OCOH) which then transfers the formate group to Ph_2SiH_2 in a catalytic manner (5 mol% of NHP-H) to afford the silyl formate intermediate $Ph_2Si(OCHO)_2$. Finally, the silyl formate intermediate formylate the amine present in the mixture to afford wide variety of formamide products with yields up to 94% (Scheme 3c) [54].

A highly active organocatalytic system based on *N*-heterocyclic carbene (IPr) also showed high reactivity for the formylation of a variety of amine substrates using CO_2 in presence of the reducing agent polymethylhydrosiloxane ($Me_3Si(OSiMeH)_nOSiMe_3$, PMHS), which is highly accessible as an abundant and nontoxic chemical waste in silicone industry (Scheme 3d) [56]. This approach disclosed an efficient catalytic system for the utilization of CO_2 at mild conditions, where the reaction can be performed at room temperature and yet affording the desired *N*-formyl products in high yields (Scheme 3d). Another interesting study involved the use of *N*-heterocyclic olefin (NHO) organocatalysts for the activation of CO_2 in the *N*-formylation reaction of amines in presence of a mixture of PMHS and 9-borabicyclo[3.3.1]nonane (9-BBN) as the reducing agents [57]. Similarly, highly effective and inexpensive thiazolium carbene-based catalysts (T-NHC) were also investigated for the *N*-formylation and *N*-methylation of amines, using PMHS as a reducing agent [58, 59]. This new catalytic system can operate under ambient conditions compared to typical NHC catalysts (under low pressures of CO_2) and employing more tolerant (to reduction) amine substrates to afford the corresponding formamide products in high yields up to 95% (Scheme 3e) [58, 59]. Interestingly, such thiazolium carbenes are inexpensive and nontoxic, and their corresponding salts are air stable and can be stored without the need to exclude moisture and oxygen [60]. More interestingly, tuning of the reaction temperature (up to 100°C) resulted in the complete reduction of the formyl group to afford the corresponding *N*-methylated products (see Sect. 3.2) [58]. Another simple and attractive approach for *N*-formylation with CO_2 and hydrosilane reducing agents was also described by using cheap fluoride and hydroxide salt catalysts. These catalysts showed high efficiency in catalyzing the reaction of various amines into formamides in excellent yields and high selectivity at room temperature and under low pressure of CO_2 (1 bar) [61]. As tetrabutylammonium fluoride (TBAF) and other fluoride salts are known to have highly nucleophilic anions, they possess high affinity for silicon and are thus frequently employed as catalysts for efficient hydrosilane reduction of carbonyls [62]. TBAF was used as a simple ammonium salt catalyst for efficient *N*-formylation of amines with CO_2 even at room temperature and atmospheric pressure. The scope of the amine substrates varies between aliphatic and aromatic amines, affording the corresponding formamide products in excellent yields with high selectivity (Scheme 3f) [61]. In line with this approach, an efficient organocatalytic approach for the utilization of CO_2 as a building block of formyl group in formamide synthesis was developed by the group of He on carboxylate-based catalyst glycine betaine (trimethylglycine TMG) in presences of diphenylsilane as reducing agent [63]. In this approach, the inner salt (or zwitterion) catalyst was used for the synthesis of a variety of formamides starting from amines under mild reaction conditions. The catalytic system showed ability to

selectively terminate the reduction step at formamide level (Scheme 3g). Moreover, aminals or *N*-methylamine products could also form selectively by applying minor modification of the reaction conditions [63]. These products, having various energy contents, correspond to two-, four-, or six-electron reduction of CO_2 with amine substrate and hydrosilane. For example, methylamines or formamides could be selectively obtained in high yields by tuning the CO_2 pressure and reaction temperature under which the reductive reaction is taking place (see Sect. 3.2). On the other hand, it has been known that oxygen-containing nucleophiles, e.g., hydroxide, alkoxide, carboxylate, or carbonate, can activate hydrosilanes and enhance their hydride-donating ability through interaction between the silicon atom and oxygen anion [64–66]. In this manner, simple and readily available inorganic bases alkali-metal carbonates such as cesium carbonates were also used to efficiently catalyze both the formylation and methylation (see Sect. 3.2) of amine substrates with CO_2 under mild conditions. Interestingly, the selectivities of different products were controlled by varying reaction temperature and reducing agent in which formamide products were obtained at room temperature when using $PhSiH_3$ as reducing agent [66].

Based on the fact that the nucleophilicity and basicity of amines could be tuned by solvation and polarization in different solvents [67, 68], the groups of Lei and Li have investigated the effect of selected solvents on the interaction of amine substrates and hydrosilanes to activate CO_2 in a catalyst-free fashion [69]. They found that the solvent plays a vital role in promoting the interaction of amines with hydrosilanes and subsequent CO_2 insertion, thus facilitating the simultaneous activation of N-H and Si-H bonds by promoting their Lewis acid/Lewis base interaction, enabling the formation of a new N-Si bond. In their report, Lei and Li proposed a reaction pathway that involves the formation of silyl carbamate which is reduced to formamide using hydrosilanes. This study showed that when using highly polar aprotic solvent, such as DMSO or DMF, up to quantitative yields of formamides were achieved in 24 h at room temperature under only atmospheric pressure of CO_2 (Scheme 3h) [69]. In the same manner, the group of Han and Song extended the investigation of the effect of solvent to the use of the biomass-derived γ-valerolactone (GVL) as an efficient catalyst and solvent for the *N*-formylation of amines with CO_2 [70]. This system showed excellent performance of GVL in the transformation of various primary and secondary amines into formamides, which are obtained in excellent yield, albeit high pressure of CO_2 (30 bar) at a temperature of 80°C has to be used (Scheme 3i). This performance was attributed to the lactone structure of dipolar aprotic GVL which played a key role in the formation of the active silyl formates intermediate and the activation of N-H bonds in amines. Interestingly, the use of other lactone-containing compounds, including γ-butyrolactone, δ-valerolactone, and ε-caprolactone, showed a similar activity to GVL in contrast to noncyclic esters, showing no activity. This can clearly indicate that solvents with high polarity could activate the N-H bond by solvation and polarization [70].

A more general approach to the direct formylation of amines in the presence of borohydrides was also achieved by developing a catalyst-free system for the

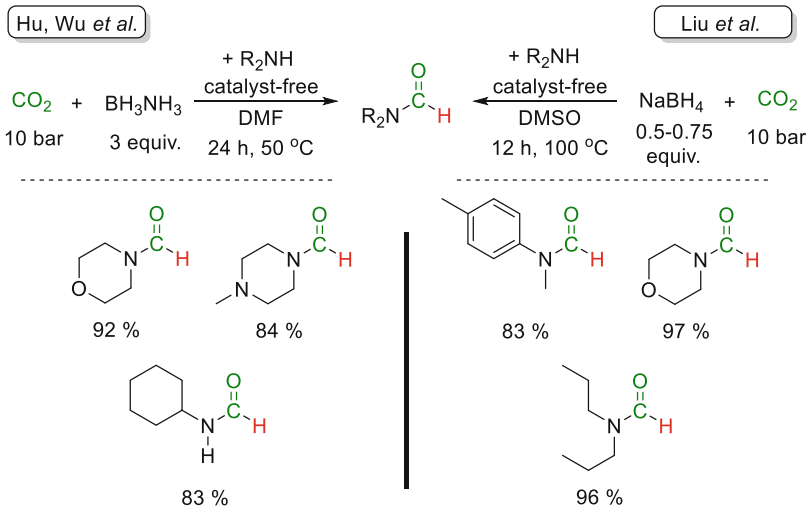

Scheme 4 Catalyst-free direct synthesis of formamide from CO_2 and amines reduced by boron hydrides

N-formylation of amine substrates using CO_2 as C1 source and ammonia borane (BH_3NH_3) as a reducing agent [71]. The latter is known as an excellent hydrogen storage material because of its high hydrogen capacity [72]. Compared to other catalytic systems employing hydrosilanes, BH_3NH_3 provide high potential in using a milder reaction conditions in an atom-economic fashion. This catalyst-free/BH_3NH_3 system was successfully applied for the *N*-formylation reaction at a low temperature of 50°C in DMF solvent where formamide products were afforded in very high yields and selectivities (Scheme 4, left) [71]. Some control experiments lead to a possible reaction mechanism involving the activation of BH_3NH_3 by DMF solvent, followed by CO_2 insertion into the B-H bond to generate a boron-formate intermediate which reacts with amines to afford the corresponding formamide final product [71]. A similar catalyst-free system was also reported using $NaBH_4$ as the reductant in DMSO solvent, in which, aliphatic and aromatic amines could react with CO_2 and $NaBH_4$ at 100°C (Scheme 4, right) [73]. Interestingly this reducing agent showed better reducing capacity compared to BH_3NH_3 enabling the use of as low as 0.5 equivalent per equivalent of the amine substrate to produce the corresponding formamides in moderate to excellent yields [73].

2.2.2 Organometallic Homogeneous Systems

In the course of studying the reactivity of non-precious transition metals in the *N*-formylation of amines using CO_2, the group of Cantat reported in 2014 the use of the first iron catalysts, able to promote the reductive functionalization using hydrosilanes as reductants [74]. They showed that iron precursor $Fe(acac)_2$

supported by tris[2-(diphenylphosphino)ethyl]phosphine (PP_3) ligand (previously used for the hydrosilylation of organic ureas to formamidines) [75] is able to catalyze the formylation of amines using $PhSiH_3$ as reducing agent at room temperature (Scheme 5) [74]. The reaction showed to be chemoselective and tolerant to various amine substrates bearing ketone and ester functionalities. These stimulating results in combination with their NHC (IPr) catalyst [56] outcompete other systems used for the formylation reaction such as TBD, $Cu(OAc)_2.H_2O$, or $Rh_2(OAc)_4$ [1, 76, 77]. In a similar approach, the use of an inexpensive $Cu(OAc)_2$-bis(diphenylphosphino) ethane/Cu(II)-dppe catalytic system showed also high reactivity for *N*-formylation reactions of various amines with CO_2 and $PhSiH_3$ at ambient condition with only 0.1 mol% catalyst loading. Here again the reaction is expected to proceed via silyl formate intermediate, formed catalytically from 1 atm CO_2 and $PhSiH_3$ at room temperature. The addition of amines to this intermediate afforded the formamide products in yield from 91 to 99% without formation of any by-product [78].

Employing PMHS as reducing agent, copper-diphosphine complexes showed also high reactivity as homogeneous catalysts for the reductive formylation of amines with CO_2 (1 bar) [76]. The latter catalytic system was found to be very active for the formylation of various amines even under very low catalyst loading, where the formamide products were obtained with high TONs up to 11,700. More specifically, the Cu complexes with phosphine ligands having ortho-phenylene structures with alkyl functionalities (Scheme 6) showed better reactivity as compared to conventional bidentate or monodentate ligands [76]. Interestingly, mechanistic investigation revealed the mechanism of this reaction and showed that the catalytically active species is a Cu-hydride-diphosphine complex. This species was generated from the Cu precursor, diphosphine ligand, and hydrosilane as the major reaction route, rather than the minor formation of a silyl formate intermediate (Scheme 6) [79].

Additional efforts were made to investigate the use of other reducing agents such as boron hydrides for the *N*-formylation reaction of amines. During their novel work

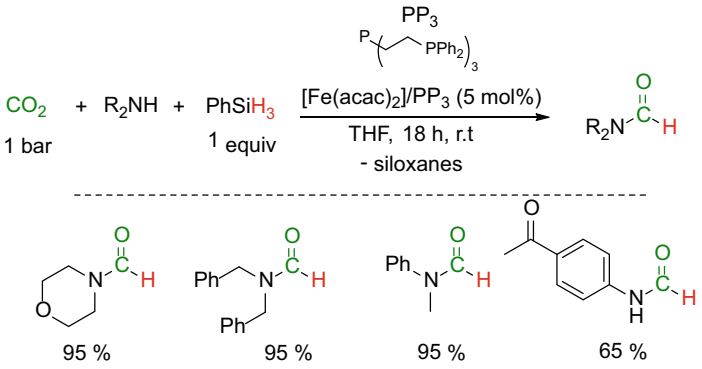

Scheme 5 First iron-catalyzed reductive functionalization of CO_2 by amines using hydrosilane as reducing agent

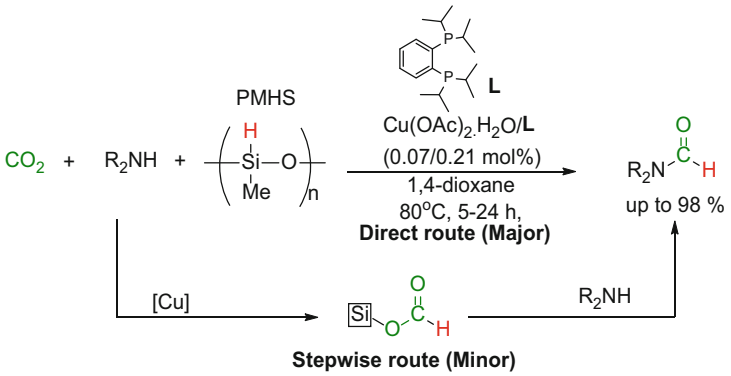

Scheme 6 Cu-catalyzed reductive formylation of amines using CO_2

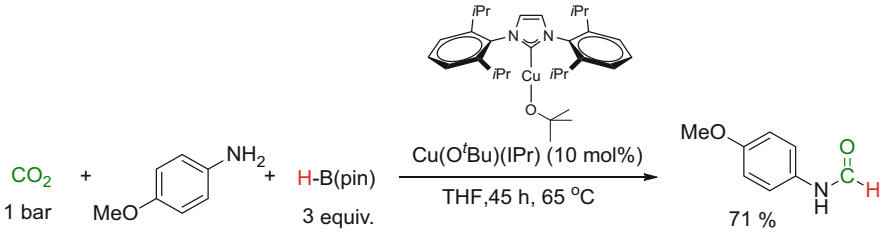

Scheme 7 One-pot synthesis of 4-methoxyformanilide starting from *p*-anisidine and CO_2

on the copper/*N*-heterocyclic carbene-catalyzed hydroboration of CO_2 to formic acid using pinacolborane HB(pin) as reducing agent, the group of Shintani and Nozaki developed a method for the synthesis of formamides by treating the in situ formed borane formate $HCO_2B(pin)$ intermediate with various amines in a two-step procedure [80]. Under mild reaction conditions, various amines were formylated by CO_2 (via borane formate) to afford the corresponding formamide products with high yields up to 98%. For example, treatment of *p*-anisidine in the presence of Et_3N with a solution of $HCO_2B(pin)$, after the catalytic hydroboration of CO_2, cleanly afforded the corresponding formamide in 84% yield. Interestingly, a one-pot procedure of the same substrates afforded the same product with a reduced yield of 71% (Scheme 7) [80].

On the other hand, the in situ synthesis of a silyl formate intermediate followed by a nucleophilic addition using amines could also be involved as a major pathway for the synthesis of formamide using CO_2 and hydrosilanes [81]. This was clearly demonstrated when silyl formates were efficiently synthesized from CO_2 and a hydrosilane under catalytic conditions and used as "formyl synthon" to sequentially produce formamides in addition to formic acid as a coproduct [77, 82]. However, this reaction was performed under 1 bar of CO_2 using the simple $Rh_2(OAc)_4$ catalyst in the presence of a base additive, typically K_2CO_3, to first afford the silyl formate intermediate. This species reacts in a subsequent step with added amines or anilines

to obtain the corresponding formamide products in moderate yield (Scheme 8). This approach is an important example, highlighting the potential of silyl formates for the synthesis of a wide range of value-added chemicals [77, 83, 84].

Another Rh-catalyzed approach encountered the synthesis and use of a series of alkyl bridged chelating bis(NHC) rhodium complexes in the reductive formylation of amines using CO_2 and Ph_2SiH_2. A rhodium-based bis(tzNHC) complex (tz = 1,2,3-triazol-5-ylidene) was identified to be highly effective at a low catalyst loading, ambient temperature, and much milder reaction conditions. Moreover, a wide range of amine substrates was efficiently formylated with CO_2 in a selective manner. Interestingly, amines bearing reducible functional groups showed high tolerance under theses reduction conditions (Scheme 9) [85]. Correspondingly, the catalyzed reaction is promoted by a silylene-rhodium dihydride $Ph_2Si{=}Ru(H)_2$

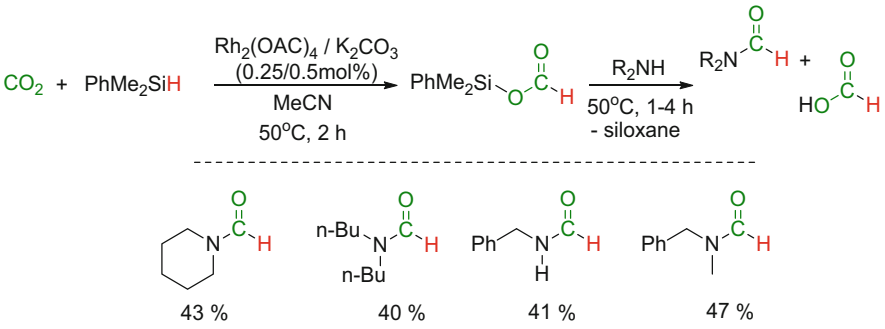

Scheme 8 Rh-catalyzed utilization of CO_2 for the synthesis of formamides via silyl formate formation/amine addition sequence

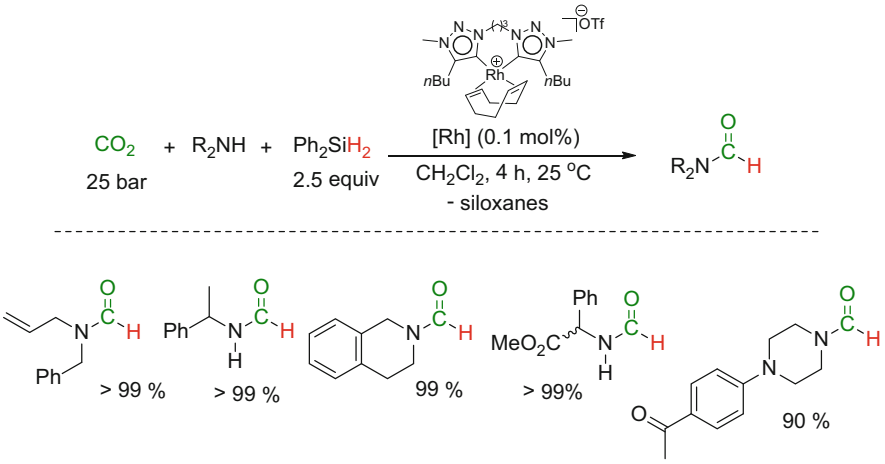

Scheme 9 Chemoselective Rh-catalyzed reductive functionalization of CO_2 with amines to formamides

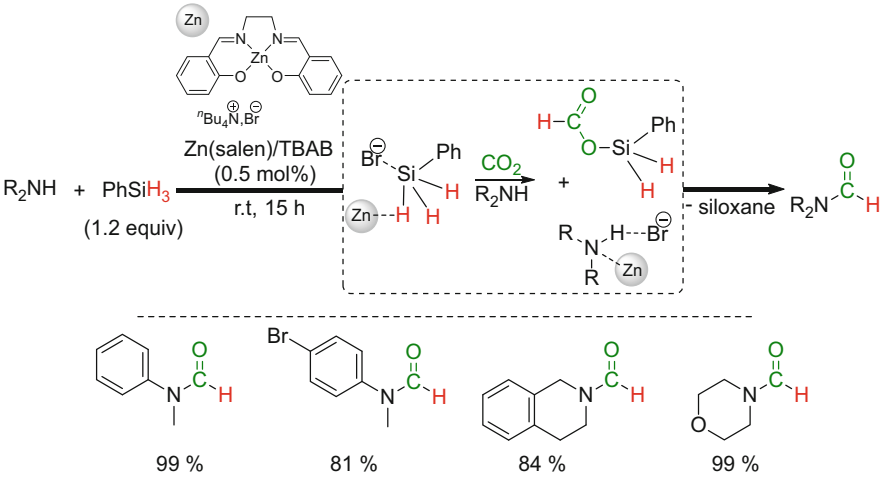

Scheme 10 Catalytic *N*-formylation of amines using CO_2 catalyzed by a Zn(salen)/TBAB system

intermediate that activates/reduces CO_2 molecules in a concerted manner. The formation of this intermediate explains the crucial use of dihydrosilanes (R_2SiH_2) instead of monohydrosilanes (R_3SiH) [85].

Zinc-catalyzed approaches were also investigated, and the Zn(salen) complex together with quaternary ammonium salts showed high efficiency as a binary catalytic system, possessing a significant synergistic effect for the *N*-formylation reaction of amines using CO_2 and hydrosilanes under solvent-free conditions [86]. This system was the first example of a metallosalen-catalyzed selective reduction of CO_2 in solution under mild conditions. Interestingly, inter- or intramolecularly cooperative effects were proposed to activate the Si-H bonds of hydrosilane, leading to CO_2 insertion and thereby activating this molecule between Lewis base and the transition metal center (LB-TM). This effect can subsequently facilitate the insertion of CO_2 to form the active silyl formate intermediate (Scheme 10). Moreover, the bifunctional Zn(salen) complexes, with two imidazolium-based ionic liquid (IL) linker units, acted intramolecularly as cooperative catalyst, resulting in facile and efficient catalyst recycling and reuse [86]. The same group showed in a follow-up investigation that a combination of a zinc phthalocyanine catalyst and a stoichiometric amount of DMF provided a simple route to formamide derivatives from amines, CO_2, and hydrosilanes in the absence of any halogenated co-catalysts [87].

2.3 *Production of Formamides Using CO_2 and H_2*

The use of molecular hydrogen in the conventional synthesis of formamides from CO_2 and amines with one or more N-H functionalities can afford the corresponding products by employing elevated temperatures ($\geq$75°C) and high pressures

$$CO_2 + H_2 + NHR_2 \rightleftharpoons [NH_2R_2][O_2CH] \longrightarrow HCONR_2 + H_2O \quad \text{(eq. 1)}$$

$$CO_2 + 2\,NHR_2 \rightleftharpoons [NH_2R_2][O_2CNR_2] \quad \text{(eq. 2)}$$

Scheme 11 Reaction pathway for the formation of formamides from CO_2 (Eq. 1); formation of the carbamates from CO_2 and amine (Eq. 2)

($\geq$60 atm). Although the approach with hydrogen gas is the most atom-economic, harsh reaction conditions prevent a broad application of this molecular reducing agent. As described in Scheme 11, the mechanism is believed to be based on the hydrogenation of CO_2 to ammonium formate as a first step, followed by the non-catalyzed thermal condensation to formamide (Scheme 11, Eq. 1) [3, 88]. For example, the preparation of formamide and dimethylformamide from CO_2/H_2 is highly efficient, in which, nearly complete conversion and selectivity are obtained in contrast to lower yields obtained for more bulky amines. Increasing the steric bulk and basicity of the used amine has a great influence on the interconnection of the species in Scheme 11, resulting in a favorable formation of solid carbamate salts from CO_2 and corresponding amines (Scheme 11, Eq. 2) [89].

2.3.1 Recent Investigations on Catalyst Development

The synthesis of formamide via hydrogenation of CO_2 in the presence of the corresponding alkylamines was reported as early as 1935 by Farlow and Adkins, using heterogeneous nickel catalysts [90]. Since then, few efforts have been made with solid catalysts as the obtained activity remained limited. The major contributions were describing the use of homogeneous systems with more active organometallic catalysts for the production of formamides from CO_2 for which representative examples are being summarized in Table 1.

One of the earliest homogeneous catalytic systems for the formation of formamides from CO_2 was presented in 1970, using a wide variety of phosphine complexes of metals as diverse as Co, Rh, Ir, Pt, Pd, Ru, and Cu with highest TONs (1,200) of DMF obtained with $[IrCl(CO)(PPh_3)_2]$ [91]. A major improvement in TON and TOF was achieved by Jessop et al. in 1994 when using supercritical CO_2, which resulted in high conversions and yields (up to 99%) and a maximum TON of 370,000 of DMF product when using $[RuCl_2(PMe_3)_4]$ precursor [92]. The use of supercritical CO_2 is thought to result in rapid diffusion and weak catalyst solvation. Moreover, the high miscibility of H_2 in $scCO_2$ could explain this high performance and high TONs [92]. Synthesis of other formamide products using similar conditions was also possible were products such as formamide, diethylformamide, and *n*-propylformamide could be produced with TONs of 500, 820, and 260, respectively [109]. In the same manner, the group of Baiker employed $scCO_2$ with the complex $[RuCl_2(dppe)_2]$ to further increase the TOF up to 360,000 h^{-1} for DMF production [93]. Interestingly, the production of *N*-formylmorpholine from morpholine was also possible with quantitative yield using $[RuCl_2(dppe)_2]$ in presence of $scCO_2$. This

Table 1 Selected catalytic systems for the production of formamides from CO_2 and H_2

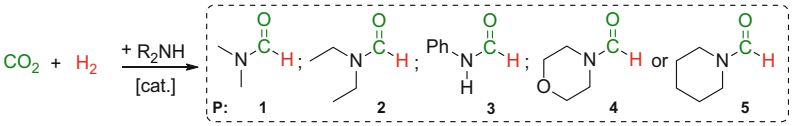

Entry	[cat.]	P	T [°C]	p_{H_2}/p_{CO_2} [bar/bar]	TOF [h^{-1}]	TON (yield)	Ref
1	[CoH(dppe)]	**1**	125	55 total	59	1,000	[91]
2	$[IrCl(CO)(PPh_3)_2]$	**1**	125	55 total	71	1,200	[91]
3	$[CuCl(PPh_3)_3]$	**1**	125	55 total	53	900	[91]
4	$[RuCl_2(PMe_3)_4]$	**1**	100	80/130	19,474	370,000	[92]
5	$[RuCl_2(dppe)_2]$	**1**	100	85/130	36,000	740,000	[93]
6	$[RuCl_2(PMe_3)_4]$	**3**	100	80/120	140	1,400	[94]
7	$[RuCl_2(dppe)_2]$	**4**	100	87/128	68,400	210,000	[89]
8	$Fe(BF_4)_2{\cdot}6H_2O/PP_3$	**1**	100	60/30	36	727	[95]
9	[(iPr-PNP)FeH(CO)(BH_4)]	**5**	120	35/35	556	8,900	[96]
10	$Co(BF_4)_2{\cdot}6H_2O/PP_3$	**1**	100	60/30	65	1,308	[97]
11	$Fe(BF_4)_2{\cdot}6H_2O$/L	**1**	100	70/30	211	4,229	[98]
12	"Si"-$[RuCl_2\{PMe_2(CH_2)_2Si(OEt)_3\}_3]$	**1**	133	85/130	1,847	110,800	[99]
13	"Si"-$[RuCl_2\{RPhP(CH_2)_3PPhR\}_2]$	**2**	110	180 total	18,400	–	[100]
14	PS-PEG-"Ru"	**1**	100	86/130	108	1,620	[101]
15	"Si"-$[RuCl_2(L)(NHC)]$	**5**	100	30/50	121	2,900	[102]
16	[RuCl(H)CO(PNP)]	**4**	120	35/35	20,208	1,940,000	[103]
17	$Cu(OAc)_2$/DMAP	**4**	90	40/40	–	(99%)	[104]
18	$CoCl_2$(iPr-PN^{H}P$^{\cdot}$)	**1**	150	30/30	–	(99%)	[105]
19	$MnBr(CO)_2$(iPr-PN^{H}P)	**4**	110	30/30	–	48 (95%)	[106]
20	$MnBr(CO)_3$(2,2′-bipyridine)	**2**	80	20/50	25	588 (72%)	[107]
21	$Ni(acac)_2$/dmpe	**4**	100	100 total	85	18,000 (90%)	[108]

PP$_3$ $P(CH_2CH_2PPh_2)_3$, *L* tris[(2-diphenylphosphino)phenyl]phosphine, *PNP* $MeN(CH_2CH_2PPh_2)_2$, *iPr-PNP* $MeN(CH_2CH_2PiPr_2)_2$, *DMAP* 4-dimethylaminopyridine, *iPr-PN^{H}P* $(iPr_2PCH_2CH_2)_2NH$, *iPr-PN^{H}P$^{\cdot}$ ortho*-$(iPr_2P)(-CH_2-NH-CH_2CH_2-PiPr_2)C_6H_4$

enabled an increase of TOF by an order of magnitude to 68,400 h^{-1} simply by adding small amounts of water to the reaction mixture to enhance the solubility of the solid carbamate formed from CO_2 and morpholine [89, 110]. The same group showed that immobilized organometallic catalysts have particularly high efficiency in this reaction, more specifically when DMF was obtained in 82% yield together with high TOF of 1,860 h^{-1} and TON of 110,800 using hybrid "Si"-$RuCl_2\{PMe_2(CH_2)_2Si(OEt)_3\}_3$ catalyst [99, 100, 111, 112]. Another immobilization approach was reported in 2003 by the group of Ikariya, describing the use of cross-linked polystyrene-poly(ethylene glycol) graft copolymer (PS-PEG) modified with

tertiary phosphines as an amphiphilic resin support for ruthenium complexes (such as $RuCl_2\{P(C_6H_5)_3\}_3$) to obtain DMF in 98% yield (TON = 1,620, TOF = 108 h^{-1}) [101]. Another interesting system was also developed based on a liquid/liquid two-phase process, resulting in the separation of the formamide product in one of the liquid phases. In 2004 Behr et al. described a biphasic reaction system for the production of DMF, consisting of an organic catalyst phase (toluene) and an aqueous extraction phase using $[RuCl_2(dppb)_2]$ as the catalyst [113]. Interestingly, Tumas and Baiker described the employment of a biphasic system, consisting of an ionic liquid as $[RuCl_2(dppe)_2]$ catalyst-host phase and $scCO_2$ as extraction phase [114]. For example, the product *N*,*N*-di-*n*-propylformamide could be separated from the catalyst by extraction with $scCO_2$, whereas the catalyst remained active for the cyclic uses in the ionic liquid phase. Another interesting direct application of a liquid/liquid phase process for the synthesis of formamide has also been developed using an homogeneous Ir/phosphine catalysts to catalyze the reaction of three gases (CO_2, H_2, and NH_3) in methanol as solvent in which different components can be separated using reactive distillation units [115].

In 2015, the group of Ding described the use of a highly efficient catalyst system based on ruthenium pincer-type complexes with a PNP (PNP = MeN $(CH_2CH_2PPh_2)_2$ ligand (Fig. 2) for *N*-formylation of various amines with CO_2 and H_2 [103]. The catalysts afforded the corresponding formamides with excellent productivity (turnover numbers of up to 1,940,000 in a single batch) and selectivity. Interestingly, this catalytic system was reused for 12 consecutive cycles for the DMF synthesis without significant loss of activity [103]. On the other hand, the group of Han reported in 2017 that the Cu–DMAP (DMAP = 4-dimethylaminopyridine) catalytic system could also catalyze *N*-formylation reaction very effectively with up to 99% yield. Together with a significant tolerance of the various amine substrates, the molecules retained its unsaturated group functionalities (e.g., carbonyl group, C=C bond, C=N bond, and ester group) [104].

On a more sustainable approach, the use of non-precious metal catalysts based on iron, nickel, and cobalt precursors is also applicable. Since 2010 such catalytic systems have been used to catalyze the formation of formamides from amines, CO_2, and H_2 (Fig. 3) [95, 97, 98]. For example, using the in situ pincer-type complex $Fe(BF_4)_2{\cdot}6H_2O/PP_3$ [PP_3 = $P(CH_2CH_2PPh_2)_3$] developed by the group of Beller, DMF was obtained in 75% yield (TON = 727), and *N*-formylpiperidine was formed in 41% (TON = 373) [95]. On the other hand, the analogous cobalt complex $Co(BF_4)_2{\cdot}6H_2O/PP_3$ afforded DMF in 73% yield (TON = 1,308) and *N*-formylpiperidine in 70% yield (TON = 1,254), employing similar reaction

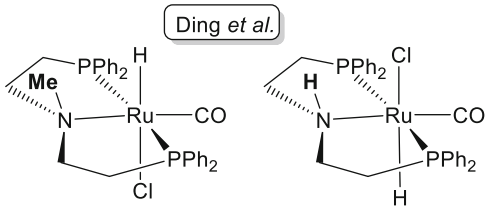

Fig. 2 Ruthenium pincer-type complexes introduced by Ding for the *N*-formylation of amines using CO_2 and H_2

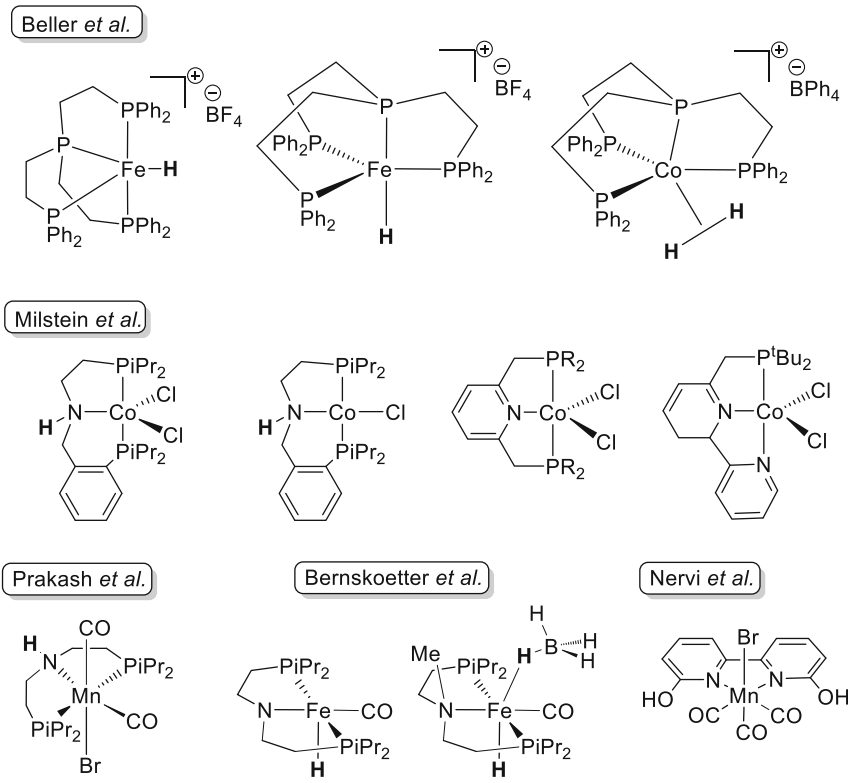

Fig. 3 Novel catalytic systems based on pincer ligand/earth-abundant metals for the *N*-formylation of amines using CO_2 and H_2

conditions [97]. Modifying the pincer ligand on the iron catalyst to the tetradentate ligand tris[(2-diphenylphosphino)phenyl]phosphine provided a significant improvement of the TONs up to 4,229 in the formation of DMF [98]. The PNP ligand was also used for a family of iron(II) carbonyl hydride species by the group of Bernskoetter. Two different types of iPr-PNP ligands (with tertiary or secondary amine moiety) were examined for formamide production using CO_2 and H_2. The iron catalyst incorporating a iPr-PNP ligand with tertiary amine was active for the *N*-formylation of a variety of amine substrates by affording the corresponding formamides with TONs up to 8,900 and conversion as high as 92% [96].

In 2017, the group of Milstein described the reactivity of a novel paramagnetic Co (II) chloride complex Co-(iPr-PN^{H}P$^{'}$) pincer-type complex (Fig. 3) for the selective synthesis of a wide range of *N*-formamides and showed that this complex could catalyze the formation of the formamide in good to excellent yield (e.g., DMF up to 99% yield, 248 TON) [105]. Despite the difficulty in assigning the reactivity of a fully characterized Co-H species, Milstein and coworkers proposed a mechanism for the formylation/hydrogenation pathways (Scheme 12). Upon treatment of the $CoCl_2$(iPr-PN^{H}P$^{'}$) complex with $NaHBEt_3$, a monochloride Co(Cl)(iPr-PN^{H}P$^{'}$)

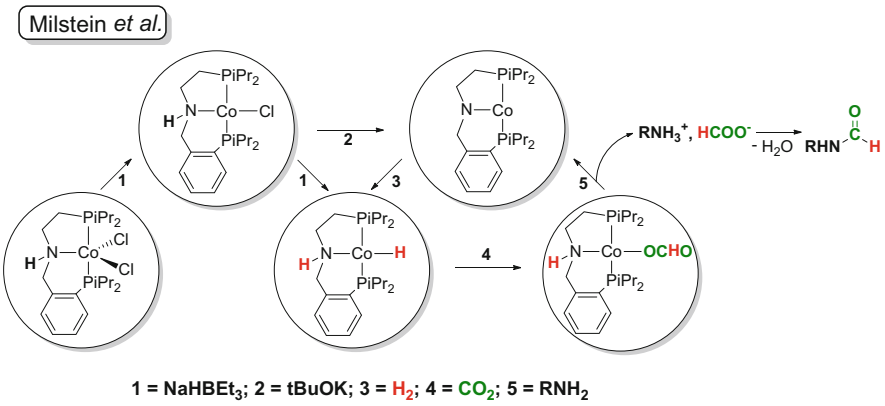

Scheme 12 Proposed mechanism of the Co-(iPr-PN^{H}P$^{\cdot}$) catalyzed *N*-formylation of amines using CO_2 and H_2

species is formed that can react with tBuOK to produce a non-chlorinated highly reactive, coordinatively unsaturated intermediate. Under H_2 pressure, a monohydride Co(H)(iPr-PN^{H}P$^{\cdot}$) is formed, by which a CO_2 molecule can insert into the Co-H bond. The presence of excess amine results in the formation of a formate salt that liberates water to construct the final formamide product [105]. In 2017, a base-metal manganese catalyst was also investigated for this reaction by the group of Prakash where iPr-PN^{H}P ligand was the key for the high reactivity of the catalyst (Fig. 3) [106]. This Mn(I)-PN^{H}P pincer catalyst was mainly investigated for the sequential one-pot homogeneous CO_2 hydrogenation to CH_3OH using H_2 in presence of amine additive for the in situ formation of a formamide intermediate. However, this well-defined catalyst was found also active for the selective synthesis of formamides (up to 95% yields) [106]. On the other hand, the group of Nervi reported the first examples of manganese catalysts with high activity for CO_2 hydrogenation to formate and formamide (588 TON of diethylformamide DEF) [107]. Compared to other reported first-row transition metal hydrogenation catalysts, these manganese complexes do not contain air-sensitive phosphine ligands. Instead, a simple bidentate *N*-donor 6,6′-dihydroxy-2,2′-bipyridine ligand was used to afford air-stable manganese complexes that can be synthesized without strict exclusion of oxygen [107]. Also in 2017, the group of Jessop investigated the activity of in situ Fe(II)- and Ni(II)-bidentate phosphine complexes for the *N*-formylation reaction using CO_2 and H_2, achieving conversions of 90–98% of amine to formamide [108]. Interestingly, such catalysts can be readily prepared from abundant iron or nickel salts such as $FeCl_2$, $Fe(OAc)_2$, $Ni(acac)_2$, $Ni(OAc)_2{\cdot}4H_2O$, and $NiCl_2{\cdot}6H_2O$ in presence of 1,2-bis(dimethylphosphino)ethane phosphine ligand (dmpe). For example, Jessop and coworkers showed that the catalytic formylation of morpholine with CO_2 and H_2 reached a TON of 18,000 and a 90% yield when using $Ni(acac)_2$/dmpe in presence of CO_2/H_2 (total 100 bar) at 100°C in DMSO as a solvent [108].

3 *N*-Methylation of Amines

3.1 N-*Methylated Amines*

N-methylated amines are one of the key structural motifs in a variety of valuable chemical compounds ranging from simple methylamines to more complex pharmaceutical, agrochemical, or biologically active compounds [116–120]. For example, methylamines (a term used generally to define the simplest C_1 alkyl amines: mono-, di-, or trimethylamines – $MeNH_2$, Me_2NH, and Me_3N) are considered important bulk chemicals with a high market value due to their importance as intermediates for the production of a wide range of agricultural chemicals, animal nutrients, catalysts, personal care electronics, resins, solvents, dyes, rubber chemicals, explosives, fuel additives as well as gas and oil treatment chemicals [121]. Industrially, methylamines are produced from ammonia and methanol over heterogeneous dehydration catalysts (Scheme 13d), whereas the *N*-methylation of structurally complex amines can be achieved using hazardous alkylating agents such as methyl iodide or dimethyl sulfate (Scheme 13c), and in few cases the use of dimethyl carbonate offers as a greener alternative (Scheme 13b) [122–128]. Eschweiler-Clarke methylation method is also one frequently used synthetic method for *N*-methylation of amines employing formaldehyde as the carbon source and formic acid as the reducing agent (Scheme 13a) [129, 130]. The first reported observation of CO_2 as C1 source for *N*-methylation reaction was described by the group of Vaska while working on DMF synthesis from dimethylamine, CO_2, and H_2 [131, 132]. However, it was only until 2013 that CO_2 utilization as an alternative route to *N*-methylated amines started to gain more attention. Since then, many research groups have dedicated intensive investigation on the use of CO_2 as a more sustainable C1 source for the construction of the *N*-methyl group compared to the traditional methylating agents (Scheme 13e) [133]. Previously, heterogeneous catalysts were rarely investigated for

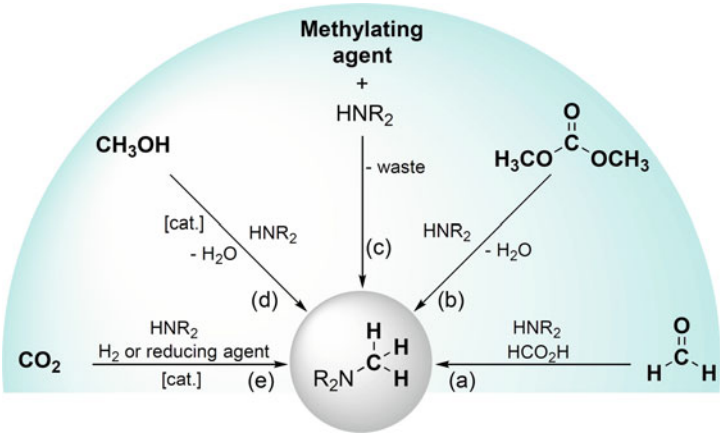

Scheme 13 Diverse approaches for *N*-methylation of amines

N-methylation reaction using CO_2 as C1 building block, with an early attempt carried out by the group of Baiker in 1995 [134–136]. In their attempts, Baiker and coworkers employed a Cu-catalyzed gas-phase approach to methylate ammonia gas using CO_2 and H_2; however, low yields, low selectivities, and the necessity of high temperatures (200–300°C) were considered as main drawbacks of such system. In this chapter we will mainly discuss the metal-free and organometallic homogeneous systems employed for *N*-methylation of amines using CO_2 knowing that, in the same period, many approaches summarizing the use of solid catalysts for *N*-methylation were also investigated by using a variety of copper-, palladium-, platinum-, rhenium-, or gold-supported catalysts [41, 137–142].

A detailed mechanism for the construction of the N-CH_3 bond from CO_2 and H_2 is yet not available; however, many reports suggest numerous bond-breaking and bond-forming steps with most of it supporting the formation of a formamide as a key intermediate toward the final *N*-methylated amine product. The formation of carbamic acid or carbamate salt or the subsequent urea (via dehydration) from CO_2 and amine has also to be considered which is influenced by many factors such as reaction pressure and temperature as well as the basicity of amine substrates [143]. Overall, these species can upon reduction be converted back to the expected formamide intermediate which is then reduced by the reducing agent to the final *N*-methylamine product (Scheme 14). One other possible pathway would be the reduction of CO_2 to methanol followed by catalytic alkylation of the amine substrate.

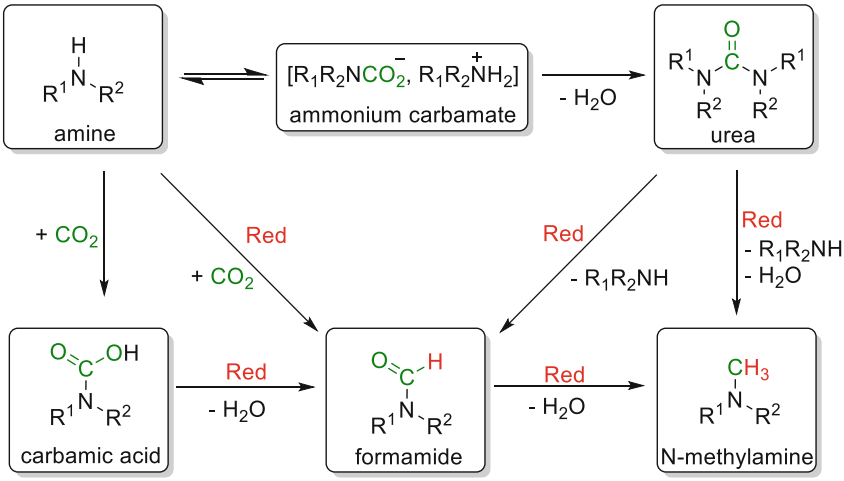

Scheme 14 Possible pathways for the catalytic *N*-methylation of amines via reductive functionalization of CO_2 in presence of a reducing agent (red: reduction step)

3.2 *Catalytic* N-*Methylation of Amines Using CO_2 and Reducing Agents (Excluding Molecular Hydrogen H_2)*

3.2.1 Metal-Free Systems

The use of silanes or boranes as reducing agent for the *N*-methylation of amines using CO_2 is an interesting synthetic approach that can be performed at mild reaction conditions ranging from mild reaction temperatures to ambient pressure of CO_2 in standard glassware apparatus. Another advantageous factor would be the functional group tolerance that can be better controlled when using a reducing agent other than H_2 together with a metal-free catalytic system. In this manner, the first attempts were reported by the group of Cantat who showed that the metal-free NHC catalytic systems could be employed for the reduction of CO_2 in the presence of amines to afford mainly formamides as the main product (see Scheme 3 in Sect. 2.2.1) together with traces of *N*-methylated products (<1%) [56, 144]. The same group was able to successfully increase the selectivities and yields of the *N*-methylated products by employing a boron hydride 9-borabicyclo(3.3.1)nonane (9-BBN) reducing agent together with the IPr catalyst to obtain *N*-methyldiphenylamine in 79% yield at a temperature of 90°C (Scheme 15a) [145]. Moreover, Cantat and coworkers showed that 9-BBN could also be used in presence of a Verkade's super-bases (VB^{Me}, Scheme 15d) to provide a high catalytic activity in the chemoselective *N*-methylation of a broad scope of substrates with up to 99% yields (TON up to 6,043 and TOF up to 2,934 h^{-1}) under mild conditions and short reaction time (in minutes) [145].

Since then, many efforts have been dedicated to study different metal-free system for this interesting *N*-methylation reaction where, remarkably, such metal-free systems were found to enable the catalytic *N*-methylation of amines with CO_2 and silanes under ambient conditions. This was again disclosed by the group of Dyson using also nucleophilic *N*-heterocyclic carbenes (NHCs) as metal-free catalysts (Scheme 15b) [56, 58, 59, 146, 147]. Such catalysts are able to activate CO_2 via imidazolium carboxylates resulting in the *N*-methylation of amine substrates in presence of Ph_2SiH_2 under ambient pressure and at mild temperatures of 50°C. A variety of *N*-methylated aromatic primary or secondary amines with up to 91% yields could be synthesized with a remarkable tolerance of a broad range of substrates/functional groups such as nitrile and nitro groups, double and triple bonds, and ether and ester-substituted amines [147]. As discussed in Sect. 2.2.1, highly effective and inexpensive thiazolium carbene-based catalysts (T-NHC) were successfully employed for the *N*-formylation of amines using PMHS as a reducing agent at a temperature of 50°C (Scheme 3e) [58, 59]. Attempts to switch the selectivity to *N*-methylated products were successful only when a temperature of 100°C was employed (Scheme 15c) to afford, for example, the *N*-methylated cinacalcet drug compound in 83% yield (Scheme 16, left) [58, 59]. Another efficient approach to *N*-methylated amines using CO_2 was described by the group of Liu where they used

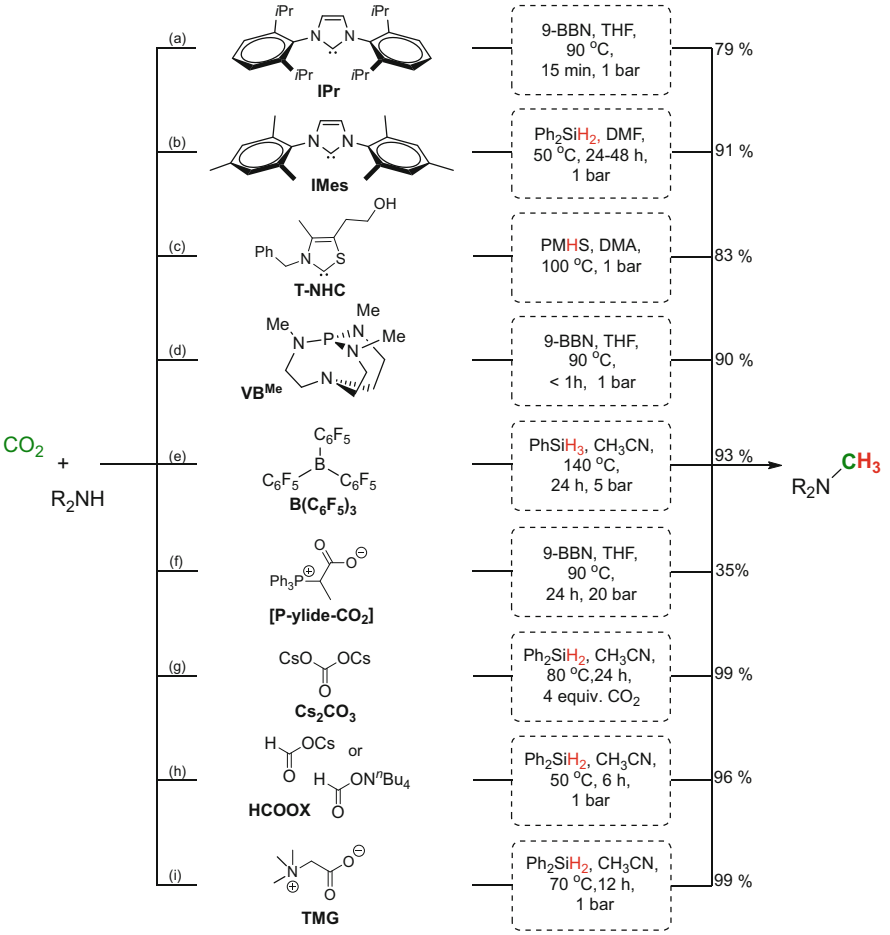

Scheme 15 Recent applications of metal-free catalytic system for the *N*-methylation of amines using CO_2 with corresponding maximum yields obtained

$B(C_6F_5)_3$ as a metal-free catalyst to catalyze the *N*-methylation of a broad range of anilines in the presence of hydrosilane $PhSiH_3$ as reducing agent (Scheme 15e) [148]. A double role is expected for the boron center of this Lewis acid which possesses an electron-deficient character for the activation of the Si-H bond as well as the activation of the amine substrates. On the other hand, the activation of CO_2 is favored by the incorporation of the strongly polar C-F bonds through electrostatic interactions. With this approach, the corresponding *N*-methylated products were formed with up to 93% yields under 5 bar pressure of CO_2, however, at 140°C reaction temperature [148]. Few investigation attempts were made to use the P-ylide-CO_2 adduct catalyst, previously described for the *N*-formylation reaction (see Sect. 2.2.1), to catalyze the *N*-methylation reaction using CO_2 and 9-BBN (Scheme 15f)

[53]. For example, the P-ylide-CO_2 adduct catalyst showed poor, but promising, activity and selectivity toward the *N*-methylated product *N*,*N*-dimethylaniline which was obtained in 35% yield.

Another interesting approach for the *N*-methylation was reported by the group of Fu and Lin in 2016 comprising the use of a simple, efficient, and readily available inorganic bases alkali-metal carbonates, especially cesium carbonate, to catalyze the *N*-methylation reactions under mild reaction conditions (Scheme 15g) [149]. High selectivities of the *N*-methylated products over the *N*-formylation products were obtained when a high temperature of 80°C was employed rather than room temperature despite the relatively longer reaction time required to obtain quantitative yields (24 h). In this manner, a "cesium effect" on the reaction was observed by comparing the catalytic activity of various alkali-metal carbonates where the corresponding solubility or nucleophilicity of cesium carbonate in the reaction solution may have a great influence on its activity. A direct application of this catalytic system was also tested for the *N*-methylation of the drug cinacalcet to afford the desired *N*-methylated product in 92% yield (Scheme 16, right) [149]. A very similar approach was also described by the group of He in 2017 by employing cesium or tetrabutylammonium carboxylate as catalysts for the efficient and selective *N*-methylation reaction (up to 96% yield) of different aromatic or aliphatic amines using atmospheric pressure of CO_2 and Ph_2SiH_2 reducing agent at only 50°C reaction temperature for 6 h (Scheme 15h) [66]. Though most of the *N*-methylation reactions proceed conventionally via a formamide intermediate, He and coworkers provided in their work some experimental evidences of a different pathway of this oxygen nucleophile-catalyzed reduction of CO_2. In this approach, it involves a reduction to the C0 species of CO_2 (i.e.,

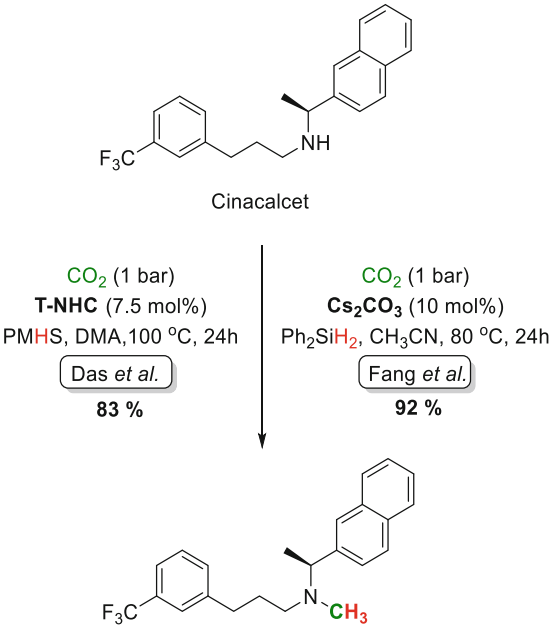

Scheme 16 Synthesis of *N*-methylated cinacalcet using CO_2 as C_1 building block

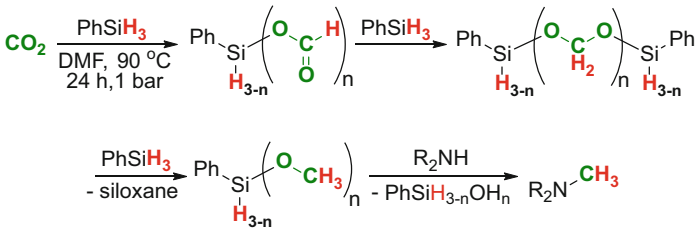

Scheme 17 Catalyst-free reductive *N*-methylation of amines using CO_2 and $PhSiH_3$ ($n = 1, 2$, or 3)

aminal) rather than the formamide as the intermediate to realize a total of six-electron reduction of CO_2 when the *N*-methylamine product is formed [66]. Another efficient carboxylate-based catalyst glycine betaine (TMG) was developed by the same group for the direct *N*-formylation or *N*-methylation of amines (Scheme 15i) [63]. This inner salt, which was used for the synthesis of a variety of formamides (Scheme 3g), could also be used to terminate the reduction steps at the *N*-methylation step by simply tuning the CO_2 pressure (from 10 to 1 bar) and temperature of the reaction (from 50 to 70°C) to afford the *N*-methylated amine products in up to 99% yields [63]. Last but not least, an exciting application of a "catalyst-free system" was introduced by the group of Chiang and Lei for the *N*-methylation of amines using only 1 bar of CO_2 and $PhSiH_3$ reducing agent to synthesize a variety of *N*-methylamine products in up to 95% yields [150]. In this work, a significant pathway was described involving the sequential formation of formoxysilane, bis(silyl)acetal, and silylmethoxide intermediates as three key steps in the formation of *N*-methylamine product (Scheme 17). The methyl group on silylmethoxide intermediate is then attacked by the nucleophilic amine substrate to afford the final *N*-methylamine product. The polar aprotic DMF solvent used in this reaction could have also played a favoring factor by promoting the activity of the Si-H bond and the solubility of CO_2 through solvation and polarization effects as described by Lei and Li (see Sect. 2.2.1) [69].

3.2.2 Organometallic Homogeneous Systems

As the utilization of CO_2 for the direct *N*-methylation of amines has been better explored and generalized starting from 2013, many reports by different research groups were published in a very short time in the following years. Many of these reports described the use of organometallic homogeneous systems for this CO_2-based *N*-methylation approach, and many of them were even so comparable in terms of efficiency and general conditions. The first homogeneous metallic system was actually reported in 2013 by the group of Cantat who described the use of zinc/*N*-heterocyclic carbene catalytic system for the direct methylation of aliphatic and aromatic amines using atmospheric pressure of CO_2 and small excess of $PhSiH_3$ reducing agent (2 equivalents) to afford the *N*-methylated products in yields up to

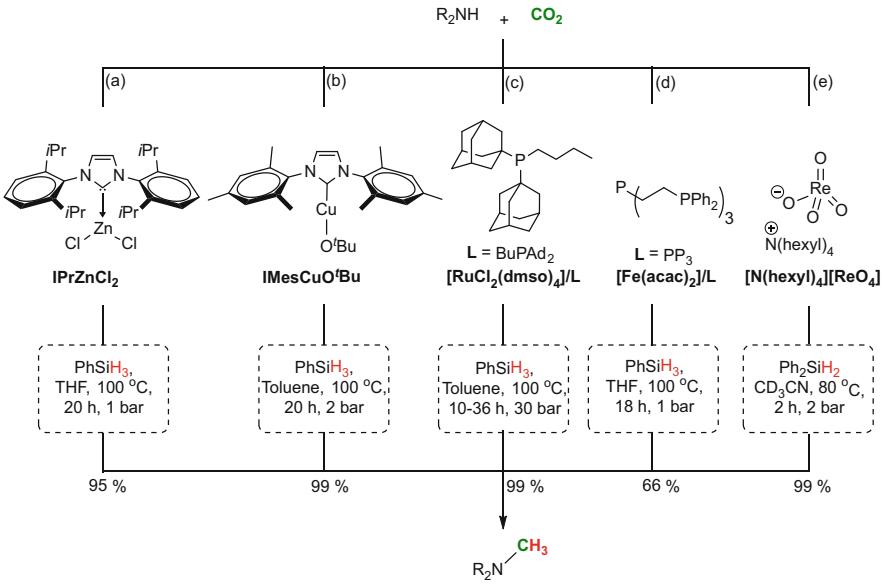

Scheme 18 Homogeneous organometallic catalytic systems for the direct *N*-methylation of amines using CO_2 and hydrosilanes as reducing agents

95% (Scheme 18a) [144]. The use of sterically congested IPr as both in situ coordinating ligand for $ZnCl_2$ or in the isolated $IPrZnCl_2$ catalyst resulted in the efficient *N*-methylation of a variety of amine substrates. A higher reactivity of aromatic amines over aliphatic ones was observed in addition to minor drawbacks in terms of selectivities of mono- and dimethylation when starting from primary amines. Interestingly, immobilized version of these catalysts were also investigated; however, lower yields of *N*-methylated products were obtained compared to the formamide ones [151]. Another very similar approach was described by the group of Cazin but this time using NHC ligand (IMes) in a Cu-metallic system ($IMesCuO^tBu$) under similar conditions using 2 bar of CO_2 and $PhSiH_3$ reducing agent to afford the *N*-methylated products in yields up to 99% (Scheme 18b) [152]. Selectivity limitations were also observed with many of the amine substrates used, for which, formamide intermediates were formed as the major product. This was resolved by the use of 4 equivalent excess of $PhSiH_3$ in addition to a base additive such as KO^tBu to promote the catalyst regeneration. Phosphine-derived ligands were also explored for different metal-catalyzed *N*-methylation of amines using CO_2. In this manner, the group of Beller described the *N*-methylation of amines using a Ru-based catalyst bearing a bulky phosphine ligand $BuPAd_2$ (Ad = adamantyl) [153]. This system can be prepared in situ starting with $[RuCl_2(dmso)_4]$ in presence of $BuPAd_2$ ligand to enable the methylation of a large variety of anilines and aliphatic amines using 30 bar of CO_2 and 4 equivalent excess of $PhSiH_3$ to afford the corresponding *N*-methylated products in up to 99% yields (Scheme 18c) [153]. Again the group of Cantat demonstrated that the iron-based catalytic system $Fe(acac)_2/PP_3$

{PP_3 = tris[2-(diphenylphosphino)ethyl]phosphine or Tetraphos} can afford promising results when employed for the direct *N*-methylation of amines using CO_2 and excess of $PhSiH_3$ to afford the *N*-methylated products in up to 66% yields (Scheme 18d) [74]. Another third-row transition metal catalytic system was also developed for the *N*-methylation reaction using CO_2. For this, García and coworkers described the use of two nickel-based catalysts $[(dippe)Ni(\mu\text{-}H)]_2$ and $[Ni(cod)_2]$/dcype (dippe = 1,2-Bis(diisopropylphosphino)ethane; dcype = 1,2-Bis (dicyclohexylphosphino)ethane) for the successful mono-*N*-methylation of aliphatic primary amines under relatively mild reaction conditions (1 bar CO_2) [154]. However, the systems revealed some drawbacks in terms of yields (moderate to good yields) and product selectivities in which different nitrogen-containing species were formed as significant side products. In 2017, the group of Love investigated the first use of a simple lipophilic perrhenate salt $[N(hexyl)_4][ReO_4]$ as a catalyst for a set of reduction reactions including reduction of organic carbonyls and CO_2 using primary and secondary hydrosilanes (Scheme 18e) [155]. This system showed promising results for the reduction of CO_2 to methanol via silyl formate and silyl acetal intermediates. On the other hand, when an amine (mainly aliphatic amines) is added under 2 bar pressure of CO_2, the *N*-methylated product is favored over methanol production. In this manner, using a set of different aliphatic amines for this *N*-methylation reaction resulted in the formation of the target *N*-methylamine products in up to 99% yields. A DFT study of the corresponding CO_2 reduction mechanism revealed that the perrhenate anion activates the silyl hydride to form an active hypervalent silicate transition state (instead of the formation of Re-H species) which enables the reduction of CO_2 by directly cleaving a Si-H bond.

3.3 Catalytic N-*Methylation of Amines Using CO_2 and H_2*

3.3.1 Organometallic Homogeneous Systems

In terms of sustainability, it is highly desired to apply more sustainable reagent for the *N*-methylation reaction starting from CO_2 as C_1 building block. However, the availability and energy requirements of the traditionally used reducing reagents (mainly hydrosilanes) remain a main limitation in the course of investigating ultimate sustainable approaches of the reduction of CO_2. In this manner the use of molecular hydrogen (H_2) instead of the traditional wasteful reducing agents (by-products and E-factor) is considered an elegant and more viable first-step approach. For example, the only by-product of the corresponding reaction would be H_2O albeit the use of high H_2 pressures/techniques as well as harsher reaction conditions in many examples. The first example for the direct *N*-methylation of primary and secondary amines with CO_2 and H_2 as the building blocks was described by the group of Klankermayer and Leitner in 2013 [156, 157]. They employed a Triphos-based [158] ruthenium system, consisting of [Ru(triphos)(tmm)] [159] and an acidic additive, as the key factor for the successful use of these simple and readily available reagents to construct the methyl group with high

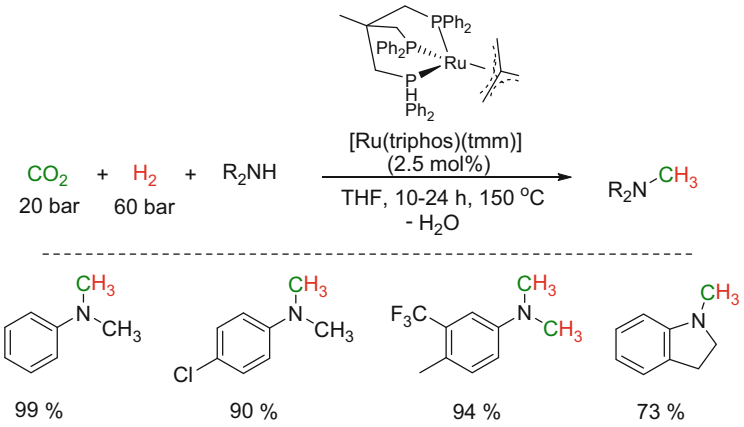

Scheme 19 Ruthenium-catalyzed *N*-methylation of amines with CO_2 and H_2 using [Ru(triphos)(tmm)]

reactivity (Scheme 19). This catalytic system was previously applied for reduction of CO_2 to methanol as well as for the hydrogenation of amides [160, 161].

The use of an acid additive was found to be crucial to activate the pre-catalyst by forming a cationic ruthenium hydride system in presence of H_2 gas. The direct *N*-methylation of different aromatic primary and secondary amines was highly reactive in presence of CO_2/H_2 (20/60 bar) in THF as solvent to afford the corresponding di- or monomethylated amines in >90% yields at 140–150°C, whereas aliphatic amines showed lower reactivity under these conditions. Interestingly, Klankermayer and Leitner showed that this system can also be applied for the dual hydrogenation/*N*-methylation of secondary amides which offers a direct access to unsymmetrical methyl/alkyl tertiary amines in a stepwise one-pot approach. In the same year, the group of Beller published a very similar approach to the *N*-methylation of aromatic and aliphatic amines using CO_2/H_2 by employing an in situ catalyst $[Ru(acac)_3]$/Triphos/H^+ [162]. Interestingly, the reactivity of this Ru-Triphos system for the *N*-methylation of aliphatic amines was significantly increased by using LiCl as additive however under relatively higher loading compared to the optimized reaction conditions (Scheme 20). The same in situ Ru-Triphos system was adopted by Han and coworkers in 2017 to extend the scope of the reaction to quinoline substrates by following the *N*-methylation/hydrogenation sequence in presence of CO_2/H_2 (20/80 bar) to afford the corresponding *N*-methyl-1,2,3,4-tetrahydroquinoline products in up to 99% yields [163].

As the chemical, industrial, and market value of alkyl amines is of great importance and has gained more attention in last few years, the group of Klankermayer and Leitner investigated the use of ammonia, CO_2, and H_2 as the only reagents for the synthesis of highly valuable trimethylamine using the Ru-Triphos catalytic system [164]. Indeed, they showed that the [Ru(triphos)(tmm)] catalyst can also be applied for the selective catalytic triple *N*-methylation of ammonia and ammonium chloride for the selective synthesis of trimethylamine. Interestingly, two different approaches can be employed (Scheme 21): (a) from ammonia in organic solvents where a Lewis

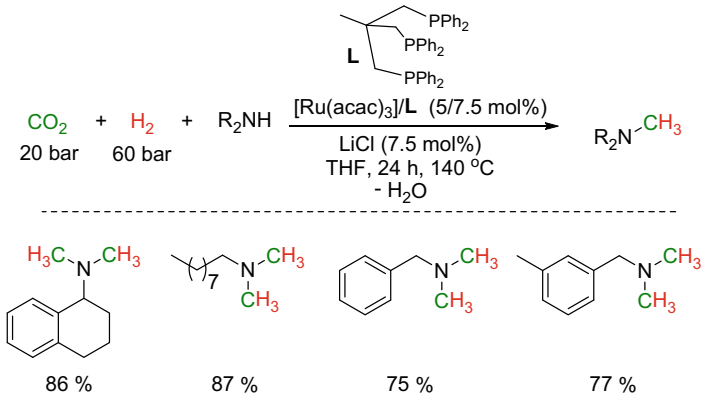

Scheme 20 *N*-methylation of amines with CO_2 and H_2 catalyzed by in situ Ru-Triphos system in the presence of LiCl additive

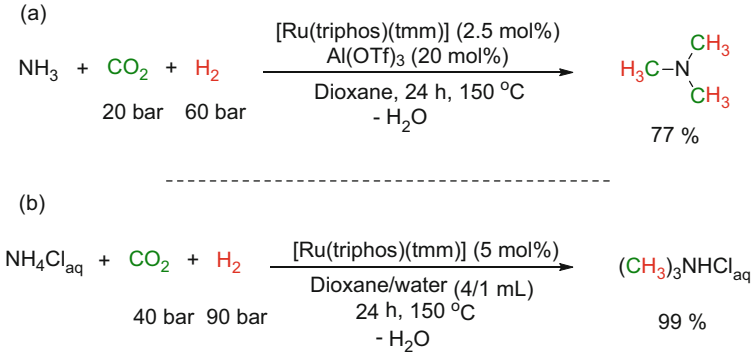

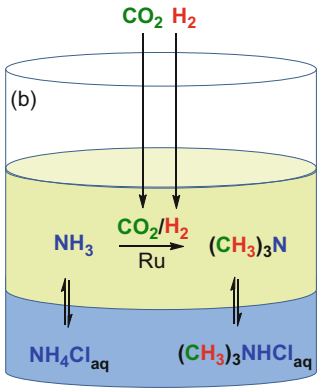

Scheme 21 Synthesis of trimethylamine TMA or its hydrochloride starting from (**a**) NH_3 or (**b**) NH_4Cl using CO_2/H_2

and/or Brønsted acid as co-catalyst is required (77% yield) or (b) from ammonium chloride in aqueous solutions in the absence of any acid additives (quantitative yields). For the latter approach, the absence of acid additives is overcome by the availability of the inherent proton from the ammonium chloride. Moreover, a biphasic aqueous/organic system with recycling potentials was achieved, from which separation and isolation of the trimethylamine product salt was readily performed (Scheme 21b) [164].

The synthesis of more complex unsymmetrical trialkylamines was also possible using the [Ru(triphos)(tmm)] catalyst via *a* non-precedent sequential reductive methylation of imines. Both isolated imines and mixture of aldehydes and amines could be applied for this reaction to afford a variety of unsymmetrical alkyl/methyl anilines in up to 97% yields at even lower temperature (100°C) compared to the general conditions applied in the initial work from the same group [165]. The choice of acid co-catalyst was crucial for this reaction where traditional protonic acid such as methanesulfonic acid (MSA) or *p*-toluenesulfonic acid (*p*-TsOH) resulted in the cleavage of the imine substrate and subsequent *N*-methylation of the resulting aniline. On the other hand, using $HNTf_2$ acid was crucial for the reaction to proceed smoothly to the desired trialkylamine product. More interestingly, this catalytic reductive utilization of CO_2 and H_2 as CH_3 unit building blocks was employed for a greener approach to synthesis an antimycotic antifungal agent named butenafine [166, 167] which is synthesized traditionally via a multistep and wasteful process [168]. The CO_2-based synthesis of butenafine can be achieved by using commercially available substrates (1-naphthalene aldehyde and 4-tert-butylbenzyl amine) to react with CO_2 and H_2 in either a one-step multicomponent coupling pathway (60% yield, Scheme 22) or starting from the corresponding isolate imine (88% yield, Scheme 22) [133, 165].

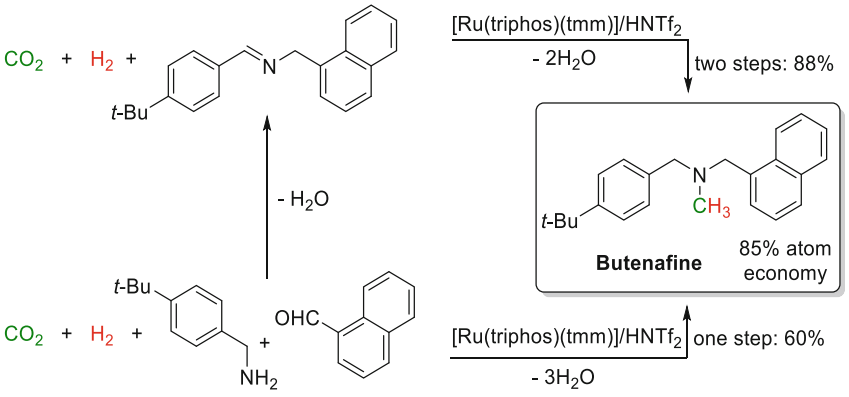

Scheme 22 Multicomponent coupling synthesis of antifungal agent butenafine via *N*-methylation using CO_2 and H_2 in one- or two-step procedure

4 Synthesis of Dialkoxymethanes

4.1 OMEs as Potential Fuel Additives

In the last century, highly efficient diesel engines have played an important role to enable effective transportation all over the planet. However, the complex combustion process with diesel fuels requires complex after gas treatment, as soot and NO_X formations have to be eliminated in modern high-performance diesel engines [169]. Efficient particulate filters allowing the reduction of soot emissions and the catalytic decomposition of NO_x, as effective technologies, are already implemented in diesel cars. However, recently alternative fuels and fuel additives paved the way to tailor the combustion process with respect to a minimal environmental impact. In this manner, oxygenated compounds such as methanol, dimethyl ether (DME), and oxymethylene ethers (OMEs) are the most promising fuel additive candidates that are able to strongly reduce soot formation [169–171]. Especially, oxymethylene dimethyl ethers such as dimethoxymethane (referred as OME_1, DMM, or methylal) and poly(oxymethylene) dimethyl ethers (OME_n) are gaining increasing attention as potential fuel additives due to their experimentally observed advantageous combustion properties [170–173]. Besides their interesting properties as fuel additives, OMEs have also gained many potentials as suitable replacements of formaldehyde solutions used for the preservation of human and animal corpses [174]. In this chapter, the CO_2-based synthetic approach of the first member in this homologous series (OME_1) will be discussed. OME_1 has been reported to represent a key molecule and building block for the synthesis of higher OMEs, in addition to many other potentials as green solvent or in pharmaceutical and perfume industries [170, 172, 173, 175].

4.2 Traditional Approaches to OME_1 Synthesis

An acid-catalyzed reaction between methanol and trioxane could afford methylal straightforward in excellent yields (Scheme 23c) [176]; however, the industrial production of OME_1 is achieved via a two-step process comprising the oxidation of methanol over silver or modified iron-molybdenum-vanadium oxide catalysts to form formaldehyde followed by the subsequent acid-catalyzed condensation of the latter with methanol to afford the corresponding OME_1 product (Scheme $23b_{1,2}$) [177–180]. Investigations on one-step direct oxidation of methanol as substrate to DMM have been also performed with a number of selective oxidation catalysts (mostly bifunctional heterogeneous catalysts) yielding DMM in up to 100% selectivity via a sequential in situ oxidative formation of formaldehyde and its subsequent condensation (Scheme 23a) [181–191].

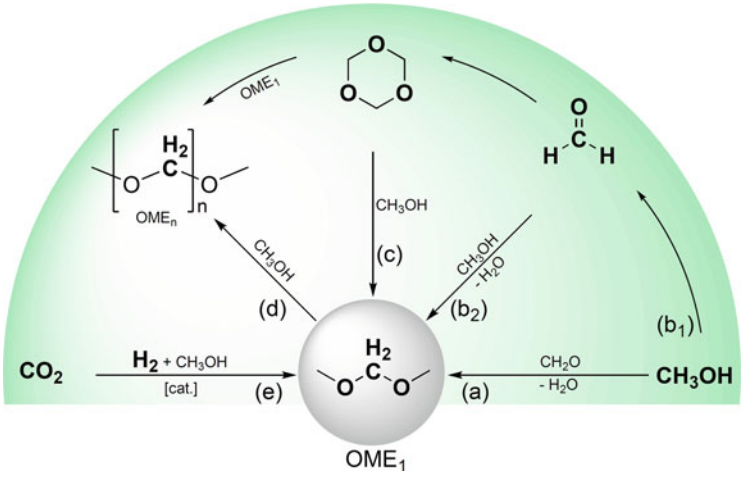

Scheme 23 Different approaches for the synthesis of OME_1 and its use in the synthesis of OME_n

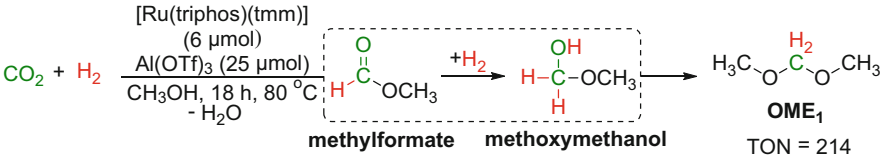

Scheme 24 [Ru(triphos)(tmm)]/$Al(OTf)_3$-catalyzed synthesis of OME_1 using methanol and CO/H_2 as C_1 synthon

4.3 Reductive Approach for the Synthesis of OME_1 and Dialkoxymethanes Using CO_2 and H_2

In 2016, the group of Klankermayer described the first reductive catalytic approach to generate OME_1 directly from MeOH by using CO_2/H_2 as C1 building blocks of the $-CH_2-$ unit as an attractive alternative route to the oxidative approaches (Schemes 23e and 24) [22].

In general, the ruthenium systems were investigated in combination with selected acidic co-catalysts using methanol, CO_2, and H_2 as substrates. The first catalytic system employed for this reaction was based on the [Ru(triphos)(tmm)] catalyst in combination with Lewis and/or Brønsted co-catalysts. The multifunctionality of the catalyst system was found to be crucial for the complex reaction sequence, comprising various hydrogenation and esterification/acetalization steps (Scheme 24). Reactions were carried out with a 20/60 bars of CO_2/H_2 (pressurized at room temperature) and reaction temperatures of 80°C. The use of the acid additive showed to be crucial for the formation of OME_1 as the absence of any acid did not result in the formation of any detectable CO_2 hydrogenation products.

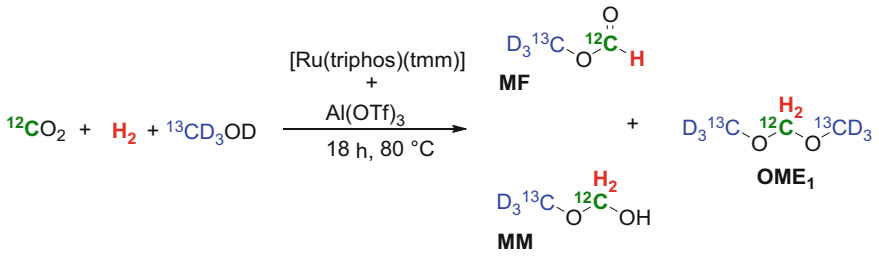

Scheme 25 Isotopic labeling observed by NMR spectroscopy for the [Ru(triphos)(tmm)]/Al(OTf)$_3$-catalyzed synthesis of DMM from ^{13}C-methanol-d$_4$

The detected methyl formate and methoxymethanol intermediates indicate a possible reaction pathway involving the hydrogenation/esterification of CO_2 to form methyl formate intermediate followed by a hydrogenation step to the hemiacetal methoxymethanol (MM) which follows a transacetalization step with methanol solvent to form OME_1 product (Scheme 24). Whereas the reduction sequence is catalyzed by the ruthenium catalyst, the esterification and acetalization steps are expected to be largely induced by the Brønsted and/or Lewis acidity of the multifunctional catalytic system. This pathway was further confirmed by a set of labeling experiments revealing that the final product OME_1 incorporated only the methyl groups generated from methanol substrate, whereas the CH_2O unit was generated from the used CO_2 and H_2 (Scheme 25).

In 2017, the same group developed a non-precious cobalt catalyst system for the selective synthesis of OME_1 from CO_2/H_2 and methanol [20]. This cobalt-based approach to OME_1 incorporated the use of a tailored system based on cobalt salts in combination with selected Triphos ligands and acidic co-catalysts to enable a smooth synthetic pathway involving the formation of methyl formate and methoxymethanol intermediates as well. $Co(BF_4)_2{\cdot}6H_2O$ was identified as the most active cobalt precursor, producing, with Triphos ligand, a highly active system for the formation of OME_1 with a TON of 373 starting from methyl formate as substrate and with a TON of 92 starting from CO_2 as the C_1 source. Compared to the ruthenium/Triphos system, the cobalt/Triphos system required a higher temperature of 100°C in addition to the use of THF as a cosolvent for this reaction. More interestingly, initial studies showed that the reactivity of the cobalt system could be enhanced by variation of the ligand sphere when using a set of other tailor-made Triphos ligands bearing different sterically hindering functionalities. For example, the use of Triphos^{Tol} ligand (1,1,1-tris(bis(4-methylphenylphosphino)methyl)ethane) for the synthesis of OME_1 from CO_2 resulted in increasing the TON from 92 to 157 (Scheme 26), affording a comparable activity to the precious metal catalyst based on ruthenium/Triphos [22].

The versatility of the novel ruthenium- and cobalt-catalyzed synthesis of OME_1 was also investigated for the synthesis of dialkoxymethanes (DAM) [20, 22]. A set of selected alcohols were investigated as substrates and showed that generally,

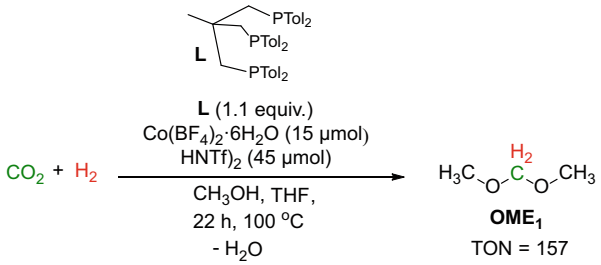

Scheme 26 $Co(BF_4)_2$/Triphos^{Tol}-catalyzed synthesis of OME_1 using methanol and CO/H_2 as C_1 synthon

Table 2 Ruthenium- or cobalt-catalyzed synthesis of dialkoxymethanes (DAM) using variable alcohols with CO_2 and molecular hydrogen

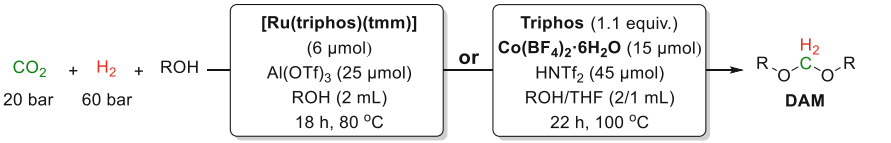

Entry	ROH	DAM	TON/Ru	TON/Co
1		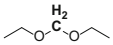	118	109
2		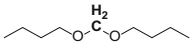	110	48
3		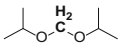	29	16

moderate to good reactivities under the conditions employed for both ruthenium and cobalt systems could be obtained (Table 2).

5 Conclusion

This short overview demonstrated that the use of CO_2 as a carbon source for catalytic transformations can provide a sustainable alternative to the conventional use of petrochemical-based building blocks within traditional synthetic pathways. Thus, the reductive functionalization and coupling of CO_2 with selected substrates in the presence of versatile reducing agents are providing a straightforward approach for the synthesis of interesting and valuable chemical products. Moreover, using molecular hydrogen for the presented reductive utilization of CO_2 would result in an atom-efficient chemical reaction with water as the sole by-product. Therefore, if the H_2 required in these reductive reactions is sourced from renewable primary energy sources, the corresponding CO_2 utilization approaches would enable to further

reduce the carbon footprint of the chemical transformation, especially when applied for processes in chemical industry. Among the target products, formamides and methylamines are considered of high market value and the corresponding synthesis of such chemical products from CO_2 and H_2 is highly advantageous both economically and environmentally. Consequently, other valuable chemical products with great potential in the fuel sector or as solvents are also accessible by using CO_2 as building block. Thus, dialkoxymethane ethers and derivatives represent important target molecules, synthesized from CO_2 in a more efficient methodology compared to traditional synthetic procedures. More interestingly, such CO_2-based approaches, when combined with bio-based substrates and green hydrogen from water electrolysis, could open a sustainable synthetic pathway for important liquid energy carriers or solvents ("biohybrid" fuels and materials).

References

1. Das Neves Gomes C, Jacquet O, Villiers C, Thuéry P, Ephritikhine M, Cantat T (2012). Angew Chem Int Ed 51:187
2. Klankermayer J, Wesselbaum S, Beydoun K, Leitner W (2016). Angew Chem Int Ed 55:7296
3. Jessop PG (2007) Homogeneous hydrogenation of carbon dioxide. In: Vries JG, Elsevier CJ (eds) The handbook of homogeneous hydrogenation. Wiley-VCH, Weinheim, p 489
4. Sakakura T, Choi J-C, Yasuda H (2007). Chem Rev 107:2365
5. Aresta M (2010) Carbon dioxide as chemical feedstock. Wiley-VCH, Weinheim
6. Peters M, Köhler B, Kuckshinrichs W, Leitner W, Markewitz P, Müller TE (2011). ChemSusChem 4:1216
7. Cokoja M, Bruckmeier C, Rieger B, Herrmann WA, Kühn FE (2011). Angew Chem Int Ed 50:8510
8. Hölscher M, Keim W, Gürtler C, Müller TE, Peters M, Leitner W (2012). Z Naturforsch B 67:961
9. Centi G, Quadrelli EA, Perathoner S (2013). Energy Environ Sci 6:1711
10. Aresta M, Dibenedetto A, Angelini A (2014). Chem Rev 114:1709
11. Barbato L, Centi G, Iaquaniello G, Mangiapane A, Perathoner S (2014). Energ Technol 2:453
12. Perathoner S, Centi G (2014). ChemSusChem 7:1274
13. Plass L, Bertau M, Linicus M, Heyde R, Weingart E (2014) Methanol as a hydrogen and energy carrier. In: Bertau M, Offermanns H, Plass L, Schmidt F, Wernicke H-J (eds) Methanol: the basic chemical and energy feedstock of the future. Springer, Heidelberg, p 619
14. Bourasseau C, Guinot B (2015) Hydrogen: a storage means for renewable energies. In: Godula-Jopek A (ed) Hydrogen production. Wiley-VCH, Weinheim, p 311
15. Ausfelder F, Beilmann C, Bertau M, Bräuninger S, Heinzel A, Hoer R, Koch W, Mahlendorf F, Metzelthin A, Peuckert M, Plass L, Räuchle K, Reuter M, Schaub G, Schiebahn S, Schwab E, Schüth F, Stolten D, Teßmer G, Wagemann K, Ziegahn K-F (2015). Chem Ing Tech 87:17
16. Junge H, Rockstroh N, Fischer S, Brückner A, Ludwig R, Lochbrunner S, Kühn O, Beller M (2017). Inorganics 5:14
17. Duan J, Chen S, Zhao C (2017). Nat Commun 8:15341
18. Yao S, Zhang X, Zhou W, Gao R, Xu W, Ye Y, Lin L, Wen X, Liu P, Chen B, Crumlin E, Guo J, Zuo Z, Li W, Xie J, Lu L, Kiely CJ, Gu L, Shi C, Rodriguez JA, Ma D (2017). Science 357:389
19. Leitner W, Quadrelli EA, Schlogl R (2017). Green Chem 19:2307

20. Schieweck BG, Klankermayer J (2017). Angew Chem Int Ed 56:10854
21. Deutz S, Bongartz D, Heuser B, Kätelhön A, Schulze Langenhorst L, Omari A, Walters M, Klankermayer J, Leitner W, Mitsos A, Pischinger S, Bardow A (2018). Energy Environ Sci 11:331
22. Thenert K, Beydoun K, Wiesenthal J, Leitner W, Klankermayer J (2016). Angew Chem Int Ed 55:12266
23. Hett R, Fang QK, Gao Y, Wald SA, Senanayake CH (1998). Org Process Res Dev 2:96
24. Kazuhiro K, Satoshi N, Masataka K, Osamu M, Hisatoshi K (1995). Chem Lett 24:575
25. Weissermel K, Arpe H-J (2008) Industrial organic chemistry3rd edn. Wiley-VCH, Weinheim
26. Jones S, Warner CJA (2012). Org Biomol Chem 10:2189
27. Bipp H, Kieczka H (2000) Formamides. Ullmann's encyclopedia of industrial chemistry. Wiley-VCH, Weinheim
28. Wuts PGM (2014) Greene's protective groups in organic synthesis5th edn. Wiley, Hoboken
29. Gerack C, McElwee-White L (2014). Molecules 19:7689
30. Olah GA, Ohannesian L, Arvanaghi M (1987). Chem Rev 87:671
31. Arpe H-J (2010) Industrial organic chemistry, vol 5. Wiley-VCH, Weinheim
32. Choi Y-S, Shim YN, Lee J, Yoon JH, Hong CS, Cheong M, Kim HS, Jang HG, Lee JS (2011). Appl Catal A Gen 404:87
33. Ortega N, Richter C, Glorius F (2013). Org Lett 15:1776
34. Tanaka S, Minato T, Ito E, Hara M, Kim Y, Yamamoto Y, Asao N (2013). Chem Eur J 19:11832
35. Kang B, Hong SH (2015). Adv Synth Catal 357:834
36. Kothandaraman J, Kar S, Sen R, Goeppert A, Olah GA, Prakash GKS (2017). J Am Chem Soc 139:2549
37. Chakraborty S, Gellrich U, Diskin-Posner Y, Leitus G, Avram L, Milstein D (2017). Angew Chem Int Ed 56:4229
38. Galindo Cifre P, Badr O (2007). Energy Convers Manag 48:519
39. Dong B, Wang L, Zhao S, Ge R, Song X, Wang Y, Gao Y (2016). Chem Commun 52:7082
40. Nale DB, Rath D, Parida KM, Gajengi A, Bhanage BM (2016). Cat Sci Technol 6:4872
41. Molla RA, Bhanja P, Ghosh K, Islam SS, Bhaumik A, Islam SM (2017). ChemCatChem 9:1939
42. Luo R, Chen Y, He Q, Lin X, Xu Q, He X, Zhang W, Zhou X, Ji H (2017). ChemSusChem 10:1526
43. He Z, Liu H, Liu H, Qian Q, Meng Q, Mei Q, Han B (2017). ChemCatChem 9:1947
44. Ju P, Chen J, Chen A, Chen L, Yu Y (2017). ACS Sustain Chem Eng 5:2516
45. Zhang Y, Wang H, Yuan H, Shi F (2017). ACS Sustain Chem Eng 5:5758
46. Mitsudome T, Urayama T, Fujita S, Maeno Z, Mizugaki T, Jitsukawa K, Kaneda K (2017). ChemCatChem 9:3632
47. Villiers C, Dognon J-P, Pollet R, Thuéry P, Ephritikhine M (2010). Angew Chem Int Ed 49:3465
48. Hao L, Zhao Y, Yu B, Yang Z, Zhang H, Han B, Gao X, Liu Z (2015). ACS Catal 5:4989
49. Maryanoff BE, Reitz AB (1989). Chem Rev 89:863
50. Li A-H, Dai L-X, Aggarwal VK (1997). Chem Rev 97:2341
51. Sun X-L, Tang Y (2008). Acc Chem Res 41:937
52. Matthews CN, Driscoll JS, Birum GH (1966) Chem Commun 736. https://doi.org/10.1039/C19660000736
53. Zhou H, Wang G-X, Zhang W-Z, Lu X-B (2015). ACS Catal 5:6773
54. Chong CC, Kinjo R (2015). Angew Chem Int Ed 54:12116
55. Lu Y, Gao Z-H, Chen X-Y, Guo J, Liu Z, Dang Y, Ye S, Wang Z-X (2017). Chem Sci 8:7637
56. Jacquet O, Das Neves Gomes C, Ephritikhine M, Cantat T (2012). J Am Chem Soc 134:2934
57. Saptal VB, Bhanage BM (2016). ChemSusChem 9:1980
58. Das S, Bobbink FD, Bulut S, Soudani M, Dyson PJ (2016). Chem Commun 52:2497
59. Bobbink FD, Das S, Dyson PJ (2017). Nat Protoc 12:417
60. Piel I, Pawelczyk MD, Hirano K, Fröhlich R, Glorius F (2011). Eur J Org Chem 2011:5475
61. Hulla M, Bobbink FD, Das S, Dyson PJ (2016). ChemCatChem 8:3338

62. Revunova K, Nikonov GI (2015). Dalton Trans 44:840
63. Liu X-F, Li X-Y, Qiao C, Fu H-C, He L-N (2017). Angew Chem Int Ed 56:7425
64. Xie W, Zhao M, Cui C (2013). Organometallics 32:7440
65. Zhao M, Xie W, Cui C (2014). Chem Eur J 20:9259
66. Liu X-F, Qiao C, Li X-Y, He L-N (2017). Green Chem 19:1726
67. Aue DH, Webb HM, Bowers MT (1976). J Am Chem Soc 98:318
68. Reichardt C (1994). Chem Rev 94:2319
69. Lv H, Xing Q, Yue C, Lei Z, Li F (2016). Chem Commun 52:6545
70. Song J, Zhou B, Liu H, Xie C, Meng Q, Zhang Z, Han B (2016). Green Chem 18:3956
71. Zhao T-X, Zhai G-W, Liang J, Li P, Hu X-B, Wu Y-T (2017). Chem Commun 53:8046
72. Zhang X, Kam L, Trerise R, Williams TJ (2017). Acc Chem Res 50:86
73. Hao L, Zhang H, Luo X, Wu C, Zhao Y, Liu X, Gao X, Chen Y, Liu Z (2017). J CO2 Util 22:208
74. Frogneux X, Jacquet O, Cantat T (2014). Cat Sci Technol 4:1529
75. Pouessel J, Jacquet O, Cantat T (2013). ChemCatChem 5:3552
76. Motokura K, Takahashi N, Kashiwame D, Yamaguchi S, Miyaji A, Baba T (2013). Cat Sci Technol 3:2392
77. Itagaki S, Yamaguchi K, Mizuno N (2013). J Mol Catal A Chem 366:347
78. Zhang S, Mei Q, Liu H, Liu H, Zhang Z, Han B (2016). RSC Adv 6:32370
79. Motokura K, Takahashi N, Miyaji A, Sakamoto Y, Yamaguchi S, Baba T (2014). Tetrahedron 70:6951
80. Shintani R, Nozaki K (2013). Organometallics 32:2459
81. Lu X-B (2016) Carbon dioxide and organometallics. Springer, Cham
82. González-Sebastián L, Flores-Alamo M, García JJ (2013). Organometallics 32:7186
83. Motokura K, Kashiwame D, Miyaji A, Baba T (2012). Org Lett 14:2642
84. Sattler W, Parkin G (2012). J Am Chem Soc 134:17462
85. Nguyen TV, Yoo WJ, Kobayashi S (2015). Angew Chem Int Ed 54:9209
86. Luo R, Lin X, Chen Y, Zhang W, Zhou X, Ji H (2017). ChemSusChem 10:1224
87. Luo R, Lin X, Lu J, Zhou X, Ji H (2017). Chin J Catal 38:1382
88. Jessop PG, Ikariya T, Noyori R (1995). Chem Rev 95:259
89. Schmid L, Schneider MS, Engel D, Baiker A (2003). Catal Lett 88:105
90. Farlow MW, Adkins H (1935). J Am Chem Soc 57:2222
91. Haynes P, Slaugh LH, Kohnle JF (1970) Tetrahedron Lett 365
92. Jessop PG, Hsiao Y, Ikariya T, Noyori R (1994). J Am Chem Soc 116:8851
93. Kröcher O, Köppel RA, Baiker A (1997) Chem Commun 453. https://doi.org/10.1039/A608150I
94. Munshi P, Heldebrant DJ, McKoon EP, Kelly PA, Tai C-C, Jessop PG (2003). Tetrahedron Lett 44:2725
95. Federsel C, Boddien A, Jackstell R, Jennerjahn R, Dyson PJ, Scopelliti R, Laurenczy G, Beller M (2010). Angew Chem Int Ed 49:9777
96. Jayarathne U, Hazari N, Bernskoetter WH (2018). ACS Catal 8:1338
97. Federsel C, Ziebart C, Jackstell R, Baumann W, Beller M (2012). Chem Eur J 18:72
98. Ziebart C, Federsel C, Anbarasan P, Jackstell R, Baumann W, Spannenberg A, Beller M (2012). J Am Chem Soc 134:20701
99. Kröcher O, Köppel RA, Baiker A (1996) Chem Commun 1497. https://doi.org/10.1039/CC9960001497
100. Schmid L, Rohr M, Baiker A (1999) Chem Commun 2303. https://doi.org/10.1039/A906956I
101. Kayaki Y, Shimokawatoko Y, Ikariya T (2003). Adv Synth Catal 345:175
102. Baffert M, Maishal TK, Mathey L, Copéret C, Thieuleux C (2011). ChemSusChem 4:1762
103. Zhang L, Han Z, Zhao X, Wang Z, Ding K (2015). Angew Chem Int Ed 54:6186
104. Liu H, Mei Q, Xu Q, Song J, Liu H, Han B (2017). Green Chem 19:196
105. Daw P, Chakraborty S, Leitus G, Diskin-Posner Y, Ben-David Y, Milstein D (2017). ACS Catal 7:2500

106. Kar S, Goeppert A, Kothandaraman J, Prakash GKS (2017). ACS Catal 7:6347
107. Dubey A, Nencini L, Fayzullin RR, Nervi C, Khusnutdinova JR (2017). ACS Catal 7:3864
108. Affan MA, Jessop PG (2017). Inorg Chem 56:7301
109. Jessop PG, Hsiao Y, Ikariya T, Noyori R (1996). J Am Chem Soc 118:344
110. Schmid L, Canonica A, Baiker A (2003). Appl Catal A Gen 255:23
111. Kröcher O, Köppel RA, Fröba M, Baiker A (1998). J Catal 178:284
112. Kröcher O, Köppel RA, Baiker A (1999). J Mol Catal A Chem 140:185
113. Behr A, Ebbinghaus P, Naendrup F (2004). Chem Eng Technol 27:495
114. Liu F, Abrams MB, Baker RT, Tumas W (2001) Chem Commun 433. https://doi.org/10.1039/B009701M
115. Pazicky M, Schaub T, Paciello R, Lissner A (2013) DE102012019441A1, 11 Apr 2013
116. Seayad J, Tillack A, Hartung CG, Beller M (2002). Adv Synth Catal 344:795
117. Pohlki F, Doye S (2003). Chem Soc Rev 32:104
118. Lygaitis R, Getautis V, Grazulevicius JV (2008). Chem Soc Rev 37:770
119. Fuglseth E, Otterholt E, Høgmoen H, Sundby E, Charnock C, Hoff BH (2009). Tetrahedron 65:9807
120. Song L, Jiang X, Wang L (2011). J Chromatogr B Anal Technol Biomed Life Sci 879:3658
121. van Gysel AB, Musin W (2000) Methylamines. Ullmann's encyclopedia of industrial chemistry. Wiley-VCH, Weinheim
122. Farkas E, Sunman CJ (1985). J Org Chem 50:1110
123. Hailes HC (2001). Appl Organomet Chem 15:315
124. Tundo P, Selva M (2002). Acc Chem Res 35:706
125. Zhao Y, Foo SW, Saito S (2011). Angew Chem Int Ed 50:3006
126. Cabrero-Antonino JR, Adam R, Junge K, Beller M (2016). Cat Sci Technol 6:7956
127. Das D, Khan HPA, Shivahare R, Gupta S, Sarkar J, Siddiqui MI, Ampapathi RS, Chakraborty TK (2017). Org Biomol Chem 15:3337
128. Zheng J, Darcel C, Sortais J-B (2014). Chem Commun 50:14229
129. Eschweiler W (1905). Ber Dtsch Chem Ges 38:880
130. Clarke HT, Gillespie HB, Weisshaus SZ (1933). J Am Chem Soc 55:4571
131. Schreiner S, Yu JY, Vaska L (1988). Inorg Chim Acta 147:139
132. Vaska L, Schreiner S, Felty RA, Yu JY (1989). J Mol Catal 52:11
133. Klankermayer J, Leitner W (2015). Science 350:629
134. Gredig SV, Koeppel RA, Baiker A (1995) J Chem Soc Chem Commun 73
135. Gredig SV, Koeppel R, Baiker A (1996). Catal Today 29:339
136. Gredig SV, Koeppel R, Baiker A (1997). Appl Catal A Gen 162:249
137. Cui X, Dai X, Zhang Y, Deng Y, Shi F (2014). Chem Sci 5:649
138. Cui X, Zhang Y, Deng Y, Shi F (2014). Chem Commun 50:13521
139. Kon K, Siddiki SM, Onodera W, Shimizu K (2014). Chem Eur J 20:6264
140. Du XL, Tang G, Bao HL, Jiang Z, Zhong XH, Su DS, Wang JQ (2015). ChemSusChem 8:3489
141. Tamura M, Miura A, Gu Y, Nakagawa Y, Tomishige K (2017). Chem Lett 46:1243
142. Toyao T, Siddiki S, Morita Y, Kamachi T, Touchy AS, Onodera W, Kon K, Furukawa S, Ariga H, Asakura K, Yoshizawa K, Shimizu KI (2017). Chemistry 23:14848
143. Hardy S, de Wispelaere IM, Leitner W, Liauw MA (2013). Analyst 138:819
144. Jacquet O, Frogneux X, Das Neves Gomes C, Cantat T (2013). Chem Sci 4:2127
145. Blondiaux E, Pouessel J, Cantat T (2014). Angew Chem Int Ed 53:12186
146. Riduan SN, Zhang Y, Ying JY (2009). Angew Chem Int Ed 48:3322
147. Das S, Bobbink FD, Laurenczy G, Dyson PJ (2014). Angew Chem Int Ed 53:12876
148. Yang Z, Yu B, Zhang H, Zhao Y, Ji G, Ma Z, Gao X, Liu Z (2015). Green Chem 17:4189
149. Fang C, Lu C, Liu M, Zhu Y, Fu Y, Lin B-L (2016). ACS Catal 6:7876
150. Niu H, Lu L, Shi R, Chiang CW, Lei A (2017). Chem Commun 53:1148
151. Yang Z-Z, Yu B, Zhang H, Zhao Y, Ji G, Liu Z (2015). RSC Adv 5:19613
152. Santoro O, Lazreg F, Minenkov Y, Cavallo L, Cazin CSJ (2015). Dalton Trans 44:18138

153. Li Y, Fang X, Junge K, Beller M (2013). Angew Chem Int Ed 52:9568
154. González-Sebastián L, Flores-Alamo M, García JJ (2015). Organometallics 34:763
155. Morris DS, Weetman C, Wennmacher JTC, Cokoja M, Drees M, Kuhn FE, Love JB (2017). Cat Sci Technol 7:2838
156. Beydoun K, vom Stein T, Klankermayer J, Leitner W (2013). Angew Chem Int Ed 52:9554
157. Klankermayer J, Beydoun K, vom Stein T, Leitner W (2015) WO2015000753A1, 8 Jan 2015
158. Bianchini C, Meli A, Peruzzini M, Vizza F, Zanobini F (1992). Coord Chem Rev 120:193
159. vom Stein T, Weigand T, Merkens C, Klankermayer J, Leitner W (2013). ChemCatChem 5:439
160. Nunez Magro AA, Eastham GR, Cole-Hamilton DJ (2007) Chem Commun 3154. https://doi.org/10.1039/B706635J
161. Coetzee J, Dodds DL, Klankermayer J, Brosinski S, Leitner W, Slawin AMZ, Cole-Hamilton DJ (2013). Chem Eur J 19:11039
162. Li Y, Sorribes I, Yan T, Junge K, Beller M (2013). Angew Chem Int Ed 52:12156
163. He Z, Liu H, Qian Q, Lu L, Guo W, Zhang L, Han B (2017) Sci China Chem 1
164. Beydoun K, Thenert K, Streng ES, Brosinski S, Leitner W, Klankermayer J (2016). ChemCatChem 8:135
165. Beydoun K, Ghattas G, Thenert K, Klankermayer J, Leitner W (2014). Angew Chem Int Ed 53:11010
166. McNeely W, Spencer CM (1998). Drugs 55:405
167. Singal A (2008). Expert Opin Drug Metab Toxicol 4:999
168. Maeda T, Yamamoto T, Takase M, Sasaki K, Arika T, Yokoo M, Hashimoto R, Amemiya K, Koshikawa S (1991) US patent 5021458, 4 June 1991
169. Lahaye J, Prado G (1983) Soot in combustion systems and its toxic properties. Nato conference series, series VI: material science. Plenum Press, New York, p 433
170. Burger J, Siegert M, Ströfer E, Hasse H (2010). Fuel 89:3315
171. Lumpp B, Rothe D, Pastötter C, Lämmermann R, Jacob E (2011). MTZ Worldwide 72:34
172. Burger J, Ströfer E, Hasse H (2012). Ind Eng Chem Res 51:12751
173. Burger J, Ströfer E, Hasse H (2013). Chem Eng Res Des 91:2648
174. Dubois J-L (2011) EP 2306816, 13 Apr 2011
175. Ströfer E, Schelling H, Hasse H, Blagov S (2006) WO2006134081, 21 Dec 2006
176. Zhu Z, Zhang J, Chen Z, He J (2012) China Patent 102557899A, 11 July 2012
177. Friedrich H, Neugebauer W (1974) US Patent 3843562, 22 Oct 1974
178. Sato S, Tanigawa Y (2000) Japan Patent 2000109443, 18 Apr 2000
179. Hasse H, Drunsel JO, Burger J, Schmidt U, Renner M, Blagov S (2012) WO2012062822, 18 May 2012
180. Hasse H, Drunsel JO, Burger J, Schmidt U, Renner M, Blagov S (2014) US Patent 20140187823, 3 July 2014
181. Fu Y, Shen J (2007) Chem Commun 2172
182. Zhan E, Li Y, Liu J, Huang X, Shen W (2009). Catal Commun 10:2051
183. Prado NT, Nogueria FGE, Nogueira AE, Nunes CA, Diniz R, Oliveira LCA (2010). Energy Fuel 24:4793
184. Guo H, Li D, Jiang D, Li W, Sun Y (2010). Catal Commun 11:396
185. Zhao H, Bennici S, Shen J, Auroux A (2010). J Catal 272:176
186. Chen S, Wang S, Ma X, Gong J (2011). Chem Commun 47:9345
187. Lu X, Qin Z, Dong M, Zhu H, Wang G, Zhao Y, Fan W, Wang J (2011). Fuel 90:1335
188. Nikonova OA, Capron M, Fang G, Faye J, Mamede A-S, Jalowiecki-Duhamel L, Dumeignil F, Seisenbaeva GA (2011). J Catal 279:310
189. Thavornprasert K-a, Capron M, Jalowiecki-Duhamel L, Gardoll O, Trentesaux M, Mamede A-S, Fang G, Faye J, Touati N, Vezin H, Dubois J-L, Couturier J-L, Dumeignil F (2014). Appl Catal B Environ 145:126
190. Li M, Long Y, Deng Z, Zhang H, Yang X, Wang G (2015). Catal Commun 68:46
191. Zhang Q, Zhao H, Lu B, Zhao J, Cai Q (2016). J Mol Catal A Chem 421:117

Top Organomet Chem (2019) 63: 77–102
DOI: 10.1007/3418_2018_18

Published online: 1 September 2018

Alkene Metathesis for Transformations of Renewables

Christian Bruneau and Cédric Fischmeister

Contents

Abstract Alkene metathesis of unsaturated bio-sourced olefins, a green and atom economic strategy, has been recently investigated with the objective of producing high-value molecules and polymer precursors. This chapter contains the recent developments in this field using terpenes, terpenoids, and fatty acid derivatives as olefin metathesis partners. The successful achievements with these renewable substrates presenting different types of carbon-carbon double bonds in self-metathesis, ring closing metathesis, cross metathesis including ethenolysis, and ring opening metathesis are presented.

Keywords Fatty acid derivatives · Olefin metathesis · Renewables · Terpenes

C. Bruneau (✉) and C. Fischmeister
Univ Rennes, CNRS, ISCR (Institut des Sciences Chimiques de Rennes)—UMR 6226, Rennes, France
e-mail: christian.bruneau@univ-rennes1.fr

1 Introduction

With the depletion of fossil resources and the concerns about climate change and environment protection, biomass is intensively considered as a sustainable source of raw materials for the chemical industry and for the production of biofuels [1–4]. Besides the very abundant carbohydrate and lignocellulosic biomass, lipids and to a lesser extend terpenes are envisioned as promising candidates for the production of biosourced compounds with a broad range of applications [5, 6]. Terpenes are of most importance in fragrance composition whereas fats and oils have already found applications as biodiesel fuel and biosourced polymers. The transformation of these renewable compounds into valuable molecules for the chemical industry using efficient and selective processes is therefore of prime importance. In this context, catalysis plays a pivotal role by offering efficient tools for converting biomass to more value-added chemicals through economically and environmentally competitive processes [7, 8]. In particular, olefin metathesis is one of the modern catalysed reactions which has impacted the world of homogeneous organometallic catalysis over the last 25 years [9–11]. Continuous improvements of catalyst performances [12] and stability with better knowledge of activation and deactivation pathways [13–15] have rendered this process compatible with the transformation of biosourced compounds of variable purity [16]. In this chapter, we will review the main recent achievements and progress obtained in the valorization of terpenes and lipids thanks to catalytic olefin metathesis.

2 Metathesis of Unsaturated Terpene Derivatives

Terpenes are found in essential oils and constitute a class of natural products that find direct applications and serve as feedstocks in flavour and fragrances industry and other potential applications due to their biological properties [17]. Terpenoids are chemically modified terpenes, essentially oxygenated derivatives such as alcohols, epoxides, ketones, aldehydes, carboxylic acids and esters. Chemical transformations of terpene derivatives have been investigated with the objective of producing new fine chemicals with high added value for diverse applications. Catalytic isomerization, rearrangements, cyclization, ring opening, hydrogenation, dehydrogenation, epoxidation, oxidation, hydration, hydroformylation and cyclopropanation are the most studied reactions [18–20]. Recent transformations of unsaturated terpenes and terpenoids based on olefin metathesis processes include ring closing metathesis of dienes, cross metathesis with ethylene and functional olefins to produce fine chemicals, ring opening metathesis and ring opening/cross metathesis for the production of reticulated polymers.

2.1 Ring Closing Metathesis

The ring closing metathesis of terpenes has been investigated with the monoterpenes citronellene **1**, linalool **2**, β-myrcene **3** and β-ocimene **4** (Scheme 1). Under RCM conditions, these terpenes containing a 1,6-diene structure eliminate isobutene and form cyclopentene derivatives from citronellene, linalool, and myrcene, and 2-methyl-1,3-cyclopentadiene in the case of β-ocimene.

The first ring closing metathesis transformations of a monoterpene have been carried out with citronellene **1** in the presence of molybdenum and tungsten catalysts. With a catalyst loading as low as 0.1 mol%, the Schrock catalyst Mo(CHC(Me)$_2$Ph)((CF$_3$)$_2$MeCO)$_2$(2,6-^{i}Pr$_2$(C$_6$H$_3$N)) **Mo1** catalysed the ring closing metathesis of (−)-citronellene at room temperature into 3-methylcyclopentene **6** in 60% isolated yield without racemization [21]. Each optically pure (*R*)- and (*S*)-citronellene enantiomer was converted into the corresponding (***R***)-**6** and (***S***)-**6** 3-methylcyclopentene in 68–70% isolated yield and 97% enantiomeric excess with retention of configuration at 90°C in 1,2,5-trichlorobenzene for 1 h in the presence of 2 mol% of WOCl$_2$(2,6-Br$_2$C$_6$H$_3$O)$_2$ **W1** as catalyst (Scheme 2) [22].

Later on, this RCM reaction was achieved with full conversion of (*R*)-citronellene **1** with 0.5 mol% of the ruthenium catalyst **Ru1** (Scheme 3) in toluene at 80°C using microwave heating for 20 min [23].

A conversion of 93% of citronellene **1** was obtained during RCM at 60°C for 6 h catalysed by 84 ppm of second-generation Hoveyda catalyst immobilized on silica

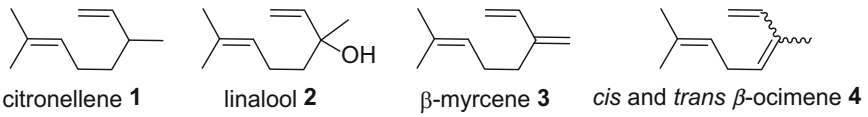

Scheme 1 Terpenes used in ring closing metathesis

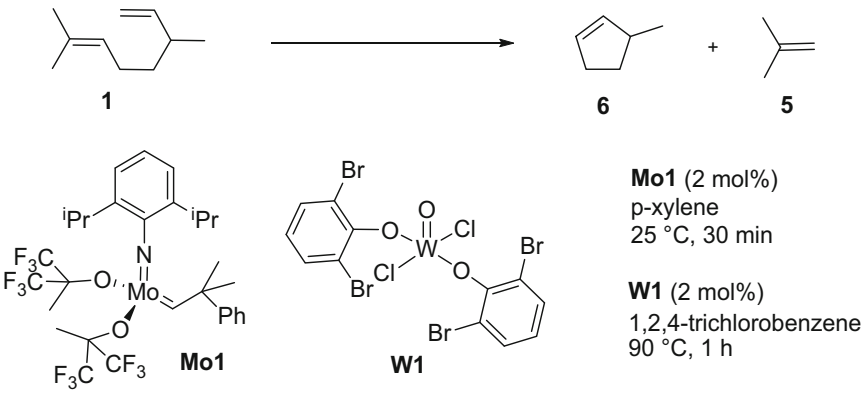

Scheme 2 Ring closing metathesis of citronellene **1** with Mo and W catalysts

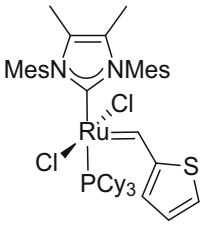

Ru1

Scheme 3 Structure of complex **Ru1**

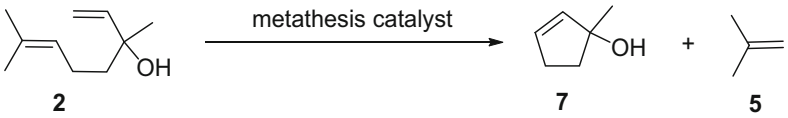

2 **7** **5**

Scheme 4 Ring closing metathesis of linalool **2**

[24, 25]. In toluene at 80°C, a TON of 16,000 was obtained with very high conversion and selectivity, whereas the reaction carried out without solvent also gave full conversion of **1** but only 30% of **6** was formed together with high amounts of oligomers, and homometathesis and cycloisomerization by-products.

Ring closing metathesis of linalool **2** leading to isobutene **5** and 1-methylcyclopent-2-en-1-ol **7** as primary products, has been very often used as a model reaction to evaluate the catalytic properties of new ruthenium catalysts (Scheme 4).

Several well-defined benzylidene ruthenium complexes and in situ generated ruthenium carbene moieties featuring a bidentate Schiff base ligand derived from salicylaldehyde [26–28], and a benzylidene ruthenium complex containing a tridentate phosphinesulfonate ligand [29] have revealed modest activities.

The most efficient ruthenium catalysts that have been used for this RCM reaction are presented in Scheme 5.

In the presence of the first-generation Grubbs catalyst **Ru3** at room temperature in $CDCl_3$, the reactivity of linalool **2** was one order of magnitude higher than that of citronellene **1**, whereas the *O*-methoxy-protected linalool presented no reactivity even at 65°C. These two results highlight the beneficial effect of the allylic alcohol functionality on the rate of the metathesis reaction as compared to isostructural terpene derivatives [30]. The second-generation Grubbs catalyst **Ru4** also gave full conversion whereas the Hoveyda–Grubbs catalysts **Ru5** and **Ru6** exhibited a slightly lower activity (Table 1 – entries 1–4) [32, 33]. Other second-generation ruthenium complexes (**Ru7**, **Ru8** and **Ru9**), equipped with a very bulky *N*-heterocyclic carbene ligand containing substituted naphthyl groups, gave full conversion with excellent yields of isolated 1-methylcyclopent-2-en-1-ol **6** under mild conditions with 1 mol% of catalyst (Table 1 – entries 5–7) [34]. With **Ru1** (Scheme 3), it was possible to reach full conversion within 10 min by increasing the catalyst loading to 0.5 mol% (Table 1 – entries 8–10) [23]. The authors confirmed that the

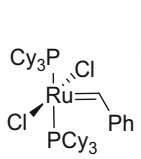

Ru3

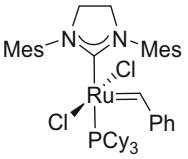

Ru4

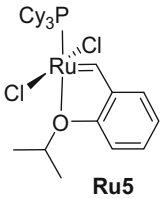

Ru5

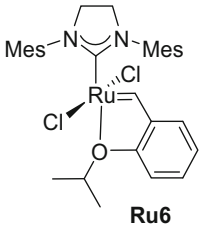

Ru6

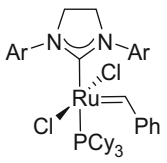

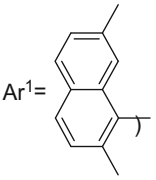

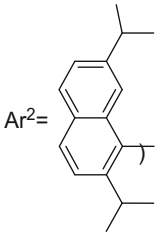

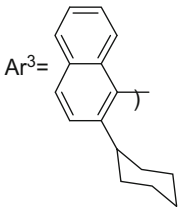

Ar= Ar^1 (**Ru7**), Ar^2 (**Ru8**), Ar^3 (**Ru9**)

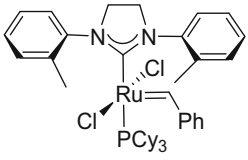

Ru10

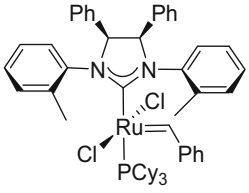

Ru11

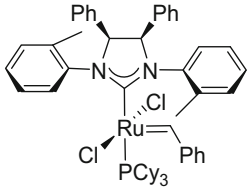

Ru12

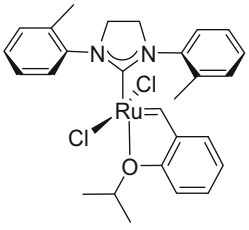

Ru13

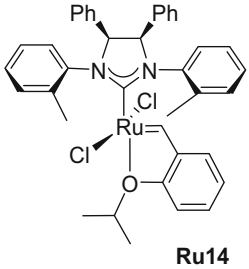

Ru14

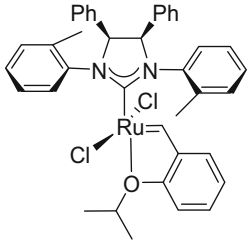

Ru15

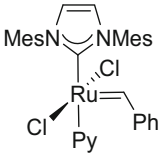

Ru16

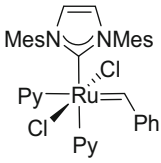

Ru17

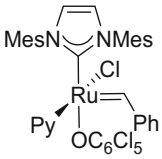

Ru18

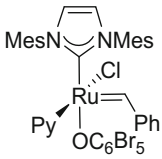

Ru19

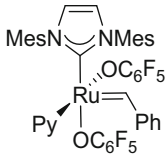

Ru20

Scheme 5 Selected ruthenium catalysts used for linalool ring closing metathesis

Table 1 Efficient ring closing metathesis of linalool **2**

Entry	Catalyst	Catalyst (mol%)	Solvent	*T* (°C)	*t* (min)	Conversion[a] or yield[b] (%)	Ref.
1	**Ru3**	5	$CDCl_3$	Rt	60	100	[17]
2	**Ru4**	5	$CDCl_3$	Rt	60	100	[17]
3	**Ru5**	5	$CDCl_3$	Rt	60	65	[17]
4	**Ru6**	5	$CDCl_3$	Rt	60	95	[17]
5	**Ru7**	1	CH_2Cl_2	Rt	30	92[b]	[31]
6	**Ru8**	1	CH_2Cl_2	Rt	6	88[b]	[31]
7	**Ru9**	1	CH_2Cl_2	Rt	6	94[b]	[31]
8	**Ru1**	0.1	Toluene	80	60	43	[8]
9	**Ru1**	0.1	DMC	80	60	40	[8]
10	**Ru1**	0.5	Toluene	80	10	100	[8]
11	**Ru10**	1	CD_2Cl_2	30	13	100	[18]
12	**Ru11**	1	CD_2Cl_2	30	7	100	[18]
13	**Ru12**	1	CD_2Cl_2	30	10	100	[18]
14	**Ru10**	0.1	CD_2Cl_2	30	60	30	[18]
15	**Ru11**	0.1	CD_2Cl_2	30	60	59	[18]
16	**Ru12**	0.1	CD_2Cl_2	30	60	33	[18]
17	**Ru13**	1	C_6D_6	60	6	100	[18]
18	**Ru14**	1	C_6D_6	60	6	100	[18]
19	**Ru15**	1	C_6D_6	60	6	100	[18]
20	**Ru13**	0.1	C_6D_6	60	6	>98	[18]
21	**Ru14**	0.1	C_6D_6	60	6	>98	[18]
22	**Ru15**	0.1	C_6D_6	60	6	90	[18]
23	**Ru6**	0.1	Neat	Rt	45	100	[19]
24	**Ru6**	0.01	Neat	Rt	60	44	[19]
25	**Ru10**	0.1	Neat	60	30	36	[19]
26	**Ru3**	0.1	Neat	45	60	55	[19]
27	**Ru16**	0.05	$CDCl_3$	Reflux	60	24	[20]
28	**Ru17**	0.05	$CDCl_3$	Reflux	60	29	[20]
29	**Ru18**	0.05	$CDCl_3$	Reflux	60	17	[20]
30	**Ru19**	0.05	$CDCl_3$	Reflux	60	34	[20]
31	**Ru20**	0.05	$CDCl_3$	Reflux	60	100	[20]

[a]Conversion determined by ^{1}H NMR or GC
[b]Isolated yield

presence the allylic alcohol functionality increased the reaction rate since the full conversion of citronellene under similar conditions required a double time of 20 min.

The RCM of linalool has been investigated with Grubbs (**Ru11** and **Ru12**) and Hoveyda (**Ru14** and **Ru15**) second-generation catalysts featuring frozen saturated *N*-heterocyclic imidazolinylidene ligands substituted on the backbone of the five-membered ring by two phenyl groups in *syn*-position and by *ortho*-tolyl groups at the nitrogen atoms with a *syn* or *anti*-conformation [35]. Full conversions of linalool were obtained with the Grubbs-type catalysts **Ru11** and **Ru12** and the less sterically

hindered catalyst **Ru10** when the reactions were performed with 1 mol% of catalyst in dichloromethane at 30°C within 7–13 min (Table 1 – entries 11–13). With a lower catalyst loading of 0.1 mol%, the higher catalytic activity of the *syn*-isomer **Ru11** was evidenced. The RCM reactions carried out at 60°C in deuterated benzene in the presence of 1 mol% of the Hoveyda-type catalysts **Ru13**, **Ru14** and **Ru15** led to full conversion within 6 min (Table 1 – entries 17–19). With these catalysts operating at 60°C, full conversion was also obtained in 1 h with 0.1 mol% catalyst loading of **Ru13** and **Ru14**, whereas the *anti*-isomer **Ru15** was less efficient giving only 90% conversion (Table 1 – entries 20–22).

With catalysts **Ru10**, **Ru11** and **Ru12**, complete dehydration of the alcohol took place after formation of 1-methylcyclopent-2-en-1-ol **7**, to give first 2-methylcyclopentadiene (2-MCPD) **8** within 2 h, and then a mixture with its isomer 1-methylcyclopentadiene (1-MCPD) **9** (Scheme 6). With the phosphine-free Hoveyda-type catalysts **Ru13**–**Ru15**, these subsequent reactions from **7** were much less pronounced.

The second-generation Hoveyda-type complex **Ru6** appeared as a good catalyst making the full conversion of **2** possible under neat conditions at room temperature with a catalyst loading of 0.1 mol% (Table 1 – entry 23) [36]. The Grubbs-type catalysts **Ru3** and **Ru10** were less efficient and dehydration of 1-methylcyclopent-2-en-1-ol **7** to methylcyclopentadienes was observed with **Ru3** and **Ru6** when the temperature was increased to 60°C.

Ruthenium complexes **Ru17**–**Ru20** equipped with a benzylidene and a pyridine ligand with at least one chloride atom substituted by another halide or an alkoxide have been evaluated in ring closing metathesis of dienes [37, 38]. In the presence of 0.05 mol% of catalyst in refluxing $CDCl_3$, linalool was converted into 1-methylcyclopent-2-en-1-ol **7**. **Ru20** featuring two pentafluorophenoxy ligands exhibited an exceptional activity leading to full conversion in 1 h, whereas the other catalyst precursors showed conversions located in the range 17–34% (Table 1 – entries 27–31). Nevertheless, all these ruthenium-pseudohalide catalysts led to 100% conversion in 15 min when the catalyst loading was as low as 0.5 mol%.

The ring closing metathesis of β-myrcene **3** has been achieved with the second-generation catalyst **Ru4** at 40°C in decalin as solvent (Scheme 7) [39]. From this

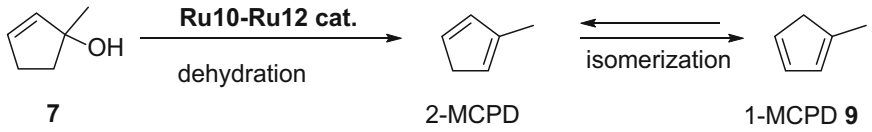

Scheme 6 Dehydration of 1-methylcyclopent-2-en-1-ol **6** catalysed by Grubbs-type catalyst

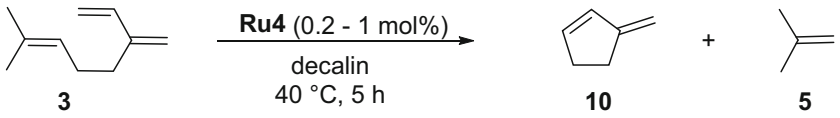

Scheme 7 Ring closing metathesis of β-myrcene **3** into 3-methylenecyclopentene **10**

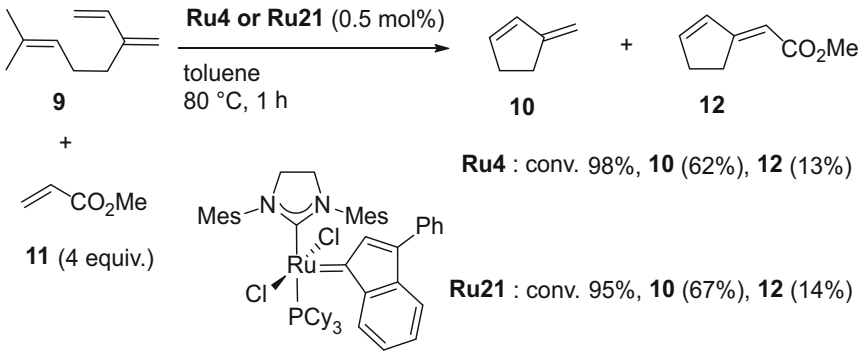

Scheme 8 Ring closing metathesis of β-myrcene in the presence of methyl acrylate

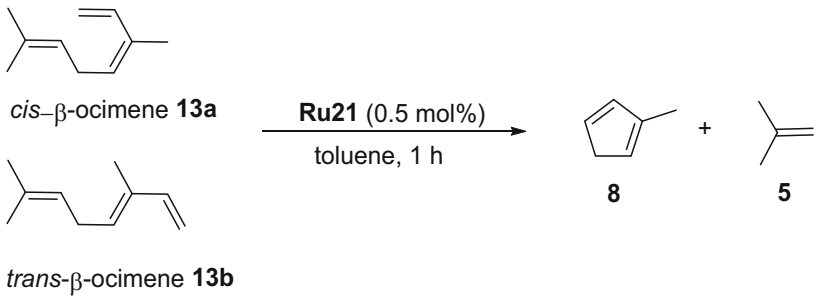

Scheme 9 RCM of cis- and trans-β-ocimene in the presence of **Ru21** as catalyst

triene **3**, full conversion into 3-methylenecyclopentene **10** was obtained in the presence of 1 mol% of catalyst.

The diene **10** was then used for controlled cationic polymerization with a catalytic system based on ^{i}BuOCH(Cl)Me/$ZnCl_2$/Et_2O in toluene.

It has been shown that, even in the presence of methyl acrylate **11** as cross metathesis partner, the ring closing metathesis of β-myrcene was favoured over the cross metathesis reaction [40]. The second-generation benzylidene and indenylidene ruthenium catalysts **Ru4** and **Ru21** led to excellent conversion of β-myrcene at 80°C in the presence of 0.5 mol% of catalyst within 1 h with production of **10** in 62–67% GC yields and the cross metathesis product **12** in 13–14% (Scheme 8).

The RCM of *cis*- and *trans*-β-ocimene **13a** and **13b**, isomers of β-myrcene (Scheme 9), has been studied in the presence of catalyst **Ru21**. The *cis*-derivative **13a** was very reactive and led to 94% conversion after 1 h at 80°C, whereas only 33% of the *trans*-isomer **13b** was converted under the same conditions. However, the expected 2-methylcyclopentadiene **8** was formed in only 24% yield indicating that side or subsequent reactions took place. As discussed earlier, both **8** and **5** have potential applications as fuels or polymer precursors [36].

2.2 Cross Metathesis

2.2.1 Cross Metathesis of Terpenes with Electron-Deficient Olefins

The second-generation Hoveyda catalysts have been found to be the most efficient catalysts for cross metathesis of terpenes and terpenoids with acrylic substrates. The cross metathesis of methyl acrylate **11a** with the diterpenes citronellal **15**, citronellol **16** and citral **17** was achieved in the presence of catalytic amounts of **Ru6** in the green solvent dimethyl carbonate (DMC) at 60–80°C leading to the cross metathesis products isolated in 42–70% yield (Scheme 10) [41]. With an acrylate as cross

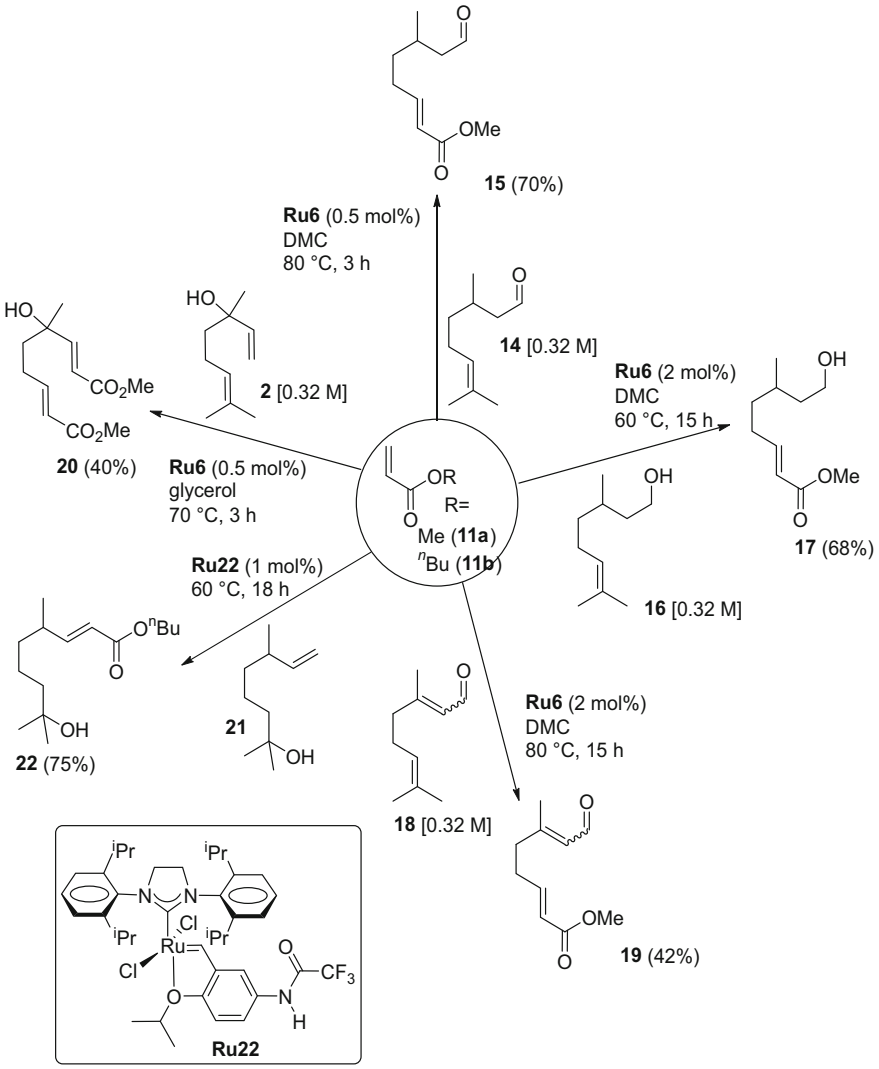

Scheme 10 Cross metathesis of terpenoids with acrylates

metathesis partner, the resulting double bond presented an *E*-configuration, exclusively. Dichloromethane [42] and glycerol [43] have also been used as solvents to perform these cross metathesis reactions with **Ru4** and **Ru6** as catalysts. In the case of linalool, the terminal and prenyl double bonds were involved in the cross metathesis process leading to the formation of the 1,9-diester **20** with two (*E*)-double bonds in 40% yield obtained with only 0.5 mol% of catalyst **Ru6** (Scheme 10) [43]. Dihydromyrcenol **21**, a diterpenoid featuring one terminal double bond, has been used in cross metathesis with *n*-butyl acrylate **11b** in the presence of 1 mol% of **Ru22** to give the (*E*)-isomer **22** in 75% yield after 18 h at 60°C without solvent (Scheme 10) [44].

Cross metathesis of the more sterically hindered methyl methacrylate **23** required more demanding conditions. It was found that the best conditions for the transformation of **14**, **16** and **18** were obtained under neat conditions at 80–90°C with catalyst **Ru6** (Scheme 11) [41]. Again, the reaction was stereoselective and only the (*E*)-isomers **24**, **25** and **26** were isolated in 75%, 70% and 40% yield, respectively. These products formally correspond to new terpenoids with an oxidized prenyl group obtained without oxidation steps. These syntheses produce isobutene as single co-product of the reaction. They are therefore much eco-friendlier than other

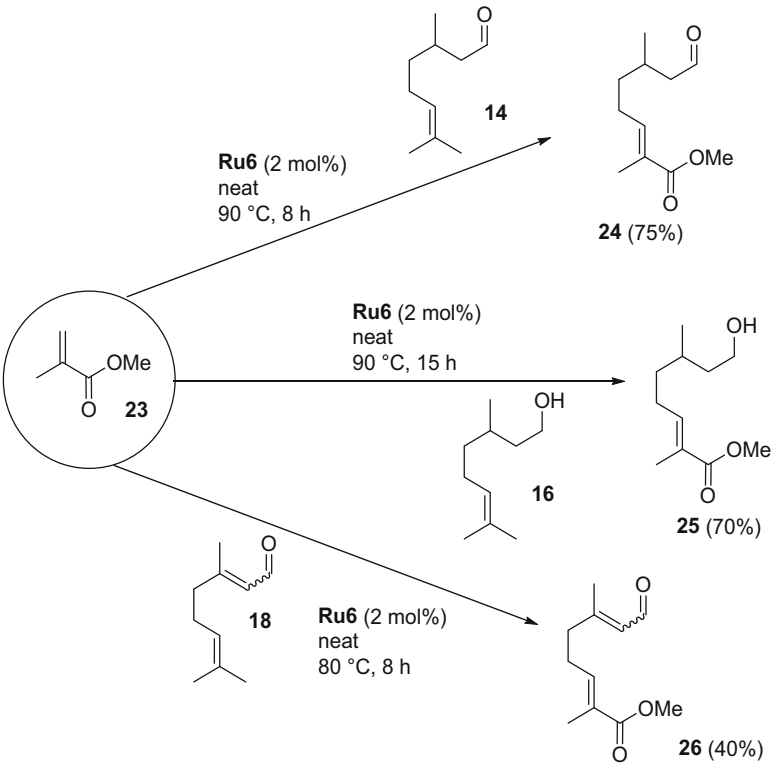

Scheme 11 Cross metathesis of terpenoids with methyl methacrylate

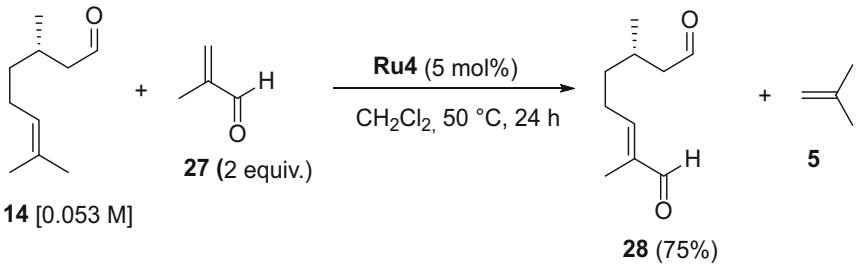

Scheme 12 Cross metathesis of (*S*)-citronellal with methacrolein

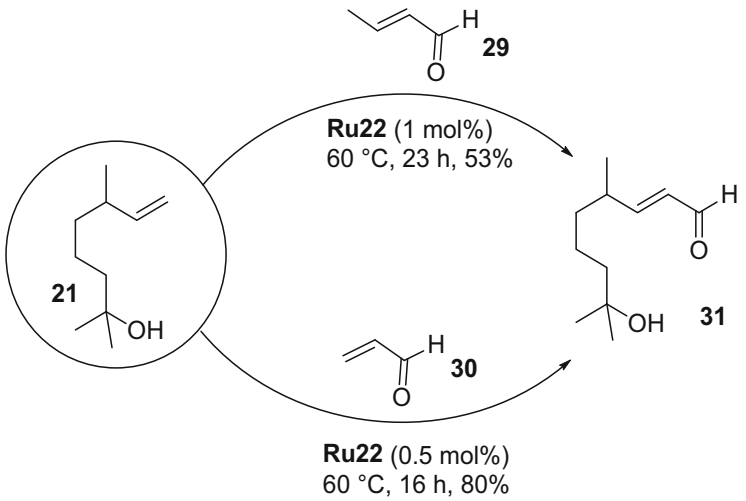

Scheme 13 Cross metathesis of dihydromyrcenol with acrylic aldehyde

multistep syntheses employing high amounts of toxic and hazardous reagents such as SeO_2, MnO_2, NaCN, $NaClO_2$ or diazomethane also generating large amounts of wastes [41].

Cross metathesis of (*S*)-citronellal **(S)-14** with methacrolein **27** was used to produce the optically pure dialdehyde **28** as the first step of the synthesis of the biologically active (−)-fusarisetin A [45]. The reaction was achieved in 75% yield with 5 mol% of the second-generation Grubbs catalyst **Ru4** in CH_2Cl_2 at 50°C for 24 h (Scheme 12).

With the catalyst **Ru22**, the cross metathesis of neat **21** performed at 60°C with the α,β-unsaturated aldehydes **29** and **30** gave the same product, namely (*E*)-8-hydroxy-4,8,dimethylnon-2-enal **31**, with high stereoselectivity (*E*/*Z* = 95:5 and 94:6, respectively), but acrolein **30** was more reactive than crotonaldehyde **29** leading to higher conversion with lower catalyst loading (Scheme 13) [44].

2.2.2 Cross Metathesis of Acyclic Terpenes with Terminal and Internal Olefins

A mixture of stereoisomers of the self-metathesis product **32** was produced in 82% yield when dihydromyrcenol **21** was treated at 80°C for 3 h with 1 mol% of catalyst **Ru22** under neat conditions (Scheme 14) [44]. When the terminal allylic alcohol **33** was used as cross metathesis partner, **34** was obtained in 43% yield after 24 h at 50°C. Cross metathesis with methyl oleate **35** featuring a *cis* internal double bond led to **36** and **37** in 61% and 71% yield, respectively. These two products correspond to the reaction of **21** with each side of the double bond of **35** (Scheme 14). In this case, the (*E*)-stereoisomers are the major ones (*E/Z* = 86:14 and 87:13) but as expected in a much less pronounced ratio than with the previous electron-deficient olefins **11a-b**, **23**, **27**, **29** and **30**.

The conjugated diene **40** was prepared in two steps from citronellal **14**. The cross metathesis of **14** with allyl chloride **38** was first carried out in the presence of 2 mol% of catalyst **Ru23** in refluxing dichloromethane for 5 h with an excess of **38** leading to the isolation of **39** in 65% yield with an *E/Z* ratio of 8.5:1. The ruthenium-catalysed dehydrochlorination reaction was then performed at room temperature with 5 mol% of [Cp*Ru(MeCN)$_3$][PF$_6$] as catalyst and provided **40** in 65% yield with an *E/Z* ratio of 8:1 (Scheme 15) [46].

The ruthenium complexes **Ru24**–**Ru25** featuring a 4-NMe$_2$-substituted and 4,5-(NMe$_2$)$_2$-disubstituted imidazolylidene carbene ligand were evaluated in the cross metathesis of citronellol benzyl ether **41** with *cis*-1,4-diacetoxybut-2-ene **42** containing an internal double bond (Scheme 16) [47]. Under the conditions reported in Scheme 16, these ruthenium benzylidene complexes led to the formation of **43** in

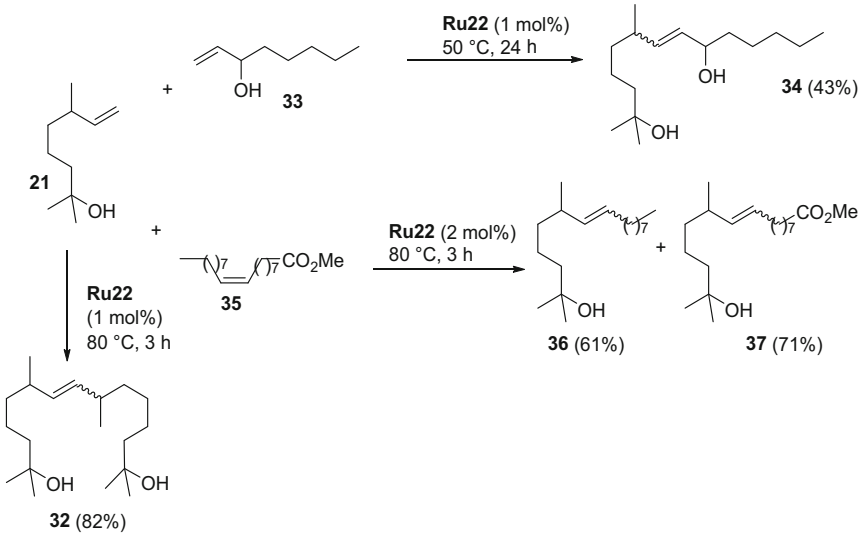

Scheme 14 Cross metathesis of dihydromyrcenol **21** with non-activated olefins

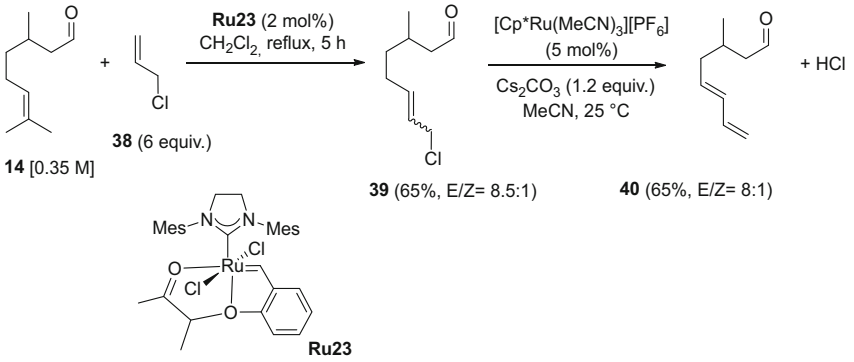

Scheme 15 Cross metathesis of citronellal with allyl chloride followed by diene formation

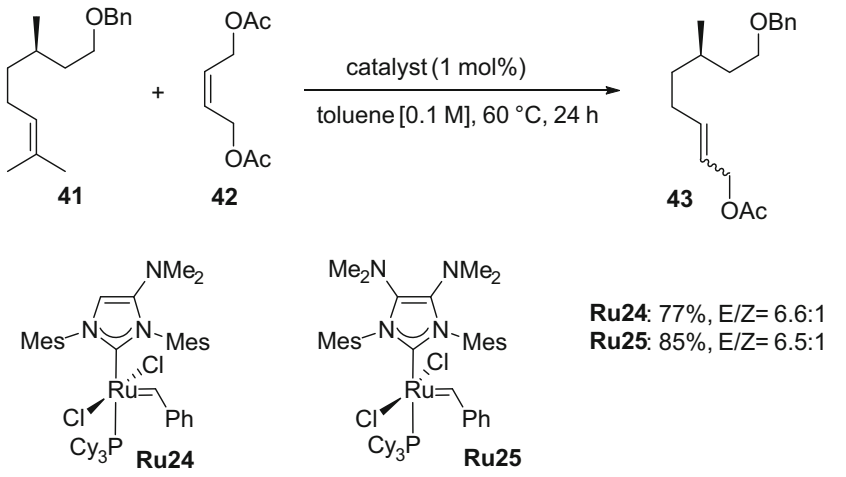

Scheme 16 Cross metathesis of citronellol benzyl ether **41** with *cis*-1,4-diacetoxybut-2-ene **42**

77% and 85% yield, respectively. It is noteworthy that under similar conditions Hoveyda-type catalysts equipped with the same *N*-heterocyclic ligands were less efficient as they delivered **43** with only 25% yield.

2.2.3 Ethenolysis: Double Bond Cleavage

Ethenolysis of terpene derivatives, which corresponds to cross metathesis with ethylene [48, 49] and cleavage of internal double bonds to produce two different products, has been used for degradation and analytical purposes rather than for target-oriented synthesis. These applications involve terpenes with a high number of isoprene motifs and are not reported in detail in this chapter. Among them, the triterpene squalene and the tetraterpene β-carotene have been selectively cleaved

into shorter polyenes with ruthenium catalysts [50, 51]. Ethenolysis has also been used to degrade polyisoprene and polyisoprene-containing copolymers in the presence of various catalysts based on molybdenum, tungsten or ruthenium [52–59]. Alkenolysis, which corresponds to cleavage with short internal alkenes, has also been investigated [60, 61] with limonene [62, 63] and β-pinene [64], which have been used to produce terpene-terminated oligomers of isoprene.

2.2.4 Cross Metathesis of Cyclic Terpenes

Cyclic terpenes are more sterically hindered than the acyclic ones, and the access to the reactive catalytic centre might be difficult in some cases. However, with the non-functional terminal olefin 1-hexene **45**, limonene **44** reacted in the presence of 2 mol% of **Ru4** at 55°C without solvent to give the cross metathesis product **46** in 40% yield (Scheme 17) [65].

This reactivity of limonene with a terminal olefin has been extended to the production of co-oligomers starting from 1,5-hexadiene in the presence of **Ru4** (1 mol% with respect to the diene) in an excess of limonene as solvent (30 equiv.) at 45°C. Polyhexadiene was formed together with hexadiene oligomers featuring one or two limonene ends [65].

It has been shown that β-pinene **47** and camphene **48** failed to give the cross metathesis reaction with *N,O*-protected allylglycine. On the other hand, the cross metathesis of these sterically hindered terpenes was possible with a large excess of the prenylglycine derivative **49** and 5 mol% of **Ru6** at 100°C leading to the modified terpenes **50** and **51** in 36% and 34% yield, respectively (Scheme 18) [66]. The cross metathesis with the aliphatic internal olefin (*Z*)-3-methylpent-2-ene **52** with β-pinene has also been carried out with 5 mol% of catalyst **Ru4** at 45°C without solvent and the two possible cross metathesis products **53** and **54** have been observed (Scheme 18) [64].

The general idea to make these cross metathesis reactions with bulky double bonds successful was to favour the productive with respect to the non-productive pathway by playing with the steric parameters of the cross metathesis partner [66, 67]. Hence, the cross metathesis of β-pinene and camphene appeared to be more efficient with a trisubstituted olefin as cross metathesis partner than with a terminal olefin. This is in line with the computational studies, which indicated that

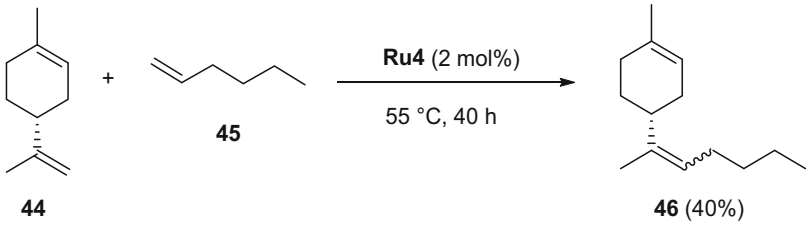

Scheme 17 Cross metathesis of (D)-limonene with 1-hexene

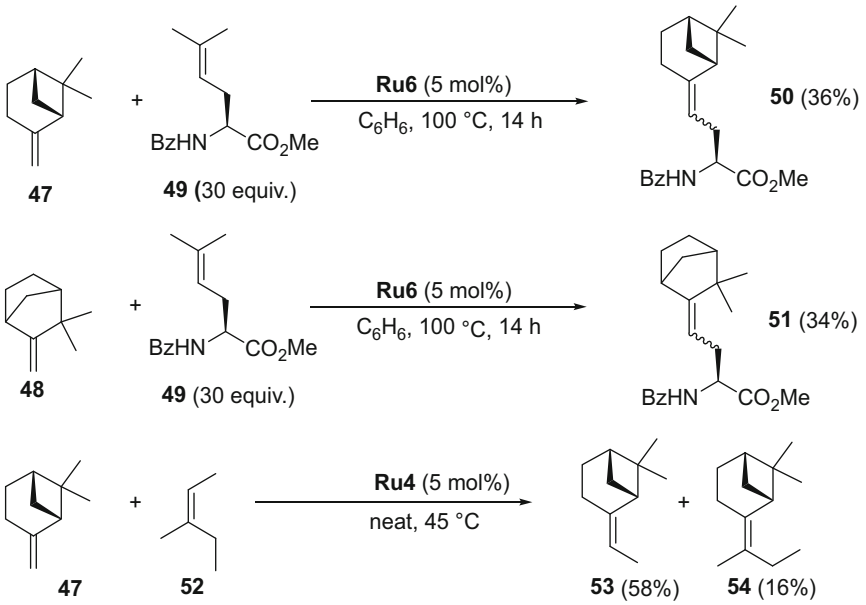

Scheme 18 Cross metathesis involving β-pinene **47** and camphene **48**

non-productive metathesis of β-pinene in the presence of another olefin takes place in the presence of second-generation ruthenium catalysts via formation of a carbene involving the pinene substrate, and that its self-metathesis does not occur because it is inhibited both by kinetic and thermodynamic factors [55].

2.3 Ring Opening Metathesis Polymerization

Ring opening metathesis of terpenes is extremely scarce. Only recently, the ring opening metathesis of the sesquiterpenes caryophyllene **55** and humulene **56** has been reported [68]. The ruthenium catalysts **Ru4** and **Ru26** appeared to be the most active for this polymerization where only trisubstituted double bonds were involved (Scheme 19). Complete conversion of **55** was achieved even with 0.04 mol% of **Ru26** at 25°C and its exocyclic methylene group was not involved in the polymerization process. These polymers are soft materials with low glass transition temperature in the range −15°C to −50°C.

Finally, functional hyperbranched polymers have been produced via ring opening metathesis polymerization of dicyclopentadiene in the presence of terpenes. D-Limonene, limonene oxide, β-pinene and carvone have been used as chain transfer agent to modify the physical properties and thermal stability of thermosets based on polydicyclopentadiene [69, 70].

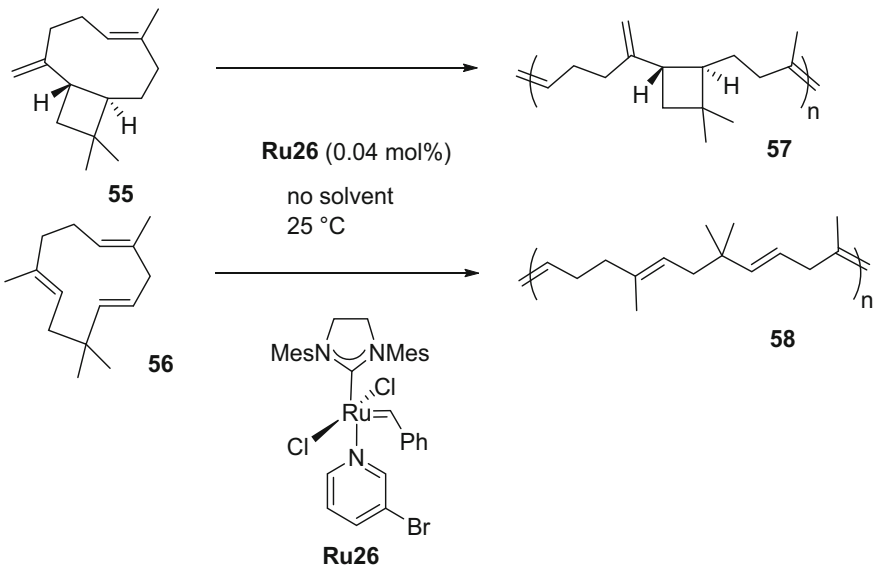

Scheme 19 Ring opening metathesis of two sesquiterpenes

3 Metathesis of Unsaturated Fatty Acid Derivatives

Triglycerides are the main components of fats and oil leading to fatty acid and esters following hydrolysis or transesterification, respectively. They originate essentially from plant seeds or algae and are composed of essentially mono- or polyunsaturated linear carbon chain and a terminal carboxylic functional group. Oleochemistry is a well-developed domain in food industry as well as in biofuels and is based on the reactivity of the terminal carboxylic functional group or carbon–carbon double bond [71–73] and in some case on the presence of other functional groups in the linear carbon chain, a typical example being castor oil [74, 75]. Among the portfolio of carbon–carbon double bond transformations, olefin metathesis appears as a very efficient and versatile catalytic transformation offering a broad range of potential applications for the transformation and valorization of fatty esters. The main transformations of fatty esters by olefin metathesis will be considered hereafter focusing on recent contributions.

3.1 Self-metathesis

The early days of olefin metathesis of fatty esters concerned essentially the self-metathesis reaction promoted by heterogeneous catalysts [76]. This reaction later developed with homogeneous catalysts offers an easy access to fatty dieters of

interest for the production of polyesters. As depicted in Scheme 20, methyl oleate **59** can be converted into dimethyl 9-octadecene-1,18-dioate **60** and 9-octadecene **61** in general in an equilibrium mixture unless polyunsaturated fatty esters are used [77]. A number of reviews cover this topic that will not be developed in this chapter [78–80].

3.2 Cross Metathesis

Cross metathesis is another important transformation that allows the introduction of a variety of functional groups [81]. In contrast to self-metathesis, cross metathesis can easily be brought to high conversion and selectivity using an excess of one of the reagents in general the less prone to self-metathesis and/or the less expensive. Two different reactions can be applied to fatty ester derivatives. The first one, cross metathesis with ethylene "*ethenolysis*", has been used in order to cleave fatty esters into two terminal olefins whereas cross metathesis with functional olefins aims at preparing bifunctional molecules as polymer precursors.

3.2.1 Ethenolysis

The ethenolysis of fatty esters has been used to shorten the chain length of fatty esters thereby producing valuable medium chain compounds for polymer industry. For instance, the ethenolysis of methyl oleate **59** produces methyl 9-decenoate **62** and 1-decene or *n*-decene **63**, two compounds with many applications in fragrance, polymers and surfactants (Scheme 21) [48, 49].

An early report by Mol in 1981 paved the way to future developments in ethenolysis of fatty esters. This work identified what will be one of the major

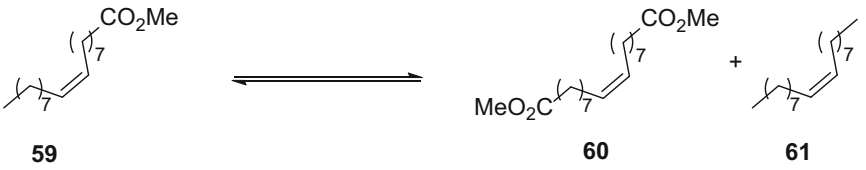

Scheme 20 Self-metathesis of methyl oleate **59**

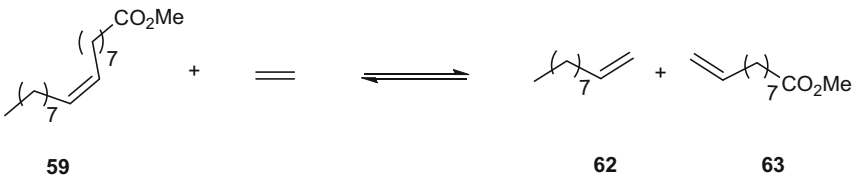

Scheme 21 Ethenolysis of methyl oleate

challenges of ethenolysis. Indeed, selectivity to the desired products **62** and **63** is hampered by self-metathesis reactions leading to undesired compounds **60** and **61**. However, the ethylene pressure is an efficient manifold to access high selectivity. For instance, a Re/Al/Sn catalyst delivered up to 29% of self-metathesis products when the reaction was conducted under 2 bar of ethylene pressure but self-metathesis was almost totally suppressed when the reaction was conducted with 50 bar of ethylene pressure [82]. Since this first report, many improvements have been achieved owing to the development of well-defined catalysts. In a thorough experimental and computational study, researchers at Dow Chemical reported a TON of 15,000 obtained with Grubbs catalyst **Ru3** in the ethenolysis of methyl oleate hence raising the issue of the economic viability of this process for which a TON of 50,000 would be required [83]. A major improvement came in 2008 when the group of Schrodi reported a TON of 35,000 and selectivity of 83% obtained with the Ru-CAAC **Ru27** (CAAC: CycloAlkylAminoCarbene) catalyst (Scheme 22) [84]. More recently, Grubbs and Bertrand studied the structure/activity relationship of a series of Ru-CAAC complexes where they reported the highest TON ever reported in ethenolysis with a slightly different catalyst **Ru28** (Scheme 22) [85]. They highlighted the dramatic influence of the feed purity. If the necessity to use low hydroperoxide-containing methyl oleate is a known issue necessitating pretreatment of the oil feed [86–90], the influence of the ethylene gas purity was studied and found to be also a major parameter to consider for achieving high TONs.

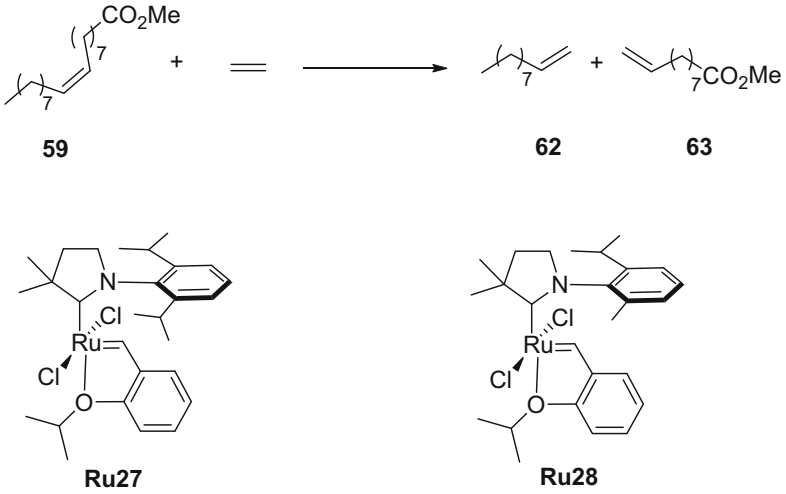

Scheme 22 Ru-CAAC catalysts in ethenolysis of methyl oleate

The highest TON still reported to date (340,000) was thus obtained at 40°C with a catalyst loading of 1 ppm and an ethylene purity and pressure of 99.995% and 10 bar, respectively. If the vast majority of ethenolysis transformation of fatty esters has been performed with ruthenium-based catalysts, this reaction was also reported with molybdenum catalysts but with moderate TONs [91].

3.2.2 Alkenolysis

Besides the cleavage by ethenolysis of fatty esters, researchers sought for a more efficient cleavage process by considering the formation of ruthenium methylidene species as the Achilles' heel of this reaction. Another type of fatty ester cleavage denoted as alkenolysis was thus investigated. In 2006, Jackson and Robinson reported the cross metathesis of natural oils with 2-butene. At that time, the purity of both methyl oleate and 2-butene was identified as a key issue for achieving high TONs. A productivity as high as 470,000 was achieved at – 5°C and Hoveyda catalyst **Ru6** with triply distilled methyl oleate and 2-butene free of 1,3-butadiene, which acted as a catalyst poison [92]. In 2012, Meier used the cross metathesis of non-purified oil-derived biodiesel with 1-hexene in order to shorten the chain length of the fatty ester chains. Best results (TONs $>$ 2000) were obtained with Umicore M51 **Ru23** [93]. It must be noted that alkenolysis was also used for the simple determination of double bond positions in long chain olefins including fatty esters [94]. Alkenolysis of fatty esters was transferred into an industrial process by Elevance in a joint venture with Wilmar. This metathesis process is used to produce chemical intermediates by cross metathesis of natural oils with 1-butene (http://Elevance.com) [95]. Very recently, Mecking extended alkenolysis to algae-based polyunsaturated fatty derivatives, in particular the penta-unsaturated eicosapentaenoic ester. Several ruthenium catalysts were evaluated in the butenolysis reaction of this compound with 2-butene searching for high conversion and selectivity. Most second-generation ruthenium catalysts were found competent for this reaction but the selectivity for the desired methyl 5-heptenoate was not exceeding 48%. However, increasing the catalyst loading to 0.2 mol% per double bond led to a selectivity of 95% for the desired product [96]. Interestingly, the self-metathesis of eicosapentaenoic acid opens the way toward the synthesis of biosourced benzene [97].

3.2.3 Cross Metathesis with Functional Olefins

Olefin metathesis has been used for the polymerization of long chain fatty esters under various manners [98]. The cross metathesis of fatty esters with functional olefins is a one stone two birds process as it shortens the carbon chain length while introducing a second functional group. The prepared homo- or hetero-bifunctional compounds are of great interest for the preparation of short chain polymer precursors. Cross metathesis with acrylic derivatives has been extensively studied for the preparation for diesters [99–102] and nitrile-esters [103–110] derivatives for the

production of polyesters and polyamides, respectively (Scheme 23). Polyamide precursors were also prepared by cross metathesis of fatty ester-derived carbamates with methyl acrylate [111]. Other cross metathesis partners such as allyl chloride, [112] acrolein [90, 113] and alkynes [114, 115] have also been used.

Following these pioneering researches on the preparation of bifunctional monomers using terminal functional olefins, several groups investigated cross metathesis reactions with internal olefins bearing one or two functional groups. As presented earlier for alkenolysis of methyl oleate, this process would be an ethylene-free process when fatty esters such as methyl oleate **59** are used. In 2011, Behr reported the cross metathesis of methyl oleate **59** with *cis*-2-butene-1,4-diyl diacetate **69** (Scheme 24). The Schiff base-ruthenium catalyst **Ru27** was found the most efficient for this reaction leading to high conversion of methyl oleate. However, high selectivity could not be obtained even with a catalyst loading of 2 mol% [116].

At the same period, this group also investigated the cross metathesis of methyl 10-undecenoate **72**, arising from the pyrolysis of castor oil, with diethyl maleate **73** leading to the diester **74** (Scheme 25) [117]. Experimental parameters as well as various ruthenium-based catalysts were investigated. Again, the best results were obtained with a high catalyst loading (4 mol%) of the indenylidene catalyst **Ru21** and the formation of the self-metathesis product of **72** could not be reduced below 25%. Similarly, the investigation of the cross metathesis of **72** with dimethyl maleate

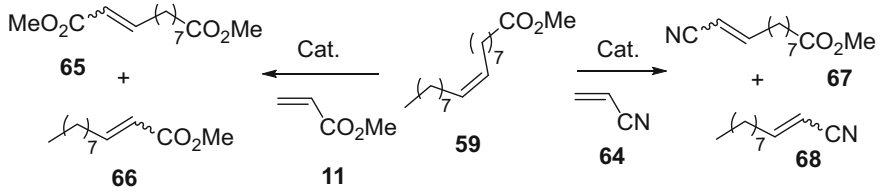

Scheme 23 Cross metathesis of methyl oleate with methyl acrylate and acrylonitrile

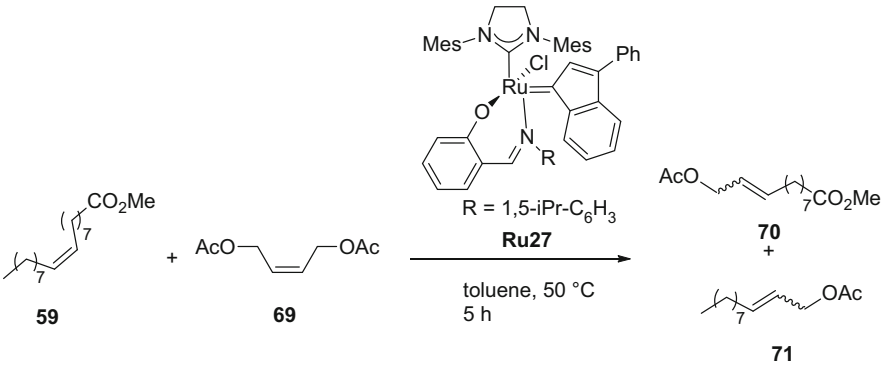

Scheme 24 CM of methyl oleate with cis-2-butene-1,4-diyl diacetate

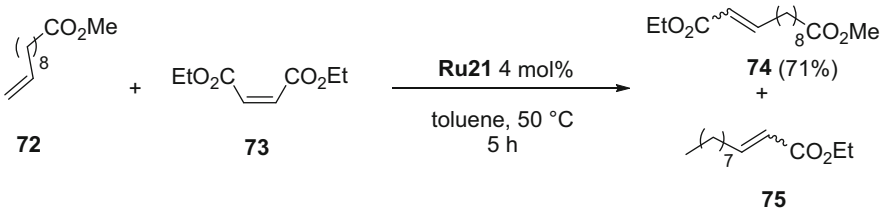

Scheme 25 CM of methyl 10-undecenoate **72** with diethyl maleate **73**

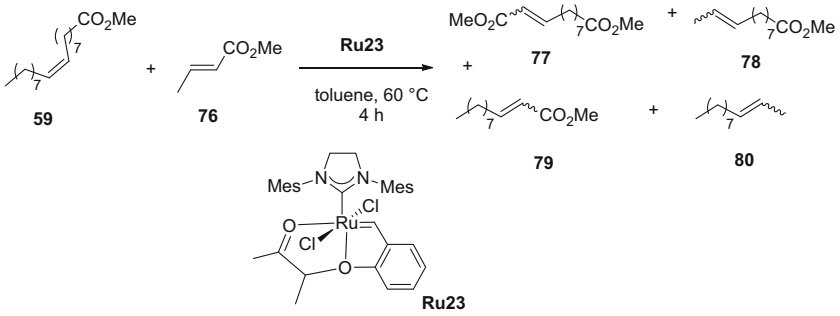

Scheme 26 CM of methyl oleate **59** with methyl crotonate **76**

and methyl acrylate **11** was realized. It was demonstrated that at 80°C in toluene, the cross metathesis with methyl acrylate was faster and required lower catalyst loading (0.5 mol%) than the cross metathesis involving dimethyl maleate [118].

The direct synthesis of bifunctional compounds incorporating a carboxylic acid function was reported by Schrekker [119]. In this comparative study, the benefit of using acrylic acid or maleic acid instead of methyl acrylate or maleate was established. Better conversion and selectivity were obtained using ultrapure methyl oleate **59** and Hoveyda catalyst **Ru6** in THF at 60°C. It is postulated that these results are likely due to the higher steric hindrance of esters vs acid.

An important contribution came in 2015 from the group of Gauvin. It was demonstrated that the use of methyl crotonate **76** as cross metathesis partner led to significant improvements in terms of activity and selectivity for the cross metathesis products (Scheme 26) [120]. As an example, a productive TON of 35,450 was obtained with 26 ppm of catalyst **Ru23**. This protocol was scaled up to 50 g using an industrial grade feed under bulk conditions at 60°C. A high conversion and selectivity for cross products of 96% and 97% were obtained, respectively.

Similarly, the group of Gauvin investigated the influence of nitrile-functionalized olefins on the outcome of cross metathesis with methyl oleate. Cross metathesis of methyl oleate was conducted with either acrylonitrile or crotonitrile (Scheme 27) [121]. Under similar conditions, i.e. **Ru23** 1 mol%, toluene, 60°C, 4 h, a higher conversion was obtained with crotonitrile (75% vs 22%) but the highest selectivity was obtained with acrylonitrile (86% vs 82%). However, higher selectivity could be

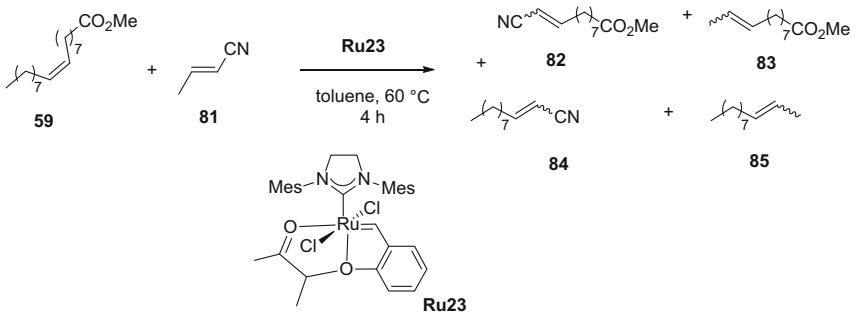

Scheme 27 Cross metathesis of methyl oleate **59** with crotonitrile **81**

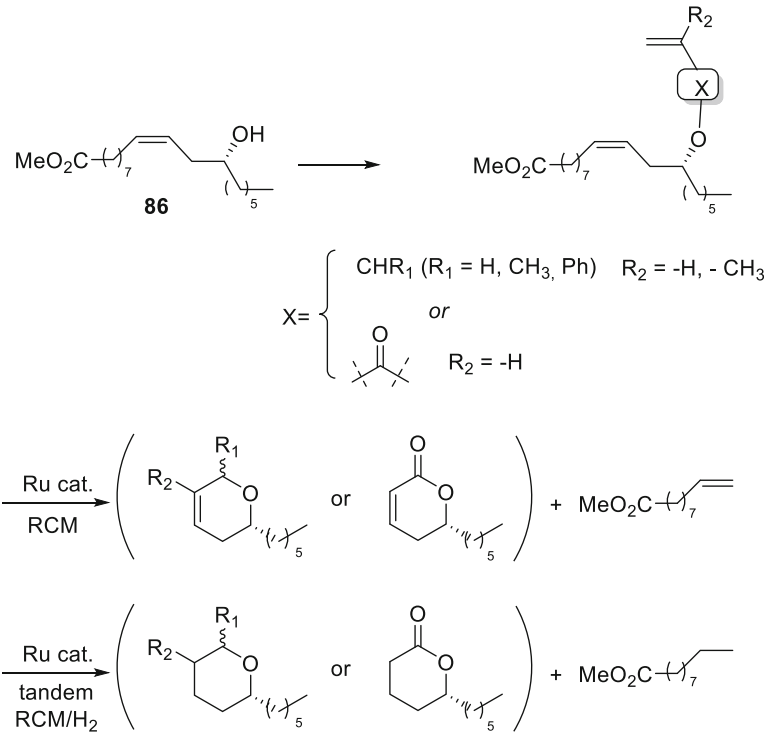

Scheme 28 High added-value compounds from methyl ricinoleate (castor oil)

obtained at 110°C but the process suffered from a rather high catalyst loading limiting the TON to values below 250.

As exemplified here above, the transformation of fatty esters by olefin metathesis aims almost exclusively at the synthesis of polymer precursors. In 2012, the use of methyl ricinoleate **86** as a platform chemical for the synthesis of high added-value chemicals was reported (Scheme 28). The synthetic strategy involved the functionalization of methyl ricinoleate using the hydroxyl group present in the

carbon chain and further ring closing metathesis. This methodology enabled the synthesis of a variety of compounds of interest for flavour or fragrance composition [122]. The ester by-products of these reactions can be directly valorized by cross metathesis transformations as described in Sect. 3.2.3.

4 Conclusion

This chapter provides an update on recent achievements in academic research on the transformation and valorization by olefin metathesis of two families of renewables with distinct fields of applications. Terpenes and terpenoids are important ingredients in flavours, fragrance and therapeutic drugs and new compounds based on these renewable chemical platforms are potentially of high interest. For these reasons, their transformation using high catalyst loadings is acceptable provided metal contaminations can be reduced by efficient and preferably eco-friendly processes or eventually in consecutive reactions when the metathesis step occurs early in a synthetic pathway.

The situation is somewhat different with fats and oils which are low-cost renewables as compared to terpenes and for which applications in polymer synthesis are the most interesting and easily accessible. Consequently, olefin metathesis applied to these compounds has to be highly efficient delivering very high productivity and selectivity in order to reach economically viable processes considering the cost of the catalysts. Typically, ppm levels of catalyst are required and despite the tremendous progress made in catalyst efficiency and robustness, this level of performance is difficult to attain. One manifold to reach high productivity is to work with high purity feed but this puts a strain on the overall cost of the process. Despite these difficulties, the evergrowing demand for biosourced compounds will undoubtedly stimulate innovation and improvement of process performances and boost the transfer of olefin metathesis technology to industrial applications.

References

1. Mika TM, Cséfalvay E, Németh A (2018) Chem Rev 118:505
2. Climent MJ, Corma A, Iborra S (2017) Gree Chem 16:516
3. Ricci M, Perego C (2012) Cata Sci Technol 2:1776
4. Gallezot P (2012) Chem Soc Rev 41:1538
5. Meier MAR, Metzger JO, Schubert US (2007) Chem Soc Rev 36:1788
6. Breitmaier E (ed) (2006) Terpenes: flavors, fragrances, pharmaca, pheromones. Wiley-VCH, Weinheim
7. Corma A, Iborra S, Velty A (2007) Chem Rev 107:2411
8. Deuss JD, Barta K, de Vries JG (2014) Cat Sci Technol 4:1174

9. Hoveyda AH, Zhugralin AR (2007) Nature 458:243
10. Grubbs RH (ed) (2003) Handbook of metathesis, vol 3. Wiley-VCH, Weinheim
11. Grela K (ed) (2014) Olefin metathesis, theory and practice. Wiley, New York, NY
12. Vougioukalakis GC, Grubbs RH (2010) Chem Rev 110:1746
13. Cavallo L (2002) J Am Chem Soc 124:8965
14. Thiel V, Hendann M, Wannowius KL, Plenio H (2012) J Am Chem Soc 134:1104
15. Bailey GA, Foscato M, Higman CS, Day CS, Jensen VR, Fogg DE (2018) J Am Chem Soc 140:6931
16. Montero de Espinosa L, Meier MAR (2012) Top Organomet Chem 39:1
17. Zwenger S, Basu C (2008) Biotechnol Mol Biol Rev 3:1
18. Swift KAD (2004) Top Catal 27:143
19. Monteiro JLF, Veloso CO (2004) Top Catal 27:169
20. Ravasio N, Zaccheria F, Guidotti M, Psaro R (2004) Top Catal 27:157
21. Sita LR (1995) Macromolecules 28:656
22. Nugent WA, Feldman J, Calabrese JC (1995) J Am Chem Soc 117:8992
23. Alexander KA, Paulhus EA, Lazarus GML, Leadbeater NE (2016) J Organomet Chem 812:74
24. Pastva J, Skowerski K, Czarnocki SJ, Zilkova N, Cejka J, Bastl Z, Balcar H (2014) ACS Catal 4:3227
25. Shinde T, Zilkova N, Hankova V, Balcar H (2012) Catal Today 179:123
26. De Clercq B, Verpoort F (2002) Adv Synth Catal 344:639
27. Opstal T, Verpoort F (2003) J Mol Catal A Chem 200:49
28. De Clercq B, Verpoort F (2001) Tetrahedron Lett 42:8959
29. Bashir O, Piche L, Claverie JP (2014) Organometallics 33:3695
30. Hoye TR, Zhao H (1999) Org Lett 1:1123
31. Schwab W, Fuchs C, Huang FC (2013) Eur J Lipid Sci Tech 115:3–8
32. Braddock DC, Matsuno A (2002) Tetrahedron Lett 42:3239
33. Braddock DC, Matsuno A (2002) Tetrahedron Lett 43:3305
34. Vieille-Petit L, Clavier H, Linden A, Blumentritt S, Nolan SP, Dorta R (2010) Organometallics 29:775
35. Perfetto A, Costabile C, Longo P, Grisi F (2014) Organometallics 33:2747
36. Meylemans HA, Quintana RL, Goldsmith BR, Harvey BG (2011) ChemSusChem 4:465
37. Conrad JC, Parnas HH, Snelgrove JL, Fogg DE (2005) J Am Chem Soc 127:11882
38. Conrad JC, Amoroso D, Czechura P, Yap GPA, Fogg DE (2003) Organometallics 22:3634
39. Kobayashi S, Lu C, Hoye TR, Hillmyer MA (2009) J Am Chem Soc 131:7960
40. Behr A, Johnen L, Wintzer A, Gümüs çetin A, Neubert P, Domke L (2016) ChemCatChem 8:515
41. Bilel H, Hamdi N, Zagrouba F, Fischmeister C, Bruneau C (2011) Green Chem 13:1448
42. Yoshikai K, Hayama T, Nishimura K, Yamada KI, Tomioka K (2005) J Org Chem 70:681
43. Al-Ayed AS (2015) Asian J Chem 27:3609
44. Borré E, Dinh TH, Caijo F, Crévisy C, Mauduit M (2011) Synthesis 13:2125
45. Xu J, Caro-Diaz EJE, Trzoss L, Theodorakis EA (2012) J Am Chem Soc 134:5072
46. Bilel H, Hamdi N, Zagrouba F, Fischmeister C, Bruneau C (2014) Cat Sci Technol 4:2064
47. César V, Zhang Y, Kosnik W, Zielinski A, Rajkiewicz AA, Ruamps M, Bastin S, Lugan N, Lavigne G, Grela K (2017) Chem Eur J 23:1950
48. Bidange J, Fischmeister C, Bruneau C (2016) Chem Eur J 22:12226
49. Spekreijse J, Sanders JPM, Bitter JH, Scott EL (2017) ChemSusChem 10:470
50. Wolf S, Plenio H (2011) Green Chem 13:2008
51. Jermacz I, Maj J, Morzycki JW, Wojtkielewicz A (2008) Toxicol Mech Methods 18:469
52. Wagener KB, Puts RD, Smith DW Jr (1991) Makromol Chem Rapid Commun 12:419
53. Korshak YV, Tlenkopatchev MA, Dolgoplosk BA, Adveikina EG, Kutepov DF (1982) J Mol Catal 15:207
54. Alimuniar A, Yarmo MA, Rahman MZA, Kohjiya S, Ikeda Y, Yamashita S (1990) Polym Bull 23:119

55. Acevedo A, Fomine S, Gutiérrez S, Tlenkopatchev MA (2014) J Organomet Chem 765:17
56. Gutierras S, Martinez Vargas S, Tlenkopatchev MA (2004) Polym Degrad Stabil 83:149
57. Ouardad S, Peruch F (2014) Polym Degrad Stabil 99:249
58. Wolf S, Plenio H (2013) Green Chem 15:315
59. Craig SW, Manzer JA, Coughlin EB (2001) Macromolecules 34:7929
60. Solanky SS, Campistron I, Laguerre A, Pilard JF (2005) Macromol Chem Phys 206:1057
61. Sadaka F, Campistron I, Laguerre A, Pilard JF (2013) Polym Degrad Stabil 98:736
62. Martinez A, Gutiérrez S, Tlenkopatchev MA (2012) Molecules 17:6001
63. Martinez A, Gutiérrez S, Tlenkopatchev MA (2013) Nat Sci 5:857
64. Gutierrez S, Tlenkopatchev MA (2011) Polym Bull 66:1029
65. Mathers RT, McMahon KC, Damodaran K, Retarides CJ, Kelley DJ (2006) Macromolecules 39:8982
66. Wang ZJ, Jackson WR, Robinson AJ (2013) Org Lett 15:3006
67. Stewart IC, Douglas CJ, Grubbs RH (2008) Org Lett 10:441
68. Grau E, Mecking S (2013) Green Chem 15:1112
69. Delancey JM, Cavazza MD, Rendos MG, Ulisse CJ, Palumbo SG, Mathers RT (2011) J Polym Sci Part A: Polym Chem 49:3719
70. Mathers RT, Damodaran K, Rendos MG, Lavrich MS (2009) Macromolecules 42:1512
71. Biermann U, Friedt W, Lang S, Lühs W, Machmüller G, Metzger JO, Rüsch Gen Klaass M, Schäfer HJ, Schneider MP (2000) Angew Chem Int Ed 39:2206
72. Behr A, Westfechtel A, Pérez Gomes J (2008) J Chem Eng Technol 5:700
73. Biermann U, Bornscheuer U, Meier MAR, Metzger JO, Schäfer HJ (2011) Angew Chem Int Ed 20:3854
74. Mutlu H, Meier MAR (2010) Eur J Lipid Sci Technol 112:30
75. Van der Steen M, Stevens CV (2009) ChemSusChem 2:692
76. Van Dam PB, Mittelmeijer MC, Boelhouver C (1972) J Chem Soc Chem Commun 1221
77. Mutlu H, Hofsäss R, Montenegro RE, Meier MAR (2013) RSC Adv 3:4927
78. Mol JC (2002) Green Chem 4:5
79. Rybak A, Fokou PA, Meier MAR (2008) Eur J Lipid Sci Technol 110:797
80. Chikkali S, Mecking S (2012) Angew Chem Int Ed 51:5802
81. Connon SJ, Blechert S (2003) Angew Chem Int Ed 42:900
82. Bosma RHA, van der Aardweg F, Mol JC (1981) J Chem Soc Chem Commun 1133
83. Burdett KA, Harris LD, Margl P, Maughon BR, Mokhtar-Zadeh T, Saucier PC, Wasserman EP (2004) Organometallics 23:2027
84. Schrodi Y, Ung T, Vargas A, Mkrtumyan G, Champagne TM, Pederson RL, Hyeok Hong S (2008) Clean 36:669
85. Marx VM, Sullivan AH, Melaimi M, Virgil SC, Keitz BK, Weinberger DS, Bertrand G, Grubbs RH (2015) Angew Chem Int Ed 54:1919
86. Couturier JL, Dubois JL, WO 2013/017786
87. Lemke DW, Uptain KD, Amatore F, Abraham T, WO 2009/020667
88. Nickel A, Ung T, Mkrtumyan G, Uy J, Lee CW, Stoianova D, Papazian J, Wei WH (2012) Top Catal 55:518
89. Bidange J, Dubois JL, Couturier JL, Fischmeister C, Bruneau C (2014) Eur J Lipid Sci Technol 116:1583
90. Bonin H, Keraani A, Dubois JL, Brandhorst M, Fischmeister C, Bruneau C (2015) Eur J Lipid Sci Technol 117:209
91. Marinescu SC, Schrock RR, Müller P, Hoveyda AH (2009) J Am Chem Soc 131:10840
92. Patel J, Mujcinovic S, Jackson WR, Robinson AJ, Serelis AK, Such K (2006) Green Chem 8:450
93. Montenegro RE, Meier MAR (2011) Eur J Lipid Sci Technol 114:55
94. Kwon Y, Lee S, Oh DC, Kim S (2011) Angew Chem Int Ed 50:8275
95. Higman CS, Lummis JAM, Fogg DE (2016) Angew Chem Int Ed 55:3552
96. Zimmerer J, Williams L, Pingen D, Mecking S (2017) Green Chem 19:4865

97. Pingen D, Zimmerer J, Klinkenberg N, Mecking S (2018) Green Chem 20:1874
98. Lu Y, Larock RC (2009) ChemSusChem 2:136
99. Rybak A, Meier MAR (2007) Green Chem 9:1356
100. Djigoué GB, Meier MAR (2009) Appl Catal A Gen 368:158
101. Rybak A, Meier MAR (2008) Green Chem 10:1099
102. Meier MAR (2009) Macromol Chem Phys 210:1073
103. Malacea R, Fischmeister C, Bruneau C, Dubois JL, Couturier JL, Dixneuf PH (2009) Green Chem 11:152
104. Miao X, Malacea R, Fischmeister C, Bruneau C, Dixneuf PH (2011) Green Chem 13:2911
105. Miao X, Fischmeister C, Dixneuf PH, Bruneau C, Dubois JL, Couturier JL (2012) Green Chem 14:2179
106. Miao X, Fischmeister C, Bruneau C, Dixneuf PH, Dubois JL, Couturier JL (2012) ChemSusChem 5:1410
107. Bruneau C, Fischmeister C, Miao WX, Dixneuf PH (2010) Eur J Lipid Sci Technol 112:3
108. Miao X, Dixneuf PH, Fischmeister C, Bruneau C (2011) Green Chem 13:2258
109. Nieres PD, Zelin J, Trasarti AF, Apesteguia CR (2016) Eur J Lipid Sci Techol 118:1722
110. Dixneuf PH, Bruneau C, Fischmeister C (2016) Oil Gas Sci Technol 71:19
111. Winkler M, Meier MAR (2014) Green Chem 16:3335
112. Jacobs T, Rybak A, Meier MAR (2009) Appl Catal A Gen 353:32
113. Miao X, Fischmeister C, Bruneau C, Dixneuf PH (2009) ChemSusChem 2:542
114. Le Ravalec V, Fischmeister C, Bruneau C (2009) Adv Synth Catal 351:1115
115. Le Ravalec V, Dupé A, Fischmeister C, Bruneau C (2010) ChemSusChem 3:1291
116. Behr A, Perez Gomes J, Beilstein J (2011) Org Chem 7:1
117. Behr A, Perez Gomes J, Bayrak Z (2011) Eur J Lipid Sci Technol 113:189
118. Behr A, Toepell S, Harmuth S (2014) RSC Adv 4:16320
119. Ferreira LA, Schrekker HS (2016) Cat Sci Technol 6:8138
120. Vignon P, Vancompernolle T, Couturier JL, Dubois JL, Mortreux A, Gauvin RM (2015) ChemSusChem 8:1143
121. Vancompernolle T, Vignon P, Trivelli X, Mortreux A, Gauvin RM (2016) Catal Commun 77:75
122. Dupé A, Achard M, Fischmeister C, Bruneau C (2012) ChemSusChem 5:2249

Top Organomet Chem (2019) 63: 103–140
DOI: 10.1007/3418_2018_19

Published online: 9 September 2018

Metal-Catalyzed Aromatic C-O Bond Activation/Transformation

Mamoru Tobisu and Naoto Chatani

Contents

Abstract Phenol derivatives have attracted significant attention as a renewable aromatic feedstock for the production of organic compounds that are required by society. However, the inertness of a C(aryl)-O bond of phenol derivatives poses a significant challenge for the direct functionalization at the ipso position. This review summarizes the recent advances in the area of catalytic transformations of unactivated phenol derivatives via the activation of C(aryl)-O bonds of aryl esters, carbamates, and ethers as well as arenols. The most intensively studied catalysts are nickel complexes, which allow a range of nucleophiles to be coupled with phenol derivatives. Group 8 and 9 metal complexes have also been used to activate C(aryl)-O bond of such phenol derivatives, and these are also covered in this review.

M. Tobisu (✉) and N. Chatani
Department of Applied Chemistry, Graduate School of Engineering, Osaka University, Suita, Osaka, Japan
e-mail: tobisu@chem.eng.osaka-u.ac.jp; chatani@chem.eng.osaka-u.ac.jp

Keywords Carbon-oxygen bond activation · Cross-coupling · Phenol derivatives · Transition metal complexes

1 Introduction

In response to the steady growth in the global population, the demand for fuels and carbon-based chemicals is predicted to continue to increase. The current production of commodity plastics and materials is now strongly dependent on nonrenewable petroleum as a feedstock, but, for a sustainable society, it will be necessary to shift to renewable resources. This green chemistry campaign has had a substantial impact on various aspects of synthetic organic chemistry. The catalytic cross-coupling of aryl halides with organometallic and organic nucleophiles is now widely recognized as one of the most reliable methods for preparing functionalized aromatic compounds both in the laboratory and in industry (Scheme 1a) [1, 2]. However, the starting aryl halides are largely derived from petroleum-based BTX (benzene, toluene, and xylenes), and this will require the development of new aromatic transformation methods using renewable aromatic building blocks. In this context, phenols represent attractive feedstock materials, since phenol derivatives are prevalent in nature. Recent advances in the depolymerization of lignin, the most abundant biomass containing benzene motifs, have also enhanced the potential utility of phenols as renewable aromatic sources [3]. It is possible to use phenols as alternatives to aryl halides in cross-coupling reactions by converting the phenolic hydroxyl group into a better leaving group, such as trifluoromethane sulfonates (triflates). However, the

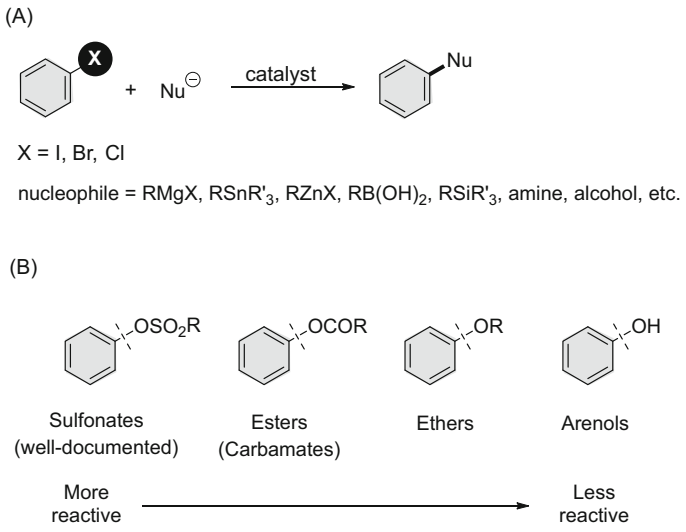

Scheme 1 (**a**) Cross-coupling of aryl halides. (**b**) Phenol-based electrophiles

advantage of using renewable phenol starting materials is offset by the issue associated with the fluorine-based wastes that are produced during the course of the reaction. The waste problem could be minimized by using nonfluorinated, less harmful leaving groups, such as carboxylates and methoxides. However, the bond dissociation energies of C(aryl)-O bonds in aryl esters and aryl ethers are much larger than those in aryl triflates, thereby posing a challenge to the use of aryl esters and ethers in cross-coupling reactions (Scheme 1b). During the past decade, significant progress has been made in the development of catalysts that can be used to activate C(aryl)-O bonds in inert phenol derivatives, and such catalysts have been used in cross-coupling reactions [4–12]. This review summarizes the catalytic transformations of aryl esters, carbamates, ethers, and arenols that involve the cleavage of C(aryl)-O bonds. The reactions are classified primarily based on the metal catalyst used, i.e., nickel, group 8 and 9 metals, and chromium.

2 Nickel Catalysis

Nickel is the most widely used metal for catalytic transformations of inert phenol derivatives, including aryl esters, carbamates, ethers, and arenols. The outstanding activity of nickel in C(aryl)-O bond activation can be attributed, in part, to its relatively electron-positive nature, which facilitates oxidative addition processes [13]. The following section overviews the nickel-catalyzed transformations, which are classified by substrates.

2.1 Reactions of Aryl Esters and Carbamates

2.1.1 Coupling with Organometallic Carbon Nucleophiles

In 1992, Snieckus reported an early example of the nickel-catalyzed cross-coupling of aryl carbamates using Grignard reagents as nucleophiles [14]. In this study, $Ni(acac)_2$ (acac = acetylacetonate) was used as the catalyst precursor without other external ligands being added, which allowed the introduction of phenyl and alkyl groups lacking β-hydrogens (i.e., methyl, CH_2SiMe_3, and vinyl) derived from Grignard reagents (Eq. 1). When Grignard regents containing a β-hydrogen such as isopropylmagnesium halides were used, the reductive cleavage of aryl carbamates occurs via β-hydrogen elimination (see Eq. 18). Since aryl carbamates can be selectively functionalized at the *ortho* position through lithiation, the overall 1,2-difunctionalization of aryl carbamates is possible using this nickel-catalyzed C(aryl)-O bond activation.

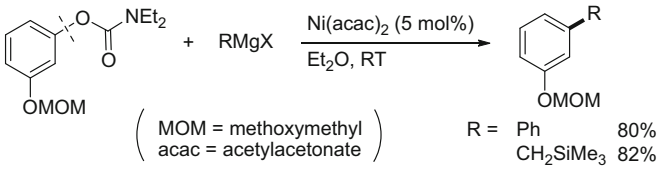

(1)

The nickel-catalyzed Kumada-Tamao-Corriu-type reaction was revisited by Nakamura, who found that the use of a well-designed P,O-bidentate ligand led to the generation of a more active catalyst (Eq. 2) [15]. They proposed that a nickel-phosphine/magnesium alkoxide bimetallic species is involved, and the C(aryl)-O bond cleavage is facilitated by a cooperative push-pull action of the nucleophilic nickel and the Lewis acidic magnesium.

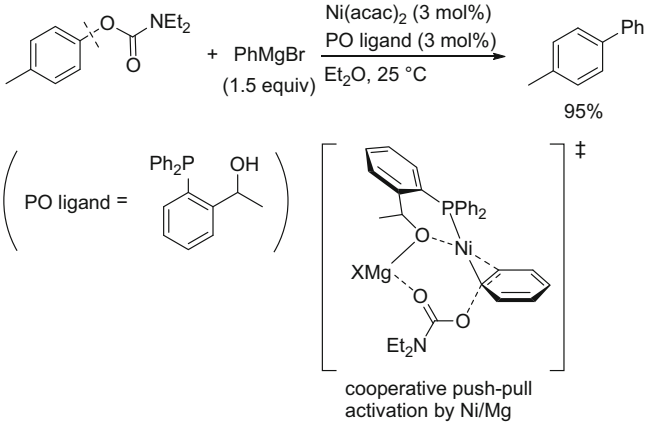

(2)

Cross-coupling of aryl pivalates with organozinc reagents can be catalyzed by a nickel catalyst bearing a PCy_3 ligand (Eq. 3) [16]. The use of pivalates is essential for suppressing an undesired C(acyl)-O bond cleavage, which is a common occurrence in the metal-catalyzed C(aryl)-O bond activation of aryl esters.

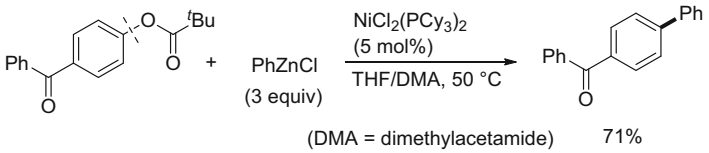

(3)

Alkylzinc reagents can also be cross-coupled with aryl pivalates when a bisphosphine ligand ($Cy_2CH_2CH_2PCy_2$) is used (Eq. 4) [17]. Various β-hydrogen-containing alkyl groups, including secondary alkyl fragments, can be introduced by this method.

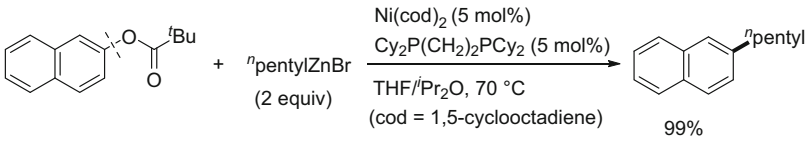

(4)

As is the case for the cross-coupling of aryl halides, arylaluminum reagents serve as viable coupling partners for nickel-catalyzed reaction of aryl carbamates (Eq. 5) [18]. Alkenyl and alkynylaluminum reagents also successfully participate in this reaction, with the formation of the corresponding cross-coupling products.

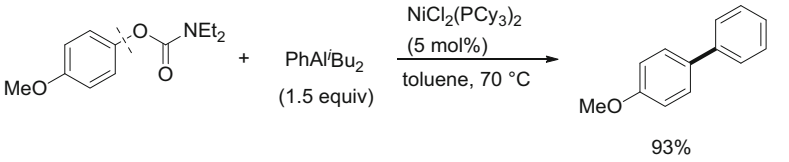

(5)

Organoboron nucleophiles are arguably among the most useful reagents in cross-coupling reactions because of their stability to air and moisture and high functional group compatibility, as exemplified by the widespread use of the Suzuki-Miyaura reaction in various areas of synthetic organic chemistry [19]. Garg and Shi independently reported the first Suzuki-Miyaura reaction of aryl esters using a Ni/PCy_3 catalyst. Garg's protocol employs arylboronic acids as a nucleophile (Scheme 2, top) [20], while Shi's uses arylboroxines, a cyclic trimer of arylboronic acids, in the

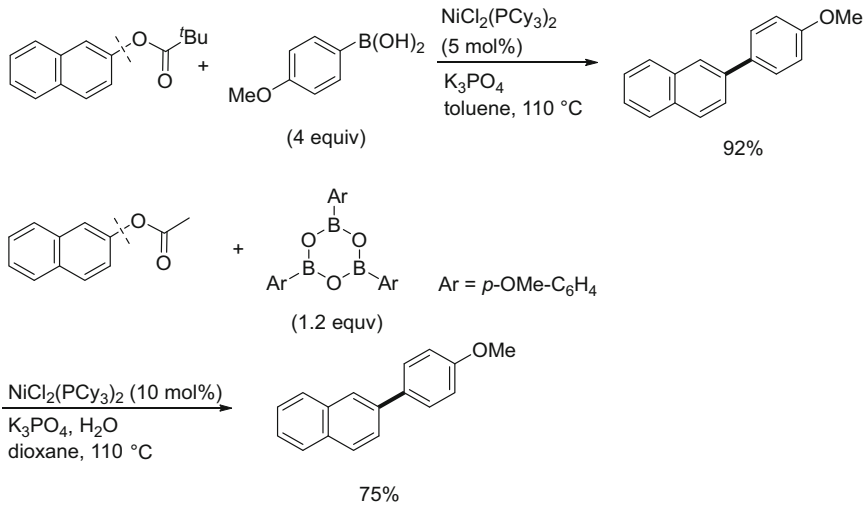

Scheme 2 Nickel-catalyzed Suzuki-Miyaura type reaction of aryl esters

presence of a controlled amount (0.88 equiv to the aryl ester) of water (Scheme 2, bottom) [21]. The latter conditions allow aryl acetates to be used for Suzuki-Miyaura coupling, which is notable, since most of the reported reactions of aryl esters have been limited to the use of aryl pivalates to suppress the undesired C(acyl)-O bond fission. This nickel/PCy_3 system is also applicable to the Suzuki-Miyaura coupling of aryl carbamates and carbonates, further demonstrating the general utility of this catalyst [22–31].

The issue of selectivity between the activation of a C(aryl)-O bond and a C(acyl)-O bond in aryl esters was investigated by DFT calculations [32]. A C(acyl)-O bond is more reactive than a C(aryl)-O bond based on the bond dissociation energies (80 kcal/mol and 106 kcal/mol). The DFT studies revealed that the oxidative addition of a C(acyl)-O bond is a reversible process and the resulting (acyl)(aryloxy)nickel intermediate is relatively resistant to transmetallation with arylboronic acid (Scheme 3, top). In contrast, although the oxidative addition of a C(aryl)-O bond requires a higher activation barrier than a C(acyl)-O bond to proceed, the subsequent transmetallation of (aryl)(acyloxy)nickel species occurs more facilely (Scheme 3, bottom). In a real system, overall selectivity is also affected by the nature of the substituent on the acyl group, with a bulky pivaloyl group being generally used in most catalytic transformations of aryl esters in order to suppress the undesired C(acyl)-O bond cleavage.

The Suzuki-Miyaura alkylation of aryl esters was reported by Rueping (Eq. 6) [33]. B-Alkyl-9-borabicyclo[3.3.1]nonanes (B-alkyl-9-BBNs), which can be readily synthesized by the hydroboration of the corresponding alkenes with 9-BBN, are widely used reagents in the alkylative cross-coupling of organic halides [34]. These reagents can also be successfully used for the alkylation of aryl pivalates in the presence of a nickel catalyst in conjunction with an *N*-heterocyclic carbene ligand, allowing a range of β-hydrogen-containing alkyl groups to be introduced.

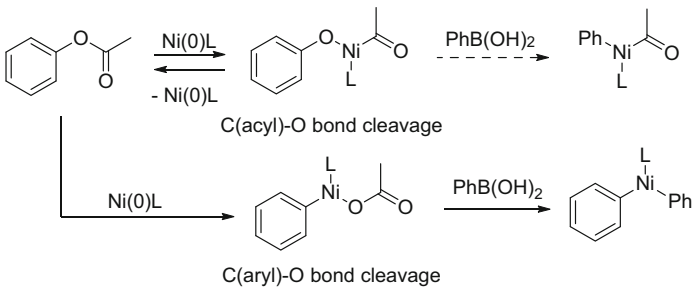

Scheme 3 Selectivity in C-O activation of aryl carboxylates

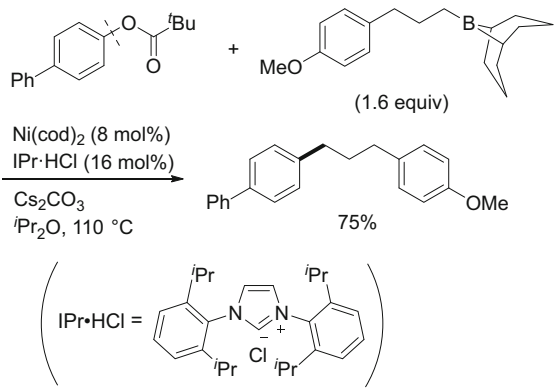

(6)

Organosilicon compounds represent another class of environmentally benign and functional group compatible nucleophiles that can be used in cross-coupling reactions [35]. Shi reported that $ArSi(OEt)_3$ can serve as a suitable coupling partner for the nickel-catalyzed cross-coupling of aryl carbamates (Eq. 7) [36]. The addition of CuF_2 is essential for this reaction, which can be rationalized by assuming the involvement of arylcopper species formed by the transmetallation of the aryl group from silicon to copper. Interestingly, iron salts have also been shown to exhibit some catalytic activity for this cross-coupling.

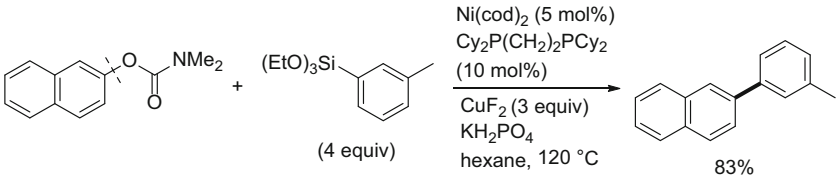

(7)

2.1.2 Coupling with C-H Bonds

In recent years, the arylation of C-H bonds, or direct arylation, has emerged as a more economical and environmentally benign alternative to the conventional cross-coupling of aryl halides and organometallic nucleophiles [37–44]. It is, therefore, natural to envision that C-O bond activation could also be combined with C-H functionalization reactions. In this context, Itami developed the cross-coupling of aryl pivalates and carbamates with azoles, such as (benz)oxazoles, (benzo)thiazoles [45], and (benz)imidazoles [46] (Scheme 4). Cyclohexyl-substituted bisphosphine $Cy_2PCH_2CH_2PCy_2$ was found to be uniquely effective for this reaction, allowing the intermediate formed by the oxidative addition of a C(aryl)-O bond of 2-naphthyl pivalate to $Ni/Cy_2PCH_2CH_2PCy_2$ to be characterized by X-ray crystallography [47]. The subsequent nickelation of a C-H bond in azoles is proposed to be a

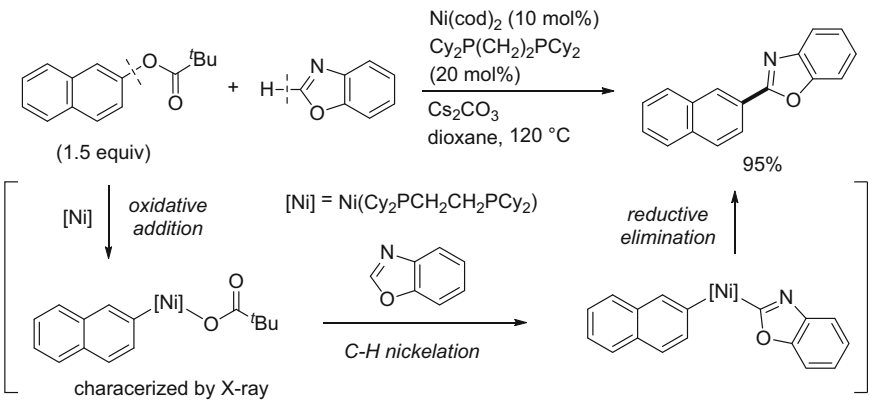

Scheme 4 Nickel-catalyzed cross-coupling of aryl esters with azoles

turnover-limiting step based on kinetic studies and kinetic isotope effect experiments. A polymer-supported bisphosphine ligand was also reported to be more effective in promoting this reaction [48].

Perfluoroarenes can serve as suitable coupling partners in nickel-catalyzed C-H arylation using aryl carbamates as the arylating reagent (Eq. 8) [49]. The use of a copper co-catalyst is required for an efficient reaction, the role of which is again proposed to generate perfluoroarylcopper species. Triisopropylsilylacetylene also undergoes cross-coupling with aryl carbamates under these conditions to form the corresponding alkynylated products.

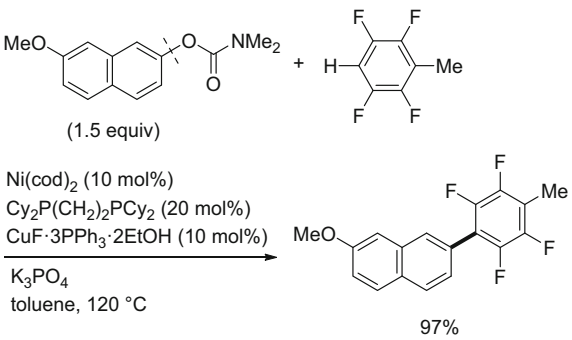

(8)

The scope of the nickel-catalyzed C-H arylation of inert phenol derivatives that have been reported to date is limited to arenes and heteroarenes bearing relatively acidic C-H bonds (i.e., azoles and perfluoroarenes). One exception to this is an intramolecular cyclization, in which aryl pivalates are coupled with a non-acidic C(aryl)-H bond (Eq. 9) [50].

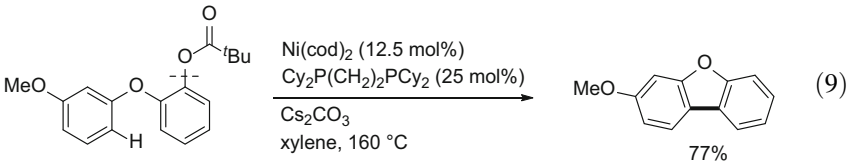

(9)

The palladium-catalyzed α-arylation of carbonyl compounds using aryl halides is a useful method for the construction of α-arylketones, esters, and amides, which has enjoyed widespread use in diverse fields [51]. The use of a suitable nickel catalyst allows aryl pivalates and carbamates to be used in the α-arylation of ketones (Scheme 5, top) [52], esters, and amides [53]. In these reactions, a unique bisphosphine ligand containing a thiophene backbone exhibits a superior activity to the more common bisphosphine ligands. An enantioselective variant was also developed using a chiral BINAP derivative as a ligand, generating a quaternary stereogenic center (Scheme 5, bottom) [54].

The Mizoroki-Heck reaction is used to formally functionalize an alkenyl C-H bond by the reaction of aryl halides with alkenes [55]. Watson developed a Mizoroki-Heck-type reaction of aryl pivalates with styrene derivatives using a nickel/dppf [dppf = 1,1′-bis(diphenylphosphino)ferrocene] system (Eq. 10) [56].

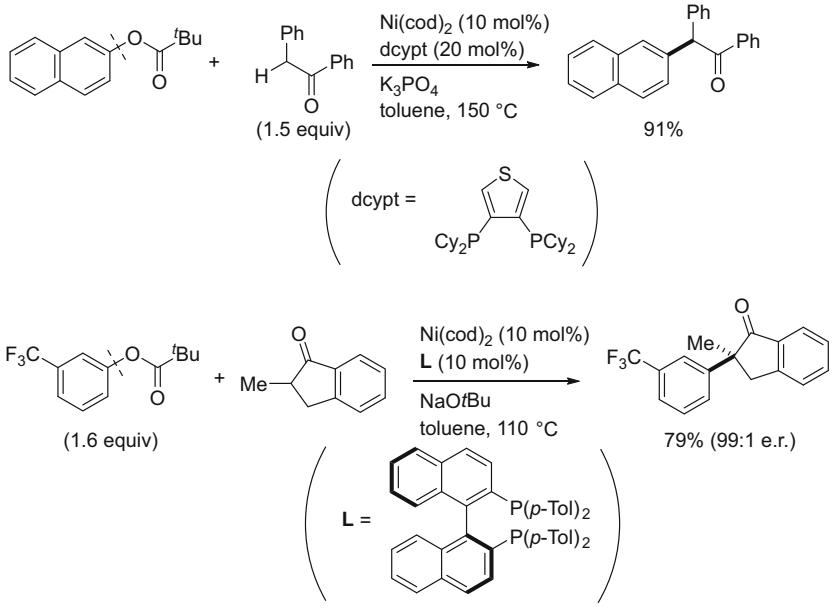

Scheme 5 Nickel-catalyzed α-arylation of ketones using aryl esters

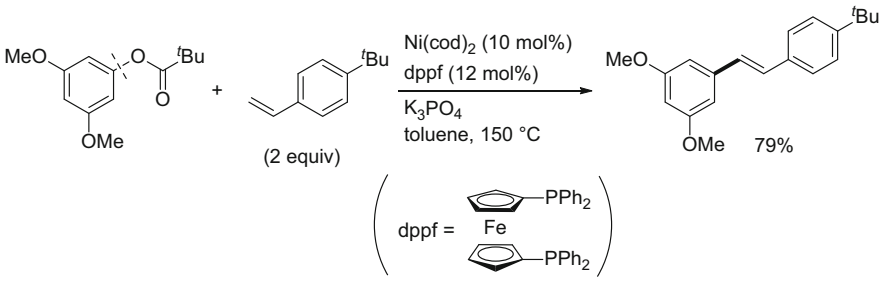

(10)

2.1.3 Other Types of Carbon-Carbon Bond Formations

The catalytic cyanation of aryl halides represents a powerful method for the synthesis of aromatic nitriles [57]. Aryl pivalates and carbamates can also be cyanated by nickel catalysis using an aminoacetonitrile derivative as a cyanide source (Eq. 11) [58].

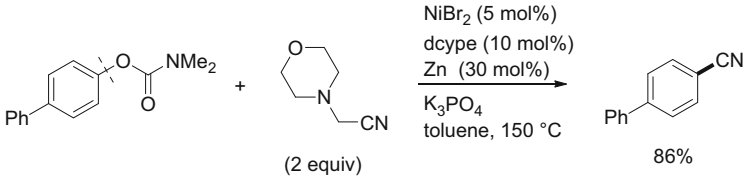

(11)

The reductive cross-coupling of two different electrophiles has emerged as a potential method that permits the use of organometallic reagents in cross-coupling reactions to be avoided [59]. To achieve useful cross-/homo-selectivity in reductive cross-electrophile coupling, it is essential to use two electrophiles that have completely different reactivity profiles, such as a combination of an aryl halide and an alkyl halide. Shi reported on the nickel-catalyzed reductive cross-coupling of aryl esters and aryl bromides using metallic magnesium as a stoichiometric reducing agent (Eq. 12) [60]. A series of mechanistic studies revealed that this reaction does not proceed through the formation of a Grignard reagent followed by the cross-coupling of aryl esters with the resulting Grignard reagent.

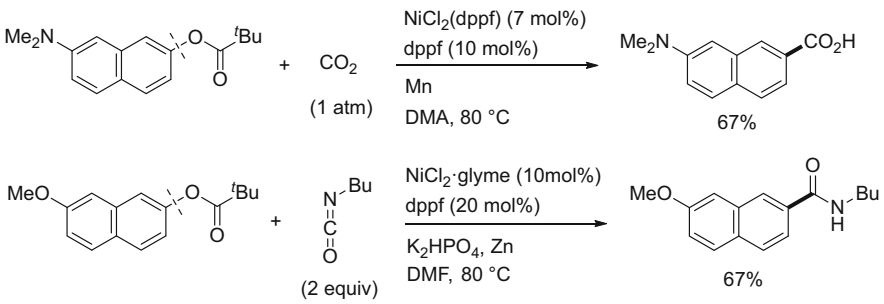

Scheme 6 Nickel-catalyzed reactions of aryl esters with CO_2 and isocyanates

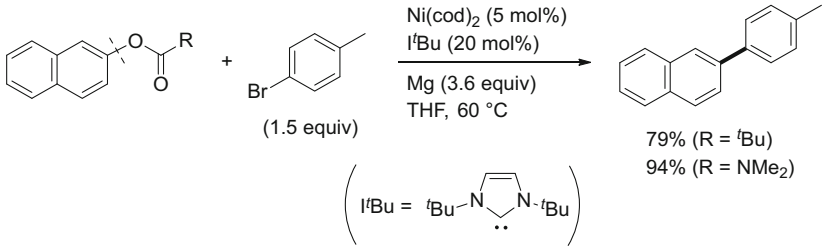

(12)

Because of its abundance and lack of toxicity, carbon dioxide (CO_2) is an ideal, renewable carbon source. Classically, CO_2 can be incorporated into organic molecules by reaction with strongly nucleophilic organometallic reagents, such as Grignard reagents. Recent progress in this field now allows the catalytic carboxylation of aryl halides using a palladium [61] or nickel [62] catalyst. The latter reaction was originally developed using PPh_3 as a ligand and metallic manganese as a stoichiometric reductant. The reduction of an oxidative addition complex [i.e., Ar-Ni(II)-X] with manganese forms an arylnickel(I) species, which is sufficiently nucleophilic to react with CO_2. This nickel system can also be used for the carboxylation of aryl pivalates by replacing the ligand with dppf (Scheme 6, top) [63]. This protocol is also applicable to the carboxylation of benzylic pivalates. The use of isoelectronic isocyanates, in place of CO_2, in the nickel-catalyzed reaction of aryl pivalates in the presence of Zn results in the formation of benzamide derivatives (Scheme 6, bottom) [64].

2.1.4 Coupling with Heteroatom Nucleophiles

In addition to carbon-carbon bond formation, cross-coupling reactions have now also become powerful tools in carbon-heteroatom bond formation, thanks to outstanding progress made in this field during the last few decades. Based on this progress, the nickel-catalyzed cross-coupling of inert phenol derivatives has also been applied to carbon-heteroatom bond-forming processes. Among the most

important is an amination reaction, given the widespread utility of the resulting aryl amines in pharmaceuticals, agrochemicals, and organic materials. Although catalytic amination of aryl halides proceeds best when a palladium-based catalyst is used [65, 66], its application to the corresponding aryl esters and carbamates calls for a nickel catalyst in conjunction with an *N*-heterocyclic carbene ligand (Eq. 13) [67–69]. A range of secondary amines can be used to form the corresponding aminated products.

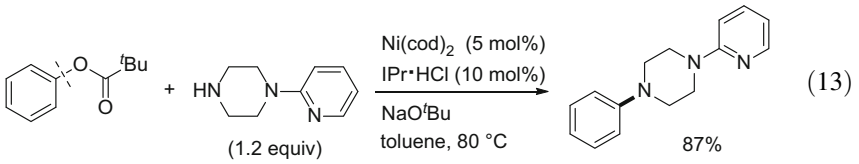

(13)

The synthesis of primary anilines is possible by using a benzophenone imine [70] as an aminating reagent (Eq. 14) [71]. The primary products are *N*-aryl imines, which ultimately give rise to primary aniline derivatives upon acid hydrolysis.

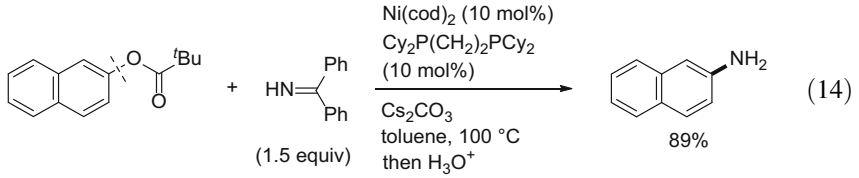

(14)

Boron is a versatile functionality, and its catalytic introduction to an aromatic ring has been a subject of considerable interest [72]. In this context, developing a method that would permit boron to be introduced into phenol derivatives via C(aryl)-O bond cleavage would be expected to be a useful tool in organic synthesis. Such a reaction was, in fact, developed using aryl carbamates as substrates and diboron reagents in the presence of a $NiCl_2(PCy_3)_2$ catalyst (Eq. 15) [73].

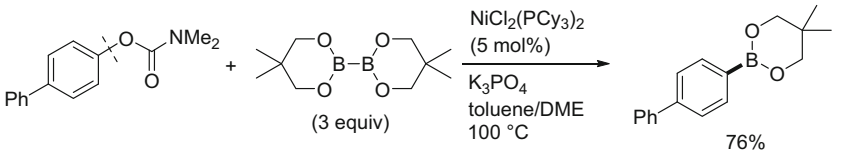

(15)

Carbon-silicon bond formation via the cleavage of C(aryl)-O bonds in aryl esters is also possible using a silylborane reagent (Scheme 7) [74]. The use of a combination of nickel and copper catalysts is effective in promoting this silylation reaction, in which an in situ generated silylcopper species is proposed to be an active nucleophile. However, recent studies suggest that the direct transmetallation from a silylborane reagent is also a viable pathway [75]. In the course of mechanistic studies of this silylation, bimetallic nickel complexes, which are relevant as an

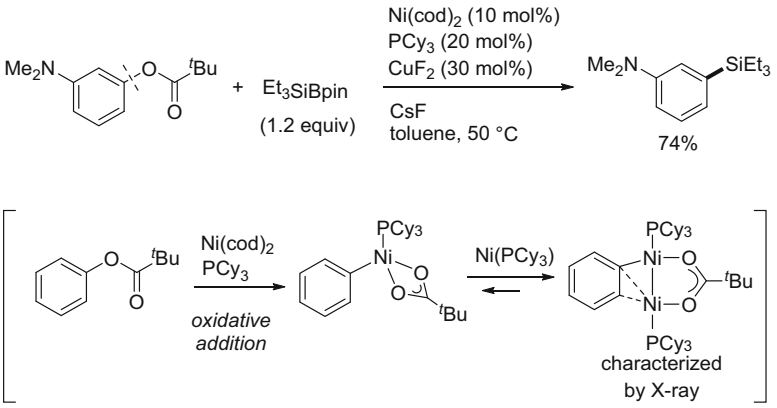

Scheme 7 Nickel-catalyzed silylation of aryl esters

intermediate in the oxidative addition of aryl pivalates to nickel(0) having a monophosphine ligand, have been successfully characterized [75].

Similarly, a stannyl group can be introduced at the ipso position of aryl pivalates by nickel catalysts (Eq. 16) [76]. In this reaction, silylstannanes function as a suitable stannane source, rather than distannanes.

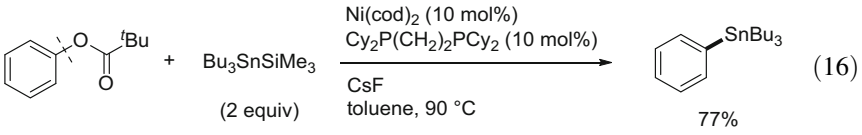

(16)

Phosphorus-based nucleophiles are also viable coupling partners in nickel-catalyzed cross-coupling of aryl esters and carbamates (Eq. 17). Diphenylphosphines [77], diphenylphosphine oxides [77], and phosphonate [78] reagents all can be successfully cross-coupled to form the corresponding aryl phosphine derivatives.

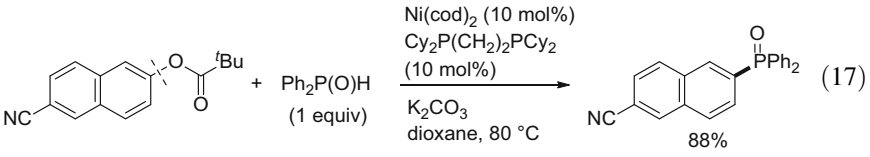

(17)

2.1.5 Reductive Cleavage

Ester and carbamate groups can function as an ortho-directing group in both transition metal-catalyzed processes and ortho-lithiation reactions. A method for removing these directing groups is important from the synthetic point of view, since

it allows these directing groups to be used as a traceless handle in arene functionalized reactions. The first example of the catalytic removal of a carbamate group was documented in the nickel-catalyzed Kumada-Tamao-Corriu-type reaction of aryl carbamates with isopropylmagnesium halides, which serves as a hydride donor via β-hydrogen elimination (Eq. 18) [14, 79].

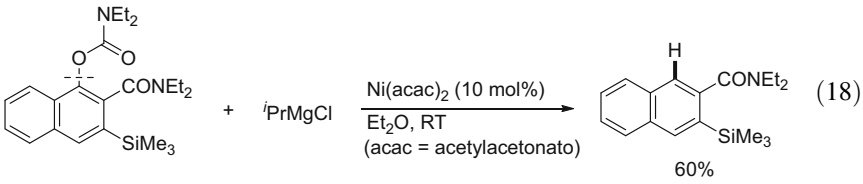

(18)

A more functional group-tolerant protocol was developed for aryl pivalates [80] and carbamates [81] using hydrosilanes as a reducing agent, in which several functional groups that react with Grignard reagents, such as esters and amides, are compatible (Eq. 19). Another functional group-tolerant protocol was developed using HCO_2Na as a reductant [82].

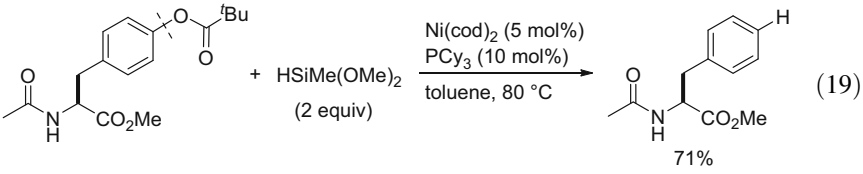

(19)

2.2 *Reactions of Aryl Ethers*

2.2.1 Coupling with Organometallic Carbon Nucleophiles

C(aryl)-O bonds of aryl ethers are much more inert and therefore more difficult to activate than those of aryl esters and carbamates. Nevertheless, as early as 1979, Wenkert reported his pioneering work on the nickel-catalyzed cross-coupling of methoxyarenes with Grignard reagents (Eq. 20) [83, 84]. This intriguing reactivity of nickel complexes to activate ether C(aryl)-O bonds did not attract significant attention at that time, and the trend in cross-coupling moved to the use of palladium catalysts and activated phenol derivatives, such as aryl triflates.

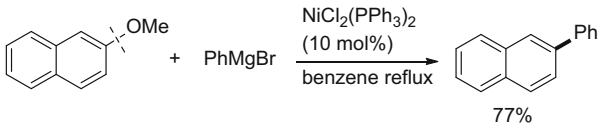

(20)

In 2004, Dankwardt revisited the Wenkert reaction in an attempt to develop modified nickel catalysts, in which alkylphosphines, such as PCy_3, P^iPr_3, $PPhCy_2$, and PPh_2Cy, could be used as excellent ligands (Eq. 21) [85]. A wide range of anisole derivatives, including those bearing an unprotected hydroxyl group, were shown to undergoing coupling with aryl Grignard reagents to form the corresponding biaryl derivatives. In addition to methyl ethers, ethoxy, methoxymethyl, aryl, and silyl ethers all successfully participated in the C(aryl)-O bond cleavage. This report by Dankwardt stimulated additional studies into the nickel-catalyzed cross-coupling of aryl ethers with aryl Grignard reagents [86–89]. Regarding the mechanism for this reaction, a unique concerted aromatic substitution pathway by anionic nickelate species via a cyclic transition state was proposed based on theoretical studies (Scheme 8) [90]. This nickel-catalyzed Kumada-Tamao-Corriu-type coupling was successfully applied to the synthesis of π-conjugated polymers via polycondensation of bifunctional aryl ethers with aromatic dimetallic compounds (Eq. 22) [91].

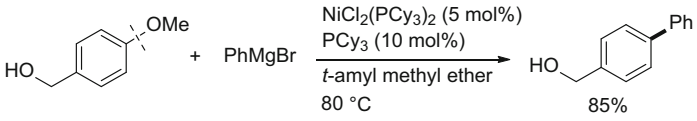

(21)

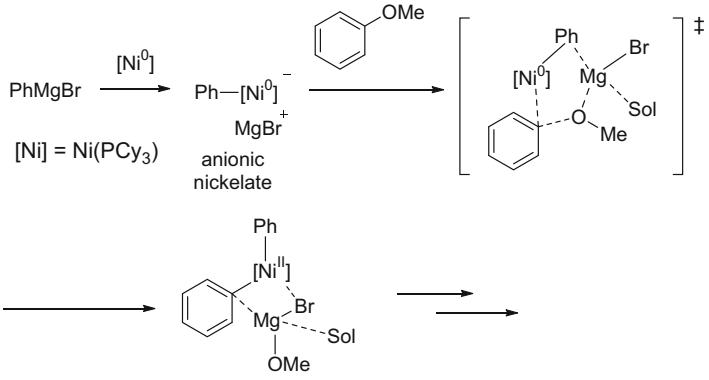

Scheme 8 Nickel-catalyzed Kumada-Tamao-Corriu type reaction of aryl ethers

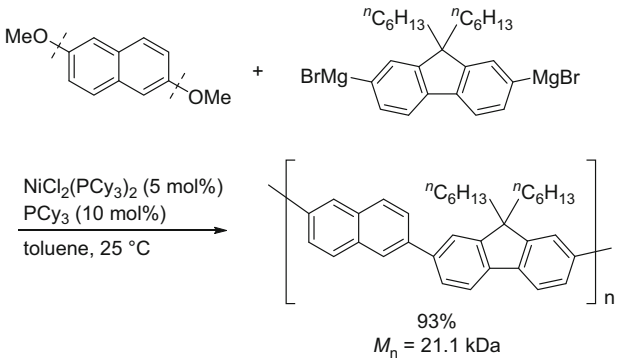

(22)

Despite the progress made in the Kumada-Tamao-Corriu-type cross-coupling of aryl ethers with aryl Grignard reagents, its application to alkylation and alkynylation reactions has lagged behind. Although MeMgX undergoes cross-coupling with aryl ethers under the same conditions as are used for aryl Grignard reagents (i.e., Ni/PCy$_3$) (Eq. 23) [92], other alkyl Grignard reagents fail to react under these conditions, and different ligands are required. An NHC ligand bearing cyclohexyl groups (ICy) is suitable for use in the cross-coupling of alkyl Grignard reagents lacking a β-hydrogen atom, such as Me$_3$SiCH$_2$MgX and ArCH$_2$MgX (Eq. 24) [93]. 1- and 2-Adamantyl and cyclopropyl Grignard reagents are also successfully cross-coupled, probably because undesired β-hydrogen elimination is suppressed by the ring strain in these cases.

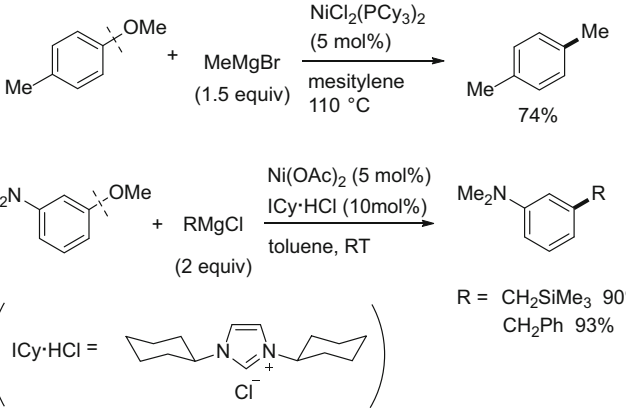

(23)

(24)

A more general protocol for alkylative cross-coupling involves the use of a nickel catalyst in conjunction with a Cy$_2$PCH$_2$CH$_2$PCy$_2$ ligand, which allows cross-coupling using alkyl Grignard reagents bearing a β-hydrogen (Eq. 25) [94]. Primary and secondary alkyl groups containing β-hydrogens can be incorporated directly at the ipso position of anisole derivatives. The type of halide atom in the Grignard reagent has a significant impact on the efficiency of the reaction, with iodide being optimal. When Grignard reagents bearing other halides, such as chlorides and bromides, are used, the addition of MgI$_2$ results in an improved reactivity.

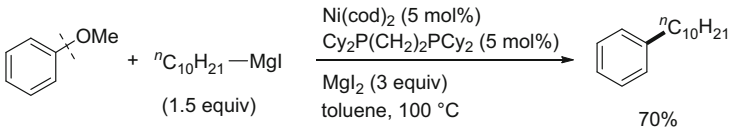

(25)

The only reported method that permits the alkynylation of anisole derivatives was accomplished by Ni/ICy-catalyzed cross-coupling using a triisopropylsilyl-substituted alkynyl Grignard reagent (Eq. 26) [95]. Although the use of this bulky silyl group at the alkyne terminal is essential for the cross-coupling to proceed, it can be readily deprotected to form a terminal alkyne. Since alkynes are amenable to diverse transformations, this protocol can be used for the construction and modification of elaborate π-systems [96].

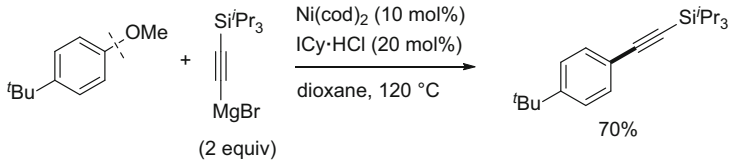

(26)

The reactions discussed thus far have focused on the transformation of aryl methyl ethers, in which a methoxy group serves as a leaving group. Diaryl ethers are, in general, more reactive substrates and can react with Grignard reagents in the presence of a suitable nickel catalyst. Dibenzofurans similarly undergo cross-coupling with Grignard reagents to form ring-opened products. For example, the nickel-catalyzed reaction of dibenzofuran with an aryl Grignard reagent leads to the formation of [1,1′:2′,1″-terphenyl]-2-ol derivatives, which can then be used for the modular synthesis of triphenylene derivatives (Scheme 9) [97].

Regarding organozinc reagents, monoanion-type zincate ArZnMe$_2$Li, which can be generated by the reaction of ArI and Me$_3$ZnLi, can serve as suitable nucleophiles in the Ni/PCy$_3$-catalyzed cross-coupling of methoxyarenes, whereas ArZnX failed to react under these conditions (Eq. 27) [98].

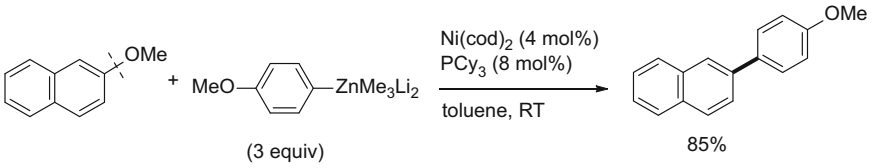

(27)

The use of a Ni/PCy$_3$ system in Suzuki-Miyaura-type cross-coupling reactions of aryl ethers was also reported, in which a range of functional groups, including ketones and esters, were found to be compatible (Eq. 28) [99]. Under these conditions, a methoxy group on π-extended aromatic rings, such as naphthalene, can be coupled efficiently, while anisole remains intact. This difference in reactivity allows for the site-selective arylation of methoxy groups based on the degree of π-extension of the parent aryl groups.

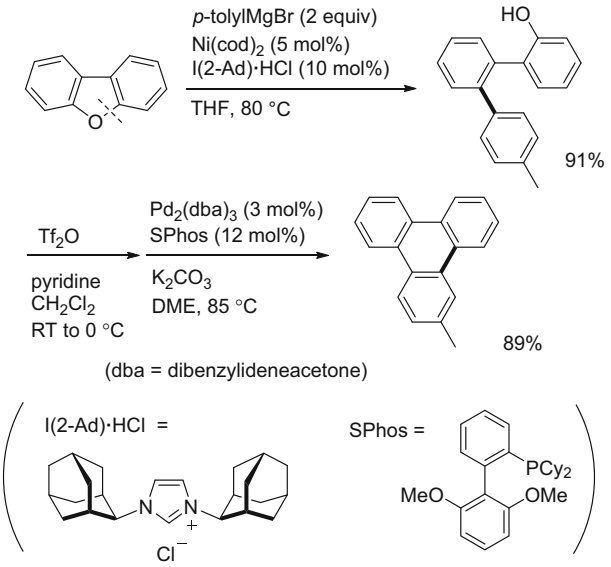

Scheme 9 Nickel-catalyzed ring-opening arylation of dibenzofurans and its application to the modular synthesis of triphenylene derivatives

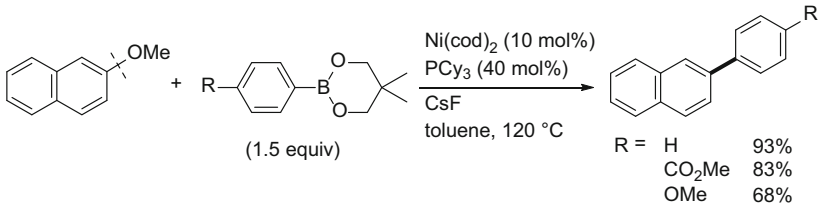

(28)

The catalytic activity for the Suzuki-Miyaura coupling of aryl ethers is dramatically improved when an ICy ligand is used, which allows the arylation of non-naphthalene substrates (Eq. 29) [100]. Theoretical studies revealed that this cross-coupling proceeds through the oxidative addition of a C(aryl)-OMe bond to Ni $(ICy)_2$ [101].

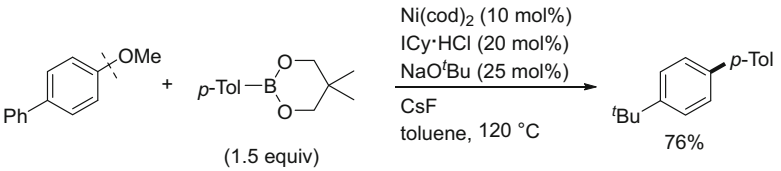

(29)

A method for the alkylative Suzuki-Miyaura coupling of aryl ethers using alkylboron reagents derived from 9-BBN was also developed (Eq. 30) [102]. β-Hydrogen-containing alkyl groups can be successfully incorporated into aryl

ethers by using a Ni/PCy_3 catalyst. A pinacol-protected boryl group does not react under these conditions, indicating that the Lewis acidic 9-BBN-based boron reagents provide assistance in the oxidative addition process by coordinating to a methoxy group.

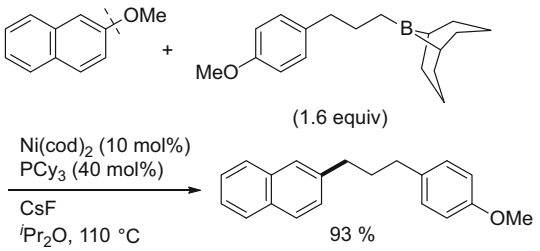

(30)

Similar to the conventional cross-coupling using aryl halides, several organometallic nucleophiles other than Grignard and organoboron reagents can also be used in the nickel-catalyzed cross-coupling aryl ethers. Reported examples include organolithium (Scheme 10) [103–105], organoaluminum (Scheme 11) [18, 106, 107], and organo rare-earth (Eq. 31) [108] reagents. It is noteworthy that no ligand is needed to promote the cross-coupling when timethylsilylmethyllithium is used as

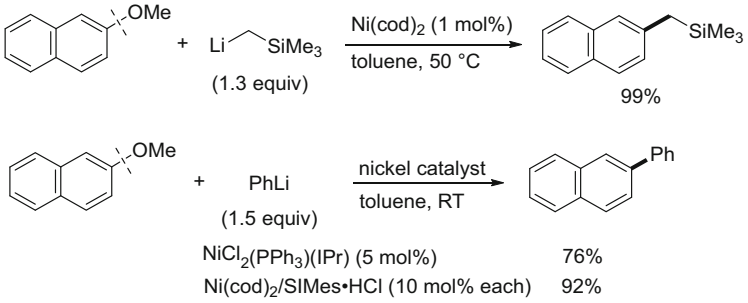

Scheme 10 Nickel-catalyzed cross-coupling of aryl ethers with organolithium reagents

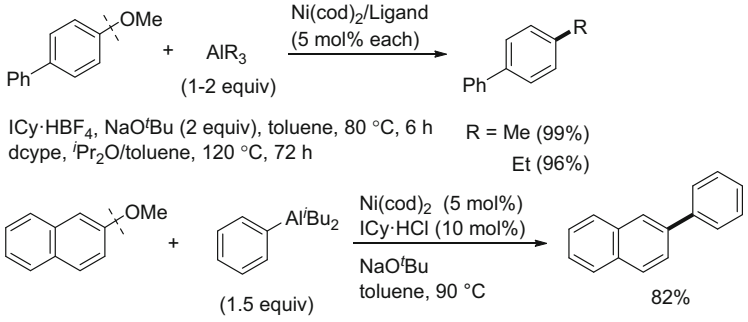

Scheme 11 Nickel-catalyzed cross-coupling of aryl ethers with organoaluminum reagents

the nucleophile. This is in sharp contrast to the other nickel-catalyzed cross-couplings of aryl ethers, which normally require strong σ-donor ligands.

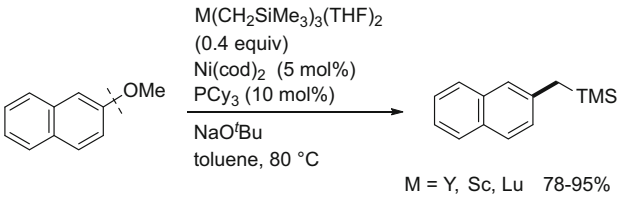

(31)

2.2.2 Reductive Coupling with Aryl Halides

As shown in Eq. (12), the nickel-catalyzed reductive cross-coupling of aryl esters with aryl bromides can be achieved when a stoichiometric amount of metallic magnesium is used as a reductant. This protocol is also applicable to methoxynaphthalene derivatives, allowing the biaryl coupling without the need for organometallic nucleophiles (Eq. 32) [60]. Although the scope of aryl ethers is limited to naphthalene derivatives, the site-selective reductive coupling of two different methoxy groups is possible based on the differences in reactivity profiles.

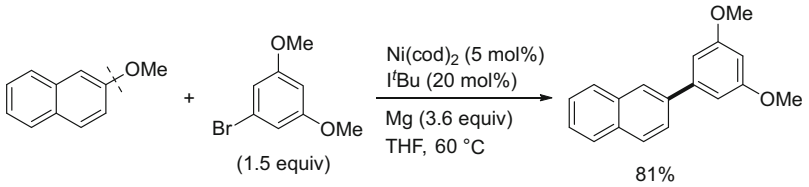

(32)

2.2.3 Coupling with Heteroatom Nucleophiles

Reactions of aryl ethers with heteroatom-based nucleophiles to produce carbon-heteroatom bonds have met with limited success. The first example in this context is the Ni/IPr-catalyzed amination of methoxyarenes, although there is considerable room for improvement in terms of efficiency (Eq. 33) [109, 110]. Recent studies revealed that siloxyarene derivatives are more reactive than methoxyarenes in Ni/NHC-catalyzed amination reactions [111].

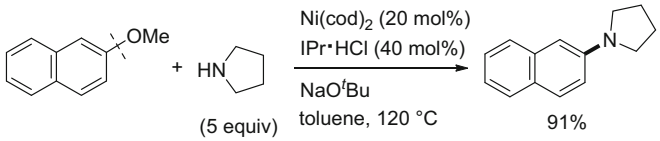

(33)

The borylation of C(aryl)-OMe bonds involves Ni/PCy_3 catalysis and a neopenthylglycol-protected diboron reagent (Eq. 34) [112]. The nature of this protecting group is important for this borylation, with a pinacol-protected diboron reagent being completely ineffective under these conditions.

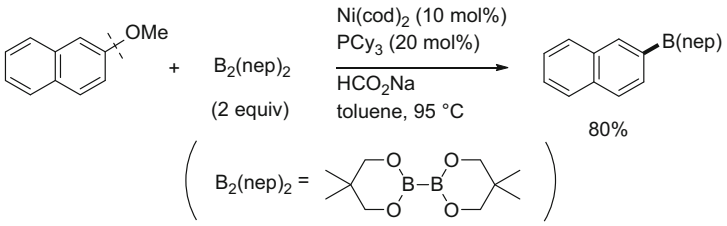

(34)

Interestingly, a reductive homocoupling product is formed when ICy is used as a ligand, in place of PCy_3, possibly through a tandem C(aryl)-OMe borylation/Suzuki-Miyaura coupling of the resulting borylated product and the starting methoxyarene (Scheme 12) [113]. The yield of the homocoupling product can be maximized by using 0.8 equiv of the diboron reagent. This protocol permits a rapid extension of π-systems using methoxyarenes.

The nickel-catalyzed borylation of aryl ethers was successfully applied to benzofuran substrates, which results in the formal insertion of a boron atom into a C2-O bond to form an oxaborin ring system (Eq. 35) [114].

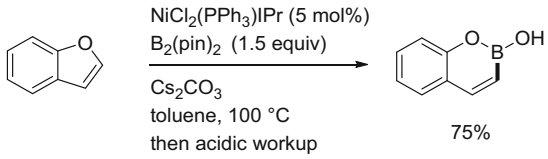

(35)

Ipso-Silylation of anisoles proceeds by nickel catalysis using silylborane as a silylation reagent (Eq. 36) [115]. A striking feature of this reaction includes (1) no

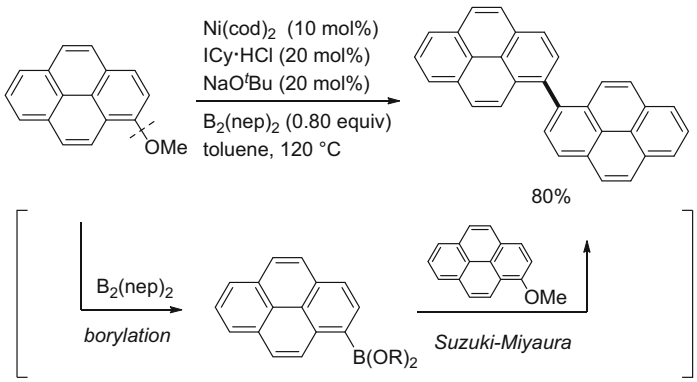

Scheme 12 Nickel-catalyzed dimerization of aryl ethers via C–O bond cleavage

ligands are necessary for an efficient reaction, and (2) the reaction takes place at ambient temperature. Although an anionic silyl-nickelate species is proposed to be involved, the details of the mechanism for the C(aryl)-O bond cleavage remain controversial [116, 117].

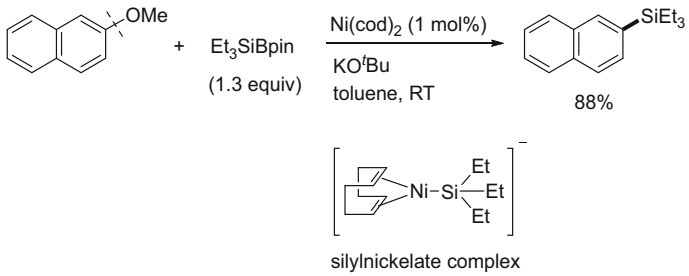

(36)

Hydrosilanes can also be used in the nickel-catalyzed silylation of aryl silyl ethers, in which a methoxy group does not undergo silylation (Eq. 37) [118].

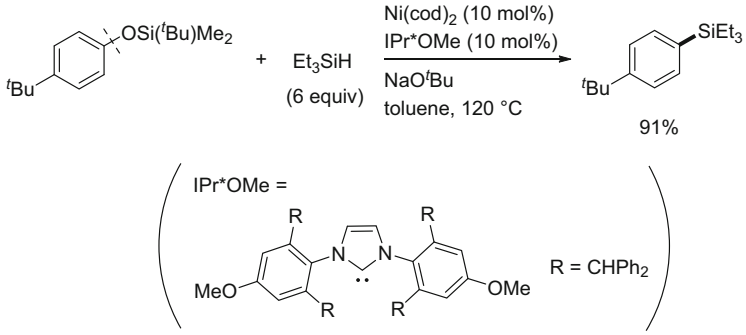

(37)

2.2.4 Reductive Cleavage

When a methoxy group, a commonly used electron-donating group, is placed on an aromatic ring, it is activated toward electrophilic aromatic substitution reactions with controlled *ortho*/*para* site selectivity. Furthermore, a methoxy group on an aromatic ring can be used as an *ortho*-directing group in lithiation and transition metal-catalyzed reactions. Therefore, a method for removing a methoxy group from an aromatic ring would be a valuable synthetic tool, since it would allow the unique features of a methoxy group to be utilized temporarily. However, the inertness of C(aryl)-O bonds in anisole derivatives makes the reductive cleavage of this bond extremely challenging among other C(aryl)-O bonds. The first direct method that was reported for removing a methoxy group from an aromatic ring involved a nickel-catalyzed reaction with hydrosilanes (Scheme 13) [80, 119]. Despite the apparent similarity to the catalytic reductive cleavage of aryl halides

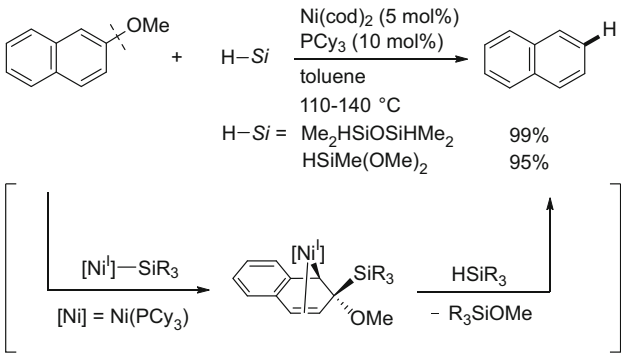

Scheme 13 Nickel-catalyzed reductive dealkoxylation of aryl ethers using hydrosilanes

with hydride donors, the proposed mechanism, which involves the oxidative addition of a C(aryl)-O bond followed by hydride transfer, is now thought to be unlikely based on several mechanistic experiments. A silylnickel(I) species is proposed to be responsible for the catalysis [120].

Hydrogen can also be used as a reducing agent for the nickel-catalyzed reductive cleavage of C(aryl)-O bonds (Eq. 38) [121]. Biaryl ethers are split into the corresponding arenes and phenols under these conditions.

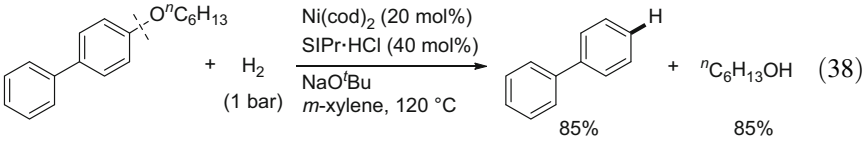

(38)

Sodium formate was also reported to serve as a hydride donor in the nickel-catalyzed reductive cleavage of aryl ethers (Eq. 39) [82].

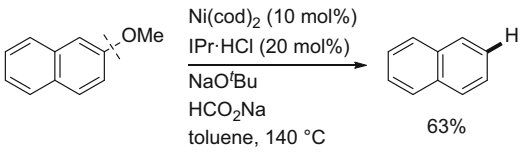

(39)

Although several hydride donors have the ability to promote the reductive cleavage of aryl ethers, the scope of the substrates is limited primarily to polyaromatic systems, such as naphthalene and biphenyl, as shown thus far. The most powerful system reported to date involves the use of diisopropylaminoborane, which is capable of removing a methoxy group on a simple benzene ring (Eq. 40) [122].

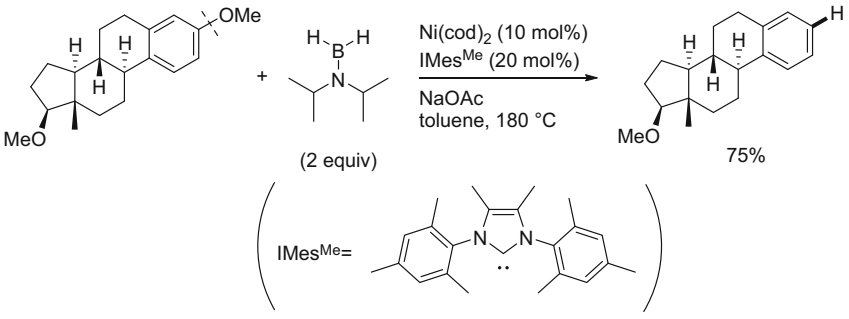

(40)

$Ti(O^iPr)_4$ is a silyl ether-specific reductant, which cannot reduce aryl methyl ethers, aryl pivalates, and aryl triflates under identical conditions (Eq. 41) [118].

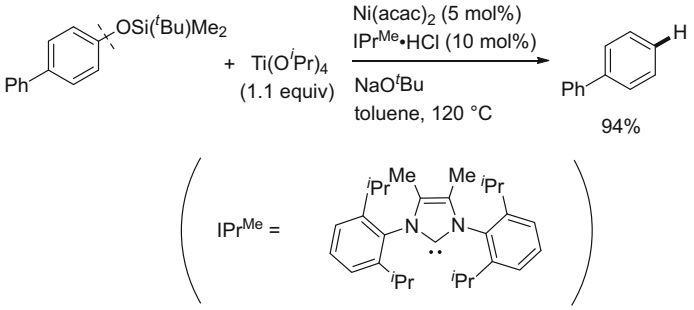

(41)

The reductive cleavage of a C(aryl)-O bond of aryl ethers can also occur in the absence of an external reducing agent. The Ni/I(2-Ad)-catalyzed reaction of alkoxyarenes provides a reduction product, possibly through a sequence comprised of the oxidative addition of the C(aryl)-O bond to nickel(0) and β-hydrogen elimination, followed by reductive elimination (Scheme 14) [123]. This proposed

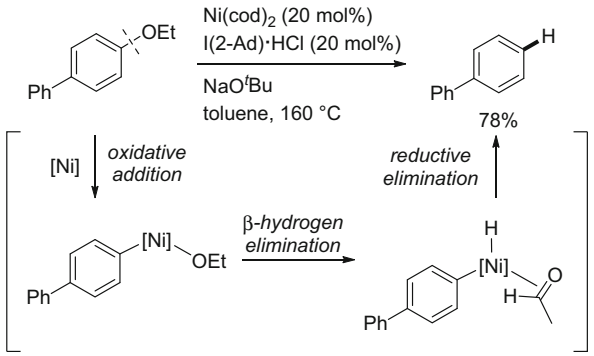

Scheme 14 Nickel-catalyzed reductive dealkoxylation of aryl ethers in the absence of external reducing agents

mechanism is supported by the results of a labelling experiment using $ArOCD_3$, which gives Ar-D with a deuterium incorporation of 96%. This protocol can be used to reduce an aryl ether moiety without affecting normally more reducible functional groups, such as carbonyl and alkene, since the reaction can be performed in the absence of any external hydride donors.

2.3 *Reactions of Arenols*

Although there have been significant advances in the cross-coupling of unactivated phenol derivatives, the most ideal substrates are phenols themselves, in terms of availability and atom economy. However, a phenolic C(aryl)-O bond is among the most difficult to cleave (Scheme 1b), and the presence of a protic OH group is frequently detrimental to the efficiency of transition metal catalysis [25, 120], both of which have hampered the direct use of phenols in cross-coupling reactions. A breakthrough finding was achieved by Shi's work on the nickel-catalyzed Kumada-Tamao-Corriu-type cross-coupling of naphthols (Scheme 15) [124, 125]. In this reaction, the formation of magnesium salts of naphthols is critical, and the use of the corresponding lithium or potassium salts leads to unsuccessful results. Although both arylation [124] and methylation [125] are possible for naphthols, provided a suitable ligand is used, phenols are unreactive under these conditions.

A method for coupling naphthols with arylboroxine reagents was developed using a Ni/PCy_3 catalyst and BEt_3 as a stoichiometric promoter (Scheme 16) [126]. Although the role of BEt_3 is not clear at present, it can activate the borate intermediate as a Lewis acid toward C(aryl)-O bond activation.

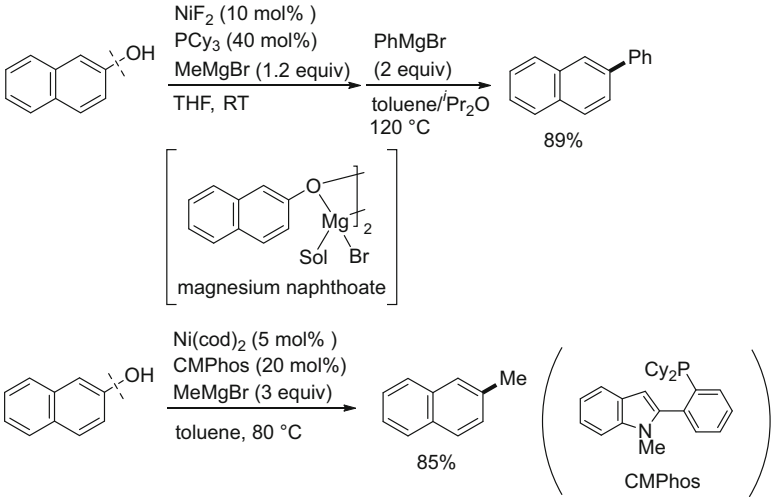

Scheme 15 Nickel-catalyzed Kumada-Tamao-Corriu type reaction of naphthols

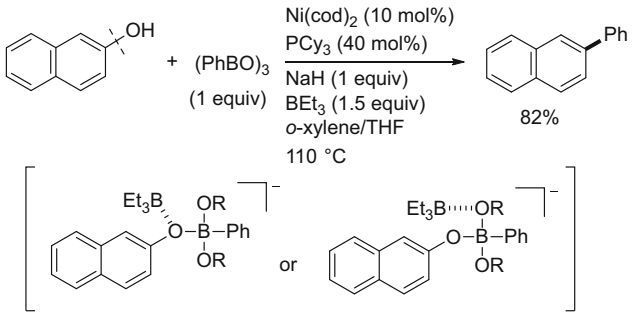

Scheme 16 Nickel-catalyzed Suzuki-Miyaura type reaction of naphthols

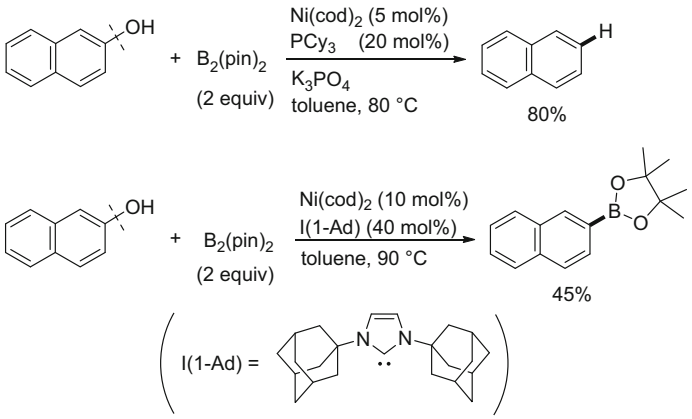

Scheme 17 Nickel-catalyzed reduction and borylation of naphthols

As discussed in Eqs. (12) and (32), the Ni/I^{t}Bu system can catalyze the reductive cross-coupling of aryl esters and ethers with aryl halides in the presence of metallic magnesium. This method was further applied successfully to naphthols substrates by changing the solvent from pure THF to a THF/toluene mixed solvent (Eq. 42) [60].

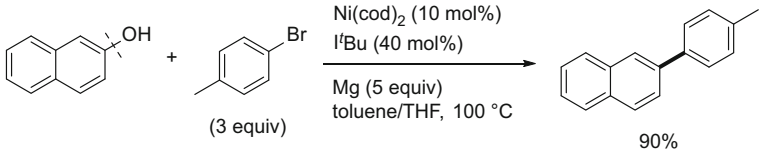

(42)

The removal of a phenolic OH group can be achieved by the nickel-catalyzed reaction of phenols with diboron reagents, in which an *O*-borylated intermediate is proposed to be involved (Scheme 17) [127]. The use of an NHC ligand, instead of PCy_3, was shown to form a borylation product rather than reduction, although one isolated example is included [128].

The reductive removal of a phenolic OH group via the use of hydrosilane reagents is also possible, in which a nickel catalyst mediates both the dehydrogenative

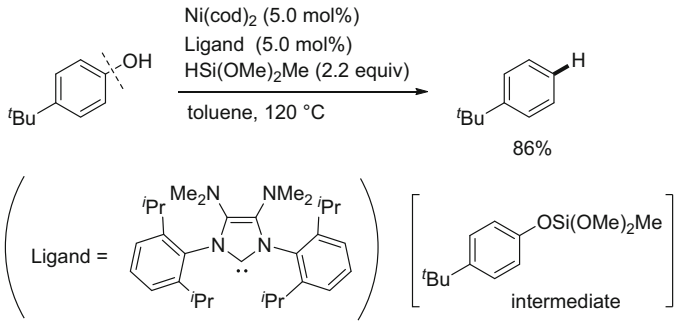

Scheme 18 Nickel-catalyzed reduction of phenols using hydrosilanes

O-silylation and the reductive cleavage of the resulting siloxyarenes (Scheme 18) [129].

3 Group 8 Metal Catalysis

3.1 Iron Catalysis

Since iron is an abundant, inexpensive, and nontoxic metal on the earth, iron catalysis has attracted a great deal of attention in organic synthesis. In this context, significant progress has been made in iron-catalyzed cross-coupling reactions of aryl halides [130–133]. However, inert phenol derivatives have not been used in such iron-catalyzed reactions, except for the cross-coupling of aryl carbamates with alkyl Grignard reagents (Scheme 19). The original conditions involved a $FeCl_2$/SIMes system, which allowed the alkylation of naphthyl carbamates and alkenyl esters

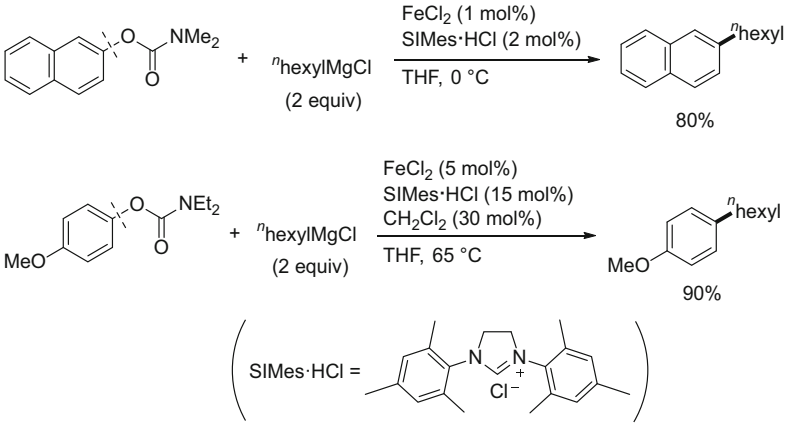

Scheme 19 Iron-catalyzed Kumada-Tamao-Corriu type reaction of aryl carbamates

[134]. A subsequent study revealed that the addition of a catalytic amount of CH_2Cl_2 permits the use of regular phenyl carbamates, although its role is not fully understood [135].

3.2 Ruthenium Catalysis

In 2004, Kakiuchi reported that anisoles bearing an *ortho* carbonyl group can be coupled with arylboronic esters in the presence of $RuH_2(CO)(PPh_3)_3$ (Scheme 20) [136–138]. The reaction represents the first Suzuki-Miyaura-type reaction of aryl ethers. An *ortho* carbonyl moiety serves as a directing group to facilitate the oxidative addition of C-O bonds, which allows for the regioselective C-O bond cleavage of diaryl ethers. The intermediate complex formed by the oxidative addition of a C(aryl)-O bond to Ru(0) was isolated and characterized by X-ray crystallography when a substrate bearing an *ortho* aryloxy group was used [139]. This method was successfully employed in the synthesis of polyaromatic compounds based on the arylation of polymethoxyanthraquinone [140–142] and methoxyfluorenones [143].

$RuH_2(CO)(PPh_3)_3$ is also known to be a powerful catalyst for use in directed *ortho* C-H bond activation reactions [38]. Therefore, both C-H and C-O bonds in the starting compound shown in Scheme 20 can be activated under such catalytic conditions. C-H bond activation is kinetically favored in this system, while C-O bond activation provides a more thermodynamically stable complex [139]. The sequential functionalization of C-H and C-O bonds proceeds in a one-pot reaction by carrying out the reaction in the presence of alkenes and boronic esters (Scheme 21). The key to the chemoselectivity in this reaction is that a ruthenium-hydride intermediate is able to react only with alkenes, whereas boronic esters undergo transmetallation only with a ruthenium-methoxide intermediate. Theoretical studies

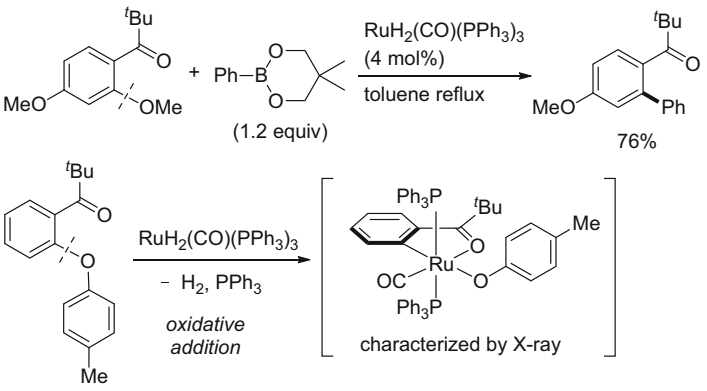

Scheme 20 Ruthenium-catalyzed Suzuki-Miyaura type reaction of aryl ethers bearing a directing group

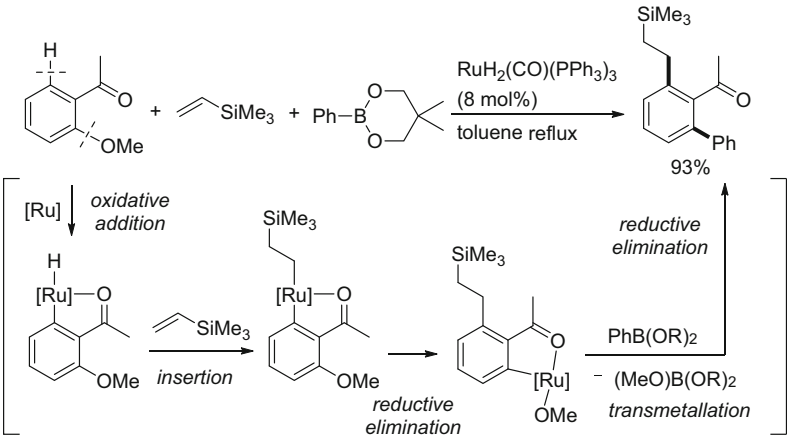

Scheme 21 Ruthenium-catalyzed directed C-H and C-O bond transformation

regarding this selectivity issue in ruthenium-catalyzed directed C-H/C-O activation have also been reported [144].

An amide [145, 146] and ester [147] moiety can also serve as a directing group in this ruthenium-catalyzed *ortho* arylation of a C(aryl)-OMe bond. When hydrosilane, instead of an arylboron reagent, is used in such amide-directed reactions, the catalytic removal of a methoxy group is also possible (Eq. 43) [148].

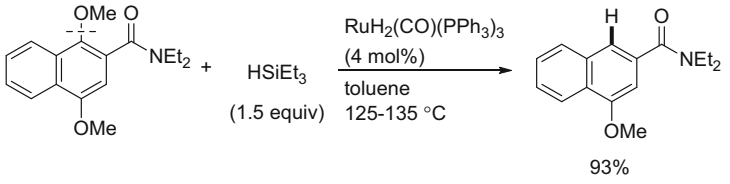

(43)

4 Group 9 Metal Catalysis

4.1 Cobalt Catalysis

Despite the significant advances in cobalt-catalyzed cross-coupling reactions [149–151], there exists only one report on the cobalt-catalyzed C(aryl)-O bond activation of unactivated phenol derivatives. Ackerman developed the cobalt-catalyzed cross-coupling of aryl carbamates with 2-phenylpyridine derivatives, in which an ortho C-H bond of 2-phenylpyridine derivatives is arylated (Eq. 44) [152]. In the nickel-catalyzed C-H/C-O coupling of unactivated phenol derivatives, the scope of the C-H bonds is limited to relatively acidic C-H bonds, such as those in azoles and

pentafluoroarenes (Scheme 4 and Eq. 8). In contrast, this reaction permits non-acidic C-H bonds to be coupled with inert phenol derivatives. One limitation is the need to use stoichiometric amount of a Grignard reagent to promote the reaction.

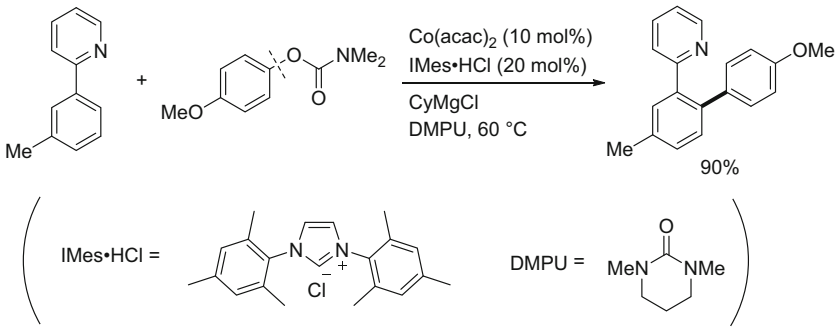

(44)

4.2 Rhodium Catalysis

Ozerov reported on the potential reactivity of rhodium in the activation of unactivated C(aryl)-O bond in reactions of rhodium complexes having a pincer-type ligand with aryl esters and carbamates, which gives oxidative addition complexes [153]. However, its application to catalytic reactions had not been reported as of 2015. The first rhodium-catalyzed cross-coupling of unactivated phenol derivatives was achieved in borylation using a diboron reagent, demonstrating that a rhodium complex can be used to activate C(aryl)-O bond without the need for a pincer-type ligand (Eq. 45) [154].

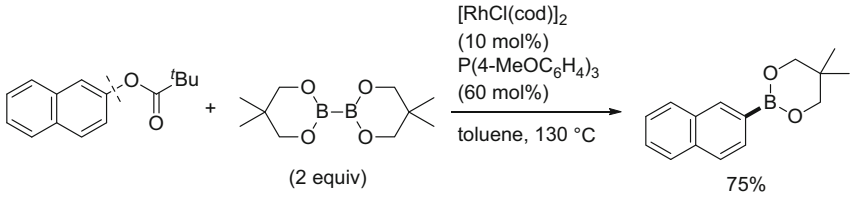

(45)

The rhodium-catalyzed Suzuki-Miyaura-type reaction of aryl carbamates was also developed using a rhodium(I) complex in conjunction of an NHC ligand bearing 2-adamantyl groups (Eq. 46) [155]. This reaction presumably proceeds through the oxidative addition of C(aryl)-O bonds to an arylrhodium(I) species, which is generated in situ.

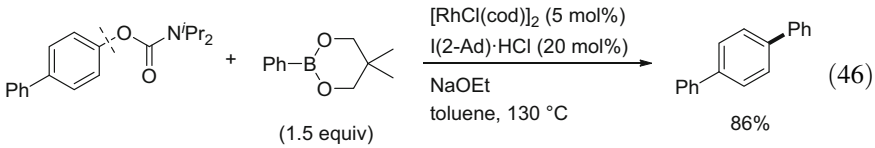

(46)

Although the development of the above-described borylation (Eq. 45) and Suzuki-Miyaura reactions (Eq. 46) demonstrated the viability of using rhodium complexes to activate inert C(aryl)-O bonds, both of the transformations can also be achieved by nickel catalysis (i.e., Eq. 15 and Scheme 2). One of the outstanding features of rhodium complexes includes their ability to activate C-H bonds [156–158], which can be merged with C-O bond activation reactions. Arenes bearing an oxazoline directing group undergo directed *ortho* arylation with aryl carbamates in the presence of a rhodium(I) catalyst and an NHC ligand (Eq. 47) [159]. Unlike the cobalt system (Eq. 44), Grignard reagents are not required for this C-H/C-O coupling, allowing a range of functional groups to be compatible. Mechanistic studies revealed that the generation of a bis-NHC complex, Rh(I)$(NHC)_2$, is essential for an efficient reaction.

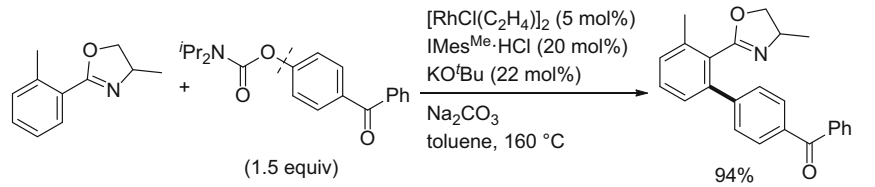

(47)

Despite the importance of the Sonogashira-type reaction in organic synthesis, methods for directly introducing an alkyne moiety to unactivated phenol derivatives are limited to the use of alkynylmagnesium (Eq. 26) [95] or alkynylaluminum (Eq. 5) [18] reagents in nickel-catalyzed reactions. It was reported that a copper co-catalyst allows a terminal alkyne to be used in cross-coupling reactions of aryl carbamates, although only two examples are shown in the paper and its synthetic potential was not investigated in detail [49]. A rhodium catalyst with a strong donating NHC ligand can mediate the alkynylation of aryl carbamates using propargyl alcohol derivatives (Eq. 48) [160]. In this reaction, the propargyl alcohol derivative initially undergoes β-carbon elimination [161] to form an alkynylrhodium(I) intermediate, which then activates a C(aryl)-O bond by oxidative addition. Since a carbamate group is a common *ortho* director, the tandem 1,2-difunctionalization of aryl carbamates is possible by sequential *ortho* functionalization/ipso-alkynylation.

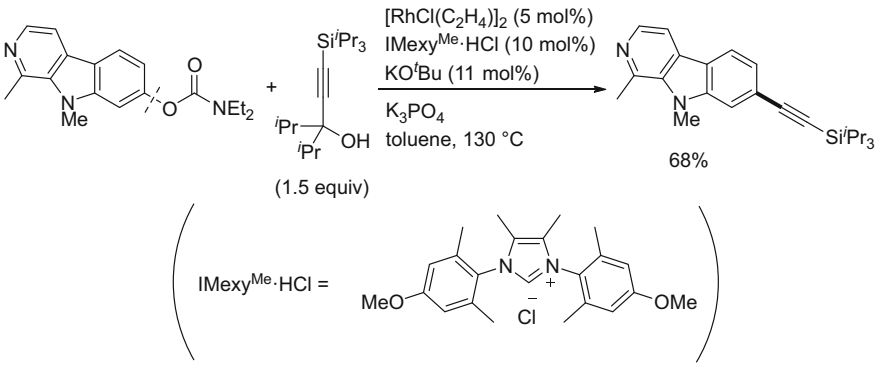

(48)

Similarly, the reductive cleavage of aryl carbamates occurs when isopropanol is used, instead of propargyl alcohol, via β-hydride elimination (Eq. 49) [162]. Compared with the other reductive cleavage methods using ^{i}PrMgX (Eq. 18) and hydrosilane (Eq. 19) by nickel catalysis, a wider range of substrates are applicable.

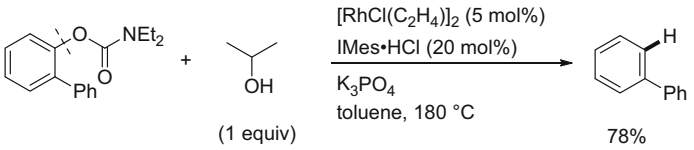

(49)

4.3 Iridium Catalysis

Nozaki reported on the iridium-catalyzed hydrogenolysis of C(aryl)-O bonds in phenols (Scheme 22) [163]. Unlike the nickel-catalyzed phenol activation, which

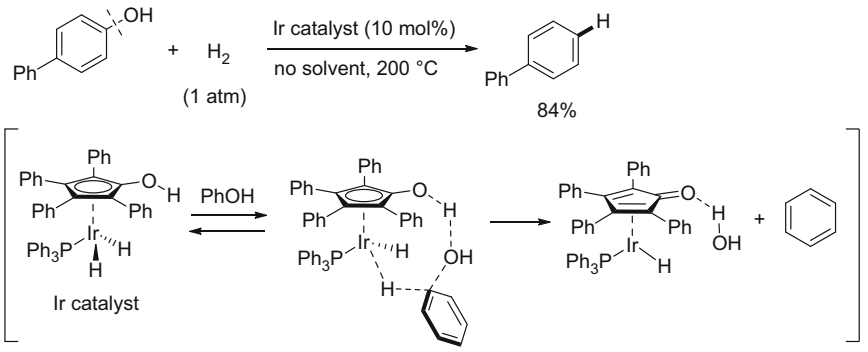

Scheme 22 Iridium-catalyzed reduction of phenols to benzenes

requires *O*-activating reagents such as boron or silicon reagents (Schemes 16 and 17), no such additives are required in this reaction. Iridium complexes containing a hydroxycyclopentadienyl ligand specifically displays catalytic activity, which can be rationalized by the involvement of a metal-ligand cooperative hydrogen transfer mechanism. An OH group on the cyclopentadienyl ligand activates phenols by hydrogen bonding, which facilitates the ipso substitution by the hydride on the iridium center.

5 Chromium Catalysis

Although the utility of organochromium(III) reagents in organic synthesis is well-recognized [164], chromium-catalyzed cross-coupling reactions remain underdeveloped [165], which is in sharp contrast to the great success achieved in the cases of other first-row transition metals, such as nickel, iron, and cobalt, as alternatives to precious metals. Zheng reported on the $CrCl_2$-catalyzed Kumada-Tamao-Corriu-type cross-coupling of anisole derivatives bearing a directing group (Eq. 50) [166]. The optimal directing group for this reaction is an imine moiety, which can be converted to a versatile formyl group upon hydrolysis. Other first-row metal salts, including $CoCl_2$, $FeCl_2$, and $NiCl_2(PPh_3)_2$, were found to be ineffective. Both aryl and alkyl Grignard reagents can be used in this transformation. Formal reductive cross-coupling using aryl bromides and stoichiometric amount of metallic magnesium was also reported [167].

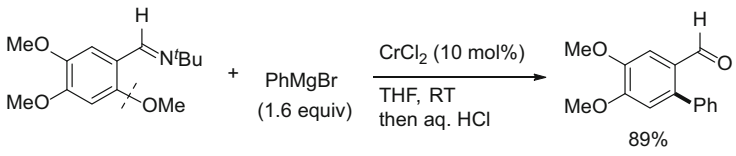

(50)

6 Summary and Outlook

This chapter provides an overview of the current state of our knowledge regarding the transition metal-catalyzed transformation of unactivated phenol derivatives via the cleavage of C(aryl)-O bonds. Since the pioneering work of Wenkert on the cross-coupling of methoxyarenes with Grignard reagents (Eq. 20), nickel complexes, in conjunction with strong σ-donor ligands, have served as the most active catalysts for use in mediating difficult C(aryl)-O bond activation processes. Tremendous advancements have been made in nickel-catalyzed cross-coupling reactions of aryl esters and carbamates, allowing a range of nucleophiles, including organometallic reagents, heteroatom nucleophiles, and even some C-H bonds, to be coupled.

Therefore, these phenol derivatives have now become viable alternatives to aryl halides.

C(aryl)-O bonds of anisole derivatives are much less reactive than the corresponding bonds of aryl esters and carbamates, and therefore the scope of the cross-coupling of anisole derivatives is much more limited. Grignard reagents are the most reliable nucleophiles for use in the nickel-catalyzed cross-coupling of anisole derivatives, in which arylation, alkylation, and alkynylation are all possible, although the range of compatible functional groups that can be used is limited. Reactions using several other nucleophiles, such as organoboron reagents and amines, have also been developed during the last decade. However, most of these reactions suffer from the limited scope of aryl ethers (i.e., the much lower reactivity of anisoles than methoxynaphthalenes), and more powerful catalysts are needed for their widespread use. What makes the rational design of a catalyst difficult is the mechanistic complexity associated with the activation of C(aryl)-O bonds of anisoles. Recent experimental and theoretical studies suggest that several new mechanistic options may be involved, other than simple concerted oxidative addition, depending on the nucleophiles used. A clearer mechanistic understanding will likely serve to accelerate the development of new catalysts for anisole transformation.

The most ideal substrates for use in cross-coupling are arenols, an OH group of which can serve as a leaving group. However, explorations of such transformations have met with strictly limited success, and the successful examples still involve in situ formation of protected phenols and/or the use of stoichiometric activators, such as BEt_3. The development of a sophisticated system based on new mechanisms will be essential for the future development of the direct transformation of phenols, as demonstrated, for example, in the iridium-catalyzed hydrogenolysis of phenols (Scheme 22).

The use of transition metals other than nickel for C(aryl)-O bond activation will definitely be important in terms of further diversifying the transformations of phenol derivatives. Although several metals have been shown to display catalytic activity for the activation of aryl esters and carbamates, and anisoles bearing a directing group, aside from nickel, simple methoxyarenes cannot be activated by these metals. In addition, the vast majority of transformations that have been developed with metals other than nickel can also be accomplished by the use of a nickel catalyst, and metal-specific transformation is expected to appear in the future studies.

With the advantage of renewability and less environmental impact of the leaving group, phenol derivatives are attractive feedstocks for use in the catalytic synthesis of aromatic compounds. Despite the significant advances over the past decade, the goal of realizing truly green processes has not yet been reached, and additional breakthroughs in catalyst development will be essential.

References

1. Miyaura N (ed) (2001). Top Curr Chem:219
2. de Meijere A, Diederich F (2004) Metal-catalyzed cross-coupling reactions2nd edn. Wiley, Weinheim
3. Sun Z, Fridrich B, de Santi A, Elangovan S, Barta K (2018). Chem Rev 118:614
4. Yu D-G, Li B-J, Shi Z-J (2010). Acc Chem Res 43:1486
5. Li B-J, Yu D-G, Sun C-L, Shi Z-J (2011). Chem Eur J 17:1728
6. Rosen BM, Quasdorf KW, Wilson DA, Zhang N, Resmerita A-M, Garg NK, Percec V (2011). Chem Rev 111:1346
7. Tobisu M, Chatani N (2013). Top Organomet Chem 44:35
8. Yamaguchi J, Muto K, Itami K (2013). Eur J Org Chem (1):19
9. Cornella J, Zarate C, Martin R (2014). Chem Soc Rev 43:8081
10. Tobisu M, Chatani N (2015). Acc Chem Res 48:1717
11. Tobisu M, Chatani N (2016). Top Curr Chem 374:41
12. Zeng H, Qiu Z, Domínguez-Huerta A, Hearne Z, Chen Z, Li C-J (2017). ACS Catal 7:510
13. Tasker SZ, Standley EA, Jamison TF (2014). Nature 509:299
14. Sengupta S, Leite M, Raslan DS, Quesnelle C, Snieckus V (1992). J Org Chem 57:4066
15. Yoshikai N, Matsuda H, Nakamura E (2009). J Am Chem Soc 131:9590
16. Li B-J, Li Y-Z, Lu X-Y, Liu J, Guan B-T, Shi Z-J (2008). Angew Chem Int Ed 47:10124
17. Liu X, Jia J, Rueping M (2017). ACS Catal 7:4491
18. Ogawa H, Yang Z-K, Minami H, Kojima K, Saito T, Wang C, Uchiyama M (2017). ACS Catal 7:3988
19. Miyaura N, Suzuki A (1995). Chem Rev 95:2457
20. Quasdorf KW, Tian X, Garg NK (2008). J Am Chem Soc 130:14422
21. Guan B-T, Wang Y, Li B-J, Yu D-G, Shi Z-J (2008). J Am Chem Soc 130:14468
22. Quasdorf KW, Riener M, Petrova KV, Garg NK (2009). J Am Chem Soc 131:17748
23. Antoft-Finch A, Blackburn T, Snieckus V (2009). J Am Chem Soc 131:17750
24. Xu L, Li B-J, Wu Z-H, Lu X-Y, Guan B-T, Wang B-Q, Zhao K-Q, Shi Z-J (2010). Org Lett 12:884
25. Quasdorf KW, Antoft-Finch A, Liu P, Silberstein AL, Komaromi A, Blackburn T, Ramgren SD, Houk KN, Snieckus V, Garg NK (2011). J Am Chem Soc 133:6352
26. Molander GA, Beaumard F (2010). Org Lett 12:4022
27. Kuwano R, Shimizu R (2011). Chem Lett 40:913
28. Baghbanzadeh M, Pilger C, Kappe CO (2011). J Org Chem 76:1507
29. Leowanawat P, Zhang N, Percec V (2012). J Org Chem 77:1018
30. Xu M, Li X, Sun Z, Tu T (2013). Chem Commun 49:11539
31. Ramgren SD, Hie L, Ye Y, Garg NK (2013). Org Lett 15:3950
32. Li Z, Zhang S-L, Fu Y, Guo Q-X, Liu L (2009). J Am Chem Soc 131:8815
33. Guo L, Hsiao CC, Yue H, Liu X, Rueping M (2016). ACS Catal 6:4438
34. Chemler SR, Trauner D, Danishefsky SJ (2001). Angew Chem Int Ed 40:4544
35. Nakao Y, Hiyama T (2011). Chem Soc Rev 40:4893
36. Shi WJ, Zhao HW, Wang Y, Cao ZC, Zhang LS, Yu DG, Shi ZJ (2016). Adv Synth Catal 358:2410
37. Rouquet G, Chatani N (2013). Angew Chem Int Ed 52:11726
38. Kakiuchi F, Kochi T, Murai S (2014). Synlett 25:2390
39. Miura M, Satoh T, Hirano K (2014). Bull Chem Soc Jpn 87:751
40. Yamaguchi J, Yamaguchi AD, Itami K (2012). Angew Chem Int Ed 51:8960
41. Chen X, Engle KM, Wang D-H, Yu J-Q (2009). Angew Chem Int Ed 48:5094
42. Lyons TW, Sanford MS (2010). Chem Rev 110:1147
43. Wencel-Delord J, Glorius F (2013). Nat Chem 5:369
44. Ackermann L, Vicente R, Kapdi AR (2009). Angew Chem Int Ed 48:9792
45. Muto K, Yamaguchi J, Itami K (2012). J Am Chem Soc 134:169

46. Muto K, Hatakeyama T, Yamaguchi J, Itami K (2015). Chem Sci 6:6792
47. Muto K, Yamaguchi J, Lei A, Itami K (2013). J Am Chem Soc 135:16384
48. Iwai T, Harada T, Shimada H, Asano K, Sawamura M (2017). ACS Catal 7:1681
49. Wang Y, Wu S-B, Shi W-J, Shi Z-J (2016). Org Lett 18:2548
50. Wang J, Ferguson DM, Kalyani D (2013). Tetrahedron 69:5780
51. Culkin DA, Hartwig JF (2003). Acc Chem Res 36:234
52. Takise R, Muto K, Yamaguchi J, Itami K (2014). Angew Chem Int Ed 53:6791
53. Koch E, Takise R, Studer A, Yamaguchi J, Itami K (2015). Chem Commun 51:855
54. Cornella J, Jackson EP, Martin R (2015). Angew Chem Int Ed 54:4075
55. Beletskaya IP, Cheprakov AV (2000). Chem Rev 100:3009
56. Ehle AR, Zhou Q, Watson MP (2012). Org Lett 14:1202
57. Ellis GP, Romney-Alexander TM (1987). Chem Rev 87:779
58. Takise R, Itami K, Yamaguchi J (2016). Org Lett 18:4428
59. Everson DA, Weix DJ (2014). J Org Chem 79:4793
60. Cao Z-C, Luo Q-Y, Shi Z-J (2016). Org Lett 18:5978
61. Correa A, Martin R (2009). J Am Chem Soc 131:15974
62. Fujihara T, Nogi K, Xu T, Terao J, Tsuji Y (2012). J Am Chem Soc 134:9106
63. Correa A, León T, Martin R (2014). J Am Chem Soc 136:1062
64. Correa A, Martin R (2014). J Am Chem Soc 136:7253
65. Surry DS, Buchwald SL (2008). Angew Chem Int Ed 47:6338
66. Hartwig JF (2008). Acc Chem Res 41:1534
67. Shimasaki T, Tobisu M, Chatani N (2010). Angew Chem Int Ed 49:2929
68. Mesganaw T, Silberstein AL, Ramgren SD, Nathel NFF, Hong X, Liu P, Garg NK (2011). Chem Sci 2:1766
69. Hie L, Ramgren SD, Mesganaw T, Garg NK (2012). Org Lett 14:4182
70. Wolfe JP, Ahman J, Sadighi JP, Singer RA, Buchwald SL (1997). Tetrahedron Lett 38:6367
71. Yue H, Guo L, Liu X, Rueping M (2017). Org Lett 19:1788
72. Mkhalid IAI, Barnard JH, Marder TB, Murphy JM, Hartwig JF (2010). Chem Rev 110:890
73. Huang K, Yu D-G, Zheng S-F, Wu Z-H, Shi Z-J (2011). Chem Eur J 17:786
74. Zarate C, Martin R (2014). J Am Chem Soc 136:2236
75. Somerville RJ, Hale LVA, Gómez-Bengoa E, Burés J, Martin R (2018). J Am Chem Soc 140:8771
76. Gu Y, Martin R (2017). Angew Chem Int Ed 56:3187
77. Yang J, Chen T, Han LB (2015). J Am Chem Soc 137:1782
78. Yang J, Xiao J, Chen T, Han LB (2016). J Org Chem 81:3911
79. Jørgensen KB, Rantanen T, Dörfler T, Snieckus V (2015). J Org Chem 80:9410
80. Tobisu M, Yamakawa K, Shimasaki T, Chatani N (2011). Chem Commun 47:2946
81. Mesganaw T, Fine Nathel NF, Garg NK (2012). Org Lett 14:2918
82. Xi X, Chen T, Zhang JS, Han LB (2018). Chem Commun 54:1521
83. Wenkert E, Michelotti EL, Swindell CS (1979). J Am Chem Soc 101:2246
84. Wenkert E, Michelotti EL, Swindell CS, Tingoli M (1984). J Org Chem 49:4894
85. Dankwardt JW (2004). Angew Chem Int Ed 43:2428
86. Xie LG, Wang ZX (2011). Chem Eur J 17:4972
87. Zhao F, Yu D-G, Zhu R-Y, Xi Z, Shi Z-J (2011). Chem Lett 40:1001
88. Iglesias MJ, Prieto A, Nicasio MC (2012). Org Lett 14:4318
89. Zhang J, Xu J, Xu Y, Sun H, Shen Q, Zhang Y (2015). Organometallics 34:5792
90. Ogawa H, Minami H, Ozaki T, Komagawa S, Wang C, Uchiyama M (2015). Chem Eur J 21:13904
91. Yang Z-K, Xu N-X, Takita R, Muranaka A, Wang C, Uchiyama M (2018). Nat Commun 9:1587
92. Guan B-T, Xiang S-K, Wu T, Sun Z-P, Wang B-Q, Zhao K-Q, Shi Z-J (2008). Chem Commun 44:1437
93. Tobisu M, Takahira T, Chatani N (2015). Org Lett 17:4352

94. Tobisu M, Takahira T, Morioka T, Chatani N (2016). J Am Chem Soc 138:6711
95. Tobisu M, Takahira T, Ohtsuki A, Chatani N (2015). Org Lett 17:680
96. Chen X-C, Nishinaga S, Okuda Y, Zhao J-J, Xu J, Mori H, Nishihara Y (2015). Org Chem Front 2:536
97. Kurata Y, Otsuka S, Fukui N, Nogi K, Yorimitsu H, Osuka A (2017). Org Lett 19:1274
98. Wang C, Ozaki T, Takita R, Uchiyama M (2012). Chem Eur J 18:3482
99. Tobisu M, Shimasaki T, Chatani N (2008). Angew Chem Int Ed 47:4866
100. Tobisu M, Yasutome A, Kinuta H, Nakamura K, Chatani N (2014). Org Lett 16:5572
101. Schwarzer MC, Konno R, Hojo T, Ohtsuki A, Nakamura K, Yasutome A, Takashima H, Shimasaki T, Tobisu M, Chatani N, Mori S (2017). J Am Chem Soc 139:10347
102. Guo L, Liu X, Baumann C, Rueping M (2016). Angew Chem Int Ed 55:15415
103. Leiendecker M, Hsiao C-C, Guo L, Alandini N, Rueping M (2014). Angew Chem Int Ed 53:12912
104. Heijnen D, Gualtierotti J-B, Hornillos V, Feringa BL (2016). Chem Eur J 22:3991
105. Yang Z-K, Wang D-Y, Minami H, Ogawa H, Ozaki T, Saito T, Miyamoto K, Wang C, Uchiyama M (2016). Chem Eur J 22:15693
106. Morioka T, Nishizawa A, Nakamura K, Tobisu M, Chatani N (2015). Chem Lett 44:1729
107. Liu X, Hsiao C-C, Kalvet I, Leiendecker M, Guo L, Schoenebeck F, Rueping M (2016). Angew Chem Int Ed 55:6093
108. Yan X, Yang F, Cai G, Meng Q, Li X (2018). Org Lett 20:624
109. Tobisu M, Shimasaki T, Chatani N (2009). Chem Lett 38:710
110. Tobisu M, Yasutome A, Yamakawa K, Shimasaki T, Chatani N (2012). Tetrahedron 68:5157
111. Wiensch EM, Montgomery J (2018). Angew Chem Int Ed 57:11045. https://doi.org/10.1002/anie.201806790
112. Zarate C, Manzano R, Martin R (2015). J Am Chem Soc 137:6754
113. Nakamura K, Tobisu M, Chatani N (2015). Org Lett 17:6142
114. Saito H, Otsuka S, Nogi K, Yorimitsu H (2016). J Am Chem Soc 138:15315
115. Zarate C, Nakajima M, Martin R (2017). J Am Chem Soc 139:1191
116. Wang B, Zhang Q, Jiang J, Yu H, Fu Y (2017). Chem Eur J 23:17249
117. Jain P, Pal S, Avasare V (2018). Organometallics 37:1141
118. Wiensch EM, Todd DP, Montgomery J (2017). ACS Catal 7:5568
119. Álvarez-Bercedo P, Martin R (2010). J Am Chem Soc 132:17352
120. Cornella J, Gómez-Bengoa E, Martin R (2013). J Am Chem Soc 135:1997
121. Sergeev AG, Hartwig JF (2011). Science 332:439
122. Igarashi T, Haito A, Chatani N, Tobisu M (2018). ACS Catal 8:7475
123. Tobisu M, Morioka T, Ohtsuki A, Chatani N (2015). Chem Sci 6:3410
124. Yu D-G, Li B-J, Zheng S-F, Guan B-T, Wang B-Q, Shi Z-J (2010). Angew Chem Int Ed 49:4566
125. Shi W-J, Shi Z-J (2018). Chin J Chem 36:183
126. Yu D-G, Shi Z-J (2011). Angew Chem Int Ed 50:7097
127. Shi W-J, Li X-L, Li Z-W, Shi Z-J (2016). Org Chem Front 3:375
128. Cao Z-C, Luo F-X, Shi W-J, Shi Z-J (2015). Org Chem Front 2:1505
129. Ohgi A, Nakao Y (2016). Chem Lett 45:45
130. Shang R, Ilies L, Nakamura E (2017). Chem Rev 117:9086
131. Sherry BD, Fürstner A (2008). Acc Chem Res 41:1500
132. Nakamura E, Hatakeyama T, Ito S, Ishizuka K, Ilies L, Nakamura M (2013). Org React 83:1
133. Sun C-L, Li B-J, Shi Z-J (2011). Chem Rev 111:1293
134. Li B-J, Xu L, Wu Z-H, Guan B-T, Sun C-L, Wang B-Q, Shi Z-J (2009). J Am Chem Soc 131:14656
135. Silberstein AL, Ramgren SD, Garg NK (2012). Org Lett 14:3796
136. Kakiuchi F, Usui M, Ueno S, Chatani N, Murai S (2004). J Am Chem Soc 126:2706
137. Kondo H, Akiba N, Kochi T, Kakiuchi F (2015). Angew Chem Int Ed 54:9293
138. Kondo H, Kochi T, Kakiuchi F (2017). Org Lett 19:794

139. Ueno S, Mizushima E, Chatani N, Kakiuchi F (2006). J Am Chem Soc 128:16516
140. Matsumura D, Kitazawa K, Terai S, Kochi T, Ie Y, Nitani M, Aso Y, Kakiuchi F (2012). Org Lett 14:3882
141. Suzuki Y, Yamada K, Watanabe K, Kochi T, Ie Y, Aso Y, Kakiuchi F (2017). Org Lett 19:3791
142. Izumoto A, Kondo H, Kochi T, Kakiuchi F (2017). Synlett 28:2609
143. da Frota LCRM, Schneider C, de Amorim MB, da Silva AJM, Snieckus V (2017). Synlett 28:2587
144. Wang Z, Zhou Y, Lam WH, Lin Z (2017). Organometallics 36:2354
145. Zhao Y, Snieckus V (2014). J Am Chem Soc 136:11224
146. Zhao Y, Snieckus V (2015). Org Lett 17:4674
147. Zhao Y, Snieckus V (2016). Chem Commun 52:1681
148. Zhao Y, Snieckus V (2018). Org Lett 20:2826
149. Gao K, Yoshikai N (2014). Acc Chem Res 47:1208
150. Moselage M, Ackermann L (2016). ACS Catal 6:498
151. Yoshino T, Matsunaga S (2018). Asian J Org Chem 7:1193
152. Song W, Ackermann L (2012). Angew Chem Int Ed 51:8251
153. Zhu Y, Smith DA, Herbert DE, Gatard S, Ozerov OV (2012). Chem Commun 48:218
154. Kinuta H, Hasegawa J, Tobisu M, Chatani N (2015). Chem Lett 44:366
155. Nakamura K, Yasui K, Tobisu M, Chatani N (2015). Tetrahedron 71:4484
156. Satoh T, Miura M (2010). Chem Eur J 16:11212
157. Kuhl N, Schröder N, Glorius F (2014). Adv Synth Catal 356:1443
158. Colby DA, Bergman RG, Ellman JA (2010). Chem Rev 110:624
159. Tobisu M, Yasui K, Aihara Y, Chatani N (2017). Angew Chem Int Ed 56:1877
160. Yasui K, Chatani N, Tobisu M (2018). Org Lett 20:2108
161. Funayama A, Satoh T, Miura M (2005). J Am Chem Soc 127:15354
162. Yasui K, Higashino M, Chatani N, Tobisu M (2017). Synlett 28:2569
163. Kusumoto S, Nozaki K (2015). Nat Commun 6:6296
164. Fürstner A (1999). Chem Rev 99:991
165. Steib AK, Kuzmina OM, Fernandez S, Flubacher D, Knochel P (2013). J Am Chem Soc 135:15346
166. Cong X, Tang H, Zeng X (2015). J Am Chem Soc 137:14367
167. Tang J, Luo M, Zeng X (2017). Synlett 28:2577

Top Organomet Chem (2019) 63: 141–174
DOI: 10.1007/3418_2018_15

Published online: 28 November 2018

Hydrogenation/Dehydrogenation of Unsaturated Bonds with Iron Pincer Catalysis

William D. Jones

Contents

Abstract This chapter examines iron pincer complexes that catalyze hydrogenation and dehydrogenation reactions of common organic compounds, focusing on work reported in the last decade. Substrates include aldehydes, ketones, alcohols, esters, nitriles, imines, amines, CO_2, formic acid, amides, alkenes, and alkynes. Hydroboration and hydrosilation catalysis with iron pincers are also summarized. Some examples of enantioselective iron catalysis using pincers and tetradentate ligands are included. Examples of C–O cleavage have also been reported, and the scope of this chemistry is presented.

W. D. Jones (✉)
Department of Chemistry, University of Rochester, Rochester, NY, USA
e-mail: jones@chem.rochester.edu

Keywords Dehydrogenation · Catalysis · Enantioselectivity · Hydroboration · Hydrogenation · Hydrosilation · Iron · Pincers

In this chapter, iron pincer complexes that catalyze hydrogenation and dehydrogenation reactions of common organic compounds are examined, focusing on work reported in the last decade. Substrates include aldehydes, ketones, alcohols, esters, nitriles, imines, amines, CO_2, formic acid, amides, alkenes, and alkynes. Hydroboration and hydrosilation catalysis with iron pincers are also summarized. Some examples of enantioselective iron catalysis using pincers and tetradentate ligands are included. Examples of C–O cleavage have also been reported, and the scope of this chemistry is presented. It is seen that recent developments in iron pincer catalysis have revealed chemistry as rich as that seen with precious metal catalysts, indicating strong promise for the development of new, reactive iron pincer catalysts.

1 Hydrogenation of Aldehydes

Hydrogenation of aldehydes using dihydrogen gas has been possible with a number of iron-containing catalysts. In 2015, Milstein reported a PNP catalyst that was effective for aldehyde hydrogenation [1]. Complex **1** serves as a catalyst precursor that can be activated by dehydrohalogenation using potassium *tert*-butoxide as base. The hydrogenation is not facile, but proceeds to completion at 40°C under 30 bar H_2 (Eq. 1), but only if substantial quantities of NEt_3 are present as additive (1 mL NEt_3/ 2 mL EtOH). As many as 4,000 turnovers were obtained under these optimized conditions. Primary alkyl aldehydes are unsuitable for this hydrogenation, however, as the base induces aldol coupling to give α,β-unsaturated alcohol products. For these hydrogenations, the borohydride derivative **2** can be used as catalyst precursor to give alcohol products in good yield. Halide-substituted benzaldehydes gave low yields of products. The derivative where the $^{i}Pr_2P$ groups were replaced by $^{t}Bu_2P$ groups showed dramatically reduced reactivity with benzaldehyde. The mechanism of this reaction will be discussed in the later section on ketone hydrogenation with this catalyst.

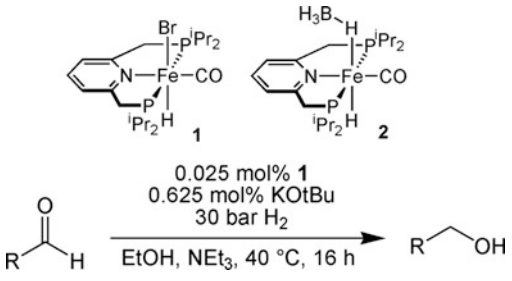

(1)

In 2015, Hu reported that the related iron PONOP complex **3** could be used for aldehyde hydrogenation [2]. With this catalyst, benzaldehyde is reduced in good yield under 8 bar H_2 at ambient temperature in the absence of base (Eq. 2). Higher catalyst loadings were employed in these reactions (5–10%). Furthermore, the catalyst selectively reduces aldehydes in the presence of ketones. This catalyst operated under more mild conditions than the iron catalysts $FeF[P(o\text{-}C_6H_4PPh_2)_3]$ and $(\eta^4\text{-cyclopentadienoneTMS}_2)Fe(CO)_3$ reported by Beller [3, 4], the former of which was also selective for aldehydes over ketones.

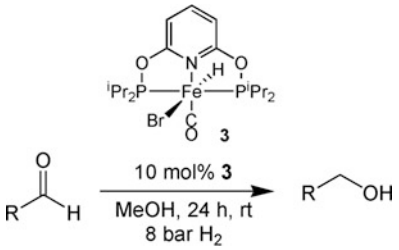

(2)

Kirchner reported a PNP pre-catalyst **4** derived from a 2,6-diaminopyridine scaffold that was exceptionally active for aldehyde hydrogenation under mild conditions (40°C, 30 bar H_2). Here, as little as 12.5 ppm of the iron catalyst could be used, and TONs of up to 80,000 were obtained (Eq. 3). DBU was added as base (1 mol%) to generate the active catalyst **5**. Note that the nitrogen groups attached to the pyridine are substituted by methyl groups, suggesting that the ligand is not redox active during the hydrogenation. Mechanistic investigations revealed that the aldehyde reacts by way of a classical Schrock–Osborn (inner-sphere) mechanism [5] in which insertion into an iron–hydride bond gives an alkoxide (Scheme 1). Replacement of the alkoxide by dihydrogen followed by deprotonation of the coordinated dihydrogen regenerates the iron hydride. The solvent ethanol plays an important role as hydrogen bonding to the alkoxide is critical to its displacement from the metal. This aspect of the mechanism was demonstrated using DFT calculations. Substrates

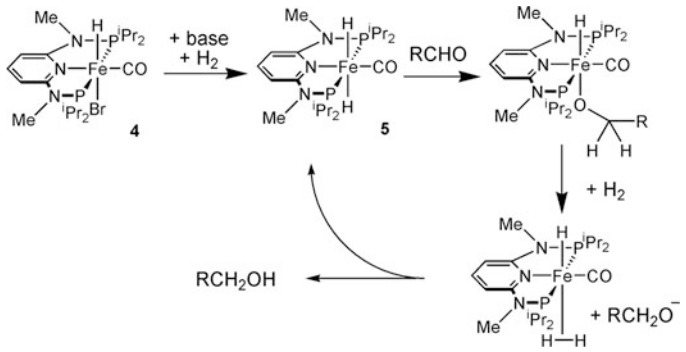

Scheme 1 Aldehyde hydrogenation by **5**

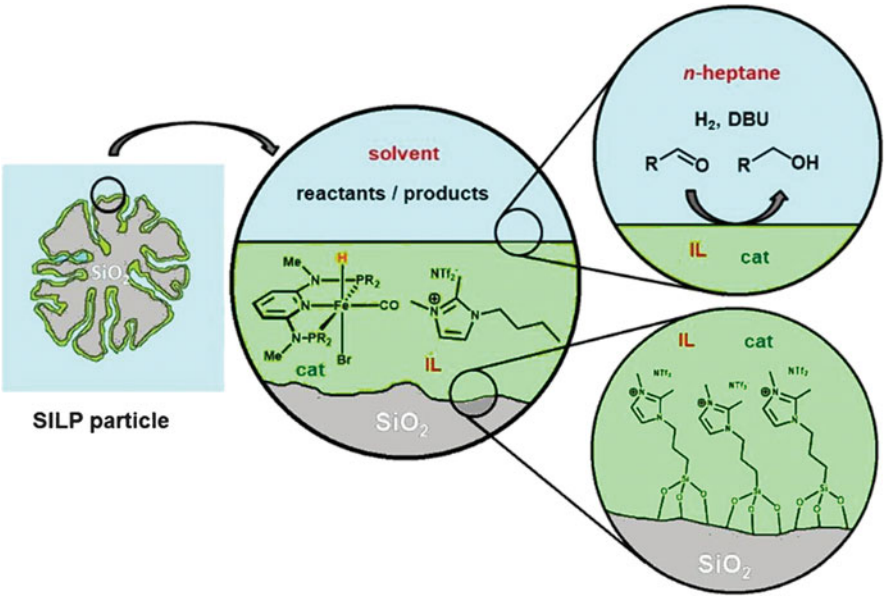

Fig. 1 A new iron-based SILP catalyst (Reproduced with permission from [7], ©2018 ACS)

that are *not* hydrogenated under the reaction conditions include acetophenone, ethyl benzoate, phenyl propyne, phenylethylene oxide, and nitrotoluene [6]. Cinnamaldehyde showed exclusive reduction of the aldehyde, leaving the olefin intact.

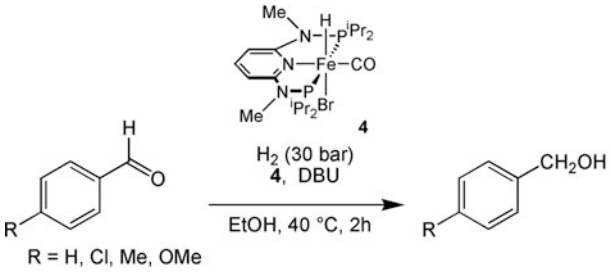

(3)

In 2018, Kirchner reported a base-tolerant supported ionic-liquid-phase (SILP) system in which an Fe(PNP) hydride was used for hydrogenation of aldehydes to alcohols. Here, the iron catalyst **4** above was combined with a dimethylimidazolium tethered to a silica gel surface in an ionic liquid solvent (Fig. 1). Exposure of this catalyst to heptane containing aldehyde and pressurizing with hydrogen led to efficient hydrogenation to the alcohol. The rates of hydrogenation are quite high (TOF = 4,000 h^{-1}), slightly lower than in the homogeneous system but with comparable TONs. Furthermore, examination of the heptane solution showed no evidence for leaching of the iron catalyst. Product (in heptane) can be isolated by just

filtering to remove the SILP catalyst. The catalyst could be recycled many times without loss of activity [7].

2 Hydrogenation of Ketones

A number of iron pincer complexes have been found to be active for ketone hydrogenation. Prior to his full report on aldehyde hydrogenation, Milstein reported in 2011 that his PNP–Fe catalyst **1** was a good catalyst for ketone hydrogenation for aryl ketones [8]. With cyclohexenone, a mixture of cyclohexanol, cyclohexanone, and cyclohexenol was obtained under the same reaction conditions (Eq. 4). *trans*-4-phenyl-3-buten-2-one also gave a mixture of products. In contrast to the aldehyde reductions, large quantities of NEt_3 were not required. Potassium t-butoxide was again needed to activate the catalyst. NMR studies of the reaction suggested that the reaction proceeds through a dearomatized intermediate – i.e., the ligand is redox active. The proposed mechanism is shown in Scheme 2.

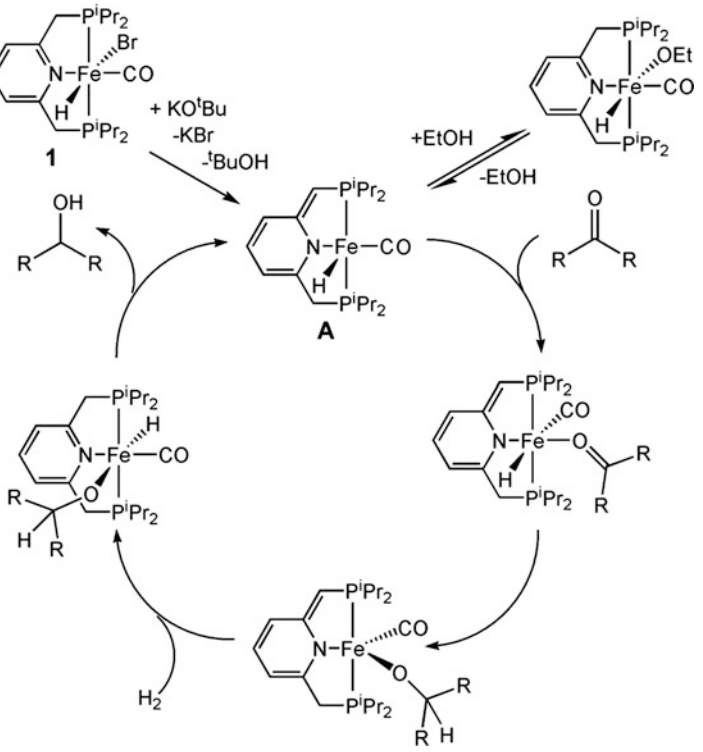

Scheme 2 Hydrogenation of ketones by **1**

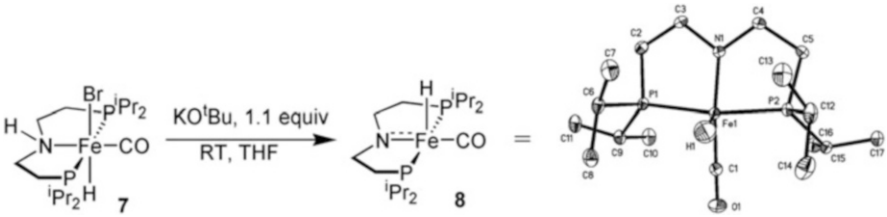

Fig. 2 Structure of catalyst **8** synthesized from **7**

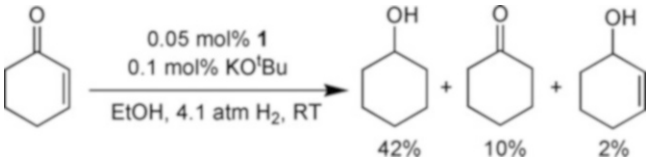

(4)

In 2012, Milstein reported that borohydride catalyst **2** could also be used for ketone hydrogenation at 40°C. The scope of reactivity was similar to that seen using catalyst **1** as precursor [9], but no base is required. The related compound with no CO ligand, but a κ^2-BH_4 ligand, showed no activity. DFT calculations on this system are discussed below.

In 2014, Jones, Hazari, and Schneider reported that the iron PNP pincer complex **6** was active for the hydrogenation of acetophenones (Eq. 5) [10]. Here, the central *N*-donor is a simple secondary amine as opposed to a pyridine as in Milstein's catalyst. An alternative derivative with bromide replacing the BH_4 ligand (**7**) was also equally active with the addition of KO^{t}Bu. In fact, the actual catalytic intermediate **8** could be synthesized, isolated, and characterized by X-ray structural determination [11]. **8** shows a square pyramidal geometry, with a short Fe–N distance of 1.86 Å and a planar nitrogen, indicative of sp^2 hybridization (Fig. 2). **8** forms a labile N–H/dihydride complex upon addition of H_2. This dihydride was proposed to reduce the ketone substrate via a concerted hydride-from-Fe and proton-from-nitrogen heterolytic H_2 transfer.

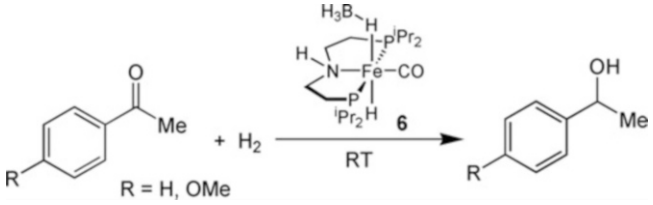

(5)

In 2014, Kirchner reported that derivatives of catalyst **4** in which the N–Me groups are replaced by N–H groups were active for ketone hydrogenation [12]. Replacement of the bromide ligand with a labile group also led to efficient catalysts. As mentioned above, the N–Me complex **4** was selective for aldehydes. Catalyst **9** gave good yields of secondary alcohols with aryl ketones (Eq. 6).

Cyclohexanone was reduced in 30% yield under similar conditions. As seen with Milstein's catalyst, *trans*-4-phenyl-3-buten-2-one also gave a mixture of products, with ketone reduction being about 4× faster than double-bond reduction. The reactions appeared to involve heterolytic dihydrogen cleavage via metal–alkoxide cooperation, with the PNP ligand not being involved in the activation of dihydrogen. The PNP ligand remains deprotonated throughout the catalytic cycle, acting as a strong electron donating anionic ligand. Protic solvent is required for the reduction to take place, with EtOH being the best solvent examined. Ethanol prevents formation of a dihydride species and is proposed to act by stabilization of a 16-electron intermediate via reversible solvent coordination.

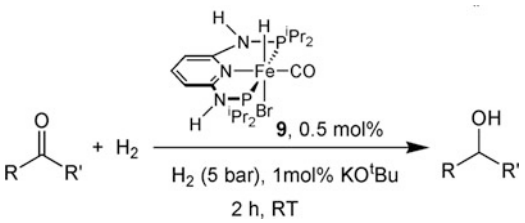

(6)

DFT calculations of Milstein's catalyst for ketone hydrogenation suggested a mechanism slightly varied from the one proposed in Scheme 2 [9]. Species **A** first rearranges (using EtOH solvent) to the aromatic tautomer (Eq. 7), which binds ethanol and then undergoes a simultaneous outer sphere dual-hydrogen transfer from the PNP arm to an incoming acetophenone carbon and the proton of the bound ethanol to the oxygen of the acetophenone ligand. The resulting ethoxide complex then adds H_2 and loses EtOH to regenerate the catalyst **A**. A year earlier, Yang had published a DFT study on this system in which he indicated that a mechanism involving acetophenone insertion into an Fe–H bond to generate an alkoxide was too high in energy [13]. He postulated a direct reduction mechanism, in which there is a direct transfer of hydride from a dihydride complex to the acetophenone carbon from the catalyst and H_2 cleavage by the hydrido–alkoxo complex without participation of the PNP ligand. Yang's study, however, used a simplified version of the catalyst with PMe_2 groups in place of the P^iPr_2 groups. In addition, Yang's mechanism goes by way of a trans-dihydride complex, which Milstein showed was inactive toward reaction with benzophenone.

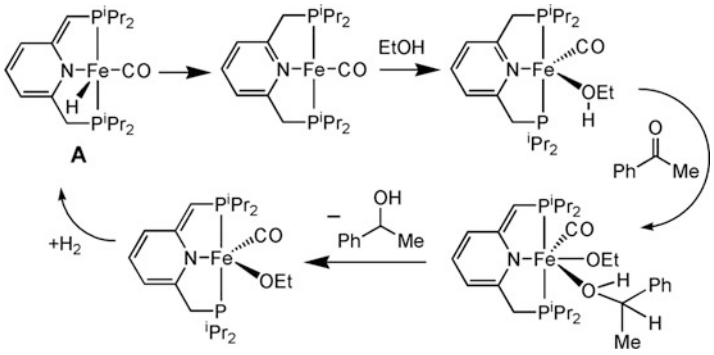

(7)

More recently, Hopmann published in 2017 a comparison by DFT of the Milstein and Kirchner catalysts, **1**, **5**, and **9** [14]. For catalysts **1** and **9**, a dihydride mechanism involving dearomatization of the PNP ligand was predicted, whereas for **5**, which cannot undergo dearomatization, the mechanism shown in Scheme 1 was found to be lowest in energy. The mechanisms for each catalyst proposed in this paper are able to explain the substrate selectivities seen in the reduction of aldehydes and ketones. For **1**- and **9**-mediated ketone hydrogenations, they predicted a reaction pathway involving hydride transfer to the free substrate, formation of an iron–alkoxide intermediate, intramolecular proton transfer from the PNP linker to the alkoxide, alcohol release, H_2 coordination to the dearomatized species, and product-mediated proton-shuttling to the PNP linker, which regenerates the active dihydride species and is rate-limiting (Scheme 3, bottom). The first step of this mechanism is as originally proposed by Yang, but the following steps are different from earlier proposals. For **5**, their

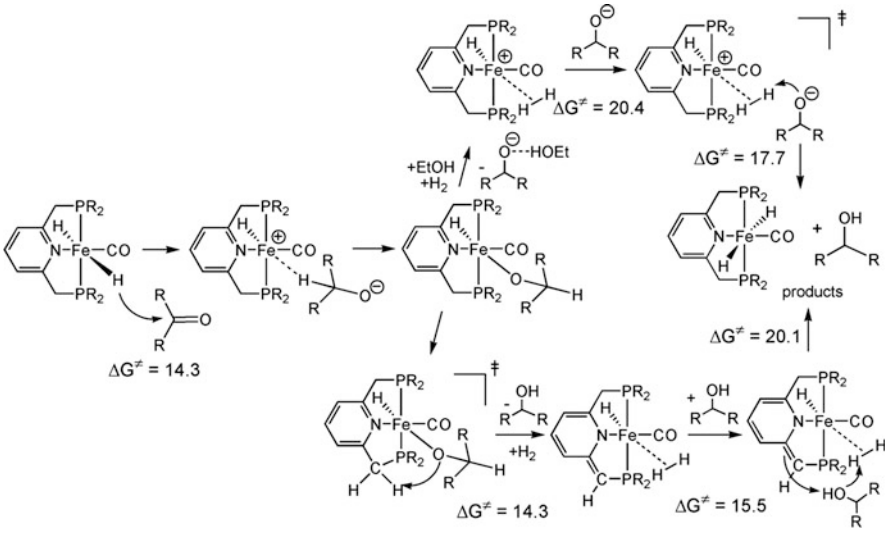

Scheme 3 DFT mechanisms for alcohol dehydrogenation

calculations support the dihydride mechanism proposed by Kirchner and coworkers, based on the original proposal by Yang. **5** forms unstable iron alkoxides, implying that the intrinsically higher reactivity of aldehydes is preserved, explaining the chemoselectivity observed in experiments. **1** and **9** convert the more reactive substrates (aldehydes and activated ketones) into low-energy stable iron alkoxides. The barriers for hydrogenation of these substrates are higher and therefore become similar to those of less reactive substrates, eliminating the expected substrate preferences, in excellent agreement with experiment.

Mezzetti examined an asymmetric derivative of the Milstein catalyst **1** for the hydrogenation of acetophenone [15]. He found that (*S*)-1-phenylethanol is produced with 48% e.e. (Eq. 8). Milstein's mechanism involving direct hydride transfer from the benzylic carbon of the ligand was the only one to reproduce the experimentally observed enantioselectivity and sense of induction.

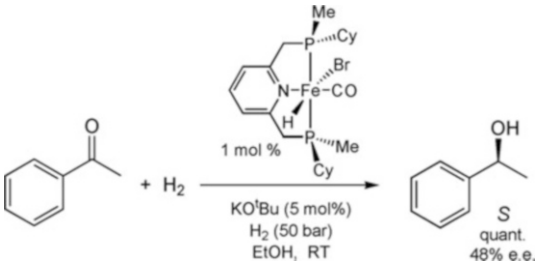

(8)

Finally, Ikariya examined an NNN pincer complex **10** for the reduction of acetophenone [16]. While the ruthenium complex gave alcohol in 36% yield, the iron complex was unreactive (Eq. 9).

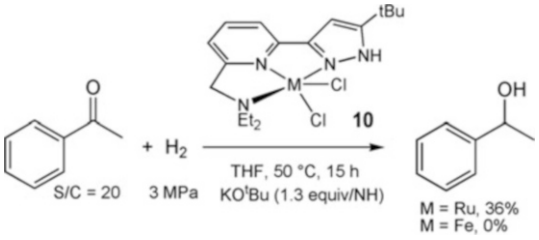

(9)

3 Dehydrogenation of Alcohols

In 2014, Hazari, Jones, and Schneider reported the dehydrogenation of primary and secondary alcohols to give esters and ketones, respectively, using the iron PNP catalyst **6** (Eqs. 10 and 11) [10]. The dehydrogenation proceeds without an acceptor, and hydrogen is removed under a slowly moving stream of nitrogen in order to drive this thermodynamically uphill reaction. Benzylic alcohols are converted in good

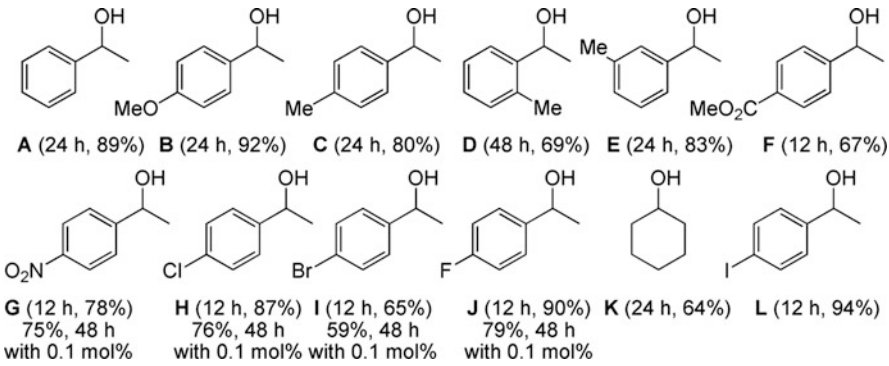

Fig. 3 Dehydrogenation of alcohols by **6**

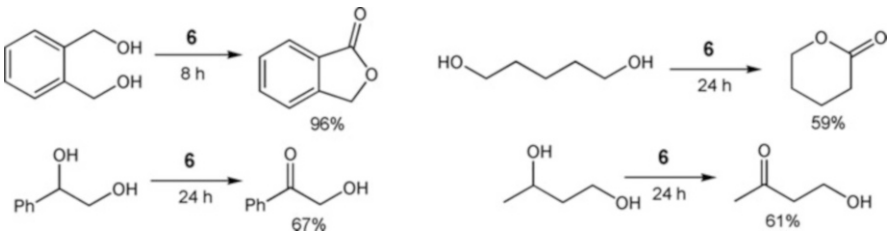

Scheme 4 Dehydrogenation reactions of diol substrates by **6**

yields with both electron-donating and electron-withdrawing substituents on the arene. Cyclohexanol is also dehydrogenated to cyclohexanone, albeit a bit more slowly (Fig. 3). Primary alcohols are dehydrogenated to give esters, as the aldehyde intermediates can form hemiacetals that are then rapidly dehydrogenated. High yields are obtained in refluxing toluene using only 0.1% catalyst loading. Use of diols leads to lactone formation, where possible. A preference is seen for dehydrogenation of secondary alcohols over primary alcohols (Scheme 4).

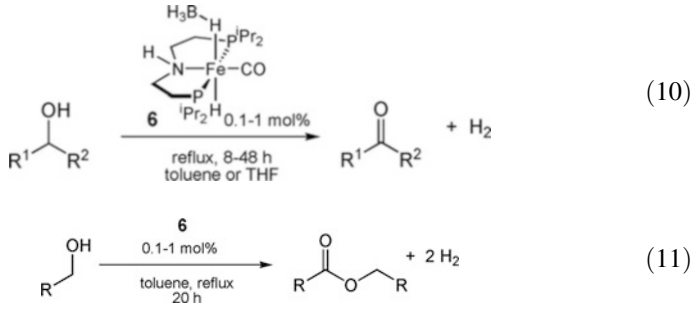

The Schneider group examined methanol dehydrogenation by DFT [10] and found strong energetic preference for a mechanism involving catalytic intermediate

8 undergoing heterolytic concerted transfer of H_2 to make formaldehyde, which rapidly formed hemiacetal. Hemiacetal dehydrogenation occurred via a similar pathway, but the heterolytic dehydrogenation was stepwise (proton transfer before hydride transfer), rather than concerted. Elimination of H_2 from (PNP)Fe(CO)H_2 was assisted by the participation of methanol in a 6-membered transition state.

As dehydrogenation is thermodynamically uphill, the reverse reaction, hydrogenation, is thermodynamically downhill. Hydrogenation of acetophenone by catalyst **8** occurred readily at room temperature giving quantitative yields of alcohol. Hydrogenation of ketones is selective, as reduction of 5-hexene-2-one gives exclusively the unsaturated alcohol and reduction of α,β-unsaturated ketone exhibits high selectivity for hydrogenation of ketone over C–C double bond (7:1).

Interestingly, Yang had predicted the ability of catalytic intermediate **8** to readily dehydrogenate alcohols by DFT prior to the above experimental report [17]. The calculations used ethanol as the substrate, producing acetaldehyde via the same pathway as found by Schneider for methanol dehydrogenation. While most of the paper dealt with the established Ru–MACHO catalyst [18], extension to the iron derivative **8** was made and found to be energetically accessible (although thermodynamically uphill by ~10 kcal/mol).

In 2015 Bonitatibus reported the dehydrogenation of alcohols using an Ir(dach) catalyst (**11a/11b**, first reported by Königsmann et al. [19]) in terms of separately extracting protons and electrons that used stoichiometric oxidants combined with a weak base [20]. Here, stoichiometric benzyl alcohol oxidation could be effected using ferrocenium as oxidant and phenoxide as proton acceptor. Reduction of the aldehyde could be effected with cobaltocene as reductant and phenol as proton donor (Scheme 5). These results were presented as being of importance for the development of reversible dehydrogenation electrocatalysts and, ultimately, the application of such catalysts in regenerative liquid fuel cells using chemically bound hydrogen for energy storage.

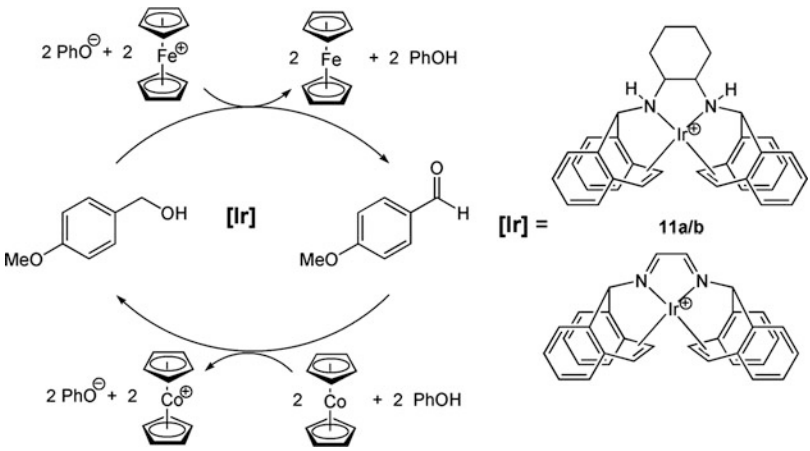

Scheme 5 Oxidative dehydrogenation of alcohols by **11a/11b**

In dehydrogenation chemistry related to that shown in Scheme 4 above, Beller reported extended studies of diol dehydrogenation to make lactones using (PNP)Fe catalyst **6** [21]. About 20 examples were reported (Eq. 12), as well as 9 examples of lactam formation from α,ω-aminoalcohols (Eq. 13). The reaction features high atom economy, as molecular hydrogen is the only stoichiometric by-product and two sequential dehydrogenation reactions can be performed in the absence of external oxidants.

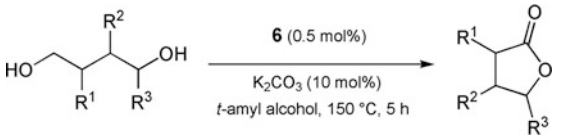

(12)

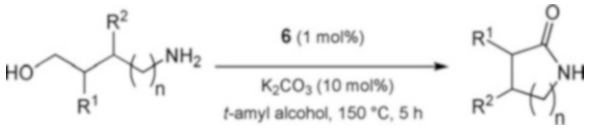

(13)

In 2017 Gauvin reported the dehydrogenation of primary alcohols by a variety of PNP iron and manganese catalysts to produce carboxylic acid salts (Eq. 14). The catalytic conditions were optimized for the acceptorless dehydrogenative coupling (ADC) of 1-butanol and water to butyric acid salt. The iron catalyst **6** was found to be a better catalyst than its manganese analog [22].

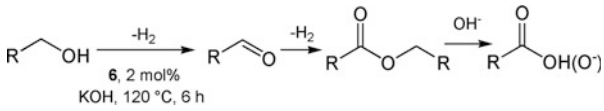

(14)

Hazari and Crabtree reported the dehydrogenation of glycerol to lactic acid using (PNP)Fe catalyst **6** [23]. This system gives superior selectivity compared with previous heterogeneous systems, but further improvements are needed to match the activity of homogeneous precious metal catalysts. The proposed mechanism involves initial primary alcohol dehydrogenation followed by dehydration/rehydration steps (Scheme 6).

4 Hydrogenation of Esters

Following on their success with the use of iron pincer complexes **1** and **2** for ketone hydrogenation, Milstein examined the use of the related $^{t}Bu_2P$-dihydride catalyst **12** for ester hydrogenation [24]. For esters where the keto group is attached to CF_3, they found that a wide range of esters could be hydrogenated to give CF_3CH_2OH and RCH_2OH in yields of 80–99% at H_2 pressures of 360 psi (Eq. 15). The proposed mechanism involved addition of the Fe–H bond across the ester C–O bond and

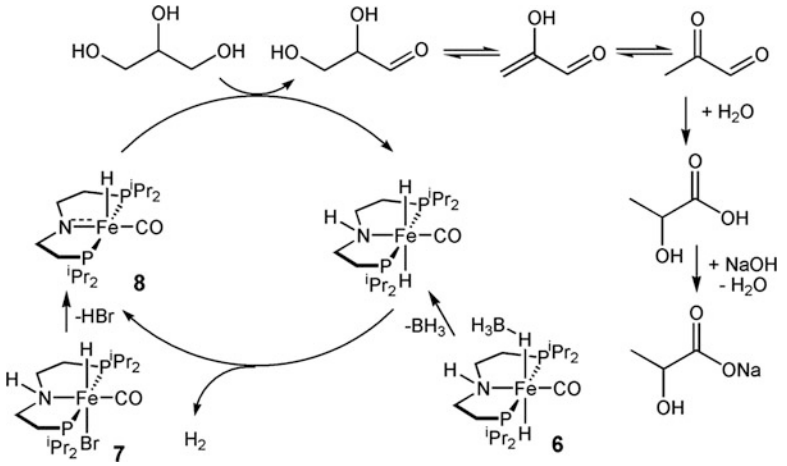

Scheme 6 Proposed mechanism for glycerol conversion to lactic acid with **8**

elimination of the hemiacetal using a hydrogen from the PNP ligand arm. The acetal then eliminated RCH_2OH while forming CF_3CHO. The latter was hydrogenated to give trifluoroethanol. The catalyst **12** is regenerated by the addition of hydrogen through metal–ligand cooperation.

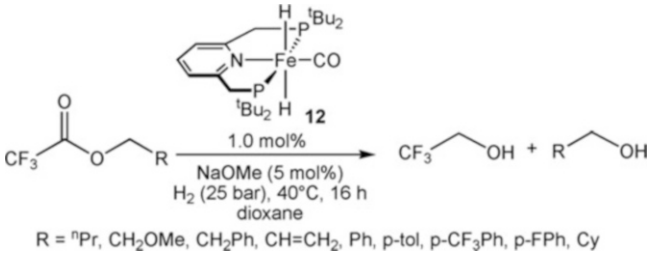

(15)

For comparison, Lefort and Pignataro reported an easy to make benchtop stable non-pincer cyclopentadienone iron catalyst for hydrogenation of trifluoroacetate esters [25]. For unactivated ester, however, no reduction was observed (Eq. 16).

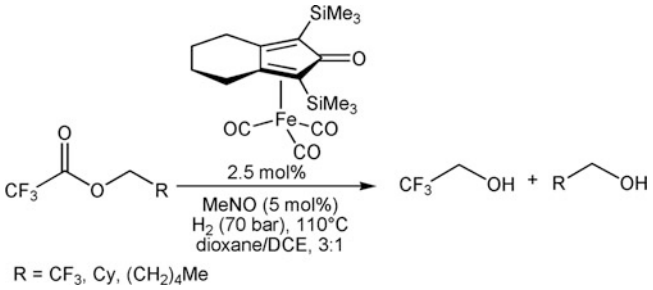

(16)

Another report appeared in 2014 by Guan et al. in which a PNP catalyst **6** was used for ester hydrogenation [26]. With this catalyst, a wide variety of methyl and ethyl esters were hydrogenated in yields of 50–95% (Eq. 17). The reaction required less pressure than the Milstein catalyst described above. The true catalyst was proposed to be the species **8** and its dihydride analog, as described above in ketone hydrogenation. However, the ester hydrogenation was reported first. Also, Beller reported almost the same ester hydrogenations using the same catalyst (**2**) at about the same time [27]. Guan also submitted a patent on this work [28].

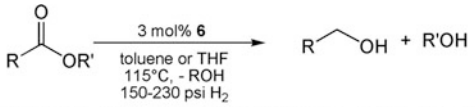

R = Ph, p-CF_3Ph, p-MeOPh, p-ClPh, p-MeO_2CPh, n-heptyl, Cy, CH_2Ph, cinnamyl;
R' = Me, Et, CH_2Ph

(17)

Beller also published a paper comparing the activity of three derivatives of these types of PNP catalysts in which the phosphine was substituted with ^{i}Pr (**6**), cyclohexyl (**13**), or Et (**14**) groups (Eq. 18). For the hydrogenation of methyl benzoate, 30 bar H_2 pressure was needed to obtain reasonable yields [29]. Table 1 shows that the PEt_2 derivative is most reactive, followed by the $P^{i}Pr_2$ catalyst, and finally by the PCy_2 catalyst. Complex **14** could even hydrogenate the ester at 40°C, albeit in lower yield. Lower H_2 pressures also resulted in lower yields. A variety of other esters were also found to be hydrogenated by **14**. Conjugated C–C double bonds were also hydrogenated (e.g., methyl cinnamate), while non-conjugated C–C bonds were untouched.

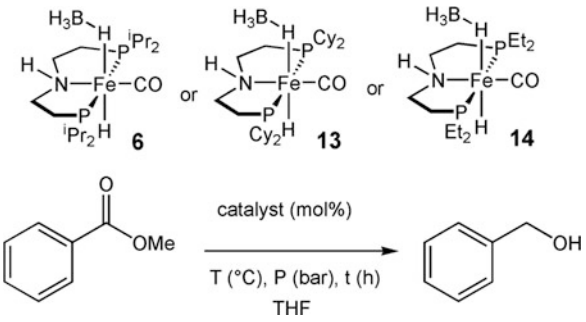

(18)

Table 1 Reduction of methyl benzoate with iron pincers

Entry	Catalyst (mol%)	P (bar)	T (°C)	t (h)	Yield (%)
1	**6** (1)	30	60	6	50
2	**13** (1)	30	60	6	30
3	**14** (1)	30	60	6	99

Methyl benzoate (0.5 mmol), **1**, **13**, **14** (0.005 mmol), THF (1 mL)

Prior to the above reports, Yang published in 2012 a DFT study [30] on the hydrogenation of dimethyl carbonate to methanol using an iron PNN catalyst **15** (Eq. 19). This study was based on experimental work by Milstein [31] using a related PNN ruthenium catalyst, which Yang also investigated by DFT. **15** was predicted to have a barrier for catalytic hydrogenation that was 3.4 kcal/mol lower than its Ru analog, but an experimental investigation with this catalyst has not appeared yet.

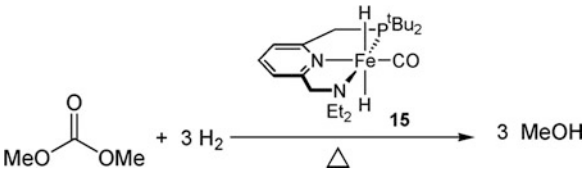

(19)

Guan also published DFT results on using complex **6** for hydrogenation of methyl benzoate to methanol and benzyl alcohol [32]. A key finding was activation of **6** to produce the dihydride by loss of BH_3. He found that addition of NEt_3 could promote this activation, allowing full conversion under conditions where only 50% yield could be obtained without NEt_3. The reaction was found to proceed via a hemiacetal intermediate, which decomposed to benzaldehyde and methanol. Two other pathways were examined and found to be higher in energy. Beller also examined this catalyst using DFT but also made a comparison of the Fe, Ru, and Os derivatives [33]. The ruthenium complex was found to be the most effective catalyst for ester reduction, followed by the iron and then the osmium complex. The ruthenium catalyst was found to be best for benzaldehyde reduction, in agreement with experiment.

5 Hydrogenation/Dehydrogenation of Nitriles and Imines/Amines

Catalyst precursor **6** was also reported by Beller to be capable of the reduction of nitriles to amines. The scope of the substrates included aryl, alkyl, heterocyclic nitriles, and dinitriles [34]. Ester, ether, acetamido, and amino substituents were not reduced in the presence of nitriles (Eq. 20). The primary amine products were obtained as ammonium salts by protonation during workup after hydrogenation. Adiponitrile was hydrogenated to 1,6-hexamethylenediamine, constituting the first homogeneous catalyst for this selective hydrogenation.

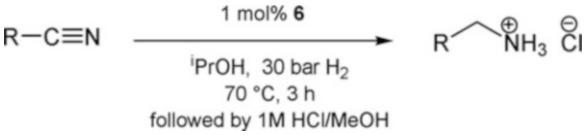

(20)

A subsequent investigation using PCy_2 and PEt_2 catalysts **13** and **14** revealed that the cyclohexyl derivative was comparable to the isopropyl derivative but that the ethyl derivative was not as effective, especially at catalyst loadings of <1% [35]. DFT calculations indicated that **14** should have the fastest rate for acetonitrile reduction, but experiments indicate that the lower stability of the complex (especially at low loadings) leads to it being a worse catalyst. Additional DFT studies compared the Fe, Ru, and Os derivatives [33]. Both the iron and ruthenium complexes were found to be competent catalysts for ester reduction, whereas the osmium complex was predicted to have a significantly higher barrier.

Milstein reported a different PNP catalyst **16** that could reduce nitriles to secondary imines [36]. High conversions and yields were obtained with aryl nitriles, although in a few cases, some hydrogenated imine and trimerized products were observed. Moderate yields were obtained with aliphatic nitriles, even at extended reaction times, and $NaHBEt_3$ could be employed in place of ^{t}BuOK (Eq. 21). The reaction proceeds by hydrogenation of nitrile to imine and amine, followed by condensation of these two products to give an aminal. Ammonia is liberated as a by-product of aminal decomposition to produce the secondary imine.

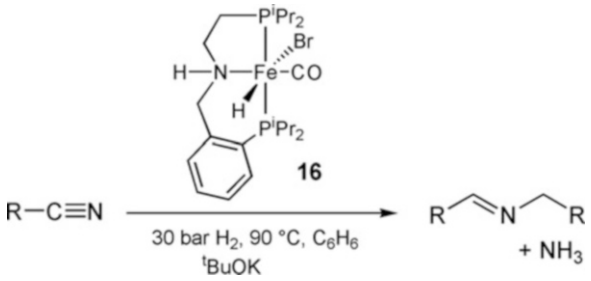

(21)

Milstein also reported the hydrogenative coupling of nitriles with amines to give secondary imines [37]. Here, catalyst **16** was employed to give cross-imines exclusively (Eq. 22). Only traces of self-coupled products were observed. The reaction proceeds via nitrile hydrogenation to form imine, which then makes the cross-aminal to yield the cross-imine selectively.

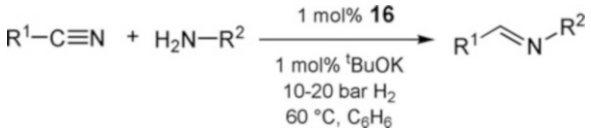

(22)

Amine dehydrogenation has been identified as a possible hydrogen storage alternative [38]. Jones reported that iron PNP catalyst **6** could be used for the dehydrogenation of nitrogen-containing heterocycles by allowing for the escape of hydrogen in this thermodynamically uphill reaction [11]. Here, tetrahydroquinolines and isoquinolines were readily dehydrogenated to give their aromatic counterparts in high yield (Eq. 23). Temperatures of ~140°C were also required to drive this

reaction. Dihydroindole and piperidine were dehydrogenated to indole and pyridine, respectively, at a slightly reduced rate. The thermodynamically favorable hydrogenation reactions could be effected at 80°C with 5–10 atm H_2 pressure using the hydrido bromide precursor to the catalyst (Eq. 24). Mechanistic studies revealed that tetrahydronaphthalene and dihydronaphthalene were not dehydrogenated, indicating a pathway involving heterolytic amine dehydrogenation to make imines, which then isomerized to permit a second equivalent of H_2 to be eliminated.

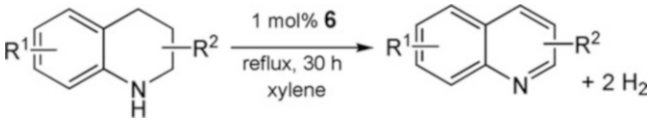

(23)

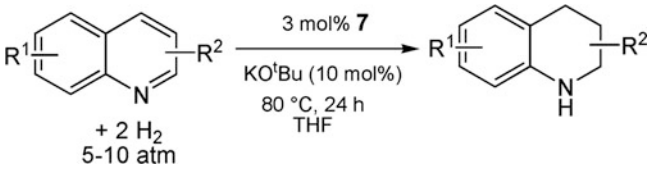

(24)

Surawatanawong investigated the mechanism of tetrahydroquinoline dehydrogenation by DFT using the active catalytic species **8** [39]. The dehydrogenation involves two main steps: (1) dehydrogenation of tetrahydroquinolines to 3,4-dihydroquinoline and (2) dehydrogenation of 3,4-dihydroquinoline to quinolone. The isomerization of 3,4-dihydroquinoline to 1,4-dihydroquinoline or 1,2-dihydroquinoline was found to be unnecessary, as **8** can dehydrogenate the C3–C4 bond of 3,4-dihydroquinoline directly (barrier = 22.8 kcal/mol). A separate report by Jones investigated the related dehydrogenation of piperidine to pyridine using **8** [40], but here isomerization to allow dehydrogenation of the N–C bond was required.

6 Hydrogenation of Amides

Langer prepared a series of five (^{R}PNP)FeH(CO)(BH_4) complexes analogous to **6** where the phosphine arms were substituted with ^{t}Bu, Cy, ^{i}Pr, Et, and Ph and examined them for amide hydrogenation [41]. Bulky ligands and less electron-donating ligands were found to result in catalyst instability to give deactivated products. The PEt_2-substituted catalyst **14** was found to be very effective for the hydrogenation of *N*-aryl benzamides to give anilines plus benzyl alcohols (Eq. 25). *N*-Methyl benzamide was only marginally reactive, but *N,N*-dimethyl benzamide showed about 50% conversion. δ-Lactams were not hydrogenated (6-membered ring), but γ-lactams (5-membered ring) were easily hydrogenated to aminoalcohols in good yield (Eq. 26). Catalyst **14** also proved superior to **6** for ester hydrogenation. Sanford also used this catalyst to hydrogenate formamides [42], and Bernskoetter

showed that the catalyst loading could be substantially reduced in amide reductions if traces of formamide were added [43].

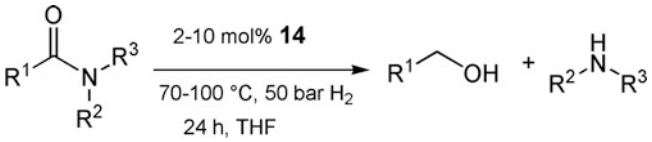

(25)

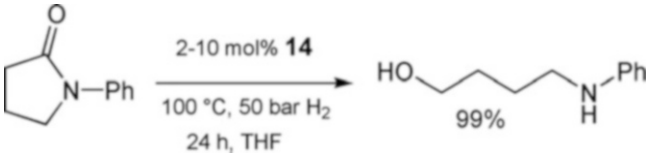

(26)

Milstein also reported that his PNP catalyst **1** with P^iPr_2 arms proved effective for hydrogenation of activated amides [44]. In particular, 2,2,2-trifluoro-*N*-phenylacetamide was hydrogenated using potassium hexamethyldisilazide (KHMDS) as base and 60 bar H_2 at 140°C. *N*-aryl amides gave good yields (Eq. 27), whereas *N*-alkyl amides gave only moderate yields of reduction products (25–35%). P^tBu_2 derivative **12** proved ineffective for this catalysis, but the BH_4 adduct of **1**, catalyst **2**, showed similar reactivity as **1**. The mechanism was thought to be similar to that proposed for trifluoromethyl-ester reduction.

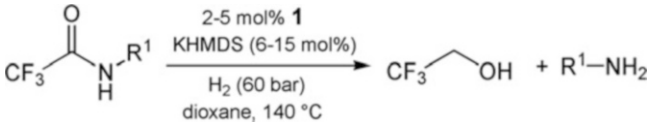

(27)

In related work, Kirchner found that benzyl alcohols can be dehydrogenated in the presence of amines to efficiently give secondary amines using iron catalyst **9** [45]. Isoelectronic manganese catalysts were also effective but produced imines rather than secondary amines. The reactions proceed without the addition of base, but molecular sieves are required to remove water. The mechanism involves alcohol dehydrogenation to make an aldehyde, which then condenses with the amine to give an imine that is hydrogenated when the iron catalyst is employed (Eq. 28).

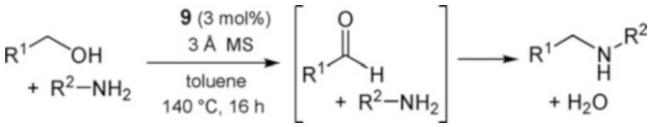

(28)

7 Hydrogenation of CO_2 and Formic Acid Dehydrogenation

These topics are being treated in other chapters in this book, so only a few representative examples will be presented here. The interested reader is referred to these other chapters for a fuller discussion.

In 2011, Milstein reported the use of iron PNP catalyst **12** for CO_2 reduction to formate [46]. He followed this with a report using pyrazine in the backbone (**17**) for CO_2 reduction [47]. Activation with base allows for the catalytic formation of sodium formate (Eq. 29). The activation proceeds by deprotonation of one of the $CH_2P^tBu_2$ arms and loss of chloride. Hydrogenation of CO_2 to formic acid is uphill thermodynamically, so this reaction must be driven to completion by deprotonation of the acid. The distal nitrogen in the pyrazine ring was found to stabilize unsaturated intermediates by coordination to a second iron center, forming 6-membered cyclic chains.

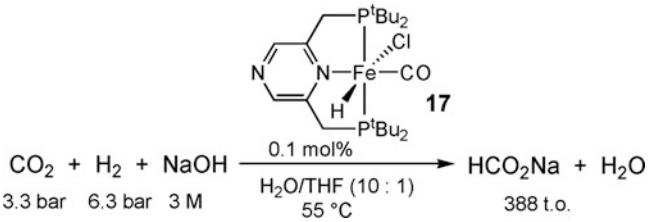

(29)

Bernskoetter and Hazari have used an iron PNP catalyst **8** for CO_2 hydrogenation to formate [48]. The catalyst uses DBU as the base to drive the reaction, as it is compatible with the catalyst. Lewis acids (Li^+, Na^+, K^+) were found to enhance the turnover numbers, giving over 3,000 turnovers with LiOTf with the PCy_2 variant of the catalyst. Use of a variant of catalyst **6** with a methyl group attached to the backbone nitrogen, **18**, led to impressive turnover numbers of 59,000 (Eq. 30). Use of a variant of catalyst **8** with CNxylyl replacing CO proved to be about 10× less reactive [49].

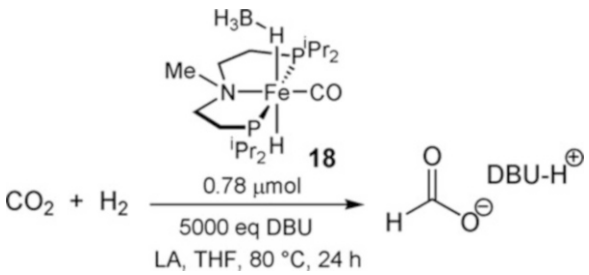

(30)

As a last representative, Milstein reported the use of catalyst **12** for the catalytic dehydrogenation of formic acid to CO_2 and H_2 [50]. Using NEt_3 as co-catalyst,

2,000 turnovers could be obtained (Eq. 31). The mechanism proceeds via protonation of **12** to generate a dihydrogen complex which then loses H_2 and coordinates formate. Decarboxylation leads directly back to **12**. This decarboxylation was proposed to occur via dissociation of formate and subsequent recoordination through the formyl hydrogen atom. Hydride transfer leads to **12** and CO_2.

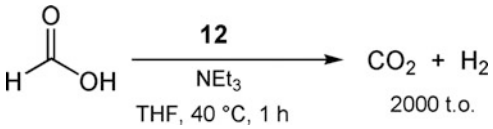

(31)

8 Hydrogenation of Alkenes and Alkynes

The efficient, mild hydrogenation of olefins by an iron complex was first reported by Chirik in 2004 using a pyridinediimine (PDI) pincer ligand [51]. The catalyst **19** effects hydrogenation of a variety of unactivated olefins with turnover frequencies as high as 1,800 h^{-1} at RT and 1 atm H_2 (Eq. 32). This work was extended to include olefins with oxygen and nitrogen containing functional groups with similar reactivity, although α,β-unsaturated ketones were observed to induce catalyst decomposition [52]. Examination of six different pyridinediimine derivatives in which steric and electronic effects of the aryl group of the PDI are varied showed that the more electron-rich iron dinitrogen complexes are effective for the catalytic hydrogenation of unfunctionalized alkenes [53].

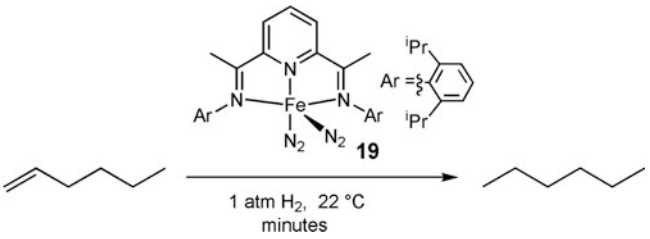

(32)

Jones examined the use of catalyst **8** for the hydrogenation of activated olefins [54]. Styrenes were reduced at room temperature in good yields (Eq. 33). The electronic effects of the arene showed dramatic changes in the rate of reaction, with electron-withdrawing groups (e.g., CF_3) dramatically increasing the rate and electron-donating groups (e.g., OMe) dramatically slowing the rate. DFT analysis of the mechanism indicated a metal–ligand cooperative stepwise hydride/proton transfer pathway (Fig. 4). The strong rate effects of donating/withdrawing groups are consistent with this mechanism. 2-Vinylpyridine was rapidly hydrogenated, and benzylideneacetone showed the ketone to react about 10× faster than the α,β-unsaturated double bond (Eq. 34).

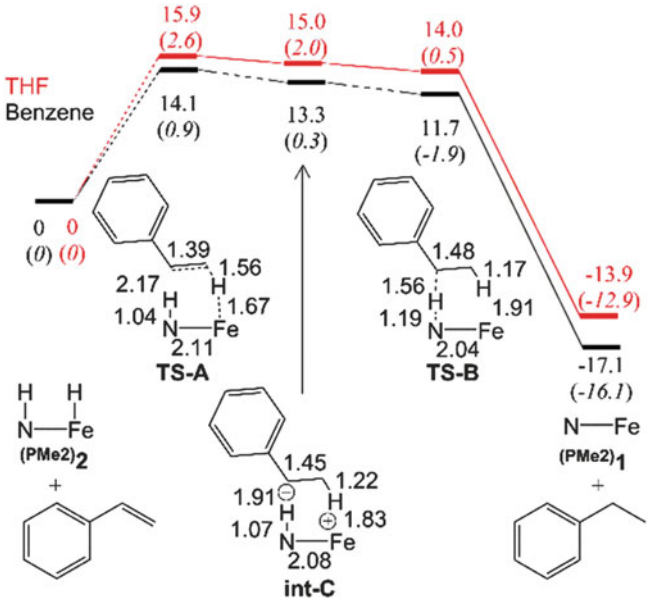

Fig. 4 Calculated potential energy diagram for the hydrogenation of styrene in benzene (lower path) and THF (upper path) by ^{PMe2}**6**. Free energies (enthalpies) are given in kcal/mol at STP (Reproduced with permission from [54], ©2016 ACS)

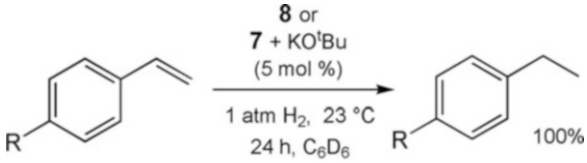

(33)

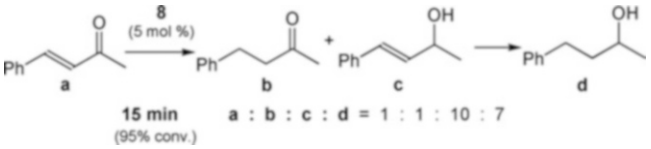

(34)

Alkynes have also been reported to be reduced by iron pincer catalysts. Milstein found that alkynes are "semi-hydrogenated" to alkenes using an acridine-based iron pincer catalyst **20** [55]. Curiously, *E*-alkenes are produced almost exclusively with a dozen different alkynes (Eq. 35). The high *E* selectivity was found to be due to rapid isomerization of the initial *Z*-olefins to the corresponding *E*-olefins. When *Z*-stilbene was stirred at 90°C with 0.6 mol% catalyst in the absence of H_2, it isomerized to *E*-stilbene.

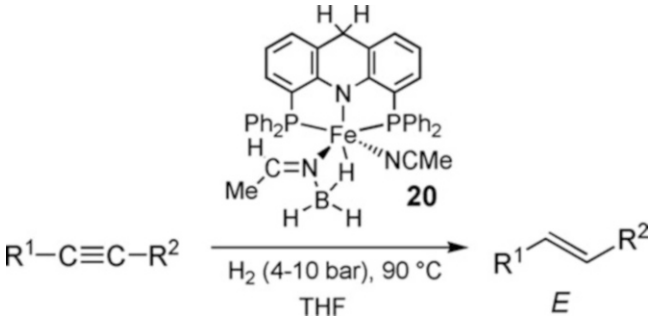

(35)

9 Olefin Hydroboration and AB Dehydrogenation

Several reports have appeared describing the addition of pinacolborane to olefins using iron pincer catalysts. Huang reported a novel PNN pincer complex **21** that served as a catalyst precursor for anti-Markovnikov hydroboration of terminal olefins with excellent efficiencies and low catalyst loadings [56]. The catalyst is activated by reduction with triethylborohydride and is far more efficient than known noble metal systems for this reaction (Eq. 36). He extended the ability to form terminal pinacolborane derivatives from *internal* olefins by combining the iron catalyst with a similarly ligated PCN–iridium catalyst that could effect double-bond isomerization, allowing the iron to capture the terminal olefin for hydroboration [57].

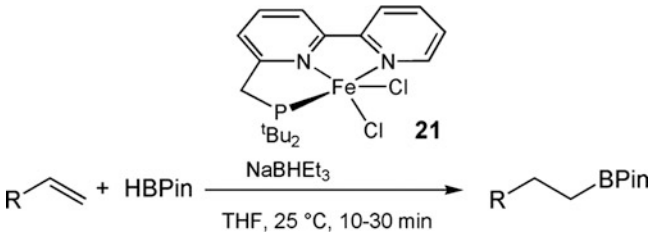

(36)

Sabo-Etienne and coworkers reported the hydroboration of styrene using an iron PCP catalyst [58]. Upon photolysis to remove CO, the iron POCOP catalyst **22** results in the dehydrogenative borylation of styrene. Only small quantities of the saturated HBpin addition product or ethylbenzene were observed (Eq. 37).

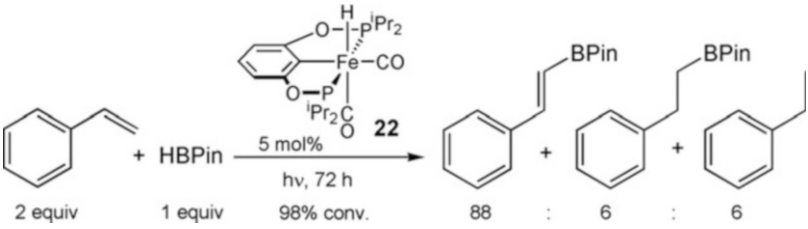

(37)

Ammonia borane is also dehydrogenated by iron POCOP complexes. Guan reported conversion of NH_3BH_3 to dehydrogenated material with the liberation of 2.3–2.5 equiv. H_2, making these the best for any known iron-based catalyst [59]. Of the three POCOP systems investigated, catalyst **23c** gave the highest conversion rates, although by only a slight amount (Eq. 38). Kinetic studies showed that the reaction was first order in iron, but zero order in $[NH_3BH_3]$, suggesting the rapid formation of an adduct with the substrate that then undergoes a unimolecular rate-determining reaction. In fact, stoichiometric experiments showed the formation of a B–H–Fe adduct. Isotope effect experiments with ND_3BD_3, ND_3BH_3, and NH_3BD_3 were consistent with both N–H and B–H bonds being broken simultaneously.

(38)

DFT calculations on this system (with P^iPr_2 replaced by PMe_2) were reported by Ushiyama [60]. He found that the barrier to dehydrogenation of NH_3BH_3 was very low (4.6 kcal/mol) for the p-MeO/PMe_2Ph derivative **23c**. They indicated that the bulky PMe_2Ph ligand repels neighboring methyl groups, allowing the AB to more easily hybridize from a staggered conformer to a planar NH_2BH_2 by releasing a proton and hydride. Subsequent dehydrogenation steps were not calculated. A second DFT study on this system appeared shortly afterward by Yang in which the B–H hydrogen moves to the iron as the N–H proton moves to the ipso carbon of the pincer ligand [61]. This pathway was found to have a barrier of 17.6 kcal/mol (Eq. 39).

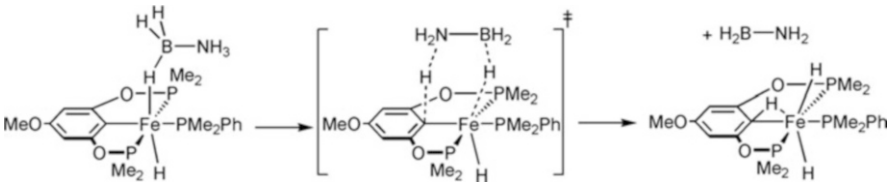

(39)

10 Asymmetric Hydrogenation of Ketones and Aldehydes

The use of pincers has been examined by several groups, but the group of R. Morris at Toronto has led the way with 3- and 4-coordinate pincers. A variant of catalyst **8** has been prepared in which the PCP ligand is deprotonated and one of the backbone arms has been made chiral (**24**) [62]. A variety of acetophenones were reduced to give products in ~90% yield and with e.e.s of ~80% (Eq. 40). TOFs of 1,000–2,000 h^{-1} were typically seen with TONs of ~1,000. Morris also performed DFT calculations on this catalyst in which outer sphere ketone reduction was proposed. The barriers for hydride attack on the ketone and H_2 splitting were close and either hydride transfer or dihydrogen splitting could determine the turnover frequency depending on the nature of the ketone [63].

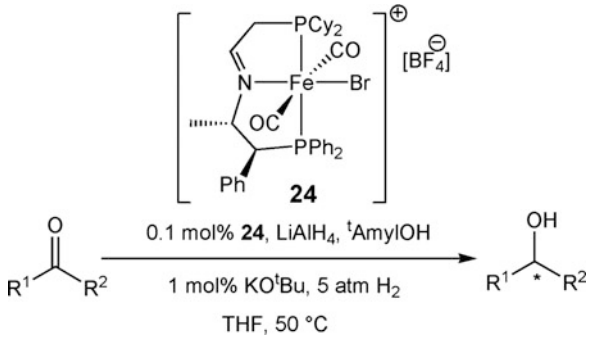

(40)

Kirchner reported hydrogenation of several acetophenone derivatives using a chiral version of catalyst **9** [64]. Here, one of the P^iPr_2 groups is replaced by a P-(*R*)-BINEPINE moiety. The catalyst was obtained as a mixture of two diastereomers (~1:1) and showed acceptable activity under mild conditions (5 bar H_2, room temperature) with yields up to 99% within 18 h (Eq. 41). However, as both diastereomers were present, no enantioselectivity was observed.

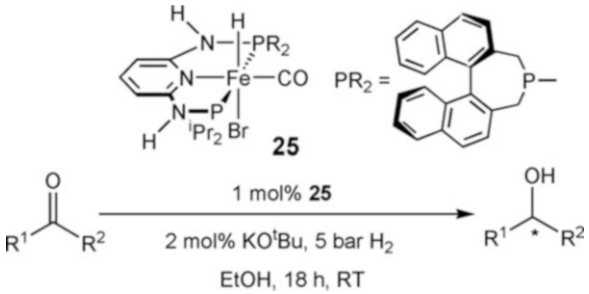

(41)

Between 2008 and 2013, Morris reported a series of articles in which tetradentate ligands on iron were examined for asymmetric ketone reductions. While these ligands are technically not pincers, they are mentioned briefly here because of their similarity to the abovementioned catalysts. The tetradentate ligands are of the PNNP variety, analogs of the Jacobsen-type ONNO epoxidation catalyst ligands. The first foray into this type of asymmetric ketone hydrogenation resulted in low e.e.s in ketone reductions using catalyst **26** (Eq. 42) [65]. Replacement of CO with CN^tBu gave higher e.e. (76%) with acetophenone. Transfer hydrogenation from ^{i}PrOH was also demonstrated with e.e.s of 80–99% with $PXyl_2$ groups on the ligand [66]. Ketimines could also be reduced by transfer hydrogenation [67].

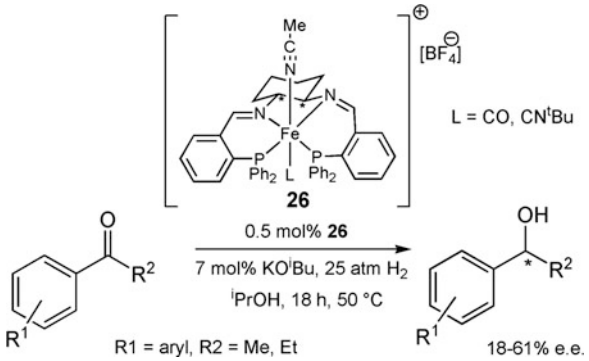

(42)

This ligand was "stripped down" to its backbone without aryl groups in the arms to give a PNNP catalyst that was very good for asymmetric transfer dehydrogenation of acetophenones (Eq. 43) [68]. Use of PEt_2 groups in the ligand permitted activation of the catalyst without addition of base [69]. The ligand was found to be non-innocent in these hydrogenations [70], with an outer sphere reduction of ketone being performed from an H–N–Fe–H moiety [71].

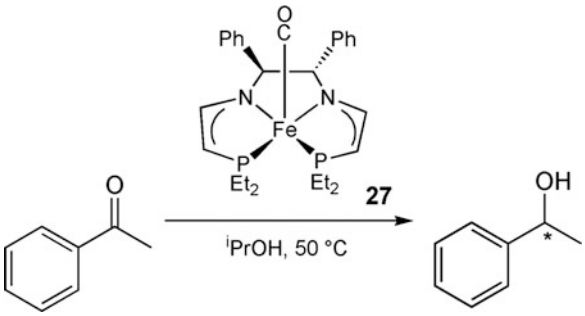

(43)

11 Hydrosilation, C–O Cleavage, and Ether Oxidation

Iron pincers can be efficient aldehyde and ketone hydrosilation catalysts. The PSiP catalyst **28** operates at 60°C to give the siloxane, which is then cleaved with a basic methanolic workup to yield the alcohol (Eq. 44) [72].

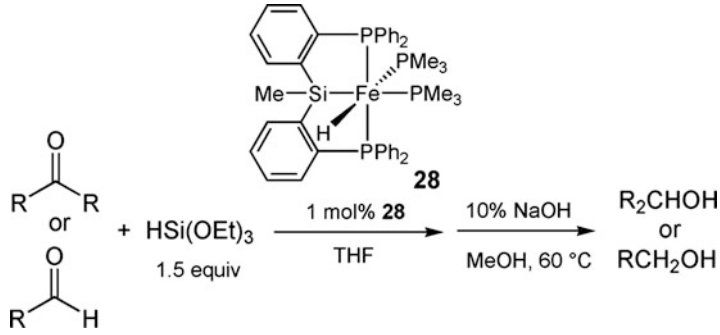

(44)

Chirik reported that iron pyridinediimine complex **19** could cleave certain C–O bonds in ethers and esters [73]. For example, catalyst **19** was found to react with diallyl ether to give an allyloxy derivative and a π-allyl adduct (Eq. 45). Allyl ethyl ether gave the same π-allyl product plus and ethoxide complex (Eq. 46). Ethyl vinyl ether also gives the ethoxide complex, but the fate of the vinyl group could not be determined.

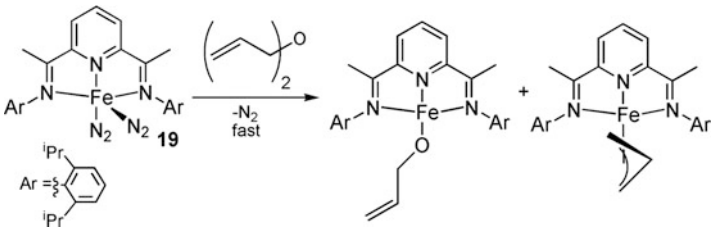

(45)

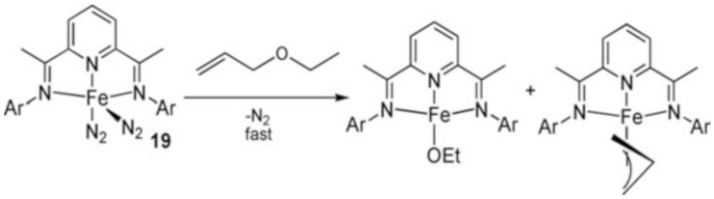

(46)

Similarly, esters undergo C–O cleavage [73]. Allyl acetate reacts with **19** to give a κ^2-acetate complex and the π-allyl complex (Eq. 47). Methyl acetate and benzoate produce the κ^2-carboxylate complexes and the (PDI)Fe–Me derivative (Eq. 48). Vinyl acetate produces the Fe(II) oxidative addition adduct (PDI)Fe(CH=CH_2)(κ^2-OAc) (Eq. 49). Phenyl acetate produces the phenoxide adduct and the methyl complex, with expulsion of CO (Eq. 50). Other acetates give mixtures of ester and acyl C–O cleavage products (Scheme 7).

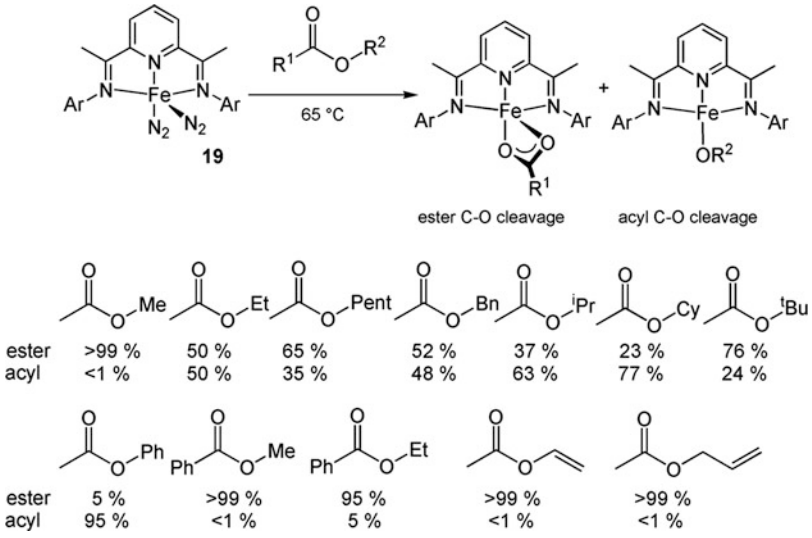

Scheme 7 C–O selectivity in ester cleavage by **19**

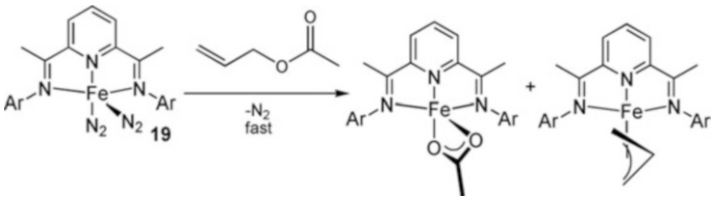

(47)

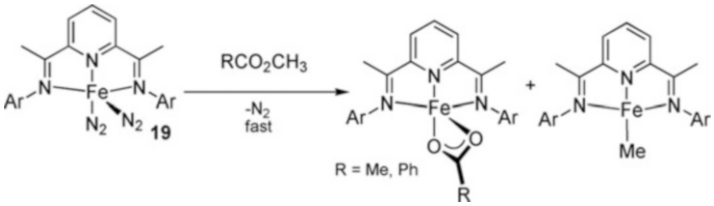

(48)

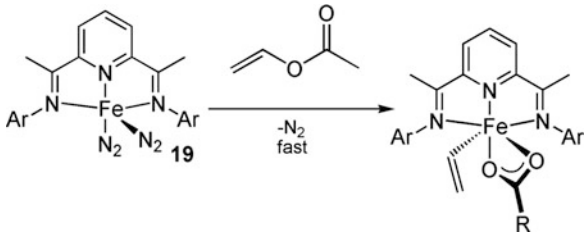

(49)

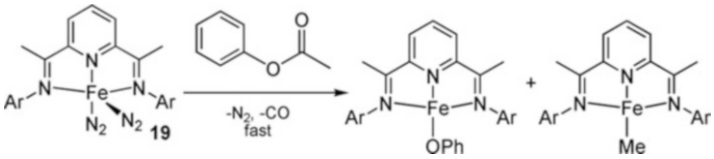

(50)

Xiao found that an NNN iron pincer complex **29** that catalyzed the α-oxidation of ethers using air [74]. Interestingly, unlike metalloenzymes, H_2 is the only by-product (Scheme 8). Mechanistic investigation provided evidence for a two-step reaction pathway which involves dehydrogenative incorporation of O_2 into the ether to give a peroxobisether intermediate. Cleavage of the peroxy bond forms two ester molecules, releasing a stoichiometric quantity of H_2 gas in each step. GC analysis established the stoichiometric formation of H_2. Tetrahydrofurans were converted to lactones (Eq. 51), and isochromans were converted to isochromanones (Eq. 52). Phthalans were oxidized to phthalides (Eq. 53).

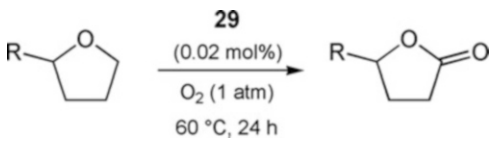

(51)

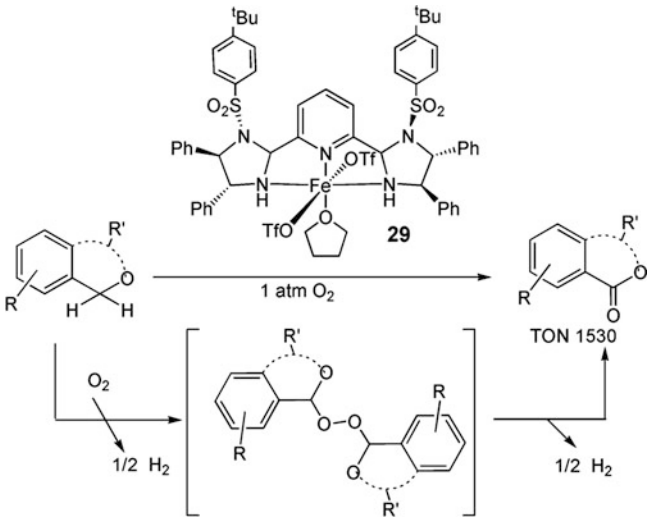

Scheme 8 Oxidation of furans and isochromans

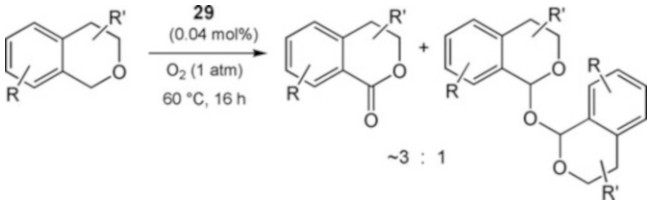

(52)

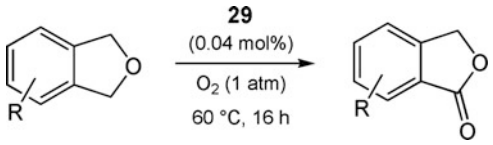

(53)

12 Reviews

A number of reviews covering portions of the above chemistry have appeared in recent years:

- Guan published a review on the synthesis and catalytic applications of iron pincer complexes [75].
- Kirchner reviewed the hydrosilation of ketones and aldehydes using iron pincer PCP catalysts in an article that included Fe, Co, Ni, and Mo catalysts [76].
- Chirik reviewed Fe and Co alkene hydrogenation using catalysts with pyridinediimine and diphosphine ligands [77].

- Milstein reviewed iron pincer catalysts where metal–ligand cooperation occurs by aromatization/dearomatization in the course of a hydrogenation reaction [78].
- Guan reviewed nickel and iron pincer complexes for the reduction of carbonyl compounds [79].
- Beller reviewed pincer complexes for hydrogenation/dehydrogenation reactions employing both noble metals and base metals [80].
- And, finally, Hu reviewed recent developments in catalytic applications of iron pincer complexes, including hydrogenation, hydrosilylation, dehydrogenation, and carbon–carbon bond forming reactions [81].

References

1. Zell T, Ben-David Y, Milstein D (2015) Highly efficient, general hydrogenation of aldehydes catalyzed by PNP iron pincer complexes. Cat Sci Technol 5:822–826. https://doi.org/10.1039/C4CY01501K
2. Mazza S, Scopelliti R, Hu X (2015) Chemoselective hydrogenation and transfer hydrogenation of aldehydes catalyzed by iron(II) PONOP pincer complexes. Organometallics 34:1538–1545. https://doi.org/10.1021/acs.organomet.5b00105
3. Wienhöfer G, Westerhaus FA, Junge K et al (2013) A molecularly defined iron-catalyst for the selective hydrogenation of α,β-unsaturated aldehydes. Chem Eur J 19:7701–7707. https://doi.org/10.1002/chem.201300660
4. Fleischer S, Zhou S, Junge K, Beller M (2013) General and highly efficient iron-catalyzed hydrogenation of aldehydes, ketones, and α,β-unsaturated aldehydes. Angew Chem Int Ed 52:5120–5124. https://doi.org/10.1002/anie.201301239
5. Schrock RR, Osborn JA (1970) Rhodium catalysts for the homogeneous hydrogenation of ketones. J Chem Soc D:567–568. https://doi.org/10.1039/C29700000567
6. Gorgas N, Stoeger B, Veiros LF, Kirchner K (2016) Highly efficient and selective hydrogenation of aldehydes: a well-defined Fe(II) catalyst exhibits noble-metal activity. ACS Catal 6:2664–2672. https://doi.org/10.1021/acscatal.6b00436
7. Bruenig J, Csendes Z, Weber S et al (2018) Chemoselective supported ionic-liquid-phase (SILP) aldehyde hydrogenation catalyzed by an Fe(II) PNP pincer complex. ACS Catal 8:1048–1051. https://doi.org/10.1021/acscatal.7b04149
8. Langer R, Leitus G, Ben-David Y, Milstein D (2011) Efficient hydrogenation of ketones catalyzed by an iron pincer complex. Angew Chem Int Ed 50:2120–2124. https://doi.org/10.1002/anie.201007406
9. Langer R, Iron MA, Konstantinovski L et al (2012) Iron borohydride pincer complexes for the efficient hydrogenation of ketones under mild, base-free conditions: synthesis and mechanistic insight. Chem Eur J 18:7196–7209. https://doi.org/10.1002/chem.201200159
10. Chakraborty S, Lagaditis PO, Forster M et al (2014) Well-defined iron catalysts for the acceptorless reversible dehydrogenation-hydrogenation of alcohols and ketones. ACS Catal 4:3994–4003. https://doi.org/10.1021/cs5009656
11. Chakraborty S, Brennessel WW, Jones WD (2014) A molecular iron catalyst for the acceptorless dehydrogenation and hydrogenation of N-heterocycles. J Am Chem Soc 136:8564–8567. https://doi.org/10.1021/ja504523b
12. Gorgas N, Stoeger B, Veiros LF et al (2014) Efficient hydrogenation of ketones and aldehydes catalyzed by well-defined iron(II) PNP pincer complexes: evidence for an insertion mechanism. Organometallics 33:6905–6914. https://doi.org/10.1021/om5009814

13. Yang X (2011) Unexpected direct reduction mechanism for hydrogenation of ketones catalyzed by iron PNP pincer complexes. Inorg Chem 50:12836–12843. https://doi.org/10.1021/ic2020176
14. Morello GR, Hopmann KH (2017) A dihydride mechanism can explain the intriguing substrate selectivity of iron-PNP-mediated hydrogenation. ACS Catal 7:5847–5855. https://doi.org/10.1021/acscatal.7b00764
15. Huber R, Passera A, Mezzetti A (2018) Iron(II)-catalyzed hydrogenation of acetophenone with a chiral, pyridine-based PNP pincer ligand: support for an outer-sphere mechanism. Organometallics 37:396–405. https://doi.org/10.1021/acs.organomet.7b00816
16. Toda T, Kuwata S, Ikariya T (2015) Synthesis and structures of ruthenium and iron complexes bearing an unsymmetrical pincer-type ligand with protic pyrazole and tertiary aminoalkyl arms. Z Anorg Allg Chem 641:2135–2139. https://doi.org/10.1002/zaac.201500558
17. Yang X (2013) A self-promotion mechanism for efficient dehydrogenation of ethanol catalyzed by pincer ruthenium and iron complexes: aliphatic versus aromatic ligands. ACS Catal 3:2684–2688. https://doi.org/10.1021/cs400862x
18. Kuriyama W, Matsumoto T, Ogata O et al (2012) Catalytic hydrogenation of esters. Development of an efficient catalyst and processes for synthesising (R)-1,2-propanediol and 2-(l-menthoxy)ethanol. Org Process Res Dev 16:166–171. https://doi.org/10.1021/op200234j
19. Königsmann M, Donati N, Stein D et al (2007) Metalloenzyme-inspired catalysis: selective oxidation of primary alcohols with an iridium–aminyl-radical complex. Angew Chem Int Ed 46:3567–3570. https://doi.org/10.1002/anie.200605170
20. Bonitatibus Jr PJ, Chakraborty S, Doherty MD et al (2015) Reversible catalytic dehydrogenation of alcohols for energy storage. Proc Natl Acad Sci U S A 112:1687–1692. https://doi.org/10.1073/pnas.1420199112
21. Peña-López M, Neumann H, Beller M (2015) Iron(II) pincer-catalyzed synthesis of lactones and lactams through a versatile dehydrogenative domino sequence. ChemCatChem 7:865–871. https://doi.org/10.1002/cctc.201402967
22. Nguyen DH, Morin Y, Zhang L et al (2017) Oxidative transformations of biosourced alcohols catalyzed by earth-abundant transition metals. ChemCatChem 9:2652–2660. https://doi.org/10.1002/cctc.201700310
23. Sharninghausen LS, Mercado BQ, Crabtree RH, Hazari N (2015) Selective conversion of glycerol to lactic acid with iron pincer precatalysts. Chem Commun 51:16201–16204. https://doi.org/10.1039/C5CC06857F
24. Zell T, Ben-David Y, Milstein D (2014) Unprecedented iron-catalyzed ester hydrogenation. Mild, selective, and efficient hydrogenation of trifluoroacetic esters to alcohols catalyzed by an iron pincer complex. Angew Chem Int Ed 53:4685–4689. https://doi.org/10.1002/anie.201311221
25. Pignataro L, Gajewski P, Gonzalez-de-Castro A et al (2016) Expanding the catalytic scope of (cyclopentadienone)iron complexes to the hydrogenation of activated esters to alcohols. ChemCatChem 8:3431–3435. https://doi.org/10.1002/cctc.201600972
26. Chakraborty S, Dai H, Bhattacharya P et al (2014) Iron-based catalysts for the hydrogenation of esters to alcohols. J Am Chem Soc 136:7869–7872. https://doi.org/10.1021/ja504034q
27. Werkmeister S, Junge K, Wendt B et al (2014) Hydrogenation of esters to alcohols with a well-defined iron complex. Angew Chem Int Ed 53:8722–8726. https://doi.org/10.1002/anie.201402542
28. Fairweather NT, Gibson MS, Guan H, Chakraborty S, Dai H, Bhattacharya P. Homogeneous hydrogenation of esters employing a complex of iron as catalyst. US provisional patent filed (serial number 61/972927) on March 31, 2014, first utility patent filed (serial number 14/664966) on March 23, 2015
29. Elangovan S, Wendt B, Topf C et al (2016) Improved second generation iron pincer complexes for effective ester hydrogenation. Adv Synth Catal 358:820–825. https://doi.org/10.1002/adsc.201500930

30. Yang X (2012) Metal hydride and ligand proton transfer mechanism for the hydrogenation of dimethyl carbonate to methanol catalyzed by a pincer ruthenium complex. ACS Catal 2:964–970. https://doi.org/10.1021/cs3000683
31. Balaraman E, Gunanathan C, Zhang J et al (2011) Efficient hydrogenation of organic carbonates, carbamates and formates indicates alternative routes to methanol based on CO_2 and CO. Nat Chem 3:609–614. https://doi.org/10.1038/nchem.1089
32. Qu S, Dai H, Dang Y et al (2014) Computational mechanistic study of Fe-catalyzed hydrogenation of esters to alcohols: improving catalysis by accelerating precatalyst activation with a Lewis base. ACS Catal 4:4377–4388. https://doi.org/10.1021/cs501089h
33. Jiao H, Junge K, Alberico E, Beller M (2016) A comparative computationally study about the defined M(II) pincer hydrogenation catalysts (M = Fe, Ru, Os). J Comput Chem 37:168–176. https://doi.org/10.1002/jcc.23944
34. Bornschein C, Werkmeister S, Wendt B et al (2014) Mild and selective hydrogenation of aromatic and aliphatic (di)nitriles with a well-defined iron pincer complex. Nat Commun 5:4111. https://doi.org/10.1038/ncomms5111
35. Lange S, Elangovan S, Cordes C et al (2016) Selective catalytic hydrogenation of nitriles to primary amines using iron pincer complexes. Cat Sci Technol 6:4768–4772. https://doi.org/10.1039/C6CY00834H
36. Chakraborty S, Milstein D (2017) Selective hydrogenation of nitriles to secondary imines catalyzed by an iron pincer complex. ACS Catal 7:3968–3972. https://doi.org/10.1021/acscatal.7b00906
37. Chakraborty S, Leitus G, Milstein D (2017) Iron-catalyzed mild and selective hydrogenative cross-coupling of nitriles and amines to form secondary aldimines. Angew Chem Int Ed 56:2074–2078. https://doi.org/10.1002/anie.201608537
38. Crabtree RH (2008) Hydrogen storage in liquid organic heterocycles. Energy Environ Sci 1:134–138. https://doi.org/10.1039/B805644G
39. Sawatlon B, Surawatanawong P (2016) Mechanisms for dehydrogenation and hydrogenation of N-heterocycles using PNP-pincer-supported iron catalysts: a density functional study. Dalton Trans 45:14965–14978. https://doi.org/10.1039/C6DT02431A
40. Bellows SM, Chakraborty S, Gary JB et al (2017) An uncanny dehydrogenation mechanism: polar bond control over stepwise or concerted transition states. Inorg Chem 56:5519–5524. https://doi.org/10.1021/acs.inorgchem.6b01800
41. Schneck F, Assmann M, Balmer M et al (2016) Selective hydrogenation of amides to amines and alcohols catalyzed by improved iron pincer complexes. Organometallics 35:1931–1943. https://doi.org/10.1021/acs.organomet.6b00251
42. Rezayee NM, Samblanet DC, Sanford MS (2016) Iron-catalyzed hydrogenation of amides to alcohols and amines. ACS Catal 6:6377–6383. https://doi.org/10.1021/acscatal.6b01454
43. Jayarathne U, Zhang Y, Hazari N, Bernskoetter WH (2017) Selective iron-catalyzed deaminative hydrogenation of amides. Organometallics 36:409–416. https://doi.org/10.1021/acs.organomet.6b00816
44. Garg JA, Chakraborty S, Ben-David Y, Milstein D (2016) Unprecedented iron-catalyzed selective hydrogenation of activated amides to amines and alcohols. Chem Commun 52:5285–5288. https://doi.org/10.1039/C6CC01505K
45. Mastalir M, Glatz M, Gorgas N et al (2016) Divergent coupling of alcohols and amines catalyzed by isoelectronic hydride Mn^{I} and Fe^{II} PNP pincer complexes. Chem Eur J 22:12316–12320. https://doi.org/10.1002/chem.201603148
46. Langer R, Diskin-Posner Y, Leitus G et al (2011) Low-pressure hydrogenation of carbon dioxide catalyzed by an iron pincer complex exhibiting noble metal activity. Angew Chem Int Ed 50:9948–9952. https://doi.org/10.1002/anie.201104542
47. Rivada-Wheelaghan O, Dauth A, Leitus G et al (2015) Synthesis and reactivity of iron complexes with a new pyrazine-based pincer ligand, and application in catalytic low-pressure hydrogenation of carbon dioxide. Inorg Chem 54:4526–4538. https://doi.org/10.1021/acs.inorgchem.5b00366

48. Zhang Y, MacIntosh AD, Wong JL et al (2015) Iron catalyzed CO_2 hydrogenation to formate enhanced by Lewis acid co-catalysts. Chem Sci 6:4291–4299. https://doi.org/10.1039/C5SC01467K
49. Smith NE, Bernskoetter WH, Hazari N, Mercado BQ (2017) Synthesis and catalytic activity of PNP-supported iron complexes with ancillary isonitrile ligands. Organometallics 36:3995–4004. https://doi.org/10.1021/acs.organomet.7b00602
50. Zell T, Butschke B, Ben-David Y, Milstein D (2013) Efficient hydrogen liberation from formic acid catalyzed by a well-defined iron pincer complex under mild conditions. Chem Eur J 19:8068–8072. https://doi.org/10.1002/chem.201301383
51. Bart SC, Lobkovsky E, Chirik PJ (2004) Preparation and molecular and electronic structures of iron(0) dinitrogen and silane complexes and their application to catalytic hydrogenation and hydrosilation. J Am Chem Soc 126:13794–13807. https://doi.org/10.1021/ja046753t
52. Trovitch RJ, Lobkovsky E, Bill E, Chirik PJ (2008) Functional group tolerance and substrate scope in bis(imino)pyridine iron catalyzed alkene hydrogenation. Organometallics 27:1470–1478. https://doi.org/10.1021/om701091z
53. Yu RP, Darmon JM, Hoyt JM et al (2012) High-activity iron catalysts for the hydrogenation of hindered, unfunctionalized alkenes. ACS Catal 2:1760–1764. https://doi.org/10.1021/cs300358m
54. Xu R, Chakraborty S, Bellows SM et al (2016) Iron-catalyzed homogeneous hydrogenation of alkenes under mild conditions by a stepwise, bifunctional mechanism. ACS Catal 6:2127–2135. https://doi.org/10.1021/acscatal.5b02674
55. Srimani D, Diskin-Posner Y, Ben-David Y, Milstein D (2013) Iron pincer complex catalyzed, environmentally benign, *E*-selective semi-hydrogenation of alkynes. Angew Chem Int Ed 52:14131–14134. https://doi.org/10.1002/anie.201306629
56. Zhang L, Peng D, Leng X, Huang Z (2013) Iron-catalyzed, atom-economical, chemo- and regioselective alkene hydroboration with pinacolborane. Angew Chem Int Ed 52:3676–3680. https://doi.org/10.1002/anie.201210347
57. Jia X, Zhang L, Qin C et al (2014) Iridium complexes of new NCP pincer ligands: catalytic alkane dehydrogenation and alkene isomerization. Chem Commun 50:11056–11059. https://doi.org/10.1039/C3CC46851H
58. Jiang S, Quintero-Duque S, Roisnel T et al (2016) Direct synthesis of dicarbonyl PCP-iron hydride complexes and catalytic dehydrogenative borylation of styrene. Dalton Trans 45:11101–11108. https://doi.org/10.1039/C6DT01149G
59. Bhattacharya P, Krause JA, Guan H (2014) Mechanistic studies of ammonia borane dehydrogenation catalyzed by iron pincer complexes. J Am Chem Soc 136:11153–11161. https://doi.org/10.1021/ja5058423
60. Kuroki A, Ushiyama H, Yamashita K (2016) Theoretical studies on ammonia borane dehydrogenation catalyzed by iron pincer complexes. Comput Theor Chem 1090:214–217. https://doi.org/10.1016/j.comptc.2016.06.017
61. Zhang Y, Zhang Y, Qi Z-H et al (2016) Ammonia-borane dehydrogenation catalyzed by iron pincer complexes: a concerted metal-ligand cooperation mechanism. Int J Hydrog Energy 41:17208–17215. https://doi.org/10.1016/j.ijhydene.2016.07.209
62. Lagaditis PO, Sues PE, Sonnenberg JF, Wan KY, Lough AJ, Morris RH (2014) Iron(II) complexes containing unsymmetrical P–N–P′ pincer ligands for the catalytic asymmetric hydrogenation of ketones and imines. J Am Chem Soc 136:1367–1380. https://doi.org/10.1021/ja4082233
63. Sonnenberg JF, Wan KY, Sues PE, Morris RH (2017) Ketone asymmetric hydrogenation catalyzed by P–NH–P′ pincer iron catalysts: an experimental and computational study. ACS Catal 7:316–326. https://doi.org/10.1021/acscatal.6b02489
64. Schroeder-Holzhacker C, Gorgas N, Stoeger B, Kirchner K (2016) Synthesis and reactivity of BINEPINE-based chiral Fe(II) PNP pincer complexes. Monatsh Chem 147:1023–1030. https://doi.org/10.1007/s00706-016-1706-x

65. Sui-Seng C, Freutel F, Lough AJ, Morris RH (2008) Highly efficient catalyst systems using iron complexes with a tetradentate PNNP ligand for the asymmetric hydrogenation of polar bonds. Angew Chem Int Ed 47:940–943. https://doi.org/10.1002/anie.200705115
66. Mikhailine A, Lough AJ, Morris RH (2009) Efficient asymmetric transfer hydrogenation of ketones catalyzed by an iron complex containing a P−N−N−P tetradentate ligand formed by template synthesis. J Am Chem Soc 131:1394–1395. https://doi.org/10.1021/ja809493h
67. Mikhailine AA, Maishan MI, Morris RH (2012) Asymmetric transfer hydrogenation of ketimines using well-defined iron(II)-based precatalysts containing a PNNP ligand. Org Lett 14:4638–4641. https://doi.org/10.1021/ol302079q
68. Sues PE, Lough AJ, Morris RH (2011) Stereoelectronic factors in iron catalysis: synthesis and characterization of aryl-substituted iron(II) carbonyl P–N–N–P complexes and their use in the asymmetric transfer hydrogenation of ketones. Organometallics 30:4418–4431. https://doi.org/10.1021/om2005172
69. Lagaditis PO, Lough AJ, Morris RH (2011) Low-valent ene–amido iron complexes for the asymmetric transfer hydrogenation of acetophenone without base. J Am Chem Soc 133:9662–9665. https://doi.org/10.1021/ja202375y
70. Mikhailine AA, Maishan MI, Lough AJ, Morris RH (2012) The mechanism of efficient asymmetric transfer hydrogenation of acetophenone using an iron(II) complex containing an (S,S)-Ph_2PCH_2CH?NCHPhCHPhN?$CHCH_2PPh_2$ ligand: partial ligand reduction is the key. J Am Chem Soc 134:12266–12280. https://doi.org/10.1021/ja304814s
71. Zuo W, Lough AJ, Li YF, Morris RH (2013) Amine(imine)diphosphine iron catalysts for asymmetric transfer hydrogenation of ketones and imines. Science 342:1080–1083. https://doi.org/10.1126/science.1244466
72. Wu S, Li X, Xiong Z et al (2013) Synthesis and reactivity of silyl iron, cobalt, and nickel complexes bearing a [PSiP]-pincer ligand via Si–H bond activation. Organometallics 32:3227–3237. https://doi.org/10.1021/om400047j
73. Trovitch RJ, Lobkovsky E, Bouwkamp MW, Chirik PJ (2008) Carbon−oxygen bond cleavage by bis(imino)pyridine iron compounds: catalyst deactivation pathways and observation of acyl C−O bond cleavage in esters. Organometallics 27:6264–6278. https://doi.org/10.1021/om8005596
74. Gonzalez-de-Castro A, Robertson CM, Xiao J (2014) Dehydrogenative α-oxygenation of ethers with an iron catalyst. J Am Chem Soc 136:8350–8360. https://doi.org/10.1021/ja502167h
75. Bhattacharya P, Guan H (2011) Synthesis and catalytic application of iron pincer complexes. Comments Inorg Chem 32:88–112. https://doi.org/10.1080/02603594.2011.618855
76. Murugesan S, Kirchner K (2015) Non-precious metal complexes with an anionic PCP pincer architecture. Dalton Trans 45:416–439. https://doi.org/10.1039/C5DT03778F
77. Chirik PJ (2015) Iron- and cobalt-catalyzed alkene hydrogenation: catalysis with both redox-active and strong field ligands. Acc Chem Res 48:1687–1695. https://doi.org/10.1021/acs.accounts.5b00134
78. Zell T, Milstein D (2015) Hydrogenation and dehydrogenation iron pincer catalysts capable of metal–ligand cooperation by aromatization/dearomatization. Acc Chem Res 48:1979–1994. https://doi.org/10.1021/acs.accounts.5b00027
79. Chakraborty S, Bhattacharya P, Dai H, Guan H (2015) Nickel and iron pincer complexes as catalysts for the reduction of carbonyl compounds. Acc Chem Res 48:1995–2003. https://doi.org/10.1021/acs.accounts.5b00055
80. Werkmeister S, Neumann J, Junge K, Beller M (2015) Pincer-type complexes for catalytic (de)hydrogenation and transfer (de)hydrogenation reactions: recent progress. Chem Eur J 21:12226–12250. https://doi.org/10.1002/chem.201500937
81. Bauer G, Hu X (2016) Recent developments of iron pincer complexes for catalytic applications. Inorg Chem Front 3:741–765. https://doi.org/10.1039/C5QI00262A

Top Organomet Chem (2019) 63: 175–192
DOI: 10.1007/3418_2018_20

Published online: 12 October 2018

Conversion of Alcohols to Carboxylates Using Water and Base with H_2 Liberation

Peng Hu and David Milstein

Contents

Abstract Production of carboxylic acids from alcohols is an important process for both industry and laboratory. Traditional methods usually require environmentally unfriendly oxidants and generate stoichiometric waste. Recently, methods using O_2 as oxidant, oxidation processes applying stoichiometric hydrogen acceptors and acceptorless dehydrogenative coupling reactions to generate carboxylic acids/carboxylic acid salts have been developed. This chapter reviews the reported results on the generation of carboxylic acids/carboxylates by acceptorless dehydrogenative coupling of alcohols and water. The chapter is according to the types of catalysts used; reaction conditions, product yields, and mechanisms are also discussed.

Keywords Alcohols · Carboxylic acids · Catalysis · Dehydrogenation · Dihydrogen

P. Hu
School of Chemistry, Sun Yat-sen University, Guangzhou, P. R. China
e-mail: hupeng8@mail.sysu.edu.cn

D. Milstein (✉)
Department of Organic Chemistry, Weizmann Institute of Science, Rehovot, Israel
e-mail: david.milstein@weizmann.ac.il

1 Introduction

Transforming alcohols to carboxylic acids represents an essential synthetic process in both industry and laboratory. Traditionally, stoichiometric strong and/or toxic oxidants (e.g., $KMnO_4$, pyridinium dichromate, iodate, or chlorite) and chlorinated solvents have been used for this transformation, which generate copious waste and suffer from low atom economy (Eq. 1) [1]. A few early examples were also reported to produce carboxylates from alcohols under harsh conditions [2, 3]. In recent years, significant efforts have been made toward "greener" methods, and methods for alcohol oxidation to carboxylic acids using O_2 were reported (for selected reviews of heterogeneous catalysts, see [4, 5]; for selected examples of heterogeneous catalysts, see [6, 7]; for examples of homogeneous catalysts, see [8, 9]), although use of O_2 under pressure may pose safety issues. During the last decade elegant dehydrogenation methods were developed. For example, homogeneous rhodium catalysts were reported for the generation of carboxylic acid salts from alcohols in basic solvents using a ketone [10, 11], O_2 (with DMSO as a sacrificial oxygen acceptor) [12] and N_2O [13] as stoichiometric hydrogen acceptors. Acceptorless dehydrogenation and dehydrogenative coupling reactions experienced rapid development in recent years [14–21]. Within this general area, carboxylic acid synthesis from alcohols using water with no added oxidant, with liberation of hydrogen gas under relatively mild conditions (Eq. 2), has been a topic of active research during the last decade, and the reported results are reviewed in this chapter.

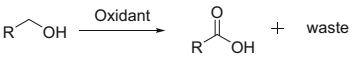

(1)

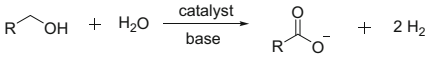

(2)

The mechanistic steps involved in the acceptorless generation of carboxylic acids from alcohols and basic water are shown in Scheme 1. In this transformation, an aldehyde intermediate is formed by catalytic dehydrogenation of the alcohol, releasing one molecule of hydrogen. Reversible nucleophilic attack by water, (or solvated hydroxide), on the aldehyde intermediate, followed by dehydrogenation of the produced gem-diol forms the carboxylic acid. Usually, the reaction is performed in a basic solution, and the produced carboxylic acid is captured by the base, leading to the corresponding carboxylic acid salt.

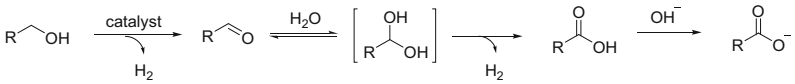

Scheme 1 General sequence of the acceptorless generation of carboxylic acid salts from alcohols and basic water

The organization of this short review follows the different types of catalytic systems and is ordered in three major parts: (1) homogeneous pincer-type catalysts – the majority of the catalysts summarized in this part are bearing cooperative pincer ligands, (2) homogeneous non-pincer catalysts, and (3) heterogeneous catalysts. Homogeneously catalyzed methanol reforming to produce H_2 and CO_2 under relatively mild conditions, which is thought to proceed via HCOOH intermediacy, was summarized in other reviews [17, 20, 21] and will not be discussed in detail in this chapter. Research covered in this chapter is until February 1, 2018.

2 Catalysis by Homogeneous Pincer-Type Complexes

Most of the catalysts summarized in this section are based on cooperative pincer ligands and follow a metal-ligand cooperation (MLC) catalytic mode. Briefly, during a MLC catalytic cycle, the cooperating ligand and the active metal center of the catalyst are both involved in bond making and breaking. MLC has become an important strategy for catalyst design and was recently reviewed in detail [22, 23].

The Milstein group reported in 2013 the homogeneously catalyzed acceptorless dehydrogenative conversion of alcohols and water to carboxylates with liberation of H_2 [24]. The reaction is performed under relatively mild conditions with high turnover numbers and product yields. Applying the pre-catalyst **1**, the actual dearomatized catalyst **2** is generated in situ under the basic conditions (Scheme 2). The unsaturated arm of the dearomatized catalyst **2** is the cooperative site of the ligand, which is involved in the catalytic cycle via an aromatization-dearomatization MLC mode.

The reaction proceeds smoothly using a low loading of complex **1** (0.2 mol%), resulting in moderate to excellent isolated yields of carboxylic acids after reflux of an aqueous solution of the alcohol and NaOH (1.1 equivalent to alcohol) for 18 h, followed by acid treatment (Fig. 1). The reaction exhibits good substrate scope of both aliphatic alcohols and benzyl alcohols. In addition, compounds bearing two hydroxyl groups also performed well, leading to dicarboxylic acid products, as shown in Fig. 1.

A labeling experiment using $^{18}OH_2$ (together with $Na^{16}OH$, the system was ~90% ^{18}O-labeled) and *n*-butanol resulted in the ^{18}O-labeled butyric acid salt (~90% ^{18}O-labeled in both O atoms), indicating that water is the eventual oxygen atom donor in formation of carboxylic acids. This labeling experiment also indicates that

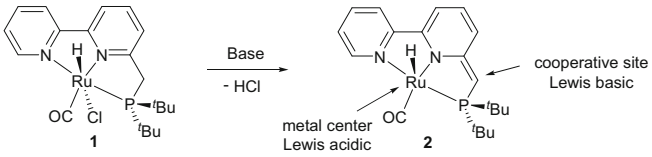

Scheme 2 Formation of the dearomatized catalyst **2** from complex **1** under basic conditions

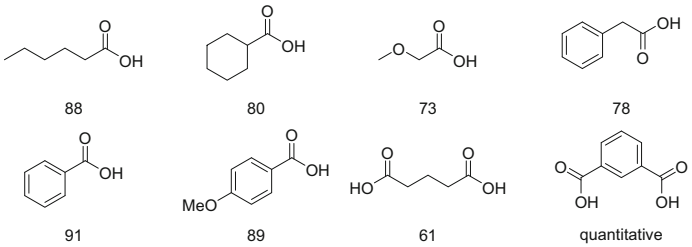

Fig. 1 Examples of carboxylic acid products and yields obtained using pre-catalyst **1**. Isolated yields (%) are presented

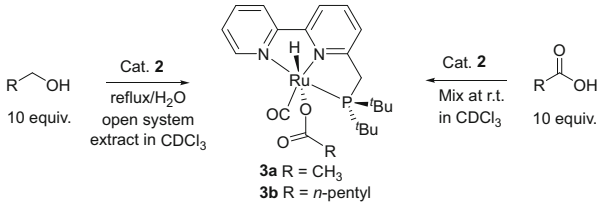

Scheme 3 Formation of a carboxylate addition complex **3** by alcohol reflux in water with complex **2** in the absence of base or by addition of a carboxylic acid to **2**[11]

formation of the gem-diol intermediate is reversible, thus resulting in labeled two oxygen atoms of the carboxylic acid salt. In the absence of base, the stable carboxylic acid adduct **3** was formed, and it was also independently prepared by treatment of complex **2** with the carboxylic acid, as shown in Scheme 3. The base NaOH scavenges the formed carboxylic acid and regenerates the catalyst. The important role of NaOH was also supported by DFT calculations reported by the Hall group [25], who suggested a four-step process for the reaction: aldehyde formation via dehydrogenation of the alcohol; gem-diol production from the aldehyde and water; carboxylic acid generation by gem-diol dehydrogenation, and carboxylate formation from carboxylic acid and base. Involvement of these organic intermediates is consistent with the proposed mechanism by the Milstein group, who suggested the organometallic intermediates shown in Scheme 4. DFT calculations by Hall indicate a modified mechanism involving a double H-transfer mechanism for alcohol activation, which has a slightly lower barrier (by 2 kcal) for aldehyde formation than a β-H elimination process involving hemilability of the bipyridine ligand [25].

Employing this reaction, amino alcohols were transformed directly to amino acid salts using complex **1** as pre-catalyst (Fig. 2) [26]. Using water/dioxane or just water as solvent, several natural and unnatural amino acid salts were prepared in excellent yields with low catalyst loading (0.1–0.5 mol%). In addition, no need for pre-protection of the amino alcohol substrates was required. The reaction enjoys a good substrate scope, both β and γ, and some other long-chain amino alcohols being suitable substrates. The concentration of base was an essential factor for the reaction; high efficiency and good yield could only be obtained by using concentrated base

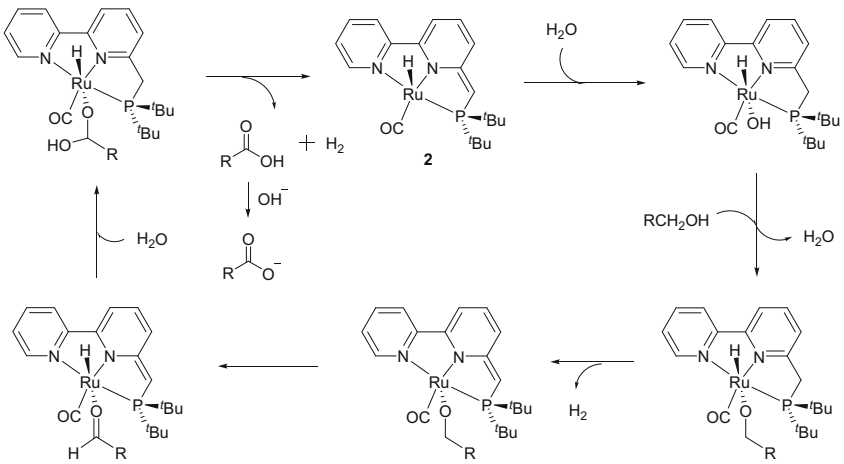

Scheme 4 Proposed mechanism of dehydrogenative carboxylic acid salt formation catalyzed by complex **2**[11]

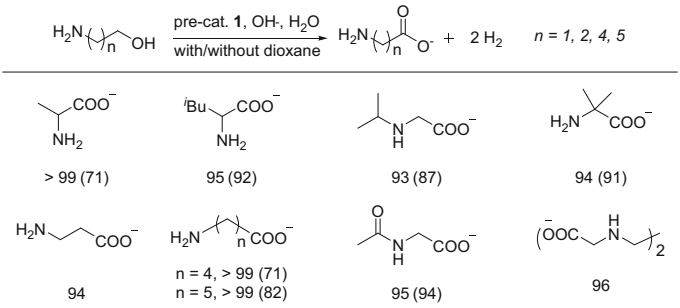

Fig. 2 Examples of amino acid salt products and yields obtained using pre-catalyst **1**. NMR yields (%) are presented. Yields in parentheses are isolated yields of the corresponding amino acids

solutions. The reason for that is likely to avoid the competing amide bond formation by dehydrogenative coupling of the amine and alcohol groups [27]. An $^{18}OH_2$-labeling experiment was also tried and showed a similar result as in the case of simple alcohols (see above) [24]. Compared with the traditional methods, such as the Strecker amino acid synthesis, which uses highly toxic cyanide salts, the present method is atom-economical and environmentally friendly and can be viewed as an alternative for amino acid synthesis.

Complex **1** was also used as a pre-catalyst for methanol reforming under mild conditions, producing H_2 and CO_2, the latter being captured by the base in the reaction system, as reported in 2014 [28]. Mild, homogeneously Ruthenium-catalyzed reforming of methanol was reported by Beller [29, 30] and Grützmacher [31] in 2013. Ru-catalyzed aldehyde-water shift reaction to form carboxylic acids was recently reported by Brewster et al. [32].

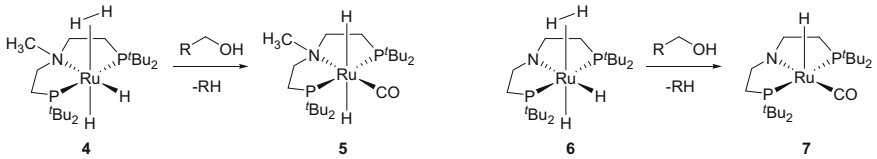

Scheme 5 Formation of complex **5** from **4**, and **7** from **6**, via alcohol decarbonylation

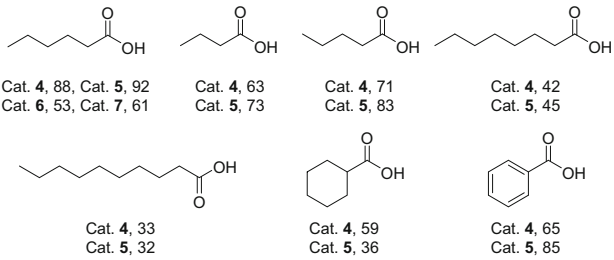

Fig. 3 Examples of carboxylic acid products and yields obtained using complexes **4** and **5**. Isolated yields (%) are presented

In 2014, Prechtl et al. developed ruthenium pincer catalysts based on aliphatic PNP-type ligands (Scheme 5) for the transformation of alcohols to carboxylates by dehydrogenation in basic aqueous solutions [33]. The carbonyl complex **5**, bearing the noncooperative Me-PNP ligand, was generated from complex **4** by an alcohol decarbonylation reaction; complex **7** was obtained from complex **6** using the same procedure.

Using a catalyst loading of 1 mol%, complexes **4**–**7** were all effective for the carboxylate formation reaction. Interestingly, use of the *N*-Me complexes **4** and **5** resulted in higher yields (Fig. 3), suggesting that MLC may not be operating in this case. Aliphatic and benzyl alcohols can be used, although the performance of long-chain aliphatic alcohols was not satisfying, probably due to their low solubility in aqueous solutions. The authors also investigated the mechanism, and carboxylic acid adducts analogous to complex **3** were observed [24]. Prechtl and coworkers also reported the mild reforming of formaldehyde to CO_2 and H_2, which proceeds even with no added base [34].

Beller's group reported in 2014 a hydrogen storage system, using ethanol as the hydrogen carrier, enabled by dehydrogenative transformation of ethanol to acetic acid salt in a basic aqueous solution (Fig. 4) [35]. Of the tested catalysts, complexes **8** and **9** showed the best results. Reported previously by the same group, complexes **9** and **10** were used as the catalysts for methanol reforming to produce H_2 in KOH aqueous solution with high TON [29]. A similar system using ethanol employing catalyst **9** (10 ppm) and NaOH (8 M) resulted in an excellent catalyst TON (80,000) after 98 h. In addition, 95% wet bioethanol, produced by fermentation, could be used directly without prior purification and performed the same as mixed ethanol/water (95:5). However, aimed as a hydrogen storage system, the conversion and the actual

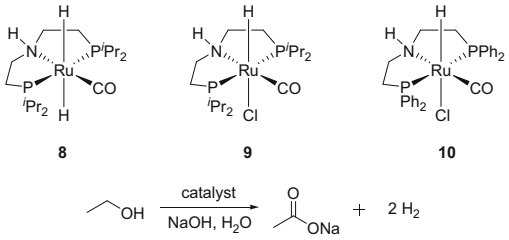

Fig. 4 PNP complexes **8**–**10** and transformation of ethanol to sodium acetate

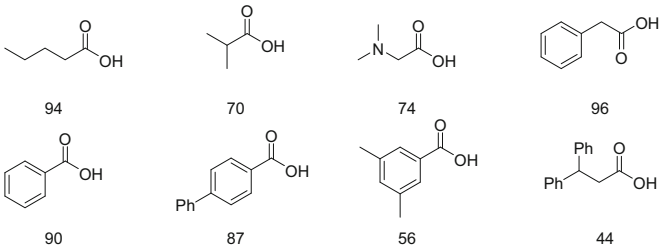

Fig. 5 Examples of carboxylic acid products and yields obtained using complex **10**. NMR yields (%) are presented

hydrogen storage capacity of the reaction, which are essential factors for the total efficiency, still need to be addressed.

In 2016, Gauvin, Dumeignil, and coworkers reported the transformation of alcohols to carboxylates [36]. Of the several tested catalysts, catalyst **10** was found to be one of the best. With a low catalyst loading of 0.1 mol%, complex **10** catalyzed the transformation of both aliphatic and benzyl alcohols (Fig. 5). In addition, the air-stable catalyst **10**, bearing phenylphosphine groups, catalyzes the reaction under air atmosphere. By applying a mixed toluene/water solvent system reported previously [28], catalyst **10** was recycled five times without significant loss of catalytic activity.

Later in 2017, Gauvin et al. reported the dehydrogenative transformation of alcohols to carboxylates, catalyzed by pincer complexes of earth abundant metals, using KOH as base (Fig. 6) [37]. Among the tested catalyst candidates, complexes **11** and **12** showed the best catalytic activity for the conversion of 1-butanol to butyric acid, leading to excellent isolated yields. Complexes **11** and **12** also catalyze the methanol reforming reaction for hydrogen production [38, 39]. Surprisingly, the reaction resulted in better yields in the absence of water, and the optimized solvent was toluene, the base serving as the source of the O atom. Some bio-sourced alcohols were also successfully utilized. In addition, C=C bonds were retained, as shown in Fig. 6.

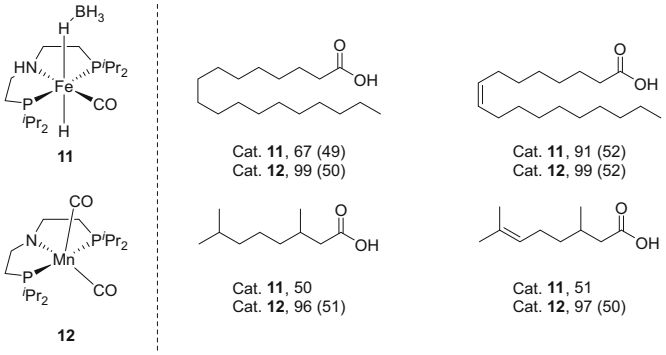

Fig. 6 Examples of carboxylic acid products and yields obtained using complexes **11** and **12**. NMR yields (%) are presented. Yields in parentheses are isolated yields of corresponding carboxylic acids

3 Other Homogeneous Catalysts

A few non-pincer-type catalysts were also reported for the conversion of alcohols to carboxylates, using water as the oxygen atom source.

Grützmacher and coworkers reported in 2013 that the Ru complex **13**, bearing the non-innocent $trop_2dad$ ligand (Fig. 7), efficiently catalyzes methanol reforming using H_2O under mild conditions, generating CO_2 and H_2. The reaction proceeds even in the absence of added base, and formic acid is believed to be an intermediate in this reaction. In this work it is reported that complex **13** catalyzes the reaction of benzyl alcohol with $^{18}OH_2$ and KO^{t}Bu as base, generating nearly fully ^{18}O-labeled potassium benzoate, in line with reversible hydration of benzaldehyde as also indicated in the general Scheme 1.

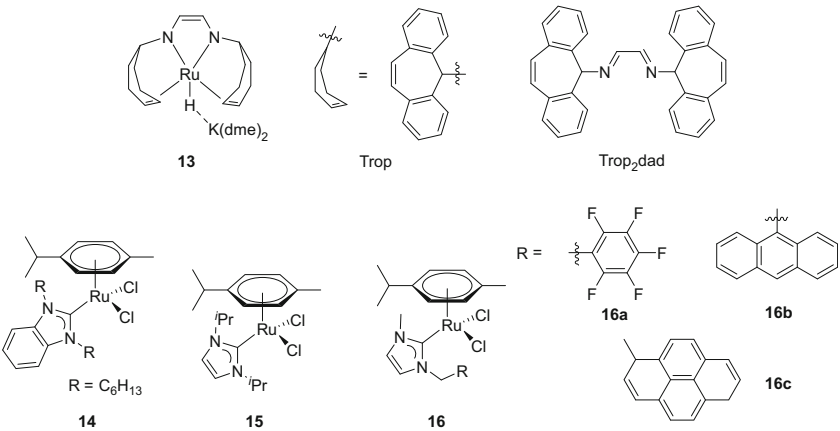

Fig. 7 Complexes **13**–**16**

In 2015, Keul and Möller reported pre-catalyst **14**, bearing a *N*-heterocyclic carbene (NHC) ligand to alleviate the problem of air sensitivity when electron-rich phosphine-based ligands are used [40]. Transformation of alcohols to carboxylates proceeded smoothly in refluxing aqueous NaOH solution under aerobic conditions, releasing H_2 as the only by-product. With a catalyst loading of 1 mol%, aliphatic and benzyl alcohols were transformed to the corresponding carboxylic acids (after acid treatment of the carboxylates) in moderate to excellent isolated yields (Fig. 8). The reaction tolerates chloro- and even bromo-substituents, as shown in Fig. 8 and Scheme 6. Interestingly, using catalyst **14** (2 mol%), biologically active alcohols were also applied as substrates, though resulting in lower isolated yields. The authors gave an example of functionalization of a polyether with hydroxyoctyl side chains, showing the negative influence of the low solubility of the substrate; using an aqueous NaOH solution, only 25% of the hydroxyl groups were transformed to carboxylic acid groups. Adding DMSO as cosolvent, 70% conversion of the hydroxyl groups was observed (Scheme 6).

A similar complex (**15**) with a different NHC ligand was reported in 2016 by Madsen et al. to catalyze the reaction in the presence of a catalytic amount of PCy_3 (in the form of $PCy_3{\cdot}HBF_4$) [41]. In the absence of water, the reaction performed well by employing complex **15** (1 mol%), $PCy_3{\cdot}HBF_4$ (1 mol%), and 1.2 equivalent

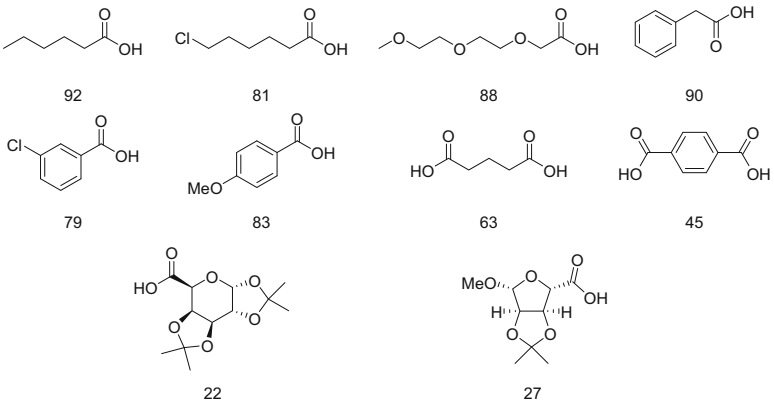

Fig. 8 Examples of carboxylic acid products and yields obtained using complex **14**. Isolated yields (%) are presented

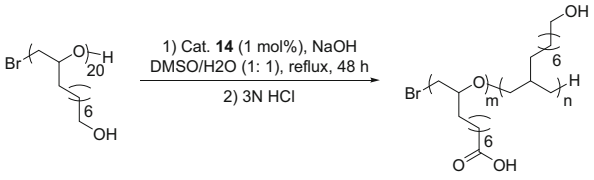

Scheme 6 Transformation of biologically active alcohols using a DMSO/water system

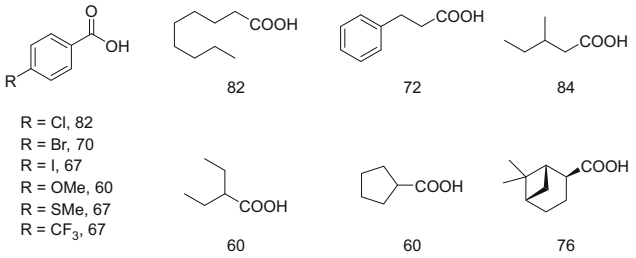

Fig. 9 Examples of carboxylic acid products and yields obtained using complex **15**. Isolated yields (%) are presented

of KOH, with toluene as the solvent. Attempts of using water as a cosolvent resulted in low yields of the corresponding carboxylate products. The reaction exhibited an outstanding substrate scope. Benzyl alcohols, aliphatic alcohols, and sterically hindered alcohols reacted well under the optimized conditions (Fig. 9). Excellent functional group tolerance was also observed, with chloro-, bromo- and iodo-substitutes as examples.

The mechanism was investigated using benzyl alcohol and hydrogen gas was collected. At the beginning of the reaction, 26% of benzaldehyde was observed. In a separate experiment, it was observed that the transformation of benzaldehyde to benzoic acid salt took place under the optimized conditions (Scheme 7). However, benzaldehyde was converted to benzoic acid salt in lower yield even in the absence of complex **15**, which indicated the possibility of involvement of a Cannizzaro reaction mechanism when benzyl alcohols are employed. Thus, conversion of the intermediate benzaldehyde may proceed via the two mechanisms at the same time. Based on the mechanistic investigation and a DFT study, the Ru-catalyzed mechanism shown in Fig. 10 was proposed for the reaction using **15** and KOH in the absence of water. The main difference of the suggested mechanism with Milstein's system is that a hydroxide ligand acts as an internal nucleophile, attacking the *cis*-coordinated aldehyde directly to generate a gem-diol species. Dehydrogenation of the gem-diol species affords the carboxylate product.

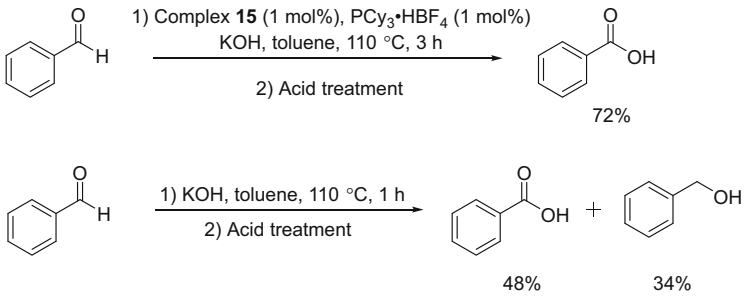

Scheme 7 Transformation of benzaldehyde to benzoic acid with and without complex **15**

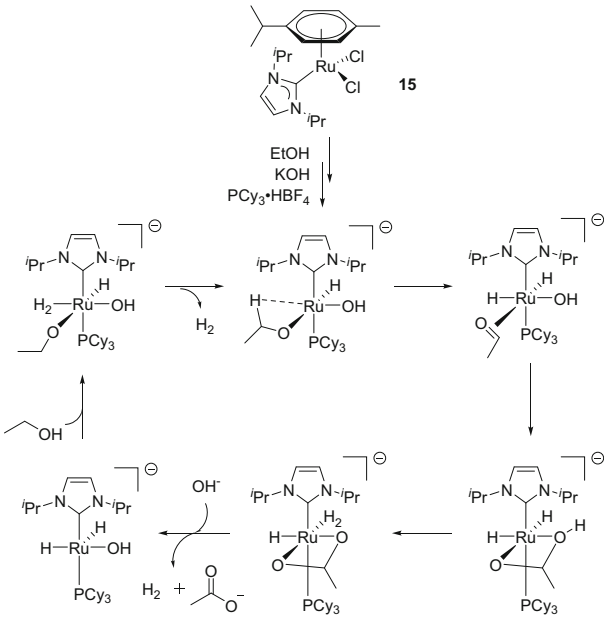

Fig. 10 Proposed mechanism using complex **15** in the absence of water

The similar complexes **16a–c** (Fig. 7) were developed by the Mata group [42]. However, use of these catalysts resulted in low conversion of alcohols to carboxylates. Interestingly, when mixed with reduced grapheme oxide, three hybrid organometallic-graphene materials of **16a–c** were obtained, leading to moderate to excellent isolated yields of aromatic carboxylic acids. Though the substrate scope was limited to benzyl alcohols, the system required just one equivalent of the weak base $CsCO_3$, which can be viewed as an advantage as compared with many other systems. Both the three hybrid organometallic-graphene catalysts could be recycled and the one based on **16c** had the best performance, without significant decrease of catalytic activity after recycling ten times. The mechanism was investigated experimentally and theoretically, suggesting that the water nucleophilic attack step to form a gem-diolate complex is the rate-determining step.

In 2016, a binuclear rhodium complex (**17**), developed by the Wang group, was reported to catalyze the formation of aromatic carboxylic acids from the corresponding alcohols [43]. Using an aqueous NaOH solution as the solvent, the reaction performed better under air and then under argon. Hydrogen was detected under argon or nitrogen, while in air, oxygen was the terminal oxidant, generating water. It was suggested that the oxygen efficiently removes the hydrogen formed in the reaction. Although no example of aliphatic alcohol was presented, the reaction exhibited good substrate scope and excellent functional group tolerance, as shown in Fig. 11. Generally, employing substrates bearing electron-withdrawing substituents resulted in lower reactivity and required longer reaction time, and an oxygen

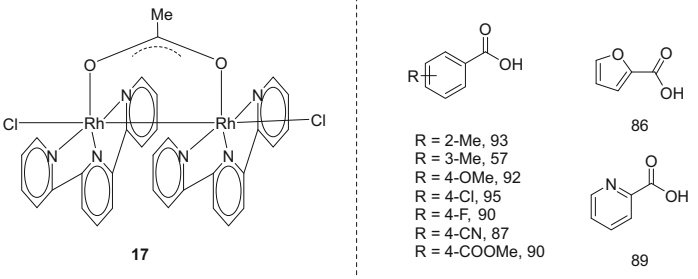

Fig. 11 Examples of carboxylic acid products and yields using complex **17**. Isolated yields (%) are presented

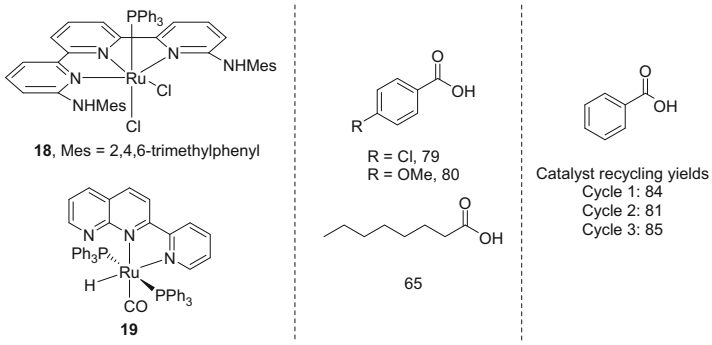

Fig. 12 Complexes **18** and **19**. Examples of carboxylic acid products and yields obtained using complex **17** as catalyst. Isolated yields (%) are presented

atmosphere was required to get a satisfactory yield. The reaction was suggested to proceed via two processes: (1) the general pathway shown in Scheme 1 as the major one and (2) the Cannizzaro reaction, which was proposed to be slow under the employed basic conditions, as the minor process. A gram-scale reaction to produce 4-methoxybenzoic acid was also presented, leading to 69% yield at a S/C ratio of 5,000:1. In addition, catalyst **17** was very stable and could be recycled for 19 times without significant loss of catalytic activity, indicating the usefulness of this catalyst system.

Szymczak reported in 2017 a ruthenium complex based on a 6,6″-bis (mesitylamino)terpyridine ligand (**18**), which catalyzes formation of carboxylates from alcohols via dehydrogenation (Fig. 12) [44]. Though with limited examples, aromatic and aliphatic primary alcohols generate the corresponding carboxylate, providing moderate to high yields of carboxylic acids after acid treatment. The pendent bulky NHMes groups are critical for the stability of complex **18**, and no decrease of reactivity was observed after three catalytic cycles, as shown in Fig. 12.

Employing complex **19**, Bera's group [45] reported that both aromatic and aliphatic primary alcohols, including several amino alcohols, were converted to carboxylates in mostly excellent GC-MS yields of the corresponding carboxylic acids. After ligand screening, the authors found that the free *N* of the ligand of complex **19** was essential for the high catalytic activity. Mechanistic investigation excluded the Cannizzaro and the Tishchenko reactions, and a similar mechanism to that shown in Scheme 1 was proposed.

In 2017, Zhang and Peng's group developed new Ru(II) complexes based on 2,6-bis(benzimidazole-2-yl)pyridine (N′NN′) ligands, of which the two complexes **20** and **21** showed good catalytic activity in the presence of base in transforming alcohols to carboxylates, in the absence of phosphine or *N*-heterocycle carbene ligands [46]. Both aromatic and aliphatic carboxylates were produced in moderate to good yields (Fig. 13). Interestingly, the reaction performed better in the absence of water, using excess alcohols as both substrates and solvents, together with 1 equivalent of $CsOH{\cdot}H_2O$. Using a low catalyst loading of 0.01 mol%, benzyl alcohol was transformed to the corresponding carboxylate in quantitative yield (based on $CsOH{\cdot}H_2O$) by complex **19** with a TON around 10,000; reusing the catalyst system after simple filtration resulted in a total yield of 98% and an increased TON of around 19,600.

In the same year, Zhang and Peng's group also developed a 2,6-bis(diethylaminomethyl)pyridine Ni(II) complex (**22**), as a catalyst of the dehydrogenative formation of carboxylates from alcohols [47]. Both aromatic and aliphatic carboxylates were formed; benzyl alcohols performed better and presented moderate to excellent isolated yields of the corresponding carboxylic acids (Fig. 14). The bases used in this study were sodium alkoxides of the corresponding alcohols,

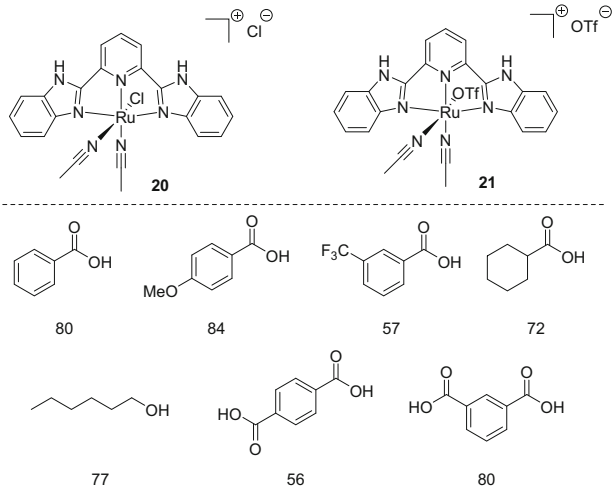

Fig. 13 Complexes **20** and **21**. Examples of carboxylic acid products and yields obtained using complex **21** as catalyst. Isolated yields (%) are presented

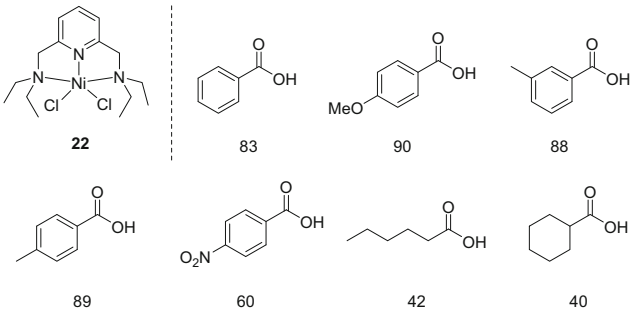

Fig. 14 Examples of carboxylic acid products and yields obtained using complex **22**. Isolated yields (%) are presented

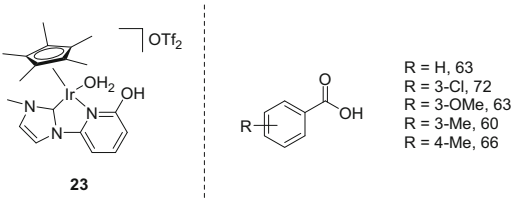

Fig. 15 Examples of carboxylic acid products and yields using complex **23**. Isolated yields (%) are presented

using excess of alcohols as the solvents. Addition of mesitylene as a cosolvent increased the product yields. Interestingly, a mechanistic study showed that stoichiometric ether was formed during the reaction, together with water, which acted as the source of oxygen atom for the formed carboxylates.

Yamaguchi and coworkers developed in 2017, a water-soluble Ir complex (**23**) that catalyzes the dehydrogenative carboxylic acids formation from alcohols in the absence of base (Fig. 15) [48]. The substrate scope was limited to benzylic alcohols, with moderate product yields, using a catalyst loading of 2–5 mol%. However, this is a unique example of dehydrogenative production of carboxylic acids form the corresponding alcohols in the absence of added base.

4 Heterogeneous Catalysts

Examples of dehydrogenative transformation of alcohols to carboxylates catalyzed by heterogeneous catalysts reported in the literature are rare. An early example appears in a patent for the generation of amino acids from amino alcohols, catalyzed by a heterogeneous Cu system, although in very low turnovers (maximum turnover number of 6) under N_2 pressure at 160°C [3]. Recently, Sajiki and coworkers studied heterogeneous systems for this transformation [49, 50]. Rh/C catalyzes the dehydrogenative transformation in basic water (Fig. 16) [49], although the

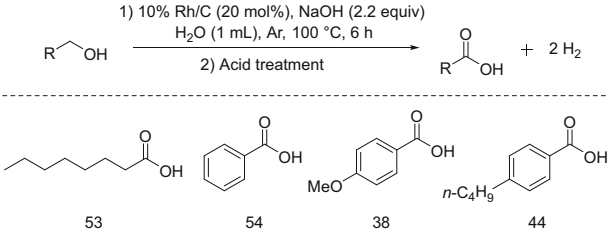

Fig. 16 Examples of carboxylic acid products and yields using Rh/C as catalyst. Isolated yields (%) are presented

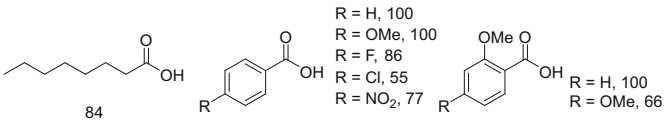

Fig. 17 Examples of carboxylic acid products and yields obtained using Pd/C as catalyst. Isolated yields (%) are presented

carboxylic acids were formed in modest yields (38–54%), in the presence of the best base tested (NaOH). Interestingly, some weak bases, including $NaHCO_3$ and NEt_3, also promoted the reaction, though with even lower yields.

In the following year, Sajiki and coworkers reported a more detailed study on the topic of carboxylic acids formation from alcohols and basic water, using metal on carbon catalysts [50]. Employing mild reduced pressure (80 kPa), much better yields were obtained, as compared with the yields under 1 atm pressure. This is likely due to the more efficient hydrogen removal under reduced pressure. The reaction is catalyzed under reduced pressure by Rh/C (10%), Pd/C (10%), Pt/C (10%), and Ru/C (10%), with Pd/C showing the best results (Fig. 17). Both aliphatic alcohols and benzyl alcohols were suitable substrates, and moderate to quantitative yields of the carboxylic acid products were obtained. In addition, the Pd/C catalyst could be reused, without any decrease of the catalytic activity after five cycles. In a mechanistic investigation, an aldehyde intermediate was observed, which transformed to the corresponding carboxylate. This investigation indicated that the reaction process was mainly based on Pd/C catalyzed dehydrogenation of alcohols with liberation of H_2, although aldehyde oxidation to carboxylic acid by O_2 could also be involved in some cases.

The Madsen group reported in 2017 a silver catalyzed dehydrogenative formation of carboxylates from primary alcohols [51]. Silver salts were used as pre-catalysts for the reaction and Ag_2CO_3 showed the best results. In the optimal conditions, Ag_2CO_3 (2.5 mol%) KOH (2.5–3 equivalent) and primary alcohols in refluxing mesitylene were used. The carboxylic acids, obtained after acid treatment of the product potassium carboxylates, were obtained in moderate to excellent yields (Fig. 18). Both benzylic and aliphatic primary alcohols were suitable substrates, and good functional group tolerance was observed. The reaction was believed to

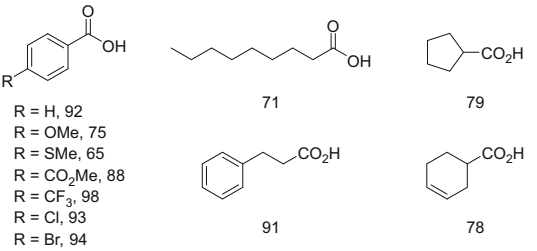

Fig. 18 Examples of carboxylic acid products and yields obtained using Ag_2CO_3 + KOH as catalyst. Isolated yields (%) are presented

proceed via dehydrogenative Cannizzaro reaction catalyzed by silver nanoparticles. Hydrogen gas was collected and tested. Formation of silver nanoparticles was confirmed by transmission electron microscopy (TEM). Silver nanoparticles produced form $AgNO_3$ and PVP (polyvinylpyrrolidone) also showed similar catalytic activity to that of Ag_2CO_3.

5 Summary and Outlook

In summary, in the relatively short period since 2013, several ligands and catalysts have been developed for the catalytic acceptorless transformation of alcohols to carboxylic acid salts using basic water and no added oxidant under relatively mild conditions, including catalysts that showed both high efficiency and good substrate scope. This success is partly due to the development of catalysts capable of function by metal-ligand cooperation (MLC). The majority of the systems are homogeneously catalyzed, and only few heterogeneously catalyzed systems were reported. Homogeneous, and particularly heterogeneous catalysts for the dehydrogenative transformations, can be robust and may be recycled, an obvious advantage for industrial applications. However, nearly all of the successful examples suffer from the need of strong bases, and when in some cases weak bases were used, low conversions and yields were observed. This is a significant disadvantage since chiral carboxylic acids, such as chiral amino acids, undergo racemization in a strongly basic environment.

Based on this situation, more efficient and robust catalysts, which are suitable for both aliphatic and aromatic alcohols and can tolerate different functional groups, are still required for lab applications. Especially, the development of catalytic systems which can use weak bases or function in the absence of base is a significant challenge. Highly efficient and reusable catalysts for industrial applications are also needed.

References

1. Tojo G, Fernandez M (2007) Oxidation of primary alcohols to carboxylic acids: a guide to current common practice. Springer, New York
2. Reid EM, Worthington H, Larchar AW (1939). J Am Chem Soc 61:99
3. Franczyk TS, Moench WL (2003) US patent 6,646,160
4. Mallat T, Baiker A (2004). Chem Rev 104:3037
5. Della Pina C, Falletta E, Rossi M (2012). Chem Soc Rev 41:350
6. Rass HA, Essayem N, Besson M (2013). Green Chem 15:2240
7. Ahmed MS, Mannel DS, Root TW, Stahl SS (2017). Org Process Res Dev 21:1388
8. Han L, Xing P, Jiang B (2014). Org Lett 16:3428
9. Jiang X, Zhang J, Ma S (2016). J Am Chem Soc 138:8344
10. Zweifel T, Naubron J-V, Grützmacher H (2009). Angew Chem Int Ed 48:559
11. Trincado M, Kühlein K, Grützmacher H (2011). Chem Eur J 17:11905
12. Annen S, Zweifel T, Ricatto F, Grützmacher H (2010). ChemCatChem 2:1286
13. Gianetti TL, Annen SP, Santiso-Quinones G, Reiher M, Driess M, Grützmacher H (2016). Angew Chem Int Ed 55:1854
14. Gunanathan C, Milstein D (2011). Acc Chem Res 44:588
15. Gunanathan C, Milstein D (2013). Science 341:1229712
16. Gunanathan C, Milstein D (2014). Chem Rev 114:12024
17. Trinicado M, Banerjee D, Grützmacher H (2014). Energy Environ Sci 7:2464
18. Younus HA, Su W, Ahmad N, Chen S, Verpoort F (2015). Adv Synth Catal 357:283
19. Huang F, Liu Z, Yu Z (2015). Angew Chem Int Ed 54:2
20. Werkmeister S, Neumann J, Junge K, Beller M (2015). Chem Eur J 21:12226
21. Alberico E, Nielsen M (2015). Chem Commun 51:6714
22. Khusnutdinova JR, Milstein D (2016). Angew Chem Int Ed 55:1854
23. Pandey P, Dutta I, Bera JK (2016). Proc Natl Acad Sci India Sect A Phys Sci 86:561–579
24. Balaraman E, Khaskin E, Leitus G, Milstein D (2013). Nat Chem 5:122
25. Li H, Hall MB (2014). J Am Chem Soc 136:383
26. Hu P, Ben-David Y, Milstein D (2016). J Am Chem Soc 138:6143
27. Gnanaprakasam B, Balaraman E, Ben-David Y, Milstein D (2011). Angew Chem Int Ed 50:12240
28. Hu P, Diskin-Posner Y, Ben-David Y, Milstein D (2014). ACS Catal 4:2649
29. Nielsen M, Alberico E, Baumann W, Drexler H-J, Junge H, Gladiali S, Beller M (2013). Nature 495:85
30. Alberico E, Lennox AJJ, Vogt LK, Jiao H, Baumann W, Drexler H, Nielsen M, Spannenberg A, Checinski MP, Junge H, Beller M (2016). J Am Chem Soc 138:14890
31. Rodríguez-Lugo RE, Trincado M, Vogt M, Tewes F, Santiso-Quinones G, Grützmacher H (2013). Nat Chem 5:342
32. Brewster TP, Goldberg JM, Tran JCD, Heinekey M, Goldberg KI (2016). ACS Catal 6:6302
33. Choi J-H, Heim LE, Ahrens M, Prechtl MHG (2014). Dalton Trans 43:17248
34. Heim LE, Schlörer NE, Choi J, Prechtl MHG (2014). Nat Commun 5:3621
35. Sponholz P, Mellmann D, Cordes C, Alsabeh PG, Li B, Li Y, Nielsen M, Junge H, Dixneuf P, Beller M (2014). ChemSusChem 7:2419
36. Zhang L, Nguyen DH, Raffa G, Trivelli X, Capet F, Desset S, Paul S, Dumeignil F, Gauvin R (2016). ChemSusChem 9:1413
37. Nguyen DH, Morin Y, Zhang L, Trivelli X, Capet F, Paul S, Desset S, Dumeignil F, Gauvin RM (2017). ChemCatChem 9:2652
38. Alberico E, Sponholz P, Cordes C, Nielsen M, Drexler H-J, Baumann W, Junge H, Beller M (2013). Angew Chem Int Ed 52:14162
39. Andérez-Fernández M, Vogt LK, Fischer S, Zhou W, Jiao H, Garbe M, Elangovan S, Junge K, Junge H, Ludwig R, Beller M (2017). Angew Chem Int Ed 56:559
40. Malineni J, Keul H, Möller M (2015). Dalton Trans 44:17409

41. Santilli C, Makarov IS, Fristrup P, Madsen R (2016). J Org Chem 81:9931
42. Ventura-Espinosa D, Vicent C, Bayac M, Mata JA (2016). Cat Sci Technol 6:8024
43. Wang X, Wang C, Liu Y, Xiao J (2016). Green Chem 18:4605
44. Dahl EW, Louis-Goff T, Szymczak NK (2017). Chem Commun 53:2287
45. Sarbajna A, Dutta I, Daw P, Dinda S, Rahaman SMW, Sarkar A, Bera JK (2017). ACS Catal 7:2786
46. Dai Z, Luo Q, Meng X, Li R, Zhang J, Peng T (2017). J Organomet Chem 830:11
47. Dai Z, Luo Q, Jiang H, Luo Q, Li H, Zhang J, Peng T (2017). Cat Sci Technol 7:2506
48. Fujita K, Tamura R, Tanaka Y, Yoshida M, Onoda M, Yamaguchi R (2017). ACS Catal 7:7226
49. Sawama Y, Morita K, Yamada T, Nagata S, Yabe Y, Monguchi Y, Sajiki H (2014). Green Chem 16:3439
50. Sawama Y, Morita K, Asai S, Kozawa M, Tadokoro S, Nakajima J, Monguchi Y, Sajikia H (2015). Adv Synth Catal 357:1205
51. Ghalehshahi HG, Madsen R (2017). Chem Eur J 23:11920

Top Organomet Chem (2019) 63: 193–224
DOI: 10.1007/3418_2018_23

Published online: 24 November 2018

Selective Transfer Hydrogenation of α,β-Unsaturated Carbonyl Compounds

Ronald A. Farrar-Tobar, Sergey Tin, and Johannes G. de Vries

Contents

Abstract Allylic alcohols are very versatile compounds which are used in a large variety of industrial processes. Transfer hydrogenation of α,β-unsaturated carbonyl compounds is a very appealing approach to obtain allylic alcohols. It avoids the use of stoichiometric and hazardous reagents such as $NaBH_4$ or $LiAlH_4$. Furthermore, compared to classical catalytic hydrogenations, these reactions do not need special equipment such as autoclaves or high-pressure reactors. Thus, protocols for transfer hydrogenation are cheaper and safer. One of the major problems in the reduction of unsaturated carbonyl compounds is to achieve high chemoselectivity. Free energy barriers for the reduction of carbonyl compounds and for the reduction of conjugated carbon-carbon double bonds are often very close in value. For that reason, mixtures of products as well as fully reduced products are often obtained making the scope of many catalysts limited. Herein we review the literature on selective transfer hydrogenation of α,β-unsaturated carbonyl compounds to the allylic alcohols using soluble

R. A. Farrar-Tobar, S. Tin, and J. G. de Vries (✉)
Department Catalysis with Renewable Resources, Leibniz Institut für Katalyse e. V., Rostock, Germany
e-mail: Johannes.devries@catalysis.de

transition metal complexes as catalysts. Ruthenium is the most employed metal in this field followed by iridium. In addition, some examples using complexes based on other transition metals including some first-row transition metals were found. This is a rapidly growing field. The review is structured according to the metals and to the hydrogen source used. In addition to these reductions catalysed by transition metal-based catalysts, there exists another type of transfer hydrogenation which follows a different mechanism which is known as the Meerwein-Ponndorf-Verley (MPV) reaction. This reaction uses metal alkoxide catalysts based on cheap metals such as aluminium. Whereas the original catalysts such as aluminium tri-isopropoxide were very slow, new variants have been developed that are much faster. The mechanisms reported for the MPV reaction and the transfer hydrogenation are briefly summarized, and the most interesting features of all references cited in this work are highlighted.

Keywords α,β-Unsaturated carbonyl compounds · Allyl alcohol · Carbonyl reduction · Chemoselectivity · Homogeneous catalysis · Iridium · Meerwein-Ponndorf-Verley · Ruthenium · Transfer hydrogenation

1 Introduction

Transfer hydrogenation allows the reduction of a large variety of compounds, such as aldehydes, ketones, imines, alkenes, alkynes, nitro-compounds, nitriles and esters in a simple and safe manner [1–4]. In particular the reduction of ketones and imines has also been performed enantioselectively using chiral transition metal-based catalysts. Using transfer hydrogenation, the use of potentially explosive hydrogen as well as the use of high-pressure equipment can be avoided. The method conforms to a number of the green chemistry principles such as less hazardous chemical synthesis, use of an innocuous solvent, use of catalysis and inherently safer chemistry. The most common hydrogen sources are iPrOH and HCOOH. To a lesser extent, other alcohols such as potentially renewable EtOH and cyclohexanol have also been studied. Also, other sources like ammonia borane or hydrazine were reported as potential sources of hydrogen for transfer hydrogenation. Depending on the hydrogen source employed, different by-products will be obtained. When iPrOH is used, acetone is obtained; when EtOH is used, acetaldehyde is the by-product which reacts further with another equivalent of ethanol; dehydrogenation of the formed hemiacetal gives ethyl acetate [5]. In case HCOOH is the source of hydrogen, CO_2 is produced [6]. With the latter two reductants, the reaction is irreversible allowing 100% conversion of the substrate. Using isopropanol, the transfer hydrogenation is an equilibrium reaction necessitating the use of a large excess of iPrOH to achieve conversions in excess of 95%. Once the catalyst is in its active state, it can reduce the substrate to the desired product via different pathways. There are three main reaction mechanisms described for these reactions [7]:

1. The inner sphere mechanism (Scheme 1). In this mechanism, the metal-halide complex **A** reacts with isopropoxide to form the isopropoxy complex **B**, which undergoes beta-hydride elimination to form the metal-hydride complex **C**. Insertion of the carbonyl compound into the metal hydride gives the new metal alkoxide complex **D**, which undergoes exchange with isopropanol to reform the metal isopropoxide complex.
2. The outer sphere mechanism (Noyori-Morris, Scheme 2) whereby the hydride of the metal is transferred directly to the substrate and the proton is either transferred from a ligated amino or hydroxy group in the ligand as in the Noyori mechanism (Scheme 2) or from the solvent as exemplified in the Dub and Gordon mechanism [8–10]. After that, the catalyst is ready to dehydrogenate the hydrogen source (isopropanol in this case) to furnish the active hydride (NH) form of the catalyst again.
3. The Meerwein-Ponndorf-Verley reaction follows a completely different mechanism [11] (Scheme 3). In this case, a carbonyl compound is coordinated to a strong Lewis acid metal complex like $Al(iPrO)_3$ forming a tetrahedral intermediate **B**. Then, a direct hydride transfer occurs from one of the alkoxide groups to the carbonyl via a six-membered transition state. After the release of one molecule of acetone, a new tridentate complex **C** is formed. Finally, the desired product is released by alkoxide exchange with another iPrOH molecule to form $Al(iPrO)_3$, closing the cycle. All steps in this mechanism are equilibria. Thus, the conversion is governed by the thermodynamic characteristics of the species involved and by the excess of reductant.

Due to the versatility of the transfer hydrogenation reaction, its application in both academia and industry is paramount. One type of substrate which is particularly challenging to be reduced via transfer hydrogenation is the α,β-unsaturated carbonyl compounds and more specifically the carbonyl bond in α,β-unsaturated aldehydes and ketones. The difference in activation energy between the reduction of the C=C conjugated double bond and the C=O bond is relatively small [12]. For that reason, mixtures of ketones, allylic alcohols and overreduced products may be obtained. However, in some cases, selectivity towards carbonyl compounds can be achieved

Scheme 1 Inner sphere mechanism

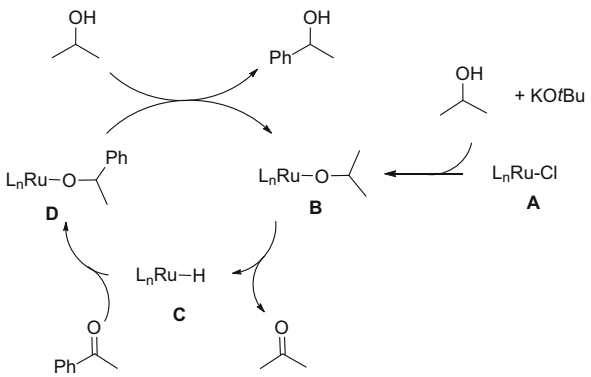

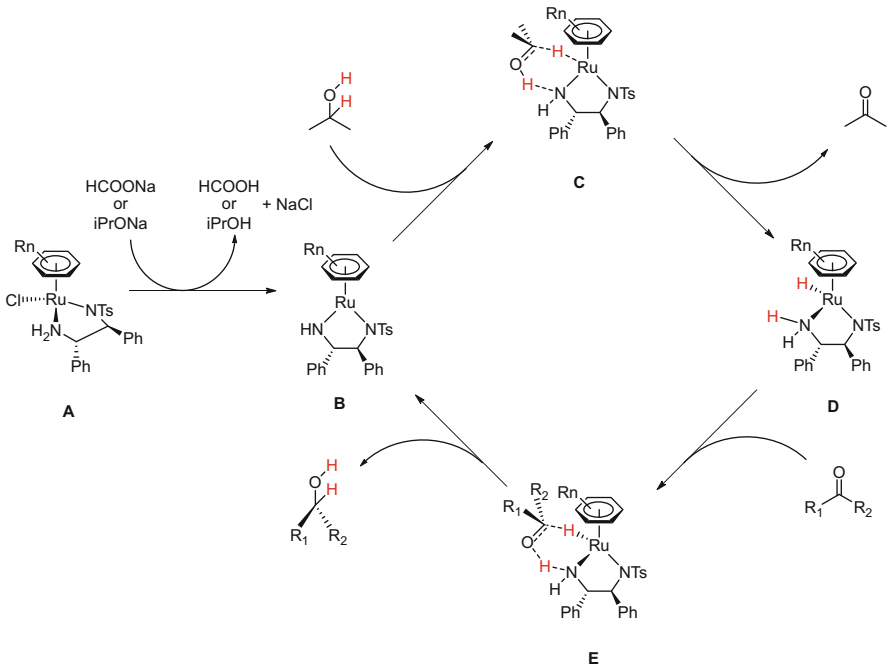

Scheme 2 Noyori-Morris outer sphere mechanism

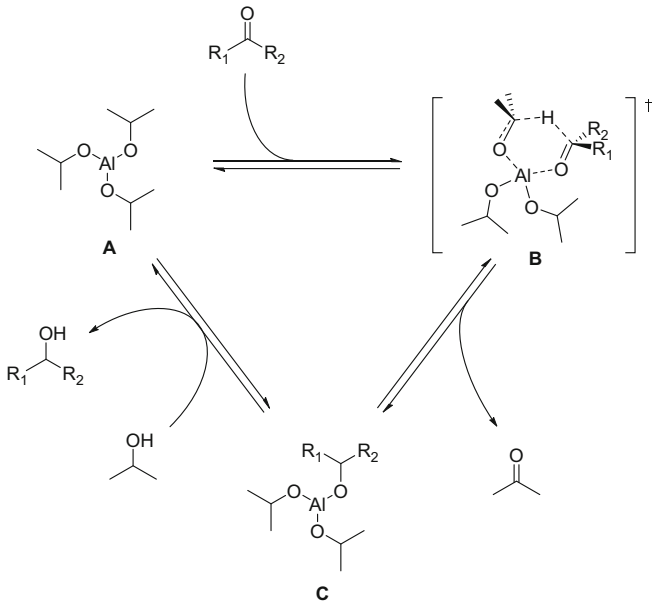

Scheme 3 Meerwein-Ponndorf-Verley mechanism

by kinetic control of the reactions. Recently, Dub and Gordon rationalized the C=O versus C=C selectivity obtained in some systems as a consequence of the C=O reduction within the outer sphere of the metal centre caused by non-innocent ligands [10]. Allylic alcohols are very important molecules in the chemical industry as they are used as intermediates in the synthesis of a large variety of commercial products. Furthermore, glycerol and monomers such as 1,4-butanediol or allyl carbonates are prepared from allyl alcohol [13]. In the fragrance industry, allylic alcohols are important intermediates [14]. In addition, allylic alcohols represent key intermediates in organic synthesis, for example, for hydroformylations [15] or ß-arylations [16]. Classic hydrogenation of this type of substrate using hydrogen gas was briefly reviewed in the context of the reduction of citral [17].

This review limits itself to homogeneous hydrogenations. Thus far, no review on the transfer hydrogenation of α,β-unsaturated carbonyl compounds has appeared. In this chapter, we cover mainly examples reported within the last 30 years and only a few relevant older ones.

2 Ruthenium Catalysts

Ruthenium-based complexes are by far the most reported catalysts in the transfer hydrogenation of α,β-unsaturated carbonyl compounds.

2.1 Chiral Metal Catalysts

2.1.1 Using iPrOH as Hydrogen Donor [18–25]

Back in the 1990s, Ryōji Noyori and co-workers developed ruthenium catalysts that were prepared from the reaction between $[Ru(Arene)Cl_2]_2$ and tosylated 1,2-diaryl ethylenediamines or 1,2-diarylaminoethanol as chiral ligands for the asymmetric transfer hydrogenation (ATH) of α,ß-acetylenic ketones (Fig. 1) [18]. They used iPrOH as hydrogen source, and the catalysis was very effective using 0.5 mol % catalyst loading at 28 °C, affording the desired unsaturated alcohols with very high enantioselectivities and yields (Table 1, entries 1–7). More than a decade later, Adolfsson's group was examining the use of the same ruthenium source combined with a hydroxy-amide ligand derived from L-alanine [19]. With these catalysts, more than ten substituted propargylic ketones were reduced to the corresponding propargylic alcohols in a TH process using iPrOH as hydrogen source in toluene. High yields and high enantioselectivities in very short reaction times were achieved. For some examples, see Table 1 (entries 9–11). To prove the robustness of the system, the reaction was scaled up to 10 mmol with substrate **7a** to give 88% yield of the desired product with 97% ee in only 30 min. The following year, Adolfsson, Pamies and Diéguez and co-workers reported more bio-based ligands for ruthenium

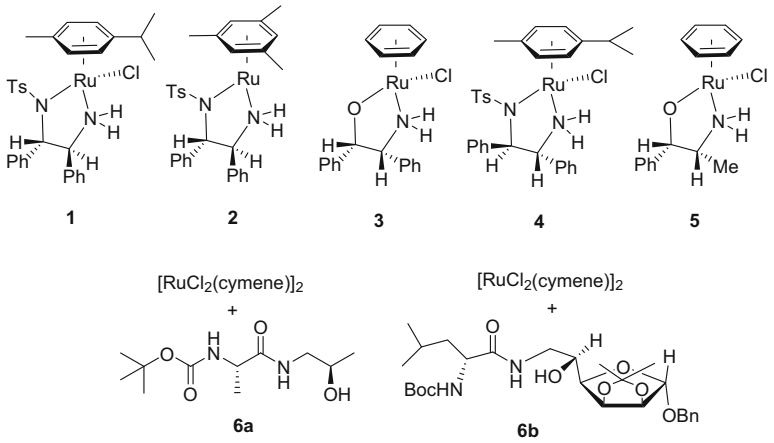

Fig. 1 Ruthenium-based catalysts for the chiral reduction of α,ß-unsaturated carbonyl compounds using iPrOH as hydrogen donor

catalysis. They synthesized a modular ligand library of α-amino acid hydroxyamides and thioamides [20]. One example of this library is the 2,3-O-isopropylidene-α-D-mannofuranoside derivative **6b** which in combination with [Ru(*p*-cymene)Cl_2]$_2$ succeeded in the TH of **7a** to afford the propargylic alcohol with 89% isolated yield and 96% ee (Table 1, entry 12). However, only 34% isolated yield was achieved when benzalacetone was the substrate. The ee was still as high as 95% (Table 2, entry 7). Interestingly, this catalyst also showed high activity for other types of transformations such as a tandem isomerization/asymmetric transfer hydrogenation of racemic allylic alcohols to the saturated alcohols and α-alkylation/asymmetric transfer hydrogenation of acetophenones and 3-acetylpyridine with primary alcohols.

A slightly lower ee was obtained when catalyst **3** was used for the reduction of deuterated cinnamaldehyde as substrate (Table 2, entry 1). Püntener and Hawaii Biotech were also working with the same catalysts targeting the reduction of substrate **8b** (Table 2, entries 2, 4) [22, 24]. In both cases, very good enantioselectivities in short reaction times were achieved. It is worth to mention that Püntener and Hawaii Biotech observed selectivity towards the more hindered carbonyl group. Also, the crystal structures of different ruthenium catalysts in this family were reported. However selectivity was slightly lower in all cases. Using Noyori's ruthenium catalyst **1**, the group of Zhaoguo Zhang selectively reduced several α-keto-β,γ-unsaturated esters with high yields and moderate enantioselectivities using iPrOH as the hydrogen source [25]. In this study, in order to achieve the desired selectivity towards the carbonyl moiety, isolating the previously activated catalyst was crucial. With this protocol, two heteroaromatic substituted substrates **8c** and **8d** were reduced to the desired unsaturated alcohols with 99% and 96% isolated yields, respectively, in only 1 h reaction time among other substrates (Table 2, entries 5–6). The observed ees were up to 65%.

Table 1 Enantioselective transfer hydrogenation of α,ß-acetylenic ketones to the corresponding chiral alcohols using ruthenium catalysts **1**, **2** and **6a** and **b** using iPrOH as hydrogen source

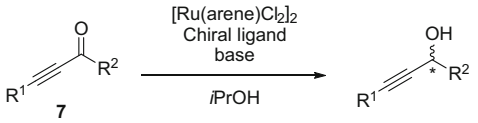

7

7a R^1 = Ph, R^2 = CH_3
7b R^1 = Ph, R^2 = $CH(CH_3)_2$
7c R^1 = Ph, R^2 = *c*-C_6H_{11}
7d R^1 = $Si(CH_3)_3$, R^2 = CH_3
7e R^1 = $Si(CH_3)_3$, R^2 = *n*-C_5H_{11}
7f R^1 = $Si(CH_3)_3$, R^2 = $CH(CH_3)_2$
7g R^1 = $Si(CH_3)_3$, R^2 = $CH(CH_3)CH(OTBS)CH(CH_3)CH_2OTBS$

Entry	Cat.	Cat. loading (mol%)	Base	Substrate	Temp.	Yield[a] (%)	ee (%)	Time (h)	Ref.
1	**1**	0.5	–	**7a**	28	>99	97[b]	20	[18]
2	**2**	0.5	KOH	**7a**	28	>99	97[b]	4	[18]
3	**2**	0.5	KOH	**7a**	28	>99	98[b]	18	[18]
4	**2**	0.5	KOH	**7b**	28	98	99[b]	5	[18]
5	**2**	0.5	KOH	**7c**	28	>99	98[b]	13	[18]
6	**1**	0.5	–	**7d**	28	>99	98[b]	12	[18]
7	**1**	0.5	–	**7e**	28	98	99[b]	15	[18]
8	**1**	0.5	–	**7f**	28	99	99[b]	12	[18]
9	**6a**	1	tBuOK	**7a**	rt	91	97	10	[19]
10	**6a**	1	tBuOK	**7b**	rt	98	99	10	[19]
11	**6a**	1	tBuOK	**7d**	rt	0	–	–	[19]
12	**6b**	0.25	tBuOK/ LiCl	**7a**	rt	89	96	10[c]	[20]

[a]Isolated yield
[b]HPLC analysis using Daicel Chiralcel OD column unless otherwise specified
[c]Time in minutes

2.1.2 Using Formic Acid as Hydrogen Donor [26–37]

Ru-arene complexes are also active in ATH when HCOOH is used as hydrogen donor. The group of Wills showed that catalysts **1** and **11** can afford enantioselectivities up to 99% when using HCOOH/Et_3N in the reduction of α,ß-acetylenic carbonyl compounds (Table 3, entries 4–6, 8–9) [26–28, 30, 36, 37]. In the same report, higher activity and increased selectivity were described when catalysts were modified by bridging the arene moiety and the diamine ligand forming catalysts **10** and **11a** (Fig. 2). This effect was rationalized by an π/CH edge/face directing effect of aryl-substituted substrates. Then, using catalyst loadings between 0.5 mol% and 10 mol%, the desired unsaturated alcohols were obtained with ee values up to 99% (Table 3, entries 1–3, 7, 10–12). Wills kept working on rationalizing the enantioselectivity of these Ru/TsDPEN complexes. This led to a

Table 2 Enantioselective transfer hydrogenation of α,β-unsaturated ketones by ruthenium catalysts in iPrOH

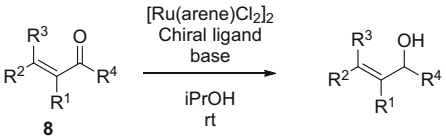

8

8a R^1 = H, R^2 = Ph, R^3 = H, R^4 = D
8b [Cycle] R^1 = Me, R^2 = H, [R^3 = $COCH_2C(CH_3)_2$ = R^4] (Ketoisophorone)
8c R^1 = H, R^2 = 2-furanyl, R^3 = H, R^4 = $COOCH(CH_3)_2$
8d R^1 = H, R^2 = 2-thiophenyl, R^3 = H, R^4 = $COOCH(CH_3)_2$
8o R^1 = R^3 = H, R^2 = Ph, R^4 = Me

Entry	Cat.	Loading (mol%)	Base	Substr.	Yield (%)	ee (%)	Time (h)	Ref.
1	**3**	1	*t*BuOK	**8a**	97[a]	72[b]	0.25	[21]
2	**3**	1	NaOH	**8b**	>99[c]	97[c]	0.5	[22]
3	**4** or **1**	5	–	**7g**	76	95	Overnight	[23]
4	**5**	0.8	NaOH	**8b**	60	[d]	3	[24]
5	**1**	1	–	**8c**	99[e]	59	1	[25]
6	**1**	1	–	**8d**	96[e]	65	1	[25]
7	**6b**	1	*t*BuOK/LiCl	**8o**	34[e]	95	10[f]	[20]

[a]Determined by GLC analysis
[b]Determined by ^{1}H-NMR analysis of the corresponding MTPA ester
[c]Conversion and ee determined by CG analysis
[d]Product identified as *R*-enantiomer without ee determination
[e]Isolated yield
[f]Time in minutes

very recent report on the TH of more challenging aryl/acetylenic ketones [29]. The strategy consisted of introducing an electron-donating group on the aryl moiety of the catalyst **11a** and **11b** (Fig. 2) combined with the use of aryl/acetyl *ortho*-substituted substrates. This allowed them to play with both electronics and sterics, thus increasing the enantioselectivity. Some examples from the scope are shown in Table 3 (entries 13–15).

Carmona and co-workers synthesized a trimeric ruthenium cluster (Fig. 2, **9**) for the transfer hydrogenation of cinnamaldehyde (**8e**) and citral (**8f**) (Table 4, entries 1–2) [31]. Substituting the arene moiety in Noyori's catalyst **1** by mesitylene gave catalyst **12** (Fig. 2) [32]. The use of 0.5 mol% of catalyst **12** in the presence of Et_3N was sufficient for the reduction of several α,ß-unsaturated carbonyl compounds to the corresponding allylic alcohols with excellent enantioselectivities (Table 4, entries 4–6). The group of Ying-Chun Chen designed and synthesized Fréchet-type core-functionalized chiral diamine-based dendritic ligands which they combined with [Ru(*p*-cymene)Cl_2]$_2$ (**13**) [33]. By modifying this type of ligands, they were able to control the solubility, which allowed them to recycle the catalyst several times. In addition, three benzalacetone derived substrates were reduced to the

Table 3 Enantioselective transfer hydrogenation of α,ß-acetylenic carbonyl compounds by ruthenium catalysts using HCOOH as hydrogen donor

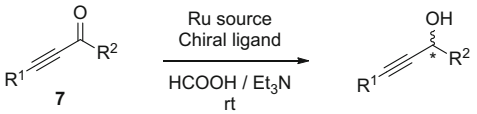

7h $R^1 = C{\equiv}C\text{-}(n\text{-}C_4H_9)$, $R^2 = n\text{-}C_3H_7$
7i $R^1 = C{\equiv}C\text{-}(CH_2)_4OH$, $R^2 = CH_3$
7j $R^1 = C{\equiv}C\text{-}(n\text{-}C_4H_9)$, $R^2 = CH_2(C_6H_5)$
7k $R^1 = C(CH_3)_2OBn$, $R^2 = (CH_2)COOCH_3$
7l $R^1 = Ph$, $R_2 = CH(CH_3)COOCH_2CH_3$
7m $R^1 = C(CH_3)_2OBn$, $R^2 = CH(CH_3)COOCH_2CH_3$
7n $R^1 = (CH_2)_2OBn$, $R^2 = (CH_2)_3COOCH_3$
7o $R^1 = Ph$, $R^2 = (CH_2)_3COC(C_6H_5)$
7p $R^1 = C(CH_3)_2OBn$, $R^2 = (CH_2)_3COCCC(CH_3)_2OBn$
7q $R^1 = Ph$, $R^2 = o\text{-}(Cl)Ph$
7r $R^1 = Ph$, $R^2 = o\text{-}(MeO)Ph$
7s $R^1 = Ph$, $R^2 = o\text{-}(BnO)Ph$

Entry	Cat.	Loading (mol%)	Substrate	Yield[a] (%)	ee (%)[b]	Time (h)	Ref.
1	**10**	10	**7h**	95	98	3	[26]
2	**10**	10	**7i**	96	>90	3	[26]
3	**10**	10	**7j**	92	98	3	[26]
4	**1**	10	**7h**	91	97	3	[26]
5	**1**	10	**7i**	89	>90	3	[26]
6	**1**	10	**7j**	90	97	3	[26]
7	**11a**	0.5	**7k**	99	99	48	[27, 28]
8	**4**	3.34	**7l**	99	98	48	[27, 28]
9	**4**	3.34	**7m**	90	99	48	[27, 28]
10	**11a**	0.2	**7n**	99	99	48	[27, 28]
11	**11a**	0.5	**7o**	96	>99	48	[27, 28]
12	**10**	0.5	**7p**	97	>99	48	[27, 28]
13	**11b**	0.1	**7q**	94	68	40	[29]
14	**11b**	0.1	**7r**	91	59	40	[29]
15	**11b**	0.1	**7s**	93	61	40	[29]

[a]Isolated yields
[b]Determined by HPLC

corresponding allylic alcohols in high isolated yields (Table 4, entries 7–9). The enantioselectivity was comparable with the one obtained with the monomeric counterpart. Ikarya, one of the pioneers of asymmetric transfer hydrogenation, and his co-workers developed a new generation of oxo-tethered ruthenium-amido complexes (Fig. 2, **11c**) [34]. This new generation was highly active allowing use of catalyst loadings down to 0.0025 mol% giving high yields and high enantioselectivities when aromatic ketones were used as substrates in TH. Also, the cyclic α,β-unsaturated ketone Seudenone **8m** was reduced at 60°C in 7 h to the corresponding enantioenriched unsaturated alcohol using 0.5 mol% catalyst loading

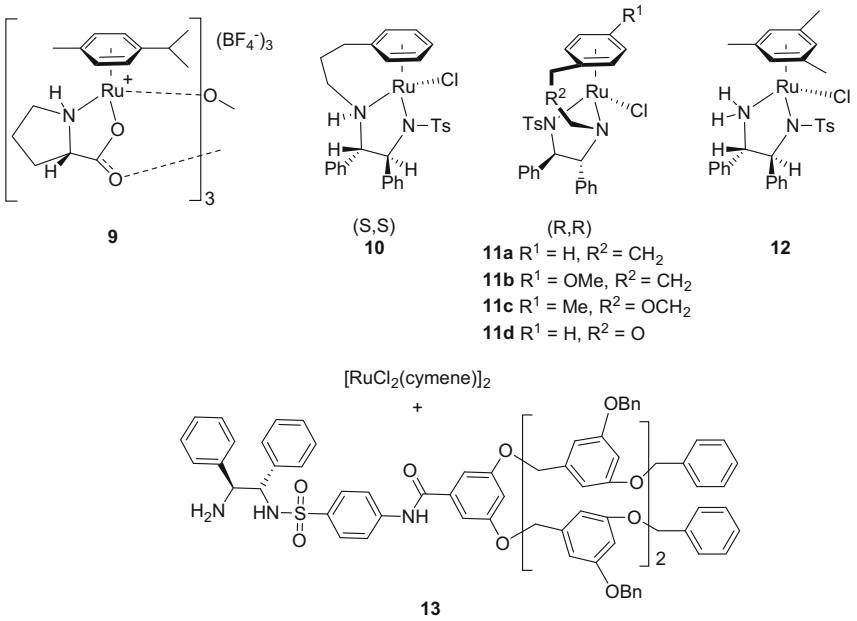

Fig. 2 Ruthenium based catalyst for chiral reduction of α,ß-unsaturated carbonyl compounds using HCOOH as hydrogen donor

with 94% yield and 96% ee (Table 4, entry 10). In the same year, Wills and his team were also modifying these tethered ruthenium complexes by introducing an ether group in the aliphatic bridge (Fig. 2, **11d**) [35]. In spite of the fact that several aromatic ketones were successfully reduced with high yields and good enantioselectivities, 13 days were necessary for the reduction of 1-acetyl-cyclohexene to the corresponding allylic alcohol (Table 4, entry 11). This result was hypothesized to be a consequence of the interaction between the ketone moiety from the substrate and the ether function of the catalyst.

2.2 Non-chiral Ruthenium Catalysts

2.2.1 Using iPrOH and Other Aliphatic Alcohols as Hydrogen Donor [38–45]

The ruthenium complexes reported for the TH of α,ß-unsaturated carbonyl compounds using alcohols as hydrogen donors are shown in Fig. 3.

Iyer and co-workers achieved good results in the TH of several α,ß-unsaturated carbonyl compounds using a very simple phosphine-free DMSO-Ru complex (Fig. 3, **14**) in combination with KOH (Table 5, entries 1–3) [38]. The fastest catalyst reported in the TH of α,ß-unsaturated carbonyl compounds was reported by

Table 4 Enantioselective transfer hydrogenation of α,ß-unsaturated carbonyl compounds by ruthenium catalysts using HCOOH as hydrogen donor

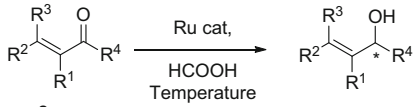

8

8b [Cycle] R^1 = Me, R^2 = H, [R^3 = $COCH_2C(CH_3)_2$ = R^4] (Ketoisophorone)
8e R^1 = R^3 = R^4 = H, R^2 = Ph
8f R^1 = R^4 = H, R^2 = $(CH_2)_2CH{=}C(CH_3)_2$, R^3 = Me
8g R^1 = R^3 = H, R^2 = Ph, R^4 = $CH(OCH_3)COOCH_3$
8h R^1 = R^3 = H, R^2 = p-MePh, R^4 = $CH(OCH_3)COOCH_3$
8i R^1 = R^3 = H, R^2 = m-MePh, R^4 = $CH(OCH_3)COOCH_3$
8j R^1 = R^3 = H, R^2 = thien-2-yl, R^4 = $CH(OCH_3)COOCH_3$
8k R^1 = H , R^3 = R^4 = Me, R^2 = Ph
8l R^1 = H , R^3 = R^4 = Me, R^2 = *p*-MeOPh
8m [Cycle] R^1 = H, [R^3 = $(CH_2)_3$ = R^4], R^2 = Me (Seudenone)
8n [Cycle] [R^1 = $(CH_2)_4$ = R^2], R^3 = H, R^4 = Me

Entry	Cat.	Loading (mol%)	Base	Temp. (°C)	Substrate	Yield (%)	ee (%)	Time (h)	Ref.
1	**9**	0.7	HCOONa	83	**8e**	41[a]	–	1	[31]
2	**9**	0.7	HCOONa	83	**8f**	82[a]	–	1	[31]
3	**12**	0.5	Et_3N	30	**8g**	>99[b]	99[c]	20	[32]
4	**12**	0.5	Et_3N	30	**8h**	>99[b]	99[c]	20	[32]
5	**12**	0.5	Et_3N	30	**8i**	>99[b]	99[c]	20	[32]
6	**12**	0.5	Et_3N	30	**8j**	>99[b]	98[c]	20	[32]
7	**13**	1	Et_3N	28	**8g**	85[d]	37[e]	28	[33]
8	**13**	1	Et_3N	28	**8k**	91[d]	75[e]	45	[33]
9	**13**	1	Et_3N	28	**8l**	54[d]	78[e]	72	[33]
10	**11c**	0.5	Et_3N	60	**8m**	94[f]	96[e]	6	[34]
11	**11d**	0.5	Et_3N	30	**8n**	99[f]	71[e]	13[g]	[35]

[a]Determined by GLC
[b]Determined by analysis of the ^{1}H-NMR of the crude product
[c]Determined by CSP-SCF
[d]Isolated yield
[e]Determined on a chiral column
[f]Determined by GC or ^{1}H-NMR spectroscopy
[g]Time in days

Baratta and co-workers (Fig. 3, **15**) [39]. Using only 0.05 mol% of **15** in combination with K_2CO_3 as base, full conversions were achieved after less than a minute of reaction time (Table 5, entries 4–5). The TOF of this system was reported to be up to 3.3×10^5 h^{-1}. This is the highest TOF reported to date in the transfer hydrogenation field. A lower TOF of 1,828 h^{-1} was observed in the TH of substrate **8o** (Table 5, entry 23) when the amine in the catalyst was substituted with a tolyl group (Fig. 3, **16**) by Gong, Song and co-workers [44]. Later, Baratta's research group reported the synthesis of catalyst **17** (Fig. 3) [40]. This catalyst showed excellent selectivity when

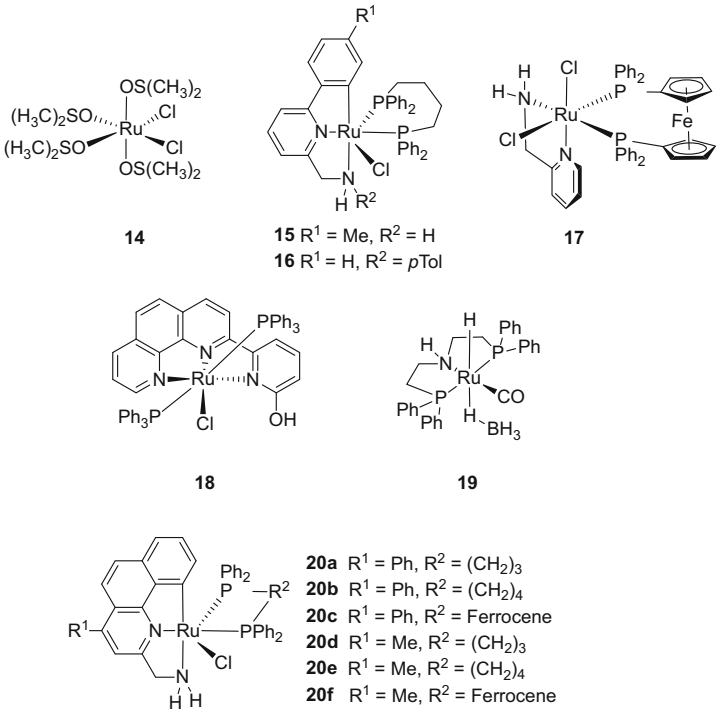

Fig. 3 Non-chiral ruthenium catalysts for transfer hydrogenation of α,ß-unsaturated carbonyl compounds using alcohols as hydrogen source

compound **8e** was reduced (Table 5, entry 6). Several new ruthenium-based complexes (Fig. 3, complex **20**) were developed in the same group in 2016 [42]. A very impressive activity was observed when aromatic ketones were used as substrates. In addition, unsaturated aldehydes **8e** and **8t** were selectively reduced to the allylic alcohols with catalyst loadings down to 0.005 mol% (Table 5, entries 14–22). However, 10–20% of different by-products including the corresponding saturated alcohols were observed depending on the substrate. A complete family of these types of systems was patented the same year [43]. S. Kundu and co-workers used an *N*,*N*,*N*-type pincer ligand which was reacted with $RuCl_2(PPh_3)_3$ giving complex **18** (Fig. 3) [41]. This complex was able to reduce benzalacetone (**8o**) to the corresponding allylic alcohol with 98% NMR yield (Table 5, entry 7). Although much more scarce than the use of iPrOH, some examples can be found in the literature of the use of EtOH as hydrogen donor. EtOH represents a cheap and green source of hydrogen. However, possible drawbacks of its use, such as catalyst poisoning by forming stable carbonyl complexes via decarbonylation of the formed acetaldehyde [46–48], and possible aldol condensations between acetaldehyde and the substrates such as the α,ß-unsaturated carbonyl compounds, have deterred most researchers. Nevertheless, de Vries and co-workers have shown that it is possible to

Table 5 Transfer hydrogenation results of α,ß-unsaturated carbonyl compounds by ruthenium catalyst using different alcohols as hydrogen donors

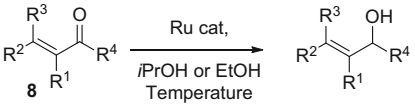

8e $R^1 = R^3 = R^4 = H$, $R^2 = Ph$
8f $R^1 = R^4 = H$, $R^2 = (CH_2)_2CH=C(CH_3)_2$, $R^3 = Me$
8o $R^1 = R^3 = H$, $R^2 = Ph$, $R^4 = Me$
8p $R^1 = R^2 = Me$, $R^3 = R^4 = H$
8q $R^1 = R^3 = R^4 = H$, $R^2 = Me$
8r $R^1 = R^3 = H = R^4 = H$, R^2 = 2,6,6-trimethylcyclohex-1-en-1-yl
8s $R^1 = R^3 = H = R^4 = H$, R^2 = furan-2-yl
8t $R^1 = Me$, $R^2 = Ph$, $R^3 = R^4 = H$

Entry	Cat.	Loading (mol%)	Base	Substr.	Temp. (°C)	Yield[a] (%)	Time (h)	Ref.
1	**14**	1.6	KOH	**8o**	83	96	25[b]	[38]
2	**14**	1.6	KOH	**8e**	83	71	24	[38]
3	**14**	1.6	KOH	**8f**	83	87	3	[38]
4	**15**	0.05	K_2CO_3	**8e**	83	>99[c]	30[d]	[39]
5	**15**	0.05	K_2CO_3	**8p**	83	>99[c]	30[d]	[39]
6	**17**	0.05	NaO*i*Pr	**8e**	83	95[c]	25	[40]
7	**18**	0.1	tBuOK	**8o**	83	98[e]	75[d]	[41]
8	**19**	0.5	–	**8e**	83	95	30[b]	[45]
9[f]	**19**	0.1	–	**8f**	78	97	10[b]	[45]
10	**19**	0.1	–	**8q**	83	89	10[b]	[45]
11	**19**	0.1	–	**8b**	83	84	30[b]	[45]
12[f]	**19**	0.1	–	**8r**	78	91	30[b]	[45]
13	**19**	0.1	–	**8s**	83	99	2[b]	[45]
14	**20a**	0.025	K_2CO_3	**8e**	82	89[c,e]	1	[42]
15	**20a**	0.01	K_2CO_3	**8t**	82	91[c,e]	2.75	[42]
16	**20b**	0.025	K_2CO_3	**8e**	82	90[c,e]	1	[42]
17	**20b**	0.01	K_2CO_3	**8t**	82	95[c,e]	1.75	[42]
18	**20c**	0.01	K_2CO_3	**8e**	82	80[c,e]	4	[42]
19	**20c**	0.005	K_2CO_3	**8t**	82	95[c,e]	2.75	[42]
20	**20d**	0.01	K_2CO_3	**8e**	82	77[c,e]	4	[42]
21	**20e**	0.01	K_2CO_3	**8e**	82	77[c,e]	4	[42]
22	**20f**	0.025	K_2CO_3	**8e**	82	84[c,e]	1	[42]
23	**16**	0.05	NaOH	**8o**	82	91[g]	1	[44]

[a]Isolated yield
[b]Time in minutes
[c]Determined by GC
[d]Time in seconds
[e]Determined by NMR
[f]EtOH used as hydrogen donor and solvent
[g]Determined by GC-Mass

use EtOH as a reductant in a base-free process for the reduction of a broad scope of α,ß-unsaturated ketones and aldehydes using Ru-MACHO-BH (**19**) as catalyst. In this work, allylic alcohols were obtained using catalyst loadings down to 0.1 mol% in short reaction times. An extract of the scope is summarized in Table 5 (entries 8–13). In some but not in all cases, higher selectivities were obtained with isopropanol as reductant.

2.2.2 Using HCOOH as Hydrogen Donor [42, 49–56]

The ruthenium complexes that have been used for the transfer hydrogenation of unsaturated carbonyl compounds using HCOOH as hydrogen donor are shown in Fig. 4. These catalysts are usually activated with different bases like NH_3, Et_3N or HCOONa. The resulting combination of HCOOH and a compatible base forms buffer solutions allowing better pH control [57]. In this context, Baratta and co-workers used the extremely active Ru-NNC phosphine-substituted complex **20b**. This catalyst was capable of reducing cinnamaldehyde and α-methyl-

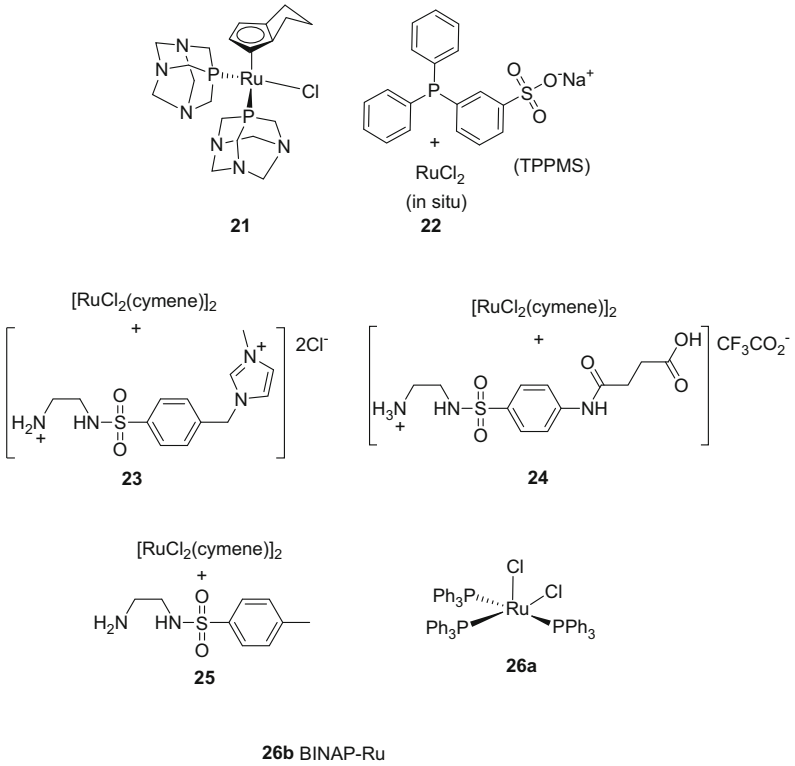

Fig. 4 Non-chiral ruthenium catalysts for the transfer hydrogenation of α,ß-unsaturated carbonyl compounds using HCOOH

cinnamaldehyde to the corresponding allylic alcohols using catalyst loadings as low as 0.05% mol (Table 6, entries 1–2) [42]. A different active ruthenium complex based on the water-soluble PTA phosphine ligand was used by Frost and co-workers (Fig. 4, complex **21**) [49]. This complex was shown to be selective for carbonyl reduction when cinnamaldehyde and benzalacetone were used as substrates (Table 6, entries 3–4). Unfortunately, rates and selectivity were dramatically lower

Table 6 Transfer hydrogenation of α,ß-unsaturated carbonyl compounds catalysed by ruthenium catalysts using HCOOH as hydrogen donor

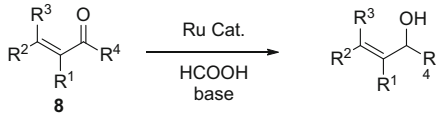

8e $R^1 = R^3 = R^4 = H$, $R^2 = Ph$
8f $R^1 = R^4 = H$, $R^2 = (CH_2)_2CH{=}C(CH_3)_2$, $R^3 = Me$
8o $R^1 = R^3 = H$, $R^2 = Ph$, $R^4 = Me$
8q $R^1 = R^3 = R^4 = H$, $R^2 = Me$
8t $R^1 = Me$, $R^2 = Ph$, $R^3 = R^4 = H$

Entry	Cat.	Loading (mol%)	Base	Temp. (°C)	Substrate	Yield (%)	Time (h)	Ref.
1	**20b**	0.05	NH_3	90	**8e**	91[a] (88[b])	10	[42]
2	**20b**	0.05	NH_3	90	**8t**	85[a]	48	[42]
3	**21**	5	HCOONa	80	**8e**	100[a,c]	6	[49]
4	**21**	5	HCOONa	80	**8o**	81[a,c]	24	[49]
5	**22**	1.5	HCOONa	80	**8e**	98[d] (92[b])	5	[50]
6	**22**	1.5	HCOONa	80	**8q**	78[d]	2.5	[50]
7	**22**	1.5	HCOONa	80	**8f**	98[d] (95[b])	7	[50]
8	**26a**	0.04	Et_3N	rt	**8f**	99[d]	30[e]	[51]
9	**26a**	0.04	Et_3N	rt	**8e**	95[b]	30[e]	[51]
10	**23**	0.5	HCOONa	80	**8e**	96[a]	30[e]	[52]
11	**23**	0.5	HCOONa	80	**8f**	96[a]	3.5	[52]
12	**23**	0.5	HCOONa	80	**8q**	96[a]	30[e]	[52]
13	**24**	0.5	HCOONa	80	**8e**	80[a]	90[e]	[53]
14	**24**	0.5	HCOONa	80	**8f**	31[a]	90[e]	[53]
15	**25**	0.45	Et_3N	rt	**8f**	99[f]	20	[54]
16	**26b**	0.5	–	40	**8o**	65[a,c,d,g]	3	[55]
17	**22**	1	HCOONa	**8e**	rt	90[a]	1	[56]
18	**22**	1	HCOONa	**8f**	rt	65[a]	1	[56]

[a]Determined by GC
[b]Isolated yield
[c]Determined by NMR
[d]Determined by GLC
[e]Time in minutes
[f]Determined by HPLC
[g]$Et_3NH^+H_2PO_2^-$ in H_2O was de hydrogen donor

when chalcone was the substrate. Different protocols like in situ catalyst formation were also investigated. For instance, Joo and co-workers used a combination of monosulfonated triphenylphosphine as its sodium salt and Ru^{2+} (**22**) in a biphasic system which allowed them to selectively reduce unsaturated aldehydes like cinnamaldehyde, citral and the challenging crotonaldehyde with very high yields (Table 6, entries 5–7) [50]. This catalyst was shown to be active at 30°C as well. Joo and his group continued studying these biphasic systems, and some years later, they observed how the rates were increased by using iPrOH as co-solvent [56]. In these reactions, the catalyst resides in the aqueous phase, while substrate and product remain in the organic layer allowing the easy separation of the catalyst from the product once the reaction is finished. In this particular case, HCOONa is in the aqueous phase, which is mixed with an organic layer of neat product or organic solvents like toluene or chlorobenzene. This protocol allowed the reduction of cinnamaldehyde to cinnamyl alcohol in 90% yield (Table 6, entry 17). The reported TOF was 160 h^{-1}. However, the selectivity was only 60% when citral (**8f**) was the substrate (Table 6, entry 18). Other in situ catalysts were reported by the group of Zhou [52, 53]. A combination of $[Ru(p\text{-cymene})Cl_2]_2$ with water-soluble monotosylated ethylenediamines was used as catalyst (Fig. 4, **23**–**24**). With this approach using a ruthenium content of 0.5 mol%, cinnamaldehyde, citral and crotonaldehyde were selectively reduced with high yields in short reaction times (Table 6, entries 10–14). A few years later, DSM patented the use of tosylated diamines as ligands for the ruthenium-catalysed transfer hydrogenation of citral and ethyl citral at room temperature (Fig. 4, **25**; Table 6, entry 15) [54]. Last but not the least, Arcelli and co-workers used commercially available $Ru(PPh_3)_3Cl_2$ to selectively reduce cinnamaldehyde and citral with catalyst loadings as low as 0.04 mol% and very short reaction times (Table 6, entries 8–9) [51]. Later, the same research group compared the activity of **26a** with that of ruthenium-BINAP [55]. In this work, a very uncommon hydrogen source consisting in a mixture of Et_3N and H_3PO_2 in water was used, which resulted in 65% yield in the TH of benzalacetone (**8o**).

3 Iridium Catalysts

Iridium is the second most used metal in homogeneous transfer hydrogenation catalysis. The high activity of the iridium-based catalysts and their high tolerance with respect to H_2O, acids and other functionalities make iridium a very appealing choice. Nevertheless, the high price of this precious metal is one of the major drawbacks.

3.1 Using iPrOH as Hydrogen Donor [58–60]

Back in 1978, James and Morris showed the feasibility of using Henbest's catalyst (Fig. 5, complex **28**) for the selective reduction of the carbonyl moiety in cinnamaldehyde, α-methyl-cinnamaldehyde and crotonaldehyde using iPrOH as hydrogen donor (Table 7, entries 5–7) [58]. Interestingly, they observed how the

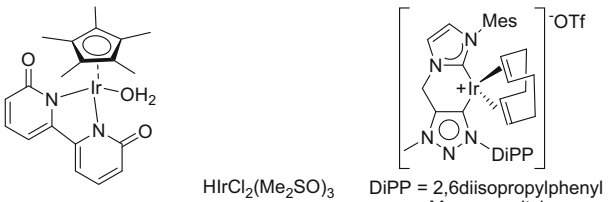

27 **28** **29**

Fig. 5 Iridium catalysts for transfer hydrogenation of α,ß-unsaturated carbonyl compounds using iPrOH as hydrogen source

Table 7 Transfer hydrogenation of α,ß-unsaturated carbonyl compounds using iridium catalysts and iPrOH as hydrogen donor

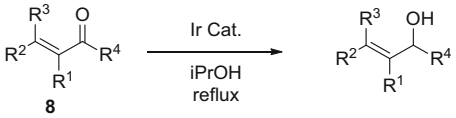

8

8e $R^1 = R^3 = R^4 = H$, $R^2 = Ph$
8f $R^1 = R^4 = H$, $R^2 = (CH_2)_2CH{=}C(CH_3)_2$, $R^3 = Me$
8p $R^1 = R^2 = Me$, $R^3 = R^4 = H$
8q $R^1 = R^3 = R^4 = H$, $R^2 = Me$
8s $R^1 = R^3 = H = R^4 = H$, R^2 = furan-2-yl
8t $R^1 = Me$, $R^2 = Ph$, $R^3 = R^4 = H$

Entry	Cat.	Loading (mol%)	Temp. (°C)	Substrate	Yield (%)	Time (h)	Ref.
1	**27**	0.2	120	**8e**	92[a]	12	[60]
2	**27**	0.2	refl.	**8f**	94[a]	6	[60]
3	**27**	0.2	refl.	**8p**	80[a]	6	[60]
4	**27**	0.2	120	**8s**	92[a]	12	[60]
5	**28**	4	refl.	**8e**	78[b]	80[c]	[58]
6	**28**	4	refl.	**8t**	90[b]	250[c]	[58]
7	**28**	4	refl.	**8q**	85[b]	50[c]	[58]
8	**29**[d]	1	refl.	**8e**	56[e]	23	[59]

[a]Isolated yields
[b]Determined by GLC and NMR
[c]Time in minutes
[d]10 mol% of *t*-BuOk was used
[e]Determined by GC

selectivity was dropping down when the water content in the system was increased. The authors attributed this to a catalyst decomposition by moisture, which was observable by a colour change of the complex from white to yellow. Best rates and selectivities were achieved when the isolated complex was used under dry conditions. After that, it was not until 2014 when another iridium-based catalyst appeared in the literature for this type of transformation. Elsevier and co-workers synthesized a variety of Ir(COD) complexes bearing carbene ligands based on the combination of 1,2,3-triazol-5-ylidene (tzNHC) and an Arduengo-type N-heterocyclic carbene (NHC) motif [59]. One of these complexes (**29**) was able to catalyse the transfer hydrogenation of cinnamaldehyde with moderate selectivity (Table 7, entry 8). Very recently in 2018, the group of Li used an iridium complex bearing a functional bipyridonate ligand (Fig. 5, **27**) for the selective transfer hydrogenation of carbonyl groups under base-free conditions of a very broad variety of unsaturated aldehydes to the corresponding allylic alcohols [60]. Some examples are summarized in Table 7 (entries 1–4). The functional group tolerance of this reaction is remarkable, especially with regard to aromatic substrates.

3.2 Using HCOOH as Hydrogen Donor [61–66]

The stability of certain iridium catalysts towards acids makes the use of HCOOH as hydrogen donor possible for the transfer hydrogenation of α,ß-unsaturated carbonyl compounds. Therefore, more examples can be found in the last decade (Fig. 6) where catalyst loadings for this type of reactions were reduced. Analogously to the previously described complexes **23**, **24** and **25** (Fig. 4) in the previous section, monotosylated ethylenediamines can also be combined in situ with $[IrCpCl_2]_2$ as a metal source to afford an active system in the transfer hydrogenation of unsaturated carbonyl compounds. These catalysts were reported by Xiao in 2006 and by Zhou in 2011 (Fig. 6, **31**, **35**, respectively) [61, 63]. In the first case, Xiao and co-workers tested a variety of rhodium, ruthenium and iridium complexes based on monotosylated ethylenediamines observing TOFs up to 132,000 h^{-1} for benzaldehyde transfer hydrogenation. In addition, complex **31** (Fig. 6) was shown to be very robust being stable in water and air while staying active for the selective transfer hydrogenation of the carbonyl group of a large range of unsaturated aldehydes. Some examples are summarized in Table 8 (entries 3–5). In more recent work, Zhou modified these monotosylated ethylenediamines finding that complex **35** was very active and very selective when cinnamaldehyde, citral and crotonaldehyde were tested as substrates (Table 8, entries 14–16) [63]. Coordination of iridium with bipyridine- and pyridine-imidazole-based ligands to create active transfer hydrogenation catalysts was pursued by different groups and companies. One example of this is the work performed by the Himeda group [62]. The main novelty of this work was the substitution of the bipyridine ligand with hydroxy groups. These moieties can be deprotonated at basic pH making the ligand much more electron donating, resulting in an increase of the TOF (complex **30**, Fig. 6). However, selectivity

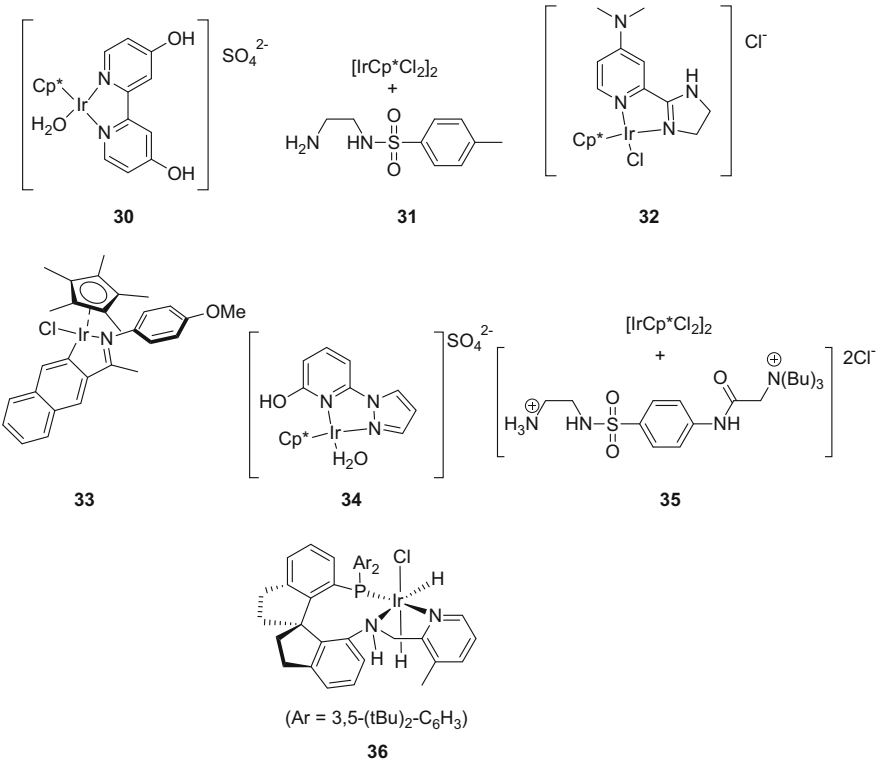

Fig. 6 Iridium catalysts for the transfer hydrogenation of α,ß-unsaturated carbonyl compounds using HCOOH

towards allylic alcohols was satisfactory in only one example, and pH 2.6 was needed for selectivity towards carbonyl reduction (Table 8, entry 1). An 85% yield was obtained and a TOF of 1,200 h^{-1} was observed.

Later in 2015, the Dalian University of Technology patented a family of pyridine-imidazole-iridium complexes for the transfer hydrogenation of α,ß-unsaturated carbonyl compounds (aldehydes and ketones) [65]. As an example, they used complex **34** for cinnamaldehyde reduction obtaining the corresponding cinnamyl alcohol in 82% yield under mild conditions (Table 8, entry 13). Recently, Tang also explored this type of complex [66]. He found that coordinating 2-(*p*-dimethylaminopyrid-2-yl)-imidazole with iridium (Fig. 6, complex **32**) resulted in a very robust complex. This complex is water and air stable and is very active for the reduction of a large variety of carbonyl compounds including cinnamaldehyde and α-methyl-cinnamaldehyde with excellent selectivities (Table 8, entries 6–7). TOFs up to 73,800 h^{-1} were observed when saturated compounds were used as substrates. Finally, iridacycles were used as catalyst in the group of Xiao [64]. In this work, complex **33** (Fig. 6) was used for the transfer hydrogenation of a large variety of substrates in H_2O buffered with the HCOOH/HCOONa couple, which also serves as

Table 8 Transfer hydrogenation of α,ß-unsaturated carbonyl compounds using iridium catalysts and HCOOH as hydrogen donor

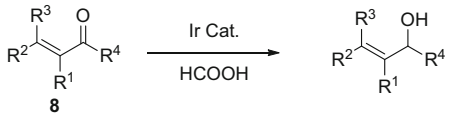

8

8e $R^1 = R^3 = R^4 = H$, $R^2 = Ph$
8f $R^1 = R^4 = H$, $R^2 = (CH_2)_2CH=C(CH_3)_2$, $R^3 = Me$
8o $R^1 = R^3 = H$, $R^2 = Ph$, $R^4 = Me$
8p $R^1 = R^4 = H$, $R^2 = R^3 = Me$
8q $R^1 = R^3 = R^4 = H$, $R^2 = Me$
8r $R^1 = R^3 = H = R^4 = H$, R^2 = 2,6,6-trimethylcyclohex-1-en-1-yl
8s $R^1 = R^3 = H = R^4 = H$, R^2 = furan-2-yl
8t $R^1 = Me$, $R^2 = Ph$, $R^3 = R^4 = H$
7a $R^1 = Ph$, $R^2 = Me$
7c $R^1 = Ph$, $R^2 = CH(CH_3)_2$
7q R^1 = *p*-MePh , $R^2 = Me$

Entry	Cat.	Loading (mol%)	Base	Temp. (°C)	Substrate	Yield[a] (%)	Time (h)	Ref.
1	**30**	0.05	HCOONa	40	**8e**	85[b]	8	[62]
2	**31**	0.02	HCOONa	80	**8e**	97	3	[61]
3	**31**	0.02	HCOONa	80	**8f**	97	4	[61]
4	**31**	0.02	HCOONa	80	**8q**	>99	1	[61]
5	**31**	0.02	HCOONa	80	**8t**	98	6[c]	[61]
6	**32**	0.02	–	80	**8e**	95	18[c]	[66]
7	**32**	0.02	–	80	**8t**	91	20[c]	[66]
8	**33**	0.1	HCOONa	80	**8e**	89	6	[64]
9	**33**	0.1	HCOONa	80	**8t**	92	6	[64]
10	**33**	0.1	HCOONa	80	**8f**	90	6	[64]
11	**33**	0.1	HCOONa	80	**8o**	58	6	[64]
12	**33**	0.1	HCOONa	80	**8r**	66	6	[64]
13	**34**	0.25	HCOONa	50	**8e**	82	4.5	[65]
14	**35**	0.1	HCOONa	80	**8e**	76[b]	3	[63]
15	**35**	0.1	HCOONa	80	**8f**	89[b]	3	[63]
16	**35**	0.1	HCOONa	80	**8e**	100[b]	20[c]	[63]
17	**36**	1	HCOONa[d]	60	**7a**	99[a] (96)[e]	8	[67]
18	**36**	1	HCOONa[d]	60	**7c**	90[a] (94)[e]	40	[67]
19	**36**	1	HCOONa[d]	60	**7q**	98[a] (97)[e]	10	[67]

[a]Isolated yield
[b]Determined by GC/HPLC
[c]Time in minutes
[d]HCOONa (0.4 mmol) combined with EtOH (5 mL)
[e]ee in brackets, determined by HPLC using a chiral column

hydrogen donor. Among other substrates, several α,ß-unsaturated aldehyde compounds were successfully reduced. An extract of these results is shown in Table 9 (entries 8–12). However, selectivity was poor when the target substrates were α,ß-unsaturated ketones instead of α,ß-unsaturated aldehydes (Table 9, entry 11). Xie and co-workers synthesized the chiral Ir-SpiroPAP complex (**36**) bearing a tridentate spiro-pyridine-aminophosphine ligand (Fig. 6) which they used for the TH of propargylic ketones [67]. This catalyst did work neither with EtOH nor with HCOOH/Et_3N but only with HCOONa in EtOH. After monitoring the reaction performed with HCOOCs in EtOH by in situ IR spectroscopy, they observed the conversion of HCOOCs and the simultaneous formation of $EtOCO_2Cs$. In addition, several alkynyl ketones were reduced with high yields and high enantioselectivities. Some examples are summarized in Table 8 (entries 17–19).

4 Iron and Other Less Common Metals as Catalysts

In addition to the abundance of Ru and Ir transfer hydrogenation catalysts in the literature, there are also publications describing the use of catalysts based on other precious metals like Rh or Ag and other transition metals like Os. Furthermore, the growing interest in greener processes as well as in cheap metals for catalysis has resulted in an exponential growth of work on catalysts based on first-row transition metals. This is also true for the transfer hydrogenation of α,ß-unsaturated compounds, and examples of the use of complexes based on Fe, Ni and more recently Mn have appeared.

4.1 Using iPrOH as Hydrogen Donor [20, 40, 45, 68–76]

One of the most well-known publications in the transfer hydrogenation field stems from the work of Morris and co-workers who reported the synthesis of the chiral amine(imine)diphosphine iron complex (Fig. 7, compound **37a**) [70]. This extremely active and fast catalyst was shown to achieve TOFs up to 242 s^{-1} at 28°C. Unfortunately, when it was tested for the reduction of **8o** as an α,ß-unsaturated ketone substrate, only 55% yield of the desired product could be obtained (Table 9, entry 8). Morris and co-workers made different modifications to the catalyst, leading to the complexes **37b**–**d**, which were patented [73–76]. However, only catalysts **37c** and **37d** were capable of converting substrate **8o** in good selectivity and yield to the desired allylic alcohol (Table 9, entries 16–17). The crystal structures of similar iron complexes bearing PNNP ligand as well as in the form of a macrocycle were reported by Mezzetti and co-workers [72]. By modifying the substituents of the isonitrile ligand, the activity and enantioselectivity of the TH of acetophenone with complexes **38a** and **38b** were shown to be greatly enhanced. In addition to the scope of ketones, the α,β-unsaturated ketone (**8o**) was reduced to the corresponding allylic

Table 9 Transfer hydrogenation of α,ß-unsaturated carbonyl compounds using catalysts based on iron, manganese, osmium and rhodium and alcohols as hydrogen donor

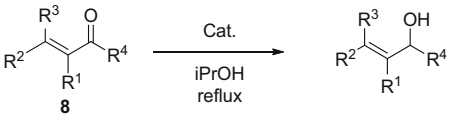

8

8e $R^1 = R^3 = R^4 = H$, $R^2 = Ph$
8o $R^1 = R^3 = H$, $R^2 = Ph$, $R^4 = Me$
8q $R^1 = R^3 = R^4 = H$, $R^2 = Me$
8r $R^1 = R^3 = R^4 = H$, R^2 = 2,6,6-trimethylcyclohex-1-en-1-yl
8t $R^1 = R^4 = H$, $R^2 = Ph$, $R^3 = Me$
8u [Cycle] $R^1 = CH_2CH(C(CH_2)CH_3)CH_2 = R^2$, $R^4 = R^3 = H$ (Perillaldehyde)
8v [Cycle] $R^3 = CH_2CH(C(CH_2)CH_3)CH_2 = R^4$, $R^1 = CH_3$, $R^2 = H$ (Carvone)

Entry	Cat.	Loading (mol%)	Base	Substrate	Yield (%)	Time (h)	Ref.
1	**39a**	2	–	**8e**	98[a]	18	[68]
2	**39a**	2	–	**8t**	97[a]	18	[68]
3	**38a**	2	–	**8u**	85[a]	18	[68]
4	**39a**	5	–	**8v**	35[a]	18	[68]
5	**39b**	2	$(CH_3)_3NO$	**8o**	22[b,c]	24	[69]
6	**39b**	2	$(CH_3)_3NO$	**8e**	99[b,c]	24	[69]
7	**40**	0.05	NaOiPr	**8e**	95[b]	30[d]	[40]
8	**37a**	0.05	t-BuOK	**8o**	55[b,e]	4[d]	[70]
9	**41**[f]	1	–	**8q**	>99[b]	2[d]	[45]
10	**42**	0.5	t-BuOK	**8o**	90[c,g]	20[d]	[71]
11	**42**	0.5	t-BuOK	**8r**	100[c,g] (90[a])[g]	1	[71]
12	**42**	0.5	t-BuOK	**8e**	92[c] (80[a])	2	[71]
13	**38a**	0.1	t-BuOK	**8o**	81[b,h]	5	[72]
14	**38b**	0.1	t-BuOK	**8o**	76[b,h]	5	[72]
15	**37b**	0.2	t-BuOK	**8o**	40[b,h]	20[d]	[74]
16	**37c**	0.07–0.2	t-BuOK	**8o**	82[i]	30[d]	[75]
17	**37d**	1.8	t-BuOK	**8o**	70[j]	130[d]	[76]
18	**43**	0.25	t-BuOK/LiCl	**8o**[k]	32[l]	3	[20]
19	**43**	0.25	t-BuOK/LiCl	**7a**[m]	90[l]	3	[20]

[a]Isolated yields
[b]Determined by GC
[c]Determined by ^{1}H-NMR
[d]Time in minutes
[e]40% ee
[f]EtOH used as hydrogen donor and solvent
[g]If room temperature was used, 16 h was enough to afford 87% GC yield using substrate **8r** and 87% isolated yield using substrate **8o**
[h]Temperature was 50°C. **38a** and **38b** gave an ee of 65% and 70%, respectively
[i]Temperature was 22°C and 5% ee was obtained
[j]68% ee
[k]82% ee
[l]Room temperature
[m]87% ee

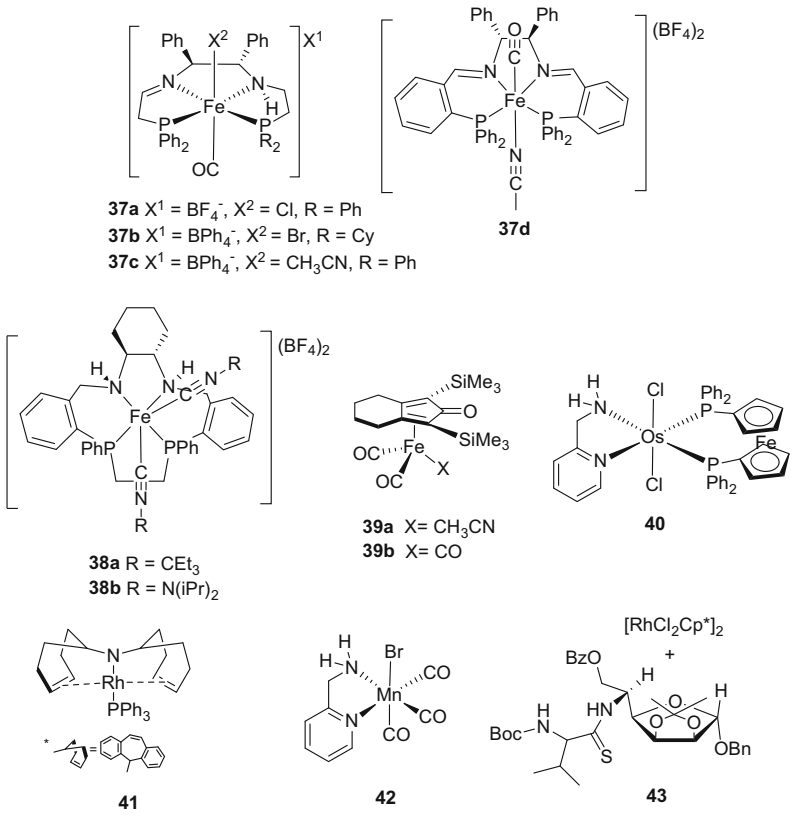

Fig. 7 Transfer hydrogenation catalysts based on iron, manganese, osmium and rhodium

alcohol with complete chemoselectivity with 81% and 76% GC yield, respectively (Table 9, entries 13–14). Other reports on iron catalysts come from Funk and co-workers who have shown that it is possible to use the Knölker complex (Fig. 7, complex **39b**) and a modified nitrile-ligated derivative (Fig. 7, complex **39a**) for the transfer hydrogenation of some α,ß-unsaturated aldehydes (Table 9, entries 1–4) [69]. Although good selectivity was obtained with some starting materials, when sterically hindered L-carvone was used as the substrate, a low yield was obtained (Table 9, entry 4). Interestingly, complex **39a** was capable of the opposite reaction (Oppenauer oxidation) when several alcohols and some α,ß-unsaturated alcohols were placed in acetone as a solvent instead of iPrOH. This capability is of course present in all transfer hydrogenation catalysts as they catalyse both hydrogenation and dehydrogenation (of isopropanol, for instance). Recently, the same research group used the Knölker catalyst **39b** for the transfer hydrogenation of cinnamaldehyde (Table 9, entry 6), where 99% yield and selectivity were achieved [69]. However, when benzalacetone (**8o**) was the substrate, only 27% of conversion with 22% selectivity was achieved (Table 9, entry 5). In this system, the use of

$(CH_3)_3NO$ was required in order to generate the 16-electron active complex by CO ligand removal through oxidation of CO to CO_2 forming $(CH_3)_3N$ as side product. Analogous to the ruthenium complex **16** described in Sect. 2.1.1, Baratta also synthesized osmium complex **40** (Fig. 7) [40]. This osmium catalyst was capable of reducing cinnamaldehyde in a selective manner with catalyst loadings as low as 0.05 mol% (Table 9, entry 7). A TOF of 8.9×10^4 h^{-1} was observed. Recently, in 2018, de Vries and co-workers employed the Rh complex **41** designed by Grützmacher (Fig. 7) in the base-free transfer hydrogenation of crotonaldehyde using EtOH as hydrogen source [45]. This reaction was complete with >99% yield in only 2 min (Table 9, entry 9). This example and the use of complex **19** reported in Sect. 2.2.1 are the only two reports on base-free transfer hydrogenation of α,β-unsaturated carbonyl compounds using EtOH as hydrogen donor. Sortais and co-workers synthesized the phosphine-free manganese-based catalyst **42** and used it successfully for the transfer hydrogenation of carbonyl groups [71]. Several compounds were reduced under mild conditions including three examples of α,ß-unsaturated carbonyl compounds: benzalacetone, ß-ionone and cinnamaldehyde (Table 9, entries 10–12). Very surprisingly, this catalyst was active at catalyst loadings as low as 0.5 mol% and remained active even at room temperature in some cases. The reported TOF was up to 3,600 h^{-1} and the TON up to 2,000. Analogous to the ruthenium complex **6b** described in the first section, Adolfsson and his team also coordinated a similar bio-based ligand to a Rh source for TH reactions (Fig. 7, **43**) [20]. The allylic alcohol was obtained in only 32% isolated yield from the TH of benzalacetone (**8o**) using this catalyst at room temperature in 3 h (Table 9, entry 18). This was mainly due to the isomerization of the formed allyl alcohol to the ketone, which was further reduced to the saturated alcohol. Propargylic ketones seemed to be much better substrates. In fact, substrate **7a** afforded propargylic alcohol in 90% isolated yield under the same conditions (Table 9, entry 19). Similar to the ruthenium analogue, this Rh catalyst was also active for the tandem isomerization/asymmetric transfer hydrogenation of racemic allylic alcohols to the enantioenriched saturated alcohols.

4.2 Using HCOOH as Hydrogen Donor [32, 77–82]

Using HCOOH as hydrogen donor is also possible with catalysts based on the first-row transition metals. One example of this is the in situ approach as reported by Beller and co-workers [79]. They combined the ligand tetraphos with $Fe(BF)_4 \cdot 6H_2O$ (Fig. 8, **50**), finding this combination a very robust and efficient catalyst for the selective reduction of a wide scope of α,ß-unsaturated aldehydes under base-free mild conditions and low catalyst loadings. Some representative examples are shown in Table 10 (entries 1–5). Scaling up the reactions to multi-gram scale without significant losses of the desired product was possible. The emerging trend on using tridentate-ligated complexes is also noticeable here. For example, the group of Hu reported iron-based PONOP complexes (Fig. 8, compounds **44a**, **44b**) and

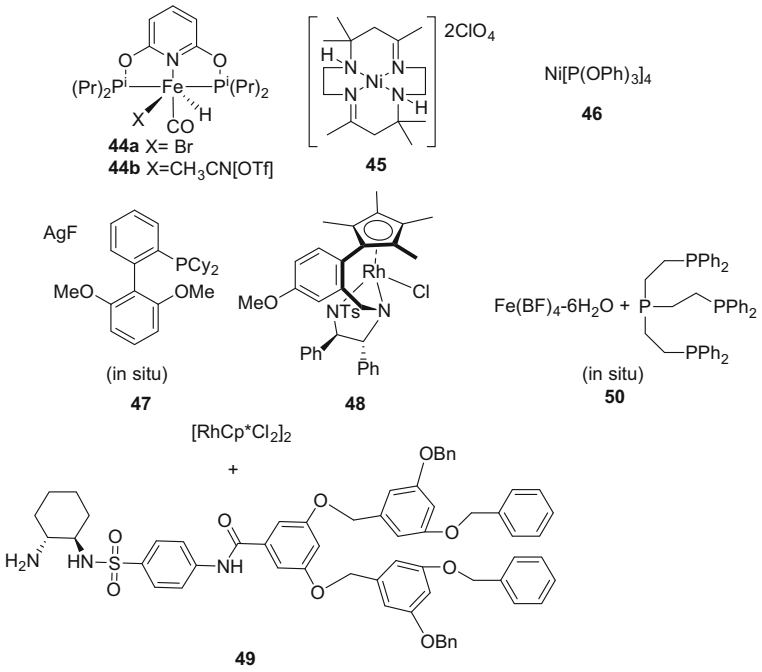

Fig. 8 Catalysts based on iron, nickel, silver and rhodium for the transfer hydrogenation of α,ß-unsaturated carbonyl compounds using HCOOH as hydrogen source

tested them for hydrogenation and transfer hydrogenation of different carbonyl compounds including α,ß-unsaturated aldehydes (Table 10, entries 6–11) [81]. A remarkable selectivity was found for the reduction of aldehydes over ketones in compounds that contained both functionalities. Interestingly, the use of H_2 gas as a reductant led to very similar yields if not lower for these α,ß-unsaturated carbonyl compounds. Some reports on Ni catalysts can also be found in the literature. For example, Iyer and Sattar used a very simple complex, $Ni[P(OPh)_3]_4$ (Fig. 8, complex **46**), for the selective transfer hydrogenation of different carbonyl compounds including benzalacetone and cinnamaldehyde (Table 10, entries 13–14) in acetic acid using $HCOONH_4$ as hydrogen source [77]. When iPrOH was tried as hydrogen source, the yields dropped. A few years later, the group of Sudalai synthesized a macrocyclic nickel(II) complex (Fig. 8, compound **45**) [78]. This Ni complex was successful at 2 mol% catalyst in the reduction of cinnamaldehyde to cinnamyl alcohol with 87% yield (Table 10, entry 12). In this work, a comparison with other hydrogen sources was also done. Using *i*PrOH as a reducing agent led to a reduced yield of cinnamyl alcohol of 53%. A number of catalysts based on late transition metals other than ruthenium and iridium can be found in the literature. For example, Li and his group screened a large variety of Ag salts, phosphine ligands, bases, additives and hydrogen sources until they found a very active combination for the transfer hydrogenation of carbonyl compounds [80]. The best combination was AgF

Table 10 Transfer hydrogenation of α,β-unsaturated carbonyl compounds by catalysts based on iron, nickel, silver and rhodium using HCOOH as hydrogen donor

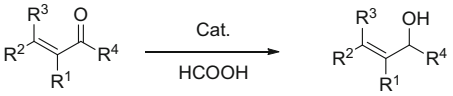

8

8e $R^1 = R^3 = R^4 = H$, $R^2 = Ph$
8f $R^1 = R^4 = H$, $R^2 = (CH_2)_2CH{=}C(CH_3)_2$, $R^3 = Me$
8o $R^1 = R^3 = H$, $R^2 = Ph$, $R^4 = Me$
8q $R^1 = R^3 = R^4 = H$, $R^2 = Me$
8r $R^1 = R^3 = R^4 = H$, R^2 = 2,6,6-trimethylcyclohex-1-en-1-yl
8s $R^1 = R^3 = R^4 = H$, R^2 = furan-2-yl
8t $R^1 = R^4 = H$, $R^2 = Ph$, $R^3 = Me$
8u Cycle $R^1 = CH_2CH(C(CH_2)CH_3)CH_2 = R^2$, $R^4 = R^3 = H$ (Perillaldehyde)
8v Cycle $R^3 = CH_2CH(C(CH_2)CH_3)CH_2 = R^4$, $R^1 = CH_3$, $R^2 = H$ (Carvone)
8w $R^1 = R^3 = R^4 = H$, $R^2 = p$-(MeO)Ph
8x $R^1 = R^3 = R^4 = H$, $R^2 = o$-(O_2N)Ph
7q $R^1 = (CH_2)_4CH_3$, $R^2 = CH(OCH_3)COOCH_3$

Entry	Cat.	Loading (mol%)	Base	Substrate	Yield[a] (%)	Time (h)	Temp. (°C)	Ref.
1[b]	**50**	0.4	–	**8e**	99[c]	2	60	[79]
2	**50**	0.4	–	**8t**	99[c]	2	60	[79]
3	**50**	0.4	–	**8u**	99[c]	2	60	[79]
4	**50**	0.4	–	**8f**	99[c]	2	60	[79]
5	**50**	0.4	–	**8s**	96	2	60	[79]
6	**44a**	5	HCOONa	**8e**	76	6	40	[81]
7	**44a**	5	HCOONa	**8w**	72	6	40	[81]
8	**44a**	5	HCOONa	**8x**	65	6	40	[81]
9	**44b**	5	HCOONa	**8e**	72	6	40	[81]
10	**44b**	5	HCOONa	**8w**	68	6	40	[81]
11	**44b**	5	HCOONa	**8x**	69	6	40	[81]
12	**45**	2	NH_3	**8e**	87	5	100	[78]
13	**46**	5	NH_3	**8o**	92	8	110	[77]
14	**47**	5	NH_3	**8e**	72	8	110	[77]
15[d]	**47**	10	DIPEA	**8e**	82	24	120	[80]
16[e]	**48**	0.5	Et_3N	**7q**	>99[f]	20	30	[32]
17[g]	**49**	0.5	HCOONa	**8o**	94	1.3	40	[82]

[a]Isolated yields
[b]Scaled up by a factor of 20 (10 mmol reaction) with no loss of yield or selectivity
[c]Determined by GC
[d]Additives: CsF (20 mol%), TfOH (10 mol%) and PhCl (7 eq)
[e]Enantioselective affording 99% ee determined by CSP-SCF
[f]Determined by ^{1}H-NMR of the crude
[g]Is enantioselective affording 52% ee determined by HPLC analysis on OD or AS column

as a source of metal, SPHOS as electron-rich ligand (Fig. 8, **47**), CsF as base and TfOH as an additive. The best hydrogen source was shown to be HCOOH-DIPEA. In addition to all these ingredients, PhCl was found to be useful as an extra additive for reducing the amount of DIPEA needed for high yields by the formation of a microscopic organic phase. Using this approach, 82% isolated yield was obtained when cinnamaldehyde was reduced (Table 10, entry 15). The low atom efficiency in regard to the number and amount of additives is a disadvantage. Since other α,ß-unsaturated aldehyde compounds like perillaldehyde or citral gave yields lower than 5%, the scope was rather limited in regard to the unsaturated carbonyl compounds. In the previously cited work of Ayad and Ratovelomanana-Vidal (Sect. 2.1.2), another chiral rhodium complex was tested for the transfer hydrogenation of substrate **7q** (Table 10, entry 16) [37]. Excellent enantioselectivity was obtained in the reduction of this starting material. Finally, analogous to the dendritic system described in Sect. 2.1.2, Jin-Gen Deng also combined a slightly modified dendrimer with Rh (III) (Fig. 8, **49**) [82]. With this catalyst, a range of prochiral ketones were reduced in water with HCOONa as hydrogen donor, achieving high yields and enantioselectivities. The measured TOFs were up to 384 h^{-1}. Interestingly, the catalyst could be precipitated from the reaction mixture by hexane addition and reused several times without loss in yield or selectivity.

5 Meerwein-Ponndorf-Verley Reactions [83–94]

The very first beginnings of the transfer hydrogenation field can be traced back to the first part of the twentieth century with the studies from Meerwein and, slightly later in the same year, from Ponndorf and Verley [83–85]. They have shown the possibility of reducing carbonyl compounds using another alcohol as a reductant via direct hydride transfer. This was possible because of the use of strong Lewis acidic metals as catalysts, i.e. Al^{3+} or Ln^{3+}. This stands in contrast to the weak acid character of the metals described in the previous sections. In regard to the mechanism of MPV reactions, the generally accepted catalytic cycle was shown in the introduction (Scheme 3) [11]. The main drawbacks of these MPV processes are the often required stoichiometric amounts of Lewis acid and the corresponding amounts of accumulated waste. A large amount of work has been performed in this area since then in order to increase the atom efficiency of the process [91, 93]. Nevertheless, in addition to waste problems, aldol condensations, Tishchenko reactions and alcohol dehydrations are observed as side reactions. Thus, highly reactive substrates like α,β-unsaturated carbonyl compounds were not considered to be good candidates for MPV reductions. Nevertheless, a number of examples has been reported. The higher activity of all complexes cited in this section in comparison with the classical $Al(OiPr)_3$ is mainly rationalized as a consequence of preventing the strong aggregation of aluminium alkoxides. Avoiding aggregation, often by ligand fine-tuning, results in more non-bridged Al alkoxides which have an accessible site for the carbonyl compound to bind to [93]. The first example of a MPV reduction of

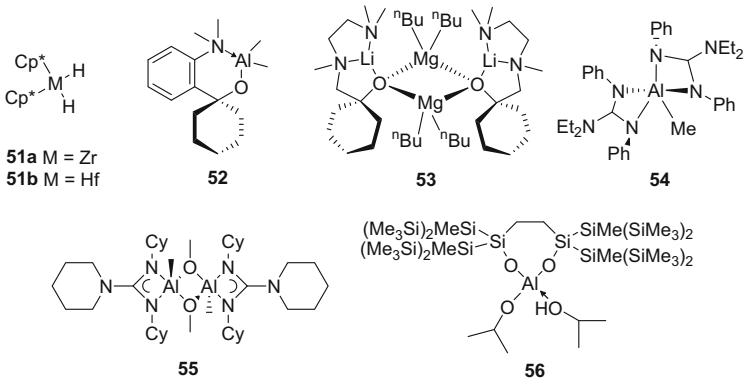

Fig. 9 Aluminium, magnesium and lanthanide complexes for Meerwein-Ponndorf-Verley reduction of α,ß-unsaturated carbonyl compounds

α,β-unsaturated carbonyl compounds comes from the work of Ishii and co-workers [86]. He and his group observed MPV reduction-type reactions when different zircocene and hafnocene complexes (Fig. 9, **51a**, **51b**) were placed in contact with α,ß-unsaturated carbonyl compounds in *i*PrOH. Some examples extracted from the scope are listed in Table 11 (entries 1–7). A major contributor in recent years has been the group of Wei who reported X-ray structures of three different types of aluminium- and magnesium-based complexes (Fig. 9, complexes **52**–**55**) [87–90]. These complexes have shown moderate to good selectivities when citral and cinnamaldehyde were used as substrates affording 68–93% NMR yields (Table 11, entries 12–19). Krempner reported the use of another aluminium-based complex containing a bis-silanol ligand (Fig. 9, complex **56**) [94]. Diffusion experiments (1H DOSY NMR spectroscopy) in C_6D_6 confirmed its monomeric structure in solution. An X-ray structure confirmed that this compound was even monomeric in the solid state. This complex was shown to be very active for a large variety of aliphatic and aromatic carbonyl compounds including some α,ß-unsaturated carbonyl compounds (Table 11, entries 1–3). The reaction could be performed with as little as 0.2 mol% catalyst loading. This method showed a high tolerance for different heteroatoms and other functional groups such as nitriles, nitro group, halides or esters. Multi-gram-scale reductions of several compounds including citral were successfully achieved affording isolated yields between 86 and 97%.

6 Conclusions

Due to its convenience, high selectivity and versatility, transfer hydrogenation has been gaining importance in the last decade. This is underlined by the increasing amount, variety and sophistication of chiral and non-chiral protocols that are being

Table 11 Meerwein-Ponndorf-Verley reduction of α,β-unsaturated carbonyl compounds

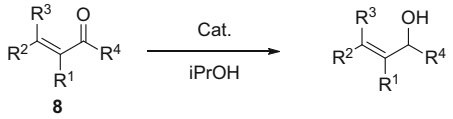

8

8e $R^1 = R^3 = R^4 = H$, $R^2 = Ph$
8f $R^1 = R^4 = H$, $R^2 = (CH_2)_2CH=C(CH_3)_2$, $R^3 = Me$
8o $R^1 = R^3 = H$, $R^2 = Ph$, $R^4 = Me$
8q $R^1 = R^3 = R^4 = H$, $R^2 = Me$
8t $R^1 = Me$, $R^2 = Ph$, $R^3 = R^4 = H$
8y [Bicyclo] [3.1.1] R^1 = 1,3-(2,2-dimethyl-cyclobutyl) = R^3, $R^3 = R^4 = H$ (Myrtenal)

Entry	Cat.	Loading (mol%)	Substrate	Yield[a] (%)	Time (h)	Temp. (°C)	Ref.
1	**56**	1	**8e**	>99	24	80	[94]
2	**56**	0.5	**8f**	>99	24	80	[94]
3	**56**	0.5	**8y**	90	24	80	[94]
4	**51a**	2	**8q**	91	8	130	[86]
5	**51a**	2	**8e**	91	8	130	[86]
6	**51a**	2	**8o**	90	8	130	[86]
7	**51a**	2	**8t**	72	8	130	[86]
8	**51b**	2	**8q**	92	8	130	[86]
9	**51b**	2	**8e**	90	8	130	[86]
10	**51b**	2	**8o**	89	8	130	[86]
11	**51b**	2	**8t**	68	8	130	[86]
12	**52**	5	**8e**	79[b]	15[c]	refl.	[87]
13	**52**	5	**8f**	73[b]	15[c]	refl.	[87]
14	**53**	5	**8e**	68[b]	4	refl.	[89]
15	**53**	5	**8f**	70[b]	4	refl.	[89]
16	**54**	10	**8e**	90[b]	2	110	[88]
17	**54**	10	**8f**	93[b]	2	110	[88]
18	**55**	5	**8e**[a]	91[b]	8	110	[90]
19	**55**	5	**8f**	89[b]	8	110	[90]

[a]Isolated yields
[b]Determined by NMR
[c]Time in minutes

developed for the transfer hydrogenation of different functionalities. The scope for transfer hydrogenation keeps growing, and examples of more selective reductions of new challenging substrates are getting published every year. Still, there is a lot of room for improvement. In the concrete case of α,β-unsaturated carbonyl compounds, more selective catalysts capable of reduction of a larger variety of structures in a selective fashion are highly desired. Most new developments are based on complexes of Ru and Ir. However examples based on more abundant metals like Fe or Mn are also starting to emerge. The Meerwein-Ponndorf-Verley reaction has taken on a new life through the development of new sophisticated ligands that prevent aggregation. This has allowed a huge increase in efficiency of these catalysts. These

new catalysts based on Al are also useful for the selective transfer hydrogenation of α,β-unsaturated carbonyl compounds using very low catalyst loadings. Thus far, iPrOH and HCOOH are the most suitable and common hydrogen sources; however, the use of other hydrogen sources such as renewable EtOH is also under development.

References

1. Ito J-I, Nishiyama H (2014). Tetrahedron Lett 55(20):3153–3166
2. Wang D, Astruc D (2015). Chem Rev 115(13):6621–6686
3. Štefane B, Wills M, Herrera RP, Miller DC, Wang L, Obora Y, Ma X, Perez F (2016) In: Guillena G, Ramón DJ (eds) Hydrogen transfer reactions. Reductions and beyond. Springer, Cham
4. Matsunami A, Kayaki Y (2018). Tetrahedron Lett 59(6):504–513
5. Pandey P, Dutta I, Bera JK (2016). Proc Natl Acad Sci India Sect A 86(4):561–579
6. Zhou J (2016). Appl Catal A 515:101–107
7. Clapham SE, Hadzovic A, Morris RH (2004). Coord Chem Rev 248(21–24):2201–2237
8. Dub PA, Ikariya T (2013). J Am Chem Soc 135(7):2604–2619
9. Dub PA, Gordon JC (2016). Dalton Trans 45(16):6756–6781
10. Dub PA, Gordon JC (2017). ACS Catal 7(10):6635–6655
11. Cohen R, Graves CR, Nguyen ST, Martin JML, Ratner MA (2004). J Am Chem Soc 126(45):14796–14803
12. Kliewer CJ, Bieri M, Somorjai GA (2009). J Am Chem Soc 131(29):9958–9966
13. Krähling L, Krey J, Jakobson G, Grolig J, Miksche L (2000) Allyl compounds. Ullmann's encyclopedia of industrial chemistry. https://doi.org/10.1002/14356007.a01_425
14. Chapuis C, Jacoby D (2001). Appl Catal A 221(1):93–117
15. Franke R, Selent D, Börner A (2012). Chem Rev 112(11):5675–5732
16. Pirnot MT, Rankic DA, Martin DBC, MacMillan DWC (2013). Science 339(6127):1593–1596
17. Stolle A, Gallert T, Schmoeger C, Ondruschka B (2013). RSC Adv 3(7):2112–2153
18. Matsumura K, Hashiguchi S, Ikariya T, Noyori R (1997). J Am Chem Soc 119(37):8738–8739
19. Shatskiy A, Kivijaervi T, Lundberg H, Tinnis F, Adolfsson H (2015). ChemCatChem 7(23):3818–3821
20. Margalef J, Slagbrand T, Tinnis F, Adolfsson H, Dieguez M, Pamies O (2016). Adv Synth Catal 358(24):4006–4018
21. Yamada I, Noyori R (2000). Org Lett 2(22):3425–3427
22. Hennig M, Puntener K, Scalone M (2000). Tetrahedron Asymmetry 11(9):1849–1858
23. Marshall JA, Bourbeau MP (2003). Org Lett 5(18):3197–3199
24. Lockwood SF, Tang PC, Nadolski G, Fang Z, Du Y, Geiss W, Williams R, Burdick W, Yang M (2006) Methods for synthesis of chiral intermediates of carotenoids, carotenoid analogs, and carotenoid derivatives. Aiea Patent WO2006039685A2
25. Guo M, Li D, Sun Y, Zhang Z (2004). Synlett 4:741–743
26. Fang Z, Wills M (2014). Org Lett 16(2):374–377
27. Fang Z, Wills M (2013). J Org Chem 78(17):8594–8605
28. Fang Z, Clarkson GJ, Wills M (2013). Tetrahedron Lett 54(50):6834–6837
29. Vyas VK, Knighton RC, Bhanage BM, Wills M (2018). Org Lett 20(4):975–978
30. Morris DJ, Hayes AM, Wills M (2006). J Org Chem 71(18):7035–7044
31. Carmona D, Lahoz FJ, Atencio R, Oro LA, Lamata MP, Viguri F, San José E, Vega C, Reyes J, Joó F, Kathó Á (1999). Chem Eur J 5(5):1544–1564
32. Monnereau L, Cartigny D, Scalone M, Ayad T, Ratovelomanana-Vidal V (2015). Chem Eur J 21(33):11799–11806

33. Chen Y-C, Wu T-F, Jiang L, Deng J-G, Liu H, Zhu J, Jiang Y-Z (2005). J Org Chem 70(3):1006–1010
34. Touge T, Hakamata T, Nara H, Kobayashi T, Sayo N, Saito T, Kayaki Y, Ikariya T (2011). J Am Chem Soc 133(38):14960–14963
35. Parekh V, Ramsden JA, Wills M (2012). Cat Sci Technol 2(2):406–414
36. Hannedouche J, Kenny JA, Walsgrove T, Wills M (2002). Synlett 2:263–266
37. Peach P, Cross DJ, Kenny JA, Mann I, Houson I, Campbell L, Walsgrove T, Wills M (2006). Tetrahedron 62(8):1864–1876
38. Iyer S, Sattar AK (2003). Indian J Chem Sect B Org Chem Incl Med Chem 42B(11):2805–2807
39. Baratta W, Siega K, Rigo P (2007). Adv Synth Catal 349(10):1633–1636
40. Putignano E, Bossi G, Rigo P, Baratta W (2012). Organometallics 31(3):1133–1142
41. Paul B, Chakrabarti K, Kundu S (2016). Dalton Trans 45(27):11162–11171
42. Baldino S, Facchetti S, Zanotti-Gerosa A, Nedden HG, Baratta W (2016). ChemCatChem 8(13):2279–2288
43. Baldino S, Baratta W, Blackaby A, Bryan RC, Facchetti S, Jurcik V, Nedden HG (2016) Preparation of benzo[h]quinoline ligands and complexes thereof. WO2016193761A1
44. Wang T, Hao X-Q, Zhang X-X, Gong J-F, Song M-P (2011). Dalton Trans 40(35):8964–8976
45. Farrar-Tobar RA, Wei Z, Jiao H, Hinze S, de Vries JG (2018). Chem Eur J 24(11):2725–2734
46. Beck CM, Rathmill SE, Park YJ, Chen J, Crabtree RH, Liable-Sands LM, Rheingold AL (1999). Organometallics 18(25):5311–5317
47. Chen Y-Z, Chan WC, Lau CP, Chu HS, Lee HL, Jia G (1997). Organometallics 16(6):1241–1246
48. Abu-Hasanayn F, Goldman ME, Goldman AS (1992). J Am Chem Soc 114(7):2520–2524
49. Mebi CA, Nair RP, Frost BJ (2007). Organometallics 26(2):429–438
50. Joo F, Benyei A (1989). J Organomet Chem 363(1–2):C19–C21
51. Bui TK, Arcelli A (1985). Tetrahedron Lett 26(28):3365–3368
52. Huo H, Zhou Z, Zhang A, Wu L (2012). Res Chem Intermed 38(1):261–268
53. Zhou Z, Huo H (2013). Curr Catal 2(1):13–16
54. Bonrath W, Medlock JA, Wuestenberg B, Schuetz J, Netscher T (2015) Selective transfer hydrogenation of citral or ethylcitral. WO2015004116, to DSM IP Assets bv
55. Khai BT, Arcelli A (1996). Tetrahedron Lett 37(36):6599–6602
56. Szatmari I, Papp G, Joo F, Katho A (2015). Catal Today 247:14–19
57. Wu X, Li X, King F, Xiao J (2005). Angew Chem Int Ed 44(22):3407–3411
58. James BR, Morris RH (1978). J Chem Soc Chem Commun 21:929–930
59. Sluijter SN, Elsevier CJ (2014). Organometallics 33(22):6389–6397
60. Wang R, Tang Y, Xu M, Meng C, Li F (2018). J Org Chem 83(4):2274–2281
61. Wu X, Liu J, Li X, Zanotti-Gerosa A, Hancock F, Vinci D, Ruan J, Xiao J (2006). Angew Chem Int Ed 45(40):6718–6722
62. Himeda Y, Onozawa-Komatsuzaki N, Miyazawa S, Sugihara H, Hirose T, Kasuga K (2008). Chem Eur J 14(35):11076–11081
63. Zhou Z, Ma Q, Zhang A, Wu L (2011). Appl Organomet Chem 25(12):856–861
64. Talwar D, Wu X, Saidi O, Salguero NP, Xiao J (2014). Chem Eur J 20(40):12835–12842
65. Wang W, Ge K, Bao M (2015) Method for preparing allyl alcohol from α,β-unsaturated aldehyde or ketone. Peop. Rep. China Patent CN104945208, to Dalian University of Technology
66. Yang Z, Zhu Z, Luo R, Qiu X, Liu J-T, Yang J-K, Tang W (2017). Green Chem 19(14):3296–3301
67. Zhang Y-M, Yuan M-L, Liu W-P, Xie J-H, Zhou Q-L (2018). Org Lett 20(15):4486–4489
68. Plank TN, Drake JL, Kim DK, Funk TW (2012). Adv Synth Catal 354(4):597–601
69. Funk TW, Mahoney AR, Sponenburg RA, Zimmerman KP, Kim DK, Harrison EE (2018). Organometallics 37(7):1133–1140
70. Zuo W, Lough AJ, Li YF, Morris RH (2013). Science 342(6162):1080–1083

71. Bruneau-Voisine A, Wang D, Dorcet V, Roisnel T, Darcel C, Sortais J-B (2017). Org Lett 19(13):3656–3659
72. Bigler R, Huber R, Mezzetti A (2015). Angew Chem Int Ed 54(17):5171–5174
73. Mikhailine A, Morris RH, Lagaditis PO, Zuo W (2013) Preparation of iron complex catalysts with unsymmetrical PNN'P ligands. WO2013173930, to University of Toronto
74. Smith SAM, Morris RH (2015). Synthesis 47(12):1775–1779
75. Mikhailine A, Lough AJ, Morris RH (2009). J Am Chem Soc 131(4):1394–1395
76. Meyer N, Lough AJ, Morris RH (2009). Chem Eur J 15(22):5605–5610
77. Iyer S, Sattar AK (1998). Synth Commun 28(10):1721–1725
78. Phukan P, Sudalai A (2000). Synth Commun 30(13):2401–2405
79. Wienhoefer G, Westerhaus FA, Junge K, Beller M (2013). J Organomet Chem 744:156–159
80. Liu M, Zhou F, Jia Z, Li C-J (2014). Org Chem Front 1(2):161–166
81. Mazza S, Scopelliti R, Hu X (2015). Organometallics 34(8):1538–1545
82. Jiang L, Wu T-F, Chen Y-C, Zhu J, Deng J-G (2006). Org Biomol Chem 4(17):3319–3324
83. Meerwein H, Schmidt R (1925). Justus Liebigs Ann Chem 444:221–238
84. Verley A (1925). Bull Soc Chim Fr 37:537–542
85. Ponndorf W (1926). Angew Chem 39:138–143
86. Nakano T, Umano S, Kino Y, Ishii Y, Ogawa M (1988). J Org Chem 53(16):3752–3757
87. Hua Y, Guo Z, Suo H, Wei X (2015). J Organomet Chem 794:59–64
88. Han H-F, Zhang S-F, Guo Z-Q, Tong H-B, Wei X-H (2015). Polyhedron 99:71–76
89. Hua Y, Guo Z, Han H, Wei X (2017). Organometallics 36(4):877–883
90. Han H, Guo Z, Zhang S, Hua Y, Wei X (2017). Polyhedron 126:214–219
91. de Graauw CF, Peters JA, van Bekkum H, Huskens J (1994). Synthesis 10:1007–1017
92. Dirk Klomp UH, Peters JA (2007) In: deVries JG, Elsevier CJ (eds) The handbook of homogeneous hydrogenation. Wiley-VCH, Weinheim, pp 585–630. https://doi.org/10.1002/9783527619382.ch20
93. Graves CR, Campbell EJ, Nguyen ST (2005). Tetrahedron Asymmetry 16(21):3460–3468
94. McNerney B, Whittlesey B, Cordes DB, Krempner C (2014). Chem Eur J 20(46):14959–14964

Top Organomet Chem (2019) 63: 225–266
DOI: 10.1007/3418_2018_22

Published online: 24 November 2018

Functionalization of C(sp^2)–H Bonds of Arenes and Heteroarenes Assisted by Photoredox Catalysts for the C–C Bond Formation

Pierre H. Dixneuf and Jean-François Soulé

Contents

Abstract The formation of C–C bonds from arenes and heteroarenes through transition metal-catalyzed C–H bond functionalizations is one of the major achievements of these last decades. It is now possible to perform such transformations under mild reaction conditions with the help of visible light photocatalysis leading to eco-friendly and safer process to build organic molecules or materials. This chapter will focus on

---

The original version of this chapter was revised. The correction to this chapter can be found at DOI 10.1007/3418_2018_25.

P. H. Dixneuf (✉) and J.-F. Soulé (✉)
Organométalliques, matériaux et Catalyse, Univ Rennes, CNRS, (UMR 6226), Institut Sciences Chimiques, Rennes, France
e-mail: pierre.dixneuf@univ-rennes1.fr; jean-francois.soule@univ-rennes1.fr

photoredox catalysis which involves a C(sp^2)–H bond functionalization step for the formation of C(sp^2)–C bonds [i.e., direct arylations and (perfluoro)alkylations] and will show how this hot topic contributes to the development of green chemistry.

Keywords C(sp^2)–H bond · C–C bond formation · MLTC photoredox catalysis · Visible light

1 Introduction

During the last two decades, catalytic C–H bond functionalizations, for cross-coupled C–C bond formation, have progressively replaced the useful metal-catalyzed cross-coupling reactions between a stoichiometric amount of an organometallic species and a (hetero)aromatic halide. The advantages involve the atom economy of the process as the C–H bond no longer needs to be transformed into a carbon–halide bond or in an organometallic reagent and the reduction of steps to lead to useful complex molecules from medicinal compounds to polyfunctional ligands and molecular materials [1–12].

The C(sp^2)–H bond functionalizations usually require previous activation by a transition metal catalyst, either via initial insertion of low-valent metal into the C–H bond such as Ru(0), Rh(I), or Ir(I) catalysts or via C–H bond deprotonation in the presence of Ru(II), Rh(III), or Ir(III) or Pd(II) catalysts. For both activation processes, the regioselectivity control is the main problem, and usually a tolerated directing group brings a suitable solution [13–15]. Whereas the metal C–H bond activation steps are relatively easily performed, the functionalization of the (M–C) carbon of intermediate requires higher energy. In addition, for the regeneration of high-valent metal catalysts, a stoichiometric amount of oxidant is often required. These drawbacks motivate the search of better C–H bond functionalizations with high regioselectivity, absence of stoichiometric amount of oxidant, and mild conditions.

Since the pioneer works by Gafney and Adamson, who showed that single electron transfer (SET) event can be initiated by the triplet charge transfer excited state of $[Ru(bpy)_3]^{2+}$ [16], the application of polypyridine-metal complexes with metal-ligand charge transfer (MLCT) properties in catalysis has become a useful alternative approach to create new C–C bonds [17–26] and more recently to functionalize C–H bonds [27–30]. The first photoredox functionalization of C(sp^2)–H bond was reported in 1984 by Deronzier with the $[Ru(bpy)_3]^{2+}$ assisting the cyclization of stilbenediazonium salts [31].

Photoredox catalysts (PC^n), such as *tris*(2,2′-bipyridine)ruthenium(II) $[Ru(bpy)_3{}^{2+}]$ or *fac-tris*(2-phenylpyridine)iridium(III) *fac*-$[Ir(ppy)_3]$, under simple irradiation by low-energy visible light lead to their long lifetime photoexcited state ($*PC^n$), resulting from electron transfer from the dπ orbital of the metal center to the π* orbital of the 2,2′-bipyridine or 2-phenylpyridine ligand (MLCT) followed by intersystem crossing. Then, photoexcited state ($*PC^n$) undergoes SET in two different scenarios:

1. *In a reductive quenching cycle*, SET occurs from an electron donor **D** to *PC^n associated with formation of reduced $PC^{(n-1)}$ followed by the reduction of an electron acceptor **A** associated with regeneration of the ground state of the catalyst photoredox (PC^n) (Fig. 1a).
2. *Oxidative quenching cycle*, SET occurs from *PC^n to an electron acceptor **A** associated with formation of the high-oxidation-state $PC^{(n+1)}$ followed by the oxidation of an electron donor **D** associated with regeneration of the ground state of the photoredox catalyst (PC^n) (Fig. 1b).

The above-generated cation or anion radicals easily decompose into carbon-centered radicals, which add regioselectively to molecules such as arenes, heterocycles, and even alkenes to form a new C(sp^2)–C bond from C(sp^2)–H bond at room temperature. These low-energy visible light photoinitiated processes offer a new life to radical generations and reactions, but more importantly they offer new ways of regioselective functionalizations of C(sp^2)–H bonds with high atom economy under very mild conditions. *They constitute an excellent, fast developing contribution to green chemistry.*

This is why this chapter will present the contributions of metal complex photoredox catalysts to functionalize, by C(sp^2)–C bond formation, the C(sp^2)–H bonds of arenes and heterocycles.

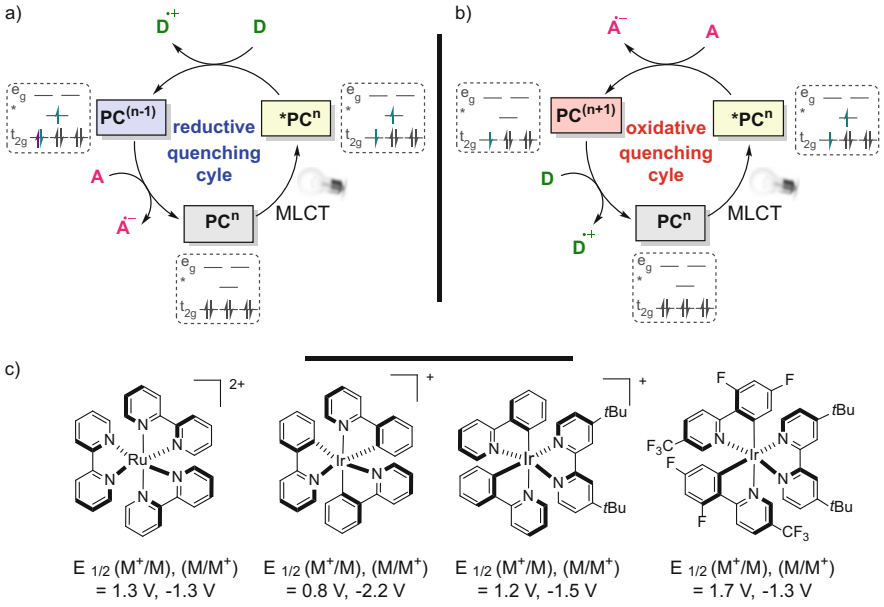

Fig. 1 ^{3}MLCT excited state: diagram of energy and electron transfer processes, (**a**) reductive quenching cycle, (**b**) oxidative quenching cycle, and (**c**) chemical structures of some common photoredox catalysts and their redox potentials in V *vs.* SCE. *SCE* saturated calomel electrode [32]

This chapter will present the different methods based on MLCT photoredox metal complexes to transform C(sp^2)–H bonds of 5-atom and 6-atom heterocycles and of functional arenes into C(sp^2)–C bonds only. The reactions will be classified by the nature of substrates and by type of functionalization: arylation, perfluoroalkylation, and alkylation. The conditions of the photoredox-catalyzed reactions will be pointed out to show the mild energy and conditions and that photoredox systems are current available keys to develop green catalysis processes.

2 Functionalizations of 5-Atom Ring Heteroarene C(sp^2)–H Bonds

2.1 Photoredox-Assisted Arylation of 5-Atom Heteroarene C(sp^2)–H Bonds

In 2013, Xue, Xiao, and co-workers demonstrated that $[Ru(bpy)_3]^{2+}$ under blue LEDs promotes the arylation of pyrroles, furans, and benzothiophene using diaryl iodonium salts as aryl radical precursors (Scheme 1) [33]. The regioselectivity of the arylation is similar to those observed with palladium catalysts in the presence of aryl halides [13], namely, at the α-positions. While the C–H arylation of heteroarenes can be performed at room temperature, a huge amount of heteroarenes (50 equivalents) is required, which make this protocol not really attractive from a synthetic point of view. The authors have proposed a mechanism based on oxidative quenching pathway.

Tobisu, Chatani, and co-workers also employed diaryliodonium salts as aryl radical precursors for the C(sp^2)–H bond arylation of heteroarenes such as pyrroles, imidazoles, and thiophenes using $[Ir(ppy)_2(bpy)]PF_6$ as photoredox catalyst (Scheme 2)

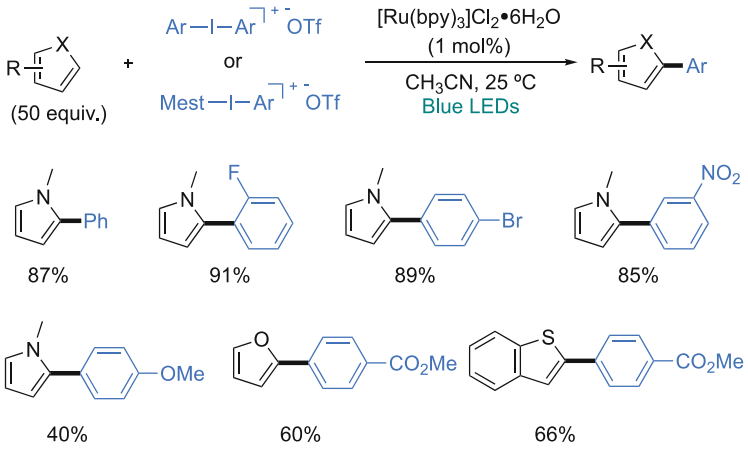

Scheme 1 $Ru(bpy)_3^{2+}$-assisted arylation of heteroarenes with diaryliodonium salts

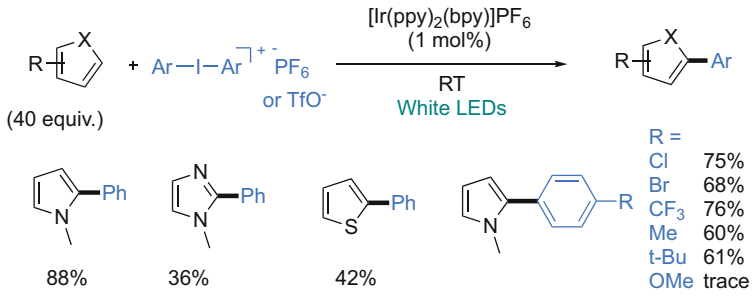

Scheme 2 [Ir(ppy)$_2$(bpy)]PF$_6$-promoted arylation of heteroarenes using diaryliodonium salts

[34]. In all cases, the arylation takes place mainly at the C2 position. A wide range of substituents at the *para* position of the diaryliodonium salts are tolerated such as chloro, bromo, trifluoromethyl, methyl, and *tert*-butyl, while *para*-methoxy-substituted diaryliodonium salts failed to react under these reaction conditions.

The generation of aryl radicals from aryl halides and pseudohalides is very challenging due to do their high reduction potentials, which are beyond the reach of many typical photoredox catalysts including Ru(bpy)$_3$. In 2016, Ackermann and co-workers reported the merge of *fac*-[Ir(ppy)$_3$] photoredox catalyst and CuI(I) to promote the C2 arylation of benzothiazole using 3-tolyl iodide (Scheme 3) [35].

In 2017, König and co-workers employed visible light photoredox catalyst [Ru(bpy)$_3$]$^{2+}$ to generate radical anions from pyrenes to promote the formation of aryl radical from aryl halides via SET event, also called sensitization-initiated electron transfer (Scheme 4) [36]. Pyrroles and indoles were arylated at the α-position using only electron-poor aryl bromides (e.g., bromobenzonitriles, bromobenzoates, and heteroaryl bromides). Again, a huge amount of heteroarenes (10 equiv.) is required. In addition, this catalytic system is also operative using aryl triflate instead of aryl halides.

Based on spectroscopic investigations, the authors proposed a catalytic cycle depicted in Fig. 2. After visible light photoexcitation of Ru(bpy)$_3^{2+}$, *Ru(bpy)$_3^{2+}$ transfers its energy to pyrene (Py). The excited Py* is then reductively quenched by *N*,*N*-diisopropylethylamine (DIPEA) to generate the radical anion [Py]$^{\bullet-}$ and the radical cation [DIPEA]$^{\bullet+}$. Then, [Py]$^{\bullet-}$ transfers one electron to the (hetero)aryl halide, yielding the (hetero)aryl radical precursor [(Het)ArX]$^{\bullet-}$ which generates the aryl radical (Ar$^{\bullet}$) and neutral Py to complete the catalytic cycle. Finally, the radical Ar$^{\bullet}$ reacts with (hetero)arenes to afford C–C coupling products. In a competing pathway, the radical Ar$^{\bullet}$ abstracts a hydrogen atom either from [DIPEA]$^{\bullet+}$or from the solvent (in this case DMSO) to give undesired reduction products and diisopropylamine.

In 2016, Natarajan et al. achieved the visible light-mediated C(sp^2)–H bond arylations of 5-atom ring heteroarenes with benzenesulfonyl chlorides at room temperature using [Ru(bpy)$_3$]Cl$_2$ as photosensitizer and blue LED irradiation (Scheme 5) [37]. The reaction occurred at the α-position and tolerated a broad

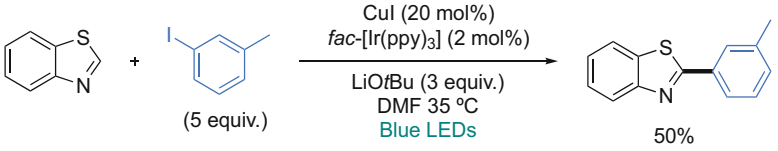

Scheme 3 Merging of *fac*-[Ir(ppy)$_3$] and Cu(I) for the C2-arylation of thiazole using aryl iodide

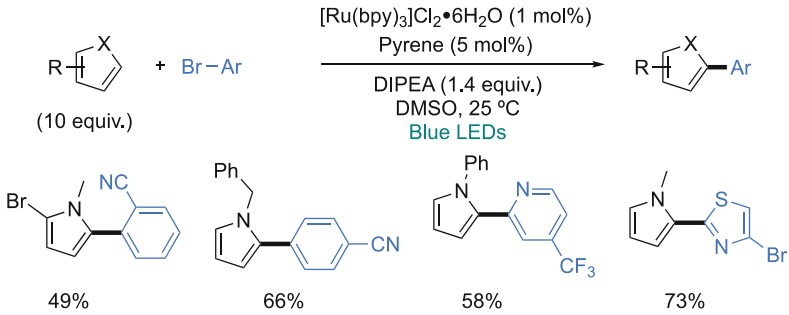

Scheme 4 Ru(bpy)$_3^{2+}$-promoted arylation of (hetero)arenes using aryl bromides and chlorides

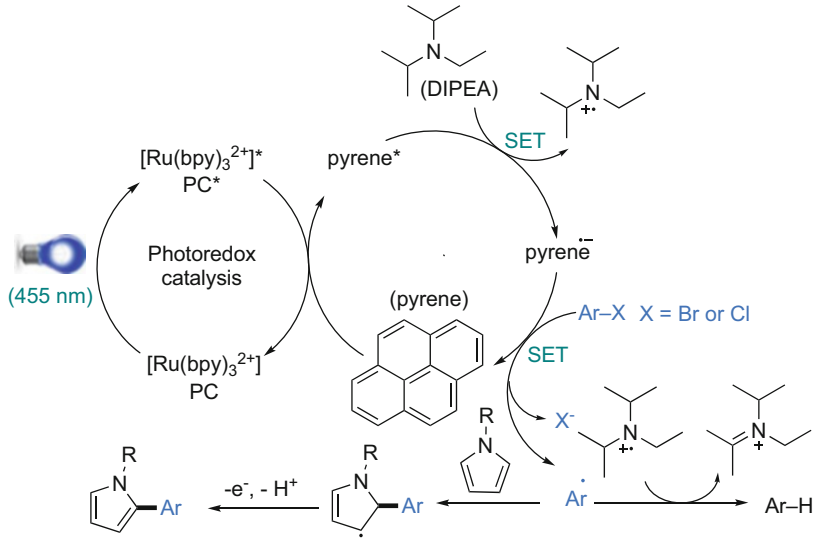

Fig. 2 Proposed catalytic cycle for pyrene sensitization-initiated electron transfer catalytic C–H arylation reactions

range of functional groups. It is noteworthy that β-arylated thiophenes are synthetized by palladium-catalyzed C–H bond desulfitative arylation [38–42]. The authors proposed a radical pathway through an oxidative quenching cycle.

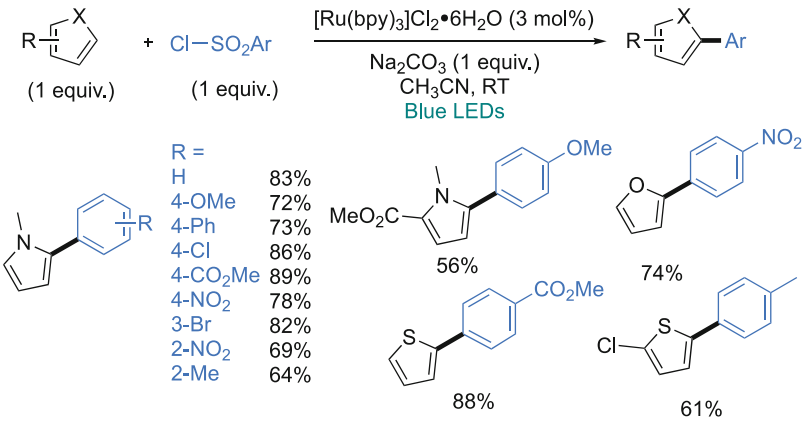

Scheme 5 $Ru(bpy)_3^{2+}$-promoted arylation of heteroarenes with arenesulfonyl chlorides

In 2016, Weaver and co-workers demonstrated that the formation of 2-azolyl radicals from 2-bromoazoles can be achieved using *fac*-[Ir(ppy)$_3$] photoredox catalysis (Scheme 6) [43]. They employed *N*-cyclohexyl-*N*-*iso*butyl-*N*-cyclohexanamine as sacrificial oxidizing agent, and an oxidative quenching cycle allows the formation of aryl radical, which could be trapped by electron-rich arenes, pyrroles, indoles, imidazoles, pyridines, and thiophenes to allow the formation of heterobiaryls in good yields. A wide range of 2-bromoazoles including the one bearing sensitive halo-bonds have been employed.

2.2 *Photoredox-Assisted Perfluoroalkylation of 5-Atom Heteroarene C(sp^2)–H Bonds*

In 2011, MacMillan and co-workers succeeded to generate $CF_3^{\bullet}$ radical from trifluoromethanesulfonyl chloride using visible light photoredox catalysis (Scheme 7) [44]. Trifluoromethylation of C(sp^2)–H bonds of 5-atom ring heteroarenes such as pyrroles, furans, thiophenes, and thiazoles at the C2 or C5 position was achieved under mild reaction conditions using 1 mol% [Ru(phen)$_3$]Cl$_2$ as photoredox catalyst. Notably, mixtures of C2 and C3 trifluoromethylated indoles were obtained depending on the N-substituents.

Oxidative quenching cycle was proposed with the generation of $CF_3^{\bullet}$ radical *via* SET reduction promoted by photoexcited *PC (Fig. 3) [45, 46].

Cho and co-workers disclosed that trifluoroiodomethane can also generate $CF_3^{\bullet}$ radical under visible light photoredox conditions allowing the C(sp^2)–H bond trifluoromethylation of 5-atom ring heteroarenes (Scheme 8) [47]. The reaction was carried out using 1 mol% [Ru(bpy)$_3$]Cl$_2$ in the presence of 2 equivalents of TMEDA (*N*,*N*,*N*′,*N*′-tetramethylethylenediamine) as base in acetonitrile under visible light. Indoles are successfully trifluoromethylated at C2 or C3 depending on the

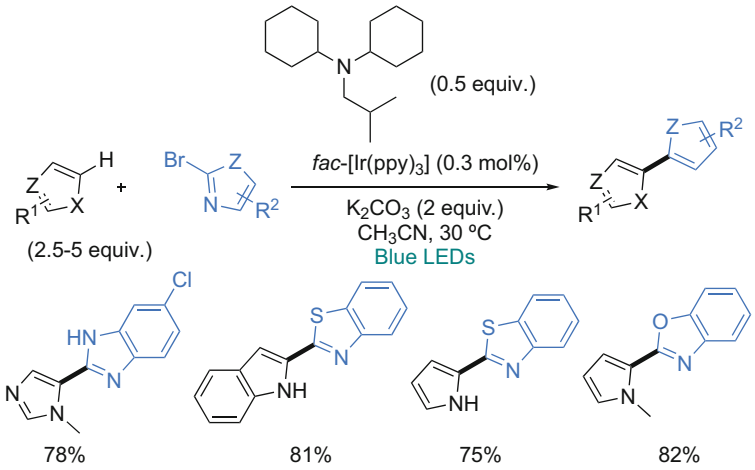

Scheme 6 Heteroarylation of (hetero)arenes with 2-bromoazoles using Ir-based photoredox catalyst

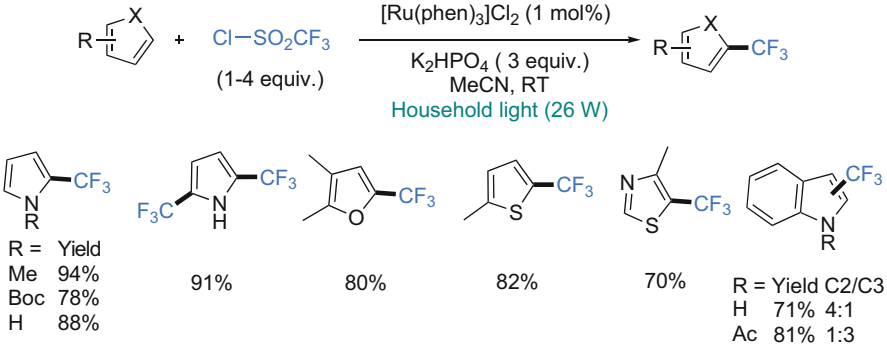

Scheme 7 $Ru(phen)_3^{2+}$-catalyzed trifluoromethylation of heteroarenes using trifluoromethanesulfonyl chloride

indolyl substituent, whereas pyrroles, thiophenes, and furans are regioselectively functionalized at the C2 or C5 position. Notably, Noël and co-workers have developed a continuous flow version of this reaction to allow the trifluoromethylation of 5-atom heteroaromatics in larger scale [48, 49].

Based on the mechanism study [49], the authors proposed a reductive quenching pathway. Indeed, the generated Ru^{3+} species is reduced by SET from TMEDA which plays the role of an electron donor (Fig. 4).

In 2013, Qing and co-workers succeeded the ethoxycarbonyldifluoromethylation of C(sp^2)–H bond heteroarenes by generating $^{\bullet}CF_2CO_2Et$ radical from ethyl difluorobromoacetate using visible light photoredox system (Scheme 9) [50]. In the presence of 1 mol% of $[Ru(phen)_3]Cl_2$ as photoredox catalyst and 4-*N*,*N*-

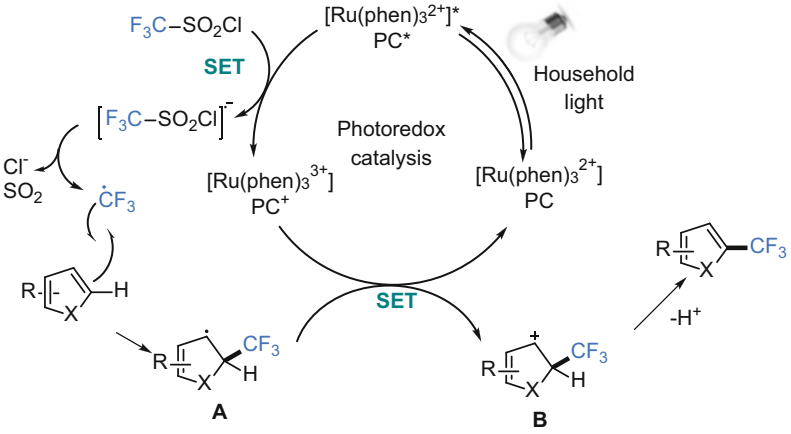

Fig. 3 Proposed mechanism for visible light-mediated trifluoromethylation of (hetero)arenes with CF_3SO_2Cl

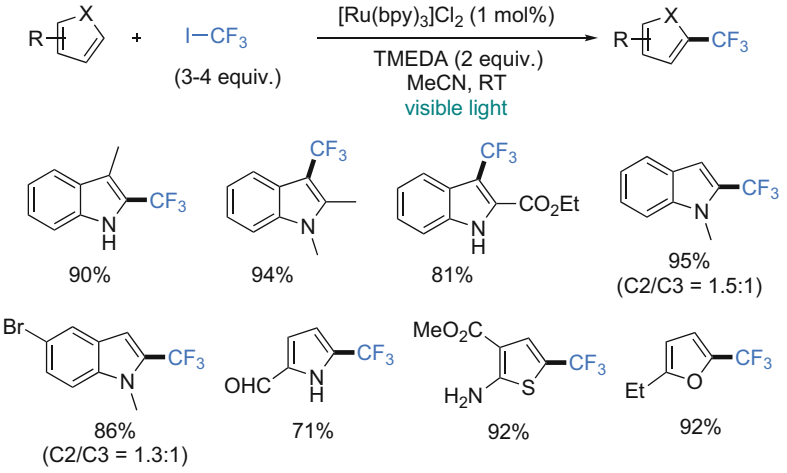

Scheme 8 $Ru(bpy)_3^{2+}$-catalyzed trifluoromethylation of heterocycles with trifluoroiodomethane

trimethylaniline as sacrificial reductant, under blue LED irradiation, a set of 3-substituted indoles are difluoromethylenated at C2 position in good to high yields. Indole led to mixture of C2 and C3 regioisomers in 5:1 ratio. Ethoxycarbonyl-difluoromethylation of benzofuran gives also mixture of C2 and C3 regioisomers, while *N*-methylpyrrole, furan, and thiophene are regioselectively alkylated at the C2 position in moderate yields. The reaction tolerates reactive functional groups (e.g., alkyl and aromatic bromides, unprotected alcohols, carboxylic acids, amides, and nitriles). Oxidative quenching pathway which enabled the generation of CF_2CO_2Et radical from ethyl difluorobromoacetate by SET has been proposed.

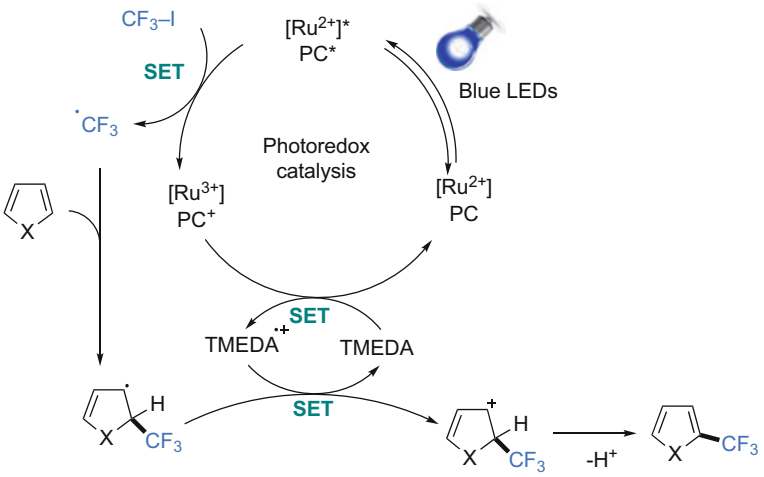

Fig. 4 Proposed mechanism for visible light-mediated trifluoromethylation of heteroarenes with CF_3I

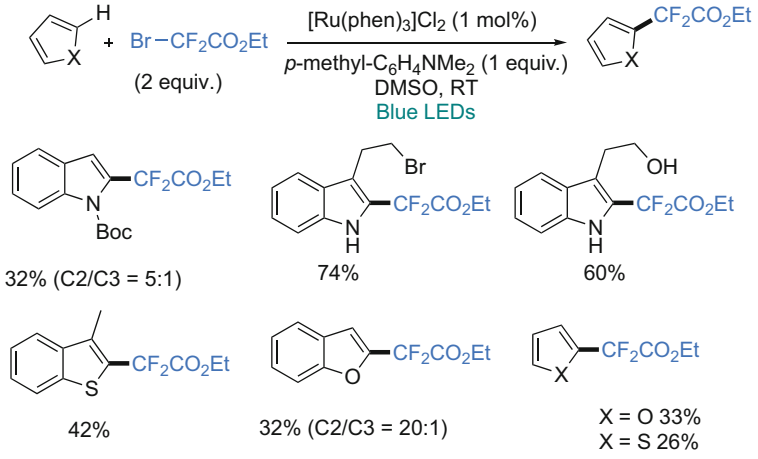

Scheme 9 $Ru(Phen)_3^{2+}$-catalyzed difluoromethylenation of heteroarenes with ethyl 2-bromo-2,2-difluoroacetate

In 2014, Wang and co-workers employed $PhSO_2CF_2I$ – a well-established difluoromethylation reagent developed by Prakash and Hu [51] in visible light photoredox-catalyzed difluoromethylation of electron-rich 5-atom ring N-, O-, and S-containing heteroarenes (Scheme 10) [52]. Pyrroles, (benzo)furans, thiophenes, and thiazoles are regioselectively difluoromethylated at α-position using 1–3 mol% of $[Ru(bpy)_3]Cl_2$ associated with K_2HPO_4 as a base in CH_2Cl_2 under visible light. Pyrazole reacts at the C5 position. Again, indole gives a mixture of C2 and C3 regioisomers, unless the C3 position is substituted.

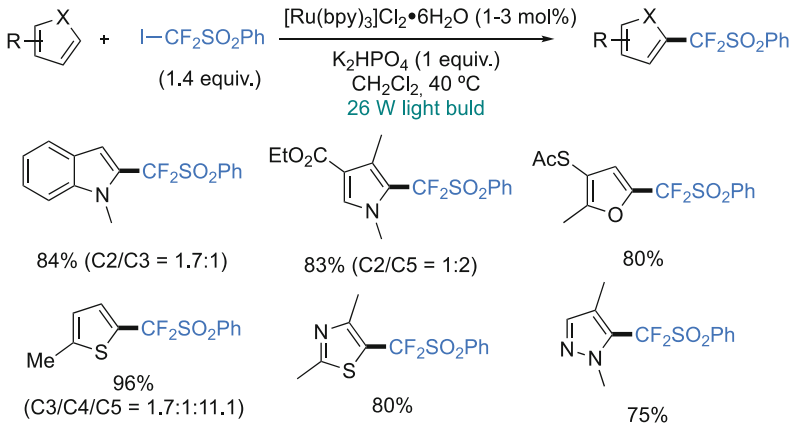

Scheme 10 $Ru(bpy)_3^{2+}$-catalyzed difluoromethylation of heteroarenes with ((difluoroiodomethyl) sulfonyl)benzene

In 2014, Liu and co-workers employed commercially available diethyl bromodifluoromethyl phosphonate as difluoromethyl radical precursor using *fac*-[Ir(ppy)$_3$] as a photosensitizer and blue LEDs as a light source (Scheme 11) [53]. A set of 5-atom heterocycles (e.g., thiophenes, selenophene, (benzo)furan, benzothiophene, indoles, etc.) is functionalized at the α-position in good yields.

In 2015, Stephenson and co-workers succeeded to generate $CF_3^{\bullet}$ radical from cheap and abundant trifluoroacetic anhydride using visible light photoredox catalysis in the presence of pyridine *N*-oxide allowing the trifluoromethylation of 5-atom ring heteroarenes (Scheme 12) [54]. A set of heteroarenes such as pyrroles, indoles, isoxazoles, caffeine, and thiophenes were trifluoromethylated at α-position using 01–1 mol% [Ru(bpy)$_3$]Cl$_2$ as photosensitizer. Interestingly, the protected boronic MIDAB (*N*-methyliminodiacetic acid) functionality is tolerated by these radical conditions, allowing further cross-coupling reactions. The reaction can be also conducted in large scale using both flow system (20 g) and batch (100 g).

Later, they discovered that the use of 4-phenylpyridine *N*-oxide instead of pyridine *N*-oxide led to better results, and they extended the reaction to C(sp^2)–H bond pentafluoroethylation and heptafluoropropylation of heteroarenes with pentafluoropropionic anhydride or heptafluorobutyryl acid anhydride (Scheme 13) [55].

The detailed mechanism is depicted in Fig. 5 [55]. In the presence of trifluoroacetic anhydride, 4-phenylpyridine *N*-oxide is acylated. This acylated species (**A**) can readily quench the photoexcited catalyst $*Ru^{2+}$, and the reduced reagent (**B**) proceeds to fragment to a carboxyl radical along with 4-phenylpyridine (PhPy). The carboxyl radical readily extrudes CO_2 to form the $CF_3^{\bullet}$ radical and its addition to the electron-rich π-system results in selective formation of the product after re-aromatization.

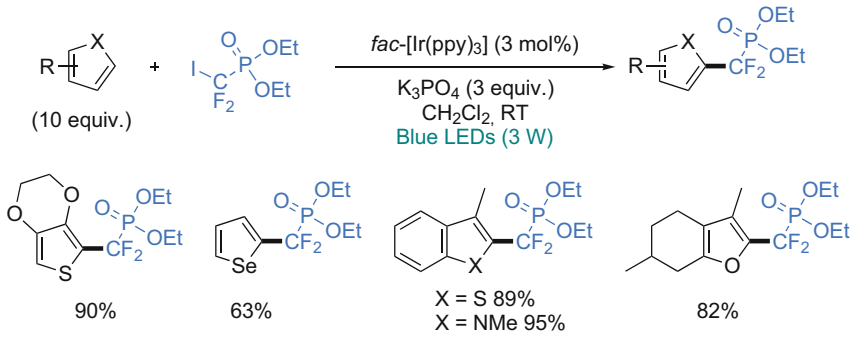

Scheme 11 *fac*-[Ir(ppy)$_3$]-promoted difluoromethylenephosphonation of heteroarenes with bromodifluoromethyl phosphonate

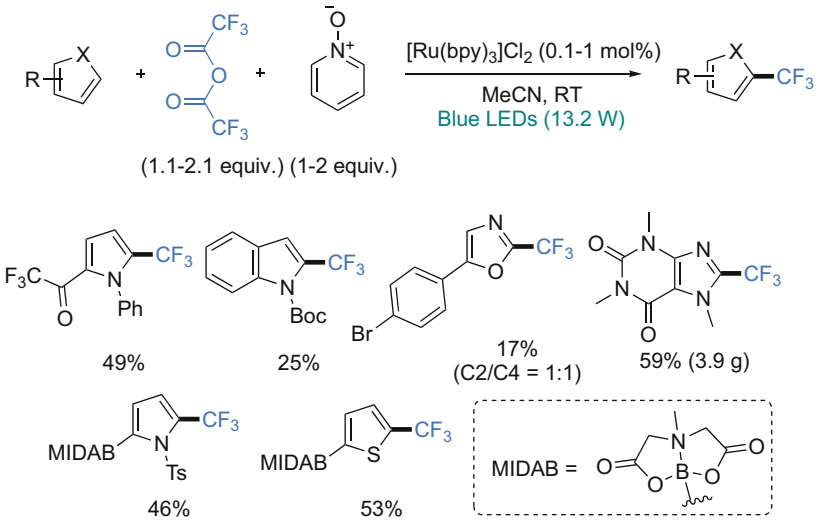

Scheme 12 Ru(bpy)$_3^{2+}$-catalyzed trifluoromethylation of heteroarenes with trifluoroacetic acid anhydride associated to pyridine *N*-oxide

2.3 *Photoredox-Assisted Alkylation of 5-Atom Heteroarene C(sp^2)–H Bonds*

The photoredox-assisted alkylation of heterocycle C(sp^2)–H bonds, to form new cross-coupled C(sp^2)–C bonds, was first initiated by the single electron transfer (SET) from the excited photoredox system under visible light to a derivative with C(sp^3)–Br bond which then generates a radical. Usually with heteroarenes, this radical adds regioselectively to an unsaturated double bond, and a C–C bond is

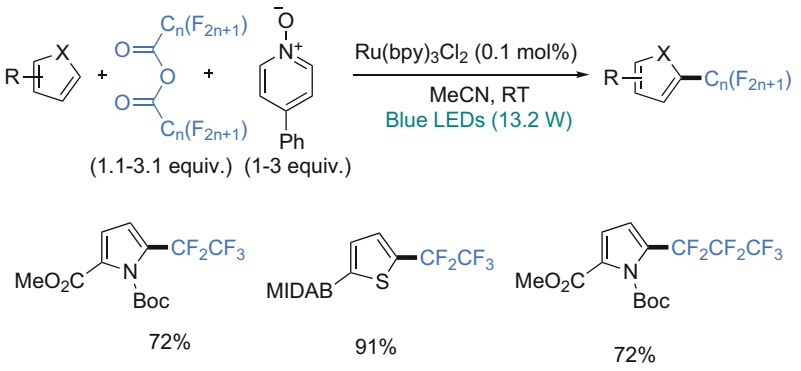

Scheme 13 $Ru(bpy)_3^{2+}$-catalyzed perfluoroalkylation of heteroarenes with anhydride associated to 4-phenylpyridine *N*-oxide

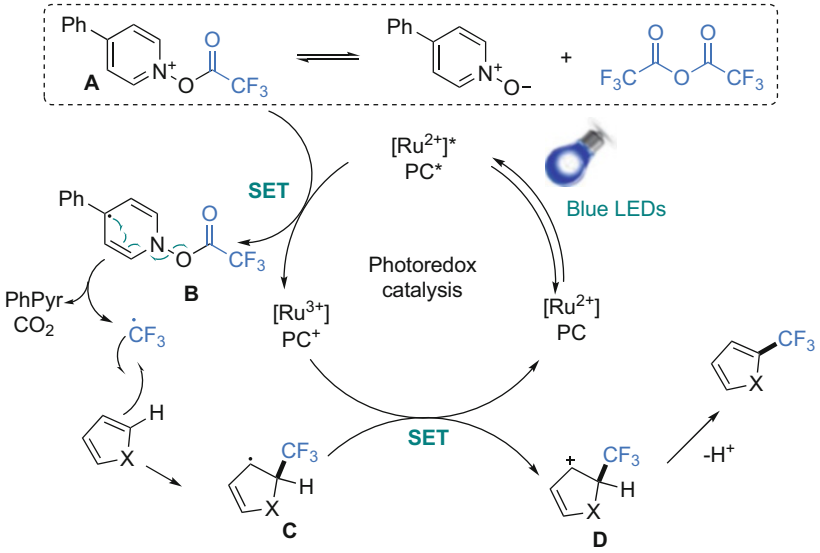

Fig. 5 Proposed mechanism for perfluoroalkylation of heteroarenes with anhydride associated to 4-phenylpyridine *N*-oxide

formed. After oxidation and deprotonation, a heteroarene with new C(sp^2)–C(sp^3) bond is obtained.

Stephenson et al. reported in 2010 the utilization of the photoredox catalyst tris (2,2′-bipyridyl)ruthenium dichloride $[Ru(bpy)_3]^{2+}(Cl^-)_2$, under visible light for the intramolecular regioselective alkylation of indoles and pyrroles containing a N-alkyl chain bearing a terminal C(sp^3)–Br bond. The excited photoredox system, under visible light from a household light bulb, is then reduced in the presence of amine NEt_3 and then allows the single electron transfer (SET) to the C(sp^3)–Br group

which generates a reactive radical. This radical adds at the heterocycle C2 with formation of a new 6-atom ring at room temperature (Scheme 14a) [56].

The same photoredox system in the presence of amine has been used by Stephenson to promote cascade radical cyclizations with successive formation of two C–C bonds to produce polycyclic heterocycle at room temperature (Scheme 14b) [56].

The reaction mechanism is presented in Fig. 6 [56]. It involves the excitation of the photoredox complex by visible light, and the excited species $[^*Ru(bpy)_3]^{2+}$ is reduced by triethylamine by one SET to produce the Ru(I) intermediate $[Ru(bpy)_3]^{+}$ species. The Ru(I) complex is able to transfer one electron to the sp^3C–Br group which generates $[Ru(bpy)_3]^{2+}$ and an electrophilic radical **A**. The latter adds regioselectively to the C2 carbon, and the resulting radical **B** can be oxidized into cation **C** by $[Ru(bpy)_3]^{2+}$ or trialkylammonium radical cation. The cation **C** by loss of a proton leads to the functionalized indole **D** or pyrrole.

The same year the Stephenson group has shown that similar conditions could be applied to the intermolecular alkylation of 5-atom heterocycles, with the help of the photoredox system $[Ru(bpy)_3]Cl_2$ under blue LED ($\lambda_{max} = 435$ nm) irradiation. The reaction is performed with bromomalonates and indoles, with 2 equiv. of amine, NEt_3 or better *p*-$MeOC_6H_4NPh_2$, in DMF at room temperature. It leads to the regioselective alkylation at C2 carbon of indoles or at C3 when C2 carbon is substituted (Scheme 15) [57]. The reaction tolerates $C(sp^2)$–Br or even primary $C(sp^3)$–Br bonds.

The mechanism of this reaction is analogous to that described in Fig. 6. The Ru $(bpy)^{1+}$ intermediate, arising from the visible light excitation of $Ru(bpy)_3^{2+}$ and one electron reduction by the amine, transfers 1 electron to bromomalonate to produce

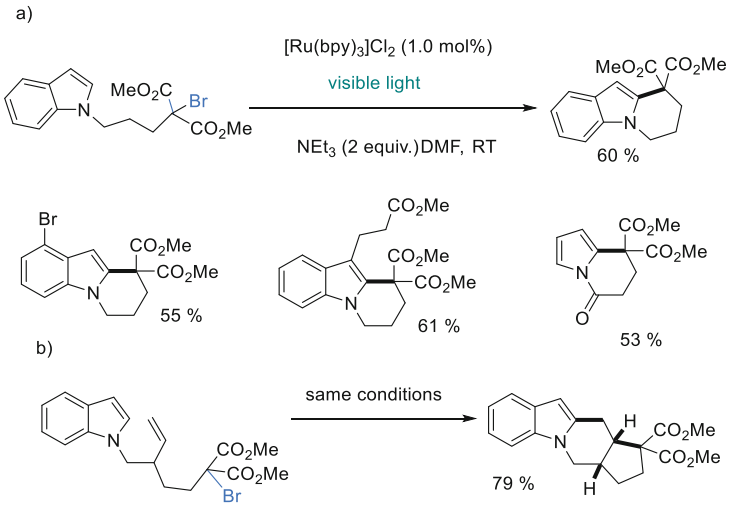

Scheme 14 Intramolecular alkylation of indoles and pyrroles at C2 promoted by $[Ru(bpy)_3]^{2+}$ photoredox and amine

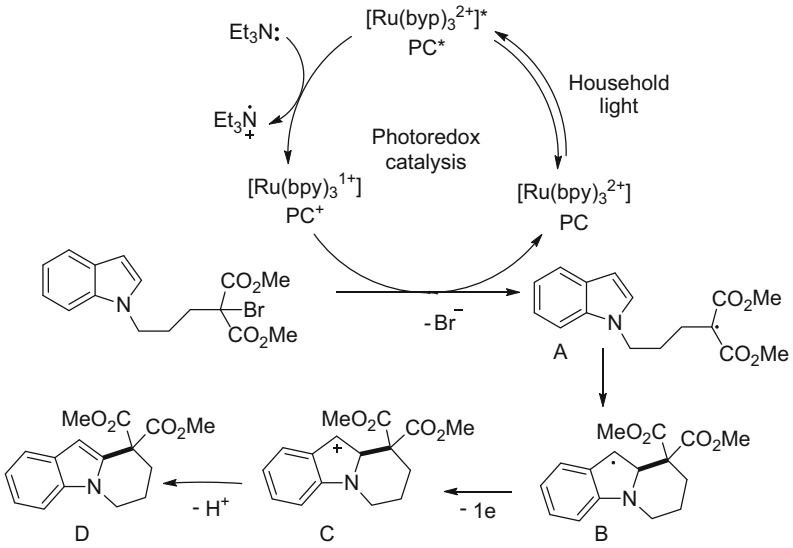

Fig. 6 Stephenson's mechanism for intramolecular alkylation at C2 of 5-atom heterocycles C(sp^2)–H bonds

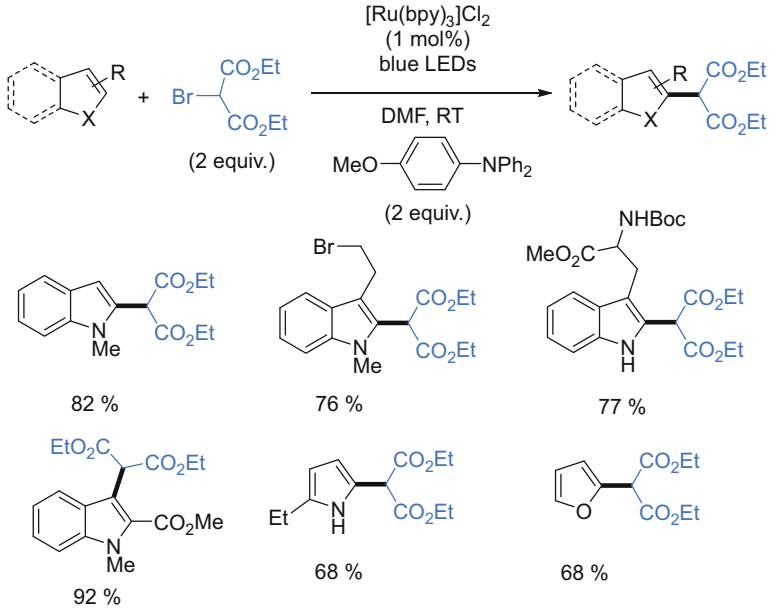

Scheme 15 Photoredox $[Ru(bpy)_3]^{2+}$ and amine for the intermolecular alkylation C2–H and C3–H bonds of 5-atom heterocycles

the $(MeO_2C)_2CH^{\bullet}$ radical which adds to the heterocycle C2 carbon bearing a C–H bond.

Later in 2016, Stephenson used the photoredox *fac*-[Ir(ppy)$_3$] complex in the presence of 1 equivalent of 2,6-lutidine which promotes the regioselective functionalization with electron-deficient radicals, generated from functional bromomalonate derivatives, of C2–H bond of heteroarenes (Scheme 16) [58]. Whereas the weakly reducing photoexcited $[*Ru(bpy)_3]^{2+}$ was almost inefficient for this reaction, the success was reached by the use of the strongly reducing complex when excited by visible light *fac*-[*Ir(ppy)$_3$], $[E_{1/2}^{IV/III*} = -1.73$ V vs SCE]. This (heterocycle)C(2)–C(sp^3) bond formation of pyrroles, thiophenes, indoles, and benzofurans tolerates chloro, allyl, *N*-Boc, and lactone groups.

This reaction was carried out in a flow process with the photoredox *fac*-[Ir(ppy)$_3$] **A**, with a 36 W blue LED. This reaction with **A** allows the transformation of 1 g of material in 4 h at room temperature with 70% yield (Scheme 17) [58]. Under the same conditions, a batch reaction with 1 g led after 8 h to 78% yield. The recovered photoredox shows that the regioselective tris alkylation of *fac*-[Ir(ppy)$_3$] **A** by the bromomalonate took place at the *para* position of the three Ir–C bonds to produce the photoredox catalyst **B** which is as efficient as its parent *fac*-[Ir(ppy)$_3$] **A** (Scheme 17) [58].

It is noteworthy that Barriault et al. showed that unactivated *primary*, *secondary*, and *tertiary* bromoalkanes could generate nucleophilic radicals for the regioselective C2 alkylation of heteroarenes with the help of gold photoredox system [Au_2(bis(diphenylphosphino)methane)$_2$]Cl_2 [Au_2(dppm)$_2$]Cl_2 irradiated with UVA LEDs

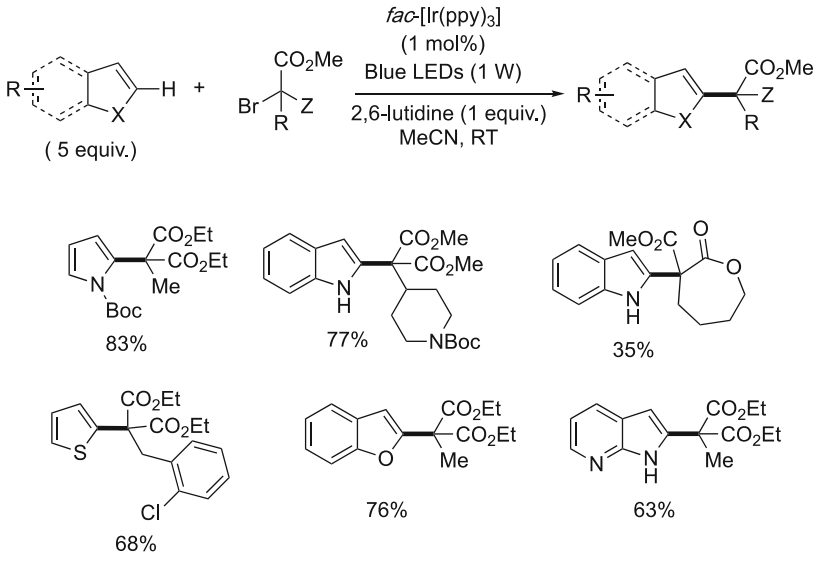

Scheme 16 Photoredox *fac*-[Ir(ppy$_3$]-promoted C2–H coupling of N, O, and S-heterocycles with bromomalonates

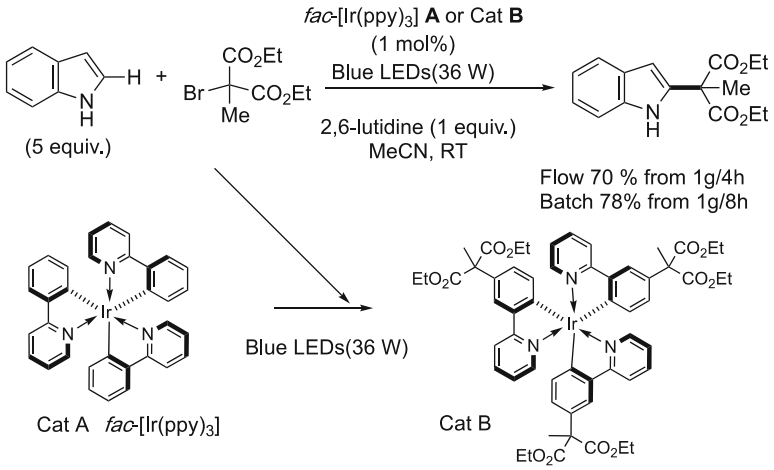

Scheme 17 Flow process promoted by *fac*-[Ir(ppy)$_3$] and modified photoredox system

(365 nm) [59]. This efficient system does not operate via MLCT as the Ru, Ir-based photoredox catalysts.

Glorius has shown in 2017 that alkylation of heteroarenes could be performed from a Katritzky salt, arising from the reaction of primary amine or amino acid with a pyrylium salt, in the presence of the photoredox complex [Ir(ppy)$_2$(dtbbpy)]PF$_6$ under visible light irradiation (Scheme 18) [60]. Thus the radical formally results from deamination of the initial amine and amino acid. The regioselective alkylation of indoles and pyrroles has been performed successfully, from amino acid-derived radicals, at room temperature in DMA. A single electron is transferred to the Katritzky salt from the light-excited [*Ir(ppy)$_2$(dtbbpy)]$^+$, the formed radical releases the deaminated radical which adds to the heteroarene at C2 position. The 2-alkylated heteroarene is generated by oxidation and deprotonation of the heterocyclic radical.

Masson et al. in 2016 have shown that the photoredox [Ru(bpy)$_3$](PF$_6$)$_2$ under visible light irradiation could promote the capture of one electron from an α-amidosulfide, with the help of oxygen, to generate beside the RS• radical an *N*-acyliminium cation. The latter is then able to perform regioselective aza-Friedel-Crafts reaction with electron-rich heterocycles, thus their alkylation, such as indoles and thiophene (Scheme 19) [61]. The reaction is performed with 10 equiv. of *t*-BuOH at room temperature as in the presence of *t*-BuOH there is decreasing of α-aminosulfide oxidation potential. Organic photoredox such as Eosin Y can perform the same alkylation of heterocycles with *N*-acyliminium cations. As the light-excited species [*Ru(bpy)$_3$]$^{2+}$ cannot directly oxidize the α-amidosulfide, it is proposed that [*Ru(bpy)$_3$]$^{2+}$ transfer one electron to oxygen to give the radical

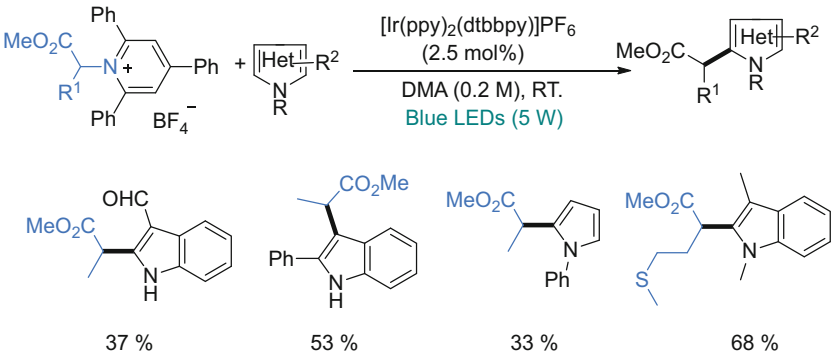

Scheme 18 Examples of alkylation of *N*-heteroarenes with radical from amino-acids *via* their Katritzky salts

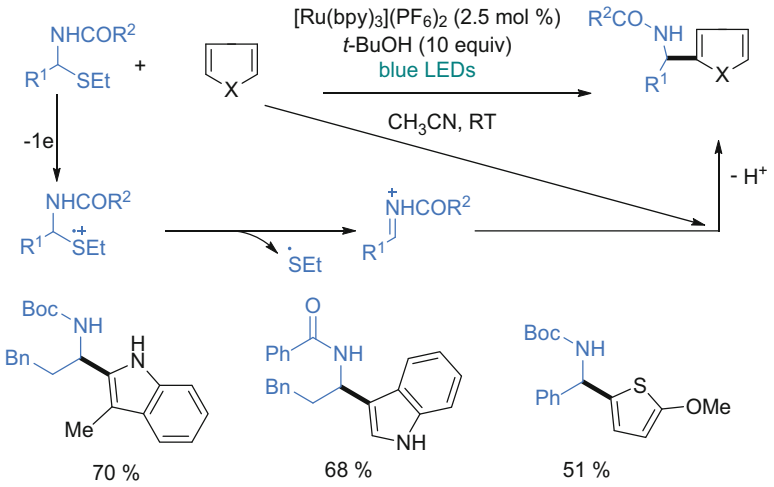

Scheme 19 Aza-Friedel-Crafts reaction of heterocycles with *N*-acyliminium cation generated from α-amidosulfides and photoredox

anion O_2-• and the $Ru(bpy)_3^{3+}$ species which then captures one electron from RCH (NHZ)SEt to produce the EtS· radical and the *N*-acyliminium cation able to add to electron-rich heteroarenes (Scheme 19) [61].

3 Functionalizations of 6-Atom Ring Heteroarenes

3.1 *Photoredox-Assisted Arylation of 6-Atom Heteroarene C(sp^2)–H Bonds*

In 2014, Xue and co-workers have employed aryldiazonium salts as aryl radical precursors in photoredox-catalyzed C–H bond arylation of pyridine, quinoline, and pyrazine derivatives (Scheme 20) [62]. The reaction was carried out in water using $[Ru(bpy)_3]Cl_2{\cdot}6H_2O$ as a photosensitizer and household light. The arylation took place at C2 position when C4-substituted pyridines are employed, while unsubstituted, C2- or C3-substituted pyridines led to mixtures of regioisomers. The authors showed that using aqueous formic acid as solvent, pyrazine and pyridazine could be also arylated.

Inspired by Deronzier for the intramolecular C–H bond arylation with diazonium stilbenes [31, 63], the authors suggested an oxidative quenching cycle as mechanism key step (Fig. 7). They proposed two possible pathways for the last step of resulting radical oxidation into carbocation intermediate: (1) a common oxidation by the strongly oxidizing $[Ru(bpy)_3]^{3+}$or (2) an oxidation by the aryldiazonium salt leading to an autocatalytic reaction.

Meanwhile, Lei and co-workers achieved the regioselective C2-arylation of isoquinolines (Scheme 21) [64]. Trifluoroacetic acid was used to in situ generate the isoquinolinium salts.

The conditions described by Tobisu, Chatani, and co-workers for the C–H arylation of 5-atom ring heteroarenes with diaryliodonium salts and $[Ir(ppy)_2(bpy)]PF_6$ as photoredox catalyst (Scheme 2) were also operative for the

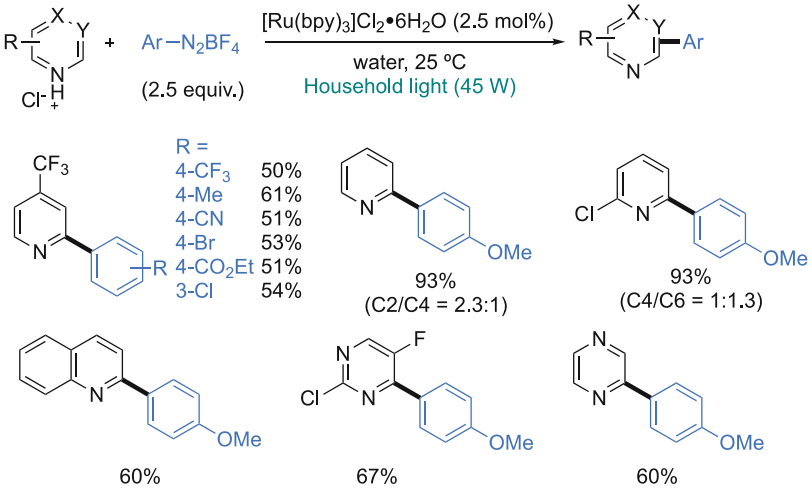

Scheme 20 $Ru(bpy)_3^{2+}$-catalyzed arylation of *N*-heteroarenes with aryldiazonium salts

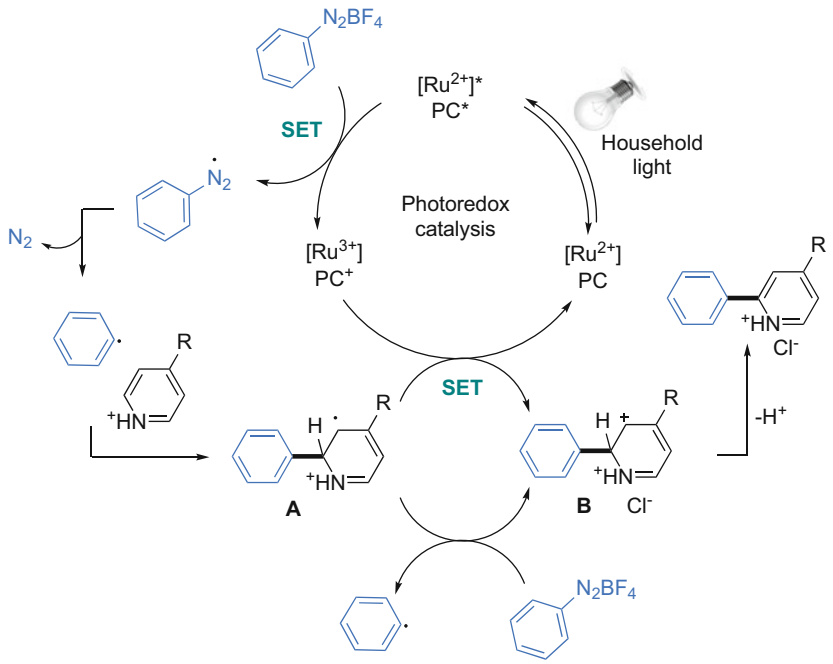

Fig. 7 Proposed mechanism for arylation of *N*-heteroarenes with aryldiazonium salts

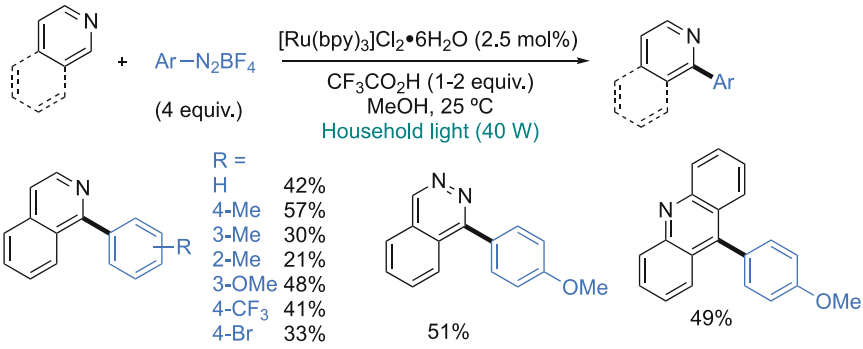

Scheme 21 $Ru(bpy)_3^{2+}$-catalyzed isoquinoline with aryldiazonium salts

phenylation of pyridines, pyrazine derivatives, albeit low yields and poor regioselectivity were observed (Scheme 22) [34].

König and co-workers applied their catalytic system based on pyrene sensitization-initiated electron transfer using $[Ru(bpy)_3]^{2+}$ to the arylation of 2,6-dimethoxypyridine with 2-bromobenzonitrile or 5-bromopyrimidine (Scheme 23) [36].

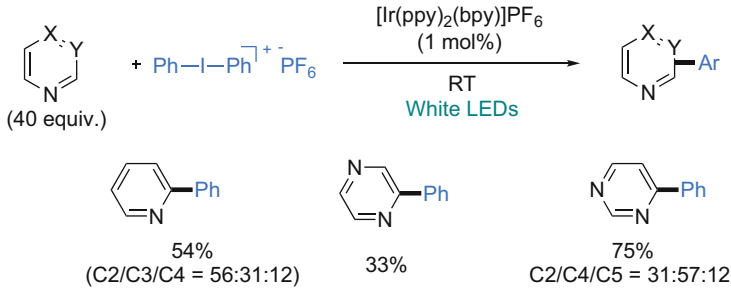

Scheme 22 [Ir(ppy)$_2$(bpy)]PF_6-catalyzed the phenylation of pyridine and pyrazine derivatives with diaryliodonium salts

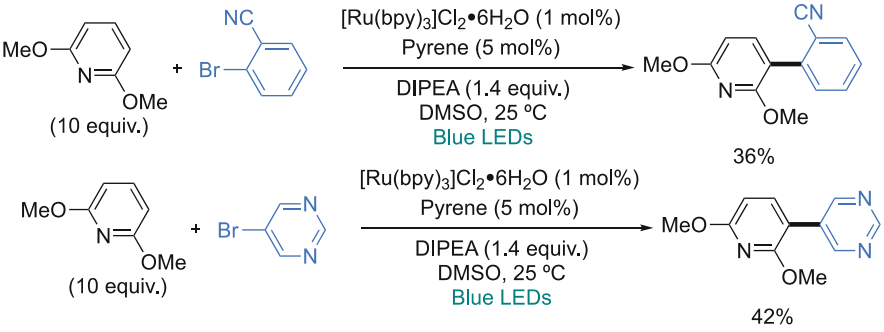

Scheme 23 $Ru(bpy)_3^{2+}$-catalyzed arylation of 6-dimethoxypyrine with aryl bromides

In 2017, Glorius and co-workers reported that the C(sp^2)–H bond arylation of pyridines using carboxylic acids is a suitable source of radicals *via* a visible light-mediated decarboxylation (Scheme 24) [65]. The key step was the formation of benzoyl hypobromite, which is in situ prepared by reaction of carboxylic acid and diethyl 2-bromo-2-methylmalonate. In the presence of photoredox system, namely, 3 mol% [Ir{dF(CF_3)ppy}$_2$(dtbbpy)]$(PF_6)_2$ under blue LED irradiation, such benzoyl hypobromite easily decomposes into aryl radical which could be trapped by heteroarenes such as pyridines derivatives. The reaction was not regioselective, and mixtures of regioisomers were obtained, except from 4-tert-butylpyridines, although a huge amount of pyridine derivatives (100 equiv.) is required.

The authors proposed a reductive quenching of PC (*Ir(III)/Ir(II)) by the benzoate anion providing aroyloxy radical (Fig. 8). The authors denied the direct decarboxylation of carboxylic acid, which required high temperature. Therefore, they proposed pathway involving bromination of radical anion of carboxylic acid generated by SET of *PC to carboxylic acid to form the benzoyl hypobromite **A**. The resulting hypobromite can be reduced by the Ir(II) ($E_{1/2}^{III/II} = -1.37$ V vs SCE) leading to intermediate **B** and its decarboxylation to afford the key aryl radical ($Ar^{\bullet}$). Finally, the aryl radical is trapped by (hetero)arene to generate the cyclohexadienyl radical **C**,

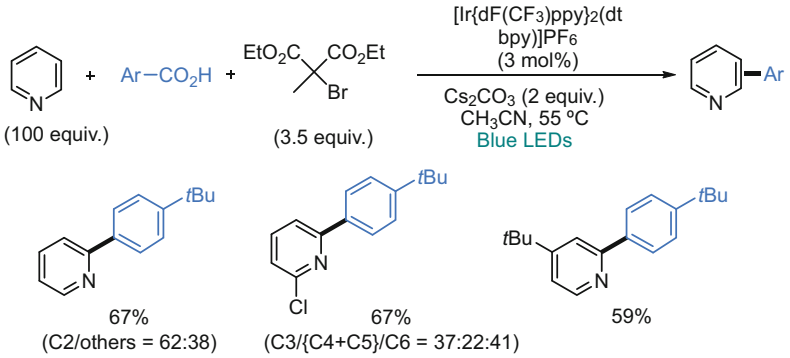

Scheme 24 [Ir{dF(CF_3)ppy}$_2$(dtbbpy)](PF_6)$_2$-catalyzed arylation of pyridine with aryl carboxylic acids

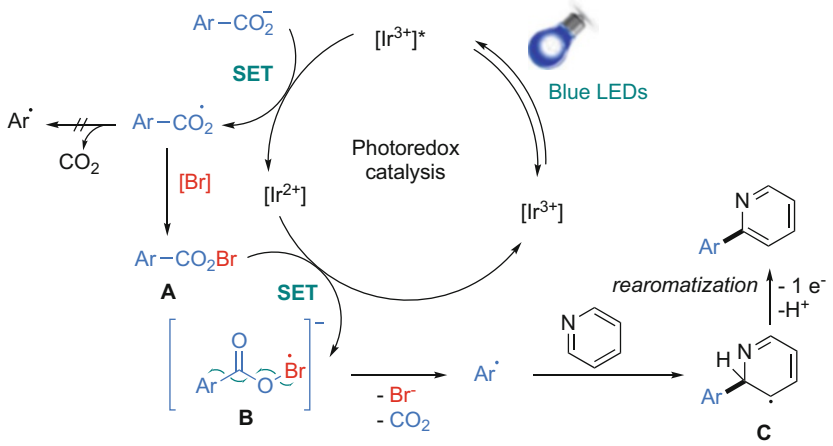

Fig. 8 Proposed mechanism for arylation with carboxylic acids

which, following oxidation to the aryl cation and deprotonation, affords the cross aryl-heteroaryl product.

3.2 Photoredox-Assisted Perfluoroalkylation of 6-Atom Heteroarene C(sp^2)–H Bonds

The trifluoromethylation of pyridines, pyrazines, pyrimidines, and pyrones using trifluoromethanesulfonyl chloride was accomplished by MacMillan and co-workers

using *fac*-[Ir(dF.ppy)$_3$] as photoredox catalyst (Scheme 25) [44]. The regioselectivity is substrate dependent, and when multi-sites are available, a mixture of regioisomers is often obtained.

The generation of $CF_3^{\bullet}$ radical from trifluoroacetic anhydride and pyridine *N*-oxide under photoredox catalysis (Scheme 12) was also applied to the trifluoromethylation of 6-atom heterocycles (Scheme 26) [54]. Pyrimidine where C2 and C5 position were blocked by methoxy substituent was successfully trifluoromethylated at C3 position. *N*-methyl pyridinones were also functionalized at the C3 position.

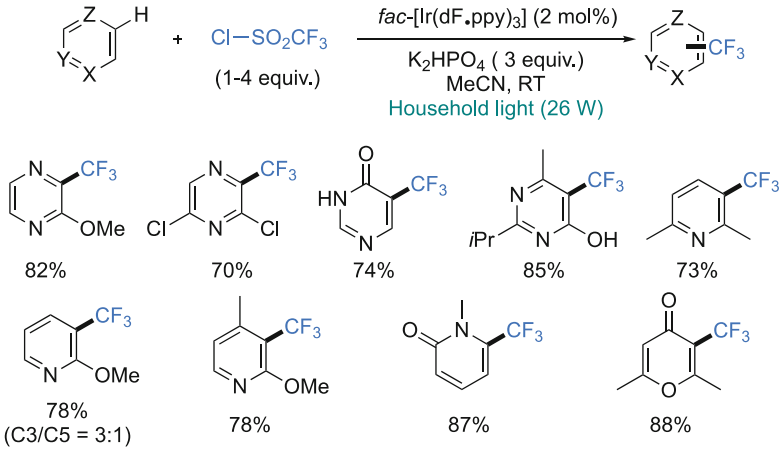

Scheme 25 *fac*-[Ir(dF.ppy)$_3$]-catalyzed trifluoromethylation of 6-atom heterocycles using trifluoromethanesulfonyl chloride

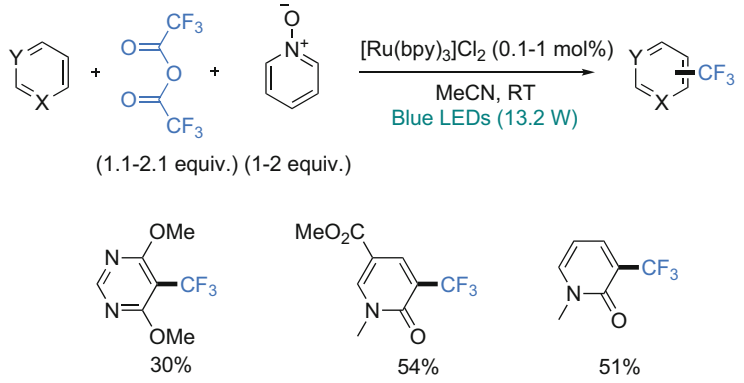

Scheme 26 Ru(bpy)$_3^{2+}$-catalyzed trifluoromethylation of 6-atom heterocycles with trifluoroacetic acid anhydride associated to pyridine *N*-oxide

In 2014, during their investigations on C(sp^2)–H bond difluoromethylation of heteroarenes from diethyl bromodifluoromethyl phosphonate as radical source (Scheme 11), Liu and co-workers showed that the reaction can be also applicable to pyridines and pyrimidine (Scheme 27) [53]. From 2-methoxy-4-methylpyridine, a mixture of C3 and C5 trifluoromethylated was obtained, while from 2,6-dimethoxypyridine, only C3-trifluoromethylated pyridine was obtained.

3.3 *Photoredox-Assisted Alkylation of 6-Atom Heteroarene C(sp^2)–H Bonds*

DiRocco et al. have found in 2014 the way to formally alkylate with small methyl or ethyl groups the C–H bond of *N*-heterocycles. They used [Ir{dF(CF_3)ppy}$_2$(dtbbpy)]PF_6 as photoredox and *tert*-butylperacetate (*t*BPA) or *tert*-amylperacetate to generate methyl or ethyl radical, respectively. These small radicals are useful to modify biologically active molecules with small alkyl groups. Thus, fasudil, camptothecin, or caffeine has been methylated that way (Scheme 28) [66].

The *t*-BuO• radical is known to produce the methyl radical and acetone. Thus on visible light, the excited {*Ir(III)} species ($E^\circ = -0.89$ V vs SCE) can transfer one electron to the protonated *t*BPA, *via* proton-coupled electron transfer (PCET) which thus provides, beside an Ir(IV) species, the *t*-BuO• radical and then methyl radical (Fig. 9) [66]. The methyl radical adds to the protonated *N*-heterocycle regioselectively at C2. After deprotonation of the resulting cation, one electron is captured by the Ir(IV) system to regenerate the Ir(III) photoredox PC and the methylated heteroarene.

Peng Liu and Gong Chen have discovered an intermolecular alkylation of 6-atom *N*-heteroarenes with alkylboronic acids with two equivalents of acetoxybenziodoxole (BI-OAc). The reaction is mediated by the photoredox system [Ru(bpy)$_3$]Cl_2 in hexafluoroisopropanol (HFIP) (Scheme 29) [67]. Aryl halide, ester, carbamate, and alkyne groups can be tolerated on the boronic alkyl group. The C2

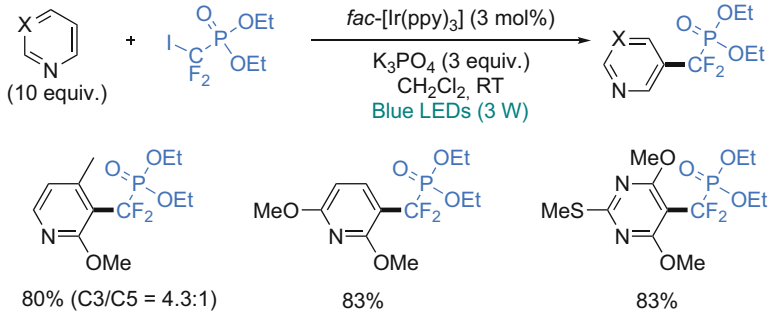

Scheme 27 *fac*-[Ir(ppy)$_3$]-catalyzed difluoromethylenephosphonation of 6-atom heterocycles with bromodifluoromethylphosphonate

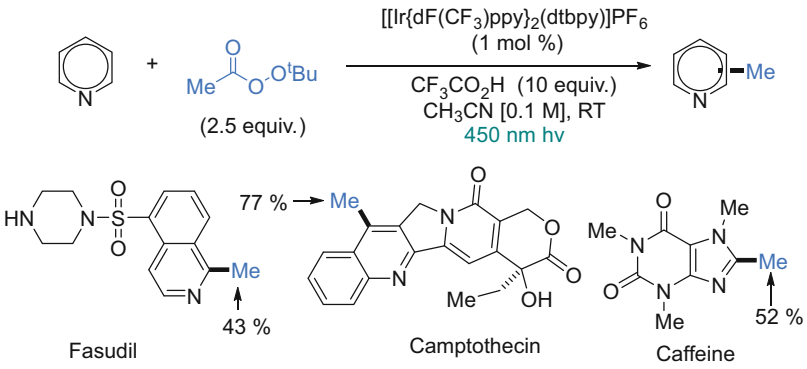

Scheme 28 Methylation of *N*-heterocycles with *tert*-butylperacetate

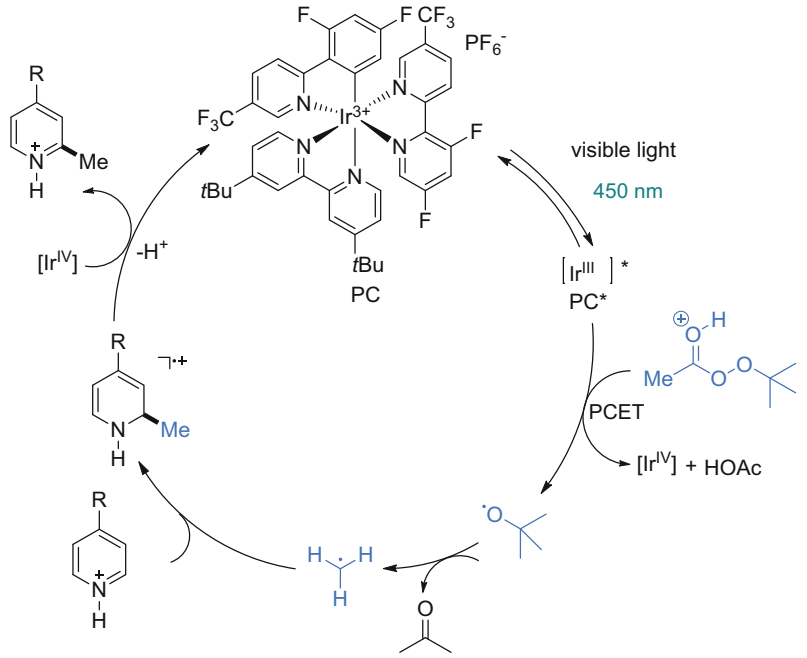

Fig. 9 Catalytic cycle for the photocatalyzed methylation of *N*-heterocycles

alkylation of 4-chloroquinoline, pyridines, phenanthroline, and quinine was selectively obtained, or at C4 when a substituent was present at C2 position.

The reaction can be explained as shown on Fig. 10 [67]. The light-excited [*Ru $(bpy)_3]^{2+}$ species transfers one electron (SET) to BI-OAc to generate acetate and a radical adding to the boronic acid to give intermediate **A**. The later gives the radical

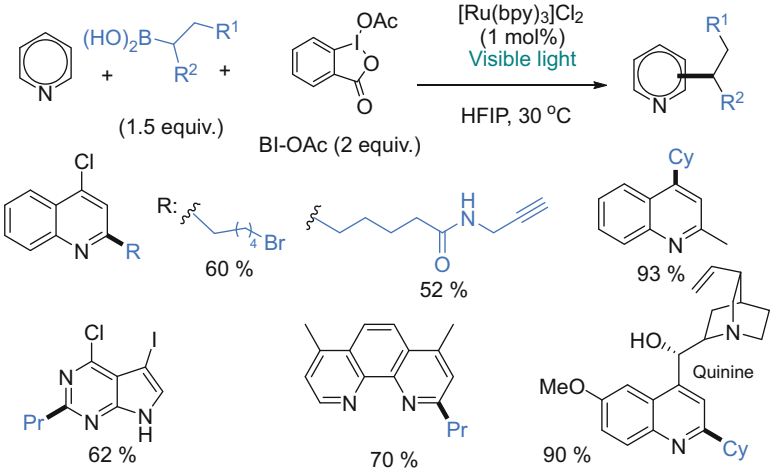

Scheme 29 Alkylation of 6-atom *N*-heteroarenes using alkyl boronic acid and hypervalent iodine

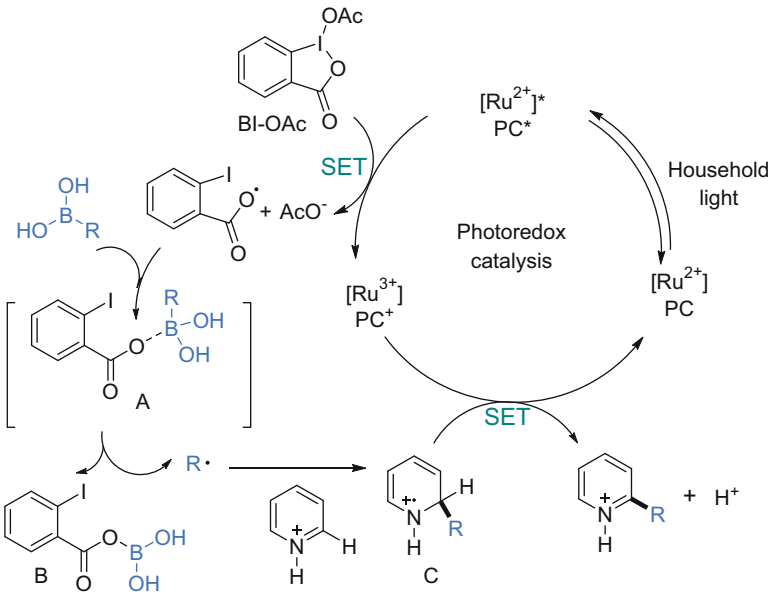

Fig. 10 Mechanism for photocatalyzed C–H bond alkylation of heteroarenes

R°, beside species **B**, which adds to the protonated *N*-heterocycle at C2 to produce **C**, which releases the protonated alkylated heterocycle**.**

MacMillan in 2015 combined the action of a metal-containing Ir(III) photoredox $[Ir(ppy)_2(dtbbpy)]PF_6$ and of a thiol ester as organocatalyst to activate

alcohols and generate a radical to directly alkylate C(sp^2)–H bonds of heteroarenes (Scheme 30) [68]. This dual photoredox-organocatalysis method is expected to generate $HOCH_2^{\bullet}$ radical from methanol which adds to the protonated heterocycle at C2 position when it is non-substituted. Thus, a variety of *N*-heterocycles have been methylated. Using a variety of primary alcohols R-CH_2OH, the $RCH^{\bullet}$-OH radicals could be generated to alkylate heteroarenes. This reaction can be performed also with diols, primary ether, and even tetrahydrofuran. The method was also applied to the alkylation of natural product derivatives such as fasudil and milrinone.

The mechanism is depicted in Fig. 11 for the methylation of pyridine with methanol. On light excitation, the photoredox {*Ir(III)} complex by SET to the heteroarene leads to a strong oxidant {Ir^{4+}} species which allows the oxidation of the deprotonated thiol organocatalyst to produce the thiyl radical **A•**. **A•** is able to capture a H atom of methanol to produce the radical $HOCH_2$• (**B**), which adds to the carbon C2 of the protonated pyridine. The generated hydroxymethyl-pyridine cation (**C**) is deprotonated and eliminates water via a spin-center shift (SCS) process and generates the radical (**D**). **D** is deprotonated and reduced by SET from excited {Ir(III)} to give the methylated product **E** and the {Ir^{4+}} oxidant.

Glorius et al. in 2017 have found the way to generate radicals by decarboxylation of simple carboxylic acids RCO_2H, with the help of the photoredox system [Ir{dF(CF_3)ppy}$_2$(dtbbpy)]PF_6, and these radicals R$^{\cdot}$ add regioselectivity to 6-atom

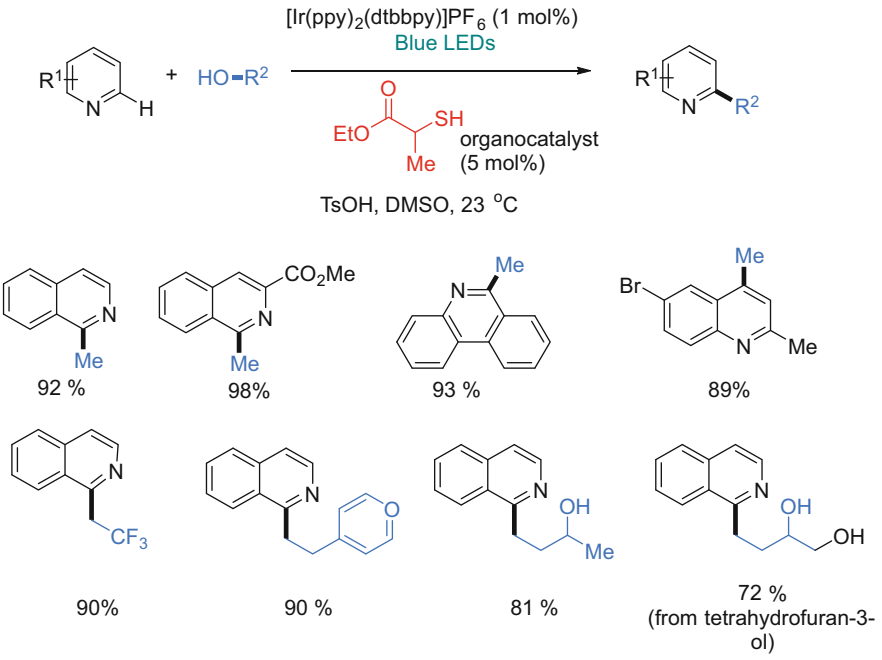

Scheme 30 Alkylation of heteroaromatic C–H bonds directly with primary alcohols via the dual photoredox and organocatalyst actions

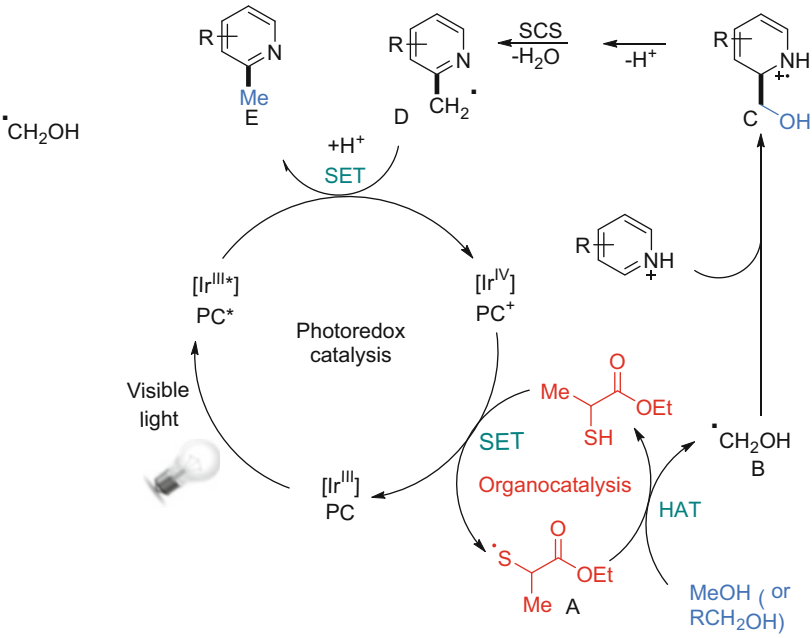

Fig. 11 Proposed mechanism for the direct methylation of pyridine at C2–H bond

heterocycles, preferentially at C2 (Scheme 31) [69]. This method which requires the presence of ammonium persulfate $(NH_4)_2S_2O_8$ offers the way to introduce a large variety of alkyl groups at C2 of heterocycles such as benzimidazole and benzothiazole, isoquinoline, and quinoxaline or fasudil derivatives. A large variety of primary, secondary, and tertiary alkyl groups of carboxylic acids can be used, but a large amount (10 equivalents) of carboxylic acid leads to reach high yields. Importantly amino acid derivatives allow the introduction of a functional alkyl group containing an amino group.

The authors proposed the mechanism depicted with cyclohexylcarboxylic acid in Fig. 12 [69]. LED irradiation ($\lambda_{max} = 455$ nm) produces a long-lived excited state {*Ir(III)} species ($E_{1/2}^{IV/*III} = -0.88$ V vs SCE in CH_3CN/H_2O), which can transfer one electron to $(NH_4)_2S_2O_8$ to give SO_4^{2-} and $SO_4^{-\bullet}$ anions, beside the $\{Ir^{4+}\}$ complex. The radical anion $SO_4^{-\bullet}$ captures the hydrogen atom from any acid RCO_2H, and then the radical $RCO_2^{\bullet}$ affords the radial R• (**A**) on decarboxylation. The R• radical adds to the *N*-heteroarenes at C2 position. The resulting radical (**B**) allows the reduction of the $\{Ir^{4+}\}$ species to regenerate the photoredox system {Ir (III)} and leads the 2-alkylated heteroarene **C**.

The 2017 Glorius's method for alkylation of 5-atom heterocycles using a Katritzky salt, simply made from primary amine and pyrylium salt (see Scheme 18), was also applicable to 6-atom heterocycles and took place selectively at

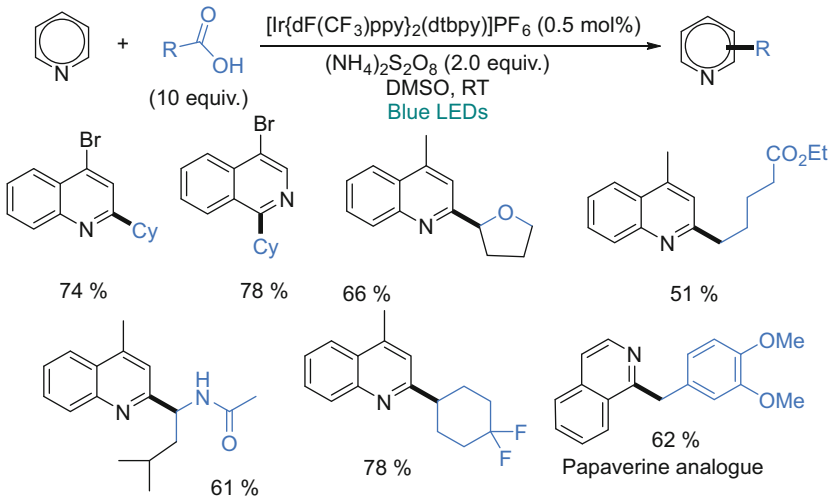

Scheme 31 Alkylation of *N*-heteroarenes with radical generated from carboxylic acids

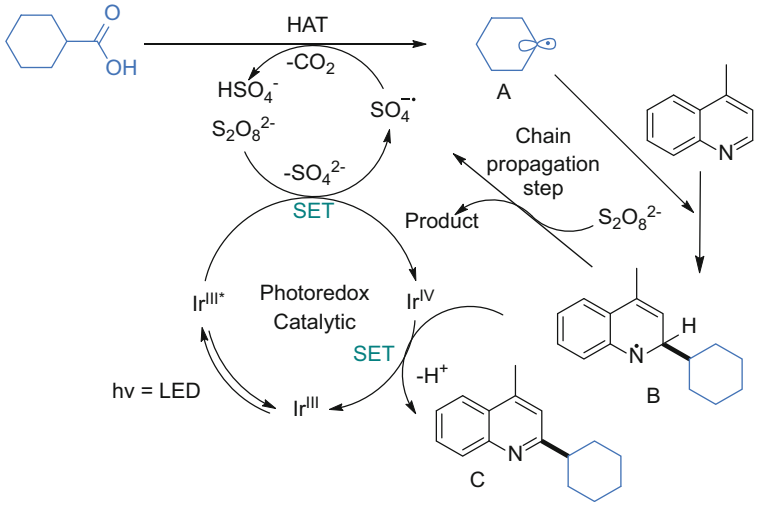

Fig. 12 Proposed catalytic cycle for alkylation of *N*-heteroarenes with carboxylic acid and $S_2O_8^{2-}$

non-substituted C2. The radical generation from amine salt is promoted by the photoredox system $[Ir(ppy)_2(dtbbpy)]PF_6$ under visible light irradiation (λ_{max} 455 nm) (Scheme 32) [60]. The reaction is efficient with a variety of alkyl groups, and it tolerates halides on the aromatic ring. The generation of the radical is initiated by SET from the excited species {*Ir(III)} to the Katritzky salt. Isoquinoline, quinoline, or phenanthroline have been selectively alkylated in good yields [60].

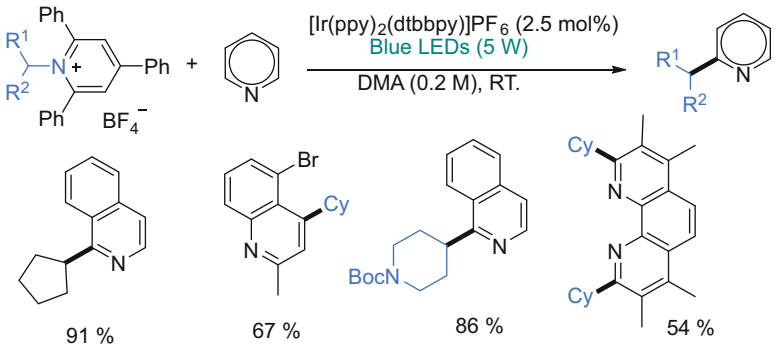

Scheme 32 Alkylation of 6-atom *N*-heteroarenes with radical from primary amines related Katritzky salts

4 Functionalizations of Arenes

4.1 Photoredox-Assisted Arylation of Arene C(sp^2)–H Bonds

Based on the pioneer Deronzier's works on the photoredox C(sp^2)–H bond cyclization of diazonium stilbenes using $Ru(bpy)_3^{2+}$ [31, 63], Sanford and co-workers developed a dual catalysis composed by palladium and photoredox catalysis for the *ortho*-directed C(sp^2)–H bond arylation of 2-arylpyridine derivatives with aryl diazonium (Scheme 33) [70]. The major advantage is that the reaction occurred at room temperature, while palladium-catalyzed direct arylation using aryl halides required 150°C. A broad range of substituted aryl diazonium salts were efficiently coupled with *N*-phenylpyrrolidone. Moreover, 2-phenylpyridines bearing halogen, trifluoromethyl, methoxy, or nitro group on the pyridine unit could be employed. Other directing groups such as amides, pyrazoles, pyrimidines, and oxime ethers also reacted under these reaction conditions.

The authors proposed two separate catalytic cycles including photoredox catalytic cycle and palladium catalytic cycle (Fig. 13) [70]. The photoreduction of the aryldiazonium salt gives aryl radical species (**A**), concomitantly affording oxidated-state photosensitizer (Ru^{3+}). Pd(II)-mediated directed C–H activation gives palladacycle, which could be oxidated by an aryl radical to give Pd(III) intermediate (**B**). Single electron oxidation of this Pd(III) by Ru^{3+} affords Pd(IV) intermediate (**C**) and regenerates the (Ru^{2+}). Finally, reductive elimination of Pd(IV) intermediate (**C**) produces the desired C–H bond arylated product and regenerates Pd(II) catalyst.

Later, Guo and co-workers extended this protocol to the *ortho*-arylation of purine nucleosides, in which the purine unit plays the role of directing group (Scheme 34) [71].

Tobisu, Chatani, and co-workers have reported one example of nondirected arylation using photoredox conditions (Scheme 35) [34]. From benzene – used as

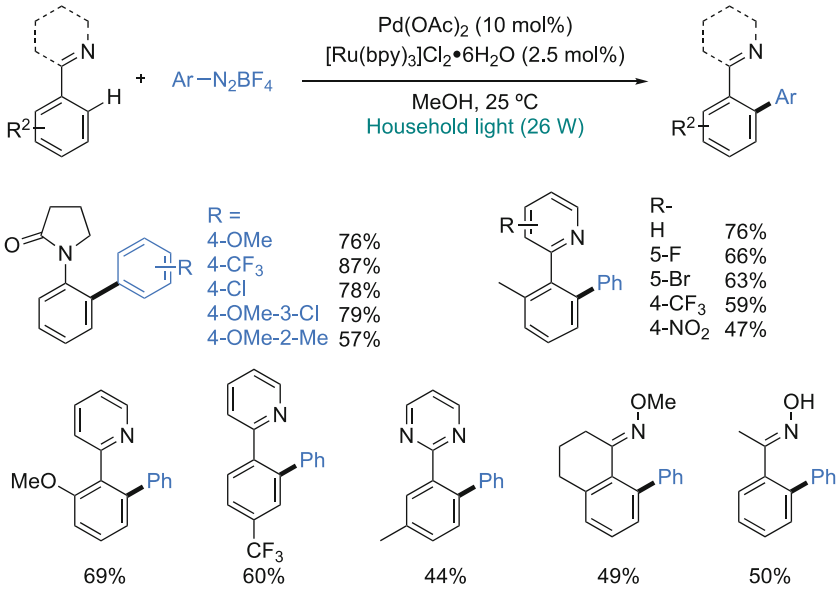

Scheme 33 Merging Pd-catalyzed C–H functionalization and visible light photocatalysis

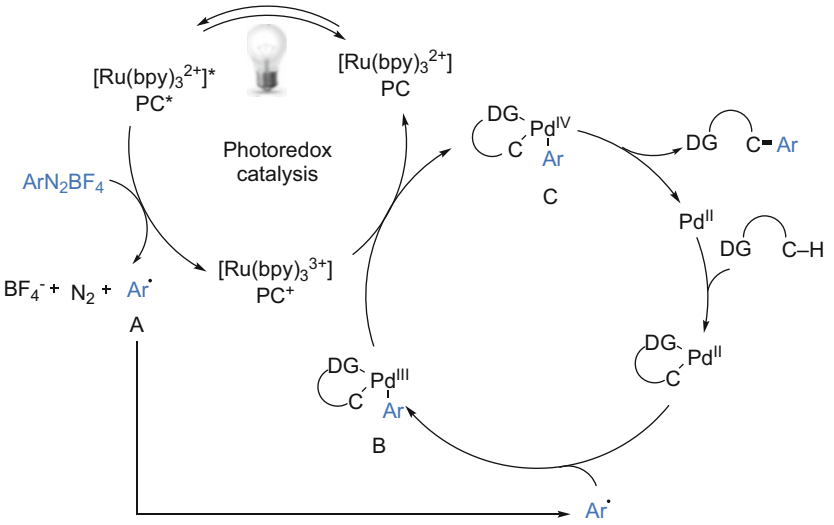

Fig. 13 Proposed catalytic cycle of C–H bond arylation *via* dual catalysis

reagent and solvent – and diphenyliodonium hexaphosphate, biphenyl was obtained in 54% yield using $[Ir(ppy)_2(bpy)]PF_6$ as photoredox catalyst.

Aryl radicals, generated from electron-poor aryl bromides using pyrene sensitization-initiated electron transfer strategy, can be trapped by electron-rich

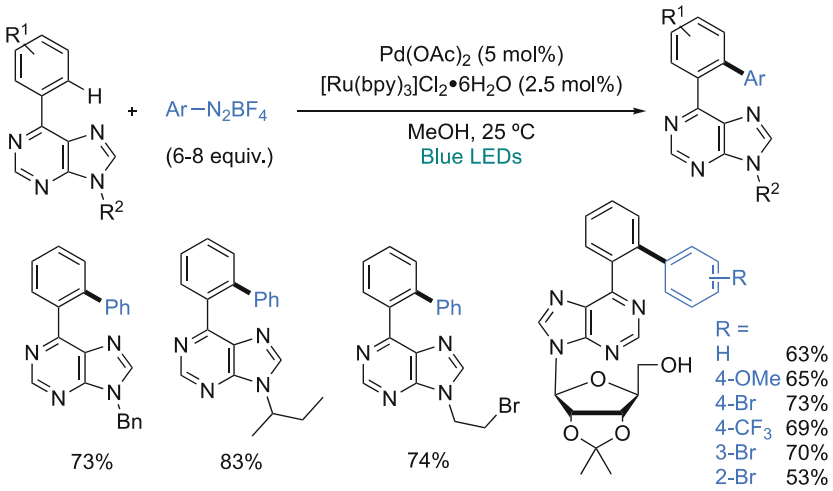

Scheme 34 Dual catalysis $Pd(OAc)_2/Ru(bpy)_3^{2+}$ for arylation of purine nucleosides using aryldiazonium salts

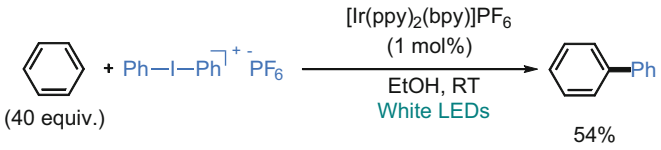

Scheme 35 $[Ir(ppy)_2(bpy)]PF_6$-catalyzed phenylation of benzene with diaryliodonium salts

arenes such as anilines, 1,3,5-trimethoxybenzene, or 1,3-dimethoxybenzene as demonstrated by König and co-workers (Scheme 36) [36]. Notably, 4-trifluoromethyl aniline is regioselectively arylated at C2-position, albeit only one example is demonstrated.

Glorius and co-workers reported photoredox-catalyzed $C(sp^2)$–H arylation of simple arenes using of aryl radical generated from decarboxylation of aryl carboxylic acids in the presence of diethyl 2-bromo-2-methylmalonate (Scheme 37) [65]. Interestingly, the reaction is not limited to the classical electron-rich arenes, but electron-deficient arenes such as 1,4-difluorobenzene and trifluorotoluene led to biaryl products in good yields, albeit 100 equivalents of arene are required.

4.2 Photoredox-Assisted Perfluoroalkylation of Arene $C(sp^2)$–H Bonds

MacMillan and co-workers have reported the first example of photoredox-assisted trifluoromethylation of arene $C(sp^2)$–H bonds using trifluoromethanesulfonyl

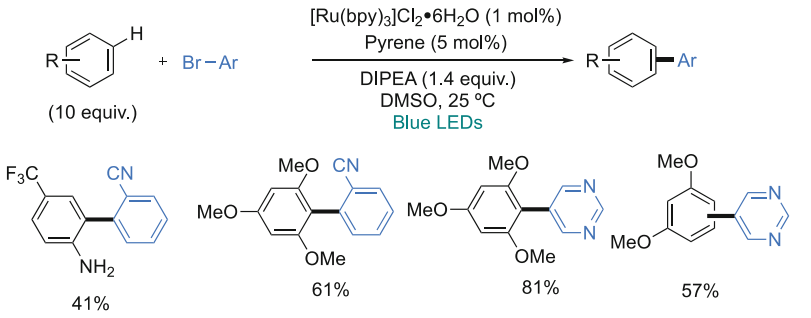

Scheme 36 $Ru(bpy)_3^{2+}$-promoted arylation of areneusing aryl bromide

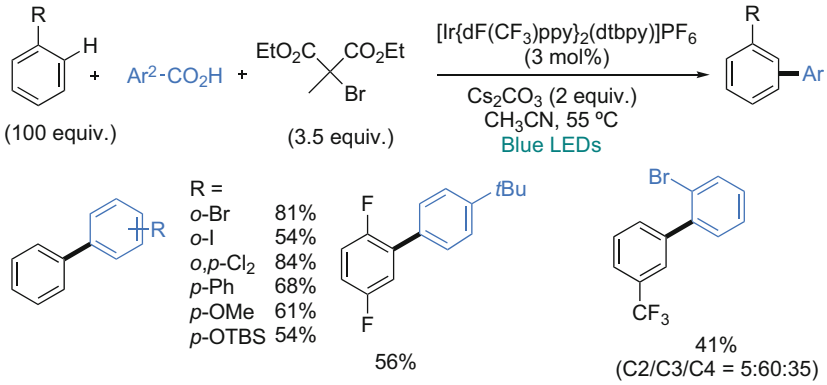

Scheme 37 [Ir{dF(CF_3)ppy}$_2$(dtbbpy)](PF_6)-catalyzed arylation of arenes with aryl carboxylic acids

chloride as CF_3 radical source (Scheme 38) [44]. Using [Ir(dF.ppy)$_3$] as photoredox catalyst, benzene was trifluoromethylated in good yield. N-Boc aniline was regioselectively functionalized at *ortho*-position. Notably, the reaction tolerates reaction functions such as C–Br, C–B, and C–Si bonds.

In 2014, Ma, Zhu, and co-workers succeeded to trifloromethylate NH_2-aniline derivatives using visible light-promoted radical C(sp^2)−H bond functionalizations (Scheme 39) [72]. They found that the Togni Reagent II was the best candidate to generate CF_3 radical – using 1.5 mol% of *fac*-[Ir(ppy)$_3$] as photocatalyst under blue LED irradiation – which is then trapped by anilines to afford C2-trifluoromethylated anilines. Anilines bearing electron-donating and electron-withdrawing groups are both trifluoromethylated. The reaction tolerates sensitive groups such as C–halo, C–OH, and C–Bpin bonds. The reaction involves an oxidative quenching pathway.

In 2017, Yang, Xia, and co-workers discovered that if benzimidazole derivatives are employed instead of anilines, the reaction led to C4-trifluoromethylated benzimidazoles (Scheme 40) [73]. A broad range of *N*-substituents (e.g., *NH*, *N*-methyl,

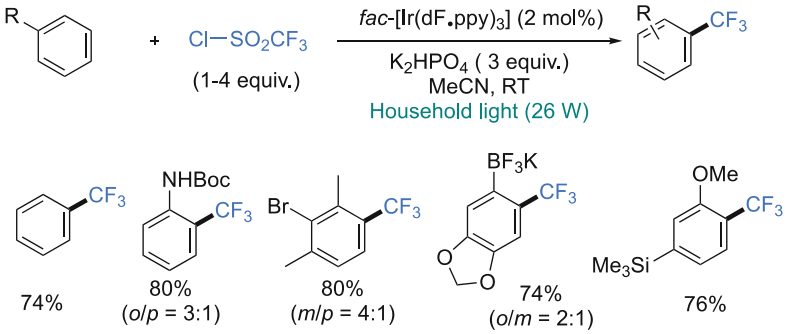

Scheme 38 *fac*-[Ir(dF.ppy)$_3$]-catalyzed trifluoromethylation of arenes using trifluoromethanesulfonyl chloride

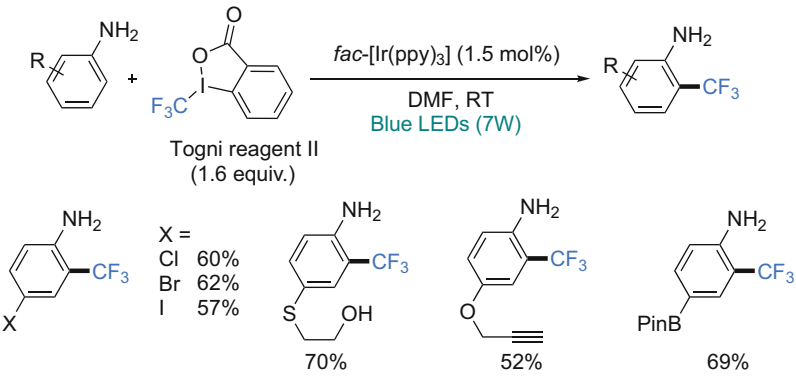

Scheme 39 *fac*-[Ir(ppy)$_3$]-catalyzed trifluoromethylation of anilines with Togni reagent

N-benzyl, *N*-phenyl, *N*-tosyl, and *N*-Boc) are tolerated. The presence of substituents on the benzene ring did not affect both yield and regioselectivity. Moreover, the reaction is not sensitive to ether, thioether, ester, chloro, heteroaryl, CF_3, and free hydroxyl groups.

Photoredox-assisted C(sp^2)–H bond trifluoromethylation of arenes was also achieved by the Stephenson's method, which generated the $CF_3^{\bullet}$ radical from irradiation under blue LEDs of the adduct composed by trifluoroacetic anhydride and pyridine *N*-oxide in the presence of [Ru(bpy)$_3$]Cl$_2$ (Scheme 41) [54]. When the substrates have multi-reactive sites, a mixture of mono- and di-trifluoromethylated arenes is often obtained.

In 2014, Liu and co-workers achieved the difluoromethylene phosphonation of arene C(sp^2)–H bonds (Scheme 42) [53]. Simple arenes such as benzene or naphthalene undergo trifluoromethylation in moderate to good yields, but the reaction is more efficient with electron-rich arenes such as trimethoxybenzene. In the presence

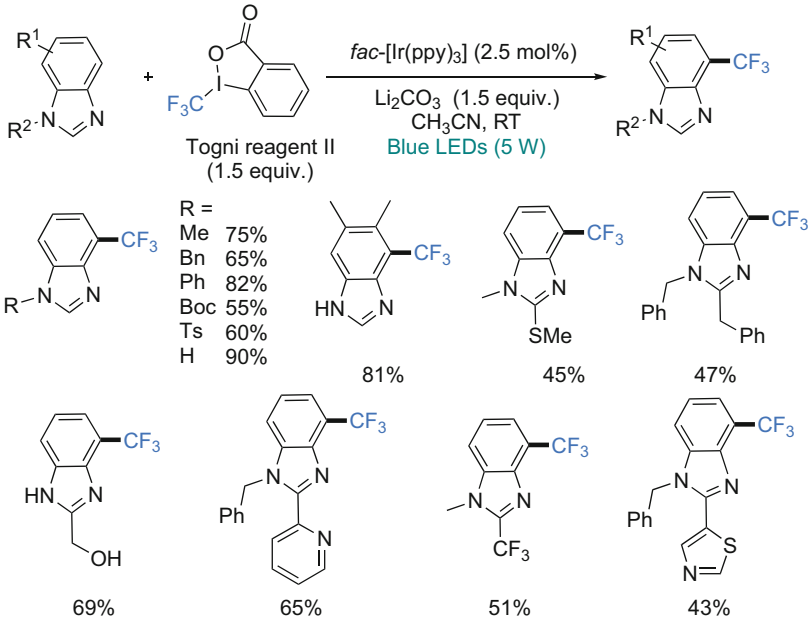

Scheme 40 *fac*-[Ir(ppy)$_3$]-catalyzed C4-trifluoromethylation of benzimidazoles with Togni reagent

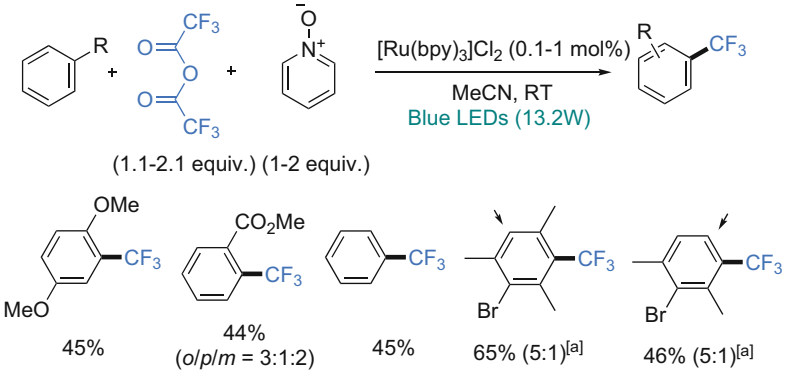

Scheme 41 Trifluoromethylation of (hetero)arenes with trifluoroacetic acid anhydride associated to pyridine *N*-oxide [a] minor doubly functionalized product, 4 equiv. of pyridine N-oxide and 8 equiv. of TFAA, 24 h

of the arenes bearing different substituents, the trifluoromethylated arenes are formed as a mixture of regioisomers.

In 2014, You and Cho et al. succeeded in the difluoromethylation of C(sp^2)–H bond of arenes with ethyl 2-bromo-2,2-difluoroacetate (Scheme 43) [74]. They

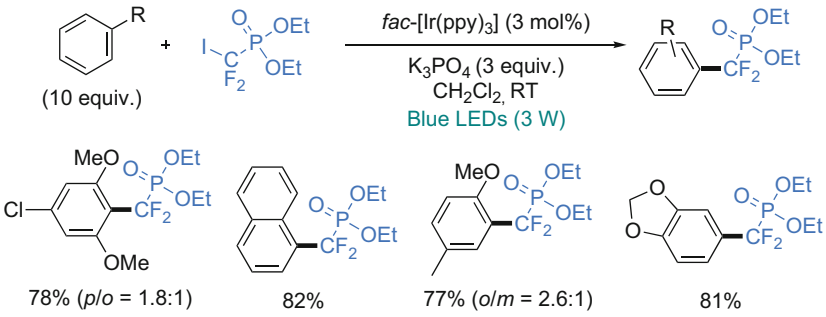

Scheme 42 *fac*-[Ir(ppy)$_3$]-promoted difluoromethylenephosphonation of arenes with bromodifluoromethylphosphonate

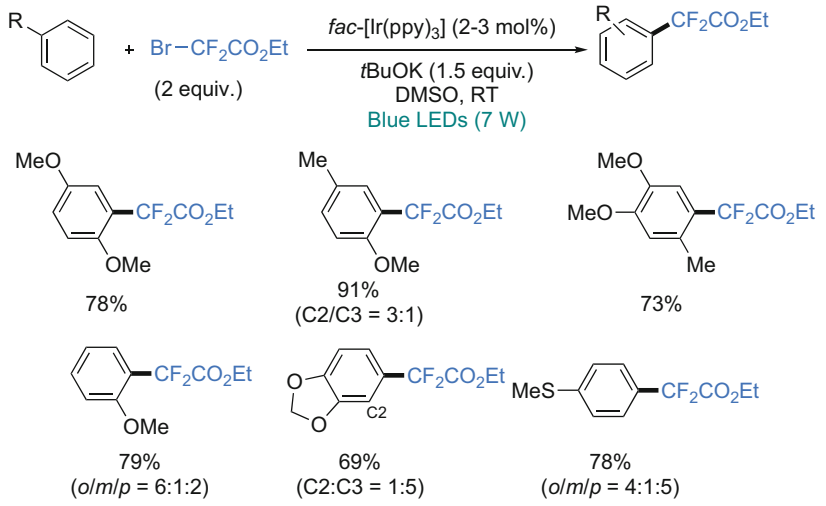

Scheme 43 *fac*-[Ir(ppy)$_3$]-catalyzed difluoroalkylation of electron-rich benzene derivatives with ethyl 2-bromo-2,2-difluoroacetate

employed *fac*-[Ir(ppy)$_3$] as photocatalyst and *t*BuOK as base in DMSO under blue LED irradiation to produce the desired difluoromethylated benzenes in good yields. The reaction is mainly limited to electron-rich benzenes, and products were often obtained as mixture of regioisomers when multi-sites are present on the arene.

4.3 Photoredox-Assisted Alkylation Arene C(sp^2)–H Bonds

In 2016, Xu Cheng et al. have shown that alpha-bromoketones could be used as radical precursors via SET from the visible light-irradiated photoredox system

[*Ru(bpy)$_3$]$^{2+}$ and that the resulting radical adds regioselectively at C2 of *N,N*-dialkylanilines (Scheme 44) [75]. This method allows the transformation of arene C(sp^2)–H bond into C(sp^2)–C(sp^3) bond. The reaction yields increase in the presence of the base NaOAc, and the simple [Ru(bpy)$_3$]Cl$_2$ photoredox system is more efficient than *fac*-[Ir(ppy)$_3$] or organic photoredox. The reaction is efficient for various alpha-bromoketones bearing halide or nitrile on the arene group and for alpha-bromoketones containing a heterocycle group such as furan or thiophene. Sunlight is also effective for this reaction and shows the robustness of the reaction intermediates.

The proposed mechanism involves the formation of the strong reducing Ru(I) species which thus allows a SET to the ArCO(Me)$_2$C-Br generating [Ru(bpy)$_3^{2+}$]. And the radical ArCO(Me)$_2$C• (**A**). The later adds regioselectively to C2 of aniline giving radical **B**. This radical **B** is able to transfer one electron to the excited photoredox [*Ru(bpy)$_3^{2+}$] to give the Ru(I) species and the cation **C**, which is easily deprotonated by NaOAc (Fig. 14) [75].

It is noteworthy that this mechanism is different from the Stephenson mechanism for alkylation of heteroarenes from alkylbromides with the same [Ru(bpy)$_3$]Cl$_2$ photoredox complex (see Fig. 6) [56], for which the reaction was performed in the presence of NEt$_3$, which is known to reduce [*Ru(bpy)$_3^{2+}$] into a Ru(I) species.

Masson et al. reported that α-amidosulfides can release one electron with the help of a photoredox partner and then generate, beside a RS• radical, a *N*-acyliminium cation allowing the alkylation of 5-atom heteroarenes (Scheme 19) [61]. They also show that the same conditions can perform the photocatalyzed aza-Friedel-Crafts

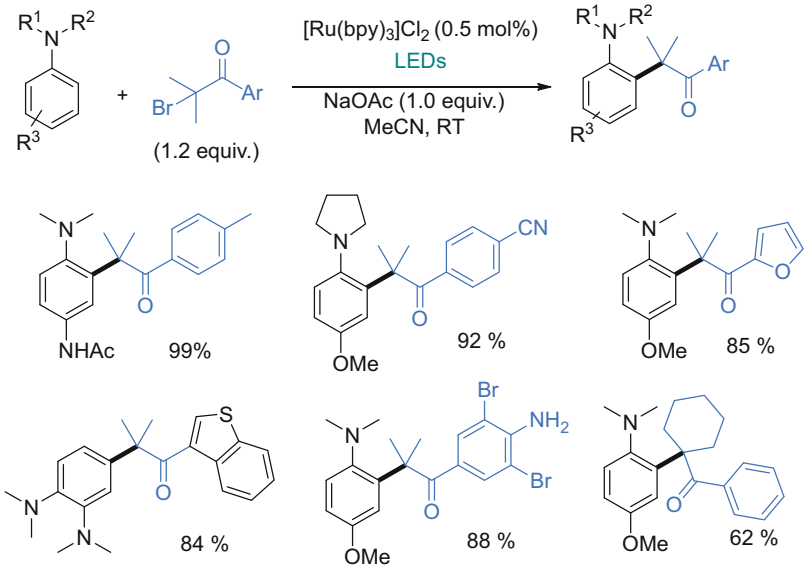

Scheme 44 Regioselective alkylation at C2 of anilines with alpha-bromoketones containing (hetero)aryl groups

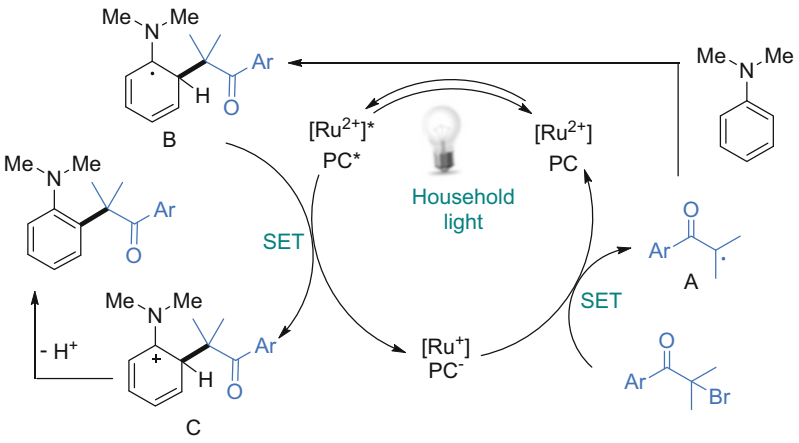

Fig. 14 Proposed mechanism for quaternary alkylation of anilines with α-bromoketones with [Ru $(bpy)_3^{2+}$] photoredox

reaction of electron-rich arenes such as trimethoxybenzene with $Ru(bpy)_3](PF_6)_2$ and thus formally the regioselective alkylation. The reaction is applicable to α-amidosulfides and α-carbamoylsulfides. Importantly chiral **α-**amidosulfides allow the selective formation of one diastereoisomer without racemization (Scheme 45) [61].

5 Conclusion

The above examples of visible light-promoted photoredox catalysis for the selective transformations of $C(sp^2)$–H bonds into $C(sp^2)$–C bonds, mostly at room temperature, show that this methodology offers one of most efficient ways for $C(sp^2)$–H bond arylation and (perfluoro)alkylation of 5- and 6-atom heterocycles and functional arenes. They require low energy and mild conditions for radical production from simple substrates and generate low by-product quantity which then offer green contribution to the catalytic processes. This methodology is a useful alternative to the metal-catalyzed C–H bond activation/functionalization. This review shows also that photoredox catalysts offer one of the best ways to produce radicals under mild conditions through SET events with the valorization of light as a green and abundant energy source.

Although a lot of efforts have been dedicated to the design of radical precursors, one of major challenge remains to control the regioselectivity of the radical additions with some substrate such as arenes in order to achieve regioselective $C(sp^2)$–H bond functionalizations. It is likely that in a close future more photoredox systems, based on MLCT metal complexes but also on functional polydentate ligands, will be

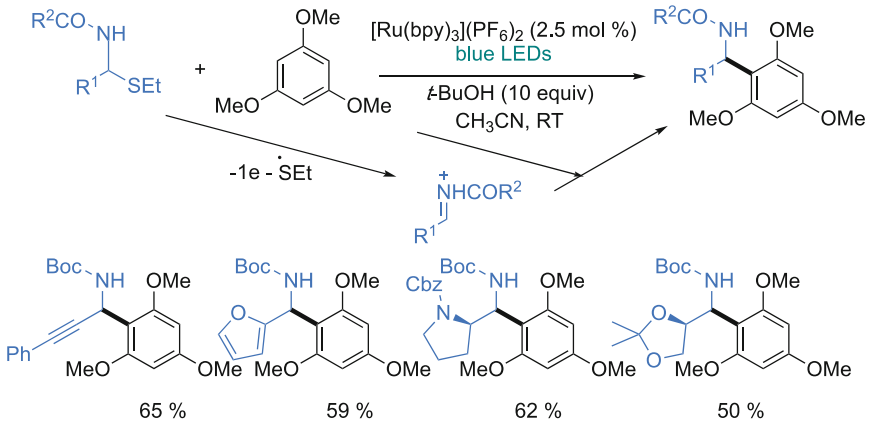

Scheme 45 Photocatalyzed aza-Friedel-Crafts reaction of trimethoxybenzene from α-amidosulfide derivatives

designed to produce new useful radicals for C–C bond formations with higher regioselectivity, but also for C–O and C–N bond formations, from C(sp^2)–H bonds.

References

1. Satoh T, Miura M (2007) Chem Lett 36(2):200–205
2. Seregin IV, Gevorgyan V (2007) Chem Soc Rev 36(7):1173–1193
3. Bellina F, Rossi R (2009) Chem Rev 110(2):1082–1146
4. Chen X, Engle KM, Wang D-H, Yu J-Q (2009) Angew Chem Int Ed 48(28):5094–5115
5. Colby DA, Bergman RG, Ellman JA (2009) Chem Rev 110(2):624–655
6. Litvinas ND, Brodsky BH, Du BJ (2009) Angew Chem Int Ed 48(25):4513–4516 S4513/4511-S4513/4512
7. Cho SH, Kim JY, Kwak J, Chang S (2011) Chem Soc Rev 40(10):5068–5083
8. Liu C, Zhang H, Shi W, Lei A (2011) Chem Rev 111(3):1780–1824
9. Yeung CS, Dong VM (2011) Chem Rev 111(3):1215–1292
10. Arockiam PB, Bruneau C, Dixneuf PH (2012) Chem Rev 112(11):5879–5918
11. Mercier LG, Leclerc M (2013) Acc Chem Res 46(7):1597–1605
12. Dixneuf PH, Doucet H (eds) C-H bond activation and catalytic functionalization Vol I (2015) & Vol II (2016) C-H bond activation and catalytic functionalization I. Springer International Publishing, Cham
13. Bheeter CB, Chen L, Soulé J-F, Doucet H (2016) Cat Sci Technol 6(7):2005–2049
14. Lyons TW, Sanford MS (2010) Chem Rev 110(2):1147–1169
15. Kuhl N, Hopkinson MN, Wencel-Delord J, Glorius F (2012) Angew Chem Int Ed 51 (41):10236–10254
16. Gafney HD, Adamson AW (1972) J Am Chem Soc 94(23):8238–8239
17. Balzani V, Juris A (2001) Coord Chem Rev 211(1):97–115
18. Yoon TP, Ischay MA, Du J (2010) Nat Chem 2:527–532
19. Tucker JW, Stephenson CRJ (2012) J Org Chem 77(4):1617–1622
20. Prier CK, Rankic DA, MacMillan DWC (2013) Chem Rev 113(7):5322–5363
21. Ravelli D, Fagnoni M, Albini A (2013) Chem Soc Rev 42(1):97–113

22. Angnes RA, Li Z, Correia CRD, Hammond GB (2015) Org Biomol Chem 13(35):9152–9167
23. Romero NA, Nicewicz DA (2016) Chem Rev 116(17):10075–10166
24. Douglas JJ, Sevrin MJ, Stephenson CRJ (2016) Org Process Res Dev 20(7):1134–1147
25. Shaw MH, Twilton J, MacMillan DWC (2016) J Org Chem 81(16):6898–6926
26. Courant T, Masson G (2016) J Org Chem 81(16):6945–6952
27. Fabry DC, Rueping M (2016) Acc Chem Res 49(9):1969–1979
28. Xie J, Jin H, Hashmi ASK (2017) Chem Soc Rev 46(17):5193–5203
29. Qin Q, Jiang H, Hu Z, Ren D, Yu S (2017) Chem Rec 17(8):754–774
30. Boubertakh O, Goddard J-P (2017) Eur J Org Chem 2017(15):2072–2084
31. Cano-Yelo H, Deronzier A (1984) J Chem Soc. Perkin Trans 2(6):1093–1098
32. Luca OR, Gustafson JL, Maddox SM, Fenwick AQ, Smith DC (2015) Org Chem Front 2 (7):823–848
33. Liu Y-X, Xue D, Wang J-D, Zhao C-J, Zou Q-Z, Wang C, Xiao J (2013) Synlett 24 (04):507–513
34. Tobisu M, Furukawa T, Chatani N (2013) Chem Lett 42(10):1203–1205
35. Yang F, Koeller J, Ackermann L (2016) Angew Chem Int Ed 55(15):4759–4762
36. Ghosh I, Shaikh RS, König B (2017) Angew Chem Int Ed 56(29):8544–8549
37. Natarajan P, Bala A, Mehta SK, Bhasin KK (2016) Tetrahedron 72(19):2521–2526
38. Yuan K, Soulé J-F, Dorcet V, Doucet H (2016) ACS Catal 8121–8126
39. Yuan K, Soulé J-F, Doucet H (2015) ACS Catal 5(2):978–991
40. Hfaiedh A, Yuan K, Ben Ammar H, Ben Hassine B, Soulé J-F, Doucet H (2015) ChemSusChem 8:1794–1804
41. Skhiri A, Beladhria A, Yuan K, Soulé J-F, Ben Salem R, Doucet H (2015) Eur J Org Chem (20):4428–4436
42. Hagui W, Besbes N, Srasra E, Roisnel T, Soulé J-F, Doucet H (2016) Org Lett 18 (17):4182–4185
43. Arora A, Weaver JD (2016) Org Lett 18(16):3996–3999
44. Nagib DA, MacMillan DWC (2011) Nature 480(7376):224–228
45. Dolbier WR (1997) Fluorinated free radicals. In: Organofluorine chemistry. Springer, Berlin, pp 97–163
46. Heaton CA, Miller AK, Powell RL (2001) J Fluor Chem 107(1):1–3
47. Iqbal N, Choi S, Ko E, Cho EJ (2012) Tetrahedron Lett 53(15):2005–2008
48. Straathof NJW, Gemoets HPL, Wang X, Schouten JC, Hessel V, Noël T (2014) ChemSusChem 7(6):1612–1617
49. Su Y, Kuijpers KPL, König N, Shang M, Hessel V, Noël T (2016) Chem Eur J 22 (35):12295–12300
50. Lin Q, Chu L, Qing F-L (2013) Chin J Chem 31(7):885–891
51. Prakash GKS, Hu J (2007) Acc Chem Res 40(10):921–930
52. Su Y-M, Hou Y, Yin F, Xu Y-M, Li Y, Zheng X, Wang X-S (2014) Org Lett 16(11):2958–2961
53. Wang L, Wei X-J, Lei W-L, Chen H, Wu L-Z, Liu Q (2014) Chem Commun 50 (100):15916–15919
54. Beatty JW, Douglas JJ, Cole KP, Stephenson CRJ (2015) Nat Commun 6:7919
55. Beatty Joel W, Douglas James J, Miller R, McAtee Rory C, Cole Kevin P, Stephenson Corey RJ (2016) Chem 1(3):456–472
56. Tucker JW, Narayanam JMR, Krabbe SW, Stephenson CRJ (2010) Org Lett 12(2):368–371
57. Furst L, Matsuura BS, Narayanam JMR, Tucker JW, Stephenson CRJ (2010) Org Lett 12 (13):3104–3107
58. Swift EC, Williams TM, Stephenson CRJ (2016) Synlett 27(05):754–758
59. McCallum T, Barriault L (2016) Chem Sci 7(7):4754–4758
60. Klauck FJR, James MJ, Glorius F (2017) Angew Chem Int Ed Engl 56(40):12336–12339
61. Lebée C, Languet M, Allain C, Masson G (2016) Org Lett 18(6):1478–1481
62. Xue D, Jia Z-H, Zhao C-J, Zhang Y-Y, Wang C, Xiao J (2014) Chem Eur J 20(10):2960–2965
63. Cano-Yelo H, Deronzier A (1987) J Photochem 37(2):315–321

64. Zhang J, Chen J, Zhang X, Lei X (2014) J Org Chem 79(21):10682–10688
65. Candish L, Freitag M, Gensch T, Glorius F (2017) Chem Sci 8(5):3618–3622
66. DiRocco DA, Dykstra K, Krska S, Vachal P, Conway DV, Tudge M (2014) Angew Chem Int Ed 53(19):4802–4806
67. Li G-X, Morales-Rivera CA, Wang Y, Gao F, He G, Liu P, Chen G (2016) Chem Sci 7 (10):6407–6412
68. Jin J, MacMillan DWC (2015) Nature 525(7567):87–90
69. Garza-Sanchez RA, Tlahuext-Aca A, Tavakoli G, Glorius F (2017) ACS Catal 7(6):4057–4061
70. Kalyani D, McMurtrey KB, Neufeldt SR, Sanford MS (2011) J Am Chem Soc 133 (46):18566–18569
71. Liang L, Xie M-S, Wang H-X, Niu H-Y, Qu G-R, Guo H-M (2017) J Org Chem 82 (11):5966–5973
72. Xie J, Yuan X, Abdukader A, Zhu C, Ma J (2014) Org Lett 16(6):1768–1771
73. Gao G-L, Yang C, Xia W (2017) Chem Commun 53(6):1041–1044
74. Jung J, Kim E, You Y, Cho EJ (2014) Adv Synth Catal 356(13):2741–2748
75. Cheng J, Deng X, Wang G, Li Y, Cheng X, Li G (2016) Org Lett 18(18):4538–4541

Top Organomet Chem (2019) 63: 267–294
DOI: 10.1007/3418_2018_14

Published online: 24 November 2018

Green Cross-Coupling Using Visible Light for C–O and C–N Bond Formation

Hong Yi, Yichang Liu, and Aiwen Lei

Contents

Abstract The development of green and sustainable approaches in organic synthesis can provide an environmentally friendly method in the industrial manufacture. Recently, visible-light-mediated photocatalysis has achieved great progress and been a powerful tool to the construction of new chemical bonds in the green synthetic community. This chapter provides an updated summary of visible-light-mediated cross-coupling for C–O and C–N bond formations. Compared with the traditional synthetic methods, the visible-light catalysis provides a new way for the useful compounds synthesis (O-containing and N-containing molecules).

Keywords C–H functionalization · C–N bond · C–O bond · Cross-coupling · Photoredox catalysis · Visible light

Hong Yi and Yichang Liu contributed equally with all other contributors.

H. Yi, Y. Liu, and A. Lei (✉)
College of Chemistry and Molecular Sciences, The Institute for Advanced Studies (IAS), Wuhan University, Wuhan, China
e-mail: aiwenlei@whu.edu.cn

1 Introduction

Visible light, a clean, inexpensive, and "almost infinitely" available source of energy, has received increasing attentions of the chemistry community. During the last decade, visible-light photoredox catalysis has shown great promise as a method to advance these goals [1–3]. Recently, visible-light photoredox catalysis has been utilized as a powerful tool to construct C–C and C–heteroatom bonds through a single-electron transfer (SET) process, playing an important role in radical-based methodologies [4–6]. In this chapter, we sum up the recent and representative C–O and C–N bond formation via visible-light-mediated cross-coupling reactions.

2 C–O Bond Formation via Visible-Light Catalysis

The development of efficient methods for the construction of C–O bonds has gained much attention from the synthetic organic chemists due to their wide occurrence in a large number of biologically active molecules and in natural products. Herein, we sum the visible-light-mediated C–O cross-coupling by different oxygen sources.

2.1 Oxygen Nucleophile (ROH, H_2O, RCOOH)

2.1.1 ROH as the Oxygen Source

The trifluoromethyl (CF_3) group is considered to be a useful structural motif in several biologically active molecules. In 2012, Koike, Akita, and co-workers reported a three-component intermolecular oxytrifluoromethylation of alkenes using [*fac*-Ir(ppy)$_3$] as the photoredox catalyst (Scheme 1) [7]. This highly efficient and regioselective radical transformation of alkenes proceeds at room temperature

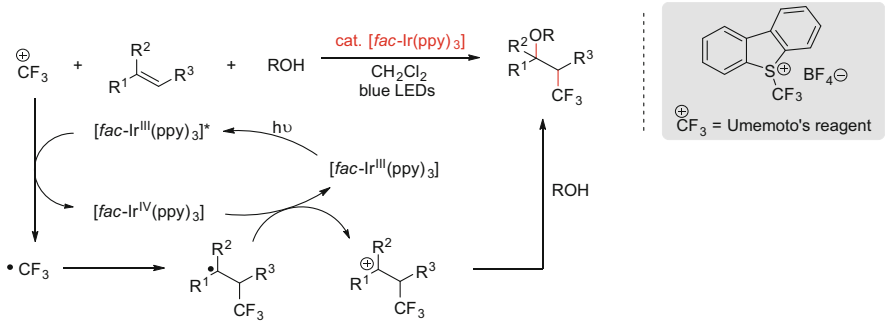

Scheme 1 Visible-light-mediated oxytrifluoromethylation of alkenes

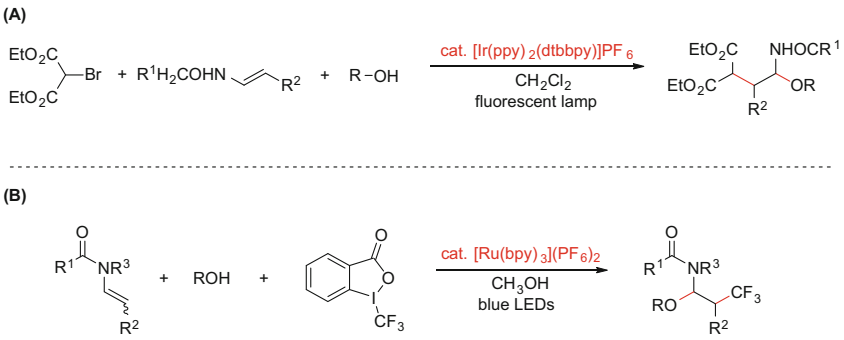

Scheme 2 (**a**) Visible-light-mediated alkylation of enamides with diethyl bromomalonate. (**b**) Photoredox-induced carbotrifluoromethylation of enecarbamates

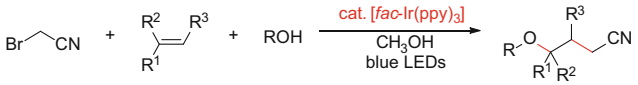

Scheme 3 Visible-light-induced alkoxycyanomethylation of alkenes

using Umemoto's reagent as CF_3 source. A variety of O functionalities such as hydroxy, alkoxy, and carboxy groups to C=C bonds has been achieved by photoredox catalysis under visible-light irradiation at room temperature. The mechanism reveals that the CF_3 radical can be formed via the single-electron transfer between Umemoto's reagent and photocatalyst. Addition of CF_3 radical to the alkenes gives the alkyl radical intermediate, which can be further oxidized to generate the cation species. Subsequent nucleophilic attack of carbocation intermediate affords the three-component coupled product.

Using alcohol as the oxygen nucleophile, Masson and co-workers developed a visible light-mediated alkylation of enamides with diethyl bromomalonate (Scheme 2a) [8]. This multicomponent domino process provides a general way to β-alkylated α-carbamido ethers in good to excellent yields under mild conditions. The easy accessibility of α-alkylated imines makes this method particularly attractive in organic synthesis. Using $[Ru(bpy)_3](PF_6)_2$ as the photoredox catalyst, Masson realized a visible-light-induced three-component synthesis of β-trifluoromethyl amines using Togni's reagent as the CF_3 source (Scheme 2b) [9]. The procedure is suitable for the completely regioselective synthesis of a wide variety of oxytrifluoromethylated carbamates. In addition, this method has also been expanded to other N and C nucleophiles. Later, Lei developed a visible-light-induced γ-alkoxynitrile synthesis via the three-component alkoxycyanomethylation of alkenes using the iridium photoredox catalyst [*fac*-Ir(ppy)$_3$] (Scheme 3) [10]. This catalytic radical difunctionalization accomplishes both alkylation and alkoxylation of alkenes in one pot. Various alcohols can serve as the alkoxy sources in the transformation.

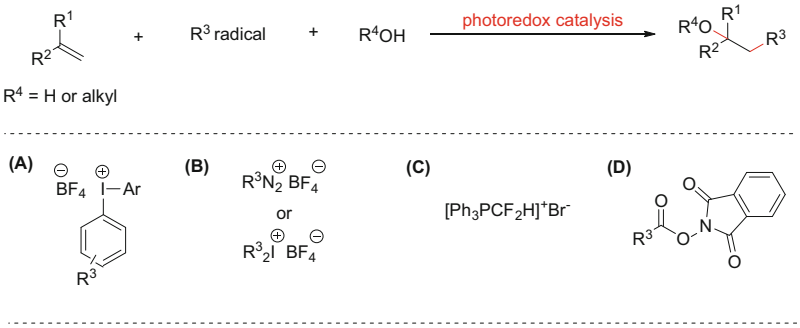

Scheme 4 Three-component couplings of styrenes via visible-light catalysis

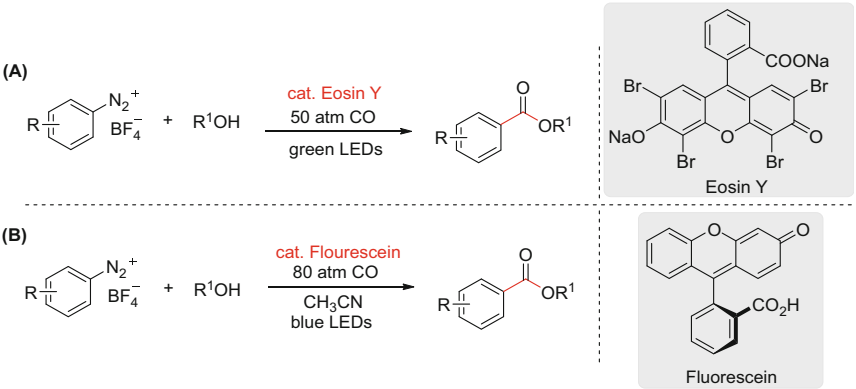

Scheme 5 Visible-light-mediated radical alkoxycarboxylation of aryldiazonium salts

In 2013, Greaney developed a three-component, photoredox-catalyzed coupling of styrenes with diphenyliodonium tetrafluoroborates and heteroatom nucleophiles such as alcohols, water, or nitriles (Scheme 4a) [11]. Subsequently, the intermolecular multicomponent oxyarylation of alkenes was developed using the gold salt and organic dye as the dual catalysts (Scheme 4b) [12]. The oxydifluoromethylation of styrenes was achieved by Qing via the visible-light catalysis. (Scheme 4c) [13]. Glorius developed a mild and overall redox-neutral method for the oxyalkylation of styrenes using visible light as energy source (Scheme 4d) [14]. The hydrogen-bonding interactions can drive direct photoinduced electron transfer between *N*-(acyloxy)phthalimides and photoexcited catalysts, which serves as a platform to access a variety of alkyl radicals.

The ester moiety has emerged as an important structural unit in a lot of natural compounds and synthetic materials. Wangelin (Scheme 5a) [15] and Xiao (Scheme 5b) [16] independently achieved the visible-light-mediated radical alkoxycarboxylation of aryldiazonium salts using CO gas. The reaction is entirely metal-free and carried out at room temperature using an organic dye as a photoredox

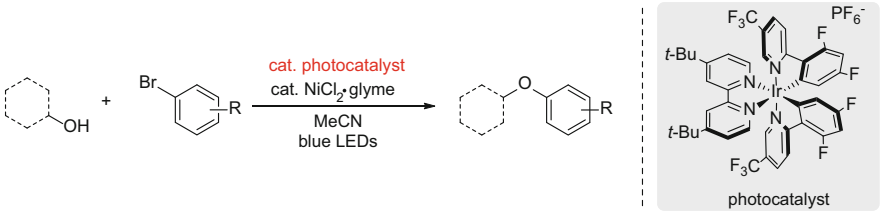

Scheme 6 Visible-light-mediated iridium photoredox and nickel dual-catalyzed cross-coupling for the formation C–O bonds

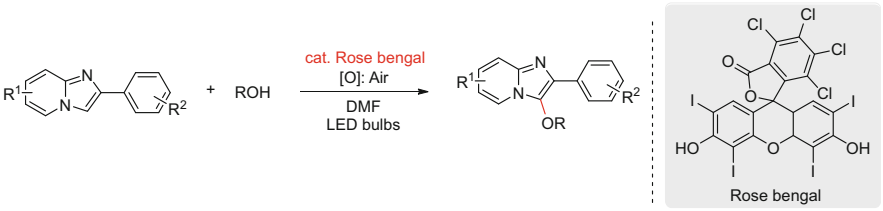

Scheme 7 Photocatalyzed C−H alkoxylation of imidazopyridines with alcohols

catalyst, which provides a wide range of alkyl benzoates. Unlike with metal-catalyzed carbonylations, *tert*-butyl esters could also be prepared in good yields. Mechanistic studies revealed that the aryldiazonium salt went through the sequential operation of SET reduction, carbonylation, and back electron transfer to give acylium cation, which underwent rapid addition to alcohols.

In 2015, MacMillan and co-workers reported the C–O bond formation between alcohols and aryl bromides via photoredox catalysis (Scheme 6) [17]. A series of substituted primary or secondary alcohols were obtained in good to excellent yields. The Ni(III) alkoxide complex was regarded as the key intermediate, which could be gained through the photoredox catalysis. It is worth mentioning that the H_2O could be used as the nucleophile in the same system.

The functionalization of imidazo[1,2-α]pyridines is synthetically attractive as this heterocyclic scaffold is widely used in biological and medicinal fields [18]. Hajra and co-workers achieved a visible-light-mediated C-3 alkoxylation of imidazopyridines with alcohols using rose bengal as an organic photoredox catalyst (Scheme 7) [19]. A wide range of functional groups could be tolerated to afford C(sp^2)–H alkoxylated products using air as the terminal oxidant.

In the past several years, Nicewicz's group has developed a series of strategies for anti-Markovnikov alkene hydro-etherification [20]. In the proposed mechanism (Scheme 8), the olefin could be oxidized to corresponding radical cation, and then the radical cation was attacked by nucleophiles. The high regioselectivity was supported by the stability of radical cation. According to this strategy, they achieved the hydro-etherification of olefins with alcohols as the nucleophiles including intramolecular (Scheme 8a) [21] and intermolecular pathways (Scheme 8b) [22]. If the

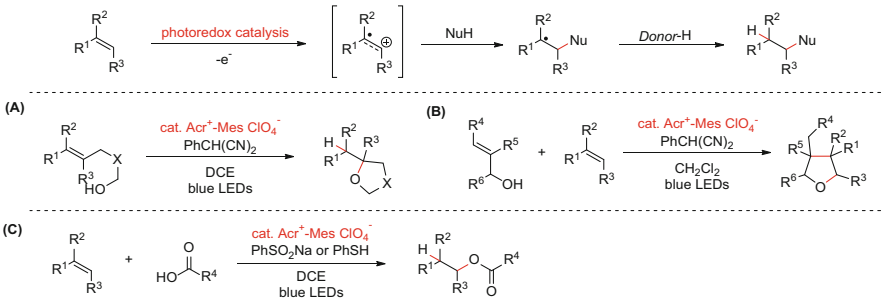

Scheme 8 Photocatalyzed hydro-etherification of olefins with alcohols or acids

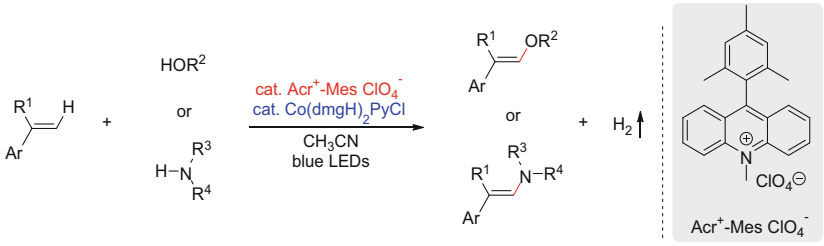

Scheme 9 Photocatalytic C–H/O(N)–H cross-coupling by using alcohols or azoles

alcohol is replaced by the carboxylic acid, the anti-Markovnikov addition of acid to alkene will be achieved in the similar approach (Scheme 8c) [23].

Inputting energy by photocatalysis and employing a cobalt catalyst as a two-electron acceptor, Lei developed a direct C–H/O–H or C–H/N–H cross-coupling with H_2 evolution for C–O and C–N bond formation (Scheme 9) [24]. A wide range of aliphatic alcohols – even long-chain alcohols – are tolerated well, providing a new route to multi-substituted enol ether derivatives using simple alkenes. In addition, this protocol can also be applied to *N*-vinylazole synthesis. This method represents a new radical alkenylation using alkene as the redox compound.

2.1.2 H_2O as the Nucleophile

Selective functionalization of unreactive C–H bonds is undoubtedly a step-economic approach to build complex molecules. In 2013, Pandey achieved a photocatalytic benzylic C–H activation for intramolecular and intermolecular C–O bond formation using 1,4-dicyanonaphthalene (DCN) as the photoredox catalyst (Scheme 10) [25]. Alkylarenes are successfully transformed into aryl ketones using water as a source of oxygen. This method can be further applied to intramolecular cyclo-etherification reactions. Later, Pandey also developed a visible-light-catalyzed

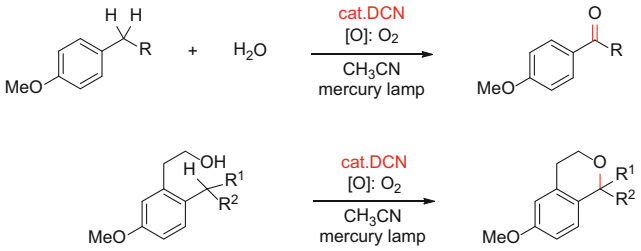

Scheme 10 Visible-light-mediated benzylic C–H functionalization

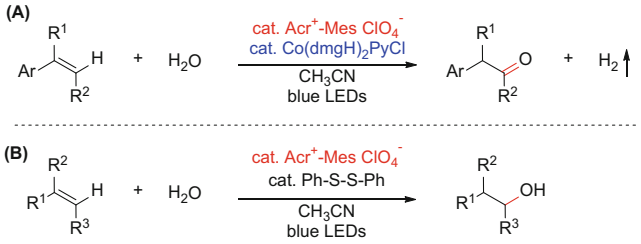

Scheme 11 (**a**) Visible-light-mediated oxygenation of styrene. (**b**) Visible-light-mediated addition of water to alkene

reaction-selective benzylic C(sp^3)−H oxidation, as well as amination using Ir(III) photoredox catalyst [26].

Oxygenation of alkenes is one of the most straightforward routes for the construction of carbonyl compounds. Lei and co-workers described a photocatalytic oxygenation of β-alkyl styrenes and their derivatives with water (Scheme 11a) [27]. This process was performed under external-oxidant-free conditions by utilizing the synergistic effect of photocatalysis and proton-reduction catalysis. Through the visible-light-induced alkene radical cation formation, the high anti-Markovnikov regioselectivity of oxidation process can be achieved. Mechanistic studies revealed that the oxygen atom of carbonyl group was originated from water. By using similar strategy, a visible-light-mediated anti-Markovnikov addition of water to alkenes by using an acridinium ion as the organic photoredox catalyst in conjunction with a redox-active hydrogen atom donor was achieved by Lei and co-workers (Scheme 11b) [28]. Both terminal and internal olefins are tolerated in this transformation to obtain corresponding primary and secondary alcohols in good yields with single regioselectivity.

Recently, Han and co-workers have developed a visible-light-mediated multicomponent oxidative trifluoromethylation of alkynes to α-CF_3-incorporated ketones from various alkynes (Scheme 12) [29]. The broad scope of functional group tolerance and the synthesis of various CF_3-incorporated heterocyclic compounds demonstrate the versatile applicability of the method. Mechanistic study reveals that H_2O can be used as a nucleophile and that enol-keto tautomerization is occurring.

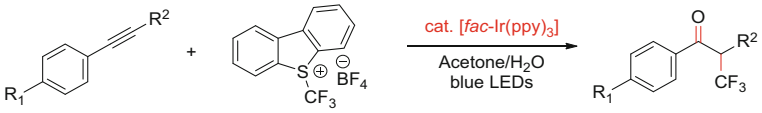

Scheme 12 Oxidative trifluoromethylation of alkynes via photoredox catalysis

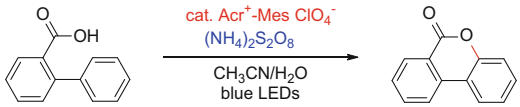

Scheme 13 Visible-light-mediated intramolecular C–O bond formation with $(NH_4)_2S_2O_8$ as a terminal oxidant

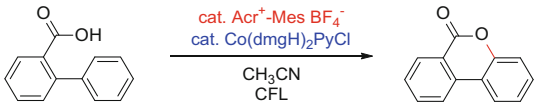

Scheme 14 Visible-light-mediated intramolecular C–O bond formation without external oxidant

2.1.3 RCOOH as the Nucleophile

Benzo-3,4-coumarin derivatives are widely found in natural bioactive compounds and material science [30]. In 2015, Gonzalez-Gomez developed a visible-light-induced dehydrogenative lactonization of 2-arylbenzoic acids under metal-free conditions. The combination of the photoredox catalyst Acr^+-Mes ClO_4^- with $(NH_4)_2S_2O_8$ as a terminal oxidant provides an economical and environmentally benign way to substituted benzocoumarins (Scheme 13) [31].

Recently, Luo, Zhu, and Lei have independently developed a practical photoredox and cobalt-co-catalyzed C(sp^2)–H functionalization/C–O bond formation reaction (Scheme 14) [32–34]. These transformations avoid the use of external oxidant with dihydrogen as the only by-product. A variety of lactone products can be successfully constructed with good functional group tolerance and high yields.

By harnessing the two discrete photochemical activation modes of (−)-riboflavin, Gilmour achieved the sequentially induced isomerization and cyclization by energy transfer and single-electron transfer (SET) activation pathways, respectively (Scheme 15) [35]. This catalytic approach has been utilized to emulate the coumarin biosynthesis pathway, which features a key photochemical E → Z isomerization step.

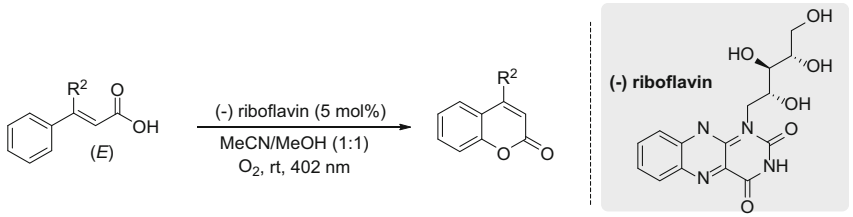

Scheme 15 Photocatalysis route to coumarins catalyzed by (−)-Riboflavin

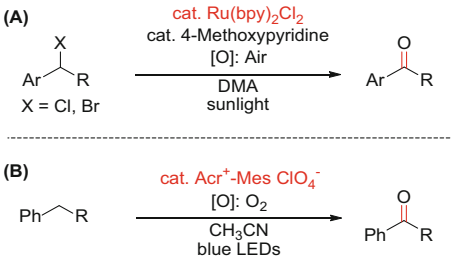

Scheme 16 Visible-light-mediated synthesis of ketones from benzylic halides or benzylic C–H bonds

2.2 *Dioxygen as the Oxygen Source*

The utilization of natural solar energy, as well as molecular oxygen as the ideal oxidant, are arguably two of the most important scientific and technical challenges due to their secure, clean, green, and sustainable characters. In these processes, the O_2 not only serves as the oxidant but also serves as oxygen source in the C–O bond coupling reactions [36–39]. In 2011, Jiao and co-workers disclosed a novel, efficient oxidation of α-aryl halogen derivatives to the corresponding α-aryl carbonyl compounds mediated by visible-light with metal photoredox system(Scheme 16a) [40]. Natural sunlight and air are successfully utilized in this approach through the combination of photocatalysis and organocatalysis. Later, Lei and co-workers demonstrated a photooxygenation of benzylic sp^3 C–H bond using O_2 (Scheme 16b) [41]. This protocol provides a simple and mild route to obtain ketones from benzylic sp^3 C–H bonds with the presence of organic photoredox catalyst. The $^{18}O_2$ labeling experiments demonstrated that the oxygen in ketone products originated from dioxygen. In 2016, Sun and co-workers described an eosin Y-catalyzed oxidation of alkynes for the synthesis of 1,2-diketones by using air as the oxidant under metal-free conditions [42].

Using air as terminal oxidant, Xiao and co-workers developed a visible-light-initiated aerobic oxidative hydroxylation of arylboronic acids (Scheme 17a) [43]. This protocol combines visible light with air in a single reaction system and shows great substrate tolerance, providing rapid and efficient access to a variety of

Scheme 17 Photocatalytic aerobic oxidative hydroxylation of aryl compounds

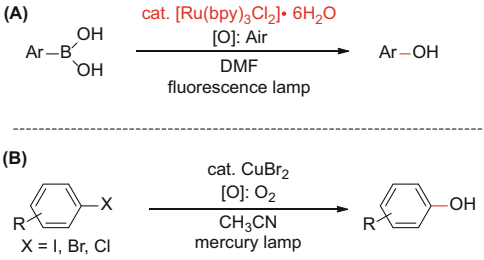

Scheme 18 Photocatalytic synthesis of α-ketoamides

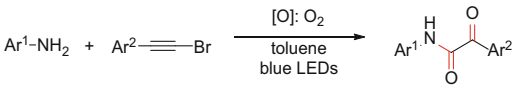

functionalized phenols. Computational and experimental investigations indicate that the boron peroxo complex is an active intermediate. Recently, Liu, Wu, and co-workers have achieved a photoredox-mediated copper-catalyzed hydroxylation of (hetero)aryl halides with O_2 (Scheme 17b) [44]. The protocol enables a variety of functionalized aryl halides (including chlorides, bromides, and iodides) to be transformed into the corresponding phenols at room temperature. The ^{18}O-labeling experiments confirmed the hydroxyl oxygen atom originated from molecular oxygen.

The development of a facile and practical platform for the synthesis of α-ketoamides has attracted more and more attention of synthetic chemists. Recently, Wang, Meng, and co-workers have developed a convenient and practical synthetic route to α-ketoamides from bromoalkynes and anilines under visible-light conditions (Scheme 18) [45]. The reaction is performed without an external photoredox catalyst at ambient conditions, and a wide range of α-ketoamides are obtained in good yields.

2.3 Other C–O Coupling Reactions by Photoredox Catalysis

In 2009, Akita and co-workers reported the oxidative coupling of enamines and aldehydes with 2,2,6,6-tetramethylpiperidinyl-1-oxy (TEMPO) under irradiation of visible light (Scheme 19) [46]. This is a new procedure to afford α-oxyaminated carbonyl compounds based on single-electron transfer mediated by photoactivated ruthenium catalyst. The visible-light irradiation is essential to generate the triplet excited state of photoredox catalyst which acts as an oxidizing agent.

Later, Koike, Akita, and co-workers developed a simple synthesis of both CF_3-containing spirooxazolines and spirooxazines from cyclic alkenes bearing an amide pendant through trifluoromethylative spirocyclization mediated by Ru(II) photoredox catalysis (Scheme 20) [47]. Regiospecific radical trifluoromethylation and anti-selective nucleophilic attack of the amide pendant to the α-CF_3-substituted carbocationic intermediate lead to the formation of CF_3-spirocycles in good to

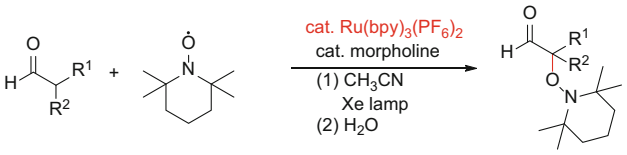

Scheme 19 Visible-light catalytic C–O cross-coupling between aldehyde with TEMPO

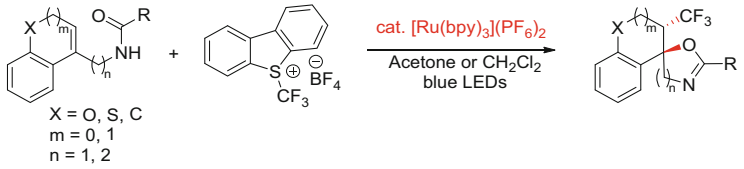

Scheme 20 Synthesis of trifluoromethylative spirocyclization mediated by ruthenium photoredox catalysis

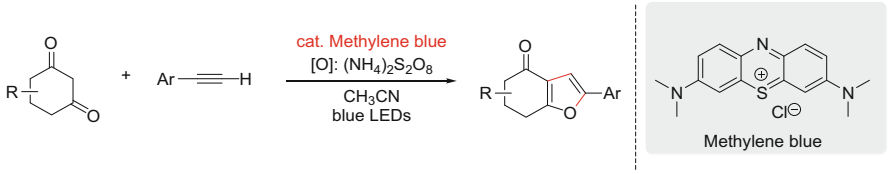

Scheme 21 Visible-light-mediated [3 + 2] cycloaddition between enols and alkynes

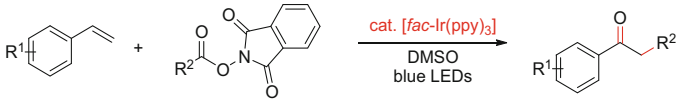

Scheme 22 Synthesis of ketones via photoredox catalysis

excellent diastereoselectivity. This method provides an easy access to antidiastereomers of CF_3-containing spirooxazolines and spirooxazines.

Lei and co-workers reported a visible-light-mediated oxidative [3 + 2] cycloaddition of enols and alkynes to access furans (Scheme 21) [48]. This transformation is well-performed by using the cheap and easy-available methylene blue as the photoredox catalyst in combination with $(NH_4)_2S_2O_8$ as a terminal oxidant. This protocol provides an atom-economical and highly selective method to construct poly-substituted furans in good yields under metal-free, mild, and simple conditions.

Glorius and co-workers reported a visible-light-mediated synthesis of ketones by the oxidative alkylation of styrenes (Scheme 22) [49]. This method allows rapid access to a wide range of α-alkyl-acetophenones in good yields and with high functional group tolerance. In addition, the developed protocol features room temperature conditions, low photoredox catalyst loadings, and the use of dimethyl sulfoxide as mild terminal oxidant and oxygen source.

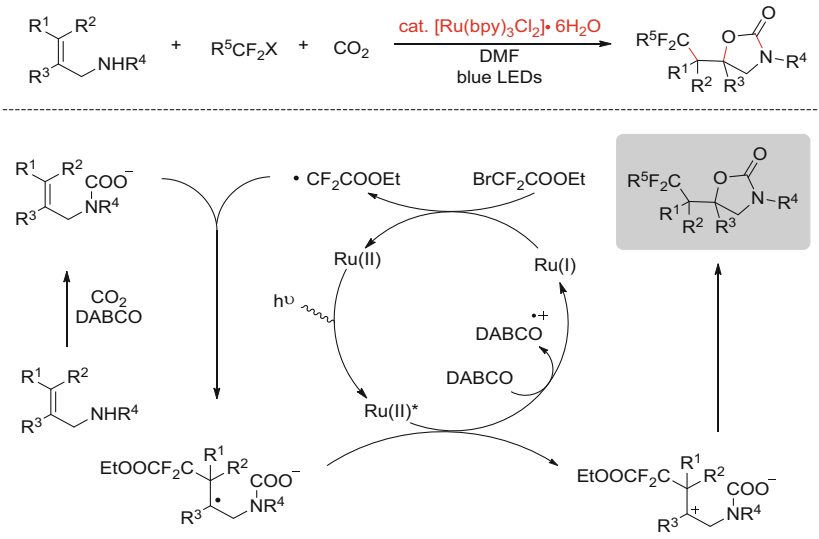

Scheme 23 Photocatalytic oxy-difluoroalkylation of allylamines with carbon dioxide

Using carbon dioxide as oxygen source, Yu and co-workers reported a selective oxy-difluoroalkylation of allylamines with carbon dioxide via visible-light photoredox catalysis (Scheme 23) [50]. These multicomponent reactions are efficient and environmentally friendly to afford a series of important 2-oxazolidinones with functionalized difluoroalkyl groups. The good functional group tolerance, broad substrate scope, easy scalability, and mild reaction conditions provide great potential for application in organic synthesis.

3 C–N Coupling via Photoredox Catalysis

The development of efficient methods to construct C−N bonds is a pivotal goal in organic synthesis owing to their ubiquitous and indispensable presence in pharmaceutical, agrochemical, and material science. The transition metal-catalyzed (Pd, Cu, and so on) cross-coupling of aryl halides (Ar–X) with azoles has served as a powerful tool for constructing C–N bonds [51, 52]. During recent research on photochemistry, visible-light photoredox catalysis can also provide optional approaches for C−N bond formation [53].

3.1 C–X/N–H Cross-Coupling Mediated by Visible Light

In 2012, Fu, Peters, and co-workers reported that Ullmann C–N coupling could be achieved by using a stoichiometric or a catalytic amount of copper under visible-light conditions (Scheme 24a) [54]. An array of data were consistent with a single-electron transfer mechanism. Later, Kobayashi's group also reported the visible-light-mediated Ullmann-type C–N cross-coupling reaction between carbazole derivatives and aryl iodides (Scheme 24b) [55]. The reaction is accomplished with the participation of an iridium-based photoredox catalyst and a copper salt under blue light-emitting diode irradiation.

Later, N-alkylation of carbazoles was achieved by using a simple precatalyst (CuI) under mild conditions (0°C) in the presence of a Brønsted base. A variety of secondary and hindered primary alkyl iodides are well tolerated (Scheme 25a) [56]. A Li[Cu(carbazolide)$_2$] complex has been crystallographically characterized,

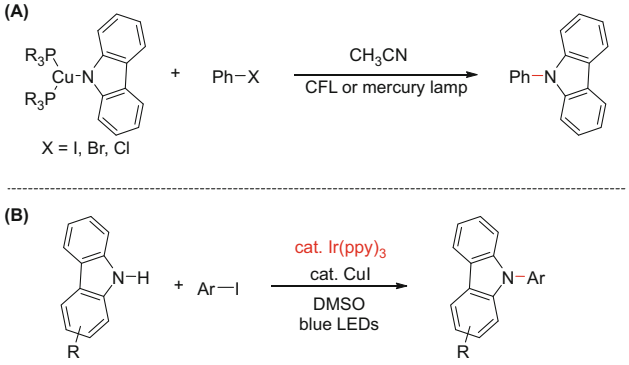

Scheme 24 Visible-light-induced C–N cross-coupling by using a stoichiometric or a catalytic amount of copper

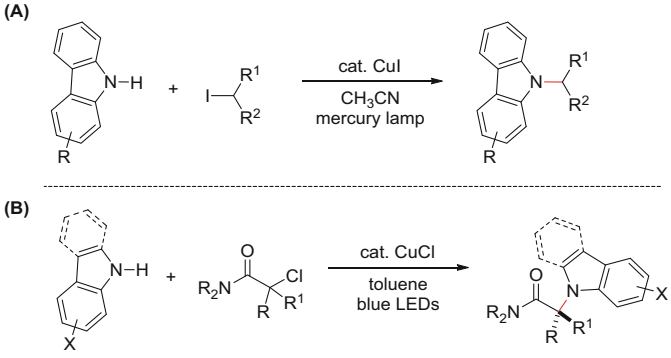

Scheme 25 (**a**) Photocatalytic C–N bond formation under mild conditions. (**b**) Photocatalytic C–N bond formation with a high enantioselectivity

Scheme 26 (**a**) Cross-coupling of alkyl halide and primary amide. (**b**) Cross-coupling of alkyl iodide and primary aliphatic amine

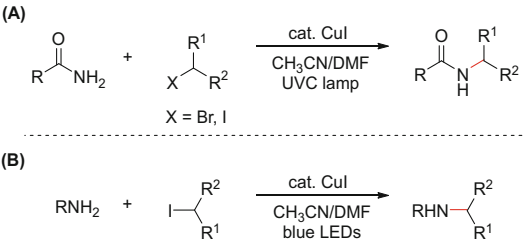

Scheme 27 Cross-coupling between aryl amide with aryl boronic acid

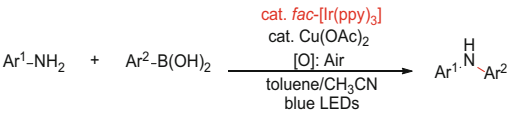

Scheme 28 Visible-light induced [3 + 2] cyclization by using a nickel catalyst

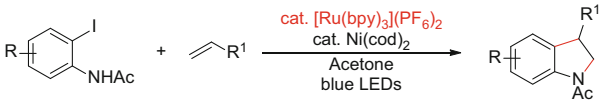

and it may serve as an intermediate in the catalytic cycle. Consequently, Fu and co-workers also achieved the enantioconvergent C–N cross-coupling reaction under the similar condition (Scheme 25b) [57]. In this work, racemic tertiary alkyl chlorides and carbazoles were used. A chiral phosphine ligand was valuable for the high yield and enantioselectivity.

Using similar system, Fu and co-workers developed visible-light-mediated cross-coupling of unactivated secondary alkyl halides and primary amides (Scheme 26a) [58]. The copper(I)-amidate complex was considered to be an important intermediate, which could be excited and then occur a single-electron-transfer (SET) process with the alkyl halide. The selective monoalkylation of aliphatic amines by unactivated, hindered halides persist as a largely unsolved challenge in organic synthesis. In 2017, Fu and co-workers also applied the copper-catalyzed and photo-induced method to cross-coupling reaction between primary aliphatic amines and secondary alkyl iodides (Scheme 26b) [59]. Good functional group tolerance, good yields are achieved in this protocol.

Besides cross-coupling reactions, an oxidative cross-coupling reaction between aryl amides with aryl boronic acids was achieved by Kobayashi and co-workers (Scheme 27) [60]. Through the productive merger of copper and iridium photoredox catalysis, the substrate scope of this oxidative coupling reaction was expanded to electron-deficient aryl boronic acids as viable starting materials.

When choosing the styrenyl olefins as the two-carbon building block, Jamison's group demonstrated an annulation reaction of 2-iodoaniline derivatives with terminal alkenes in 2015 (Scheme 28) [61]. Using a nickel/NHC catalytic system, 2-substituted indolines could be synthetized in this high regioselective protocol.

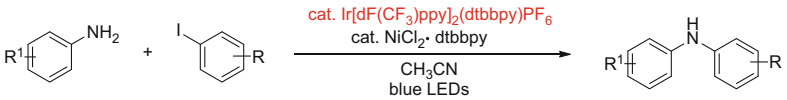

Scheme 29 C–I/N–H cross-coupling by using the photoredox and nickel catalyst system

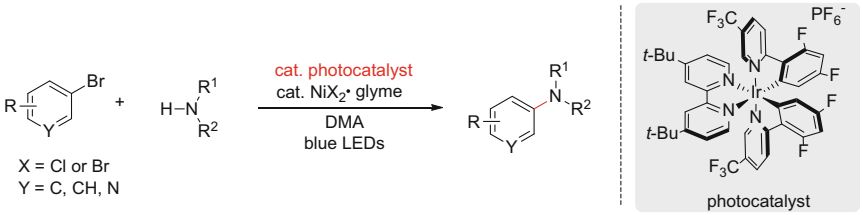

Scheme 30 Visible-light-induced C–N bond cross-coupling between aryl bromide and amine

Using a mixed photoredox and nickel catalyst system, Johannes and co-workers developed a visible-light-promoted iridium photoredox and nickel dual-catalyzed cross-coupling procedure for the formation of C–N bonds (Scheme 29) [62]. With this method, various aryl amines were chemoselectively cross-coupled with electronically and sterically diverse aryl iodides and bromides to forge the corresponding C–N bonds. The coupling reactions were carried out at room temperature without the rigorous exclusion of molecular oxygen, thus making this newly developed Ir-photoredox/Ni dual-catalyzed procedure mild and simple.

Buchwald, MacMillan, and co-workers achieved a visible-light-induced cross-coupling of aryl bromides and amines to form C–N bonds through the merger of iridium photoredox and nickel catalysis under ligand-free conditions (Scheme 30) [63]. This strategy represents a complementary approach to traditional ligated-palladium catalysis through the use of a distinct mechanistic pathway for reductive elimination, which will likely be broadly applicable across a range of substrate classes.

3.2 C–H/N–H Cross-Coupling Mediated by Visible Light

3.2.1 C–H/N–H Cross-Coupling Reaction

The direct C–H/N–H cross-coupling for C−N bond formation is quite appealing in terms of atom and step economy. In 2015, Pandey and co-workers reported a synthetically valuable cross-dehydrogenative benzylic C(sp^3)–H amination reaction via visible-light photoredox catalysis (Scheme 31a) [64]. This protocol employs DCA (9,10-dicyanoanthracene) as a visible-light-absorbing photoredox catalyst and an amide as the nitrogen source without the need of any transition metal. Using photocatalytic strategy, Lei and co-workers also developed a simple and mild

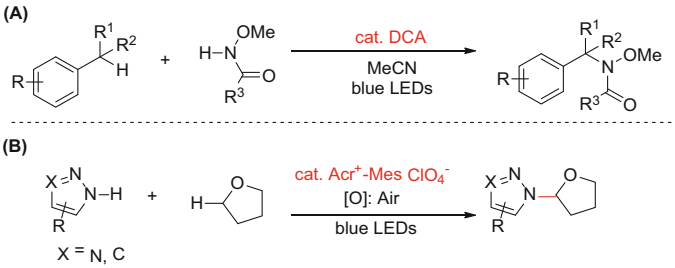

Scheme 31 (**a**) Benzylic C(sp^3)–H amination via photoredox catalysis. (**b**) C(sp^3)–H amination of THF via photoredox catalysis

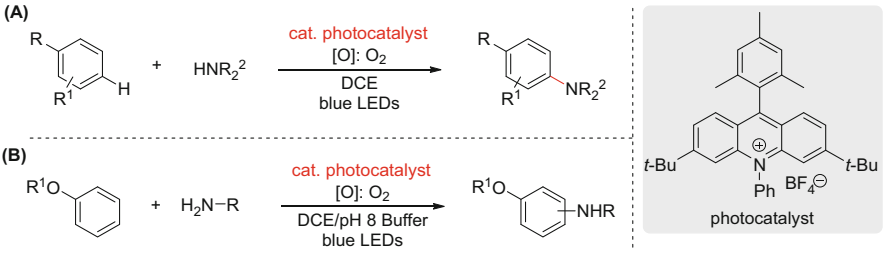

Scheme 32 (**a**) Visible-light-mediated C–N bond construction between aromatics with heteroaromatic azoles. (**b**) Visible-light-mediated C–N bond construction by using primary amines

catalytic oxidative amination of tetrahydrofuran mediated by visible-light catalysis with organic photoredox system (Scheme 31b) [65]. The C(sp^3)–H bond of tetrahydrofuran was activated using molecular oxygen as a benign oxidant. In addition, a variety of azoles could be tolerated, providing a green route for N-substituted azoles.

Direct cross-coupling between simple arenes and heterocyclic amines under mild conditions is undoubtedly important for C–N bonds construction. In 2015, Nicewicz and co-workers achieved a photoinduced site-selective C–H amination of simple arenes (Scheme 32a) [66]. This method provides a high site selectivity and tolerates comprehensive functional groups. An organic photoredox-based catalyst system, consisting of an acridinium photooxidant and a nitroxyl radical, promotes site-selective amination of a variety of simple and complex aromatics with heteroaromatic azoles. In addition, ammonia can be used for nitrogen source to form anilines, without the need for prefunctionalization of the aromatic component. Later, Nicewicz also developed a direct aryl C−H amination with primary amines using organic photoredox catalysis with an acridinium photoredox catalyst under an aerobic atmosphere (Scheme 32b) [67].

Carbazoles have attracted great interest for a variety of applications in organic and medicinal chemistry as well as in material science [68]. You, Cho, and co-workers developed an intramolecular C–H bond amination of N-substituted 2-amidobiaryls for the synthesis of carbazoles (Scheme 33) [69]. Under visible light and an aerobic atmosphere, the transformation requires only catalytic amounts of $Pd(OAc)_2$ and [Ir(dFppy)$_2$phen]PF_6.

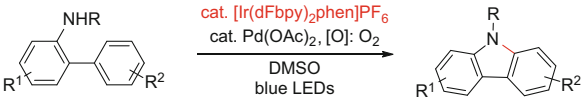

Scheme 33 Intramolecular C–N bond formation via photoredox catalysis

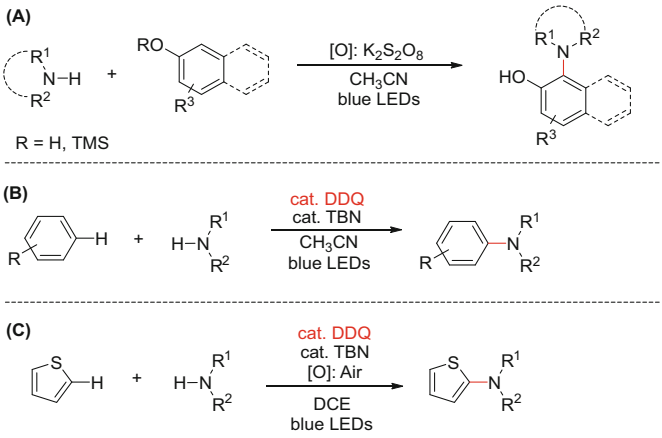

Scheme 34 (**a**) C–H amination between phenols and cyclic anilines induced by visible light. (**b**) C–H amination of benzene derivatives induced by visible light. (**c**) C–H amination between thiophenes and azoles induced by visible light

In 2016, Xia and co-workers developed a cross-dehydrogenative coupling (CDC) amination between phenols and cyclic anilines induced by visible light (Scheme 34a). This protocol provides a direct way to C–N bonds under transition-metal-free conditions [70]. Later, König's group achieved a C–H amination of benzene derivatives using DDQ as photoredox catalyst under aerobic conditions (Scheme 34b) [71]. Electron-deficient and electron-rich benzenes react as substrates with moderate to good product yields. The amine scope in this process was more comprehensive, such as pyrazoles, Boc-amines, carbamates, sulfonamides, and urea. Using DDQ as the photoredox catalyst, Lei and co-workers also reported a photoinduced C–N oxidative cross-coupling between thiophenes and azoles (Scheme 34c) [72]. A series of thiophene C2-amination products could be gained in moderate to good yields. In this process, *tert*-butyl nitrite (TBN) served as the electron transfer mediator and O_2 as the terminal oxidant to regenerate the photoredox catalyst DDQ and revive the photocatalytic cycle.

Recently, Lei and co-workers reported a selective C(sp^2)–H amination of arenes (alkyl-substituted benzenes, biphenyl, and anisole derivatives) accompanied by hydrogen evolution by using heterocyclic azoles as nitrogen sources (Scheme 35) [73]. The reaction is selective for C(sp^2)–H bonds, providing a mild route to *N*-arylazoles. It is interesting that this system works without the need for any sacrificial oxidant and is highly selective for C(sp^2)–H activation.

Scheme 35 Visible-light-mediated C(sp^2)–H amination of arenes

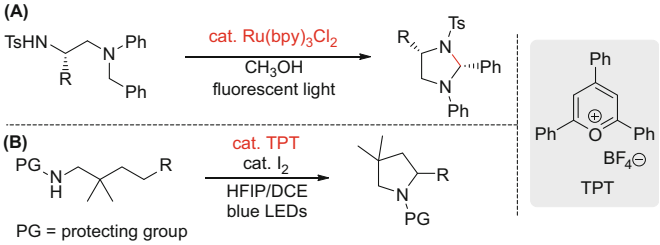

Scheme 36 (**a**) Intramolecular cyclization under visible-light-induced condition. (**b**) Visible-light-mediated C–N bond formation by 1,5-HAT process

3.2.2 Cyclization Reaction via C–H/N–H Coupling

In 2011, Xiao's group developed an efficient method to synthesize tetrahydroimidazole derivatives under the intramolecular cyclization strategy (Scheme 36a) [74]. This photoredox catalytic reaction exhibited high diastereoselectivity and afforded the desired products in good yields. Recently, Reiher, Muñiz, and co-workers have developed an intramolecular benzylic C–H amination via the cooperative interplay between molecular iodine and photoredox catalysis (Scheme 36b) [75]. Iodine serves as the catalyst for the formation of a new C–N bond by activating a remote Csp^3–H bond (1,5-HAT process) under visible-light irradiation.

Indoles are heterocyclic motifs that are embedded in a large number of bioactive natural products and pharmaceuticals. In 2012, Zheng's group presented a mild aerobic oxidation reaction for the construction of *N*-arylindole derivatives (Scheme 37) [76]. Moderate to good yields were afforded by this reaction protocol. It was worth nothing that the substrates without any hydrogen atom on the C2 could take part in a 1,2-carbon shift and a brand-new C–C bond was formed. In the proposed mechanism, the amine was initially oxidized into nitrogen-centered radical cation by a photoexcited $[Ru(bpz)_3](PF_6)_2$. Then, the benzylic radical was subsequently formed through electrophilic addition of nitrogen-centered radical cation to a tethered alkene. The desired *N*-arylindole product was finally afforded via the further oxidation and aromatization.

The oxidative [4 + 2] annulation reaction represents an elegant and versatile synthetic protocol for the construction of six-membered heterocyclic compounds. Recently, Lei and co-workers have developed a photoinduced oxidative [4 + 2] annulation of N–H imines and alkenes by utilizing a dual photoredox/cobaloxime

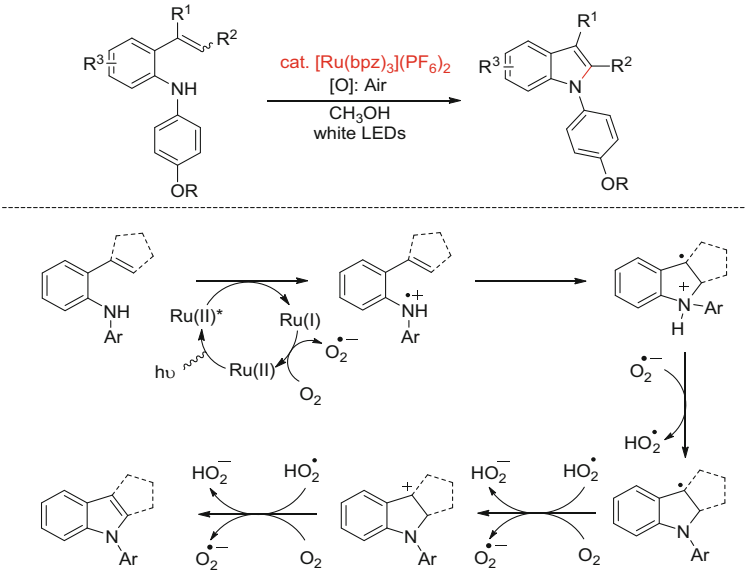

Scheme 37 Photocatalytic intramolecular cyclization to construction of *N*-arylindoles

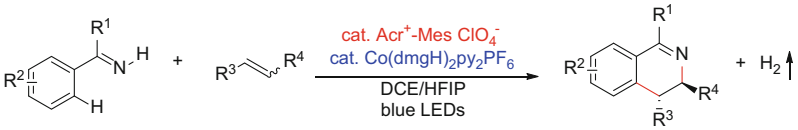

Scheme 38 Visible-light-induced [4 + 2] cyclization with a dual photoredox/cobaloxime catalytic system

catalytic system (Scheme 38) [77]. Various multi-substituted 3,4-dihydroisoquinolines can be obtained in good yields and high regioselectivity. This method not only obviated the need of stoichiometric amounts of oxidants but also exhibited excellent atom economy by generating H_2 as the only by-product. Almost at the same time, Li and co-workers achieved the [4 + 2] annulation under the external oxidant-free condition. A new cobalt catalyst was used in the reaction system [78].

3.3 C–N Coupling Reactions via Nitrogen Radical

The development of methods for the efficient and selective construction of arylamine motifs from simple building blocks is desirable but still challenging. In 2014, Sanford and co-workers reported a visible-light photocatalyzed method for the C–H amination of arenes and heteroarenes (Scheme 39a) [79]. A key enabling

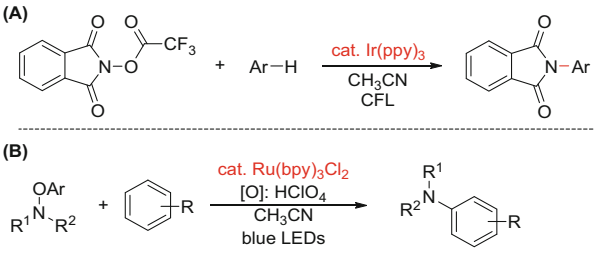

Scheme 39 (**a**) C–H amination by using *N*-acyloxyphthalimides under a visible-light-mediated condition. (**b**) C–H amination by using *O*-aryl hydroxylamines under a visible-light-mediated condition

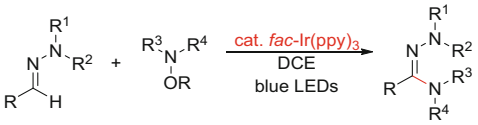

Scheme 40 Visible-light-mediated amination of hydrazones

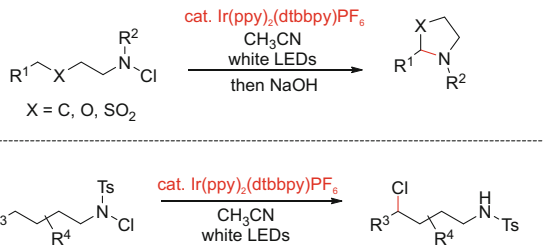

Scheme 41 Visible-light-induced amidation and chlorination of *N*-chlorosulfonamides

advance in this work is the design of *N*-acyloxyphthalimides as precursors of nitrogen-based radical intermediates for these transformations. A broad substrate scope is presented, including the selective meta-amination of pyridine derivatives. Later, Leonori demonstrated a visible light-mediate amination of aromatics via aminium radicals using $Ru(bpy)_3Cl_2$ as the photoredox catalyst (Scheme 39b) [80]. This approach provides fast access to aryl amines from unfunctionalized aromatic compounds.

In 2016, Yu, Zhu, and co-workers developed a reductive single-electron transfer (SET) amination of aldehyde-derived hydrazones through visible-light-promoted photoredox catalysis (Scheme 40) [81]. This direct transformation of hydrazones into the corresponding hydrazonamide through selective carbon-hydrogen (C–H) bond functionalization offers an entirely new substrate class to direct C–H amination.

In 2015, Yu and co-workers reported a visible-light-induced C(sp^3)–H amidation and chlorination of *N*-chlorosulfonamides (Scheme 41) [82]. This remote C(sp^3)–H functionalization can be achieved in weak basic solution at room temperature with 0.1 mol% of the iridium photoredox catalyst. A variety of nitrogen-containing heterocycles and chlorides can be prepared by using this method.

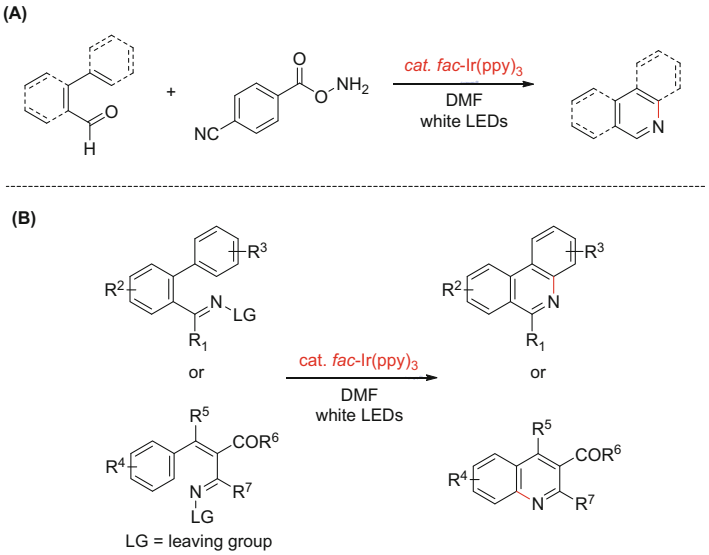

Scheme 42 (**a**) Synthesis of phenanthridines and quinolines from aldehydes and *O*-acyl hydroxylamines. (**b**) Visible-light-induced iminyl-radical formation

Later, Yu and co-workers also developed a visible-light-promoted and one-pot synthesis of phenanthridines and quinolines from aldehydes and *O*-acyl hydroxylamines (Scheme 42a) [83]. In this process, the *O*-acyl oxime was generated in situ from *O*-(4-cyanobenzoyl)-hydroxylamine with aldehydes catalyzed by Brønsted acid. A variety of phenanthridines and quinolines were prepared assisted by Brønsted acid and the iridium photoredox catalyst under visible-light irradiation. Using similar strategy, Zhang, Yu, and co-workers established a unified strategy involving visible-light-induced iminyl-radical formation for the construction of pyridines, quinolines, and phenanthridines from acyl oximes using *fac*-[Ir(ppy)$_3$] as a photoredox catalyst (Scheme 42b) [84]. These reactions proceeded with a broad range of substrates at room temperature in high yields.

Using the organic dye eosin Y as the photoredox catalyst, Leonori reported a photoredox transition-metal-free way for the generation of amidyl radicals (Scheme 43a) [85]. This activation mode represents a general strategy for the implementation of intramolecular hydroamination reactions as well as intermolecular N-arylation processes. These transformations exhibit a broad scope and can also be used in the late-stage modification of complex and high-value N-containing molecules. Later, Leonori also developed a visible-light-mediated radical cascade process for the preparation of polyfunctionalized nitrogen heterocycles (Scheme 43b) [86]. This divergent strategy features the oxidative generation of iminyl radicals and subsequent cyclization/radical trapping, which allows the effective construction of highly functionalized heterocycles.

Using iminyl radical as the key intermediate, Fu and co-workers developed a simple visible-light-promoted intramolecular α-C(sp^3)–H imination of tertiary

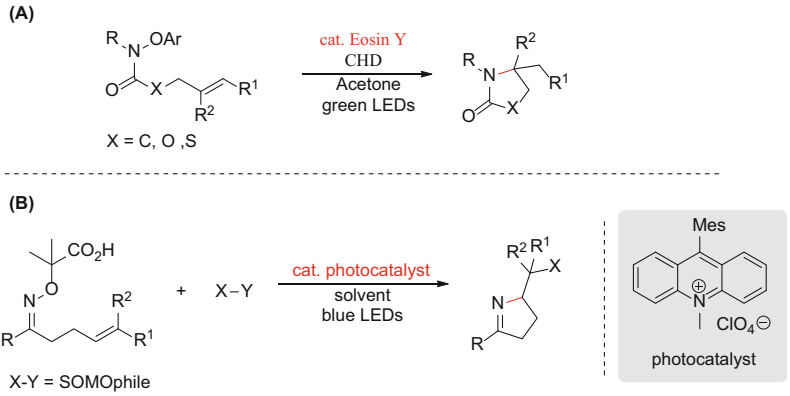

Scheme 43 Visible-light-mediated radical cyclizations

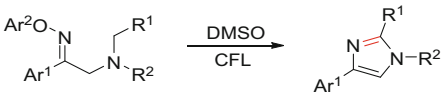

Scheme 44 Visible-light-promoted α-C(sp^3)–H amination of tertiary aliphatic amines

aliphatic amines containing β-*O*-aryl oximes (Scheme 44) [87]. The reaction was performed good reactivity at room temperature with tolerance of some functional groups. Importantly, photoredox catalyst, oxidant, and additive are not required in this selective C–H functionalization reaction.

The N–N precursors could be used as the nitrogen sources and applied in C–N coupling reactions. Xiao and co-workers achieved a nitrogen radical cascade reaction of hydrazones, which could build the 1,6-dihydropyradazines in a mild condition (Scheme 45a) [88]. And the intermolecular process was proved by Zhu and co-worker in the same year (Scheme 45b) [89]. The *N*-aminopyridinium salts are seen as the precursors for nitrogen radicals, which are easily gained upon single-electron reduction. Studer used this kind of strategy to structure the C–N bond between *N*-aminopyridinium salts with arenes or heteroarenes (Scheme 45c) [90].

Recently, Knowles and co-workers developed a photocatalytic intermolecular hydroaminations of unactivated olefins with secondary alkyl amines (Scheme 46) [91]. In this process, carbon-nitrogen bond formation proceeds through a key aminium radical cation intermediate that is generated via electron transfer between an excited-state iridium photocatalyst and an amine substrate.

In 2015, Zhou and co-worker developed a visible-light-induced radical coupling reaction of vinyl azides and α-carbonyl benzyl bromides (Scheme 47a) [92]. This method provides an efficient route to polysubstituted quinolines via a C–C and C–N bond formation sequence. Using the azide as nitrogen source, König and co-workers also reported a visible-light-mediated C–H amidation of heteroarenes with benzoyl azides (Scheme 47b) [93]. In this process, benzoyl azides were used for the direct and atom economic C–H amidation of electron-rich heteroarenes in the presence of

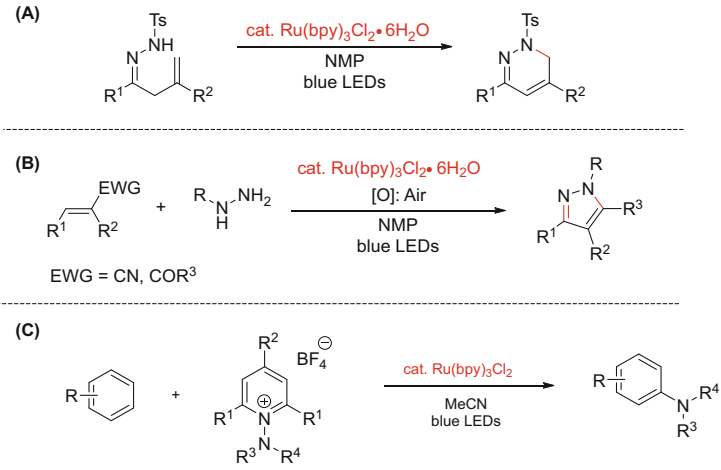

Scheme 45 Nitrogen radical reaction via the visible-light-induced process

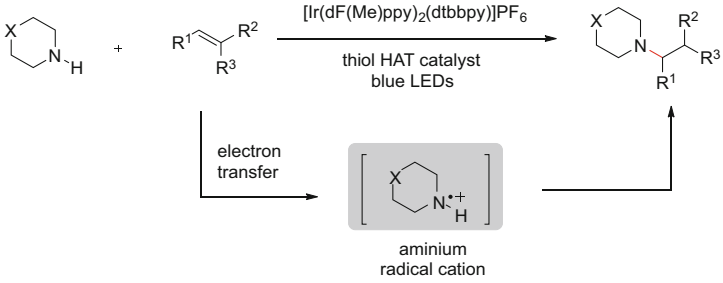

Scheme 46 Photocatalytic intermolecular hydroaminations of unactivated olefins

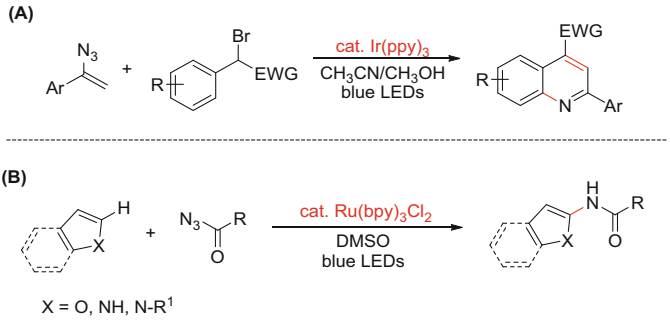

Scheme 47 (**a**) Radical coupling reaction of vinyl azides and α-carbonyl benzyl bromides. (**b**) Visible-light-mediated C–H amidation of heteroarenes with benzoyl azides

phosphoric acid, the ruthenium photoredox catalyst, and visible light. The reaction allows the use of aryl, heteroaryl, or alkenyl acyl azides and has a wide scope for heteroarenes, including pyrroles, indole, furan, benzofuran, and thiophene derivatives, which can afford good regioselectivities and yields.

3.4 *Others C–N Coupling Reactions Mediated with Photoredox Catalyst*

In 2014, Lei and co-workers described a visible-light-mediated decarboxylation/oxidative amidation of α-keto acids with amines using $[Ru(phen)_3]Cl_2$ as the photoredox catalyst (Scheme 48) [94]. Various functional groups are well-tolerated in this reaction and thus provide a new approach to developing advanced methods for aerobic oxidative decarboxylation.

In 2013, MacMillan and co-workers developed a direct, asymmetric α-amination of aldehydes via a combination of photoredox and organocatalysis (Scheme 49) [95]. This method provides an access to complex N-substituted α-amino aldehydes. Later Meggers and co-workers achieved an efficient photo-mediated enantioselective radical amination of 2-acyl imidazoles catalyzed by achiral-at-metal rhodium complex [96].

Hwang reported a visible-light-initiated copper(I)-catalyzed oxidative C–N coupling of anilines with terminal alkynes (Scheme 50a) [97]. The α-ketoamides can be directly prepared using commercially available alkynes and anilines at room temperature using O_2 as the oxidant. Using similar catalytic system, Hwang also demonstrated an oxidative C–N coupling of 2-aminopyridine with terminal alkynes mediated by visible light (Scheme 50b) [98]. This method works well for a wide range of substrates including electron-deficient 2-aminopyridines and various terminal alkynes. The mechanistic investigation illustrated that the copper(II)-superoxo or copper(II)–peroxo complex was most probably responsible for the oxidative cleavage of triple bonds in terminal alkynes.

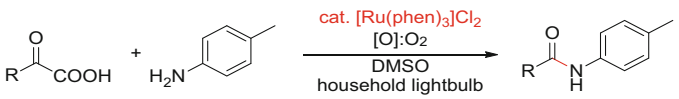

Scheme 48 Visible-light-mediated decarboxylation/oxidative amidation of α-keto acids

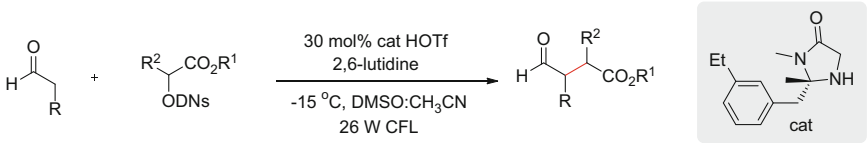

Scheme 49 Asymmetric α-amination of aldehydes via photoredox catalysis

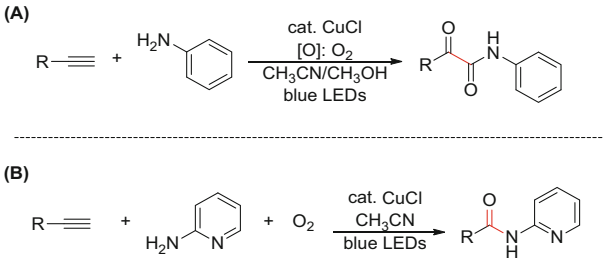

Scheme 50 Copper(I)-catalyzed oxidative C–N coupling of anilines with terminal alkynes

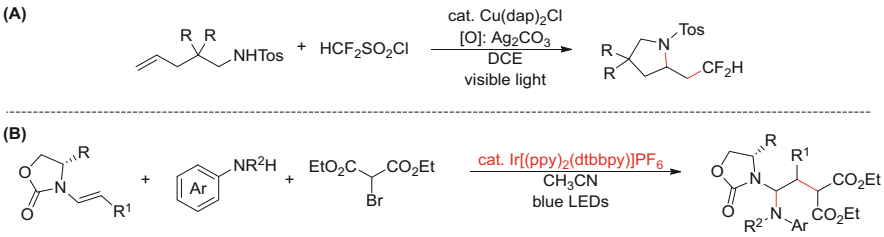

Scheme 51 (**a**) Photoredox-catalyzed aminodifluoromethylation of unactivated alkenes. (**b**) Photocatalytic approach to *N*-acyl-*N*′-aryl-*N,N*′-aminals

Visible-light-mediated difunctionalization of alkenes also provides a direct route for C–N bond formation [99]. In 2015, Dolbier, Jr and co-workers reported a photoredox-catalyzed aminodifluoromethylation of unactivated alkenes using HCF_2SO_2Cl as the HCF_2 radical source (Scheme 51a) [100]. Sulfonamides were active nucleophiles in the final step of a tandem addition/oxidation/ cyclization process to form pyrrolidines, and esters were found to cyclize to form lactones. A variety of pyrrolidines and lactones were obtained in moderate to excellent yields. Recently, Kimber have developed a photocatalytic approach to synthetically valuable *N*-acyl-*N*′-aryl-*N,N*′-aminals (Scheme 51b) [101]. The reaction has been shown to be compatible with electron-rich and electron-deficient arylamines, and moderate to good levels of diastereoselectivity can be attained using a chiral enamide. The method went through the addition of a radical precursor to enamides, with subsequent interception of the cationic iminium intermediate by using an arylamine.

4 Conclusions

Visible-light-mediated photocatalysis has proved to be a powerful tool to the construction of new chemical bond. It has attracted widely research interest from all around the world. In the past several years, various kinds of chemical substances,

including small organic molecules and transition metal complexes, have been applied as photosensitizers for the discovery of new synthetic methods and the exploration of their mechanism. This chapter provides an updated summary of visible-light-mediated cross-coupling for C–O and C–N bond formations. Compared with the traditional synthetic methods, visible-light catalysis provides new ways for the useful compounds synthesis (O-containing and N-containing molecules). There are still many unexplored methods and unknown insightful mechanism left, such as the improvement of efficiency of the visible-light catalysis, the extension of substrate scope, the application for the synthesis of complex molecules or nature products, and the understanding of single-electron transfer process. To reach these challenges, no doubt that the photoredox catalysis, because of its very mild conditions, usually room-temperature operations, will allow important improvements in organic synthesis of complex molecules and molecular materials.

References

1. Xuan J, Xiao WJ (2012). Angew Chem Int Ed 51:6828–6838
2. Zeitler K (2009). Angew Chem Int Ed 48:9785–9789
3. Prier CK, Rankic DA, MacMillan DW (2013). Chem Rev 113:5322–5363
4. Romero NA, Nicewicz DA (2016). Chem Rev 116:10075–10166
5. Narayanam JM, Stephenson CR (2011). Chem Soc Rev 40:102–113
6. Xi Y, Yi H, Lei A (2013). Org Biomol Chem 11:2387–2403
7. Yasu Y, Koike T, Akita M (2012). Angew Chem Int Ed 51:9567–9571
8. Courant T, Masson G (2012). Chem Eur J 18:423–427
9. Carboni A, Dagousset G, Magnier E, Masson G (2014). Org Lett 16:1240–1243
10. Yi H, Zhang X, Qin C, Liao Z, Liu J, Lei A (2014). Adv Synth Catal 356:2873–2877
11. Fumagalli G, Boyd S, Greaney MF (2013). Org Lett 15:4398–4401
12. Hopkinson MN, Sahoo B, Glorius F (2014). Adv Synth Catal 356:2794–2800
13. Ran Y, Lin QY, Xu XH, Qing FL (2016). J Org Chem 81:7001–7007
14. Tlahuext-Aca A, Garza-Sanchez RA, Glorius F (2017). Angew Chem Int Ed 56:3708–3711
15. Majek M, Jacobi von Wangelin A (2015). Angew Chem Int Ed 54:2270–2274
16. Guo W, Lu LQ, Wang Y, Wang YN, Chen JR, Xiao WJ (2015). Angew Chem Int Ed 54: 2265–2269
17. Terrett JA, Cuthbertson JD, Shurtleff VW, MacMillan DW (2015). Nature 524:330–334
18. Baviskar AT et al (2015). ACS Med Chem Lett 6:481–485
19. Kibriya G, Samanta S, Jana S, Mondal S, Hajra A (2017). J Org Chem 82:13722–13727
20. Margrey KA, Nicewicz DA (2016). Acc Chem Res 49:1997–2006
21. Hamilton DS, Nicewicz DA (2012). J Am Chem Soc 134:18577–18580
22. Grandjean JM, Nicewicz DA (2013). Angew Chem Int Ed Engl 52:3967–3971
23. Perkowski AJ, Nicewicz DA (2013). J Am Chem Soc 135:10334–10337
24. Yi H et al (2017). Angew Chem Int Ed 56:1120–1124
25. Pandey G, Pal S, Laha R (2013). Angew Chem Int Ed 52:5146–5149
26. Pandey G, Laha R, Singh D (2016). J Org Chem 81:7161–7171
27. Zhang G et al (2016). J Am Chem Soc 138:12037–12040
28. Hu X, Zhang G, Bu F, Lei A (2017). ACS Catal 7:1432–1437
29. Malpani YR, Biswas BK, Han HS, Jung YS, Han SB (2018). Org Lett 20:1693–1697
30. Li Y, Ding YJ, Wang JY, Su YM, Wang XS (2013). Org Lett 15:2574–2577
31. Ramirez NP, Bosque I, Gonzalez-Gomez JC (2015). Org Lett 17:4550–4553

32. Shao A, Zhan J, Li N, Chiang CW, Lei A (2018). J Org Chem 83:3582–3589
33. Yang Q, Jia Z, Li L, Zhang L, Luo S (2018). Org Chem Front 5:237–241
34. Zhang M, Ruzi R, Li N, Xie J, Zhu C (2018). Org Chem Front 5:749–752
35. Metternich JB, Gilmour R (2016). J Am Chem Soc 138:1040–1045
36. Ohkubo K, Fujimoto A, Fukuzumi S (2011). Chem Commun 47:8515–8517
37. An J, Zou Y-Q, Yang Q-Q, Wang Q, Xiao W-J (2013). Adv Synth Catal 355:1483–1489
38. Yadav AK, Yadav LDS (2016). Green Chem 18:4240–4244
39. Griesbeck AG, Cho M (2007). Org Lett 9:611–613
40. Su Y, Zhang L, Jiao N (2011). Org Lett 13:2168–2171
41. Yi H, Bian C, Hu X, Niu L, Lei A (2015). Chem Commun 51:14046–14049
42. Liu X, Cong T, Liu P, Sun P (2016). J Org Chem 81:7256–7261
43. Zou YQ et al (2012). Angew Chem Int Ed 51:784–788
44. Zhang X et al (2018). Org Lett 20:708–711
45. Ni K, Meng LG, Wang K, Wang L (2018). Org Lett 20:2245–2248
46. Koike T, Akita M (2009). Chem Lett 38:166–167
47. Noto N, Miyazawa K, Koike T, Akita M (2015). Org Lett 17:3710–3713
48. Shao A, Luo X, Chiang CW, Gao M, Lei A (2017). Chem Eur J 23:17874–17878
49. Tlahuext-Aca A, Garza-Sanchez RA, Schafer M, Glorius F (2018). Org Lett 20:1546–1549
50. Yin ZB et al (2018). Org Lett 20:190–193
51. Monnier F, Taillefer M (2009). Angew Chem Int Ed 48:6954–6971
52. Wolfe JP, Wagaw S, Marcoux J-F, Buchwald SL (1998). Acc Chem Res 31:805–818
53. Chen JR, Hu XQ, Lu LQ, Xiao WJ (2016). Chem Soc Rev 45:2044–2056
54. Creutz SE, Lotito KJ, Fu GC, Peters JC (2012). Science 338:647–651
55. Yoo WJ, Tsukamoto T, Kobayashi S (2015). Org Lett 17:3640–3642
56. Bissember AC, Lundgren RJ, Creutz SE, Peters JC, Fu GC (2013). Angew Chem Int Ed 52: 5129–5133
57. Kainz QM, Matier CD, Bartoszewicz A, Zultanski SL, Peters JC, Fu GC (2016). Science 351: 681–684
58. Do HQ, Bachman S, Bissember AC, Peters JC, Fu GC (2014). J Am Chem Soc 136: 2162–2167
59. Matier CD, Schwaben J, Peters JC, Fu GC (2017). J Am Chem Soc 139:17707–17710
60. Yoo WJ, Tsukamoto T, Kobayashi S (2015). Angew Chem Int Ed 54:6587–6590
61. Tasker SZ, Jamison TF (2015). J Am Chem Soc 137:9531–9534
62. Oderinde MS et al (2016). Angew Chem Int Ed 55:13219–13223
63. Corcoran EB et al (2016). Science 353:279–283
64. Pandey G, Laha R (2015). Angew Chem Int Ed 54:14875–14879
65. Zhang L, Yi H, Wang J, Lei A (2017). J Org Chem 82:10704–10709
66. Romero NA, Margrey KA, Tay NE, Nicewicz DA (2015). Science 349:1326–1330
67. Margrey KA, Levens A, Nicewicz DA (2017). Angew Chem Int Ed 56:15644–15648
68. Schmidt AW, Reddy KR, Knolker HJ (2012). Chem Rev 112:3193–3328
69. Choi S, Chatterjee T, Choi WJ, You Y, Cho EJ (2015). ACS Catal 5:4796–4802
70. Zhao Y, Huang B, Yang C, Xia W (2016). Org Lett 18:3326–3329
71. Das S, Natarajan P, Konig B (2017). Chem Eur J 23:18161–18165
72. Song C, Yi H, Dou B, Li Y, Singh AK, Lei A (2017). Chem Commun 53:3689–3692
73. Niu L, Yi H, Wang S, Liu T, Liu J, Lei A (2017). Nat Commun 8:14226
74. Xuan J, Cheng Y, An J, Lu LQ, Zhang XX, Xiao WJ (2011). Chem Commun 47:8337–8339
75. Becker P, Duhamel T, Stein CJ, Reiher M, Muniz K (2017). Angew Chem Int Ed 56: 8004–8008
76. Maity S, Zheng N (2012). Angew Chem Int Ed 51:9562–9566
77. Hu X, Zhang G, Bu F, Lei A (2018). Angew Chem Int Ed 57:1286–1290
78. Tian WF, Wang DP, Wang SF, He KH, Cao XP, Li Y (2018). Org Lett 20:1421–1425
79. Allen LJ, Cabrera PJ, Lee M, Sanford MS (2014). J Am Chem Soc 136:5607–5610

80. Svejstrup TD, Ruffoni A, Julia F, Aubert VM, Leonori D (2017). Angew Chem Int Ed 56: 14948–14952
81. Zhang M et al (2016). Org Lett 18:5356–5359
82. Qin Q, Yu S (2015). Org Lett 17:1894–1897
83. An XD, Yu S (2015). Org Lett 17:2692–2695
84. Jiang H, An X, Tong K, Zheng T, Zhang Y, Yu S (2015). Angew Chem Int Ed 54:4055–4059
85. Davies J, Svejstrup TD, Fernandez Reina D, Sheikh NS, Leonori D (2016). J Am Chem Soc 138:8092–8095
86. Davies J, Sheikh NS, Leonori D (2017). Angew Chem Int Ed 56:13361–13365
87. Li J, Zhang P, Jiang M, Yang H, Zhao Y, Fu H (2017). Org Lett 19:1994–1997
88. Hu XQ et al (2016). Nat Commun 7:11188
89. Ding Y, Zhang T, Chen QY, Zhu C (2016). Org Lett 18:4206–4209
90. Greulich TW, Daniliuc CG, Studer A (2015). Org Lett 17:254–257
91. Musacchio AJ, Lainhart BC, Zhang X, Naguib SG, Sherwood TC, Knowles RR (2017). Science 355:727–730
92. Wang Q, Huang J, Zhou L (2015). Adv Synth Catal 357:2479–2484
93. Brachet E, Ghosh T, Ghosh I, Konig B (2015). Chem Sci 6:987–992
94. Liu J et al (2014). Angew Chem Int Ed 53:502–506
95. Cecere G, Konig CM, Alleva JL, MacMillan DW (2013). J Am Chem Soc 135:11521–11524
96. Shen X, Harms K, Marsch M, Meggers E (2016). Chem Eur J 22:9102–9105
97. Sagadevan A, Ragupathi A, Lin C-C, Hwu JR, Hwang KC (2015). Green Chem 17: 1113–1119
98. Ragupathi A, Sagadevan A, Lin CC, Hwu JR, Hwang KC (2016). Chem Commun 52: 11756–11759
99. Gentry EC, Knowles RR (2016). Acc Chem Res 49:1546–1556
100. Zhang Z, Tang X, Thomoson CS, Dolbier Jr WR (2015). Org Lett 17:3528–3531
101. Koleoso OK, Elsegood MRJ, Teat SJ, Kimber MC (2018). Org Lett 20:1003–1006

Top Organomet Chem (2019) 63: 295–296
DOI: 10.1007/3418_2018_25

Published online: 23 January 2019

Correction to: Functionalization of C(sp^2)–H Bonds of Arenes and Heteroarenes Assisted by Photoredox Catalysts for the C–C Bond Formation

Pierre H. Dixneuf and Jean-François Soulé

Correction to:
Chapter "Functionalization of C(sp^2)–H Bonds of Arenes and Heteroarenes Assisted by Photoredox Catalysts for the C–C Bond Formation" in:
Pierre H. Dixneuf and Jean-François Soulé,
Top Organomet Chem,
DOI: 10.1007/3418_2018_22

There was a correction received for Fig. 1 and it was updated in this chapter later.

The updated online version of this chapter can be found at
DOI 10.1007/3418_2018_22

Index